Viability Assessment of a Repository at Yucca Mountain

Total System Performance Assessment

U.S. Department of Energy
Office of Civilian Radioactive Waste Management

Volume 3
DOE/RW-0508

DOE/RW-0508/V3

Viability Assessment of a Repository at Yucca Mountain

Volume 3: Total System Performance Assessment

December 1998

U.S. Department of Energy
Office of Civilian Radioactive Waste Management
Yucca Mountain Site Characterization Office

This publication was produced by the U.S. Department of Energy
Office of Civilian Radioactive Waste Management.

For further information contact:
U.S. Department of Energy
Yucca Mountain Site Characterization Office
P.O. Box 30307
North Las Vegas, Nevada 89036-0307

or call:
Yucca Mountain Information Center
1-800-225-6972

or visit:
Yucca Mountain Site Characterization Project website
http://www.ymp.gov

♻ Printed with soy ink on recycled paper.

CONTENTS

CONTENTS (Continued)

Page

CONTENTS (Continued)

Page

CONTENTS (Continued)

Page

CONTENTS (Continued)

CONTENTS (Continued)

CONTENTS (Continued)

CONTENTS (Continued)

Page

FIGURES

FIGURES (Continued)

FIGURES (Continued)

FIGURES (Continued)

FIGURES (Continued)

FIGURES (Continued)

FIGURES (Continued)

Page

FIGURES (Continued)

FIGURES (Continued)

FIGURES (Continued)

FIGURES (Continued)

FIGURES (Continued)

TABLES

TABLES (Continued)

ACRONYMS

ASTM	American Society for Testing and Materials
CCDF	Complementary Cumulative Distribution Function
CFR	*Code of Federal Regulations*
CRWMS	Civilian Radioactive Waste Management System
DOE	U.S. Department of Energy
EIS	Environmental Impact Statement
EPA	U.S. Environmental Protection Agency
LA	License Application
M&O	Management and Operating Contractor
NRC	Nuclear Regulatory Commission
TSPA	Total System Performance Assessment
USGS	U.S. Geological Survey
VA	Viability Assessment
YMP	Yucca Mountain Site Characterization Project

Measurements

Btu	British thermal unit
cm	centimeter
Eh	redox potential
ft	foot
g	gram
in.	inch
kg	kilogram
km	kilometer
kPa	kilopascal
kV	kilovolt
kVA	kilovolt-ampere
lin ft	linear feet
m	meter
mL	milliliter
mm	millimeter
MPa	megapascal

MTHM	metric tons of heavy metal
MTU	metric tons of uranium
MVA	megavolt-ampere
nm	nanometer
pH	hydrogen-ion activity
ppm	parts per million
ppmv	parts per million by volume
psi	pounds per square inch
wt	weight

OVERVIEW

The U.S. Congress directed the U.S. Department of Energy (DOE) to include in the Viability Assessment (VA) for a repository at Yucca Mountain, Nevada,

> ...a total system performance assessment based upon the design concept and the scientific data and analysis available by September 30, 1998, describing the probable behavior of the repository in the Yucca Mountain geological setting relative to the overall system performance standards. (Energy and Water Development Appropriations Act 1997)

This volume presents the results of the Total System Performance Assessment (TSPA) conducted for the VA. This TSPA is one of an iterative series of analyses conducted for Yucca Mountain over the life of the Yucca Mountain Site Characterization Project (YMP). The next TSPA in the series is planned to support the Secretary's decision on site recommendation and the License Application (LA).

The TSPA for the VA (TSPA-VA) analyzes the probable behavior of the reference design for the engineered repository components in the expected natural conditions at the Yucca Mountain site. It also includes sensitivity and uncertainty analyses to illustrate the relative importance of the various TSPA components and parameters. This aspect of the TSPA is particularly useful as a management tool for identifying and prioritizing future work, as reported in Volume 4.

This volume summarizes the TSPA work performed for the VA. Readers wanting all of the supporting information on how the TSPA for the VA was developed and performed are referred to the *Total System Performance Assessment-Viability Assessment (TSPA-VA) Analyses Technical Basis Document* (CRWMS M&O 1998i).

HOW THE TOTAL SYSTEM PERFORMANCE ASSESSMENT VOLUME IS ORGANIZED

Overview–This overview presents a summary explanation of TSPA, the general role of TSPA in repository development, the contents of the TSPA for the proposed repository system at Yucca Mountain. The section then summarizes results of the TSPA, and provides a perspective on the work remaining to support a decision on site recommendation and the LA.

Section 1–General Description of the TSPA Process. Because the subject of TSPA is both important and complex, Section 1 explains in some detail what TSPA is and why it is applicable to repository development and also discusses, from the perspective of the international radioactive waste management community, the general approach for performing a total system performance assessment.

Section 2–Yucca Mountain TSPA for the Viability Assessment. This section states the objectives of the TSPA for the VA and then describes the specific way in which the general TSPA approach was adapted for the TSPA-VA. Next is a general description of how, based on current knowledge, the repository system is interpreted and represented in the TSPA. This description traces the eventual release of radionuclides to the biosphere in terms of the four key attributes of the repository safety strategy. The section then explains the method applied to actually build the computer model used for the TSPA, and how the uncertainty and the variability were treated in the analyses. It concludes with a synopsis of TSPA results.

Section 3–Development of the TSPA-VA Components. The entire system that comprises the TSPA-VA is represented as a series of models or TSPA "components" representing the processes that are expected to influence the system performance. This section presents a detailed description of how each component was developed and also provides some results of analyses for specific aspects of individual components.

Section 4–Base Case Definition and Results. This section explains how and which aspects of the various TSPA components were combined into a total-system model. It then reports TSPA results in terms of an expected "base case" and also as a probabilistic sequence of results. Also shown are the effects of disruptive events, such as volcanism and seismicity. Finally included are analyses of selected design options to the reference design, such as the use of backfill.

Section 5–Sensitivity Analyses for TSPA-VA Components. For each of the TSPA components, this section discusses factors about which there are significant uncertainties in our understanding, and it examines their relative importance to repository system performance. It also examines how sensitive those factors are to changes in the values assigned to them.

Section 6–Summary and Conclusions. In contrast with the previous section that deals with the uncertainty and sensitivity of various aspects of individual components, this section takes the approach of looking at uncertainty from a total system perspective. It then discusses the additional work recommended by the results of the TSPA-VA, by the Performance Assessment Peer Review Panel, and by Nuclear Regulatory Commission (NRC) to improve confidence in the TSPA to support the decision on site recommendation and the LA. These recommendations are then incorporated, along with other considerations outside of the purview of the TSPA, into the LA Plan in Volume 4.

EXPLANATION OF A TOTAL SYSTEM PERFORMANCE ASSESSMENT

The general TSPA process was developed as a cooperative effort involving professionals throughout the international community of radioactive waste management. This process can be visualized as a series of levels going up a pyramid (Figure O-1). The base of the pyramid is built using all of the data and information collected by scientists and engineers involved in site characterization and engineering design. The base is very large because it represents the composite of all the information gathered by a repository program. All of this information feeds, on a very small scale, the conceptualization of how various processes work. An example of this scale is a description of the movement of water molecules as they pass between rock and fractures.

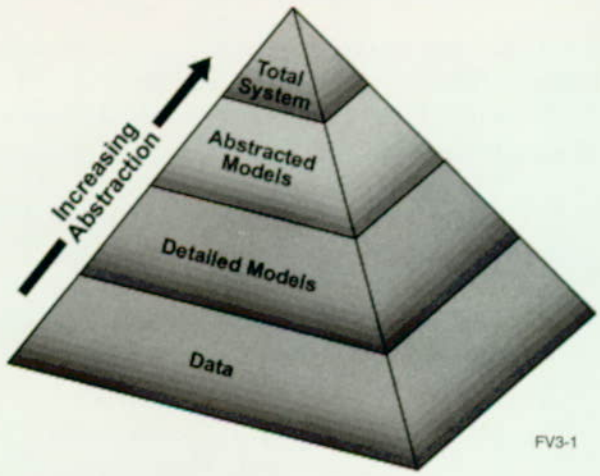

Figure O-1. Performance Assessment Information Flow Pyramid
The process of beginning with many pieces of data from multiple sources and capturing the key attributes of the system through several simplifying stages is represented by the Performance Assessment Information Flow Pyramid.

The specific aspects for describing a process on a larger scale are then extracted and incorporated into a computer model. An example is a model for all water flow above the water table, which would incorporate flow interactions between the rock matrix and the rock fractures as well as many other specifics needed to describe how water flows throughout the rock mass. Every piece of information is not generally used, or needed, in the computer model. Only information determined to be the primary driver for the process makes it up the next level of the pyramid.

This abstraction or progressive simplification to a more compact and usable form is depicted by the slightly smaller width of the pyramid. The models that eventually analyze the evolution through time of all the various components of the system are

generally the most compact or abstracted models of all. Abstraction is necessary for many reasons. One of these reasons is that many of the models are much too large to be run efficiently even on very large computers.

The TSPA must be probabilistic (as opposed to deterministic) to capture the uncertainty and variability in the behavior of the repository system, and thus to determine what is the "probable" behavior of the system under defined conditions. The models are run many times using many combinations of parameters. Each of the combinations of parameters has some definite possibility of representing the actual performance of the repository. These probabilistic analyses are intended to reflect the range of behaviors or values for parameters that could be appropriate, knowing that perfect or complete knowledge of the system will never be available and that the system is inherently variable.

A final reason to use abstraction is that, in some cases, an overly complex model would overrepresent the actual state of knowledge about a process, so a simpler model is more appropriate.

The visualization of the TSPA process is shown in Figure O-2. Here, collection of site data and incorporation of the data (or estimates, where data are not available) first into conceptual models, then into mathematical equations, next into computer (numerical) models, and, finally, into a total system model is illustrated. The figure is a more graphic representation of the process that is depicted using the TSPA pyramid in Figure O-1.

HOW THE REPOSITORY SYSTEM IS VISUALIZED IN THE TOTAL SYSTEM PERFORMANCE ASSESSMENT FOR THE VIABILITY ASSESSMENT

In general, the repository system is visualized as a series of processes linked together, one after the other, spatially from top to bottom in the mountain. From a computer modeling point of view, it is important to break the system into "bite-size" portions that relate to the way information is collected. In reality, the operating repository system will be completely interconnected, and essentially no one process will be independent of other processes. However, the complexity of the system demands some idealization of the system be developed for an analysis to be performed.

The component models are shown on Figures O-3 through O-7 in their relative spatial sequence. Each model in the sequence provides input to the model following it and receives the output of the preceding model or models. The shape of the component model icons shown on these figures is determined by the key attribute of the repository safety strategy they feed. As discussed in Section 2.2.1, the four key attributes are the following:

- Limited water contacting waste packages
- Long waste package lifetime
- Slow release of radionuclides from waste package
- Reduction in the concentration of radionuclides during transport from the waste package

An additional set of icons is used to depict the models associated with off-normal or disruptive events like volcanism, seismicity, nuclear criticality, and human intrusion. These events, if and when they occur, would affect the nominal case processes. The details of the model construction and the input and output parameters are contained in Section 3. The following is an abbreviated description of the expected behavior of the major components.

Limited Water Contacting Waste Package. The changes in climate over time provide a range of conditions that determines how much water falls onto the ground surface and infiltrates (Figure O-3). Based on current scientific understanding, the assumption in the TSPA is that the current climate is the driest that the Yucca Mountain site will ever encounter. All future climates are assumed to be either similar to current conditions or wetter. The water that is not lost back to the atmosphere by evaporation or

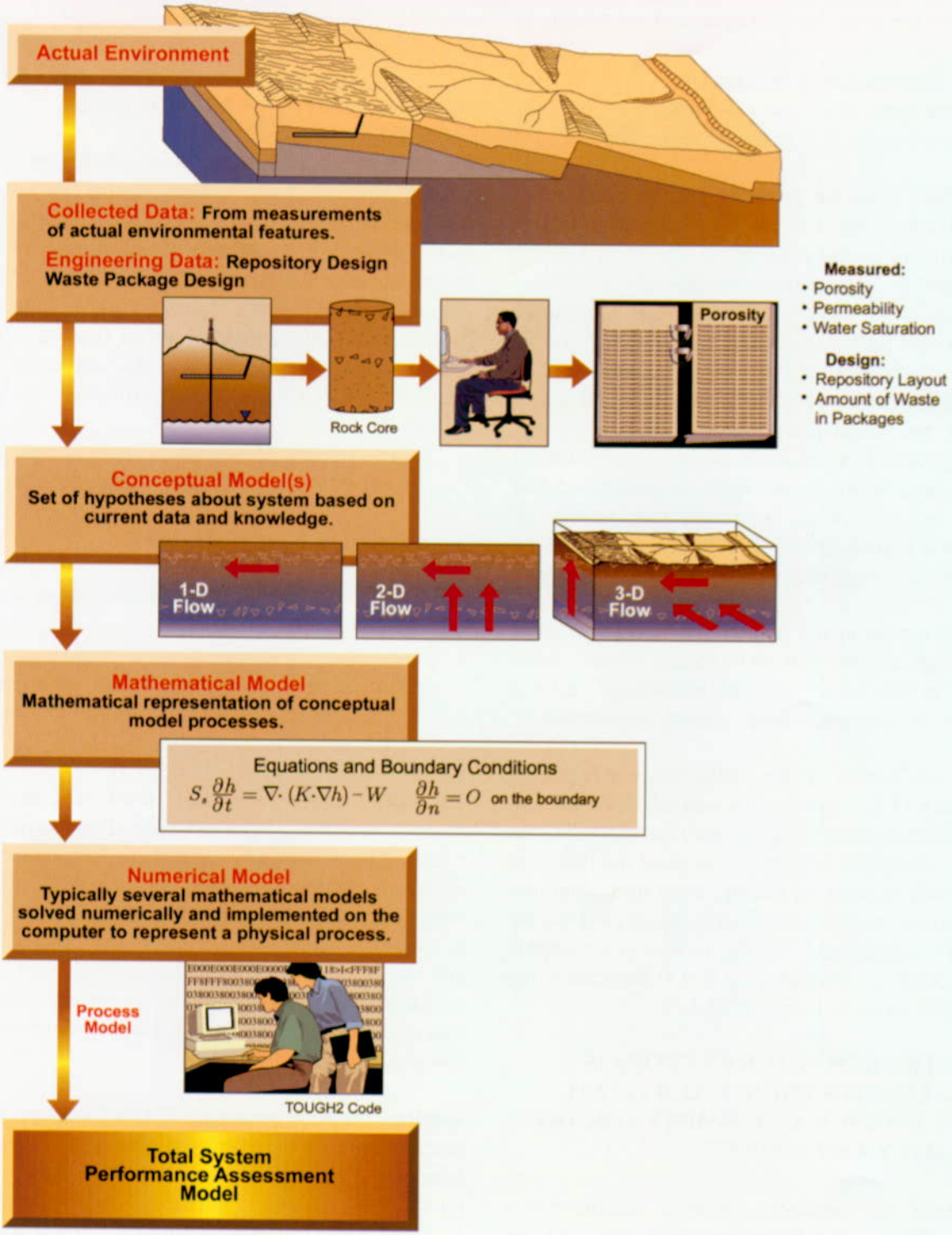

Figure O-2. Generalized Performance Assessment Approach
The generalized performance assessment approach is to develop conceptual models from site and engineering data, to represent the conceptual models using mathematical and numerical systems and to perform a calculation, the outcome of which can be used to describe the performance of the system being studied.

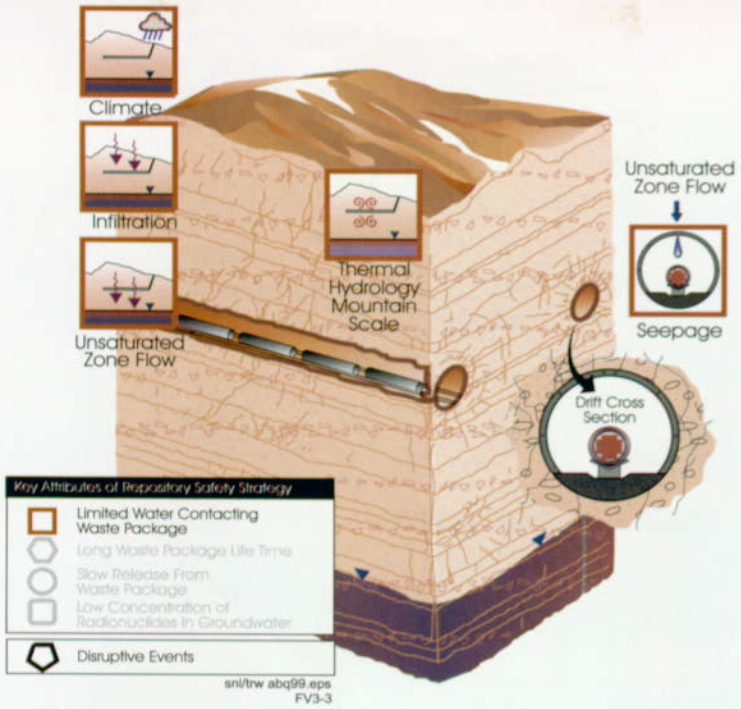

Figure O-3. Limited Water Contacting Waste Package
The five models represented by icons on this figure are used in calculations concerning water movement. Water that falls as precipitation can enter the rock of the mountain by infiltration and may eventually contact waste packages through seeps.

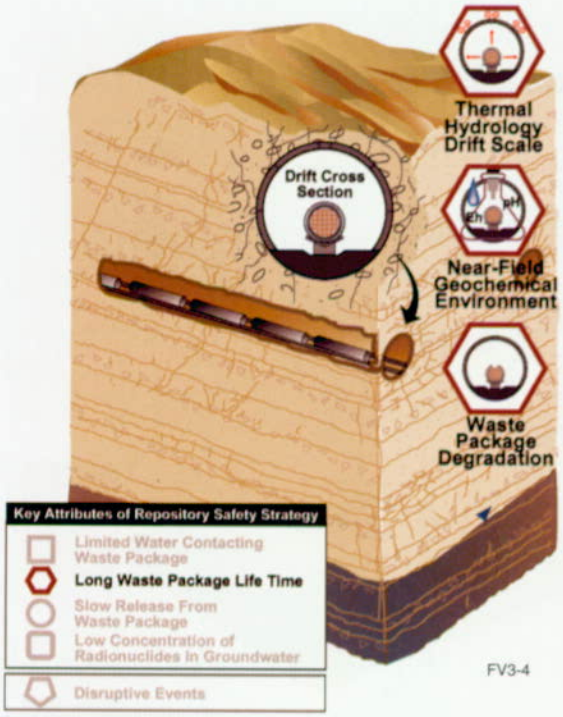

Figure O-4. Long Waste Package Life Time
The three models represented by icons on this figure are used in calculations concerning thermal and chemical environments and the impact of these environments on waste package life time.

Figure O-5. Slow Release from Waste Package
The three models represented by icons on this figure are used in calculations concerning degradation of cladding and the waste form and chemical conditions that affect the rate of release of waste from the waste package.

Figure O-6. Low Concentrations of Radionuclides in Groundwater
The three models represented by icons on this figure are used in calculations concerning the concentration of radionuclides in groundwater and their availability to contribute to exposure of individuals in the accessible environment.

Figure O-7. Disruptive Events
The four models represented by icons on this figure are used in calculations concerning performance of the engineered and natural systems during disruptive events that could release radionuclides.

transpiration enters the unsaturated zone flow system. Water infiltration is affected by a number of factors related to the climate state, such as increase or decrease in vegetation on the ground surface, total precipitation, air temperature, and run-off.

Water generally moves downward in the rock matrix and fractures. The rock mass at Yucca Mountain is composed of volcanic rock that is fractured to varying degrees as a result of contraction during cooling of the originally nearly molten rock and also due to extensive faulting in the area. Water flowing in the fractures moves much more rapidly than the water moving through the matrix. In some locations, some of the water collects into locally saturated zones in the rock or is diverted laterally by differences in the rock properties. The overall unsaturated flow system is very heterogeneous, and the location of flow paths and velocities and volumes of groundwater flowing along these paths are expected to change many times over the life of the repository system.

The thermal heat generated by the spent nuclear fuel in the repository causes the temperature of the surrounding rock to rise from the time of emplacement until about 3,000–4,000 years after repository closure. The water and gas in the heated rock are driven away from the repository during this thermal pulse. The thermal output of the waste decreases with time; eventually, the rock mass returns to its original temperature, and the water and gas flow back toward the repository. After the water returns to the repository walls, it begins to drip into the repository but only in a relatively few places. The number of seeps that can occur and the amount of water that is available to drip is restricted by the low volume of water flowing through Yucca Mountain, which is located in a semiarid region. Drips also can occur only if the hydrologic properties of the rock mass cause the water to concentrate enough to feed a seep. Over time, the number and location of seeps increase and decrease, corresponding to increased or decreased infiltration based on changing climate conditions.

Long Waste Package Lifetime. Because the repository is located above the water table in the unsaturated zone, the most important process controlling waste package lifetime is whether or not water drips on the package (Figure O-4). The location of the seeps providing dripping water depends to some extent on the natural conditions of the rock but also on the alterations caused by repository construction. Alterations such as increased fracturing may be caused by mechanical processes related to drilling the drifts or by thermal heating and expansion of the drift wall. The alterations in the seepage can also be caused by chemical alterations occurring as the engineered materials dissolve in water and re-precipitate in the surrounding rock, closing the pores and/or the fractures. The chemistry in the drift is continually changing because of the complex interactions among the incoming water, circulating gas, and materials in the drift (e.g., concrete from the liner or metals in the waste package). The chemical evolution is strongly influenced by heat during the thermal pulse.

In the reference design, the radioactive waste emplaced in the repository will be enclosed in a two-layer waste package. The layers will be constructed of two different materials that are expected to fail at different rates and from different mechanisms from each other as they are exposed to various repository conditions. The outer layer is made of carbon steel and the inner layer of a high-nickel alloy metal. Where water drips onto the waste packages, the packages corrode and eventually are breached. The breaches are thought to occur as deep, narrow pits or as broader areas called patches. The changing thermal, hydrologic, and chemical conditions in the repository all influence the corrosion rate of the waste packages.

Slow Release of Radionuclides from Waste Package. When water eventually enters a waste package through the patches or pits, it can contact the spent nuclear fuel contained within the waste package. The majority of radioactive waste material comes from commercial reactors, but there is also some material in the form of defense high-level radioactive waste and DOE reactor fuels. However, the influence of the commercial spent nuclear fuel dominates long-term performance of the repository system, so waste from other sources is not included further in this overview discussion.

The water first contacts the very thin layer (about 0.7 mm) of a zirconium alloy that covers the surface of most of the fuel elements. This layer, called cladding, must be breached by mechanical or chemical processes before the radioactive fuel pellets can be exposed. Then the individual fuel elements start to degrade, making the radionuclides available for transport away from the waste form (Figure O-5). The degradation process may involve several stages because the waste forms are sometimes altered to different chemical phases before they reach a phase that will allow the nuclides to be released from the waste. Also, different radionuclides have different chemical properties themselves, so the reaction rates of the individual nuclides with water are greatly variable. In general, however, once the waste form begins to alter, it takes about 1,000 years for the commercial waste forms to completely degrade. The result is that certain nuclides are released much earlier than others are. The results of the TSPA show this effect, as different nuclides become the key contributors to dose rate over time.

To move out of the waste package, the radionuclides are either picked up and carried away from the waste form in flowing water or they move in a thin film of water by diffusion. To escape, the nuclides must exit through a pit or patch in the waste package and move out into the waste emplacement drift.

Low Concentration of Radionuclides During Transport. After escaping from the waste package, the radionuclides can then advance through materials on the drift floor, which are mainly concrete and the corrosion products from the waste package. At this point, the nuclides may either adhere to some of the materials on the drift floor, continue to move in the water, or become attached to extremely small particles of clay, silica, or iron called "colloids." Because of their molecular charge and physical size, these colloidal particles move through the rock mass under the

repository somewhat differently than noncolloidal particles.

The radionuclides move downward beneath the repository at different rates based on the chemical characteristics of the nuclides and of the rock they are passing through and on the velocity of the water in which they are contained (Figure O-6). The rock underlying the repository is unsaturated, and the water movement behaves as described earlier. Some water moves rapidly in fractures and some much more slowly in the rock matrix. The transport rate also depends on the tendency of the individual nuclide to interact with the rock through which it moves. Some radionuclides adhere to some minerals in a process called sorption and are bound in the rock for long periods. Sorption can be irreversible in some instances, and the nuclide is bound permanently in the rock. In other cases, the nuclides may desorb at a future time and again move through the system. Other types of nuclides move more quickly through the rock with little or no interaction that delays their transport.

When the radionuclides reach the water table, they are caught in the saturated zone flow system. Beneath Yucca Mountain, the water in the saturated zone flows in a generally southerly direction toward the Amargosa Valley. Nuclide sorption also occurs in the rocks and alluvium along the flow paths in the saturated zone. Because of the differences in chemistry between the unsaturated and saturated zone rock and water, the rates, durations, and nuclides involved in sorption are different for the two regions. As the radionuclides move in the saturated zone along different paths and through different materials, they gradually become more dispersed and the concentration of the nuclides in any volume of water decreases.

If the radionuclides are pumped out of the saturated zone by water wells, the radioactive material can cause doses to humans in several ways. For example, the water from the well could be used to irrigate crops that are eaten by individuals or livestock; to water stock animals that provide milk or meat food products; or to provide drinking water. Also, if the water pumped from irrigation wells evaporates on the ground surface, the nuclides may be left as fine particulate matter that could be picked up by the wind and then inhaled by humans.

Disruptive Events. The key attributes of the system, given in the previous sections, describe the continually ongoing processes that are expected to occur in and around the proposed repository system. The term used to denote the sequence of anticipated conditions is "nominal case." In contrast, "disturbed case" refers to discrete, unanticipated events that disrupt the nominal case system (Figure O-7). The disruptive events include the following:

- Formation of a volcano through or adjacent to the repository
- Earthquake
- Human intrusion into the repository
- Nuclear criticality

Yucca Mountain is in a terrain that has experienced volcanic activity in the geologic past. The rocks in which the repository will be constructed are volcanic in origin. However, scientific studies of the timing, volume, and other aspects of volcanism have concluded that volcanic activity in this area has been waning in the recent geologic past and that the probability of volcanic activity as a repository-disturbing event is highly unlikely. However, for completeness, part of the TSPA analysis is an assessment of the consequences of a small cinder cone formed by a dike that flowed up through, or close to, the repository drifts.

In contrast, earthquakes happen frequently in and around Yucca Mountain. The effects of an earthquake important to postclosure repository performance primarily result from ground motions rather than from direct offset along a fault. The primary effect of ground shaking is to hasten rockfall into the drift.

Human intrusion is treated in a very simplistic manner as an event in which the contents of a

waste package are released to the water table through the borehole of a well drilled directly through the repository. Providing a "reasonable" (i.e., testable) forecast of future human activity is very difficult, if not impossible. The impact of such human intrusion is not included directly in the final presentation of results but is compared against the TSPA results to determine the potential level of influence. In other words, the probability of human intrusion occurring is assumed to be absolute, so it is simply the possible consequences that are evaluated.

In the TSPA calculations, the effects of nuclear criticality are assessed in the waste package and in the rock surrounding the repository. In these analyses, a series of unlikely events is assumed to occur. These unlikely events (such as filling the waste package with water or concentrating specific radionuclides in the rock mass) lead to the concentration of certain nuclides, that, in specific low probability environments, might lead to a nuclear criticality. The result is a change in the nuclear material to more highly radioactive forms. The introduction of these new radionuclides into the source term is then compared against the base case to determine if the relative change in dose rate is significant.

RESULTS OF ANALYSES

Although the TSPA is usually discussed in terms of a sequence of processes linked one after the other in space (as described in the earlier section), this approach does not readily convey how all of the processes evolve with time. This next section describes the results at various time intervals of interest, attempting to show the evolution in both time and space for the reference design and for the range of nominal-case conditions. However, the assumptions underlying the modeling development drive the results. Different sets of assumptions can give different results. The intent of this TSPA is not only to show how the system is thought to behave but also to provide information on how much uncertainty is associated with each TSPA component, as discussed later. Many of the results shown include a great deal of conservatism and also some large ranges of uncertainty. These areas of conservatism and uncertainty will help drive the specific issues that the YMP will address in the time before the LA. The results discussed below focus on the forecasted average behavior of the system. This average behavior by itself cannot fully represent the ranges of uncertainty and variability in the system and its possible future states. The full range of behavior is discussed in Section 4.

One aspect of the system that is often unclear is that, while results of the analyses are presented so that they show how the system fails over time, there are even larger parts of the system that remain essentially unaltered. Although this fact is reflected indirectly in the results, it is rarely shown explicitly. The sequence of results in the Figures O-8, O-9, O-11, and O-12 show schematically what a waste package might look like at certain time periods. However, the schematics are only representative of those packages that experience dripping water. The percentage of all packages that experience significant corrosion of the resistant inner high-nickel alloy layer is expected to be small. Even though the location and number of seeps changes with time, the majority of packages will likely never experience any significant seepage at all, even in a million years. Most packages will continue to look essentially like the one depicted in Figure O-8 and not like the ones shown in subsequent figures depicting the TSPA results.

Waste Emplacement to Several Thousand Years after Repository Closure. As the waste packages are emplaced in the drifts, their combined heat output causes the drift-wall temperatures to rise and the water and gas in the rock is driven away from the repository. This process progressively dries out the rock mass farther and farther away from the repository. At 100 to 200 years after closure, the surfaces of some of the individual waste packages start to cool below boiling, and the humidity in the drift climbs from preclosure values of about 50 percent to nearly 100 percent. Depending upon the local conditions around each waste package, the degradation of the carbon steel outer layer begins somewhere between a hundred years and several thousand years. The fluids that

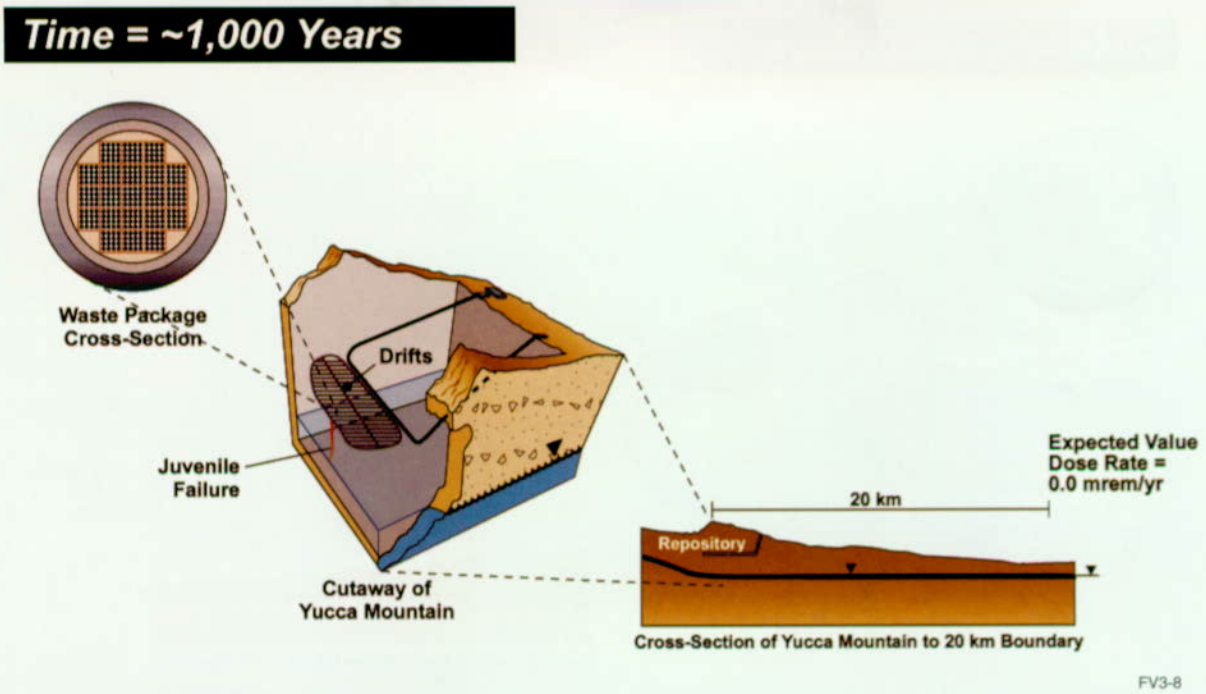

Figure O-8. Potential Radionuclide Release Conditions at About 1,000 Years
Elements of the engineered and natural barrier systems showing potential radionuclide release conditions and the resulting dose rate at the 20-km (12-mile) boundary about one thousand years after waste emplacement.

were driven away by the thermal pulse begin to move back toward the repository. Some of the areas that cool more quickly, particularly those toward the edges of the repository, start to experience dripping water. The packages in these areas have accelerated degradation of the outer barrier so that the inner layer of corrosion-resistant metal is exposed.

In Figure O-8, the cut-away of the repository shows schematically the release for one package in the repository. This release represents a single early failure from processes other than corrosion, such as failure caused by a manufacturing defect or a very large rockfall. Of course, the failed package fortuitously must be located under one of the relatively infrequent seeps for the waste form to be altered and the radionuclides to be picked up and carried away from the drift. Even with the early failure added to the analysis, there is not enough time for the nuclides to be carried to an area where it would be available to humans. Therefore, as shown in the final panel of Figure O-8, there is no dose consequence for any of the cases calculated during this period in the region 20 km (12 miles) downgradient of the repository. The schematic picture of the waste package in Figure O-8 shows the lack of corrosion failures.

Several Thousand Years to 10,000 Years after Closure. By this time, the rock surrounding the drift has returned to its original temperature, and the fluid-flow patterns have been reestablished. Some permanent alterations of the rock may remain (such as microfracturing caused by thermal expansion), but this does not appear to be significant in terms of repository performance. The outer layer of the waste package is continuing to corrode. Dripping conditions now occur at discrete locations throughout the repository. Where the entire thickness of the outer layer has been worn away corrosion of the inner-barrier material is initiated (Figure O-9). In the cases where the inner layer has been perforated, the water can enter the waste packages through small openings, alter the fuel, and move out of the engineered barrier system. The repository cutaway in Figure O-9 shows a few paths along which

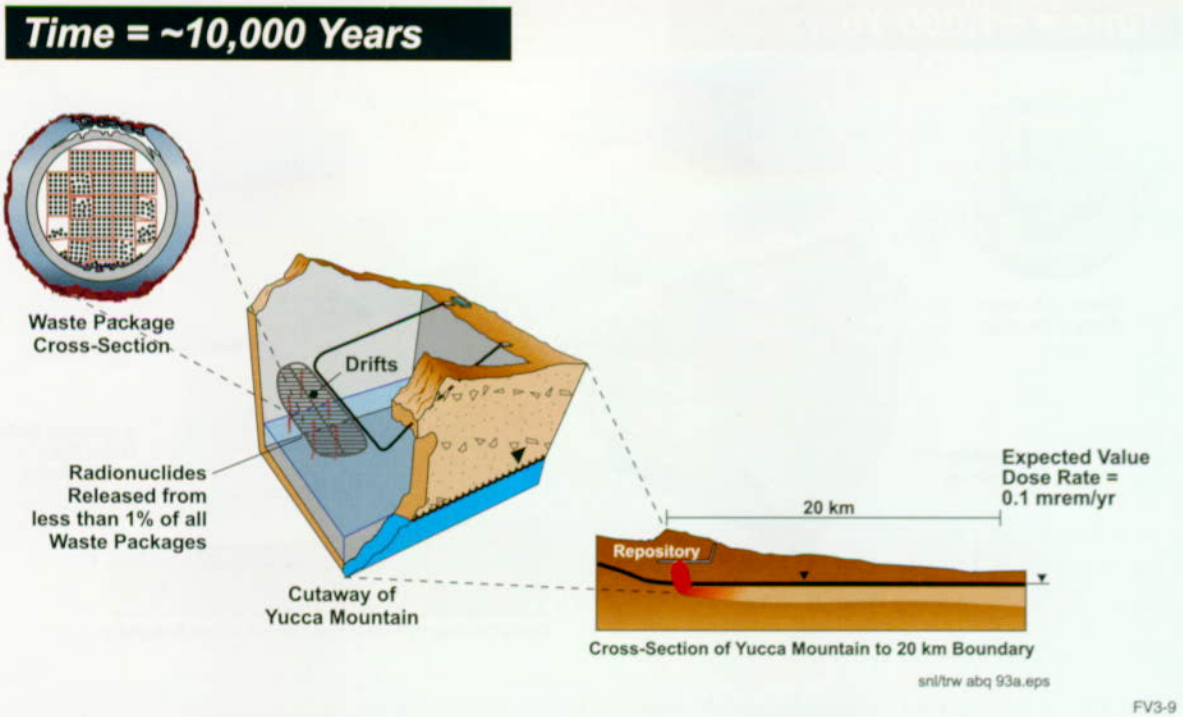

Figure O-9. Potential Radionuclide Release Conditions at About 10,000 Years
Elements of the engineered and natural barrier systems showing potential radionuclide release conditions and the resulting dose rate at the 20-km (12-mile) boundary about ten thousand years after waste emplacement.

nuclides are being released into the rock under the repository. At this time, the expected value for the number of breached waste packages is less than 1 percent of the total emplaced packages. The expected value for the peak dose rate from a plume in the saturated zone 20 km (12 miles) south-southeast of the repository is calculated to be 0.1 mrem/year. This value is 0.03 percent of the average background radiation from nonmedical sources in the United States, which is about 300 mrem/year. The primary nuclides contributing to the dose rate are technetium-99 and iodine-129.

Another way to assess the benefit of the repository system is to show the radionuclide release information in the context of how much radioactivity remains isolated in the repository versus how much has escaped. Figure O-10 illustrates how the total inventory in the repository at the time of closure (30 years) decays with time, and what amount of the total inventory has escaped from the repository at discrete times over 10,000 years. Using the value for the total amount of radioactivity in the repository at 30 years after waste emplacement, by about 300 years after closure the decay process has decreased the radioactivity to about 2 percent of the original amount. At 1000 years the amount has decreased further to 0.8 percent, and at 10,000 years the remaining portion of the original total inventory is only about 0.2 percent. Of the 0.2 percent remaining at 10,000 years, 0.00003 percent has gotten to the edge of the repository, 0.00002 percent has reached the water table, and 0.000001 percent has been transported 20 km (12 miles) south of the edge of the repository, where is assumed to be accessible to humans.

Ten Thousand to 100,000 Years after Closure. The natural conditions in the rock remain unchanged from the previous period except for the likelihood of a change in climate. The likelihood is that, when the climate changes, a significant increase in infiltration has occurred, causing more water to flow through Yucca Mountain, more seeps into the repository to occur, a larger percentage of packages to fail, and more radionuclides to be transported along the unsaturated and saturated zone pathways. The progression of corrosion of

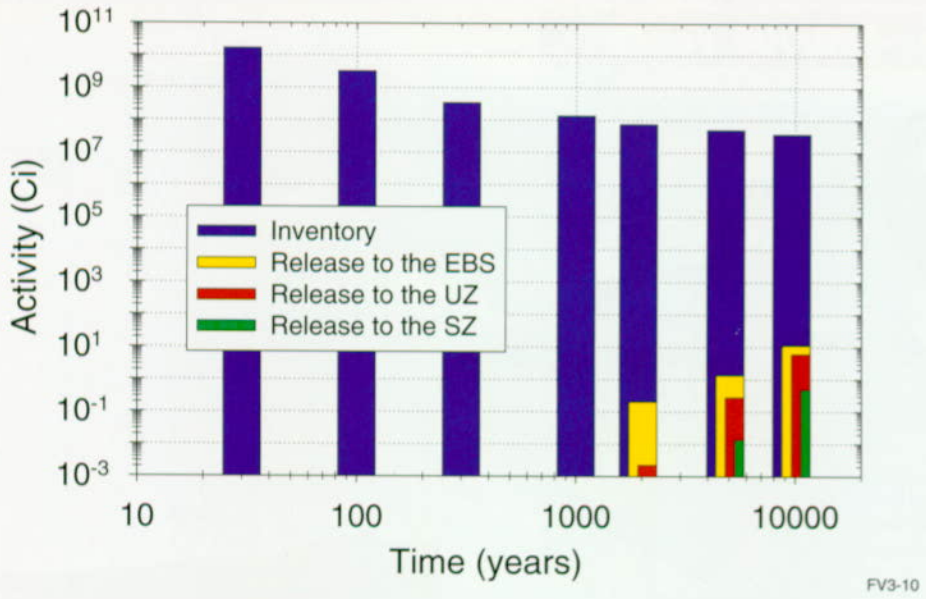

Figure O-10. Progressive Loss of Radioactivity Due to the Decay Process
The blue portion of the bar shows how much of the total radioactivity (in Curies) remains in the system at several points in time. The yellow portion shows the percentage of the remaining radioactivity that has passed through the floor of the repository into the underlying rock, the green indicates the amount of radioactivity that has reached the water table, and the red shows the amount that has moved to the accessible environment 20 km (12 miles) south of the repository.

the packages experiencing dripping water is shown in Figure O-11.

Those nuclides that at earlier times are limited in their release from the spent nuclear fuel elements because of their chemistry become larger contributors to the dose rate. In particular, neptunium-237 becomes the dominant isotope controlling dose rate. The number of packages failing by the end of this time is about 6 percent of the total number. The expected-value peak dose rate at 20 km (12 miles) is 30 mrem/year, or about 10 percent of the background radiation from natural sources in the United States.

One Hundred Thousand to 1 Million Years after Closure. The individual waste packages that are contacted by seeps continue to slowly corrode. By 1 million years, even some packages (around 1–2 percent) that have not been wetted by dripping are breached. The number of packages releasing nuclides by 1 million years after closure is about 30 percent of the total (Figure O-12). Dose rates at the 20-km (12-mile) point continue to climb as more packages release their inventory, until a maximum is reached at approximately 300,000–400,000 years. The expected value for peak dose rate at this time is 200 mrem/year. Neptunium-237 remains the main contributor to the dose rate, but plutonium attached to colloids is the dominant contributor in about 8 percent of the cases.

BASES FOR BUILDING CONFIDENCE IN THE TOTAL SYSTEM PPERFORMANCE ASSESSMENT

The confidence that can be placed in the results is a direct function of the confidence placed in the scientific and engineering data and their appropriate incorporation in process and TSPA models used to calculate repository behavior. The task of the YMP site characterization and design organizations is to describe the processes likely to occur at the proposed repository site and then design a system that works in the range of conditions specific to that site. The task of the TSPA is to give feedback to the site and design organizations on the adequacy of the information at

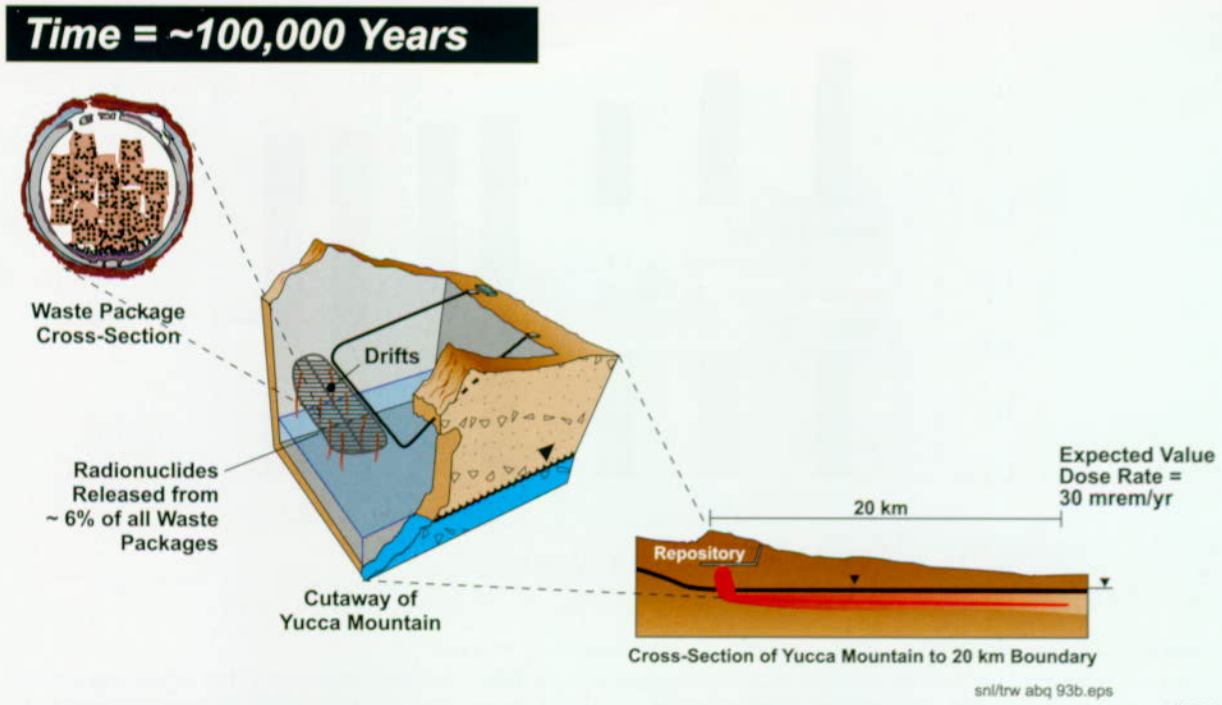

Figure O-11. Potential Radionuclide Release Conditions at About 100,000 Years
Elements of the engineered and natural barrier systems showing potential radionuclide release conditions and the resulting dose rate at the 20-km (12-mile) boundary about 100,000 years after waste emplacement.

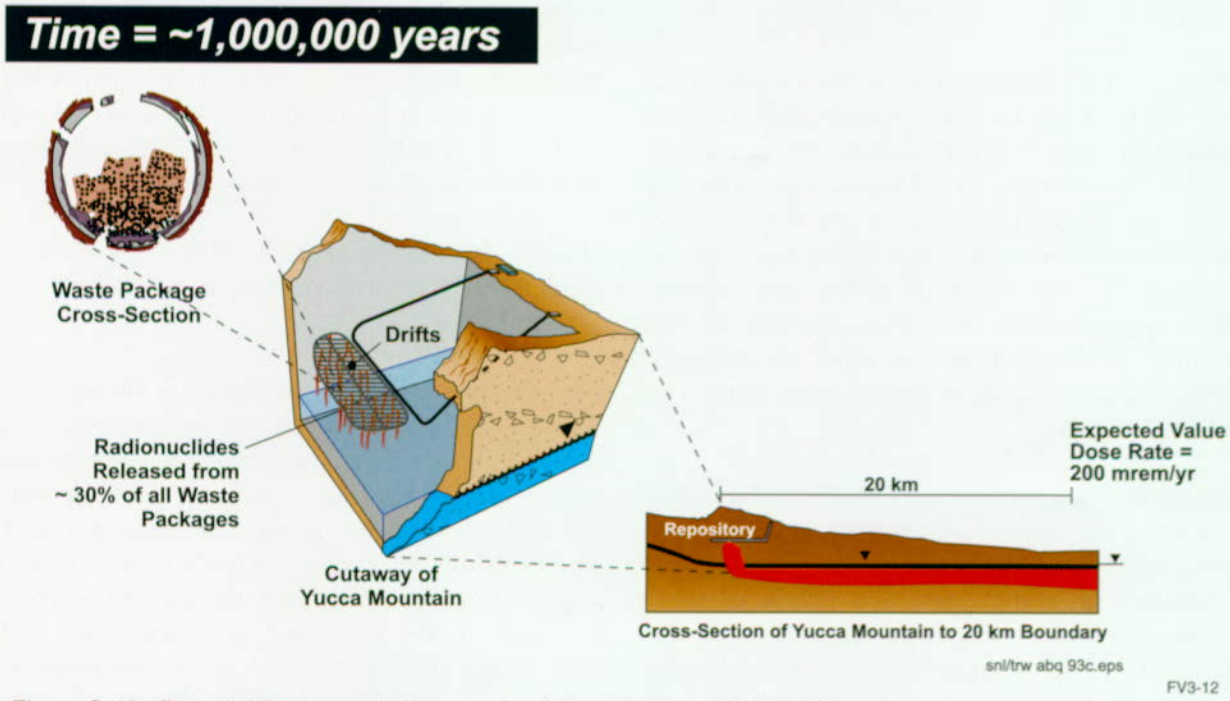

Figure O-12. Potential Radionuclide Release Conditions at About 1 Million Years
Elements of the engineered and natural barrier systems showing potential radionuclide release conditions and the resulting dose rate at the 20-km (12-mile) boundary about 1 million years after waste emplacement.

any one time and to help determine when new information is unlikely to change the results significantly. In other words, TSPA is a tool that is used to help answer the question "when is enough, enough?" It will never be possible, or necessary, to delete all uncertainty from the TSPA analyses. The forecasts based on the TSPA analyses will always be subject to uncertainty about future events and conditions. They will also depend on the natural variability in the site and design components. The information and understanding about the Yucca Mountain site and the design elements of the proposed repository has progressed a great deal in the past few years. The information has come from many sources, including site and laboratory investigation, computer simulations, and expert judgment.

However, there are still some important areas in which additional work could decrease uncertainty about specific processes that are important to repository performance. This can be accomplished, in part, by performing uncertainty and sensitivity analyses. They are the mechanism for aiding management in determining where more information is needed for the LA, or conversely, where existing information is adequate, or that additional data are unlikely to change the results. There are a number of ways to gain additional confidence. From a site-characterization perspective, adding confidence can include the following:

- Conducting additional, highly focused studies at the site to obtain specific information
- Surveying the national and international scientific literature to glean additional relevant information
- Conducting studies of natural analogs where nature has already performed the experiments in the earth over geologic time scales (the Oklo natural nuclear "reactor" in Gabon is such an example)

The design organization may also develop and implement different or additional engineered structures or components to deal with aspects of the natural system where uncertainty cannot be decreased for any number of reasons. In these cases, additional studies also may be done to ensure that the behavior of the engineered constituent in the range of natural conditions is as expected.

The sensitivity of repository performance to any specific type of information strongly depends on the way performance is being measured. The question to be answered, in terms of how performance is being measured determines the relative importance of the components. An example of how different performance criteria change the relative importance of the various parts of the system is shown by the variability in the specific TSPA parameters' importance at different times. A different suite or priority of parameters is seen in the uncertainty analyses for 10,000 years versus those for 100,000 or 1 million years.

Mathematical methods of assessing parameter sensitivity, such as regression analyses, are used in the TSPA. In general, the sensitivity analyses do not show, in an absolute sense, the parameters that are most important to performance. Rather, they show, in a relative way, the parameters in which uncertainty most affects the results. In some cases, if future studies could reduce the range in uncertainty, the parameter might no longer appear as a parameter to which performance is highly sensitive. Conversely, if a parameter or component is assigned an inappropriately low uncertainty range, it might not show up as a particularly important parameter. These analyses must be performed with care to gain the necessary understanding about the parameters that are most important to actual repository performance and to identify those parameters that need additional study to achieve the confidence to support the LA. The results of the TSPA uncertainty and sensitivity analyses are provided in the next section in the context of the work that is most important for improving the confidence in the TSPA for the site recommendation and the LA.

GUIDANCE FOR THE LICENSE APPLICATION

This last section focuses on the additional areas where work could increase confidence in certain processes and parameters for the LA. The focus for additional work is directed at the site characterization, design, and performance assessment organizations. For each change in the representation of a natural process or an engineered barrier, the change must be implemented in the TSPA models. Each TSPA model must then be tested to make sure that it is an adequate abstraction of the best understanding of the important features of the process it represents.

Based on the sensitivity and uncertainty analyses of the TSPA results (discussed in Sections 5 and 6 of this volume) and also based on the judgment of the TSPA analysts (discussed in Volume 4), the following aspects of the TSPA components have been determined to be most significant to the dose rates at 20 km (12 miles) from the Yucca Mountain repository. In some cases, the TSPA results point to very specific aspects or parameters used to represent the TSPA components, which, in turn, are captured in the principal factors of the repository safety strategy. Where this information is a subset of a principal factor, the factor with which it is associated is shown in parentheses. The results are shown for three different time periods, since the relative importance of different aspects of the modeled system changes as the system evolves.

Postclosure to 10,000 Years after Closure

- Availability of water to contact the waste package (seepage into drifts)
- Occurrence of premature package failures (loss of integrity of outer waste package barrier or of inner waste package barrier due to manufacturing flaws or mechanical effects)
- Rates of waste package degradation (loss of integrity of outer waste package barrier or of inner waste package barrier due to environmental conditions)
- Rate of cladding failure (integrity of spent nuclear fuel cladding)
- Availability of water to contact exposed waste form surfaces
- Timing and magnitude of climate change (precipitation and infiltration to depth)
- Degree of mixing in the unsaturated zone

10,000 to 100,000 Years after Closure

- Fraction of waste packages under seeps (dripping onto waste packages)
- Rate of waste package degradation
- Amount of water seeping into the drifts (dripping onto waste packages)
- Rate of cladding degradation (integrity of spent nuclear fuel cladding)
- Dilution of nuclides in the unsaturated and saturated zones (transport through the unsaturated zone, transport in the saturated zone)
- Solubility of neptunium-237
- Formation and transport of radionuclide-bearing colloids
- Biosphere dose conversion factor

100,000 to 1 Million Years after Closure

- Fraction of waste packages under seeps (dripping onto waste packages)
- Timing and magnitude of superpluvial climate (precipitation and infiltration to depth)
- Rate of waste package degradation (integrity of inner waste package barrier)
- Amount of water seeping into the drifts (dripping onto waste packages)

- Amount of water seeping into the degraded waste packages (seepage into waste package)
- Cumulative amount of degraded cladding (integrity of spent nuclear fuel cladding)
- Dilution of nuclides in the unsaturated and saturated zones (transport through the unsaturated zone, transport in the saturated zone)
- Neptunium solubility
- Biosphere dose conversion factors (biosphere transport uptake)

The details about which TSPA parameters that feed these factors could be improved is contained in different parts of this document, including Sections 3, 4, 5, and 6. Prioritization of those factors, using input from the TSPA-VA results and other considerations, such as cost, schedule, as well as the plans to address these important parameters and factors is contained in Volume 4.

INTENTIONALLY LEFT BLANK

1. INTRODUCTION

This volume reports the development of TSPA for the VA. This first section defines the general process involved in developing any TSPA, it describes the overall TSPA process as implemented by programs in the United States and elsewhere in the world, and discusses the acceptability of TSPA as a process or tool for analyzing a nuclear waste repository system.

Section 2 discusses the more specific use of the TSPA process for the TSPA-VA for Yucca Mountain, including goals, approach, and methods. It also includes a very brief synopsis of TSPA-VA results. Section 3 briefly discusses each of the component models that comprise the TSPA-VA. Each TSPA component model represents a discrete set of processes. The TSPA-VA components are: unsaturated zone flow, thermal hydrology, near-field geochemical environment, waste package degradation, waste form alteration and mobilization, unsaturated zone transport, saturated zone flow and transport, and biosphere. For each of these components, this section introduces the conceptualization of each individual process, describes the data sources, and discusses model parameter development and computer methods used to simulate each component. Section 4 explains the mechanics of how the individual TSPA components were combined into a "base case" and then provides the "expected value" results of a deterministic base case analysis. Section 4 also contains a description of the probabilistic analyses and results that help determine the relative importance of the various TSPA components and the data used to describe the components. Section 5 addresses sensitivity studies run for each of the TSPA components to understand how uncertainty in various parameters within a component change the TSPA results. Section 6 presents the findings of the sensitivity studies run on the various components in Section 5, and prioritizes the findings of the entire set of uncertainty and sensitivity studies of the components relative to each other. Section 6 also discusses the DOE assessment of potential activities to increase the confidence in future TSPAs based on the results of TSPA-VA, gives a synopsis of the insights provided by the TSPA Peer Review Panel, includes a discussion of comments received by DOE from NRC, and closes with concluding remarks.

1.1 DEFINITION OF PERFORMANCE ASSESSMENT AND TOTAL SYSTEM PERFORMANCE ASSESSMENT

Performance assessment and TSPA are terms with very specific meanings in the high-level radioactive waste management community. The process of constructing and implementing a TSPA is often described as a pyramid, where detailed information representing the various processes and components of a total system are distilled and linked into progressively more abstracted models used to analyze system performance.

1.1.1 Explanation of a Total System Performance Assessment

Performance assessment is a method of forecasting how a system or parts of a system designed to contain radioactive waste will behave over time. Its goal is to aid in determining whether the system can meet established performance requirements. A TSPA is the subset of performance assessment analyses in which all of the components of a system are linked into a single analysis.

The word "forecast" rather than "predict" is used to describe the expected outcome of a TSPA. "Predict" implies "inference from facts or accepted laws of nature." Forecast has a similar meaning but also implies anticipating eventualities and differs from predict in being usually concerned with probabilities instead of certainties (Merriam-Webster 1993, p. 457). As discussed in Section 1.3, incorporation of probabilities and uncertainty is a critical aspect of TSPA, which allows determination of reasonable assurance, as defined by regulatory agencies. However, it must be noted that NRC uses the term "predictive models" to express uses what NRC anticipates in 10 CFR 60.102 (a)(2).

The process of performance assessment is somewhat different from a safety assessment and a probabilistic risk assessment. Safety assessments

use a conservative "bounding" assessment of the entire system; performance assessments analyze the best understanding of the system and its components (NEA 1995, pp. 28-36). In a safety assessment, a given process or event is assumed to happen, regardless of the likelihood of its occurrence. A performance assessment incorporates more information than a safety assessment by assuming that some processes or events are more likely to happen than others and treating them accordingly in mathematical modeling (however, for some processes or events where information is limited, bounding analyses may be used in the performance assessment). The benefit of a performance assessment in this case is that a more realistic and, therefore, more defensible case is used. It must be noted that, in the community of nuclear waste management professionals, this distinction between a safety assessment and a performance assessment has become blurred, such that in informal usage they are often used interchangeably. However, it is important to differentiate the two philosophies, that is, use of "conservative" bounding cases versus use of the most realistic models possible. In addition, a safety case, as made before a licensing authority, could include both safety assessments and performance assessments, as defined above.

"Probabilistic risk assessment" is a term generally applied to safety studies of nuclear power plants or other engineered systems, but can be applied to any system that could fail in identifiable ways. Although this type of analysis incorporates variations in probability for different processes, the system and the time periods are very different than for a performance assessment. A probabilistic risk assessment is usually performed for discrete events of limited duration involving an engineered system and its components. Natural events such as earthquakes and volcanic eruptions are considered initiating events that may have an effect on overall system behavior, but are not a part of the system. The components can be tested on a time scale similar to that for the operational life of the system. Therefore, a set of requirements and specifications for these components is available, and the analyses are performed against criteria that have been or can be tested and validated.

A performance assessment treats both the engineered and natural system components. The engineered system is to some extent controllable, but the natural system is not. The responses of the total system extend over periods beyond those for which data have been or can be obtained.

1.1.2 The Performance Assessment Pyramid

The process for constructing a TSPA is shown in Figure 1-1 and described in more detail in Section 1.3. The Performance Assessment Pyramid shows how more detailed underlying information builds the technical basis for the total system models. The breadth of the lowest level of the pyramid represents the complete suite of process and design data and information (i.e., field and laboratory studies that are the first step in understanding the system). The next higher level indicates how the data feed into conceptual models that visualize the operation of the individual system components. Most of the information at these lower levels is reported in detail in Volumes 1 and 2.

The next higher level represents the synthesis of information from the lower levels of the pyramid into computer models. At this point, the subsystem

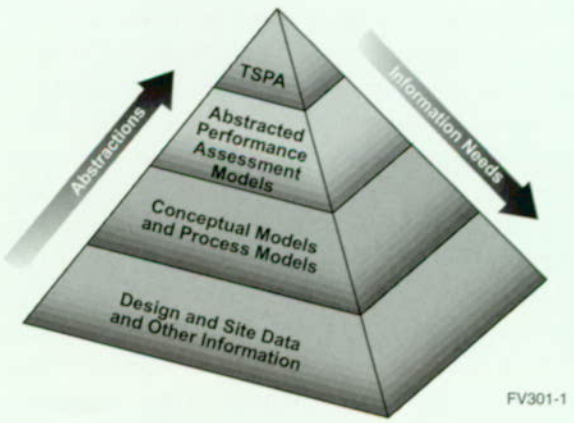

Figure 1-1. Performance Assessment Information Flow Pyramid
The performance assessment information flow pyramid shows how more detailed underlying information builds the technical basis for the total system models. Detail is reduced going up the pyramid; however, key attributes of the system are captured in the TSPA models.

behavior may be described by linking models together into representations, as described in Section 3; at this point performance assessment modeling is usually thought to begin. The term "abstraction" is used at this point to indicate the extraction of essential information. The TSPA models are usually referred to as abstracted models.

The upper level shows the final level of distillation of information into only the most critical aspects to represent the total system. At this point, all of the models are linked together, as discussed in Sections 3.3 and 4.1. These are the models used to forecast system behavior and estimate the likelihood that the behavior will comply with regulations and ensure long-term safety.

As information flows up the pyramid, it generally is distilled into progressively more simplified forms, or becomes more abstracted, as indicated in Figure 1-1. However, abstraction is not synonymous with simplification. If a particular component model can not be simplified without losing essential aspects of the model, it ceases to move up the pyramid and becomes part of the TSPA calculation tool. Thus, an abstracted model in a TSPA may take the form of something as simple as a table of values that were calculated using a complex computer model, or the abstraction may take the form of a fully three dimensional computer simulation. It must be noted that even the most complex models of specific processes are still an abstraction of reality.

There are also some considerations that dictate the level of complexity used to represent a process. One is the sensitivity of the results of the TSPA to that particular process. The more sensitive the process or parameter, the more detailed the model representation tends to be. However, the degree of complexity is also limited by the state of knowledge concerning the model. It is very important not to misrepresent the degree of understanding about a process by embedding it in an overly complicated computer model.

1.2 PHILOSOPHY OF TOTAL SYSTEM PERFORMANCE ASSESSMENT

The TSPA has become the internationally recognized method for analyzing system behavior for nuclear waste repositories. It is important to understand why TSPAs are performed, the unique nature of a TSPA compared to other types of analyses, and why the confidence in TSPA as a process has been established at such a global level.

1.2.1 Why Total System Performance Assessments Are Performed

Performance assessments are used to forecast how a specific system and all of its components evolve over time. Comparing the results to performance requirements allows analysts to estimate whether the amount of harmful material that may become accessible in the environment is acceptably low. The requirements, usually in the form of regulatory criteria, are generally established by governmental oversight agencies. The ultimate determination of whether a system complies with the requirements lies with the legally responsible regulatory group. The task of those proposing a nuclear waste repository is to provide reasonable assurance that the safety standard will be met, which in turn requires that they

- Understand the proposed system and all of its components
- Can demonstrate the capability to model the system
- Can adequately account for and treat the uncertainties in the analysis
- Can show that the information in the model provides reasonable assurance that safety standards will be met

In addition to providing a tool for determining whether a system meets regulatory requirements, TSPA also provides a rigorous method for aiding management in establishing the priority of information-gathering activities during the site selection, site characterization, and design phases.

As more information is gathered, the TSPA process iterates to incorporate revised and updated information into successive TSPA models and allows a program to progress toward more reasonable and defensible total-system models. Results of each TSPA, particularly the sensitivity and uncertainty studies, provide information about the relative importance of ongoing or proposed information-gathering activities addressing site characterization and design development. Each successive TSPA requires that the total system models become more representative. Several TSPAs by the YMP have been completed to date on the Yucca Mountain repository system (Sinnock et al. 1984; Barnard and Dockery 1991; Barnard et al. 1992; Eslinger et al. 1993; Wilson et al. 1994; Andrews et al. 1994; CRWMS M&O 1995). These efforts, along with studies done by other organizations (NRC 1995; Kessler and McGuire 1996), have contributed to the iterative process of the TSPA for the VA.

A TSPA is unique because it is the analysis that links all the system components together. This linkage is important because it allows each component to be viewed in the context of the behavior of the entire system. Even the simplest system has various aspects that are easier to understand when studied separately. For example, waste package material degradation may be characterized by laboratory tests of corrosion. However, the geologic system in which the waste package is to be emplaced may be analyzed using field studies of the host rock for properties that are only observed on a large scale, such as fracture density, as well as laboratory studies of other aspects, such as water chemistry. In a functioning system, these elements provide feedback to one another. The interaction of the water with the corroded waste package would likely change the water chemistry, which may in turn change the fractures and the way water flows through them. This very simple example shows an obvious potential for feedback. When a very complex system with numerous components is simulated as a single system in a TSPA, interactions among the components that would not otherwise be observed are often found in the analysis.

As discussed in Volume 1, the repository safety strategy for the YMP relies on a multiple barrier system. This isolation strategy means that the components of the natural and engineered systems work together to form a series of barriers. Because the behavior of each component in the series is governed by a different set of physical or chemical processes, this strategy provides a strong argument that the entire system is very unlikely to fail in response to a single mechanism. Also, the use of different types of barriers precludes reliance on complete knowledge about any one process. Therefore, the incorporation of multiple barriers helps to answer the question that frequently arises, how can the analysis account for what is not known? Given the uncertainty inherent in a forecast, one way to deal with an unanticipated response by one component of the system is to have multiple additional components that will still operate as barriers.

The concept of "reasonable assurance," used by NRC in its regulation of nuclear facilities and activities does not require absolute certainty in the results of an analysis. The incorporation of uncertainty into the TSPA, using various mathematical methods, allows the regulator and others to determine if the goal of reasonable assurance has been met. The study of uncertainty is documented in Section 4.3; however, some of the general methods of treating uncertainty include developing distributions to represent various types of data and also assigning probabilities to different conceptual models to encompass a range of potential behaviors or responses of certain components.

1.2.2 Why Total System Performance Assessments Are the Appropriate Tool for Analyzing Repository Systems

A question that often arises is whether or not performance assessment is a useful tool for the purpose of analyzing safety. The consensus of the international waste management community is that, in the realm of providing reasonable assurance, performance assessment is an adequate tool. In support of this consensus, the Nuclear Energy Agency Radioactive Waste Management Committee and the International Atomic Energy

Agency International Radioactive Waste Management Advisory Committee issued a collective opinion that they

> ...confirm that safety assessments are available today to evaluate adequately the potential long-term radiological impacts of a carefully designed radioactive waste disposal system on humans and the environment, and consider that appropriate use of safety assessment methods, coupled with sufficient information from proposed disposal sites, can provide the technical basis to decide whether specific disposal systems would offer to society a satisfactory level of safety for both current and future generations (NEA 1991a, p.7).

Although TSPAs can never be proven to be absolutely valid, many environmental problems require modeling of long-term interactions of man-made and geologic systems. Using the term "model" acknowledges that whether the descriptions of geologic features, events, and processes are unique and represent absolute reality will never be known. "Validation" of a long-term predictive model means that, on the basis of tests of the assumptions, inputs, outputs, and sensitivities, the model adequately reflects the recognized behavior of the portion of the system it is intended to represent. Adequacy is driven by the needs of the application for which the model is developed (Boak and Dockery 1998, p. 178–180).

Scientists assessing long-term risk use the following mechanisms to establish the adequacy of their models (Boak and Dockery 1998, pp. 181–182):

- Expert judgment to assign appropriate ranges of parameters where data are sparse, controversial, or unobtainable
- Conservatism in assigning parameter values and process descriptions, including ignoring some potentially mitigating processes
- Stochastic simulation to assess the effect of uncertainty in descriptions and the sensitivity of performance predictions to uncertainty and to examine alternative scenarios and process models

The following measures are undertaken to demonstrate that the effort to ensure validity has been comprehensive (Boak and Dockery 1998, p. 182):

- Documentation of the model structures, including justification for assumptions and simplifications as well as the examination of alternative conceptualizations for the system
- Review by the scientific community and those who have a stake in the decisions that these models support

Uncertainty is an inherent part of all total system studies. Information gathering activities are directed at reducing uncertainty as much as is practical. However, because of natural variability in the systems being studied and limited understanding about how processes will operate in the future, uncertainty will always have to be included explicitly in TSPA calculations.

1.3 GENERIC APPROACH FOR CONDUCTING A TOTAL SYSTEM PERFORMANCE ASSESSMENT

The TSPA process has been adopted and used throughout the global community for determining how a given waste management system might behave under a range of possible future conditions (NEA 1991b, pp. 24–25). A relatively standardized set of steps has been outlined to guide the performance assessment process, as shown below. The questions to be answered from the requirements form the basis for the details of the performance assessment, including the choice of models, parameters, and boundary conditions. The specifics of the requirements determine aspects of the system that are most sensitive to varying conditions. The steps shown below are not necessarily sequential; they may be performed in parallel. The entire process is iterative, and individual steps can be iterated within themselves.

Figure 1-2 shows the steps in the process of an iterative, total system performance assessment. The five steps shown in that diagram are defined below, and their implementation is discussed in Sections 3, 4, and 5.

1.3.1 Develop and Screen Scenarios

Scenario development in the context of a performance assessment has a very specific meaning. A scenario is a path that, using something resembling an event tree, connects a series of features, events, and processes that could result in a release of waste to the environment. Scenario development is a bookkeeping method that helps a licensing applicant demonstrate that they "thought of everything." Guidance concerning the suite of possible scenarios exists in the form of a Nuclear Energy Agency scenario report (NEA 1991c) that contains a general list of scenario classes.

Scenario development has different uses at different phases of a program. In the first stage of development, all potential pathways are developed. Potential scenarios are organized into a series of feasible futures and demonstrate what has been considered for inclusion in the TSPA. Scenario development helps a program develop logical and effective site characterization and design activities. As more site-specific information is gained, scenarios are screened and the event trees are "pruned" to discard futures that, for one reason or another, are not applicable to that site or design. In the later stages of a program, scenarios assist in ensuring that all connections among the processes are maintained. Scenarios also help describe the details of the conceptual and computer models that must be developed, and they provide a record of what has been considered and discarded in the analysis. The record is needed to make the logic behind the TSPA traceable for other analysts and the regulator. This information is contained in Section 2.2.

1.3.2 Develop Models

In this step, models are developed to represent important scenarios. The models are usually implemented in computer codes. Alternative computer models are also constructed for different conceptual models of how a system behaves. Complex process models provide the details of physical processes at more fundamental levels and correlate with the second and third levels of the performance assessment pyramid discussed in Section 1.1.2. The models developed at this level are discussed in Section 3.

System-level models contain fewer details but are required for reproducing the essential phenomena of the process. These models are often used at the highest level of the performance assessment pyramid, when the concept of abstraction is introduced.

1.3.3 Estimate Parameter Ranges and Uncertainties

The parameters used in the models described in Section 1.3.2 have natural variability. For example, in a rock mass, the pore space naturally varies from place to place. There is also uncertainty in these parameters that arises from incomplete knowledge, as would happen when the future state of a parameter must be estimated from assumptions rather than from measurements, or when possible incorrect measurements must be adjusted. This uncertainty is accounted for by developing distributions of values for the parameters rather than using any single value. The distributions also are assigned specific shapes that reflect the likelihood of any one value in the distribution occurring. Therefore, these probability distribution functions are used when many computer runs are made, and each run samples from the parameter distributions to allow many possible combinations of values. This method allows less likely values to be used infrequently and highly probable values to be used more often. However, the value selected by the simulation for a specific parameter may restrict the physically possible range of values for another parameter. Correlations among these related parameters also must be maintained mathematically.

Not all parameters have distributions of values. Some parameters may have only a single value, information on the parameter may be extremely

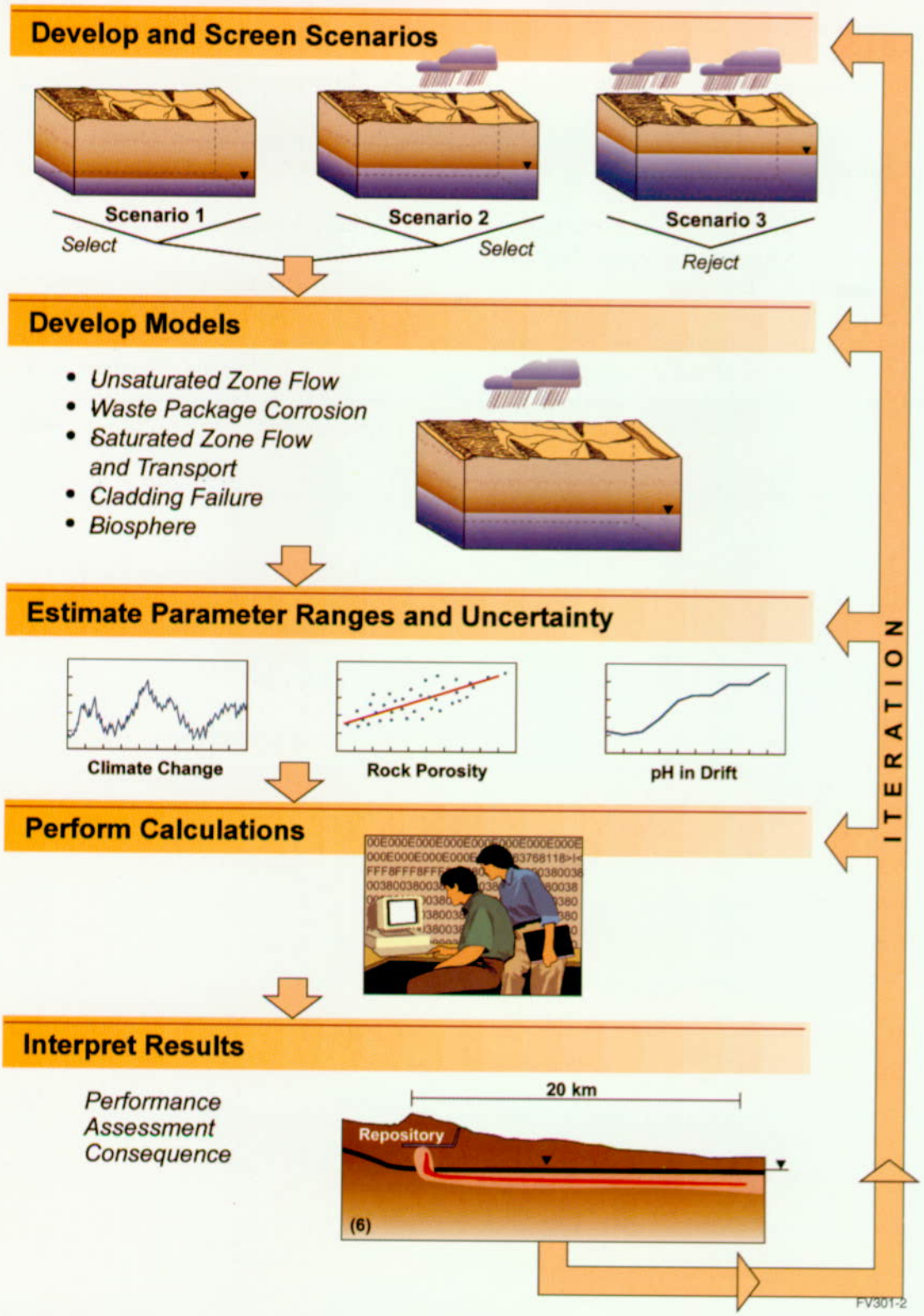

Figure 1-2. Major Steps in a Generic Performance Assessment
This figure illustrates the standardized sequence of steps in a generic performance assessment. The entire process is iterative between steps and also within individual steps.

limited, or the parameter may be very insensitive, making it unnecessary or inefficient to use a distribution in the calculations. The distributions of values for important variables are discussed in Section 3.

1.3.4 Perform Calculations

At this point, the work contained in the third or fourth tiers of the performance assessment pyramid has been completed. The next step is to run the subsystem or total system analyses using the distributions of data where distributions are available or necessary. The results of these calculations are reported in Section 4.2 for the total system. Sections 3 and 5 include the results of subsystem analyses.

1.3.5 Interpret Results

This final step is very important. The results themselves can be used for the following:

- Further develop or screen scenarios.
- Guide future testing for site characterization, design, and TSPA model development.
- When sufficiently mature, determine whether the system satisfies regulatory requirements.

2. YUCCA MOUNTAIN SITE CHARACTERIZATION PROJECT TOTAL SYSTEM PERFORMANCE ASSESSMENT FOR THE VIABILITY ASSESSMENT

The concept of TSPA and the generic TSPA process are described in Section 1 of this volume. The acceptability of TSPA as a tool for analyzing a nuclear-waste repository system was also described in that section. Section 2 of this volume discusses the more specific use of the TSPA process for Yucca Mountain, including the goals, approach, and specific method. The technical basis for this volume is provided in the *Total System Performance Assessment-Viability Assessment (TSPA-VA) Analyses Technical Basis Document* (CRWMS M&O 1998i).

The objectives of the TSPA for the VA are discussed in Section 2.1. The primary objective, to describe the probable behavior of the Yucca Mountain repository system, was a mandate from the U.S. Congress. To accomplish this objective, available scientific information about the natural geologic setting was used in the TSPA, along with data about the engineered components and their interactions with the geologic setting. Several general assumptions were made in the TSPA because as yet there are no standards to evaluate system performance. These assumptions relate to:

- The appropriate measure of performance
- The time scale of regulatory concern for the analysis

Although a "base case" was used in the TSPA to describe probable behavior of the Yucca Mountain repository system, alternative interpretations were considered to evaluate the significance of the uncertainty in the base case. An important goal throughout the process was to provide the TSPA information in a "transparent" document that describes the assumptions, results, and conclusions of the analyses.

Section 2.2 contains a general discussion of the approach used to analyze the Yucca Mountain repository system in the TSPA-VA. Building the capability for an integrated system analysis requires significant input from many individual disciplines. In addition, the analyses have benefited from comments received from both internal and external reviewers of previous system analyses conducted for the Yucca Mountain repository. Sources of data and information for constructing the TSPA-VA include previous TSPAs; documented models of the principal components; workshops to abstract, or simplify, the process model components; expert elicitations of key model components; and external review. The eight principal model components are the result of addressing the goal of the Yucca Mountain repository system of minimizing the exposure of humans to radioactive materials. The presence of water is a key factor in initiating release of radionuclides from waste packages and moving them through the environment to a contact point with humans. For this reason, the evaluation of the model components focused on the ability either to keep water from contacting the waste or to minimize releases of radioactivity from the repository if waste packages are breached.

Section 2.3 is a detailed description of the methodology used to analyze the repository system in the TSPA. The previous section discussed the process model components as individual models. This section provides a road map for reassembling, or coupling, the component models into one integral whole. Presented in the section is an overview of the TSPA-VA method for mathematical and numerical modeling of the individual processes, including their uncertainty, and the approach for combining them into an overall model and computer code. This overview includes discussions about information flow between the models and the architecture of the computer program for the TSPA-VA that facilitates the information flow. Also discussed in this section is the method for presenting the key results; in particular, how to show the influence of uncertainty on the performance predictions, and the relationship of uncertainty to the base case.

Section 2.4 summarizes the base case, or the expected performance of the repository system, based on the results of the TSPA-VA. The

expected performance is presented as a series of time slices that demonstrate the system's response to the proposed design concept.

2.1 OBJECTIVES OF TOTAL SYSTEM PERFORMANCE ASSESSMENT FOR THE VIABILITY ASSESSMENT

The overall scope and objective of the TSPA for the VA are contained in the Energy and Water Development Appropriations Act (1997):

> ...a total system performance assessment based upon the design concept and the scientific data and analysis available by September 30, 1998, describing the probable behavior of the repository in the Yucca Mountain geological setting relative to the overall system performance standards.

Assessing the performance of the system requires the following:

- Assimilating all the available scientific data and analyses that describe the geological setting into which the design concept is to be placed
- Defining the design concept that is to be used
- Describing the probable behavior of the repository system
- Identifying the performance standards by which the TSPA will be judged

The total system is comprised of geological and engineering components. Therefore, the TSPA uses the available scientific information about naturally occurring physical and chemical processes at the Yucca Mountain site, which are summarized in Volume 1. In addition, the TSPA includes the design concepts and scientific information about physical and chemical processes caused by the system engineered components, which are summarized in Volume 2.

Currently, there are no overall system-performance standards for the Yucca Mountain repository. The U.S. Environment Protection Agency (EPA) is developing applicable site-specific standards based on the recommendations in a congressionally mandated National Academy of Sciences' report, *Technical Bases for Yucca Mountain Standards* (National Research Council 1995). NRC is revising its licensing regulations. DOE anticipates that both EPA and NRC will develop system-level requirements for evaluating the suitability of the Yucca Mountain repository system for nuclear-waste disposal. This system-level guidance likely will focus on protecting humans from the potential health risks associated with excessive exposure to ionizing radiation at some distance downgradient from the repository.

In the absence of final regulatory guidance, the appropriate measure of system performance is assumed to be the exposure rate to radionuclides for average members of a critical population that may live 20 km (12 miles) downgradient from the repository. This distance was chosen to correspond to Lathrop Wells, the closest existing public or private well to the site, near the intersection of U.S. Highway 95 and Nevada State Route 373. The controlled-area boundary for the DOE Nevada Test Site also is approximately 20 km (12 miles) from the repository. Because the downgradient irrigation wells nearest to the repository are approximately 30 km (18 miles) from the site (near Amargosa Farms), this 20-km (12-mile) distance is believed to be sufficiently conservative for analysis. NRC has used this distance in its performance-assessment calculations (McCartin and Baca 1998).

Not only the geographic domain of interest but also the period of regulatory concern for the analysis must be defined. The previous EPA regulation (40 CFR 191) limited the time to 10,000 years after the facility is permanently closed. The recommendations of the National Academy of Sciences noted that the period of regulatory concern was properly an environmental policy and societal decision that was the responsibility of the implementing agency, in this case EPA. Because there is no formal guidance, the TSPA analyses

examined the 10,000-year period. To evaluate the consequences caused by the repository beyond that period, the analyses are extended to 100,000 and 1 million years in determining when the peak radionuclide doses or peak risk occurs.

DOE also has the goal to assess total system performance quantitatively defining the significance of each of the key components in the repository-safety strategy to assist in a systematic refocusing of the project resources. The statutory goal of the TSPA is to address the probable behavior of the repository system. However, the available scientific information can also suggest alternative interpretations that may also be plausible. When propagated through a quantitative tool such as performance assessment, these alternative interpretations can illustrate the significance of the uncertainty in the base case interpretation chosen to represent the probable behavior of the repository. The information about uncertainty will assist DOE in defining the work required either to minimize uncertainty or to modify the repository design to accommodate for this uncertainty before submitting the LA for constructing the repository system. The quantitative performance analyses assist in identifying those areas where additional scientific and technical work are required to evaluate the site and to prepare a complete, cost-effective, and timely license application. The additional scientific investigations and design analyses believed to be necessary for developing the LA are summarized in Volume 4.

Another indirect use of the TSPA is to provide a vehicle for prelicensing discussions with NRC. The NRC pre-licensing program concentrates on resolving the key technical issues most important to repository performance. An important role of the TSPA is to evaluate the potential significance of these issues to find a common basis for understanding the need for additional scientific and technical work.

Although the goal of the TSPA is to provide a quantitative assessment of the probable behavior of the repository system, it is important to recognize the uncertainties inherent in such analyses. EPA and NRC have recognized the care required in defining the degree of confidence needed from the analyses. EPA stated that,

> Because of the long time period involved and the nature of the events and processes of interest, there will inevitably be substantial uncertainties in projecting disposal system performance. Proof of the future performance of a disposal system is not to be had in the ordinary sense of the word in situations that deal with much shorter time frames. (40 CFR 191.13[a])

NRC also underscored this point in its discussion of reasonable assurance in 10 CFR 60.101(a)(2):

> The Commission anticipates that licensing decisions will be complicated by the uncertainties that are associated with predicting the behavior of a geologic repository over the thousands of years during which HLW [high-level radioactive waste] may present hazards to public health and safety. (48 FR 28194 1983; 10 CFR 60)

These inherent uncertainties were recognized in developing the analysis tools that are described in Sections 2.3 and 3 of this volume. The potential effects of many of these uncertainties are presented in Sections 4.3-4.5 and 5.

Given the uncertainty involved in a postclosure performance assessment, an important goal is to produce a transparent document describing the assumptions, the intermediate steps, the results, and the conclusions of the analyses. External review groups have defined what they mean by transparent. The Nuclear Waste Technical Review Board states that "transparency is the ease of understanding the process by which a study was carried out, which assumptions are driving the results, how they were arrived at, and the rigor of the analyses leading to the results" (NWTRB 1998, p. 21). The TSPA Peer Review Panel notes that "transparency is achieved when a reader or reviewer has a clear picture of what was done in the analysis, what the outcome was, and why" (Whipple et al. 1997a, pp. 9–10).

For the reader to have confidence in the analyses, the presentation must illustrate with sufficient clarity the following attributes:

- The conceptual basis for the individual components in the quantitative analyses (i.e., how the system is intended to work, which is presented in Section 2.2)
- How the individual components are combined into an assessment of system behavior (Sections 2.3 and 4.1)
- The scientific understanding used to develop the quantitative analysis tools that describe the system's expected evolution (Sections 3.1-3.8)
- The system's expected evolution as defined by the spatial and temporal response of the system to waste emplacement (Sections 4.1 and 4.2)
- Uncertainty in the system's expected evolution and the significance of that uncertainty to the system performance goals (Sections 4.3-4.5, 5.1-5.8)

Section 2.2 presents a discussion of *what* is being analyzed as part of the TSPA for the Yucca Mountain repository system. This discussion includes *how* the repository system is intended to work and is closely aligned with the repository safety strategy and the principal factors affecting postclosure performance.

Section 2.3 describes how the repository system has been analyzed in the TSPA. Section 3 describes how separate components of the system model have been assembled and the technical and scientific bases for the models used in the analyses.

2.2 TOTAL SYSTEM PERFORMANCE ASSESSMENT APPROACH

2.2.1 Development of an Integrated Total System Performance Assessment Approach

The Yucca Mountain repository system is a combination of integrated processes that can be summarized in 1 basic tenet, 4 key attributes, and 19 principal factors. The basic objective of the waste disposal system is to contain and isolate the radioactive wastes so that the dose impact to humans is attenuated to a relatively benign level. This tenet manifests itself in the following four key attributes of the DOE repository safety strategy:

- Limited water contacting the waste packages
- Long waste package lifetime
- Low rate of release of radionuclides from breached waste packages
- Radionuclide concentration reduction during transport from the waste packages

The four attributes are associated with 19 principal factors, which are listed in Table 2-1. Also shown in this table are the corresponding TSPA model components analogous to these principal factors.

Building an integrated system analysis capability requires input from the many disciplines that comprise the system. The construction also benefits from comments from internal and external reviewers of previous system analyses conducted for the Yucca Mountain repository. The analyses documented in this volume of the VA have benefited from such interactions. The final approach and methods used in the analyses have been developed over the last two years, following completion of the *Total System Performance Assessment - Viability Assessment (TSPA-VA) Plan* (CRWMS M&O 1996f) and the *Total System Performance Assessment - Viability Assessment (TSPA-VA) Methods and Assumptions* (CRWMS M&O 1997m). The major sources of information that form the bases for the methods, assumptions,

Oversight

NRC Technical Exchanges, Appendix 7 Meetings
NWTRB Panel Meetings, Reports to Congress
TSPA Peer Review Interim Reports 1, 2, and 3
State of Nevada; Affected Units of Local Government
Public

Prior TSPAs

DOE TSPA-91, 93, 95
NRC IPA-1, -2, -3
EPRI TSPA Phases 1, 2, and 3

Expert Elicitation

Probabilistic Volcanic Hazard Assessment
Probabilistic Seismic Hazard Assessment
Unsaturated Zone Flow Expert Elicitation
Saturated Zone Flow and Transport Expert Elicitation
Near-Field Environment Expert Elicitation
Waste Package Degradation Expert Elicitation
Waste Form Alteration and Mobilization Expert Elicitation

Process Model Abstraction Workshops

Unsaturated Zone Flow
Thermal Hydrology
Near-Field Geochemical Enviroment
Waste Package Degradation
Waste Form Degradation and Radionuclide Mobilization
Unsaturated Zone Transport
Saturated Zone Flow and Transport

Site and Design Models

Unsaturated Zone Flow Model
Seepage Model
Near-Field Environment Model
Corrosion Model
Unsaturated Zone Transport Model
Saturated Zone Flow and Transport Model

Site and Design Information

Site Description Document
Repository Design
Waste Package Design
Laboratory Data
In situ Data
Analog Data

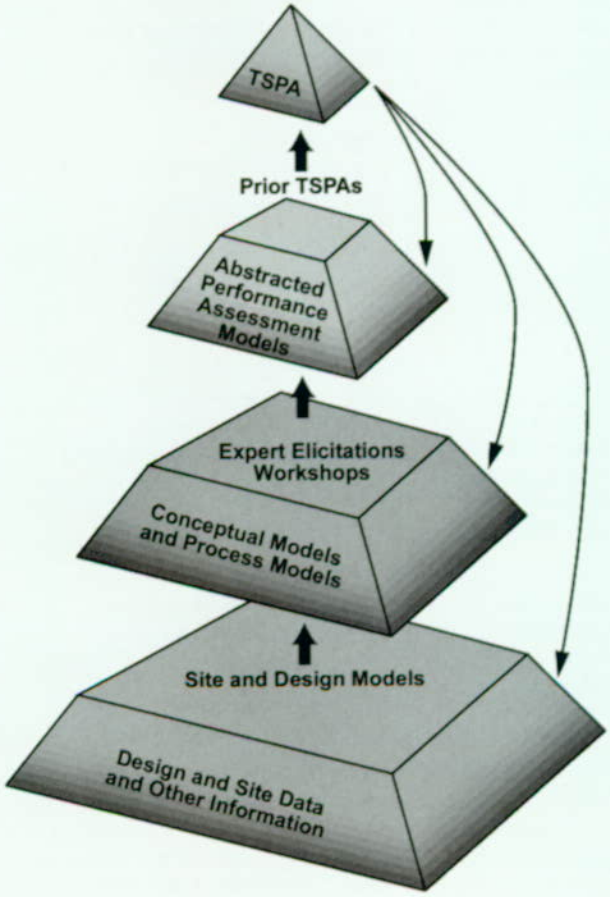

Figure 2-1. Major Sources of Information Used in the Development of the Total System Performance Assessment for the Viability Assessment
This figure illustrates the numerous internal and external sources of information used to develop the models used in the quantitative prediction of postclosure performance.

Table 2-1. Principal Factors Affecting Expected Postclosure Performance for the Viability Assessment Reference Design and Their Corresponding Total System Performance Assessment for the Viability Assessment Model Components and Nuclear Regulatory Commission Key Technical Issues

Attributes of the Repository Safety Strategy[a]	Principal Factors[a]	TSPA Model Components	NRC Key Technical Issue[b]
Limited water contacting waste packages	Precipitation and infiltration of water into the mountain	Unsaturated Zone Flow	Unsaturated and Saturated Flow under Isothermal Conditions
	Percolation to depth		
	Seepage into drifts	Seepage	Repository Design and Thermomechanical Effects
	Effects of heat and excavation on flow		
	Dripping onto waste package	Thermal Hydrology – Mountain Scale Thermal Hydrology-Drift Scale	Thermal Effects on Flow
	Humidity and temperature at waste package		
Long waste package lifetime	Chemistry on waste package	Near-Field Geochemical Environment	Evolution of the Near-Field Environment
	Integrity of waste package outer barrier	Waste Package Degradation	Container Life and Source Term
	Integrity of waste package inner barrier		
Low rate of release of radionuclides from breached waste packages	Seepage into waste package		
	Integrity of spent nuclear fuel cladding	Waste Form Degradation Radionuclide Mobilization and Engineered Barrier System Transport	
	Dissolution of UO_2 and glass waste form		
	Solubility of neptunium-237		
	Formation of radionuclide-bearing colloids		
	Transport within and out of waste package		
Radionuclide concentration reduction during transport from the waste packages	Transport through unsaturated zone	Unsaturated Zone Transport	Unsaturated and Saturated Flow under Isothermal Conditions and Radionuclide Transport
	Transport in saturated zone	Saturated Zone Flow and Transport	
	Dilution from pumping		
	Biosphere transport	Biosphere Transport and Uptake	

[a]See Rev. 2 of the DOE repository safety strategy (DOE 1998)

[b]NRC realigned its prelicensing program to focus all its activities on resolving the 10 key technical issues it considered to be most important to repository performance. The Key Technical Issues consist of the following: 1) Total System Performance Assessment (NRC 1998a); 2) Unsaturated and Saturated Flow Under Isothermal Conditions (NRC 1997e; 1997f); 3) Evolution of the Near-Field Environment (NRC 1997c); 4) Container Life and Source Term (NRC 1998b); 5) Repository Design and Thermal-Mechanical Effects (NRC 1997a); 6) Thermal Effects on Flow (NRC 1997b); 7) Radionuclide Transport (Sagar 1997); 8) Structural Deformation and Seismicity (NRC 1997d); 9) Igneous Activity (NRC 1998d); 10) Activities Related to Development of NRC High-Level Radioactive Waste Regulations (Sagar 1997). The first nine of these directly or indirectly related to performance assessment. The last one also relates to performance assessment to the extent this tool is used as a basis for setting and showing compliance with regulatory standards. These key technical issues are summarized in NRC staff reports (such as Sagar 1997) and a series of issue resolution status reports, the primary mechanism by which NRC will provide DOE with feedback on the resolution of the key technical issues.

and component models used in the TSPA documented here are illustrated in Figure 2-1 and Table 2-2. The major sources include the following:

- Previous DOE- and non-DOE-sponsored TSPAs of Yucca Mountain
- Documented models describing each of the principal components of the TSPA
- Workshops on abstractions of individual process model components used in TSPA
- Expert elicitations of key process model components used in TSPA
- External reviews of TSPA plans, methods, and assumptions

Table 2-2. Principal Sources of Information Used in the Development of the Total System Performance Assessment Model for the Viability Assessment Reference Design

Attributes of the Repository Safety Strategy	Principal Factors	Process Model Abstraction Workshop	Process Model Expert Elicitation	Described in Section
Limited water contacting waste packages	Precipitation and infiltration into the mountain	Unsaturated Zone Flow Model Abstraction/Testing (CRWMS M&O 1997t)	Unsaturated Zone Flow Expert Elicitation (CRWMS M&O 1997n)	3.1
	Percolation to depth			
	Seepage into drifts			
	Effects of heat and excavation on flow	Thermal Hydrology Model Abstraction/Testing (CRWMS M&O 1997l)	N/A*	3.2
	Dripping onto the waste package		Near-Field Environment Expert Elicitation (CRWMS M&O 1998d)	3.2
	Humidity and temperature at the waste package			
Long waste package lifetime	Chemistry on the waste package	Near-Field Geochemical Environment Abstraction/ Testing (CRWMS M&O 1997d)	NA*	3.3
	Integrity of outer waste package barrier	Waste Package Degradation Abstraction/Testing (CRWMS M&O 1997h)	Waste Package Degradation Expert Elicitation (CRWMS M&O 1998b)	3.4
	Integrity of inner waste package barrier			
Low rate of release of radionuclides from breached waste packages	Seepage into waste package	Waste Form Degradation and Radionuclide Mobilization Abstraction/Testing (CRWMS M&O 1997o)	N/A*	3.5
	Integrity of spent nuclear fuel cladding		Waste Form Degradation and Radionuclide Mobilization Expert Elicitation (CRWMS M&O 1998k)	
	Dissolution of UO_2 and glass waste forms			
	Solubility of neptunium-237			
	Formation of radionuclide-bearing colloids			
	Transport within and out of the waste package		N/A*	
Radionuclide concentration reduction during transport from the waste packages	Transport through unsaturated zone	Unsaturated Zone Transport Model Abstraction/Testing (CRWMS M&O 1997p)	N/A*	3.6
	Transport in saturated zone	Saturated Zone Flow & Transport Model Abstraction/Testing (CRWMS M&O 1997s)	Saturated Zone Flow & Transport Expert Elicitation (CRWMS M&O 1998g)	3.7
	Dilution from pumping		N/A*	
	Biosphere transport and uptake	Biosphere Model Abstraction/Testing (CRWMS M&O 1997a)	N/A*	3.8

* This principal factor was not the subject of an expert elicitation.

- NRC Issue Resolution Status Reports which address the status of key technical issues that are assessed in the TSPA

Each of these sources is described in the following paragraphs. In addition, indirect information derived from other radioactive and non-radioactive waste programs has been used in the development of the approach and methodology used in TSPA-VA. The more detailed technical basis is presented in the *Total System Performance Assessment-Viability Assessment (TSPA-VA) Analyses Technical Basis Document* (CRWMS M&O 1998i).

DOE contractors completed previous TSPA analyses in 1991, 1993, and 1995. These analyses are documented in *TSPA 1991: An Initial Total-*

System Performance Assessment for Yucca Mountain (Barnard et al. 1992), *Total-System Performance Assessment for Yucca Mountain- SNL Second Iteration (TSPA-1993)* (Wilson et al. 1994) and *Total-System Performance Assessment - 1995: An Evaluation of the Potential Yucca Mountain Repository* (CRWMS M&O 1995). The general objective of these scoping analyses was to refine the methods and approach that would be applied in the development of the site recommendation and, ultimately in the LA. An additional objective of these studies was to assist DOE in prioritizing design and scientific investigations on the key components that most significantly impact performance. The knowledge gained in these analyses has assisted DOE in prioritizing the models to include in the TSPA analyses and prioritize the data gathering activities needed to support these models.

Other TSPA analyses, not sponsored by DOE, have been conducted by the Electric Power Research Institute and by NRC. The Electric Power Research Institute's most recent iteration of a TSPA is documented in *Yucca Mountain Total System Performance Assessment, Phase 3* (Kessler and McGuire 1996). NRC has also conducted a recent TSPA (NRC 1995). NRC is conducting an iterative performance assessment (named IPA-3.1.3) in parallel with the DOE TSPA for the VA. Preliminary results of these analyses were reported in a technical exchange held in March 1998 (McCartin and Baca 1998). Each iterative analysis of total system performance, whether performed by DOE and its contractors, NRC and its contractors, or the Electric Power Research Institute and its contractors, leads to improved insights about the expected behavior of the Yucca Mountain repository system. In addition, a review of the conceptual models and parameters used in the analyses provides a basis for defining the significance of the range of uncertainties examined. In general, all of these analyses converge on a few key components that are analogous to the principal factors identified in Table 2-1. These factors are reflected in the NRC key technical issues and recently developed issue resolution status reports that address portions of the key technical issues.

TSPAs are based on a number of building blocks. Principal among these are models that describe how Yucca Mountain behaves in the presence of a repository and how the engineered system behaves within the environmental setting caused by the mountain. These process models indicate that each model is designed to describe the behavior of individual and coupled physical and chemical processes. A significant portion of the DOE site characterization program has been aimed at developing the scientific bases for the most reasonable representation of the Yucca Mountain site and its associated engineered barriers. This scientific basis serves as the foundation for the process models used in the TSPA. The basis for these models is described in more detail in Volumes 1 and 2, and their use in the TSPA is discussed in Section 3 of this volume.

To ensure that this TSPA would be based on the most current scientific knowledge (as defined in the objectives set forth for the VA), a series of workshops were held in 1997 to bring together YMP scientists, engineers, and performance-assessment analysts. These individuals consisted of DOE, national laboratory, U.S. Geological Survey (USGS), and managing and operating (M&O) contractor scientists and engineers. Observers at these workshops included technical staffs of regulatory agencies (such as NRC and EPA) and their contractors, external oversight groups such as the Nuclear Waste Technical Review Board and the Advisory Committee on Nuclear Waste, and the TSPA Peer Review Panel. The aim of these workshops was to develop a strategy for identifying and incorporating the relevant aspects of the individual process models into the TSPA analyses. In addition to defining the appropriate approach for abstracting the important elements of each process model, these workshops assisted DOE in defining and prioritizing the major technical issues that were believed to need addressing in the TSPA. Many of these issues correspond directly with the key technical issues raised by NRC. Each workshop culminated in a plan for incorporating that component in the TSPA and linking that component to other portions of the TSPA. These plans are referenced in Table 2-2 and are summarized in the *Total System*

Performance Assessment - Viability Assessment (TSPA-VA) Methods and Assumption (CRWMS M&O 1997m). The approach and methods to implement these plans are discussed in more detail in Section 3.

Acknowledging diverse technical and scientific opinions is an important part of any engineering and scientific endeavor as controversial as analyzing the design and performance of a potential disposal facility for high-level radioactive waste. In addition to the workshops, DOE sponsored five expert elicitations on key process models for the TSPA. The goal of these elicitations was to solicit the judgment of nationally and internationally recognized scientists in quantifying the uncertainty associated with each of these process models and uncertainty in the parameter values used in those models. The process followed the procedures and approaches for eliciting expert judgments that have been formalized in documents such as DOE guidance for the formal use of expert judgment (DOE 1995) and the NRC Branch Technical Position on the use of expert elicitation in the high-level radioactive waste program (Kotra et al. 1996). The assessments and probability distributions that resulted from the elicitations provide a reasonable aggregate representation of the knowledge and uncertainties about issues in evaluating the various processes important to repository performance. The five areas evaluated, in the elicitations were:

- Unsaturated zone flow (CRWMS M&O 1998g)
- Waste package degradation (CRWMS M&O 1998b)
- Saturated zone flow and radionuclide transport (CRWMS M&O 1998g)
- Near-field environment (CRWMS M&O 1998d)
- Waste form degradation (CRWMS M&O 1998k)

The major conclusions of these elicitations are described in Section 3. In addition to these elicitations, DOE conducted external elicitations of the potential hazards associated with either volcanic- or seismic-induced events. The use of these results in the analysis of the potential effects of disruptive scenarios is described in Section 4.4. All of these elicitations helped refine the range of models and parameters that have been considered in the TSPA.

In addition to DOE-sponsored development of the TSPA models, several external oversight groups provided input throughout the process of defining and implementing the approach and methods. These groups include NRC and its contractor, the Center for Nuclear Waste Regulatory Analysis; the NRC Advisory Committee for Nuclear Waste; and the congressionally chartered Nuclear Waste Technical Review Board. An independent peer review panel was convened to comment on development of the TSPA-VA. This panel will review this TSPA to assist DOE in developing more robust performance assessments for the site recommendation report and the LA, which in the current plan occur in the 2001-2002 time frame. These organizations have published a range of technical comments on the TSPA plan and the methods and assumptions documents and have conducted numerous briefings over the last 2 years on the progress of the TSPA. Examples of these comments may be found in the following publications: *Total System Performance Assessment 1995 Audit Review* (Baca and Brient 1996), *NRC High-Level Radioactive Waste Program Annual Progress Report Fiscal Year 1996* (Sagar 1997), *Report to the U.S. Congress and The Secretary of Energy - 1996 Findings and Recommendations* (NWTRB 1997), *Report to the U.S. Congress and The Secretary of Energy - 1997 Findings and Recommendations* (NWTRB 1998), *First Interim Report Total System Performance Assessment Peer Review Panel* (Whipple et al. 1997a), *Second Interim Report Total System Performance Assessment Peer Review Panel* (Whipple et al. 1997b), and *Third Interim Report Total System Performance Assessment Peer Review Panel* (Whipple et al. 1998).

These comments have aided in defining the most appropriate means of describing and analyzing the performance of the Yucca Mountain site and the engineered barriers associated with the reference design and design options. A number of recommendations, however, could not be fully addressed in this TSPA, and will be carried forward to aid the design and planning for the TSPA supporting the site recommendation and LA.

2.2.2 Components of the Yucca Mountain Repository System Evaluated in the Total System Performance Assessment

The Yucca Mountain repository system consists of the geologic setting and engineered barriers that, considered together, are aimed at reducing the exposure of humans to radioactive materials to acceptable levels. This section briefly describes the key aspects of the individual component models identified in Table 2-1 and Figure 2-2.

The model components related to the first key attribute in the repository safety strategy—limit the amount of water contacting waste package—include climate, infiltration, unsaturated zone flow, seepage, and mountain-scale thermal hydrology. Together, these components define the temporal and spatial distribution of water flow through the unsaturated tuffs above the water table at Yucca Mountain and the temporal and spatial distribution of water seeps into the repository drifts. There could be long-term (thousands to hundreds of thousands of years) climate variations. In addition, the thermal regime generated by the decay of the radioactive wastes can mobilize water over the first hundreds to thousands of years. For these reasons, the amount of water flowing in the rock and seeping into drifts is expected to vary with time.

The model components related to the second key attribute of the repository safety strategy—extend the time the waste packages contain waste—include all of the above components plus drift-scale thermal hydrology, near-field geochemical environment, and waste package degradation. Together, these components define the spatial and temporal distribution of the times when waste packages are expected to breach. The thermal, hydrologic, and geochemical processes acting on the waste package surface are the most important environmental factors affecting the waste package containment time. As noted in Volume 2 and Section 4.4, the mechanical degradation processes are insignificant in affecting the containment time. In addition, the degradation characteristics of the waste package materials significantly impact the timing of waste package breaches.

The environmental processes acting on the waste package surface as well as the timing and extent of waste package degradation are directly related to the selected design. Reviewing the key aspects of the VA reference design as they relate to the expected behavior of the repository system is appropriate. Details of the reference design are contained in Volume 2 and are not repeated here. A schematic of the reference waste package design, including the types of waste forms to be emplaced in the Yucca Mountain repository, is depicted in Figure 2-3. Of greatest relevance to performance is that the waste package reference design which consists of two dual-barrier metals—an outer metal consisting of 10 cm (4 in.) of low carbon steel and an inner metal of 2 cm (0.8 in.) of corrosion-resistant high-nickel alloy American Society for Testing and Materials (ASTM) B 575 N06022 (Alloy 22) (ASTM 1994). Volume 2 of this document gives a more detailed description of the properties of these materials and how they are used to construct the waste package. The principal waste forms to be disposed of within these waste packages consist of the following:

- Commercial spent nuclear fuel derived from pressurized water reactors or boiling water reactors
- DOE-owned spent nuclear fuels including N-Reactor fuel from Hanford, research reactor fuel, and naval spent nuclear fuel
- High-level radioactive waste in the form of glass logs placed in stainless-steel canisters from Savannah River, South Carolina; West Valley, New York; Hanford, Washington; and Idaho National Engineering and Environmental Laboratory, Idaho

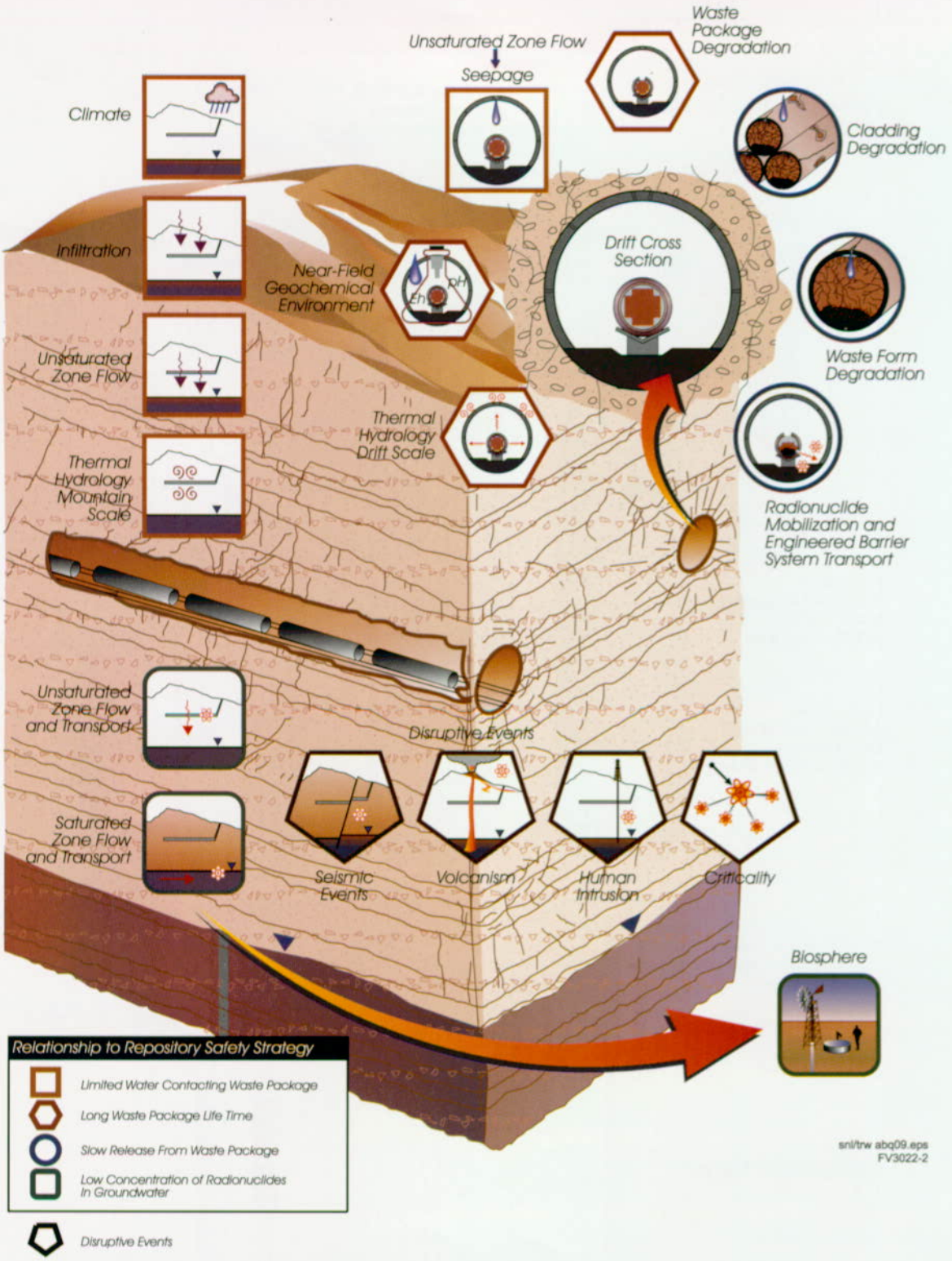

Figure 2-2. Major Components of the Total System Performance Assessment for the Viability Assessment Shown are the individual component models that together must be analyzed in evaluating the behavior of the Yucca Mountain repository system. These components comprise the individual building blocks of the TSPA analysis. The components are correlated to the four attributes of the repository safety strategy.

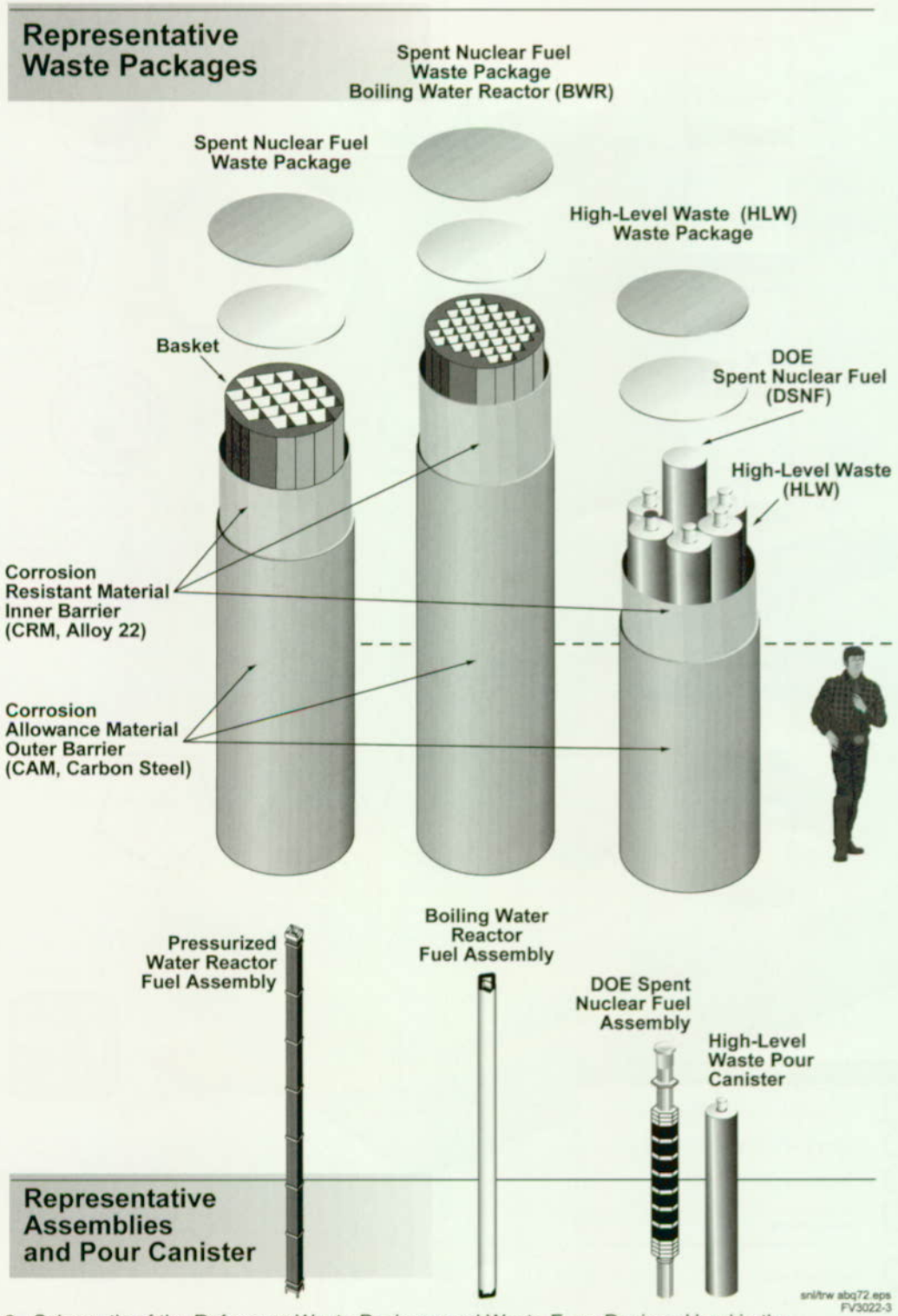

Figure 2-3. Schematic of the Reference Waste Package and Waste Form Designs Used in the Total System Performance Assessment for the Viability Assessment

This figure illustrates the three major waste form types: commercial spent nuclear fuel (existing as either pressurized water reactor fuel or boiling water reactor fuel), high-level radioactive waste, or DOE-owned spent nuclear fuel. Also illustrated is how these waste form types would be configured in the VA waste package design. More details are presented in Section 5.1 of Volume 2.

- DOE-owned stabilized excess weapons-grade plutonium

The waste packages are designed to contain up to 21 pressurized-water reactor assemblies, 44 boiling-water reactor assemblies, 5 glass logs and co-disposal of DOE-owned spent nuclear fuel assemblies and direct disposal of other canisterized DOE spent nuclear fuels including Naval spent nuclear fuel.

A schematic of the reference repository and engineered barrier system designs is depicted in Figure 2-4. Potential design option features are discussed in Volume 2 and Section 4.5. Key aspects of the repository and engineered barrier system reference design that influence the long-term performance of the disposal system include the following:

- Areal thermal loading, which corresponds to the spacing between waste packages and between emplacement drifts
- Size of the drifts
- Lining of the drifts for mechanical stability
- Characteristics of the engineered materials placed in the drifts to support the waste package (the waste package supports and inverts)

The model components related to the third key attribute—slow release of radionuclides from breached waste packages—include all of the above components plus seepage into the waste package, cladding degradation, colloid formation and stability, waste form degradation, and transport within the waste package. Together, these components lead to a determination of the spatial and temporal distribution of the mass of radioactive wastes released from the waste packages. Each component depends on the thermal, hydrologic, and geochemical conditions inside the waste package, which change with time.

The model components related to the fourth key attribute of the repository safety strategy—low concentration of radionuclides in groundwater—include all of the above components plus radionuclide transport through the engineered barrier system, the unsaturated zone, and the saturated zone; dilution from pumping; and radionuclide transport in the biosphere. Together, these components cause the spatial and temporal variation of radionuclide concentrations in groundwater. The groundwater concentration ultimately yields the mass of radionuclides that may be ingested or inhaled by individuals exposed to that groundwater, which in turn causes a level of radiological dose or risk associated with that potential exposure. Radionuclide transport may either be by advection (radionuclide movement which occur with the bulk movement of the groundwater) or diffusion (radionuclide movement which occurs because of a concentration gradient). The concentration depends on both the mass release rate of the radionuclides as well as the volumetric flow of water along the different pathways in the different components. If the volumetric flow of water from the pumping centers is greater than the volumetric flow in which the radionuclides are contained, then dilution of radionuclide concentrations can occur at the pumping well.

Each of these key attributes and TSPA model components are used to describe the expected or probable (e.g., base case) behavior of the Yucca Mountain repository system. These components describe the features, events, or processes that are expected to occur throughout the period of interest. Other features, events, or processes can occur that could alter the behavior of the system. However, these features, events, or processes have a sufficiently low probability of occurring over the period of interest that they are not considered in the expected behavior. They may be essentially classified as unanticipated processes and events. Examples of such disruptive events include igneous activity, seismic activity, criticality events, and human intrusion. The potential consequences associated with unanticipated processes and events are considered in the TSPA analyses.

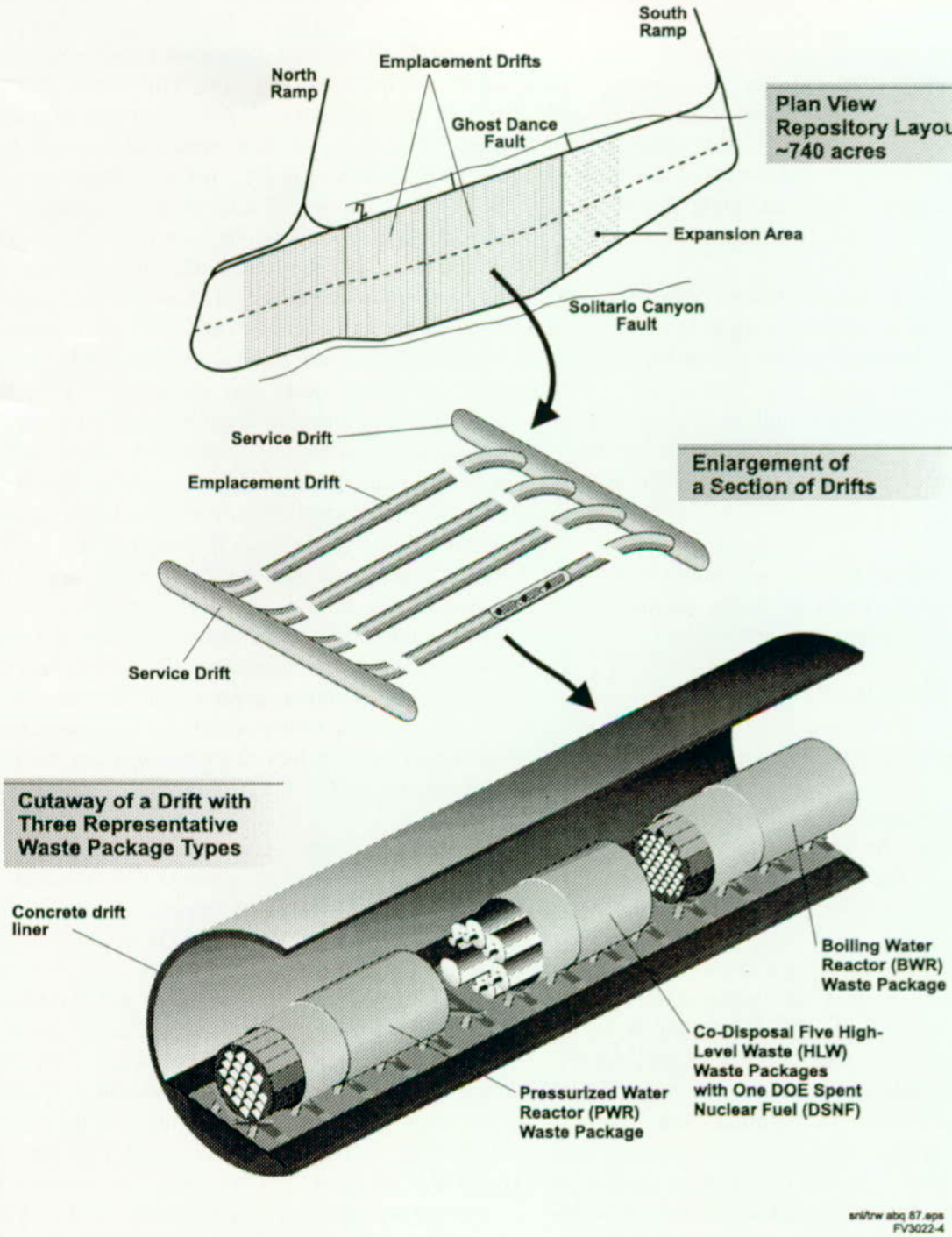

Figure 2-4. Schematic of the Reference Repository and Engineered Barrier System Designs Used in the Total System Performance Assessment for the Viability Assessment
This figure illustrates the general drift layout within Yucca Mountain to contain the 70,000 metric tons of waste. Also illustrated is the emplacement of the waste packages on supports placed on the drift inverts. More details of the reference design are presented in Sections 4.2 and 5.2 of Volume 2.

2.2.3 Conceptual Description of Processes Relevant to an Evaluation of Postclosure Performance

TSPA is an analysis of the long-term behavior of the repository system and the uncertainty in the analysis of that behavior. Before discussing how the analysis is performed (see Section 2.3), it is important to describe what is being analyzed. To describe what is being analyzed, it is necessary to describe the overall repository system and the components relevant to the evaluation of the repository system behavior.

The major components to be considered in the assessment of system performance and the relationship of those components to the repository safety strategy were presented in the previous sections. Described in this section are the key concepts of how the repository system is intended to work.

The basic principle of the Yucca Mountain repository safety strategy is to keep water away from the wastes. If water does contact the wastes, then the other principle of the safety strategy is to minimize the release rate of the radioactivity from the engineered barriers and reduce the concentration of any dissolved radionuclides as they migrate from the repository. The discussion that follows will focus on the small group of radionuclides that are mobile in the Yucca Mountain environment. Other radionuclides that either are very insoluble and/or highly retarded in the Yucca Mountain environment pose little risk to the environment.

Because the repository is approximately 300 m (1,000 ft) beneath the land surface and the wastes are all solids, the primary means for the radioactive constituents of the wastes to contact the biosphere, and ultimately humans, is along groundwater pathways. The wastes pose minimal risks to humans unless the following occur:

- Waste forms are exposed to water.
- Radionuclides within these waste forms are dissolved in the water.
- Dissolved radionuclides are transported with the water.
- Radionuclide-containing water is discharged, either naturally or at a pumping well, from the aquifer.
- Humans or any part of the food chain uses this water.

If water is kept away from the wastes, the wastes pose little or no threat to humans.

The presence of water is of primary concern as it contacts the waste and as any dissolved radionuclides migrate within the groundwater to expose humans to the potential effects of radiation. One of the reasons for the primary issue being related to aqueous processes is that in TSPA-VA the performance measure of concern is doses to individuals. Although gaseous transport of some radionuclides (notably iodine-129 and carbon-14) can occur, doses attributed to these release and transport mechanisms are insignificant. In following the water movement through Yucca Mountain, the major components and processes affecting the long-term isolation of radioactive wastes in the Yucca Mountain repository system are described. Also presented is a sketch of how this repository system is intended to work and a series of illustrations that picture the basic concepts that will be quantified in the TSPA.

In addition to tracking the movement of water through the repository system, the following discussion addresses a range of spatial and temporal scales. Being explicit in the definition of the scale being used is important because processes that might be explained at a spatial scale of kilometers must also be discussed at the scale of millimeters. Also, although time scales on the order of days and years are familiar concepts, it is sometimes difficult to extrapolate to the thousands or tens of thousands of years of importance in geologic systems. The discussion has been divided into six topics:

- Water movement in the unsaturated rocks above the repository

- Water and water vapor movement around the repository drifts
- Water movement within the engineered barrier system
- Water movement and radionuclide migration out of the engineered barrier system
- Water movement and radionuclide migration through the unsaturated tuffs below the repository
- Water movement and radionuclide migration through the saturated zone aquifers and biosphere

Each of these areas is discussed below.

2.2.3.1 Water Movement in the Unsaturated Tuffs Above the Repository

Figure 2-5 illustrates the key concepts associated with water movement in the unsaturated zone at

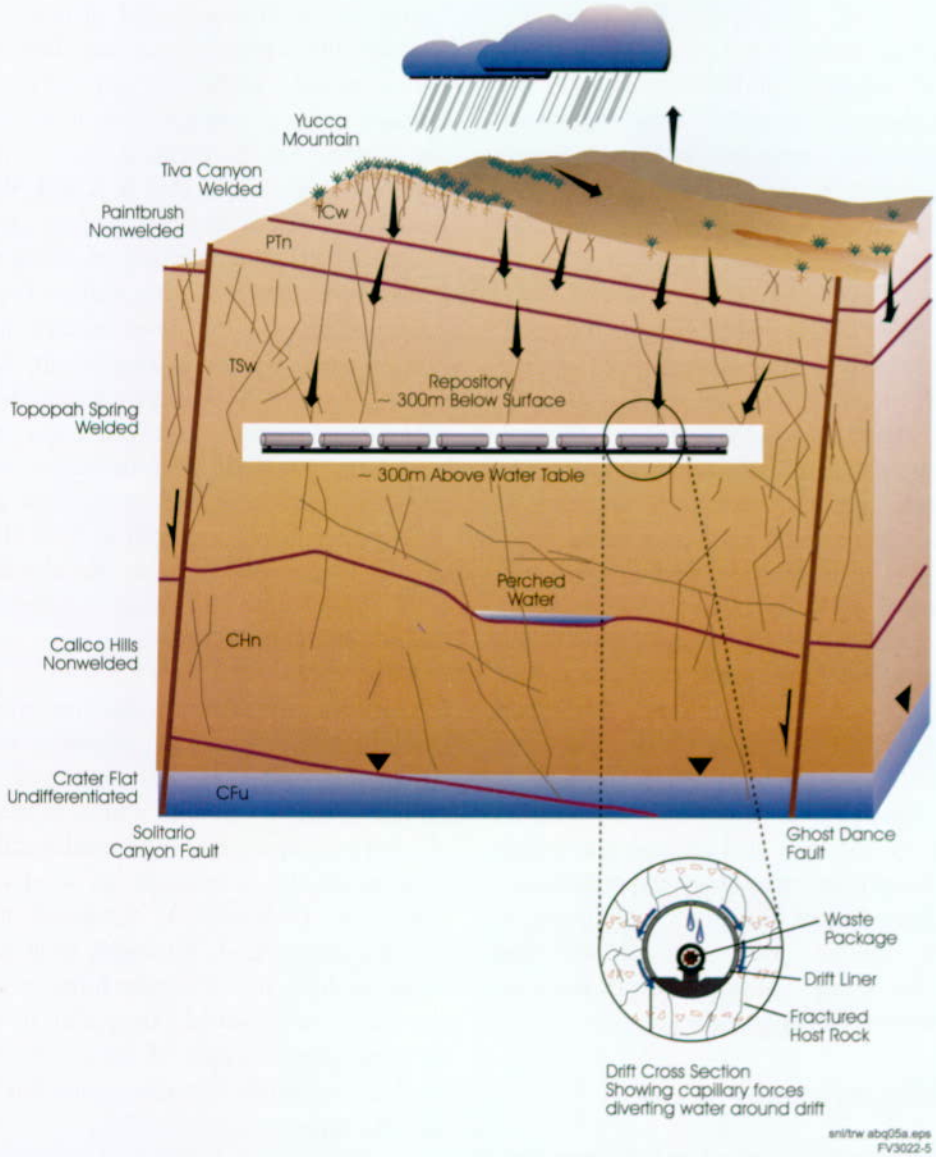

Figure 2-5. Conceptual Illustration of Water Movement Through the Unsaturated Tuffs at Yucca Mountain
Shown is the gravity-driven flow of water through the geologic units overlying the repository and the effects of capillary forces which prevent a significant fraction of the volumetric flow from entering the drifts.

Yucca Mountain. Water at the repository horizon in the unsaturated zone at Yucca Mountain has as its source precipitation at the surface. This precipitation occurs as rainfall and snow and varies over time and space. The spatial variability is defined by precipitation being generally higher at higher elevations, such as along the crest of Yucca Mountain, and lower at lower elevations. The temporal variability is characterized annually by most of the precipitation occurring in the winter months or during brief summer thunderstorms, with the precipitation being higher during El Niño years. Because of long-term (thousands of years) climatic variations, the average precipitation in southern Nevada is expected to increase from current conditions. These long-term, transient precipitation changes may be affected by human-induced changes.

A significant fraction of the rainfall and snowmelt on the surface of Yucca Mountain either runs off into the washes that bisect the mountain, evaporates from the surface, or transpires from the native plants in the area (Volume 1, Section 2.2.3.2). The remaining water continues downward through the soil horizon and eventually infiltrates into the rock. The net amount of total precipitation that infiltrates is called net infiltration. The net infiltration varies with space and time. The spatial variability is caused by variations in precipitation, soil conditions (permeability, thickness, and antecedent water content), geographic conditions (slope angle and slope direction), and vegetation conditions. The temporal variability is caused by the variability in precipitation.

The net infiltration of water moves downward through the unsaturated zone, driven primarily by gravity (Volume 1, Section 2.2.5.1). In the unsaturated zone, this downward movement of water is called percolation flux to distinguish it from infiltration, or movement of water in the soil horizon. Some lateral diversion of water occurs as it moves downward from the soil horizon through the unsaturated zone. This lateral diversion is caused by the eastward dip of the geologic strata and the heterogeneities in the rock because of the different welded and nonwelded tuffaceous lithologic units between the surface and the repository. Although the water may be spatially and temporally distributed at depth, this distribution is generally a subdued reflection of the infiltration distribution at the surface because gravity drainage drives the groundwater flow system in the unsaturated zone (CRWMS M&O 1997n).

Water movement or flux in the unsaturated, fractured tuffs occurs in the matrix and the fractures of the rock. Generally, the welded tuff layers have more of the total flux within the fractures because the permeability of the matrix is low, while the non-welded lithologic layers have more of the total flux within the matrix. The capillary forces tend to cause the water to move from the fractures, which are characterized as having a low suction, into the matrix, which has a high suction. This process is called matrix imbibition. The process is more prevalent in rock units with lower matrix saturation (e.g., the Tiva Canyon welded unit) and less significant when the matrix saturation is higher (e.g., the Topopah Spring welded units) or the fracture spacing is large (e.g., the Paintbrush non-welded unit) (Volume 1, Section 2.3.2.2). Although most of the flux occurs in the fractures, most of the water resides in the matrix.

2.2.3.2 Water and Water Vapor Movement Around the Repository Drifts

Figure 2-6 illustrates the key concepts associated with water movement around the repository drifts after waste emplacement at Yucca Mountain. Without heat-producing wastes in the drifts, the water in the unsaturated rocks around the repository drifts will tend to stay in the rocks and flow around the drifts rather than drip into the drifts. Water stays in the rocks because the rock's capillary forces, including the fractures that contain most of the water flux, are greater than the gravitational forces required for causing a seep unless the fractures are almost fully saturated (see Section 3.1).

The characteristics of the rock around the repository openings may change with time. The fracture permeability could increase because of mechanical stress relaxation following the construction of the

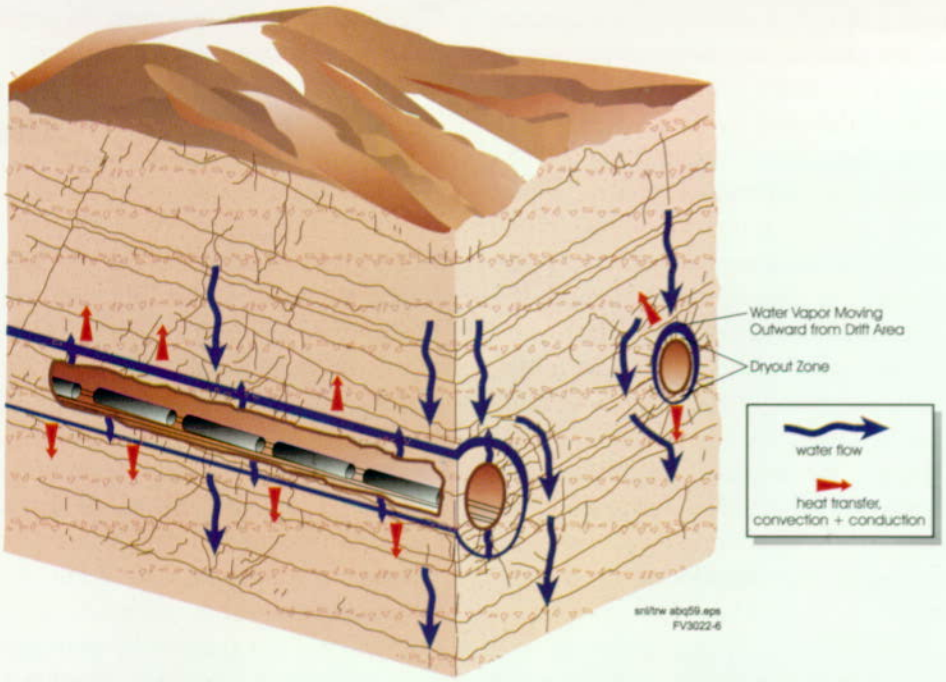

Figure 2-6. Conceptual Illustration of Water and Water Vapor Movement Around the Repository Drifts During the Thermal Period
Shown is the movement of water vapor away from the repository drifts and recondensation in the cooler zones overlying and adjacent to the drifts. This figure represents a time period that extends for several hundred years following waste emplacement.

repository drifts and ultimately the collapse of the drifts. The fracture permeability could decrease because the interaction of emplaced materials causes fractures to plug. The capillary suction of the fractures could either increase or decrease because of these same processes. However, these changes are expected to be within the range of natural variability existing before construction of the facility. The net amount of seepage and the fraction of the repository area in which seepage is expected to occur are important factors in the overall performance assessment, because they determine the likelihood that individual waste packages will be contacted by seepage water (see Section 3.1.1.4).

Water seepage from the rock into the drifts will be affected during the operational phase of the facility by the ventilation of the repository. The ventilation will take moisture from the drifts and the rock in the form of water vapor.

Following waste emplacement, the heat generated by radionuclide decay will drive moisture in the rock away from the heat source, that is, away from the spent nuclear fuel containers in drifts. This water recondenses in areas of lower temperature above, below, and between the hotter drifts. During the first few hundreds to thousands of years, there will be little or no seepage of liquid water into the drifts, because the water is generally being driven away. During this time, water in the drifts is in the form of water vapor or humid air. During the early periods, the relative humidity in the drifts is reduced, but the relative humidity eventually increases to close to 100 percent.

The distribution of liquid water and humid air within and around the repository drifts is variable in space and time. The spatial variability is caused by heterogeneity in the rock properties and variations in the ambient percolation flux. In addition, differences in the thermal output of different waste packages cause a range of thermal-hydrologic conditions in the repository. For example, cooler

regions are expected along the edges of the repository. The temporal variability in water movement around the drifts is caused in the short term (hundreds of years) by the thermal output of the wastes that eventually declines to minimal values; in the long term, the water movement is controlled by the climatic variability discussed above.

2.2.3.3 Water Movement Within the Engineered Barrier System

Figure 2-7 illustrates the key concepts associated with water movement within the drifts and the contact of water with the waste package. Water in aqueous or vapor form can cause degradation of the metallic waste package barrier. The dominant degradation mode of the outer mild steel is by aqueous or humid air corrosion. At low relative humidities and in the absence of liquid water, the corrosion rate of mild steel is generally low; however, at high relative humidities or in the presence of liquid water, this metal can corrode, exposing the inner corrosion-resistant metallic barrier composed of a high-nickel alloy, Alloy 22.

The Alloy 22 layer generally degrades only in the presence of liquid water (i.e., when water drips directly on the waste package). Alloy 22 is generally immune to localized pitting and crevice corrosion and most failures will be by slow general corrosion.

The degradation rates of the carbon steel and high-nickel alloys are also affected by the temperature of the waste package surface, the chemistry of the water in contact with the waste package surface, and the degradation characteristics of the metals themselves. Because these environmental parameters are spatially variable and because the metal fabrication is variable, the waste package degradation is also expected to be variable in space and time. Not all of the waste packages are expected to be breached at the same time. In addition, the temporal variability in degradation rate implies that, once a single opening exists through the metallic waste package, it takes additional time before more openings exist through the waste package.

Until the same waste package has been sufficiently degraded to allow an opening to form through the two metallic barriers, there is no possibility for water to come into contact with the wastes. During this period, the wastes are completely contained within the waste package. Once an opening exists, some of the seepage water falling on the waste package could enter the package.

2.2.3.4 Water Movement and Radionuclide Migration out of the Engineered Barrier System

Figure 2-8 illustrates the key concepts associated with water moving into the waste package and contacting the waste form. Also illustrated is migration through the engineered barrier system of radionuclides that may exist as either dissolved species or adsorbed onto colloidal particles.

After waste package has been breached, water may enter the waste package and contact the waste forms. For commercial spent nuclear fuel and many types of DOE-owned spent nuclear fuel, this water will first come into contact with the Zircaloy cladding around the spent nuclear fuel pellets. Zircaloy is a highly corrosion-resistant metal alloy; it is even more resistant to the effects of generalized or localized corrosion than is Alloy 22. (Although Zircaloy has been considered as a candidate waste package material, the high cost of this alloy precludes its use in the VA reference design.) Zircaloy eventually will degrade with time under several different mechanisms, but for a certain period it will prevent water from directly contacting the wastes. For high-level radioactive waste, a stainless-steel pour canister surrounds the waste glass. For much of the DOE-owned spent nuclear fuel, the wastes are contained within aluminum or Zircaloy cladding of questionable integrity, which in turn are planned to be placed in stainless steel or other metal alloy canisters. Aluminum and stainless steel are not as corrosion resistant as Zircaloy and do not provide significant protection for the wastes contained within them.

When the material surrounding the actual waste form has degraded, the wastes are exposed to the environment inside the waste package and liquid

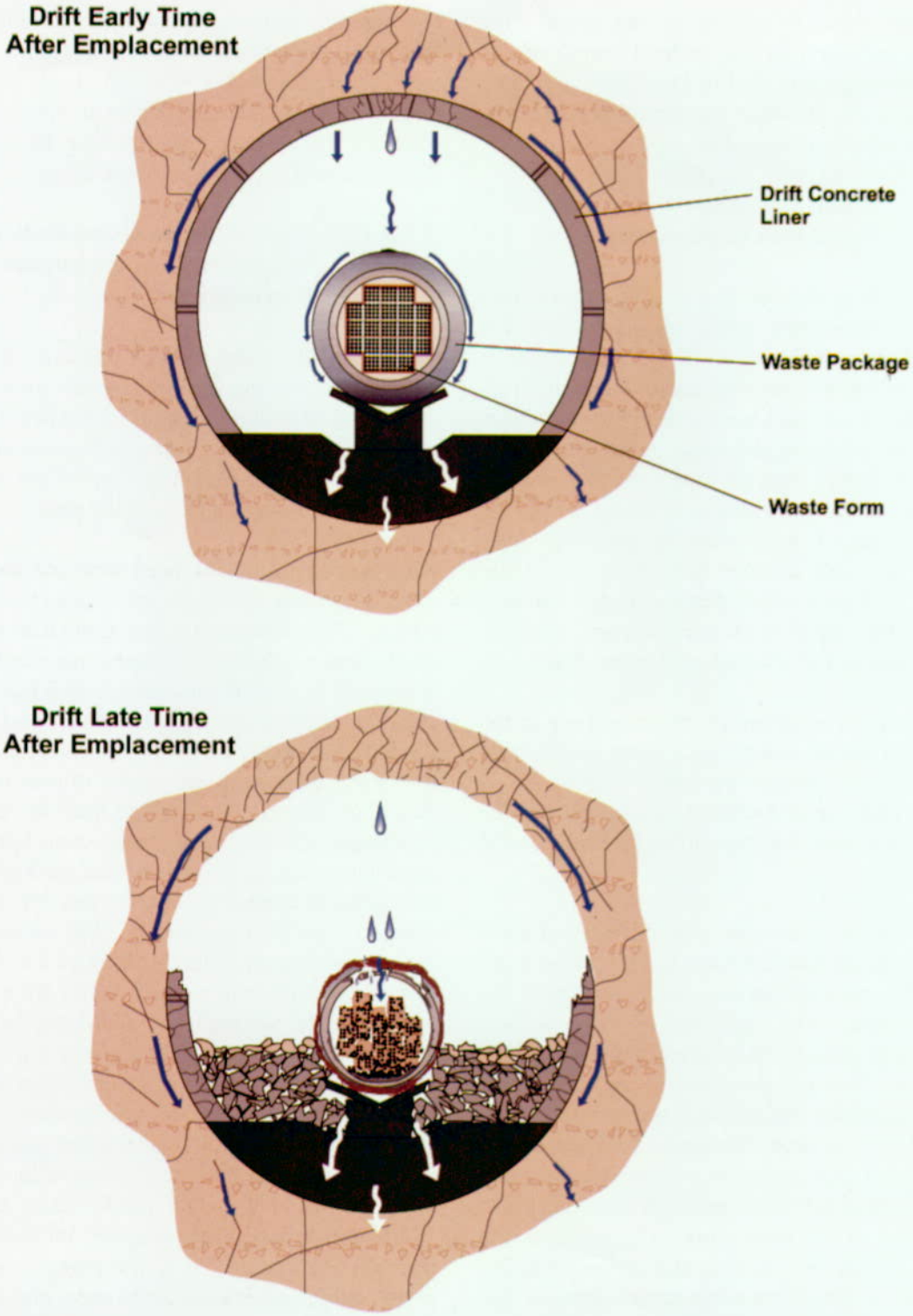

Figure 2-7. Conceptual Illustration of Water Movement into and Within the Engineered Barrier System
Shown is the movement of water between the drift walls and the waste package prior to the degradation of the waste packages. Also shown is the movement of water through degraded waste packages following the breach of the outer and inner containers by aqueous corrosion. The time for an initial breach of a waste package can vary from several thousand to several million years.

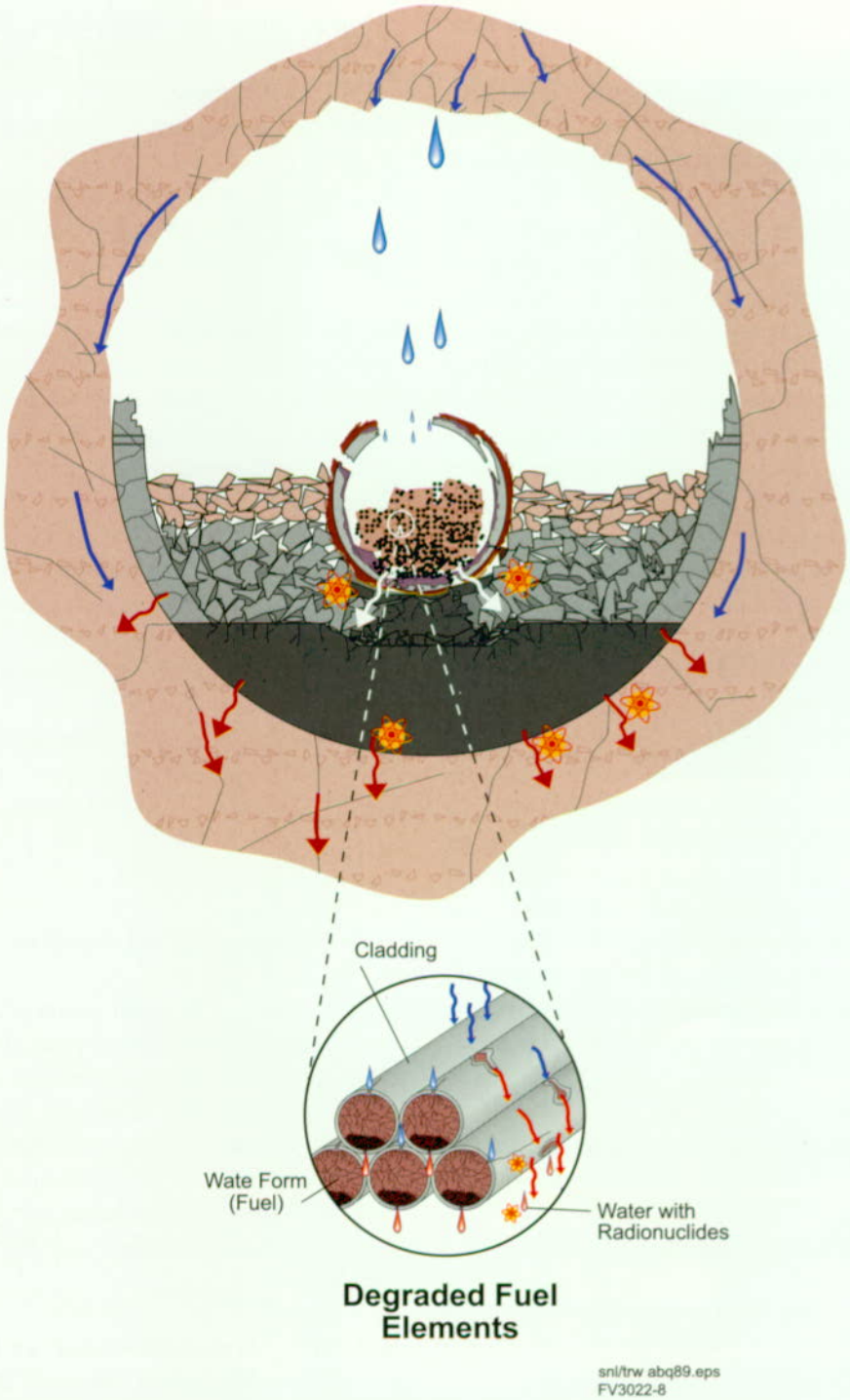

Figure 2-8. Conceptual Illustration of Water Movement and Radionuclide Transport out of the Engineered Barrier System

Shown are potential water pathways within the waste package that may lead to water coming into direct contact with the waste. These pathways would not be initiated until the waste package has been breached, which may take several thousands to millions of years. Once radionuclides have been dissolved in the water, they may be transported along discontinuous pathways within the waste package, through the waste package, and through the drift inverts into the unsaturated tuffs.

water can contact a portion of the exposed waste. If water contacts the waste form, the radionuclides can dissolve in the water. Some radionuclides are highly soluble in water, while others are very insoluble in the water that is likely to contact the waste. Some radionuclides may be attached to very small colloids that may also be mobile in the water.

When radionuclides are released from the solid waste form into the mobile liquid phase, they are available for transport. The transport mechanism depends on the distribution of water on the waste form surface and between the waste form surface and the outer edge of the degraded waste package. If water has dripped into the waste package, it is possible that advective transport of radionuclides to the edge of the waste package could occur. If the water has not dripped into the waste package, then a continuous, interconnected water film along which radionuclides may diffuse is required.

After radionuclides are transported through the degraded internal material of the waste package to the edge of the waste package, they may be transported through the degraded invert materials beneath the waste package. Radionuclides may be transported through the degraded invert by either moving water if there is seepage water, or diffusion through the pores of the invert materials. The radionuclides transported through the degraded invert are ultimately released to the tuff rock units to be transported in the unsaturated zone below the repository and ultimately to the saturated zone.

The rate at which radionuclides are released and transported from the repository depends on the following:

- Degradation rate of the engineered barriers
- Dissolution rate of the waste forms
- Form of the released radionuclides
- Solubility of the aqueous radionuclides
- Rate of water movement and volume of water that flows through the engineered barriers

In the absence of any water seepage coming into direct contact with the wastes, radionuclide releases from the engineered barriers will be minimal, with the possible exception of gaseous releases of radionuclides which are of no significant consequence to the public.

2.2.3.5 Water Movement and Radionuclide Migration Through the Unsaturated Tuffs Below the Repository

Figure 2-9 illustrates the key concepts associated with water movement in the unsaturated rocks beneath the repository and the migration of radionuclides in these rocks. After the dissolved or colloidal radionuclides are released into the unsaturated tuffs beneath the repository, they may be transported with the water to the water table. The rate at which these radionuclides are transported to the water table is a function of the following:

- Percolation flux in the unsaturated tuffs
- Distribution of the percolation flux between fractures and matrix
- Effective velocity of the groundwater within the fractured rocks
- Adsorption of radionuclides within the rock

Because each of these characteristics of the natural environment is variable in space and time, radionuclide transport is also variable. Part of the temporal variability relates to long-term climatic changes that not only change the percolation flux through the system but also cause the water table beneath Yucca Mountain to rise (in the case of wetter climates) or fall (in the case of drier climates).

2.2.3.6 Water Movement and Radionuclide Migration Through the Saturated Zone Aquifers and Biosphere

Radionuclides that are transported through the unsaturated zone are released to the saturated aquifers beneath the repository. Figure 2-10 illustrates the key concepts associated with water

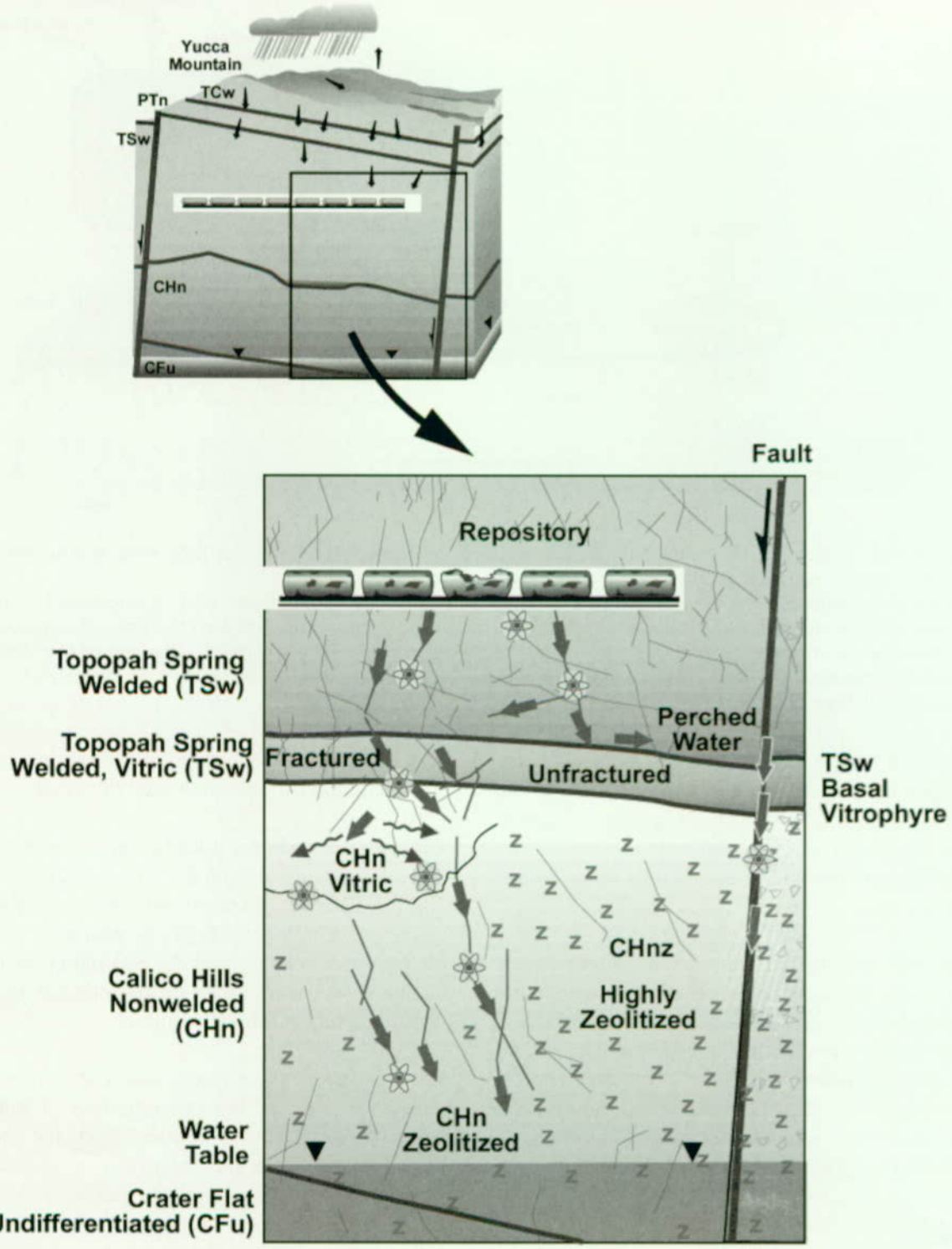

Figure 2-9. Conceptual Illustration of Radionuclide Transport Through the Unsaturated Tuffs at Yucca Mountain Shown is the gravity-driven transport of radionuclides through the unsaturated zone. Also illustrated are retardation mechanisms that delay the arrival of radionuclides to the saturated aquifers located several hundred meters beneath the repository. The mean advective travel time through the unsaturated zone is on the order of several thousand years for unretarded radionuclide species in the current climate.

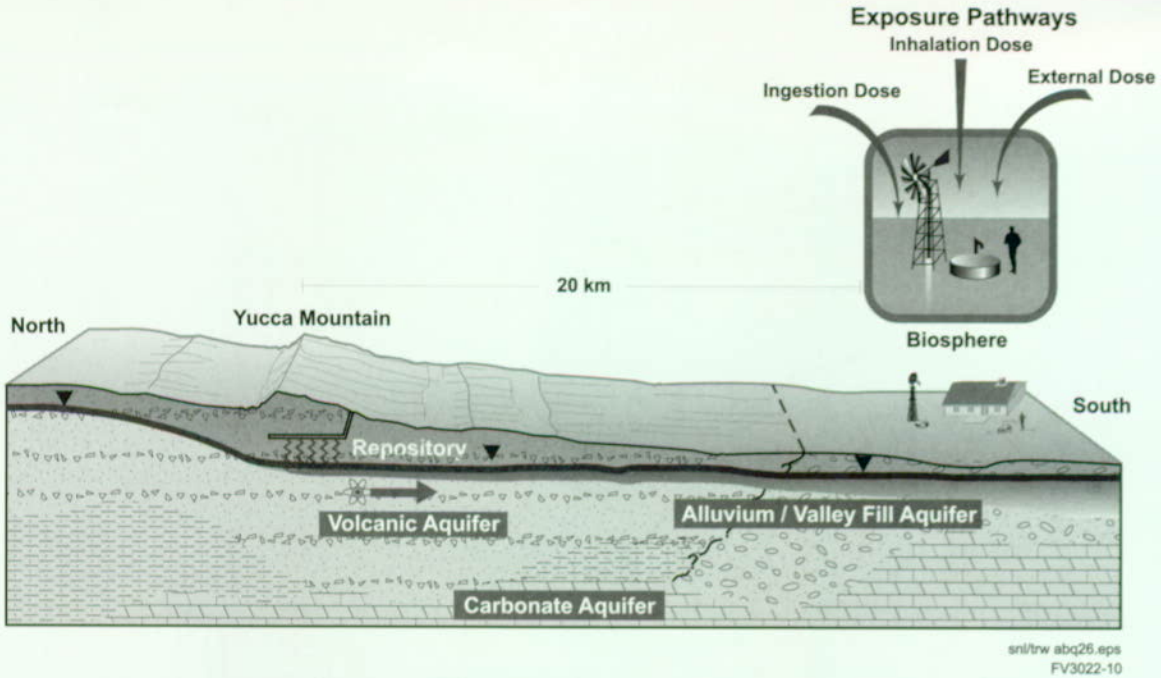

Figure 2-10. Conceptual Illustration of Radionuclide Transport Through the Saturated Tuffaceous and Alluvial Aquifers and the Biosphere
Shown is the lateral migration of any dissolved radionuclides that reach the water table downgradient from the repository. The mean advective travel time through the saturated zone to a point 20 km (12 miles) downgradient is on the order of several thousand years for unretarded species in the current climate. Also shown are potential biosphere pathways by which radionuclides that are dissolved in water may be extracted from the alluvial or tuff aquifers and come into contact with humans.

movement in the saturated aquifers beneath and downgradient from the Yucca Mountain site and the migration of radionuclides in these aquifers. Also illustrated are the pathways by which any dissolved radionuclides may come into contact with humans.

When the radionuclides reach the saturated zone, they will be transported laterally within the saturated zone. The general direction of groundwater flow in the saturated zone is to the southeast, and then possibly to the south and southwest. The concentration of the radionuclides in the saturated zone aquifers at any point downgradient from the repository is a function of the following:

- Radionuclide concentrations in the water that enters the saturated zone
- Dispersion of these radionuclides as they are transported
- Adsorption of these radionuclides on the mineral surfaces along the flow path

The time for radionuclides to reach any specified point downgradient from the repository, such as the 20-km (12-mile) point chosen for evaluating the system performance, depends primarily on the groundwater velocity and the retardation of radionuclides which may sorb on the mineral surfaces within the tuff or alluvial aquifers.

There is minimal risk associated with radionuclide releases as long as the concentration of radionuclides in water that is pumped from the aquifers downgradient from the repository is sufficiently low. Should radionuclides reach a location downgradient from the repository where water is pumped from the aquifer, the potential exists for radionuclides to come into contact with humans through biosphere pathways. The principal biosphere pathways to humans consist of the following:

- Direct consumption of water containing dissolved radionuclides
- Watering of livestock and the subsequent consumption of meat or milk
- Consumption of crops and animal products produced using water containing dissolved radionuclides
- Direct exposure to contaminated soil
- Inhalation of dust that may contain attached radionuclides

The previous discussion outlined how the various components of the Yucca Mountain repository system fit together to describe how the system is intended to work. The general conceptual aspects of each key component and processes that affect the expected behavior of the repository system have been described. The next section (Section 2.3) describes the approach used to assemble the representations of the individual components into a description of the entire system. The details of each of the component models used in the TSPA and the scientific bases for these models are presented in Section 3 and the *Total System Performance Assessment-Viability Assessment (TSPA-VA) Analyses Technical Basis Document* (CRWMS M&O 1998i).

2.3 METHODOLOGY

This section presents an overview of the method for mathematical and numerical modeling of each process and component introduced in Section 2.2, including their uncertainty, and the approach for combining them into an overall model and computer code. This overview includes discussions about information flow between the models (Section 2.3.1) and the computer code architecture that facilitates the information flow (Section 2.3.2). This section provides a road map of how to recouple the component models into one integral whole, to reassemble the analyzed pieces and pass information between them to develop reasonable assessments of overall system performance. The method for correctly coupling the component models to make robust predictions of repository behavior is comprised of the basic activities outlined in Section 1.3. More detail on these activities as they apply to the Yucca Mountain TSPA is given in *Total System Performance Assessment - Viability Assessment (TSPA-VA) Methods and Assumptions* (CRWMS M&O 1997m).

In addition to modeling and analyzing the system, the TSPA methodology presents the key results, focusing on the influence of uncertainty on the performance predictions. As mentioned in Section 2.2, the 1997 Energy and Water Appropriations Act requests an analysis of the "probable behavior of the repository." The base case models described in Section 3 are intended to represent this probable behavior. The exact definition of "base case" depends on the choice of parameter ranges for each component model. In this context, the use of the term "range" is important. In particular, the TSPA-VA base case parameter sets and conceptual models encompass a range of uncertainty for the various parameters rather than just one realization of the parameters. Given the base case definitions of these various parameter ranges for the model components, a base case TSPA model is constructed to predict overall repository performance (see Section 2.3.3). This model represents an assessment of the likely or probable range of future behavior for the overall repository system, which is essentially a combination of the likely ranges of behavior for the various component models, processes, and corresponding parameters.

In addition to base case repository performance, behavior that is considered less likely is captured in the sensitivity cases for alternative models and parameter ranges of the various processes (see Section 5). Besides alternative models and parameter ranges, other sensitivity cases (features, events, and processes not included in the base case) examine the effect of repository design options (see Section 4.5) and disruptive events such as volcanism (see Section 4.4).

Because of the inherent uncertainty in the performance predictions, the TSPA-VA results are provided in two main forms:

- Probability distributions, such as complementary cumulative distribution functions (CCDFs), for peak dose rate to a receptor 20 km (12 miles) downgradient of the repository, during a certain time (see Section 4.3).[1]

- Time histories over 10,000 years, 100,000 years, and 1 million years of the dose rate at 20 km (12 miles) downgradient of the repository, for specific samplings of the input parameters. A dose-rate realization generated by using the expected values from all input parameter distributions is used to describe and explain future repository behavior, in particular, how the various components and subsystems interact with one another (see Section 4.2).

Various sensitivity analysis methods for determining the most influential system parameters are also used (Section 4.3). These analyses include methods for displaying the results in a way that most transparently demonstrates the key natural and engineered barrier parameters and features (e.g., plots of correlation coefficients versus time). This helps prioritize future site-characterization efforts and delineate best possible design options.

2.3.1 Information Flow Between Component Models

A stylized conceptualization of the TSPA-VA model hierarchy and information flow is shown in Figures 1-1 and 2-1. These figures indicate a continuum of information and models, from the most basic, detailed level to the level of the total system model. The data and associated conceptual and process-level models rest at the base of the pyramid. These process-level models may be simplified or abstracted,[2] if necessary, because of computational constraints or lack of information. The abstracted performance assessment models may have a one-to-one correspondence with the detailed process-level models or may represent a combined subsystem model[3] covering several aspects of the overall system. The performance assessment models form the components of the overall TSPA model at the top of the pyramid. Total-system model simulations can then be performed in the computationally intensive probabilistic framework necessitated by a Monte Carlo approach to performance assessments.[4]

For this model simplification process, there are two key factors in accurately representing the performance of the overall system. First, information

---

[1] For example, based on uncertainty in the input parameters, the analysis consists of randomly sampling all input parameters 100 times to generate 100 realizations of repository performance. Each realization, being a unique combination of the input parameters, will produce a different prediction of dose rate versus time. From each of these 100 dose rate histories, the peak dose that occurred at any time during a specific time period is selected, for example, during the first 10,000 years after closure of the repository. These peak doses are then plotted as a probability distribution to answer the following question: What is the probability of exceeding dose rate x during the first 10,000 years?

[2] The word *abstraction* is used to connote the development of a simplified mathematical and/or numerical model that reproduces and bounds the results of an underlying detailed process model.

[3] Examples of various subsystems include the engineered barrier system, the unsaturated zone, and the saturated zone.

[4] Much of the modeling of the repository and its components is complex, uncertain, and variable, involving a variety of coupled processes (thermal-hydrologic-chemical and thermal-hydrologic-mechanical) operating in three spatial dimensions on a variety of different materials (e.g., fuel rods, waste packages, invert, and host rock) and changing over time. For these reasons, it is often necessary to make some simplifications to the detailed process-level models. The need for simplification is particularly evident in TSPA, which has a significant component of probabilistic risk analysis. The general approach of using probabilistic risk analysis is appropriate because of the inherent uncertainties in predicting physical behavior many thousands of years into the future in a geologic system with properties that can never be fully characterized deterministically. Because of the large number of uncertain parameters in the component TSPA models, probabilistic risk analysis involves a Monte Carlo method of multiple realizations of system behavior, which requires significant computational resources. For this reason, and because the lack of certain data makes some detailed models difficult to quantify, model abstractions are often employed.

passed up the model pyramid must be consistent. For example, an infiltration flux used to generate liquid flow fields from the detailed process model for the unsaturated zone must be used in all subsequent analyses based on those particular flow fields. The same flux must be used when calculating seepage flux in the abstracted seepage subsystem model (see Section 3.1) and when calculating thermal-hydrologic response (temperature and relative humidity) in the near-field environment (see Section 3.2). Second, the parameters that most affect performance in the detailed process models must be appropriately represented in the subsequent subsystem and total system models, including the appropriate uncertainty range of the parameters.

A key feature of the methodology is how to pass uncertainty at one level to uncertainty at another level. As Figure 1-1 illustrates, transfer of uncertainty must go in both directions, from bottom up and from top down. When analyzing uncertainty at the bottom levels (data, conceptual models, and process models), the analyses look at the effect of uncertain parameters on surrogate or subsystem performance measures such as the amount of fracture flow in the unsaturated zone. The sensitivity of the surrogate measure to component model uncertainty is then used to decide whether to carry this uncertainty through to the total system analyses. However, sometimes important parameters at the subsystem level prove to be unimportant at the overall system level and then this information is passed down the pyramid to indicate the relative unimportance of collecting more physical data about this parameter.

Traceability of data transfer amongst models and quality assurance of the data are very important aspects of the information flow process. The *Total System Performance Assessment-Viability Assessment (TSPA-VA) Analyses Technical Basis Document* (CRWMS M&O 1998i), which supports the TSPA results presented here, explicitly identifies the source and status of data, computer codes, and computer input and output files used in the VA. The *Total System Performance Assessment-Viability Assessment (TSPA-VA) Analyses Technical Basis Document* (CRWMS M&O 1998i) will form the basis for development of the DOE TSPA data qualification plans. Following prescribed procedures, DOE is reviewing the data, assumptions, computer codes, and information used in the TSPA analyses to ensure the models are valid, defensible, and appropriate. DOE has developed a transition plan to take the TSPA reported here to qualified status for the LA. To be fully qualified, there must be clear documentation that the TSPA models are supported by qualified data and the numerical models and computer codes are documented and appropriately controlled.

Figure 2-11 is a more detailed, but still simplified, look at information flow among the eight key component models: unsaturated zone flow (and seepage), thermal hydrology, near-field geochemistry, waste package degradation, waste form alteration and mobilization, unsaturated zone transport, saturated zone flow and transport, and biosphere. It does not show all of the couplings among TSPA-VA component models but does illustrate major model connections, abstractions, and information feeds. "Response surface" means a multidimensional table of output from one model to be used as input in another model. When interpolating among points in the table, linearity is generally assumed. Usually a response surface has more than one dependent variable (e.g., both time and percolation flux). However, in the usage in Figure 2-11, sometimes time is the only independent variable, and interpolation is not even necessary between the time points (e.g., the data are provided directly "as is" to the next model).

Figure 2-12 is a more detailed description of information flow in the TSPA-VA, showing the principal pieces of information passed between the various component models. These details of information flow are explained in greater depth in the discussion of the TSPA-VA code architecture in the Section 2.3.2 and in the description of the TSPA-VA base case in Section 4.1. The conceptual and experimental basis for this depiction of information flow is given in detail in Section 3. For example, the division of the repository horizon into six regions based on thermal-hydrologic response and infiltration flux is

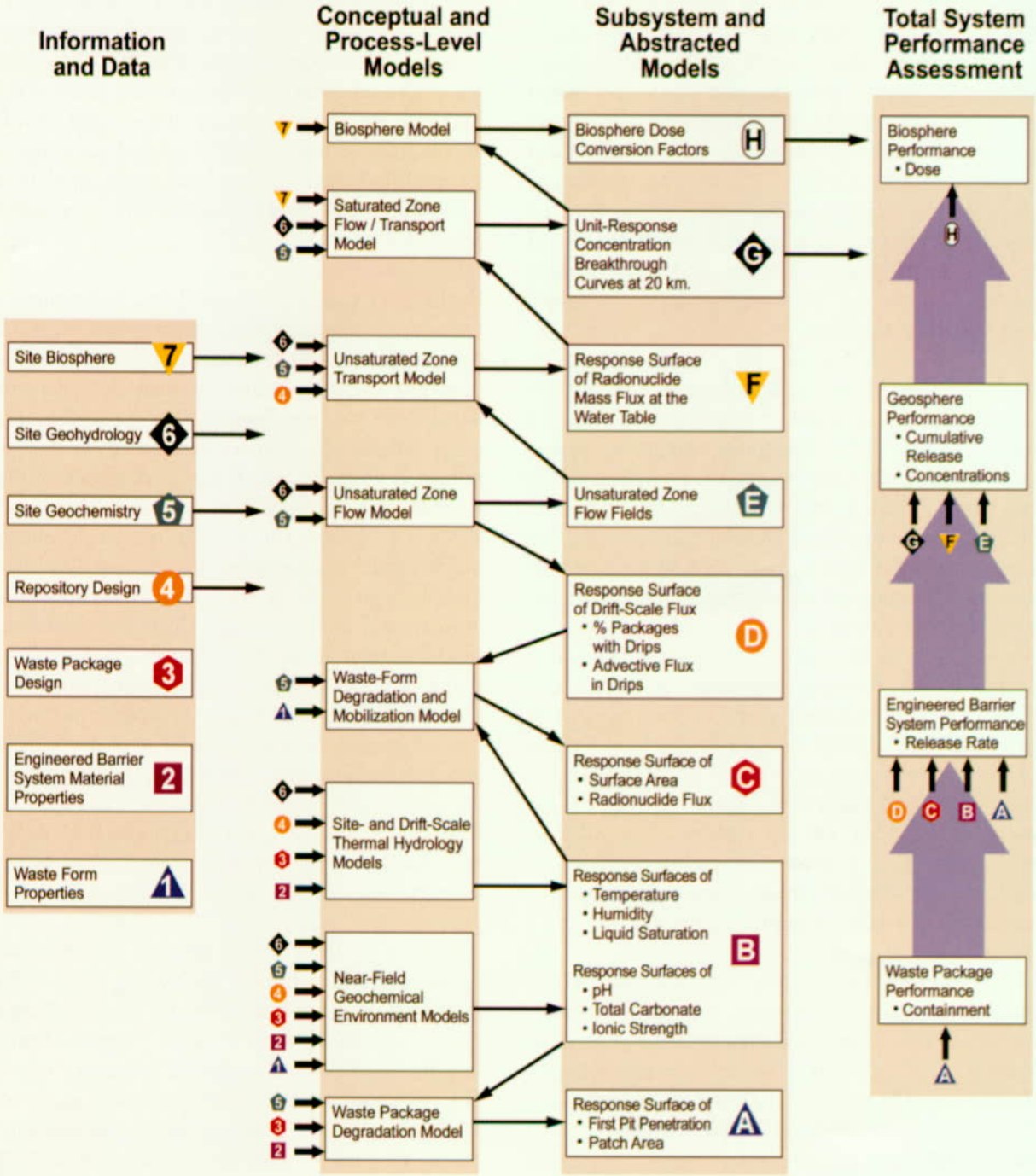

Figure 2-11. Simplified Representation of Information Flow in the Total System Performance Assessment for the Viability Assessment Between Data, Process Models, and Abstracted Models

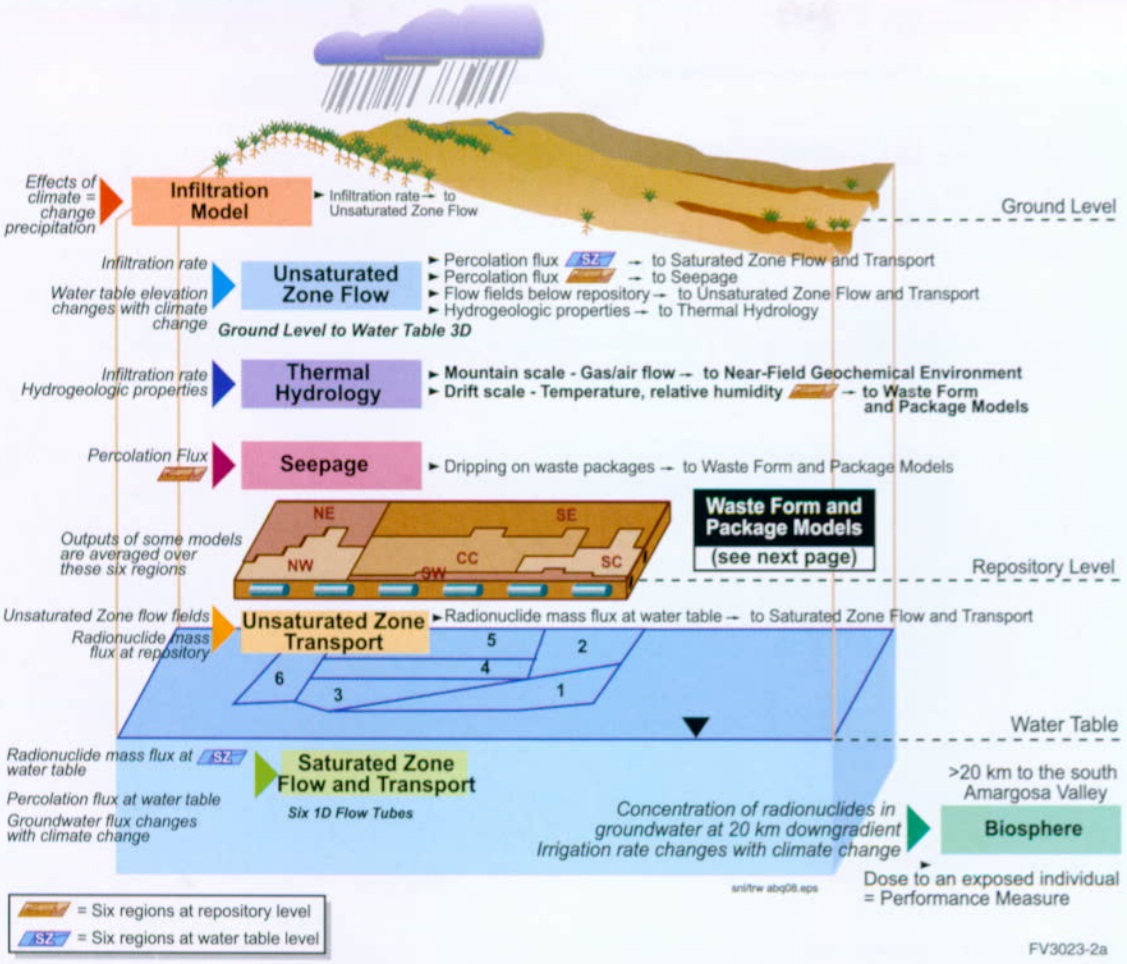

Figure 2-12a. Detailed Representation of Information Flow in the Total System Performance Assessment for the Viability Assessment
This figure is in two parts with the detail of the waste package and waste form models shown in Figure 2-12b.

discussed in Section 3.2; and the division of the saturated zone water table into six regions, unrelated to the six repository regions, based on stratigraphy and other factors is discussed in Section 3.7.

The decoupling of the physical-chemical processes into component models, shown in Figures 2-11, 2-12, and 2-2, is facilitated by a natural division of the repository system into a series of sequentially linked spatial domains (e.g., the waste package, emplacement drift, host rock near the drift, unsaturated zone between the drift and the water table, saturated zone, and biosphere). This division works best from the standpoint of radionuclide transport, which is the primary consideration of the TSPA models. The TSPA-VA model architecture and information flow becomes, therefore, a sequential calculation in which each spatially based transport model may be run in succession, with output as "mass versus time" from an upstream spatial domain serving as the input of mass versus time for the spatial domain immediately downstream.

2.3.2 Code Architecture

The overall model architecture and information flow, discussed in the previous section, forms the basis for the architecture of the overall TSPA-VA computer code. The executive driver program or integrating shell that links all the various component codes is RIP V5.19.01 (Golder Associates, Inc. 1998). It is a probabilistic sampling program that ties all the component

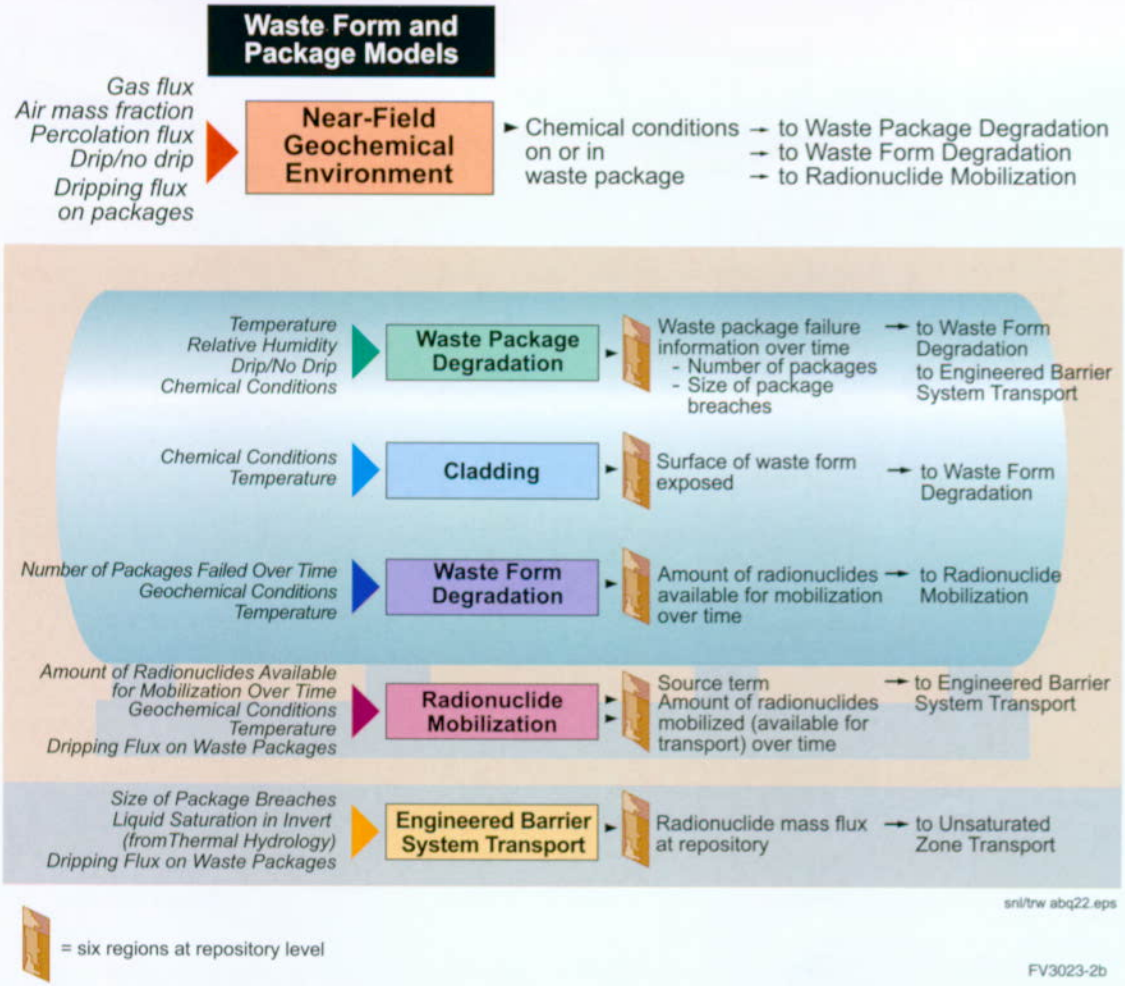

Figure 2-12b. Detailed Representation of Information Flow in the Total System Performance Assessment for the Viability Assessment

models, codes, and response surfaces together in a coherent structure that allows for consistent parameter sampling among the component models. The RIP program is used to conduct either single-realization runs of the entire system (see Section 4.2) or multirealization runs of the system (see Section 4.3). The latter realizations yield a probability distribution of dose rate in the biosphere that shows uncertainty in dose rate based on uncertainty in all the component models.

Because of the need to conduct multiple realizations of the total system behavior, RIP is generally designed to model various components in a simplified fashion. However, the current version of RIP has some very useful features such as cells and environments, that allow certain processes to be modeled in reasonable detail. The RIP program is also very flexible in representing various component processes in the total system model. The four ways that component models may be coupled into RIP, from most complex to least complex, include the following:

- External function calls to detailed process codes
- RIP cells, which are basically equilibrium batch reactors that, linked in series, can provide a reasonably accurate description of engineered barrier system transport
- Response surfaces, which take the form of multidimensional tables representing the

results of modeling with detailed process models before running the RIP TSPA code

- Functional or stochastic representations of a component model directly built into the RIP architecture

The method used for each TSPA-VA component model is described briefly below and in greater detail in the corresponding sections of Section 3.

As described above for the third coupling method, much of the computational work that goes into the TSPA-VA models is done outside of RIP, before running the actual total system computations. For example, the unsaturated zone flow fields were computed using Transport of Unsaturated Groundwater and Heat TOUGH2 (Pruess 1991), a three-dimensional, finite-volume numerical simulator, with about 80,000 grid blocks representing the entire unsaturated zone model domain (for the dual-permeability model). Similarly, the waste package degradation histories for various values of the uncertain input parameters were run before the RIP runs with a FORTRAN-based simulator called WAPDEG, on UNIX and PC workstations. Other component models that were also run outside of RIP are listed below. The results of these detailed process-level runs were provided as multi-dimensional tables that are read into RIP at run time.[5]

Figure 2-13, in conjunction with Figure 2-12, provides a better understanding of the TSPA-VA code architecture, that is, the actual computer codes used and the connections (information transfer) between codes. It includes both the codes run before the RIP program and those run in real time that are coupled to (external function calls) or within (cells and tables) the RIP program. Based on the schematic information transfer shown in Figure 2-13, some response surfaces generated by codes external to RIP only provide data to other codes external to RIP (e.g., chemical-composition response surfaces (pH) from the near-field geochemical model will directly feed the external model for waste package degradation, WAPDEG). Other response surfaces, such as liquid saturation, temperature, and seepage flux, will provide data directly into RIP as response surfaces that influence such things as waste form degradation rates. Not all couplings or all models are shown in Figure 2-13, but most are shown (e.g., near-field geochemical modeling is too complex to show all of its aspects in this figure–see Section 3.3).

Coupling of the various models is affected by the climate model, which impacts almost all the other models in one way or another, because it alters water flow throughout the system. The climate is assumed to shift in a series of step changes between three different climate states: present-day dry climate, long-term-average climate (about twice the precipitation of dry climate), and super-pluvial climate (about three times the precipitation of dry climate). These climate shifts are implemented as a series of steady-state flow fields in the unsaturated and saturated zones (including changes in the water-table elevation). Within the RIP program, these shifts require coordination among the coupled submodels because they must all simultaneously change to the appropriate climate state.

In general terms, the coding methods and couplings to be used for the major components are as follows:

- Mountain-scale, unsaturated zone flow (see Section 3.1) is modeled directly with the three-dimensional, site-scale, unsaturated zone flow model developed by YMP, using a volume-centered, integral-finite-difference, numerical flow simulator, called TOUGH2 (Pruess 1991). Steady state flow is assumed, and three-dimensional flow fields are generated for three different infiltration boundary conditions, three different climate states, and several values of rock properties.

[5] Examples of these multidimensional tables include (1) liquid flux and velocity fields for the unsaturated zone as a function x,y,z,t and uncertain parameters such as infiltration flux and (2) package failures versus time as a function of uncertain parameters such as corrosion rate of the corrosion-resistant metal that forms the inner barrier of the waste package.

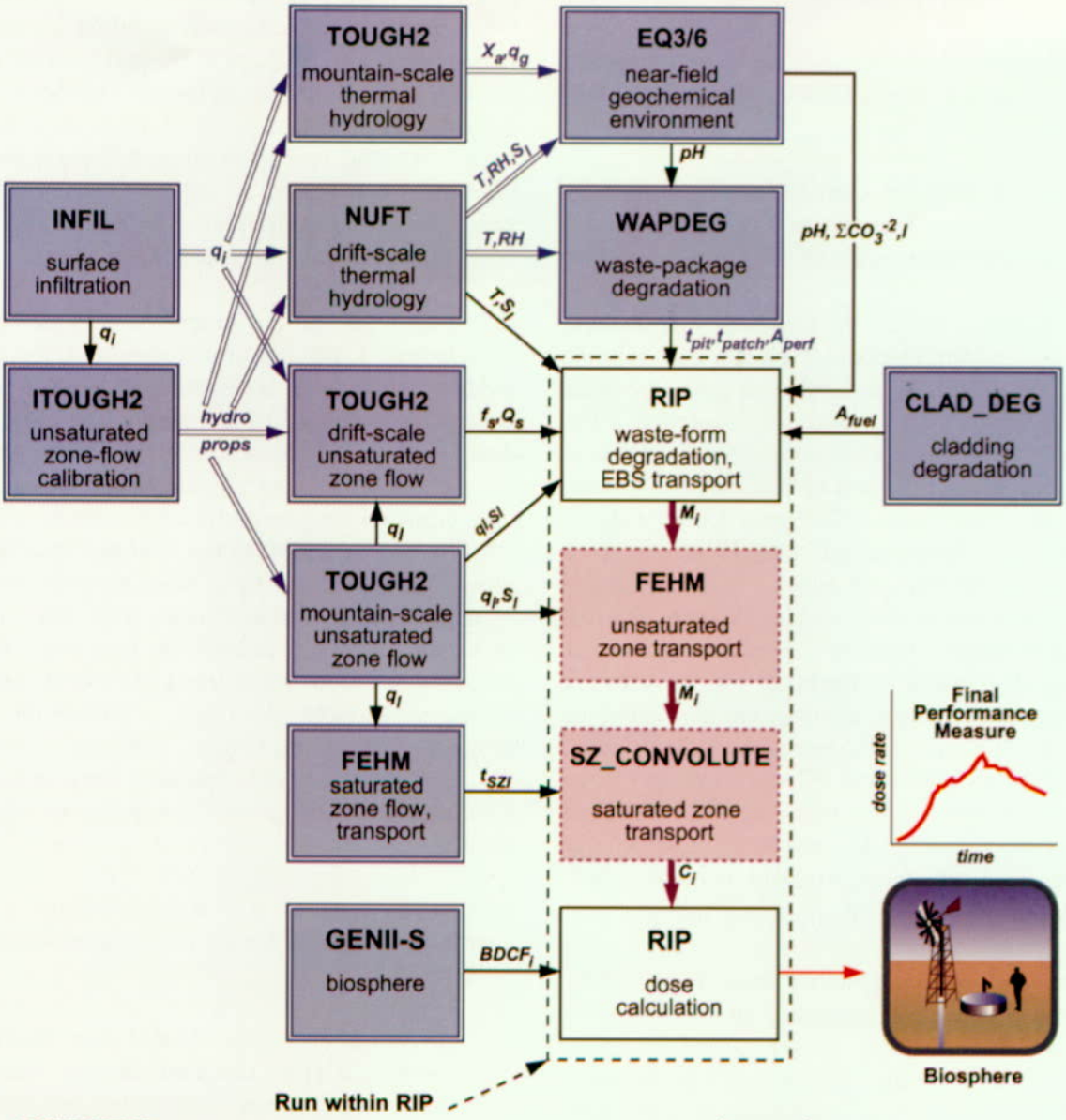

OUTPUT Parameters

T	Temperature	Q_S	Seep flow rate
RH	Relative humidity	pH	pH
S_l	Liquid saturation	ΣCO_3^{-2}	Carbonate concentration
X_a	Air mass fraction	I	Ionic strength
q_g	Gas flux	t_{pit}	Initial-pit-penetration time
q_l	Liquid flux	t_{patch}	Initial-patch-penetration time
q_i	Infiltration flux	A_{perf}	Perforated container area
M_i	Radionuclide mass flux	A_{fuel}	Exposed fuel area
C_i	Radionuclide concentration	t_{SZi}	Saturated zone transport time
f_S	Fraction of WPs with seeps	$BDCF_i$	Biosphere dose conversion factor
		EBS	Engineered Barrier System

Legend

- *External Process Model*
- *RIP Cells*
- *Rip Calls External Code*
- *Response Surface Between Process Models*
- *Response Surface from Process Model to RIP*
- *Between RIP Cells and External Code*

Figure 2-13. Total System Performance Assessment for the Viability Assessment Code Configuration: Information Flow Among Component Computer Codes

These "pre-generated" flow fields (i.e., developed externally and before the RIP simulations) are then placed in a library of files to be read by the Finite Element Heat and Mass (FEHM) code for unsaturated zone transport during the real time RIP simulations. Fracture and matrix liquid fluxes, along with liquid saturation, are passed to FEHM in these tables. To generate the library of flow fields, an inverse model, ITOUGH2 (Finsterle et al. 1996), is used to calibrate the model-predicted liquid saturations to measured liquid saturations in the matrix. This calibration is done when generating the flow fields for the three different infiltration conditions and the different fracture properties at current dry-climate conditions. For future-climate conditions, flow fields are generated based on the dry-climate calibrations. Climate change is modeled within TSPA-VA unsaturated zone calculations by assuming a series of step changes in boundary conditions, meaning that different flow fields are provided at the appropriate time with the assumption of instantaneous pressure equilibrium.[6] The unsaturated zone flow fields are also provided to the TOUGH2 drift-scale seepage models, to the saturated zone streamtube models, and to the engineered barrier system transport models. Unsaturated zone hydrologic properties are passed to the drift-scale, thermal-hydrology model.

- Seepage of water into emplacement drifts (i.e., drift-scale, unsaturated zone flow-see Section 3.1) is also modeled externally and before the RIP simulations using TOUGH2 on a finely discretized grid around the drift. Simulations are conducted over a heterogeneous fracture permeability field (based on permeability measurements in the Exploratory Studies Facility), at a variety of percolation rates (from the mountain-scale, unsaturated zone flow model) and a variety of mean values and standard deviations for the fracture permeability distribution and the fracture "alpha" distribution (see Section 3.1). These simulations become an uncertain response surface of seepage flux into the drift as a function of percolation flux and a response surface of the number of packages that are dripped on (by seeps) as a function of percolation flux. Both of these response surfaces are input directly into RIP.

- Mountain-scale, unsaturated zone thermal hydrology (see Section 3.2) is modeled with the TOUGH2 code using two-dimensional cross sections taken from the three-dimensional, site-scale, unsaturated zone flow model. Output is several histories of air mass fraction and gas flux as a function of time near the drift, which is provided directly to the near-field geochemical process models.

- Drift-scale, unsaturated zone thermal hydrology is modeled with the finite-difference computer program NUFT (Nitao 1998) in one, two, and three dimensions before the RIP simulations. The drift-scale thermal-hydrology model uses a complicated set of embedded abstractions at different levels of spatial and process detail (e.g., conduction-only versus conduction and convection), as described in Section 3.2. Outputs include:

[6] According to the particular history of climate changes sampled by the RIP TSPA model at the beginning of a given realization, the unsaturated zone flow field library is interrogated for a different flow field every time during the simulation that a step change is indicated. This change in a flow field is assumed to apply instantaneously to the transport model. The validity of this approach is discussed briefly in Section 3.6 and in more detail in the *Total System Performance Assessment-Viability Assessment (TSPA-VA) Analyses Technical Basis Document* (CRWMS M&O 1998i). The durations of each of the three climate states are uncertain parameters sampled at the beginning of each realization of the total system model. However, the sequence of these alternating climate states is the same for all realizations. More details are given in Sections 3.7 and 4.1.1.

– Waste package surface temperature (T_{wp}) and waste package surface relative humidity (RH_{wp}) for seven different package types within six discrete spatial regions of the repository (see Figure 2-12 for an illustration of the six regions).[7] These values are provided to WAPDEG.

– Average waste form temperature (T_{wf}) and liquid saturation in the invert (S_l) in each of the six regions. These values are provided to the waste form degradation and engineered barrier system transport models in the RIP program.

– Average drift-wall temperature (T_{dw}), relative humidity, and liquid saturation in the invert in the "CC" region of the repository (Figure 2-12). These values are provided to the near-field geochemical models. The outputs are in the form of response surfaces or multi-dimensional tables.

- Near-field geochemical environment (i.e., drift-scale thermal chemistry) is modeled in the base case calculations outside of the RIP simulations by assuming a certain scenario for water flow through the drift and the types of materials the water contacts. Equilibrium batch-reaction calculations with EQ3/6 (Wolery 1992a; Wolery and Daveler 1992) are performed at several places within the drift and then the output from one batch calculation is passed to the input of the next batch calculation at a different spatial location (see Section 3.3 for details). Output is a response surface of various chemical composition parameters. These values are provided both to the waste package degradation model WAPDEG, which is run outside of the RIP program, and to RIP directly as input tables for the waste form degradation and colloid models within RIP.

- Waste package degradation is modeled outside of, and before, RIP runs using a computer code named WAPDEG (CRWMS M&O 1998j), which includes corrosion-rate variability both on a given package and from package-to-package (see Section 3.4). Output is in the form of several tables, read into the RIP program at run time, of the cumulative number of package failures per time, average patch area per package versus time, and average pit area per package versus time. Early or "juvenile" failures, because of the combined effects of large rockfalls, high seismic activity, or possibly undetected material defects, are input directly into RIP as probability distributions.

- Cladding degradation by physical-chemical processes such as creep rupture is modeled outside of RIP runs and then input directly into RIP as a percentage value of failed cladding versus time (exposed waste form area versus time; see Section 3.5). Other cladding degradation modes such as mechanical failure are also input directly into the RIP program, based on other simulations (CRWMS M&O 1998i, Section 6.3.1.1.7).

- Waste form degradation is modeled as an equation within the RIP program using empirical degradation-rate formulas developed from available data and experiments for the three different waste form types: commercial spent nuclear fuel, DOE spent nuclear fuel, and high-level radioactive waste (see Section 3.5). Output from the waste form degradation model is the mass of waste form exposed per time and the volume of water in contact with this waste form versus time, which is used directly in the RIP waste form cells. There are a variety of these waste form cells in the RIP program, corresponding to three different waste form types and several different seepage scenarios. The amount of inventory that can

[7] Waste form surface temperature is actually assumed to be equal to the waste package surface temperature.

ultimately enter each waste form cell is a linear function of the number of packages emplaced in each inventory/seepage/thermal-hydrologic environment. There are 72 such environments, representing the product of 6 thermal-hydrologic regions (discussed above), 3 inventory types, and 4 seepage environments (see Section 4.1.7). The entire waste inventory is composed of hundreds of different types of radionuclides. Of these hundreds, 39 were found to be present in sufficient quantity to warrant modeling in the near-field model components of the TSPA. Of these 39, only the nine most important radionuclides—most important from the standpoint of delivering, or potentially delivering, the greatest dose rate at the biosphere location 20 km (12 miles) downgradient of the repository—were tracked through all the system models. These nine radionuclides are: technetium-99, iodine-129, neptunium-237, plutonium-239, plutonium-24, uranium-234, carbon-14, selenium-79, and protactinium-231.[8]

- Engineered barrier system transport is modeled directly within RIP at run time using the RIP cells algorithm. The modeling is based on an idealized representation (basically a linked series of equilibrium batch reactors) of waste form, waste package, and invert, and how radionuclides move through them via diffusion and advection (see Section 3.5). Output from engineered barrier system transport is radionuclide mass flux (for each of the nine radionuclides) at each time step, passed during the RIP simulations to the directly coupled, three-dimensional, dual-permeability, FEHM particle tracker (Robinson et al. 1997) used for unsaturated zone transport. As shown in Figure 2-12, the repository area is divided into six distinct regions based on infiltration and thermal hydrology, which was modeled with six distinct source-term groups within RIP. The mass releases from these six source-term groups are spread uniformly across the grid blocks in FEHM that reside within the corresponding areas of the six regions. A key part of engineered barrier system transport is waste form or radionuclide mobilization, which is a direct function of both seepage flux and radionuclide solubility in the groundwater. Solubility is input directly into the RIP program as probability density functions (see Section 3.5).

- Unsaturated zone transport is modeled at run-time using the directly coupled, three-dimensional, dual-permeability, finite-element code FEHM (Zyvoloski et al. 1995), which is accessed as an external function by the RIP program. Flow fields and property sets are accessed directly by FEHM from table files residing in the run-time file directory. The unsaturated zone transport model is based on the unsaturated zone flow model and uses the same flow fields (generated by the TOUGH2 unsaturated zone flow code) and the same climate states. As with unsaturated zone flow, a dual-permeability model is assumed, and transport is modeled with the FEHM particle tracker in three dimensions. The FEHM particle tracker transports particles on the same dual-permeability TOUGH2 spatial grid as used in the flow model (using the same material properties, infiltration, and liquid saturation). When the climate shifts, a new TOUGH2 flow field is provided from

[8] The nine radionuclides were chosen based on six criteria (not necessarily in order of significance): high solubility, low sorption affinity, size of inventory (plus ingrowth generated by parent radionuclides), high biosphere dose conversion factor, half-life long enough to survive transport, and existence as colloidal particles. Also, based on previous Yucca Mountain TSPAs (Wilson et al. 1994; CRWMS M&O 1995; NRC 1995; Kessler and McGuire 1996), a number of radionuclides in the list of 39 were inconsequential in their dose effects. Tests of the validity of using only nine radionuclides are presented in Chapter 6 of the *Total System Performance Assessment-Viability Assessment (TSPA-VA) Analyses Technical Basis Document* (CRWMS M&O 1998i).

the run-time file directory, and the particles are assumed to be instantly traveling with the new velocities. In addition, for multirealization runs, a matrix of uncertain property values is created before simulation time by the RIP program and then accessed by FEHM during the simulations. The FEHM code steps through the uncertainty matrix row by row, where each row represents one realization of the uncertain unsaturated zone transport parameters, including K_ds for each radionuclide, matrix diffusion coefficients, dispersivity, and K_c values for the plutonium colloids.[9] Output from the FEHM code at each time step is mass flux from the fractures and matrix within each of the six water-table regions (see Figure 2-12 for a depiction of the six water table regions, which have no particular correspondence to the six repository regions). The location of these output grid points is a vertical function of the climate state, increasing in elevation for wetter climates. The fracture and matrix mass fluxes from FEHM are mixed together in a RIP mixing cell and then fed to the saturated zone convolution integral SZ_CONVOLUTE at each RIP time step (see Chapter 8 of CRWMS M&O 1998i).

- Saturated zone transport is modeled by one-dimensional, effective-continuum, flow-and-transport simulations through six streamtubes using the FEHM computer program. The streamtubes extend from the bottom of the repository at the water table to the 20-km (12-mile) distance downgradient. The locations and directions of the six streamtubes, and the lithology along their flow paths, are determined with a three-dimensional computer model for saturated zone flow, based on the FEHM code and the three-dimensional, site-scale geologic framework model (see Section 3.7.1.3). These flow and transport simulations are done outside the RIP program for each of the nine radionuclides over 100 realizations of uncertain saturated zone model parameters. These uncertain parameters include effective porosity in the tuff and alluvium; K_ds in the tuff and alluvium, colloid K_c, longitudinal dispersivity, fraction of flowpath in the alluvium, and dilution factor (which mimics transverse dispersivity). The choice of six streamtubes is based in part on lithology at the water table and in part on the dilution factors recommended by the saturated zone expert elicitation panel (CRWMS M&O 1998g).[10] The saturated zone expert elicitation panel also recommended the value for the Darcy liquid flux in the dry climate (0.6 m/year), which was used for all realizations in all streamtubes. Output from the FEHM streamtube simulations is concentration versus time at 20 km (12 miles) for a constant mass-release-rate source term. These breakthrough curves reside in files in the RIP run time directory and are accessed when needed by the SZ_CONVOLUTE external function (which convolves, or integrates, the real source term with the pregenerated unit breakthrough curves) called by the RIP program. For the case of 100 realizations, 6 streamtubes, and 9 radionuclides, there are 5,400 files of breakthrough curves.

- Biosphere transport is modeled within TSPA calculations using biosphere dose-conversion factors that convert saturated zone radionuclide concentration to individual radiation dose rate. The biosphere dose-conversion factors are developed

[9] K_d is the ratio of the mass of a given radionuclide sorbed or residing on the immobile rock phase to the mass dissolved in the aqueous phase. K_c is the ratio of the mass of a given radionuclide sorbed or residing on colloidal particles to the mass dissolved in the aqueous phase.

[10] The expert panel recommended dilution factors for transport within streamtubes that have the approximate area and liquid flux as the streamtubes chosen for the TSPA-VA model.

outside the RIP program using a computer program named GENII-S (Leigh et al. 1993). The factors are then entered as table values in the RIP front-end menus. These factors are multiplied by the concentrations in the saturated zone streamtubes to compute individual doses, which are the end product of the calculations.

- Disruptive events to be considered are seismic activity, igneous activity (indirect and direct volcanic effects), nuclear criticality, and human intrusion. Models for these events are not shown in Figure 2-13; however, at least one of these events, indirect volcanism, is modeled with the RIP program using a modified source term, specifically different solubilities (because of different mineral phases) for some of the actinides. An example of an indirect volcanic effect is the contact of a magmatic dike with waste packages in which the waste form is recrystallized into other mineral phases that then dissolve at an increased or decreased rate in comparison to the nondisturbed case. Direct volcanic effects (i.e., radionuclides carried by ash plumes from volcanic eruptions) are modeled completely outside the RIP program using the code ASHPLUME (LaPlante and Poor 1997) (see Section 4.4). The codes and methods used in modeling other disruptive events—seismic effects, criticality, and human intrusion— are discussed in Section 4.4.

2.3.3 Treatment of Uncertainty

This section describes the various types of uncertainty represented in the TSPA-VA models and how these uncertainties affect the predictions of performance. Section 2.3.3.1 lists the four major types of uncertainty, describes the differences between uncertainty and variability, and introduces the modeling tools (e.g., Monte Carlo sampling) for analyzing uncertainty. Section 2.3.3.2 describes how one type of uncertainty, conceptual model uncertainty, is handled in TSPA-VA and how this leads to a definition of the TSPA-VA base case. Section 2.3.3.3 gives more details on how uncertainty is handled in the base case and how the base case might be used to explore the "probable" behavior of the repository. A description then follows about the "expected-value" realization, which is used in Section 4 to show how the various component models interact with one another. Finally, Section 2.3.3.4 describes the various sensitivity analysis methods employed in TSPA-VA to determine the most important model parameters affecting the total system performance.

2.3.3.1 Uncertainty Versus Variability

A variable feature, event, or process is one that varies over space or time. Examples include the porosity of a hydrogeologic layer and the temperature and near-field geochemical environment in the repository drifts. If perfect information (complete knowledge) were available, such parameters would best be represented by distributions over space and time.

Uncertainty relates to lack of knowledge regarding a feature, event, or process—one whose properties or future outcome cannot be predicted beforehand. Four types of uncertainty are typically considered: value uncertainty, conceptual model uncertainty, numerical model uncertainty, and uncertainty regarding future events. The treatment of a feature, event, or process as purely variable or purely uncertain can lead to significantly different modeling results. In general, variability can serve to either dilute or concentrate contamination from a repository in either time or space. Uncertainty in the treatment of a feature, event, or process results in uncertain forecasts of future repository behavior. Uncertainty and variability are related in that spatial and temporal variability are generally very uncertain. If the variability can be appropriately quantified or measured, then a model usually can be developed to include this variability. If the variability cannot be physically quantified or measured, then it should be treated as uncertainty (lack of knowledge). However, the ability to model some types of spatial variability can be limited not only by measurement deficiencies but also by computational resources. An example of this is fracture permeability in the volcanic tuffs. Fracture lengths and apertures in the tuff units

occur randomly over a wide variety of spatial scales, from the very large such as distinct fault zones (e.g., the Ghost Dance), to the very small (e.g., cracks on the order of millimeters in length and submicron in width). It is relatively easy to measure air permeabilities (but not necessarily liquid permeabilities) in these large faults and to include these discrete features in numerical models. It is much harder to include spatial heterogeneity on the millimeter scale in the overall flow-and-transport numerical models because of the difficulties of in situ measurement, the inability to comprehensively characterize small-scale permeability over the entire mountain, and a lack of computers large enough to model flow and transport on such a fine scale over the entire mountain. In addition to these considerations, the appropriate quantification of the spatial variability in the models is very much a function of what performance measure is desired at the output side of the model. If a well pumps water over a 100-m (330-ft) screened interval, the appropriate discretization of the spatial variability may be on the order of 10 m (33 ft) per numerical grid block. If it is desired to measure dripping into the drifts, the appropriate discretization of the grid cells may be on the centimeter scale.

Two basic tools used in the TSPA to deal with uncertainty and variability are probability theory and alternative conceptual models. The former is used for uncertainty in specific model parameters and the latter for uncertainty in the understanding of a key physical-chemical process controlling system behavior. In particular, uncertain processes often require different conceptual models. For example, different concepts of matrix-fracture coupling in the unsaturated zone lead to different flow and transport models. Sometimes conceptual models are not mutually exclusive (e.g., both matrix and fracture flow might occur), and sometimes they do not exhaustively cover all possibilities (matrix and fracture flow apparently do, although the definition of "matrix" depends on the length scale used in the model). These problems indicate that the use of alternative conceptual models, while often necessary to characterize some types of uncertainty, is not always as rigorous as one might like—an unfortunate result of insufficient knowledge in some areas.

For the treatment of uncertainty in specific model parameters and for alternative conceptual models that have been weighted beforehand with specific probabilities, the Monte Carlo sampling method has been used in all TSPAs to date and is the primary method of uncertainty analysis used for this TSPA. The method involves random sampling of the probability distributions for all uncertain input parameters (including any index parameters that might be used to weight alternative conceptual models). Then, numerous realizations of the repository system are calculated based on the sampled realizations of all the inputs. Each total system realization has an associated probability so that there is some perspective on the likelihood of that set of circumstances occurring.[11] The Monte Carlo method yields a range for any chosen performance measure (e.g., peak dose rate to an individual within a given time period at a given location) along with a probability for each value in the range. In other words, it gives an estimate of repository performance plus "error bars" on the estimate. The performance measures and associated probabilities have traditionally been presented as CCDFs that show the probability of exceeding a given performance measure value.

2.3.3.2 Weighting of Alternative Conceptual Models

In many subsystems of the overall TSPA system, there are plausible alternative models or assumptions. In some cases, these alternatives form a continuum, and sampling from the continuum of

[11] In the standard Monte Carlo method, each realization is equally likely, so the probability is 1 divided by the number of realizations. In more elaborate variants, for example using "importance sampling," some realizations can be less probable than others. The TSPA-VA uses a variant of the Monte Carlo method, called Latin Hypercube Sampling, which better models the tails of the input probability distributions when the number of realizations is small.

assumptions fits naturally within the Monte Carlo framework of sampling from probability distributions. In other cases, the assumptions or models are discrete choices. In particular, some processes are so highly uncertain that there is not enough data to justify developing continuous probability distributions over the postulated ranges of behavior. In other words, a high degree of sampling is unwarranted, and it is better just to look at two or three cases that are assumed to encompass (bound) the likely behavior.

There are two possible approaches to incorporating discrete alternative models within the TSPA: weighting all models into one comprehensive Monte Carlo simulation (lumping), or keeping the discrete models separate and performing multiple Monte Carlo simulations for each discrete model (splitting). There are advantages and disadvantages to both approaches. Lumping has the conceptual advantage that a single CCDF can be said to include all the system uncertainty. Splitting can lead to a profusion of cases that makes it difficult to quantify the relative importance of the various discrete assumptions. The main disadvantage of lumping is the concern that individual cases with poor performance might be diluted within a multitude of more favorable cases. In other words, there could be a combination of the discrete assumptions with poor performance that might not be obvious under the lumped approach but that would stand out if that combination were presented separately. Another potential disadvantage of lumping occurs if there is no good justification for the probabilities used—if the weighting of the alternatives is artificial, then the results will be artificial as well.

For this TSPA, a combination of the two approaches is used. In particular, the TSPA-VA "base case" model, defined in detail in Sections 4 and 4.1, can be considered an implementation of the splitting approach, because it is based on a limited range of uncertainty. Based on expert judgment (and to some extent on finite time and resources that can be applied to the VA effort), the TSPA-VA base case is a best estimate as to the more likely ranges of model behavior and parameter ranges. Some alternative models are not included in the base case and some parameter ranges of the included models have been narrowed. The level of uncertainty included in the TSPA-VA base case model is based on the current level of knowledge regarding the various processes controlling system behavior. In several instances, the range of uncertainty is set quite large, in a "conservative" manner. Because of this narrowed range of models and parameters, the base case CCDF is conditional (shown in Section 4.3), meaning that it is conditional on certain models and parameters being held constant or having their variance restricted. As described at the beginning of Section 2.3, the primary type of CCDF used to portray repository performance is a CCDF of the peak dose rate occurring within a given time span at a given location, such as the peak dose rate at 20 km (12 miles) that occurs at any time during the first 10,000 years.

Some of the most important processes and parameters (i.e., having the greatest effect on performance or dose rate) not included in the base case also warrant a separate presentation of their uncertainty in the form of several conditional CCDFs based on alternative process models. Alternative models of water seepage into the drift and of fracture-matrix flow in the unsaturated zone are treated in this manner (see Section 5.1). Also, for design options, such as drip shields and ceramic coatings on the waste packages, there is no reasonable conceptual justification for lumping them together into a single probability distribution. Therefore, they must be presented as conditional CCDFs—conditional on the given repository and/or waste package design.

2.3.3.3 Uncertainty and the Base Case

Because of the significant amount of uncertainty in most of the component models, the variance associated with most models and parameters can only reasonably be restricted, but not wholly eliminated. Thus, the base case necessarily encompasses much of the underlying uncertainty. It includes some of all four types of uncertainty: value or parameter uncertainty, conceptual model uncertainty, numerical model uncertainty, and future-event uncertainty. Therefore, the base case

by itself also represents the "lumping" approach. Uncertainty not lumped into the TSPA-VA base case is captured discretely in alternative models, alternative features, and alternative events. These alternatives that have been "split" off of the base case, and their effects on performance are described separately as either alternative conditional CCDFs or, as alternative single-realization time histories of performance. Examples of this for the TSPA-VA, with respect to each of the four types of uncertainty, include the following:

- Parameter uncertainty: widened parameter ranges for the cladding degradation models (Section 5.5)
- Conceptual model uncertainty: alternative process models for unsaturated zone flow and seepage (Section 5.1)
- Numerical model uncertainty: one-dimensional flow and transport used in the saturated zone because of uncertainty regarding numerical dispersion in three-dimensional models (Section 3.7)
- Future-event uncertainty: disruptive events, such as volcanism (Section 4.4)

A total "lumped" CCDF, including all of the uncertainty in TSPA-VA, is not presented because of difficulties (i.e., uncertainty) in assigning probabilities to some of the alternatives.

A final type of uncertainty, already mentioned, but not included in the above four and not a candidate for lumping, is "design" uncertainty. This uncertainty is driven by the uncertainty in the natural-system parameters and processes. It represents the desire to design the safest repository possible within certain cost restrictions. However, the "best" design at any given time (for example, the VA design) may not represent the best design in the future (for example, the LA design) because new knowledge may be acquired based on additional site characterization and additional TSPA analyses. Either of these factors can lead to a new repository and/or waste package design. This type of uncertainty for the VA is examined in the form of various "design options" (Section 4.5).

The 1997 Energy and Water Appropriations Act asks for the "probable behavior of the repository in the Yucca Mountain geological setting." However, it does not define the word "probable" in this context. Any of the random outcomes in the base case CCDF, or for that matter, any of the random outcomes in the alternative CCDFs could be considered "probable", since they all have a finite probability. A more explicit interpretation of the word "probable" might be either "representative" or "most probable". Regarding the latter, the most probable behavior is clearly the "mode" of a CCDF.[12] Since we do not present the total "lumped" CCDF that includes all alternatives, the most probable behavior could be taken as the mode of the base case CCDF. However, other points on the output CCDF are more often chosen as being "representative" of the likely or probable behavior of a stochastic system, including the expected-value (i.e., the mean or average of all peak dose rates) and the median (i.e., the 50th percentile value, above which lie half of the peak dose rates and below which lie the other half). Both the mean and the median of the base case peak-dose-rate CCDF, along with the entire CCDF, are presented in this document to demonstrate probable future repository behavior (see Section 4.3). In addition, other types of analyses are presented, as discussed below.

The CCDFs of peak dose rate are the most important measure of repository performance since they represent the peak, or highest, dose rate within a given time frame. However, to illustrate how the various component and subsystem models interact with one another, it is also useful to display one or more realizations of dose rate versus time over specific time periods. Perhaps the most useful realization of the input parameters for this purpose

[12] In the theory of probability, the "mode" of a distribution is the point with the highest probability or highest likelihood of occurrence.

is the expected values (means) of all the input parameters. This single realization is useful because it is time independent; that is, the same values of the input parameters can be used regardless of the time span of interest, whether it be 10,000 years, 100,000 years, or 1 million years. This single realization is called the "expected-value realization" in the rest of this document. (It is not the realization of the input parameters that produces the expected value or mean peak dose rate on any of the peak dose-rate CCDFs because those realizations differ according to the period being examined.)

The expected-value realization for the TSPA-VA base case is examined in Section 4.2 with respect to how it shows the influence of the various base-case component models on each other and on total system performance. The expected-value realizations for alternative models and designs are shown in Section 5 and compared to the expected-value base-case realization. This is one useful way to look at the sensitivity of total-system and subsystem performance to various models and parameters (see Section 2.3.3.4).

In addition to examining the behavior of the expected-value realization, it is also useful to examine the behavior of realizations that lie close to both tails (i.e., both the upper and lower extreme) of the various input parameters. This is usually done one input parameter at a time; that is, all parameters except one are sampled at their expected values. The parameter of interest is then sampled at either its 5th percentile probability or its 95th percentile probability.[13] This is useful because the behavior of the various component models and their influence on one another can be quite different at these values than for the expected-value realization. It is also useful to display these more extreme time histories on the same graph as the expected-value time history because together they give a good indication of the complete range of influence of each of the input parameters on total repository performance during the specified time period, whether it be over the first 10,000 years, 100,000 years, or 1 million years after closure. This type of analysis is presented in Section 5 for the most influential parameters of the various base-case component models.

2.3.3.4 Presentation and Analysis Techniques for Uncertainty

One goal of the TSPA-VA is to evaluate the performance and associated uncertainty for the reference repository design (see Volume 2) and various design options (see Section 4.5). Another important goal is to determine the characteristics of the engineered and natural systems that have the most influence on repository performance. This information provides input to the design and site-characterization organizations about additional data that could provide the greatest improvement in confidence about the repository. Beyond these formal goals, there is the simple need to understand the results and make them clear to all interested parties. A number of methods are used to explain the results and quantify the sensitivities.

Total system performance is a function of sensitivity (i.e., if a parameter is varied, how much do the performance measures change?) and uncertainty (i.e., how much variation of a parameter is reasonable?). For example, the TSPA results could be very sensitive to a certain parameter, but the value for the parameter is exactly known. In the uncertainty analysis techniques described below, that parameter would not be regarded as important. Many parameters in the TSPA-VA analyses do, however, have uncertainty associated with them and do end up with a high ranking for their importance to performance. On the other hand, the level of their ranking can depend on the width of the assigned uncertainty range. Therefore, uncertainty analyses must be carefully interpreted (i.e., the width of the uncertainty ranges must be considered). Most of the important parameters with possibly limited uncertainty ranges in the base case are examined in alternative models that either expand the range of their parameters beyond the expected range of uncertainty or change the

[13] Other samplings are possible, such as the 1st and 99th percentiles. We have chosen 5th and 95th as being representative of "extreme" behavior.

weighting of the parameter distribution. For example, this type of analysis is performed for alternative models of seepage (Section 5.1) and cladding degradation (Section 5.5).[14]

System performance also may be sensitive to repository design options, but models and parameters for these various options are not assigned any uncertainty. Therefore, even though they can be important (see Section 4.5), they do not show up in the tables of key parameters based on uncertainty analysis.

The determination of the parameters or components that are most important depends on the particular performance measure being used. This point was demonstrated in the 1993 TSPA (Andrews et al. 1994; Wilson et al. 1994) and the 1995 TSPA (CRWMS M&O 1995). For example, these two TSPAs showed that the important parameters are different for 10,000-year peak doses than for 1-million-year peak doses.

Some methods for investigating sensitivity are discussed below:

- **Scatter plots**—Scatter plots are a good qualitative method of looking for sensitivities based on multi-realization simulations of the system. The final results (e.g., dose rate) are plotted against the input parameters and visually inspected for trends. If there is a visible trend, it is an indication of sensitivity. The performance measures can also be plotted against various subsystem outputs or surrogate performance measures (e.g., waste package lifetime) to determine whether that subsystem or performance surrogate is important to performance.

- **Regression analysis**–In regression analysis, a mathematical relationship between the outputs (performance measures) and inputs (model parameters) of a Monte Carlo simulation is developed. Typically, a method called stepwise linear regression is used in which only a subset of the input parameters is used for the regression, with parameters added one at a time based on calculated correlation coefficients. Parameters that have little influence on the performance measure are those that, when added, only marginally change the variance of the output. This method produces a ranking of input parameters according to their impact on the performance and a quantitative measure of the impact (basically, the correlation coefficient for the performance measure versus the input parameter). A more detailed description of regression analysis is presented in Section 4.3 and in the *Total System Performance Assessment-Viability Assessment (TSPA-VA) Analyses Technical Basis Document* (CRWMS M&O 1998i).

- **Differential analysis**—Another quantitative method for ranking important parameters is differential analysis, in which the partial derivatives of the performance measure with respect to the input parameters are calculated to find the amount that performance is affected when one parameter is varied while the others are held constant. A significant drawback of this method is that it is local, that is, the derivatives are calculated about a point in the parameter space and only represent the sensitivity at that point. In contrast, regression analysis of Monte Carlo results is more global; that is, the sensitivities are determined and ranked taking into account the whole parameter space.

[14] The parameter uncertainty ranges established for the base case are usually based on site characterization data and expert judgment. Often times these ranges are expanded beyond the existing data in order to "bound" possible behavior. In such a case, if the performance is not sensitive to the given parameter, then there is generally no point in future sensitivity analyses for this parameter. On the other hand, if the performance is found to be sensitive to the parameter within the base case range, it is often useful to expand the range to quantify the effect of uncertainty beyond the "expected" base case range.

- **Alternative models or parameter sets**—A useful but less systematic method of sensitivity analysis is to look at discrete cases, for example, some discrete sets of input parameters (as opposed to a systematic sampling) or some discrete choices of alternative models for a given process or subsystem. This method provides qualitative information about the sensitivity to the changes in assumptions (i.e., do the results change a little or a lot?) but not the same type of quantitative ranking produced by the previous two methods. This method is used frequently in Section 5.

2.4 DESCRIPTION OF BASE CASE RESULTS

The following paragraphs provide a brief summary of the expected TSPA-VA base case results for the current understanding of the natural system described in Volume 1 and the reference design described in Volume 2. These results are discussed in a series of time slices that synthesize the system response to the proposed design concept. Although there is uncertainty in the probable sequence of events occurring after repository closure, this is a general description that captures the essence of system behavior as modeled in the TSPA. The responses described for each of the periods indicated below are generally applicable. However, various areas of the repository will experience somewhat different conditions over different periods. More detailed descriptions of the expected behavior and the assumptions underlying the results are presented in Sections 3, 4, and 5.

2.4.1 Time of Waste Emplacement to Time of Repository Closure

In the TSPA-VA base case calculations, conditions around each waste package will be controlled by the large heat output from decay of the short-lived radionuclides. The temperature on the waste package surfaces will be high, around 200°C (392°F) for the hottest waste package. The relative humidity in the drifts is expected to be low, less than 50 percent. The water in the rock will start to be driven away from the drifts because the temperature next to the drift wall is above boiling. Under these conditions, minimal dry oxidation of the carbon steel outer layer of the waste package is expected. However, the waste packages will remain intact, allowing no release of radionuclides.

2.4.2 Time of Repository Closure to Several Hundred Years After Closure

Following repository closure, after an initial period of increasing temperatures, the temperatures around each waste package will begin to decline, although the waste package surface temperature still will be generally above boiling. As the temperature decreases, the relative humidity will increase. The carbon steel outer container material will start to corrode under these humid air conditions. Because the waste package and drift temperatures will be above boiling, the air will be humid and drips will not be present.

The lining around the drifts will start to collapse and its absence will be reflected in the change in chemistry of incoming water and gas, since they will no longer pass through any concrete before dripping into the drift. Water will be being driven away from the drifts, and the liquid saturation in the rock matrix will be reduced from about 90 percent (under ambient preconstruction conditions) to less than 20 percent. The rock out to 10 m (3.3 ft) from the repository will be heated above the boiling temperature of water. Only minimal degradation of the carbon steel material of the outer waste package will occur. For this reason, the waste packages are expected to be intact, and there will be no release of radionuclides.

2.4.3 Several Hundred Years to Several Thousand Years After Closure

As discussed in Volume 1, Section 2.2.6.1, after a few thousand years the ground support of the repository drifts would be expected to have failed and most of the repository drifts would be expected to have sufficient rockfalls that a portion of the waste package would be covered by debris. The crushed rock around the waste package would insulate the waste package. Given that the thermal output from the individual waste packages is

significantly reduced by this time period, the effects of this on the thermal and hydraulic environment near the waste package is expected to be small. The possible effects of these rockfalls on the waste package degradation are also expected to be minimal because at this time the bulk of the carbon steel on the outer barrier of the waste package is still intact.

During the period of several hundreds to several thousands of years after closure, the temperature on the waste package surfaces will drop below boiling, causing the relative humidity in the drift to rise to almost 100 percent. Also, the rock temperature around the repository generally will drop below boiling at about 1000 years. Under these conditions, aqueous (in the presence of drips) corrosion of the layer of carbon steel that forms the outer barrier of the waste package can begin. So dripping water is likely to begin falling on some of the waste packages; but whether and exactly where these dripping conditions occur is uncertain.

The degree of degradation of the outer carbon steel layer of the waste package is expected to be variable from place to place in the repository and on the surface of each waste package. As a result, some carbon steel on some waste packages may corrode sufficiently to expose the underlying, corrosion-resistant, nickel-base alloy (Alloy 22) layer to aqueous or humid air conditions. However, the corrosion resistance of the Alloy 22 metal precludes significant degradation of this metal under the likely hydrologic and geochemical conditions at the interface of the two metal barriers.

With the possible exception of some unexpected early failures of a few waste packages, possibly caused by very large rockfalls or undetected poor welds of Alloy 22 metal combined with unexpected rapid degradation of the carbon steel, there will be no release of radionuclides during this period. For prematurely failed waste packages, if water contacts the waste, the waste can be altered and radionuclides released from the waste package to the invert and the unsaturated tuffs around the drift wall. Because only a few waste packages are even considered to fail prematurely, these releases will be small.

2.4.4 Several Thousand Years to Ten Thousand Years After Closure

Temperatures in the drift and the surrounding rock will continue to decline, liquid saturation in the rock matrix will continue to increase, and the dripping conditions will continue to be reestablished over a broader area. The environment around the repository will return to its original temperature by 3000–4000 years. However, other properties of the rock mass around the drifts may be altered from the pre-waste emplacement conditions. The variability in the ambient rock property conditions and the uncertainty in the changes induced in response to coupled thermal, hydrologic, mechanical, and chemical processes induced by the presence of the repository are difficult to define quantitatively. Therefore, as a first approximation, the TSPA simply represents the variability that could be induced by these coupled processes by using the values for rock properties based on the natural variability in properties currently present at Yucca Mountain.

There will be sufficient corrosion of the carbon steel outer barrier on virtually all of the waste packages to expose the underlying layer of corrosion-resistant Alloy 22 metal. The degradation of Alloy 22 depends on the presence of water and is a function of the geochemical conditions on the metal's surface. These conditions and the degradation rates are variable, so there may be sufficient degradation to allow small openings through some of the waste packages.

If some waste packages have openings through them, water may contact the exposed waste form surface. The majority of the commercial spent nuclear fuel waste forms is protected by a highly corrosion-resistant Zircaloy cladding. Although some types of cladding may be degraded prematurely (e.g., stainless-steel cladding), the Zircaloy cladding is expected to remain intact for tens of thousands of years. Therefore, only a small fraction of the waste form surface will be exposed and in contact with water. Any water that enters

the waste package will be expected to take a circuitous route as it flows through individual fuel rods within the waste package; however, this flow path is difficult to define. The conservative assumption used in the TSPA-VA allows the water to contact the entire exposed waste form surface.

Once water contacts the waste form surface, the spent nuclear fuel or glass will degrade, releasing some radionuclides to the aqueous phase. The degradation of the waste forms will go through many different geochemical alteration phases, some of which will tend to retain partially soluble radionuclides while others may form colloidal particles. In addition, the actual mobile concentration of radionuclides will depend on the solubility of the radionuclides in water.

More than 99 percent of the radionuclides released into solution by degradation of the waste form will be immobile within the geologic setting. Most are insoluble in the Yucca Mountain waters and will remain near the waste form. Others have an affinity for the metal components of the waste package or other engineered barrier materials or sorb strongly to the minerals in the rock. Only a small fraction of these radionuclides is mobile enough to move in the system.

This small fraction of radionuclides may be transported by water moving out of the repository, down through the unsaturated rock, and then in the groundwater flow below the water table. Some of these radionuclides will move more slowly than others because they sorb to the minerals in the unsaturated and saturated zone rocks to some degree. The radionuclides of concern during this period are highly mobile radionuclides, technetium-99 and iodine-129. These radionuclides may then be transported 20 km (12 miles) to a hypothetical well used as a representative location for the assessment of consequences or dose rates. The water flow velocities through the unsaturated and saturated zones at Yucca Mountain control the time it takes for these radionuclides to reach the hypothetical well 20 km (12 miles) downgradient. These transport times depend on rainfall in the region and the recharge to the flow system and, therefore, depend on the climate. When the change between the present-day dry climate and the assumed, long-term average climate occurs, the transport times are significantly reduced.

The likely dose rate at the hypothetical well during this period, considering all of the above processes, is 0.1 mrem/year (Figure 4-26). This value is about 0.03 percent of the average value for background radiation from nonmedical sources in the United States (about 300 mrem/year [NCRP 1987, p. 149]).

2.4.5 Ten Thousand Years to Several Tens of Thousands of Years After Closure

During this period, the natural environment near the drifts generally will have returned to ambient conditions, except that some permanent changes in rock properties around the drifts may have occurred and the climate and corresponding surface infiltration are anticipated to be different than current conditions. Degradation of the corrosion-resistant Alloy 22 barrier will continue to occur, predominantly in the areas of the repository that experience dripping conditions. Degradation of the Zircaloy cladding will also continue.

Radionuclide releases from the engineered barrier system will continue. The release rate of highly soluble species is controlled by the waste package failure rate. The release rate of less soluble species (such as neptunium-237) will be controlled by the cumulative fraction of waste packages that will have failed and the fraction of the waste package surface that will have been degraded. Over this period, the soluble radionuclides will still control the dose rate of several millirems per year at 20 km (12 miles) from the repository.

2.4.6 Several Tens of Thousands of Years to One Hundred Thousand Years After Closure

The degradation of the corrosion-resistant Alloy 22 barrier will continue, as will degradation of the Zircaloy cladding. As more inventory becomes available for transport with increased waste package failure and more water enters each waste

package that has failed, the solubility-limited radionuclides, in particular neptunium-237, will begin to control the dose rate. The anticipated dose rate is about 30 millirems/year (Figure 4-26).

2.4.7 Several Hundred Thousand Years After Closure

As time continues, more waste packages will fail, more cladding will be degraded, and more water will enter the failed waste packages and, it is assumed, will contact the exposed waste. As a result, the expected value for the dose rate at a well located 20 km (12 miles) downgradient will continue to increase to more than 100 mrem/year. A major glacial cycle is likely to occur, causing superpluvial conditions in the semiarid region around Yucca Mountain. A wetter climate would increase still further the fraction of waste packages being dripped on and the amount of water that drips into the drifts and into the waste packages. At the time this climate change occurs, the dose rate would be expected to increase still further to several hundred millirems per year.

This synopsis of results should not be read in isolation but must consider the technical bases presented in Sections 3 and 4—and in more detail in the *Total System Performance Assessment-Viability Assessment (TSPA-VA) Analyses Technical Basis Document* (CRWMS M&O 1998i)—and the uncertainty in these results described in Sections 4.3 and 5.

3. DEVELOPMENT OF TOTAL SYSTEM PERFORMANCE ASSESSMENT COMPONENTS FOR THE VIABILITY ASSESSMENT

Because of the difficulty in handling the complexity of the repository system in an analysis, the Yucca Mountain total system was divided into individual parts to make each set of TSPA-VA analyses manageable. Each individual part represents a major process area. The component models that define the process areas are discussed in this section. However, because of the need for brevity, the component models are not described in great detail. The details of each component model are thoroughly documented in the *Total System Performance Assessment-Viability Assessment (TSPA-VA) Analyses Technical Basis Document* (CRWMS M&O 1998i). The process models are listed in Table 3-1, along with their corresponding section numbers in this volume and chapter numbers in the *Total System Performance Assessment-Viability Assessment (TSPA-VA) Analyses Technical Basis Document* (CRWMS M&O 1998i). By necessity, the detailed documentation for the component models is many pages longer than the sections in this volume; each chapter of the *Total System Performance Assessment-Viability Assessment (TSPA-VA) Analyses Technical Basis Document* (CRWMS M&O 1998i) is published as a separate volume. In addition to the process areas discussed in this section, the effects of disruptive events (volcanism, seismicity, human intrusion, and nuclear criticality) on repository performance are discussed in Section 4.

It must be noted that the various TSPA component models are represented using different computer codes. The variations in the codes, in terms of their architecture, requires that the form of the input and output parameters is different from code to code. For this reason, in some cases, the models require somewhat different forms for what would appear to be the same input and output parameters. The specific parameters used in the TSPA-VA are given in the *Total System Performance Assessment-Viability Assessment (TSPA-VA) Analyses Technical Basis Document* (CRWMS M&O 1998i).

Although all of the processes will be strongly interrelated in the actual repository system, the assumption was made that the components could be treated separately if a consistent set of boundary conditions and scenarios was rigorously maintained among all the related components. This section addresses the conceptualization of eight component models and the implementation of these components into the performance assessment analyses. It also provides the results and interpretations of the analyses associated with the component. Section 4 describes how these components were recombined into the total-system model, and Section 5 discusses the sensitivity of the total-system results to various aspects of these components.

The four attributes of the Yucca Mountain repository safety strategy and the NRC key technical issues were discussed in Section 2.2.1. The relationships among the four attributes, the NRC key technical issues, and the TSPA model components are shown in Tables 2-1 and 2-2.

Table 3-1. Component Models for Process Areas and Corresponding Documentation

Process Area	TSPA-VA Section	Technical Basis Document Chapter
Unsaturated zone flow	3.1	2 (B00000000-01717-4301-00002)
Thermal hydrology	3.2	3 (B00000000-01717-4301-00003)
Near-field geochemical environment	3.3	4 (B00000000-01717-4301-00004)
Waste package degradation	3.4	5 (B00000000-01717-4301-00005)
Waste form degradation and radionuclide mobilization	3.5	6 (B00000000-01717-4301-00006)
Unsaturated zone transport	3.6	7 (B00000000-01717-4301-00007)
Saturated zone flow and transport	3.7	8 (B00000000-01717-4301-00008)
Biosphere	3.8	9 (B00000000-01717-4301-00009)

To assure that the TSPA is based on the most current scientific knowledge, eight workshops were held in 1997 to bring together YMP scientists, engineers, and performance assessment analysts. The aim of these workshops was to help define and prioritize the important technical issues to be addressed in the TSPA-VA. The general format of the workshops is described in Section 2.2.1. The workshops are summarized in the discussion of the construction of the conceptual models in Sections 3.1– 3.8.

In addition to the workshops, DOE sponsored five expert elicitations on key process models for the TSPA. The goal of these elicitations was to solicit the panel members' judgment in quantifying the uncertainty associated with the process models. These elicitations are listed in Table 3-2. Information on the results of the expert elicitations and their subsequent use in the TSPA model components is summarized, where relevant, in the discussion of the construction of the conceptual model in Sections 3.1–3.8.

Table 3-2. Expert Elicitations for the Total System Performance Assessment for the Viability Assessment

Process Model	Elicitation	Documentation
Unsaturated zone flow (Section 3.1)	Unsaturated Zone Flow	CRWMS M&O 1997n
Thermal hydrology (Section 3.2)	Near-Field Environment	CRWMS M&O 1998d
Waste package degradation (Section 3.4)	Waste Package Degradation	CRWMS M&O 1998b
Waste-Form Degradation and Radionuclide Mobilization (Section 3.5)	Waste-Form Degradation and Radionuclide Mobilization	CRWMS M&O 1998k
Saturated Zone Flow and Transport (Section 3.7)	Saturated Zone Flow and Transport	CRWMS M&O 1998g

3.1 UNSATURATED ZONE FLOW

Unsaturated zone flow at Yucca Mountain will play an important role in repository performance. Water seeping into drifts and dripping onto waste packages can accelerate waste package degradation and radionuclide mobilization. In addition, water moving through fast pathways from the repository to the water table via fractures can decrease the transport time of radionuclides to the accessible environment.

Four distinct components of unsaturated flow are considered in the TSPA for the VA: climate, infiltration, mountain-scale flow of water, and seepage into repository emplacement drifts. These components include processes at several scales. At the global scale is climate, including changes in solar heating caused by changes in the earth's orbit and inclination, and formation of huge ice sheets during glacial periods. There are also important regional-scale (hundreds of kilometers) climate effects, such as the "rain shadow" caused by the Sierra Nevada mountain range and the proximity of the polar jet stream, that make climate variations at Yucca Mountain different from the global average. Infiltration and flow through the mountain, or mountain-scale flow, are modeled at the scale of the site. The YMP infiltration model covers an area approximately 10 km × 20 km (6.2 miles × 12.4 miles), while the site-scale flow model for the unsaturated zone encompasses a volume approximately 5 km × 9 km × 800 m (3.1 miles × 5.6 miles × 2,600 ft). The site-scale models include effects of surface topography and subsurface hydrogeologic layering. The drift scale is the scale of an emplacement drift, approximately 5 m (17 ft) in diameter. At the drift scale, a seepage model evaluates the interaction of percolating water with an emplacement drift and the amount of water that seeps into the drift. Variations in permeability on scales of a few meters up to about 10 m (several feet up to about 30 ft) are important in modeling seepage. Processes at the scale of individual fractures, in particular those affecting fracture-matrix coupling, or water flow between fractures and the porous rock matrix, are important both to seepage and mountain-scale flow. Fracture-scale processes are not modeled explicitly, but are represented by parameters in the continuum flow models. Some of the important processes for unsaturated zone flow are pictured in Figure 3-1. Yucca Mountain climate is illustrated in Figure 3-2.

The unsaturated zone hydrologic modeling studies and analyses presented in this section were prepared with the view of addressing selected aspects of the NRC Key Technical Issue on

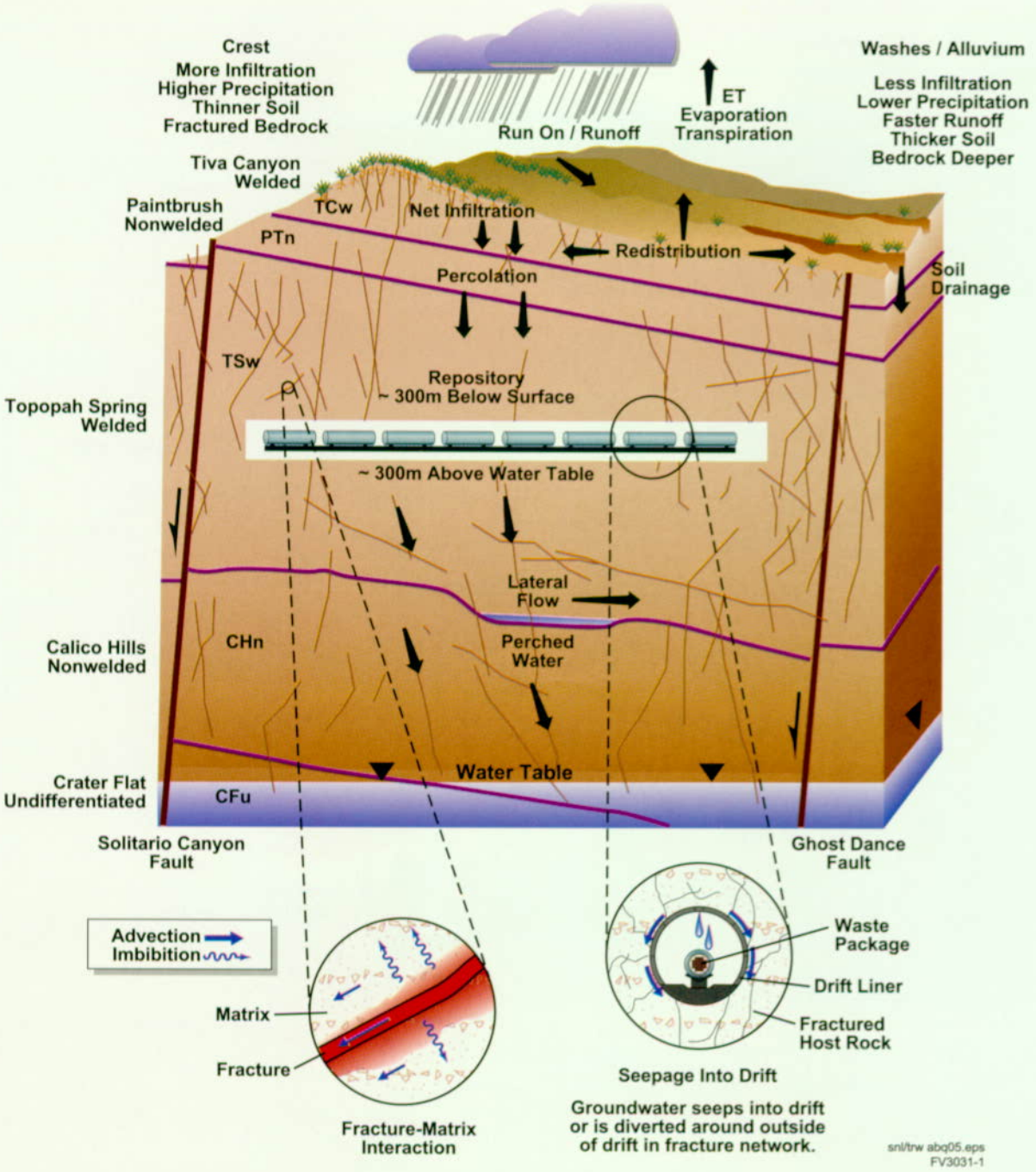

Figure 3-1. Conceptual Drawing of Unsaturated Zone Flow Processes at Different Scales
Mountain-scale and drift-scale models capture these processes except for fracture-scale processes, which are captured as parameters in continuum flow models.

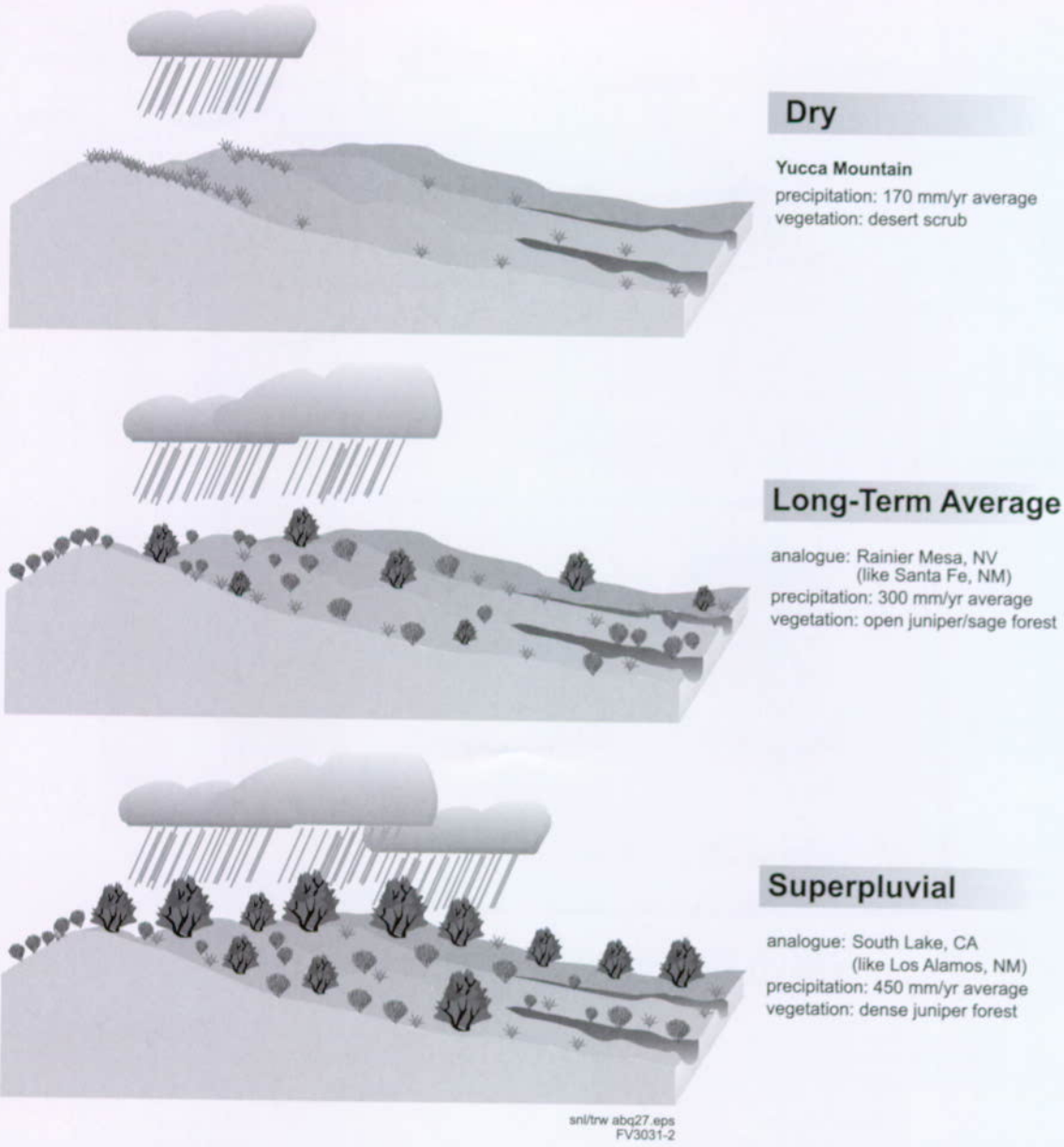

Figure 3-2. Conceptual Drawing of Projected Climates for Yucca Mountain
Climate change was modeled as three discrete climate states.

Unsaturated and Saturated Flow under Isothermal Conditions (NRC 1997e; 1997f). Specifically, the information presented is pertinent to four of the eight subissues of this key technical issue, consisting of: range of future climates, hydrologic effects of climate change, amount and distribution of present-day infiltration, and amount and distribution of groundwater percolating through the repository horizon.

Unsaturated zone flow is closely related to other model components, including thermal hydrology, the engineered barrier system, unsaturated zone transport, and flow and transport in the saturated zone. The relationships among the four subcomponents of unsaturated zone flow, and relationships with the other TSPA components, are shown in Figures 3-3–3-6.

Sections 3.1.1 and 3.1.2 summarize development of the climate, infiltration, mountain-scale flow, and seepage models, including the important processes, assumptions, and model implementation. Section 3.1.3 presents results based on the flow models for the unsaturated zone and interpretations relevant to repository performance. Additional information on unsaturated zone flow can be found in Chapter 2 of the *Total System Performance Assessment-Viability Assessment (TSPA-VA) Analyses Technical Basis Document* (CRWMS M&O 1998i).

3.1.1 Construction of the Conceptual Model

Previous TSPAs have determined that unsaturated zone flow is an important contributor to repository performance (Wilson et al. 1994, Sections 14.6.3, 15.5.4; CRWMS M&O 1995, Sections 9.2.5, 9.3.7). Calculated peak doses are sensitive to the current percolation rate at the repository horizon, the amount of increase in the percolation rate under future wetter climate conditions, the partitioning of flow between matrix and fractures, and the amount of seepage into emplacement drifts.

An unsaturated zone flow workshop was held in December 1996 to supplement the previous TSPA determinations about unsaturated zone flow. A

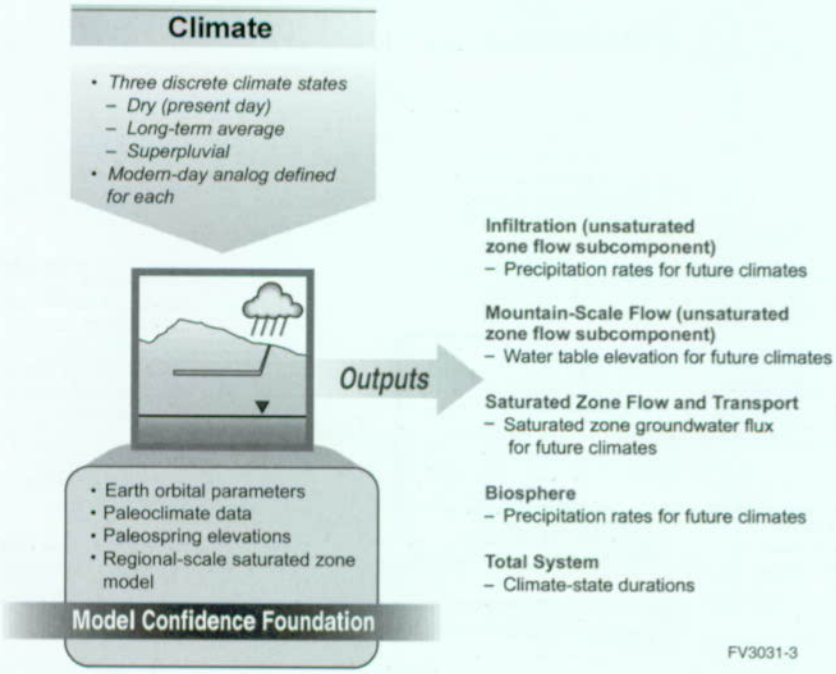

Figure 3-3. Coupling of the Climate Subcomponent to Other Unsaturated Zone Flow Subcomponents and to Other Total System Performance Assessment for the Viability Assessment Components
The three discrete climates are illustrated in Figure 3-2.

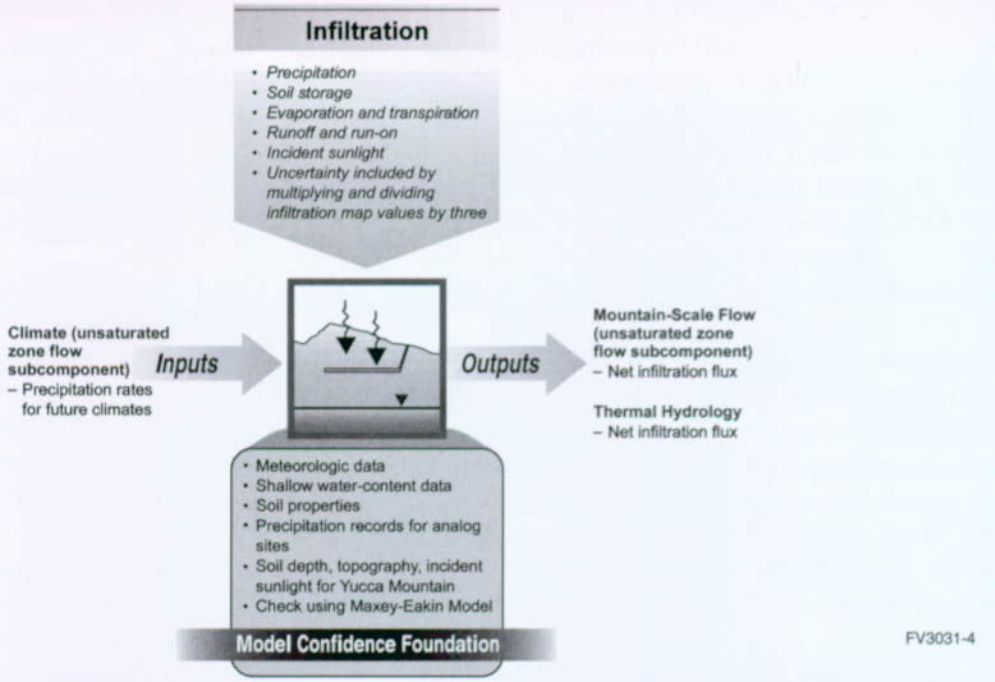

Figure 3-4. Coupling of the Infiltration Subcomponent to Other Unsaturated Zone-Flow Subcomponents and to Other Total System Performance Assessment for the Viability Assessment Components
Infiltration variability over the site is captured in the model, which covers 228 square kilometers (88 square miles) around Yucca Mountain.

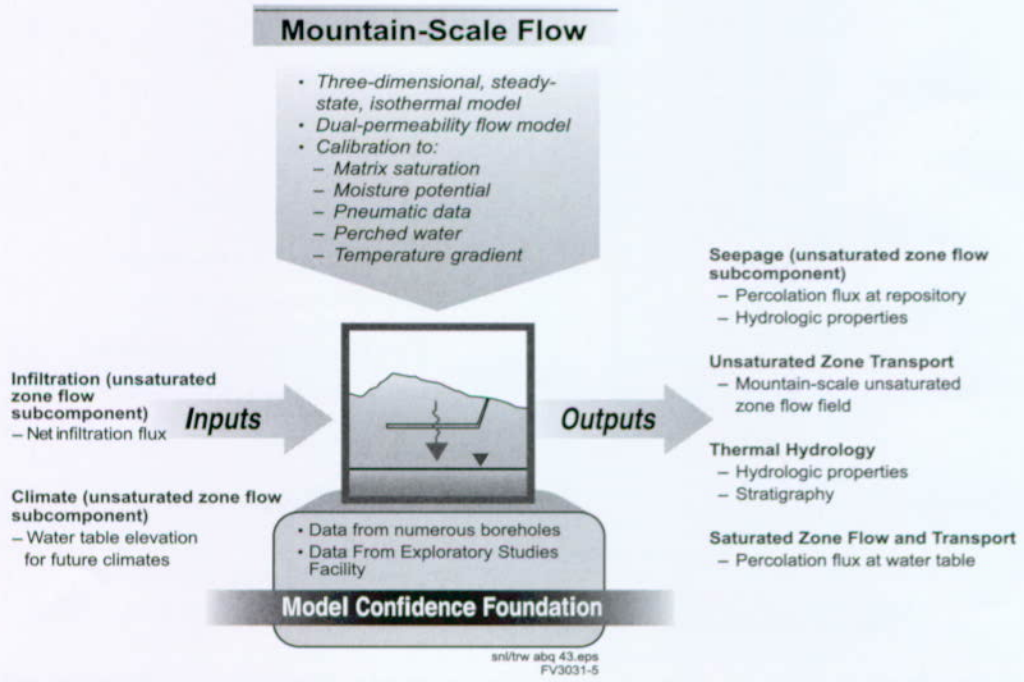

Figure 3-5. Coupling of the Mountain-Scale Flow Subcomponent to Other Unsaturated Zone Flow Subcomponents and to Other Total System Performance Assessment for the Viability Assessment Components
The three-dimensional mountain-scale flow model was used directly and not abstracted.

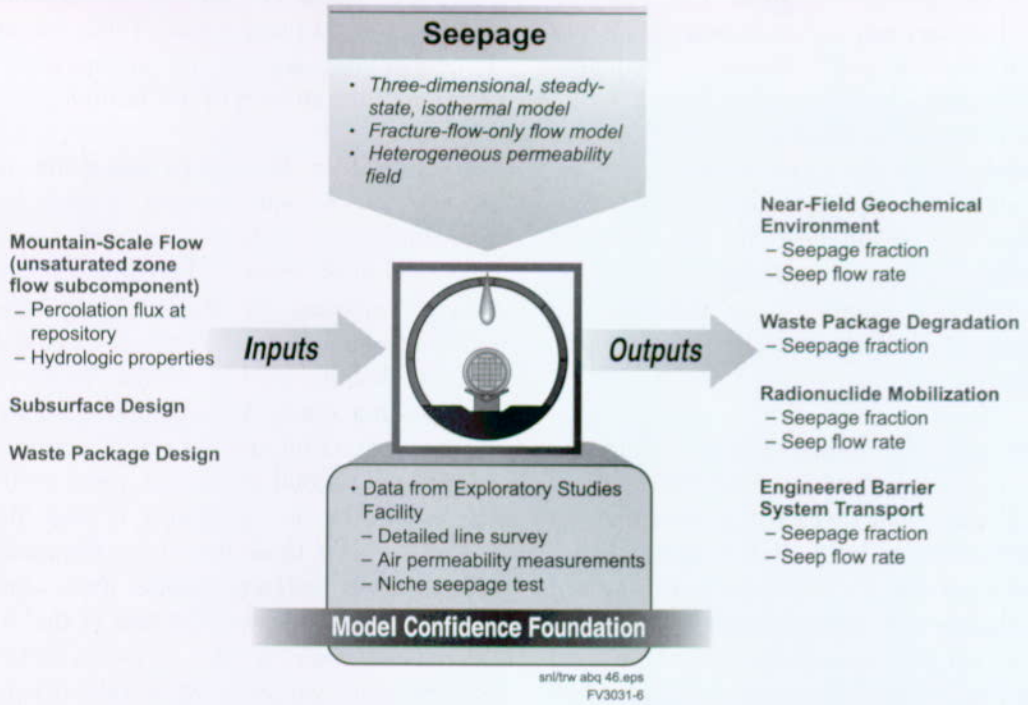

Figure 3-6. Coupling of the Seepage Subcomponent to Other Unsaturated Zone Flow Subcomponents and to Other Total System Performance Assessment for the Viability Assessment Components
The output "seepage fraction" means the fraction of waste packages receiving drips from seeps.

large portion of the workshop was a discussion of the current knowledge of unsaturated zone flow in Yucca Mountain and the important issues for evaluating unsaturated zone flow. The participants compiled a list of these issues and discussed priorities and approaches for dealing with them in the TSPA-VA (Table 3-3). The issues and priorities developed at the workshop largely determined the methods used for modeling unsaturated zone flow in TSPA-VA. Sections 3.1.2.1 and 3.1.2.2 discuss future climate and infiltration. Section 3.1.2.3 discusses issues related specifically to the unsaturated zone flow at the mountain scale. Section 3.1.2.4 discusses issues related to seepage.

In addition, YMP conducted an unsaturated zone flow model expert elicitation (CRWMS M&O 1997n). Project data and models were presented to a group of experts (mostly from outside the YMP) for their evaluation. The experts were asked to evaluate data and provide estimates of uncertainty in surface infiltration and deep percolation. Probability distributions for infiltration and percolation were elicited from each expert. The mean values

Table 3-3. Unsaturated Zone Flow Abstraction/ Testing Workshop

UNSATURATED ZONE FLOW ABSTRACTION/TESTING WORKSHOP
December 11–13, 1996, Albuquerque, NM
(CRWMS M&O 1997t)

PRIORITIZATION CRITERIA
- Does the issue have a strong effect on:
  - Percolation flux at the repository?
  - Seepage into the drift?
  - The partitioning of flow between the fractures and matrix?
- Will the issue be important to flow and transport below the repository?

Highest Priority Issues
- Infiltration and future climate
- Model calibration
- Lateral flow and perched water below the repository
- Flow channeling and seepage into the drift

Analysis Plans
- Sensitivity studies conducted on the site-scale model to determine abstraction methods for unsaturated zone flow
- Seepage into drifts under pre-waste-emplacement conditions
- Testing of perched-water concepts and their implications for TSPA-VA calculations
- Sub-grid-scale fractures and model calibration

of estimated net infiltration ranged from 3.9 mm/year (0.15 in./year) to 12.7 mm/year (0.50 in./year); the mean values of estimated percolation flux at the repository horizon ranged from 3.9 mm/year (0.15 in./year) to 21.1 mm/year (0.83 in./year). These values are commensurate with the current modeled average infiltration of approximately 8 mm/year (0.3 in./year) for the simulated repository region and the modeled spatial variation in percolation flux ranging from near zero to approximately 20 mm/year (0 to 0.8 in./year) (see Section 3.1.2.2)

The experts generally agreed that the infiltration map used shows the general variability of infiltration by location, but several suggested that the map should have more infiltration beneath washes with thin alluvial cover. The experts also agreed that net infiltration is characterized by episodic major storms but that most of the infiltration from each storm is attenuated within the system. Most of the experts agreed that contrasts in the hydrologic properties between units would likely cause lateral diversion of flow above the repository, particularly at the Tiva Canyon welded to Paintbrush nonwelded contact (Figure 3-1); however, the amount of diversion would be limited to scales of several meters to tens of meters. This finding is consistent with the results of the mountain-scale flow simulations, which show nearly vertical flow above the repository. The experts did not address the issue of lateral diversion caused by perched water below the repository. Based on the low matrix permeabilities in the Topopah Spring welded unit, the experts also agreed that the flow in the Topopah Spring welded unit is predominantly in the fractures. This finding is consistent with YMP simulated results. Finally, the experts recommended a number of additional modeling and data-collection activities to improve estimates of infiltration, percolation, and seepage. Many of these recommendations have already been incorporated into this TSPA or are planned in future work.

3.1.1.1 Climate

"Climate" refers to the meteorological conditions that characteristically prevail in a particular region. For this TSPA, climate conditions at Yucca Mountain must be known to determine the hydrology within and around Yucca Mountain. In particular, the amount of precipitation largely determines the amount of infiltration.

The climate in the Yucca Mountain region is presently warm and semiarid, with mean annual temperature of 16°C (61°F) and mean annual precipitation of about 170 mm/year (6.7 in./year). Climate proxies, or the physical remains of substances that carry the imprint of past climates, indicate that the climate in the Yucca Mountain region is not static. For example, climate proxies indicate that during the last glacial period, between 35,000 and 10,000 years ago, most of the world was drier, but the southwest United States was wetter. At that time, the Yucca Mountain region contained wetlands and streams; there were springs at the mouth of Crater Flat and in the Amargosa Desert; there was a lake in Death Valley (Lake Manley) that was over 90 m (295 ft) deep; and sufficient vegetation existed to support a variety of herbivores ranging from mammoths to sheep (CRWMS M&O 1998m, Chapter 4).

Future climate is estimated based on what is known about past climate, with consideration given to climate impacts caused by human activities. Calcite in Devils Hole, a fissure in the ground approximately 40 km (25 miles) southeast of Yucca Mountain, provides the best-dated record of climate change over the past 500,000 years. The record shows continual variation, often with very rapid jumps, between cold glacial climates (for the Great Basin, these are called pluvial periods) and warm interglacial climates similar to the present. The fluctuations average about 100,000 years in length. Because this basic time scale has been corroborated by other climate proxies (e.g., oxygen-isotope variations in marine sediments), it has been selected as the average climate cycle (CRWMS M&O 1998m, Section 4.2.3).

Climate conditions specific to the Yucca Mountain region were estimated from other, more local, climate proxies. Packrat middens are deposits consisting of plant macrofossils cemented by packrat urine that can be dated by radiocarbon methods. Plant life during the last pluvial period

has been reconstructed by analyzing packrat middens. This reconstruction shows an open juniper forest in the lower elevations and a montane conifer forest in the higher elevations of the Yucca Mountain region. From modern locations with open juniper forests, it can be inferred that temperature was then approximately 6 C° (11 F°) colder, and precipitation was approximately two times greater than modern averages. From global climate proxies, in combination with the record from Devils Hole, the last glacial or pluvial period appears to be a rather typical climate, approaching a long-term average climate in the Yucca Mountain region (CRWMS M&O 1998m, Section 4.2.4).

Climate proxies indicate that the last glacial period was not the most extreme climate in the record. The next-to-last glacial period, occurring approximately 150,000 years ago, and a glacial period occurring approximately 600,000 years ago appear to have been markedly colder and wetter. These extreme glacial climates are referred to as super-pluvials. During the next-to-last glacial period (150,000 years ago), Lake Manley in Death Valley reached a depth of over 125 m (410 ft). Lake sediments deposited by Owens Lake, north of Death Valley, hold ostracod and diatom remains of species that now live in Canada. Other evidence suggests that the vegetation in the region was mainly a dense juniper forest. This evidence supports the inference (with somewhat less confidence than inferences for the most recent glacial period) that temperature was approximately 10°C (18°F) colder, and precipitation was approximately three times greater than modern averages (CRWMS M&O 1998m, Section 4.2.3).

The wetter environments of the past suggest that more groundwater flowed beneath Yucca Mountain. Several lines of evidence indicate that the water table was 80 to 120 m (250 to 400 ft) higher during the last pluvial period. The first indication is the presence of spring deposits at the mouth of Crater Flat that have been dated to approximately 13,000 years ago. In addition, a strontium-isotope ratio characteristic of the saturated zone has been found in pore waters of rocks over 80 m (250 ft) above the present water table at Yucca Mountain, and carbon-isotope differences have been found as well. Lastly, water-table rises in this range have been obtained in saturated zone groundwater modeling of future climates. Note that the repository is planned to be over 300 m (1,000 ft) above the present water table, so the repository would still be well above the water table even with a rise of 120 m (400 ft) (CRWMS M&O 1998m, Sections 5.2.6 and 5.2.7).

3.1.1.2 Infiltration

Net infiltration is the penetration of water through the ground surface and to a depth where it can no longer be withdrawn by evaporation or transpiration by plants. Once water has entered bedrock or has penetrated below the root zone in soil (a depth of approximately 6 m, or 20 ft, at Yucca Mountain) it has infiltrated. The conceptual model used for infiltration calculations is based on evidence from field studies at Yucca Mountain, combined with established concepts in soil physics and hydrology (Flint et al. 1996). The overall framework of the conceptual model is provided by the hydrologic cycle, including processes on the surface and just below the surface that affect net infiltration.

Important infiltration processes include precipitation (rain and snow); runoff and run-on (flow of surface water off one place and onto another); evaporation; transpiration (removal of moisture from soil by plants); and redistribution of moisture by flow in the shallow subsurface. Localized precipitation depends on meteorological factors, and geographic location and elevation. The generation of runoff depends on precipitation intensity, shallow moisture conditions, soil depth, soil porosity, soil permeability, bedrock permeability, and ground-surface slope. Run-on depends mostly on material surface properties, topography, and channel geometry. Evaporation depends on the amount of sunlight, temperature, and the evaporative capacity of the atmosphere. Transpiration depends on the type of vegetation present. Redistribution of moisture by flow in the shallow subsurface in response to gravity and capillary pressure is strongly dependent on soil and bedrock properties. The removal of water

through evaporation and transpiration (together called evapotranspiration) is closely coupled with redistribution of moisture in the shallow subsurface.

The conceptual model of infiltration was developed based on analysis of an 11-year record of moisture measurements from 99 boreholes on Yucca Mountain (Flint and Flint 1995). Relative changes in water-content profiles were compared to precipitation records, estimates of evapotranspiration, physiographic setting, bedrock geology, and soil cover. Results from field studies indicate that high soil saturation leading to net infiltration primarily occurs during a series of winter storms producing moderate precipitation. These storms tend to occur more frequently during winters with an active El Niño pattern. The timing, intensity, and duration of precipitation; storage capacity of the soil; and evapotranspiration determine the availability of water for net infiltration. In the upland areas of Yucca Mountain with shallow soil cover, the amount of net infiltration depends on the effective conductivity of the underlying bedrock. Lower conductivity leads to moisture being held longer in the soil, where it can potentially be lost to evapotranspiration. During winter, when potential evapotranspiration is at a minimum, smaller amounts of precipitation are needed to develop and maintain saturated conditions at the soil-bedrock contact.

3.1.1.3 Mountain-Scale Unsaturated Zone Flow

Unsaturated zone flow is the percolation of groundwater through rocks above the water table. Unsaturated zone flow varies with the rock strata through which the water flows (CRWMS M&O 1998m, Sections 5.3.4.2, 5.3.4.3). As depicted in Figure 3-1, the unsaturated zone in Yucca Mountain is composed of alternating layers of welded and nonwelded tuffs. The terms welded and nonwelded refer to the degree of consolidation of the rock when it was formed from volcanic ash millions of years ago. Welded tuff is hard, dense rock but is typically very fractured. The welded tuff rock matrix is relatively impermeable, but the total permeability is high because of the fractures. Nonwelded tuff is softer and typically less fractured. Its matrix permeability is much higher than that of welded tuff matrix, but its total permeability is typically lower. A special case is zeolitic nonwelded tuff, which was altered during the original cooling in such a way that its matrix permeability is very low (similar to the matrix permeability of welded tuff). Zeolitic tuff may also have little fracturing so that its total permeability is very low. Perched-water zones, or localized saturated regions above the water table, have been observed on the zeolitic tuff in several boreholes.

Fractures play an important role in unsaturated zone flow (CRWMS M&O 1998m, Section 5.3.4.3.2). This role is especially important when considering radionuclide transport from a nuclear-waste repository. Flow in fractures is typically much faster than flow in the porous matrix, potentially leading to much faster travel to the water table. A few years ago, most flow in Yucca Mountain was thought to be through the porous rock matrix. This is not consistent with recent higher estimates of infiltration. The current estimate for present-day net infiltration over the repository area is about 8 mm/year (0.3 in./year) and the estimate is much higher for the wetter future climates. The rock matrix flow capacity is much less than 8 mm/year (0.3 in./year) in the welded tuff, implying that most of the flow is moving through fractures. Because the matrix pores are not saturated with water, it is inferred that the flows in fractures and matrix are only weakly coupled; otherwise, the matrix pores would be saturated.

The equivalent-continuum model, in which the fracture and matrix flows are strongly coupled, was widely used for modeling unsaturated zone flow when net infiltration at Yucca Mountain was thought to be 1 mm/year (0.04 in./year) or less. This model was used in the 1993 TSPA (Wilson et al. 1994, Chapter 14) and the 1995 TSPA (CRWMS M&O 1995, Section 4.2). Two other models of fracture-matrix unsaturated flow that have been used in past TSPAs are the generalized equivalent-continuum model in the 1995 TSPA (CRWMS M&O 1995, Section 7.2) and the Weeps model in the 1993 TSPA (Wilson et al. 1994,

Chapter 15). The generalized equivalent-continuum model is a modification of the equivalent-continuum model in which the fracture and matrix flows are strongly coupled, but fractures are assumed to flow more easily above a matrix-saturation threshold. The Weeps model does not consider the rock matrix and assumes that all significant flow is through the fractures.

The generalized equivalent-continuum model and the Weeps model overcome one of the problems with the equivalent-continuum model because they reasonably can be applied with the higher infiltration rates being used now. Most recent modeling (Bodvarsson et al. 1997, Chapter 6) has used the dual-permeability model, which is a more general model in which the fracture-matrix coupling can be strong or weak, depending on the parameter values used. The dual-permeability model has the flexibility to represent almost the entire range of possible flow behavior through variation of fracture-matrix coupling strength. This allows flow behavior to change continuously from the equivalent-continuum model, which is dominated by matrix flow, to a Weeps-type flow almost entirely within the fracture network.

In this TSPA, unsaturated zone flow, unsaturated zone transport, and thermal hydrology are modeled using the dual-permeability model. Thermal hydrology uses the generalized equivalent-continuum model as well (see Section 3.2). In the dual-permeability model, fracture-matrix coupling strength is used as an adjustable calibration parameter that is set so that net infiltration can be relatively high, as implied by the infiltration model, with matrix saturation in the model near observed values and with measured and inferred values of all matrix and fracture hydrologic properties.

The data used to develop the mountain-scale calibrated flow fields for the unsaturated zone come from several surface-based drillholes and from the Exploratory Studies Facility, which is an 8-km (5-mile) long tunnel through Yucca Mountain. These data include rock-matrix saturations, water potentials (the ability for rock to hold water), and temperatures; perched-water locations and amounts; chemical composition and isotopic abundances of groundwater and mineral deposits; air permeability and air-pressure measurements; rock types and mineralogy; fault locations and offsets; fracture density and orientations; and matrix permeability and saturation/desaturation parameters. More detailed information on data and the calibration procedure are found in Bodvarsson et al. (1997, Chapter 6) and CRWMS M&O (1998m, Section 5.3.4.4).

The effects of discrete fractures and other small-scale features are not included in the dual-permeability model and may be important. The dual-permeability model (as well as the equivalent-continuum model and the generalized equivalent-continuum model) represents flow through the myriad individual fractures and matrix blocks by approximating them as continuous flow fields. The Weeps model is a simplified version of a discrete-fracture flow model and some of its implications are different from those of continuum models. The effects of discrete fractures are not considered directly in this TSPA, and it is uncertain whether some of their effects might be important. This TSPA uses an alternative flow model called the dual-permeability/Weeps model, which is similar to the Weeps model in many respects but which still treats fractures as a continuum rather than as discrete flow paths.

3.1.1.4 Seepage into Drifts

Seepage is the movement of liquid water into emplacement drifts. The basic conceptual model for seepage is that openings in unsaturated media act as capillary barriers and divert water around them. This capillary barrier effect has been tested in the Exploratory Studies Facility by niche tests in which water is injected above a niche (a side tunnel off the main tunnel). Results from the tests indicate that most of the water does not seep into an opening just 2 ft below (CRWMS M&O 1998i, Section 2.4.4.9). In addition, no natural seeps into the Exploratory Studies Facility tunnel have been observed, although the lack of seeps may be partially caused by drying from tunnel ventilation.

For seepage to occur in the conceptual model, the rock pores at the drift wall must be locally saturated. Drift walls can become locally saturated by either disturbance to the flow field caused by the drift opening or variability in the permeability field that creates channelized flow and local ponding. Of the two reasons, the variability effect is more important. Drift-scale flow calculations made with uniform hydrologic properties suggest that seepage will not occur at expected percolation fluxes. However, calculations that include permeability variations do predict seepage, with the amount depending on the hydrologic properties and the incoming percolation flux (CRWMS M&O 1998i, Section 2.4.4).

For the drift-scale flow model used for calculating seepage, the fracture hydrologic properties were defined in the same way as for the mountain-scale flow model (Bodvarsson et al. 1997, Chapter 7). Additional information needed to define the variability of the fracture-permeability field by location was taken from a series of air-permeability tests conducted at the location of the drift-scale thermal test in the Exploratory Studies Facility (CRWMS M&O 1998i, Section 2.4.4.2.1).

As with the modeling of mountain-scale flow, the dual-permeability model is preferred for modeling seepage at the drift scale. However, to simplify the drift-scale calculations, effects of the rock matrix were not considered, and flow was calculated using a model for only the fracture continuum (CRWMS M&O 1998i, Section 2.4.4). This simplification is conservative compared to the dual-permeability model because the effect of including the matrix would be to decrease the fracture flow and reduce the amount of seepage (the large capillary suction in matrix pores prevents matrix flow from seeping into drift openings). Another simplification is to assume steady-state conditions. It is uncertain whether there is episodic flow at the repository and what its effect on seepage would be. Also, as with the modeling of mountain-scale flow, discrete-fracture effects are potentially important.

In the seepage modeling, drift collapse and thermal alteration of hydrologic properties are not considered. It is expected that the drifts will only be stable for a few hundred to a thousand years. Therefore, long-term repository performance will depend on the amount of seepage into a drift filled with rockfall rubble, rather than into an open drift. In addition, thermal-mechanical and thermal-chemical effects could alter the hydrologic properties around the drifts, possibly even permanently. The impact of these effects is uncertain.

3.1.2 Implementation of the Performance Assessment Model

3.1.2.1 Climate

Climate calculations are based on a long-term average climate, with relatively short periods of drier or wetter climates. The typical climate, defined to be the long-term average climate, is like the most recent glacial or pluvial period; the drier climate is similar to present day climate; the wetter climate is the superpluvial climate (Figure 3-2). Several factors led to this strategy. First, there is a great deal of uncertainty in estimating future climate, and a complex climate model would give the impression of a greater knowledge of, and certainty about, future conditions. Second, although this TSPA could have been based on a worst-case climate, a superpluvial climate is atypical and seen only rarely in the climate record. Basing the TSPA on a superpluvial climate would be misleading. Third, modeling groundwater flow with a three-dimensional model is complex and time consuming. Because of this complexity, only three discrete climate states were considered.

Models of human impact on future climates, caused by global warming from increased atmospheric carbon dioxide, are speculative, although they are supported by some global-climate modeling and the general increase in global temperature noted this century. At Yucca Mountain the effect of global warming is estimated to increase average precipitation to a level similar to the long-term average. This estimate is based on atmospheric model input and resembles near-continuous El Niño conditions at Yucca Mountain and the near doubling of precipitation that accompanies these conditions. Therefore, any global-warming impact on future climates is

considered to be within the bounds of paleoclimate ranges (CRWMS M&O 1998i, Section 2.4.1.1). However, infiltration might be different because the temperature would be higher (expected to be about 2 C°, or 4 F°, warmer than currently and more than 5 C°, or 9 F°, warmer than the long-term average), but effects of these temperature differences were neglected for TSPA-VA. These effects will be addressed in future TSPAs, as appropriate.

The modeled climate, then, alternates between three states: dry or present-day climate; long-term average climate; which is about twice the dry-climate precipitation; and superpluvial climate, which is about three times the dry-climate precipitation. The length of the first dry climate, or current climate, is sampled uniformly between 0 and 10,000 years, with an expected value of 5,000 years. The length of subsequent dry climates is sampled uniformly between 0 and 20,000 years, with an average of 10,000 years. The duration of long-term average climates is sampled uniformly between 80,000 and 100,000 years, with an average of 90,000 years. The duration of the superpluvial climates is sampled similarly to dry climates, from 0 to 20,000 years. Dry and long-term average climates alternate from the time of repository closure until the long-term average climate that spans the 250,000-year mark. The last part of that long-term average period is replaced by a superpluvial climate of the sampled duration. Then the climate model returns to alternating dry and long-term average climates until the long-term average climate that spans the time of 400,000 years after the first superpluvial. The end of that long-term average climate is again replaced by a superpluvial, and then back to dry, followed by alternating long-term average and dry climates. About 90 percent of the time is spent in the long-term average climate.

The data used in the climate model are summarized in Table 3-4. Additional information on the various components is found in the sections about the models using climate information (see Section 3.7 for additional information about the multiplier for saturated zone flux).

Table 3-4. Data Summary for the Climate Model

Climate Parameter	Dry (Present Day)	Long-Term Average	Super-pluvial
Precipitation	Current distribution	2 × current	3 × current
Water-table rise	0	80 m (260 ft)	120 m (390 ft)
Saturated zone flux	Current distribution	3.9 × current	6.2 × current
Duration	0–10,000 years for current; 0–20,000 years for future dry climates	80,000–100,000 years	0–20,000 years

The connections between climate and the other subcomponents of unsaturated zone flow, and the other TSPA components, are shown in Figure 3-3.

3.1.2.2 Infiltration

Distributed net infiltration rates by location were determined for each of the three climate states using the YMP infiltration model (Flint et al. 1996; CRWMS M&O 1998m, Section 5.3.4.1). The infiltration model simulates the water content of the soil profile at each location by determining water balance using precipitation input, a model for evapotranspiration, and available water in the soil profile.

The model covers an area of 228 km^2 (88 $miles^2$) around Yucca Mountain, using a regular grid with 30-m (98-ft) spacing. The inputs to the model include daily precipitation; ground-surface elevation; bedrock geology and hydrologic properties; soil type and hydrologic properties; soil depth; and identification of each location as ridge top, side slope, terrace, or channel (Flint et al. 1996, pp. 69–83).

The infiltration model was calibrated using the records of measured water-content profiles from shallow boreholes and records of daily precipitation. Model calibration consisted of qualitative and quantitative comparisons of measured versus simulated water-content changes for the soil profile. The model calibration process adjusted the parameters for evapotranspiration so that a satisfactory fit between measured and simulated time-dependent changes in soil moisture was obtained

for all borehole locations (Flint et al. 1996, pp. 84–85).

Daily precipitation data were obtained using available records or generated using a stochastic model of daily precipitation. Most of the long-term precipitation records in the Yucca Mountain region (southern Nevada and southeastern California) are less than 50 years old. Precipitation models were used to generate longer precipitation sequences and allow the simulation of paleoclimates that do not have present-day analogs. To represent the dry, present-day climate, daily precipitation records from a weather station located approximately 15 km (9 miles) east of the repository site were used. Although this station is lower in elevation than the repository site (1,000 m, or 3,300 ft, versus 1,500 m, or 4,900 ft), it provides the longest, almost-continuous record of daily precipitation near the repository. The precipitation values were scaled upward to compensate for the difference in elevation (Flint et al. 1996, p. 71). The stochastic precipitation model estimated the 100-year-average precipitation to be 150 mm/year (6 in./year), slightly lower than the recently observed average of 170 mm/year (6.7 in./year) (CRWMS M&O 1998m, Section 5.3.4.1.5.1).

Present-day analogs were chosen to represent the wetter future climates. For the long-term average climate, daily precipitation records from Rainier Mesa were used. This weather station is approximately 40 km (25 miles) north of Yucca Mountain and at higher elevation (2,200 m, or 7,200 ft). For the superpluvial climate, records from South Lake, California, were used. South Lake is located on the eastern slope of the Sierra Nevada at an even higher elevation (2,700 m, or 8,900 ft). These analog sites have not been rigorously evaluated for predictions of the expected characteristics of future climates (for example, the expected seasonal distribution of precipitation). The modeled 100-year-average precipitation based on the precipitation record was found to be 289 mm/year (11.4 in./year) for the Rainier Mesa site and 427 mm/year (16.8 in./year) for the South Lake site (CRWMS M&O 1998m, Section 5.3.4.1.5.3).

Because net infiltration is an important contributor to unsaturated zone flow and seepage into drifts, uncertainty about infiltration and how that uncertainty affects repository performance must be considered. By extension, infiltration contributes to other components that use the results of the unsaturated zone flow modeling. For TSPA-VA, uncertainty about infiltration was included by creating three different infiltration maps: the base infiltration map calculated using the infiltration model, and two other maps made by uniformly multiplying or dividing the base map by three. The same procedure was followed for the three climate states, for a total of nine infiltration maps. The factor-of-three increase or decrease was constrained by comparing the calculated mountain-scale flow fields with observations. The flow model was expected to reproduce the observed temperature gradient, which is a function of net infiltration. Infiltrating water introduces an advective component to the ambient heat balance, changing the temperature profile from what it would be if heat transfer were by thermal conduction only (see Bodvarsson et al. 1997, Chapter 11). If increases are greater than about a factor of three, the flow model cannot reproduce the observed temperature gradient for the unsaturated zone. The factor of three reduction has no definite basis, but was done simply to have symmetry in the amount of increase and decrease.

To incorporate the three infiltration maps into a Monte Carlo framework, they were assigned probabilities. Because the base infiltration map represents the current best estimate of infiltration, the probabilities were assigned so that the base infiltration was equal to the statistical mean. The probability for the high infiltration case (base map times three) was determined by balancing the recommendations made by the participants in the unsaturated zone flow model expert elicitation (CRWMS M&O 1997n, Table 3-1) with information such as the temperature gradient implications. A 10 percent probability was assigned to the "base infiltration multiplied by three" case. The requirement that the "base infiltration" case be the mean of the infiltration distribution then uniquely determines the other two probabilities to be 60 percent for the "base infiltration" case and

30 percent for the "base infiltration divided by three" case. The same probabilities are used for the other climate states, and the infiltration rates were assumed to be perfectly correlated among climates (Table 3-5). For example, when climate changes from dry to long-term average with dry-climate infiltration equal to base infiltration divided by three, then long-term average and superpluvial infiltration are also base infiltration divided by three. A more quantitative basis for infiltration probability distributions could be achieved by running the infiltration model in a stochastic mode to derive infiltration uncertainty from input-parameter uncertainties. Estimates of net infiltration for future climates could be improved by inclusion of the effects of temperature and vegetation changes. Note that in addition to the probabilities, Table 3-5 gives the net infiltration averaged over the repository area for each case.

The connections between infiltration and the other subcomponents of unsaturated zone flow, and the other TSPA components, are shown in Figure 3-4.

3.1.2.3 Mountain-Scale Unsaturated Zone Flow

The YMP three-dimensional, site-scale flow model for the unsaturated zone (Bodvarsson et al. 1997) was used in calculating mountain-scale, unsaturated zone flow for this TSPA. Three-dimensional modeling was needed primarily because of flow characteristics below the repository, where significant lateral flow is believed to occur because of low-permeability zeolitic layers and perched water. The model uses the dual-permeability conceptual model, as discussed in Section 3.1.1.3. The direct use of the three-dimensional, mountain-scale flow model eliminated the need to test simplified abstractions against more complex process models. The models were tested directly against site data as part of the calibration procedure. The following paragraphs summarize the most important features of the mountain-scale flow model for the unsaturated zone.

The mountain-scale flow model for the unsaturated zone is based on site data that include core measurements of porosity, permeability, saturation, and moisture potential; perched-water observations; fracture-frequency data from the Exploratory Studies Facility; air pressure monitoring and air permeability tests; and geochemical data. These data were used to estimate hydrologic parameters through direct calculations and calibration methods. In addition, a geologic-framework model was used to define the proper stratigraphy for the unsaturated zone flow model. Numerous sensitivity analyses have been performed to understand the importance of infiltration, hydrologic parameters, fracture-matrix interactions, and features such as faults and perched water.

The YMP site-scale flow model for the unsaturated zone, including its calibration procedures and sensitivity analyses, was used to develop a base case, mountain-scale model for unsaturated zone flow. Although there are considerable data for calibrating the mountain-scale flow model, there can not be enough data to eliminate all uncertainty. Thus, more than one calibrated model can fit the available data. The base case includes uncertainty in both infiltration (Section 3.1.2.2) and hydrologic parameters that were determined to be important through sensitivity analyses (CRWMS M&O 1998i, Section 2.4.3.2). In the base case, the only

Table 3-5. Average Net Infiltrations and Probabilities for the Infiltration Cases

	Dry (Present Day)	Long-Term Average	Superpluvial	Probability (All Climate States)
Low infiltration (base infiltration ÷ 3)	2.6 mm/year	14 mm/year	37 mm/year	30%
Base infiltration	7.7 mm/year	42 mm/year	110 mm/year	60%
High infiltration (base infiltration × 3)	23 mm/year	125 mm/year	340 mm/year	10%

Note: 25.4 mm = 1 in.

hydrologic parameters varied are the air-entry parameter for fractures (α_f) and the fracture-matrix coupling strength. The fracture air-entry parameter governs capillary pressure in the fractures, and the fracture-matrix coupling strength governs how easily water flows between fractures and the rock matrix. The fracture air-entry parameter is directly proportional to the effective fracture aperture.

For each hydrogeologic unit a range of uncertainty was developed for the fracture air-entry parameter based on measurements of fracture density and air permeability. The fracture-matrix coupling strength was not varied independently but was used as a calibration variable. The fracture-matrix coupling strength was constrained to have only three different values (for welded tuff, nonwelded nonzeolitic tuff, and nonwelded zeolitic tuff) in a given calibration. These three values were chosen to optimize the match with observed borehole matrix saturations and water potential. Additional information on parameters and calibration can be found in CRWMS M&O (1998i, Section 2.4.3).

The base case includes the following independently calibrated models:

- Base infiltration divided by 3 and the fracture air-entry parameter at a minimum for each layer
- Base infiltration divided by 3 and the fracture air-entry parameter at a maximum for each layer
- Base infiltration and the fracture air-entry parameter at the nominal "best estimate" for each layer
- Base infiltration multiplied by 3 and the fracture air-entry parameter at a minimum for each layer
- Base infiltration multiplied by 3 and the fracture air-entry parameter at a maximum for each layer

Five models were used, rather than the full matrix of nine combinations, to reduce computational requirements. Flow was calculated for each of the five models for the three climate states: dry (present-day), long-term average, and superpluvial. The probabilities for each case are given in Table 3-6. The probabilities for the infiltration cases are discussed in Section 3.1.2.2. The probabilities for minimum and maximum fracture air-entry parameter values are equal because, based on the way the ranges were defined, there is no reason to favor one over the other.

Table 3-6. Probabilities for the Mountain-Scale Unsaturated Zone Flow Cases

	Minimum α_f	Nominal α_f	Maximum α_f
Low infiltration (base infiltration ÷ 3)	15%	not considered	15%
Base infiltration	not considered	60%	not considered
High infiltration (base infiltration × 3)	5%	not considered	5%

Note: α_f = fracture air-entry parameter

In addition to the base case, an alternative model called the dual-permeability/Weeps model was considered. This model has a significantly reduced fracture-matrix coupling strength to induce more fracture flow. The biggest difference between the base case model and the dual-permeability/Weeps model is that the dual-permeability/Weeps model shows flow predominantly in fractures even in nonwelded hydrogeologic units while the base case shows flow in nonwelded nonzeolitic units predominantly in the rock matrix.

The connections between mountain-scale flow and the other subcomponents of unsaturated zone flow, and the other TSPA components, are shown in Figure 3-5.

3.1.2.4 Seepage into Drifts

The method for modeling seepage into the emplacement drifts is shown in Figure 3-7. The method is summarized as follows:

- The calculation of seepage into drifts is based on a three-dimensional, fracture-continuum flow model that includes a spatially variable permeability field.

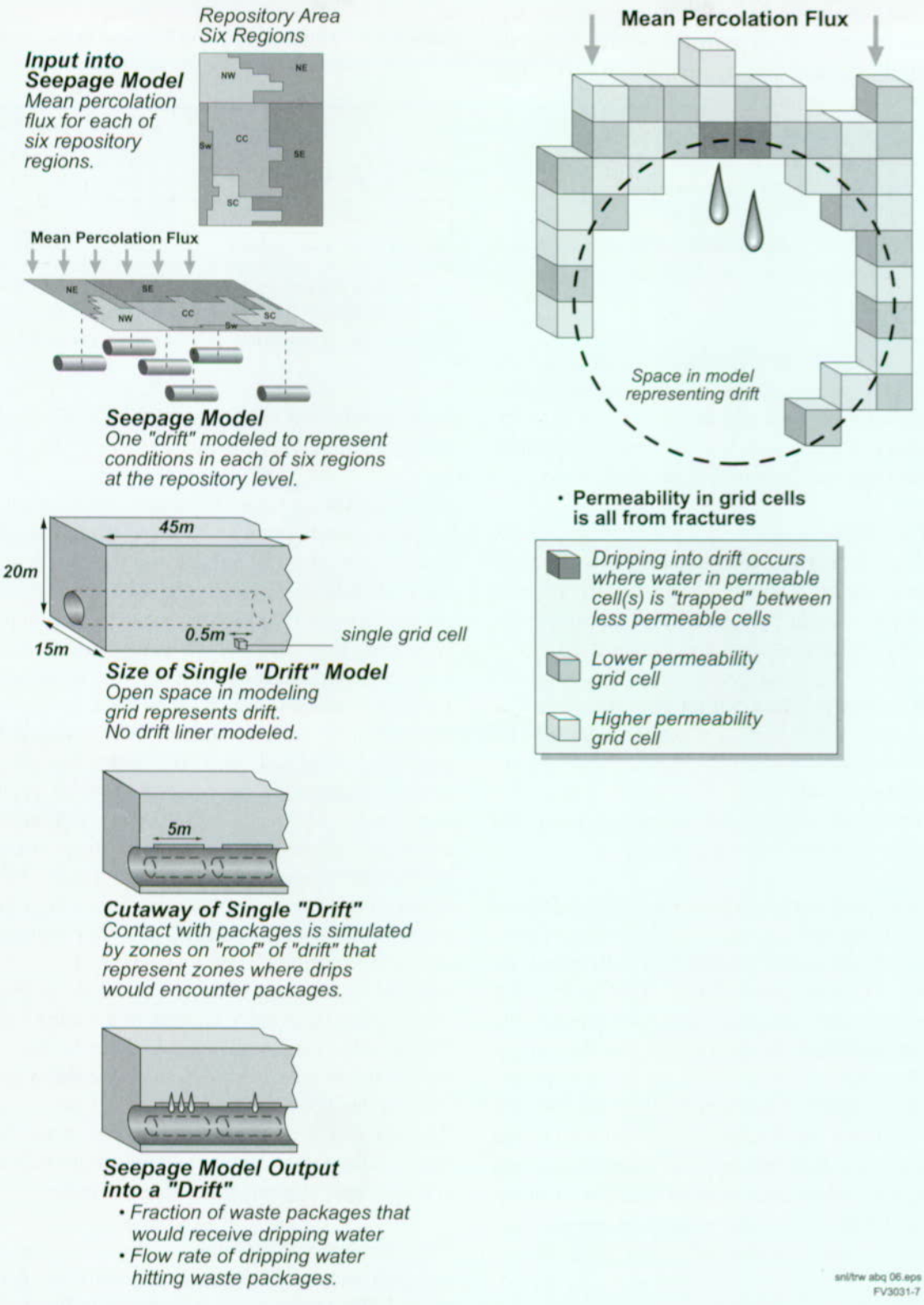

Figure 3-7. Illustration of the Method Used for Calculating Seepage for Total System Performance Assessment for the Viability Assessment
This model calculates two quantities: seepage fraction and seep flow rate.

- Using the three-dimensional process model, the amount of seepage into drifts is calculated as a function of percolation flux. The following quantities are calculated:
  - Seepage fraction, or the fraction of waste packages contacted by seeps
  - Seep flow rate, which is the rate of water flow onto a waste package that is contacted by one or more seeps
- In calculating seepage fraction and seep flow rate, a waste package is conservatively represented by an area of 5 m × 5 m (16 ft × 16 ft), which is approximately the length of a waste package and the width of the drift.
- The TSPA models of near-field processes (e.g., near-field geochemical environment and waste package degradation) include spatial variability by considering six repository regions, as shown in Figure 3-7.
- Percolation flux through fractures is averaged over each of those six regions. The average flux is used to calculate the seepage fraction and seep flow rate, using the functional dependence obtained from the process-model calculations.

Seepage fraction and seep flow rate are not defined as simple functions but rather as probability distributions with mean and standard deviation that are functions of percolation flux. The probability distributions for seepage are developed by assigning distributions to two of the key input parameters that are uncertain in the process model: the mean fracture permeability (k_f) and the air-entry parameter for fractures (α_f). Similar to the mountain-scale flow model, the distributions are discrete; the values and probabilities are summarized in Table 3-7. The parameter ranges and probabilities were developed from data on air permeability and fracture density (CRWMS M&O 1998i, Section 2.5.2.2).

Table 3-7. Probabilities for the Process-Model Cases Used to Develop Seepage Distributions

	$\alpha_f = 3\times10^{-4}$ Pa^{-1}	$\alpha_f = 10^{-3}$ Pa^{-1}	$\alpha_f = 3\times10^{-3}$ Pa^{-1}
Mean $k_f = 10^{-14}$ m^2	6.25%	12.5%	6.25%
Mean $k_f = 10^{-13}$ m^2	12.5%	25%	12.5%
Mean $k_f = 10^{-12}$ m^2	6.25%	12.5%	6.25%

Note: k_f is fracture permeability and α_f is fracture air-entry parameter; Pa = pascal is a unit of measure for pressure, equal to 1.5×10^{-4} pounds per square inch.

Nine parameter combinations were used for seepage calculations. Results from the three-dimensional process model were combined with the probabilities shown in the table to develop the probability distributions of seepage fraction and seep flow rate from which values were sampled. The seepage quantities were determined separately for each of the six repository regions; however, the values for the various regions were assumed to be perfectly correlated, and the values for different climate states were also assumed to be perfectly correlated. The values for the six regions were correlated because the probability distributions of hydrologic properties shown in Table 3-7 are assumed to represent uncertainty in the appropriate values, not spatial variability. The values for different climates were correlated to avoid unphysical behavior such as a decrease in seepage when going from a dry climate to a wetter climate. The correlations simplify the analyses because they reduce the number of independent seepage parameters in the TSPA calculations to just two (seepage fraction and seep flow rate), rather than the 36 there could potentially have been (those two times six repository regions times three climates).

The connections between seepage and the other subcomponents of unsaturated zone flow, and the other TSPA components, are shown in Figure 3-6.

3.1.3 Results and Interpretation

3.1.3.1 Infiltration

Net infiltration near the repository at the surface as calculated by the infiltration model is shown as the left map in Figure 3-8 Shown are results for the long-term average climate and for the mean (base) infiltration case. In this and most of the remaining figures in this section, the long-term average climate is used for illustration because it is in effect most of the time (approximately 90 percent of the time, on average) for the TSPA simulations.

Some features of the infiltration model can be seen in the figure:

- The modeled infiltration is highly heterogeneous and clearly correlated with topographic features.
- The highest net infiltration occurs along Yucca Crest (the vertical blue band near the center of the map).
- Net infiltration is lower in washes (the roughly horizontal red bands).

The higher net infiltration along the crest and lower net infiltration in the washes are caused by the amount of alluvial cover present. Along the crest, less alluvial cover allows more water to penetrate into the bedrock without being evaporated, but the opposite tends to be true in the washes, where thick

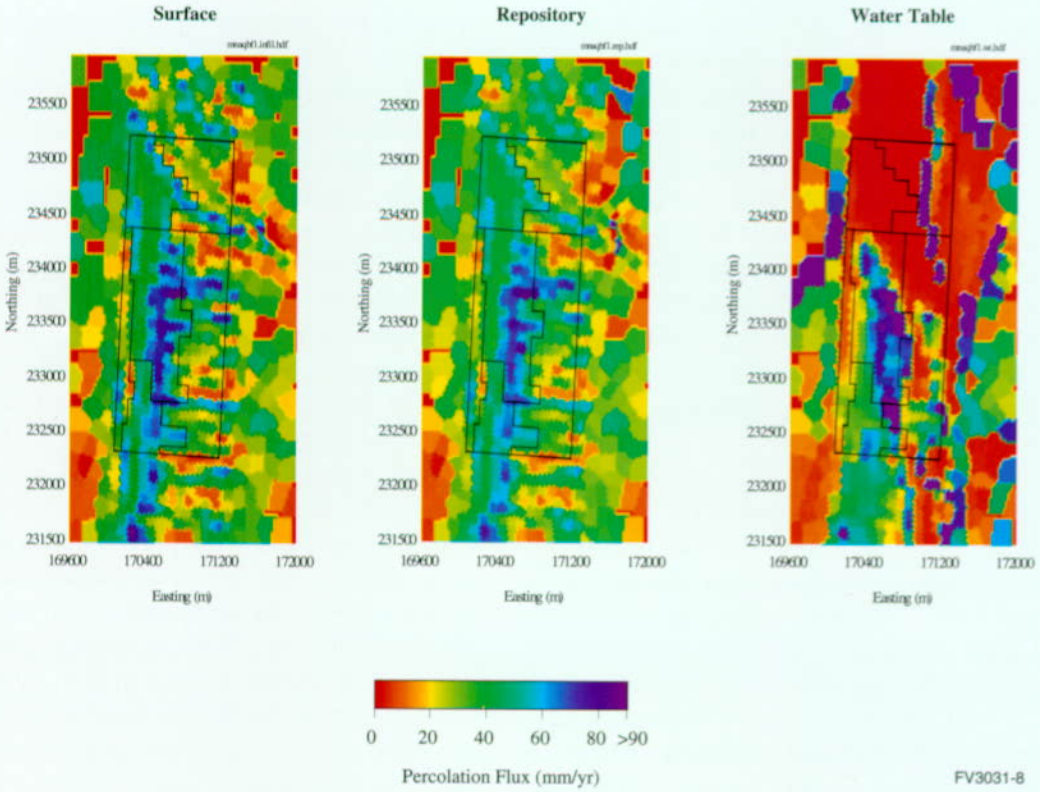

Figure 3-8. Total Percolation Flux at Three Elevations
Total percolation flux (fracture + matrix) at three elevations using long-term average climate, mean infiltration, and base case hydrologic properties. Note that percolation flux at the repository is nearly the same as at the surface, but at the water table the percolation flux is distributed much differently because of lateral flow in the northern part of the repository. An outline of the six regions at the repository level over which data are averaged is placed on each map for reference.

alluvium can store water from storm events long enough for it to be removed by evaporation or transpiration.

3.1.3.2 Mountain-Scale Unsaturated Zone Flow

Important results from the mountain-scale flow model for the unsaturated zone are percolation fluxes at the repository horizon and at the water table. These values are shown as the center and right maps in Figure 3-8 for the mean-infiltration, base case model using the long-term-average climate. The location of the repository is shown in each map, as well as the six regions that were defined to account for variations in percolation by location at the repository. The division into regions was defined to limit the variation in percolation within each region. The number of regions was arbitrarily chosen. The center map of percolation flux at the repository level is nearly the same as the left map of surface infiltration, indicating nearly vertical flow from the surface to the repository. However, the right map of percolation flux at the water table is quite different from the other two, indicating significant nonvertical flow between the repository and the water table. In particular, in the large red area to the north, the percolation flux at the water table is low because it is underneath the perched water body; most of the flow is across the top of the perched water and down to the water table at the vertical blue band.

Figure 3-9 shows calculated flow paths of hypothetical tracers (substances with no retardation effect, no hydrodynamic dispersion, and no matrix diffusion) in two west-east, vertical cross sections (labeled north and south). For each cross section, tracers were released at two surface locations above the east and west ends of the repository. White symbols on the cross sections indicate a higher concentration of the tracer in fractures, while black symbols indicate a higher concentration in the matrix; diamonds indicate particles released at the western location and triangles indicate particles released at the eastern location. In both cross sections, flow is nearly vertical above the repository, except for some lateral movement above and in the Paintbrush nonwelded unit (see Figure 3-1 for location of units). In addition, the flow is contained primarily in the fractures of the welded units and in the matrix of the nonwelded units. In the north cross section, a significant amount of lateral diversion occurs below the repository at the location of the perched water (see Bodvarsson et al. 1997, Chapter 13). Tracers released along the west end of the repository traverse above the perched water for hundreds of meters to the east before reaching the water table. Some of these tracer particles also partition into the matrix upon reaching the perched water and traverse laterally below the perched water. In the south cross-section, although perched water is not prevalent, some lateral diversion beneath the repository still occurs, caused by the contact between the Calico Hills vitric and zeolitic units, where there is a large difference in matrix permeability. The south cross-section shows lateral flow diverting downward at the Ghost Dance fault.

A useful way to compare multiple flow fields is a graph showing the distribution of time for water to travel from the repository to the water table. For example, Figure 3-10 shows the cumulative distribution of travel times (called a "breakthrough curve") for the mean infiltration, base case simulations using the present-day, long-term average, and superpluvial climates. Results show that net infiltration has a strong influence on travel time because higher infiltration results in faster water flow, particularly in the nonzeolitic nonwelded rock. The median arrival times are approximately 2,000, 200, and 90 years for the present-day, long-term average, and superpluvial infiltration rates, respectively. The first arrival times at the water table are very early as a result of fast flow through fractures. In fact, the cumulative breakthrough curves show a bimodal distribution, with over 20 percent of the water for the long-term average and superpluvial simulations taking less than 1 year to reach the water table.

Figure 3-11 shows breakthrough curves for the five base case flow fields for the long-term average climate, illustrating the effects of uncertainty in infiltration and fracture hydrologic properties. The upper parts of the curves represent water particles

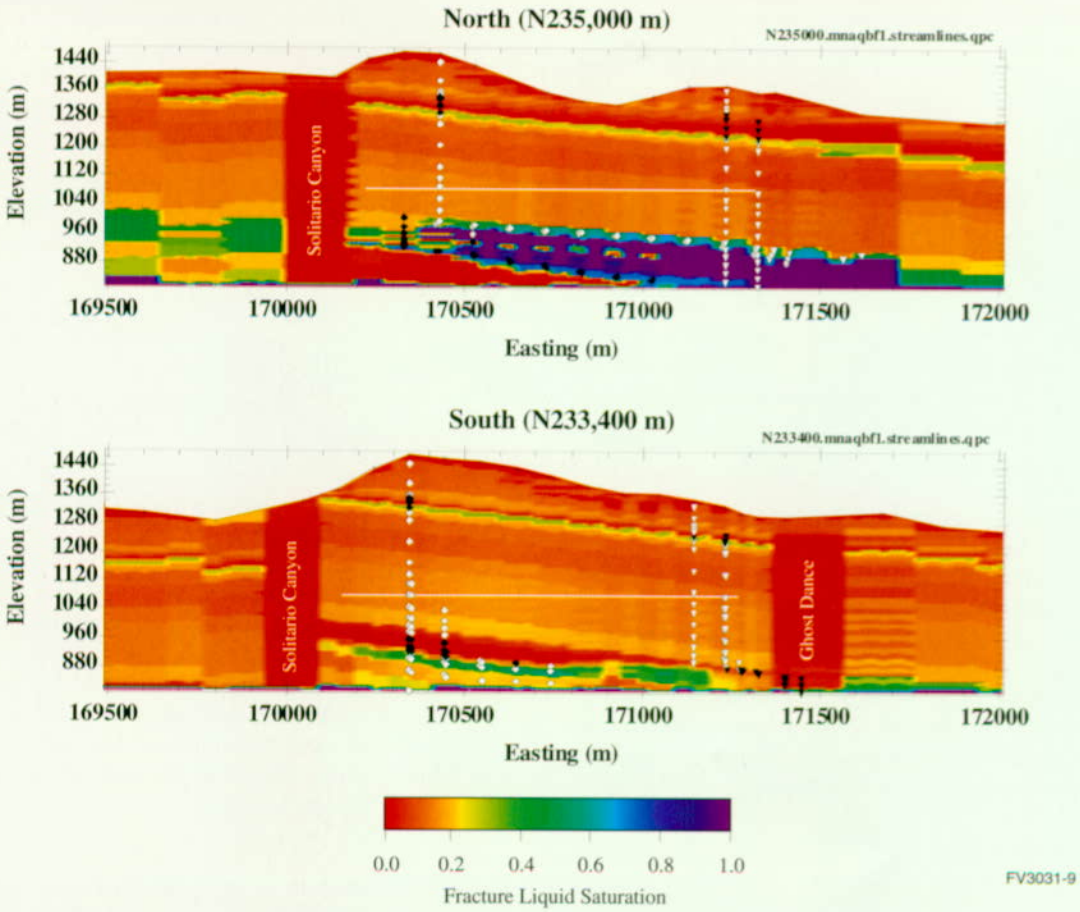

Figure 3-9. Selected Water-Flow Paths From Ground Surface to Water Table
West-east cross sections through the mountain-scale unsaturated zone flow model showing selected water-flow paths from ground surface to water table, using long-term-average climate, mean infiltration, and base case hydrologic properties. See Figure 3-8 for location of cross sections with regard to north-south coordinates. The white symbols denote flow primarily in the fractures, and the black symbols denote flow primarily in the matrix. The background color indicates fracture liquid saturation; dark blue shows perched-water location. The Solitario and Ghost Dance faults are indicated. The white line represents the repository location.

that spent at least part of their time flowing in the matrix between the repository and the water table. The lower parts of the curves represent water particles that were able to travel very quickly in fractures from the repository to the water table. There is a strong dependence of travel time on net infiltration but little dependence on fracture properties (as represented by the fracture air-entry parameter, α_f). It is worth noting that the very fast fracture flow does not represent a significant impact on repository performance because travel times from the repository to the water table of 1 year or 100 years are basically indistinguishable in a repository simulation of 10,000 years or more.

Figure 3-12 shows a comparison between the base case model and the dual-permeability/Weeps model for the base infiltration map and long-term average climate. The dual-permeability/Weeps model shows considerably more fast flow through the fractures. Over 50 percent of the particles arrive at the water table before 1 year, and the majority of the remaining particles do not arrive until after several hundred years.

These mountain-scale flow results indicate that net infiltration and fracture-matrix partitioning of flow have a significant influence on the percolation flux and groundwater travel times in the unsaturated

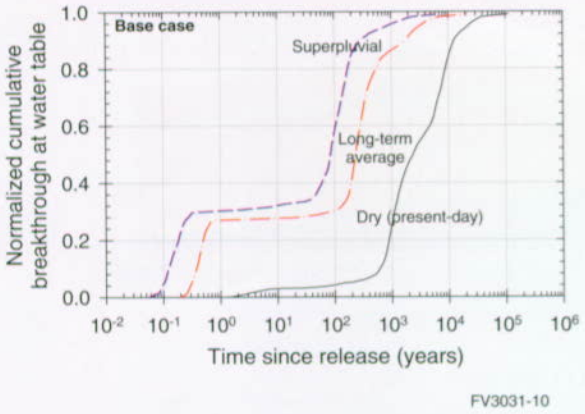

Figure 3-10. Breakthrough Curves for Three Climate States

Comparison of travel times of a hypothetical unretarded tracer, released uniformly over the area representing the repository and traveling from the repository to the water table. Breakthrough curves representing arrival times of the tracer at the water table are given for the three climate states using mean infiltration, base case hydrologic properties, and no dispersion or matrix diffusion.

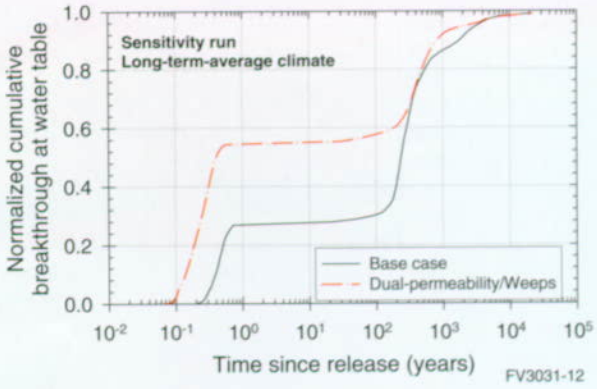

Figure 3-12. Comparison of Base Case and Dual-Permeability/Weeps Model

Comparison of travel times of a hypothetical unretarded tracer, released uniformly over the area representing the repository and traveling from the repository to the water table. Breakthrough curves representing arrival times of the tracer at the water table are given for two alternative hydrologic-property sets using long-term average climate, mean infiltration, and no dispersion or matrix diffusion.

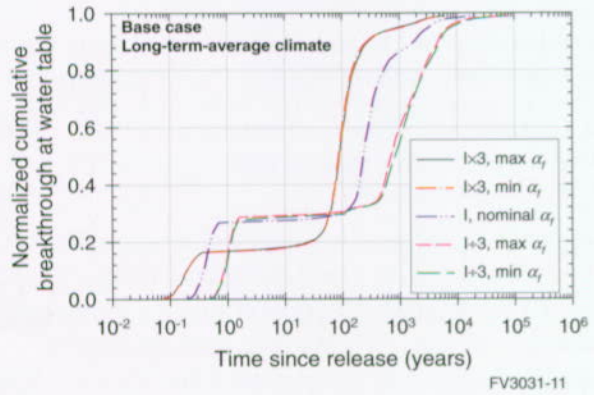

Figure 3-11. Breakthrough Curves for Five Base Case Property Sets

Comparison of travel times of a hypothetical unretarded tracer, released uniformly over the area representing the repository and traveling from the repository to the water table. Breakthrough curves representing arrival times of the tracer at the water table are given for the five base case hydrologic-property sets using long-term average climate and no dispersion or matrix diffusion. The effects of varying infiltration rates and hydrologic properties can be seen by comparison of the curves.

zone. The amount of percolation flux at the repository affects performance through seepage and its influence on the engineered systems. Lateral diversion near the perched water has a large effect on the distribution of percolation flux at the water table, which subsequently affects the distribution of radionuclides at the water table. Note that changes in the distribution of radionuclides at the water table will only affect repository performance to the extent that saturated zone travel times or concentrations are different for the different locations (see Section 3.7).

A range of infiltration rates in present-day and future climate scenarios have been considered that give a broad distribution of travel times, and alternative conceptual models (e.g., the dual-permeability/Weeps model) have been considered that provide a range of fracture-matrix partitioning of flow. By this means, uncertainty in mountain-scale flow simulations for the unsaturated zone has been captured, while retaining the realism inherent in the three-dimensional, site-scale flow model for the unsaturated zone.

3.1.3.3 Seepage into Drifts

Figure 3-13 shows the final result of the seepage modeling. On the top is a graph illustrating the distribution of seepage fraction, or fraction of waste packages contacted by seeps. On the bottom is a graph illustrating the distribution of seep flow rate, which is the rate of water flow onto a waste package that is contacted by seeps (the sum of the flows if contacted by more than one). Each graph shows a curve representing the mean value as a function of fracture percolation flux (only the fracture component of percolation flux is used in calculating seepage because matrix flow is not expected to seep into openings). In addition, curves at the 5th and 95th percentiles of the distributions are shown, to indicate the width of the uncertainty band around the mean. With the assumptions that have been made for this TSPA, there is a great deal of uncertainty about seepage, particularly in the fraction of waste packages contacted by seepage. The wide range of seepage fraction results because some combinations of the parameters shown in Table 3-7 cause a relatively large amount of seepage in the three-dimensional process model (especially low values of mean fracture permeability combined with large values of fracture air-entry parameter), while other combinations cause relatively little seepage in the model (especially large values of mean fracture permeability combined with low values of fracture air-entry parameter). If some of the combinations could be ruled out, perhaps with additional data collection or analysis, the uncertainty range could be narrowed. With additional work, it may be possible to rule out some combinations based on correlations between fracture permeability and fracture air-entry parameter (theoretically, they are both related to fracture aperture).

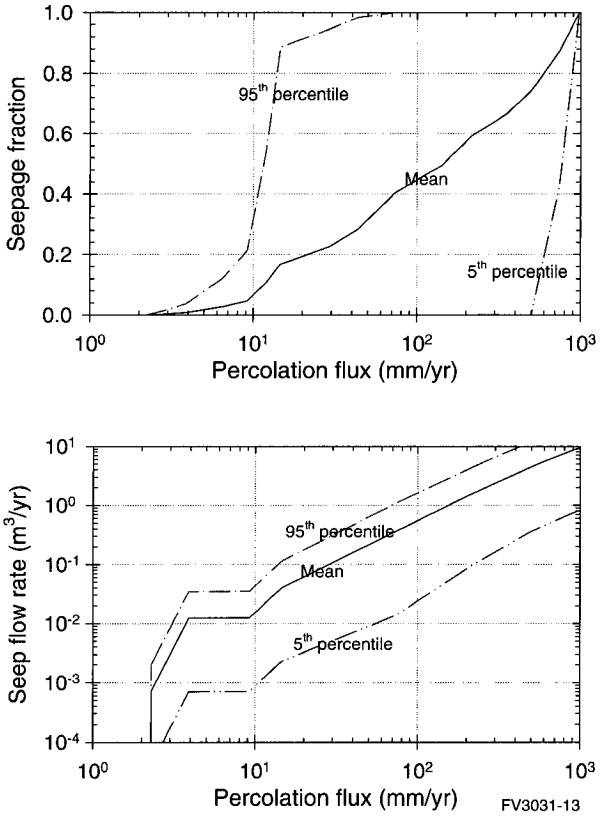

Figure 3-13. Calculated Seepage Fraction and Seep Flow Rate as Functions of Percolation Flux
Shown are the 5 percent, mean, and 95 percent values of the distributions from which the seepage parameters are sampled.

3.2 THERMAL HYDROLOGY

Thermal hydrology refers to the study of the effects of heat on hydrology. The Yucca Mountain repository will hold radioactive wastes that emit a large amount of heat from radioactive decay. This heat will influence conditions in the emplacement drifts (near-field conditions) and away from the drifts (far-field conditions). The thermal disturbance to the mountain will depend on how much waste is placed, or loaded, within a given repository area and the heat output of the waste. The areal mass loading for the reference design is specified as 85 metric tons of uranium (MTU)[1] per acre, which has an initial heat output of approximately 100 kW/acre. This loading will cause a significant disturbance in the repository environment for thousands of years after waste emplacement.

[1] The acronyms MTU and MTHM are equivalent for the once-through nuclear fuel cycle (no reprocessed fuel) and can be used interchangeably. MTHM, metric tons heavy metal, is the total amount of heavy metal initially contained in nuclear fuel. For reprocessed nuclear fuels; the initial heavy metal loading contains both uranium and plutonium. For once through nuclear fuels, the initial heavy metal loading consists of only uranium. Thus, for the United States nuclear industry, which uses a once-through fuel cycle, metric tons heavy metal equals metric tons uranium (MTHM = MTU).

The unsaturated zone at the Yucca Mountain site contains in situ water and gas within the pores that will react to the heat generated by radioactive waste. In general, the influence of radioactive decay heat includes vaporization of in situ liquid water, transport of water vapor away from the heat source, condensation of water vapor in cooler regions, and condensate flow driven by gravity and capillary forces. Thermal gradients affect gas and liquid flow in the rock matrix and in fractures, and flow between fractures and matrix. The decay-heat characteristics of the individual waste packages strongly affect the emplacement-drift thermodynamic environment (temperature and relative humidity, partitioning of water between liquid and steam, and flow of water into or out of the drift). The resulting thermodynamic conditions will affect the performance of the repository, particularly of the engineered barrier system, by influencing all of the near-field components of the TSPA-VA.

After waste emplacement, heat will flow from the repository by conduction through the rock and by advection, which means by movement with the gas and water. Through these processes, there will be movement of water vapor, liquid water (both ambient percolating water and heat-mobilized condensate), and heat. Heating will result in elevated temperatures and drying in both the surrounding host rock and regions well away from the repository. The progression of thermal-hydrologic processes through time is pictured in Figure 3-14. Thermally driven mechanical and chemical processes can potentially cause permanent changes to the fluid-flow characteristics of the entire mountain (for example, by changing permeability and porosity).

Thermal-hydrologic processes occur at two important scales: that of the emplacement drifts (a few meters to tens of meters) and that of the mountain (hundreds of meters to thousands of meters). Thermal-hydrologic processes at the drift scale include waste package interactions with other waste packages and the surrounding drift walls and floor. Thermal-hydrologic processes at the mountain scale include the influence of heat on liquid and gas movement above and below the repository. Some of the important processes are illustrated in Figure 3-15. The "drift-scale" thermal-hydrologic model includes processes at both drift and mountain scales; it provided information to the models of the near-field geochemical environment, waste package degradation, waste form degradation and radionuclide mobilization, and transport of radionuclides within the engineered barrier system. A separate mountain-scale model provided information to models of the near-field geochemical environment (Figures 3-16 and 3-17). Thermal-hydrologic processes at both the drift and mountain scales affect fluid flow and transport in the unsaturated zone; however, for the TSPA-VA it was assumed that there will not be permanent alteration of the hydrologic properties because of thermal-hydrologic-mechanical or thermal-hydrologic-chemical processes and thus the influence of thermal-hydrologic processes would be short-lived. With this assumption, thermal disturbances to seepage into drifts and radionuclide transport from the repository to the water table would only be important during the early period when no waste packages have failed, except for possibly a few juvenile failures. Therefore, thermal effects on seepage and radionuclide transport were neglected.

The thermal-hydrologic modeling studies and sensitivity analyses presented in this section were prepared with the view of addressing selected aspects of the NRC Key Technical Issue on Thermal Effects on Flow (NRC 1997b). Specifically, the information presented is pertinent to two of the three subissues of this key technical issue, namely, sufficiency of thermal-hydrologic modeling to predict the nature and bounds of thermal effects on flow in the near-field and adequacy of total system performance assessment with respect to thermal effects on flow.

Sections 3.2.1 and 3.2.2 summarize the processes, assumptions, and implementation of the thermal-hydrologic models used in the TSPA-VA. Section 3.2.3 presents results from the models and related interpretations. Additional information on the thermal-hydrologic component can be found in Chapter 3 of the *Total System Performance Assessment-Viability Assessment (TSPA-VA) Analyses Technical Basis Document* (CRWMS

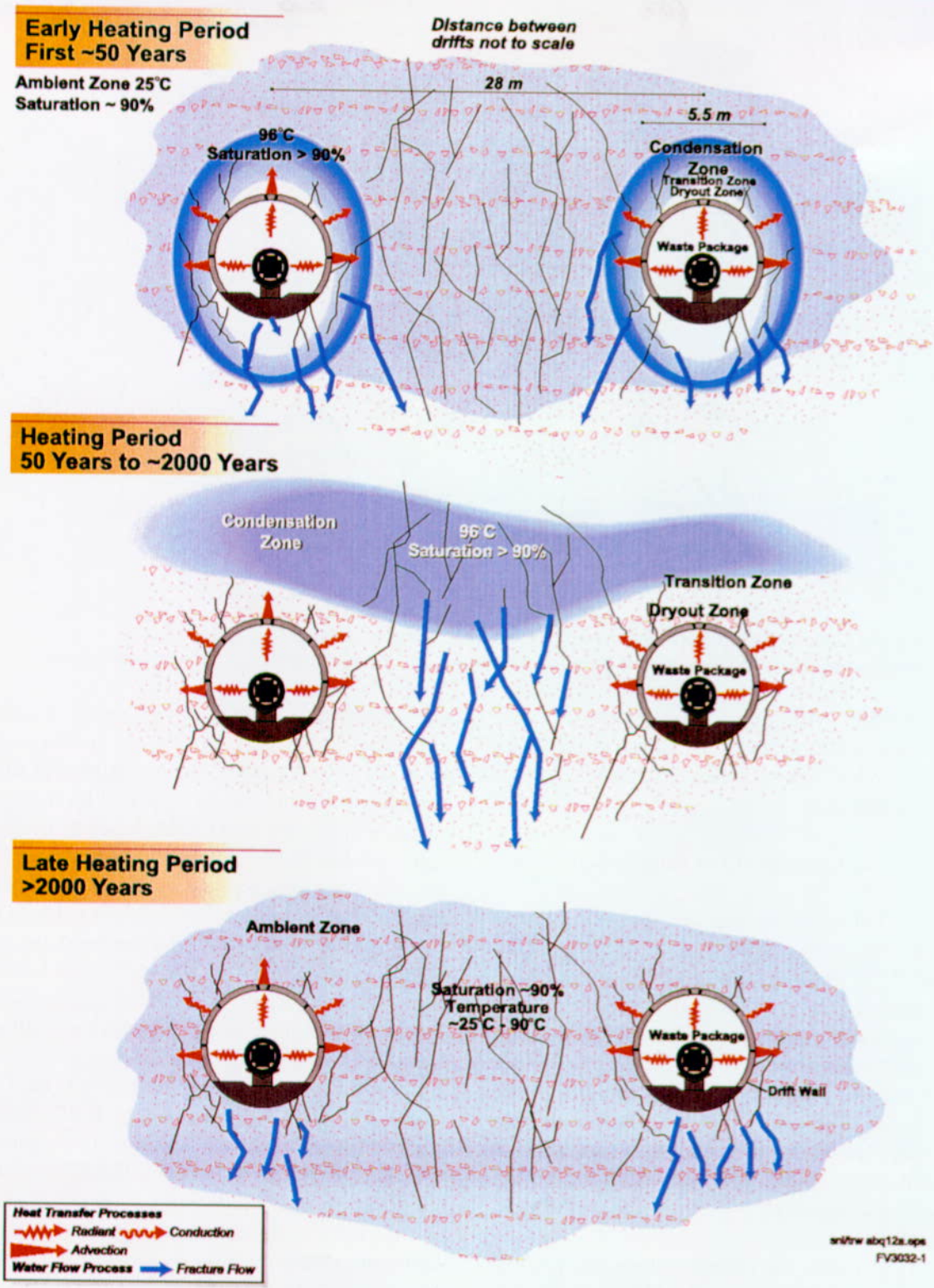

Figure 3-14. Conceptual Drawings of Thermal-Hydrologic Processes at Three Stages
Heat drives water away from the drifts; water vapor condenses in cooler rock. The condensation zone moves away from the drifts initially, and eventually returns toward the drifts. At all stages water movement in fractures is important.

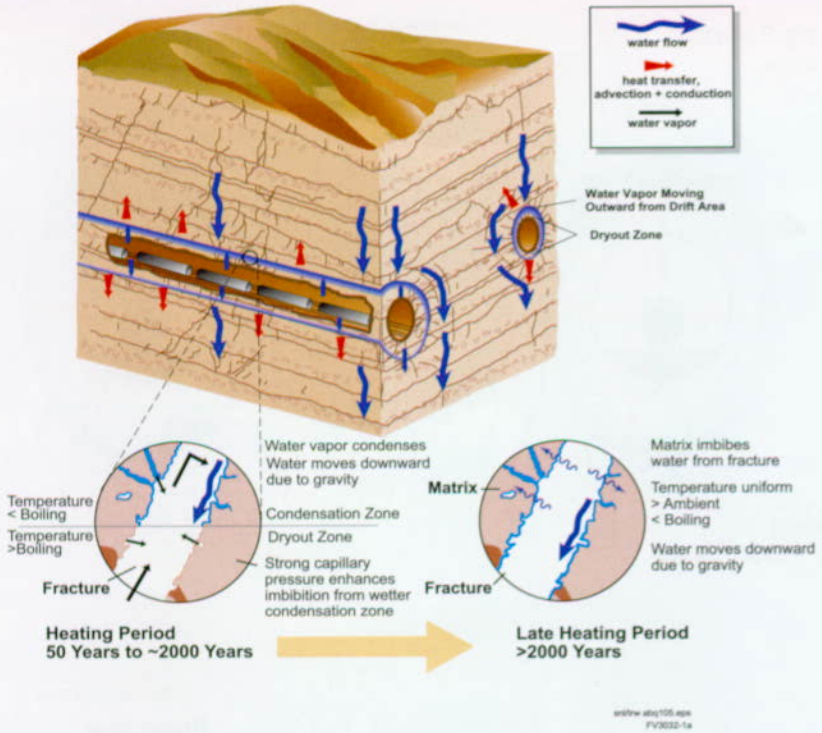

Figure 3-15. Conceptual Diagram Illustrating Flow of Liquid Water and Water Vapor in Fractures
Condensation of vapor and imbibition of water from fractures into the rock matrix are important processes.

M&O 1998i). Additional information on YMP thermal hydrology can also be found in the *Yucca Mountain Site Description* (CRWMS M&O 1998m, Chapter 7).

3.2.1 Construction of the Conceptual Model

Previous TSPAs have included the influence of thermal effects on predictions of radionuclide releases from the repository and subsequent doses to the public. Many of the model assumptions and simplifications in previous TSPA thermal analyses have been improved for the TSPA-VA. These improvements include assumptions about dimensionality and the conceptual flow model for heat and mass transfer. In addition, many recently acquired thermal and hydrologic data have been used in the TSPA-VA.

In the 1993 TSPA, thermal-hydrologic calculations used a model based solely on conduction (Wilson et al. 1994, pp. 10-1 to 10-36). Drift-scale and mountain-scale calculations used three-dimensional models for two different initial thermal loads. The two thermal-load values (heat generated per repository area), were 57 and 114 kW/acre. Effects on the repository-system hydrology (for example, the extent of rock drying) were inferred from the distance and location of the region where pore water is expected to boil. This approach has limited applicability because it does not explicitly couple heat transfer to fluid flow. Without this coupling, the nature of dry-out and condensation zones may not be properly represented (see Figure 3-15).

In the 1995 TSPA, drift-scale thermal-hydrologic calculations used a two-dimensional model for areal mass loadings of 25 and 83 MTU/acre (CRWMS M&O 1995, pp. 4-1 to 4-39). The calculations were based on the equivalent-continuum model assumption for heat and fluid flow (that is, hydraulic properties of both fractures and rock matrix were combined into a single equivalent continuum). Net infiltration rates of 0.05 and 0.3 mm/year (0.002 and 0.01 in./year) were modeled for a homogeneous, layered system. This modeling was limited because it did not allow for variations in waste package contents or the development of large-scale features such as preferential

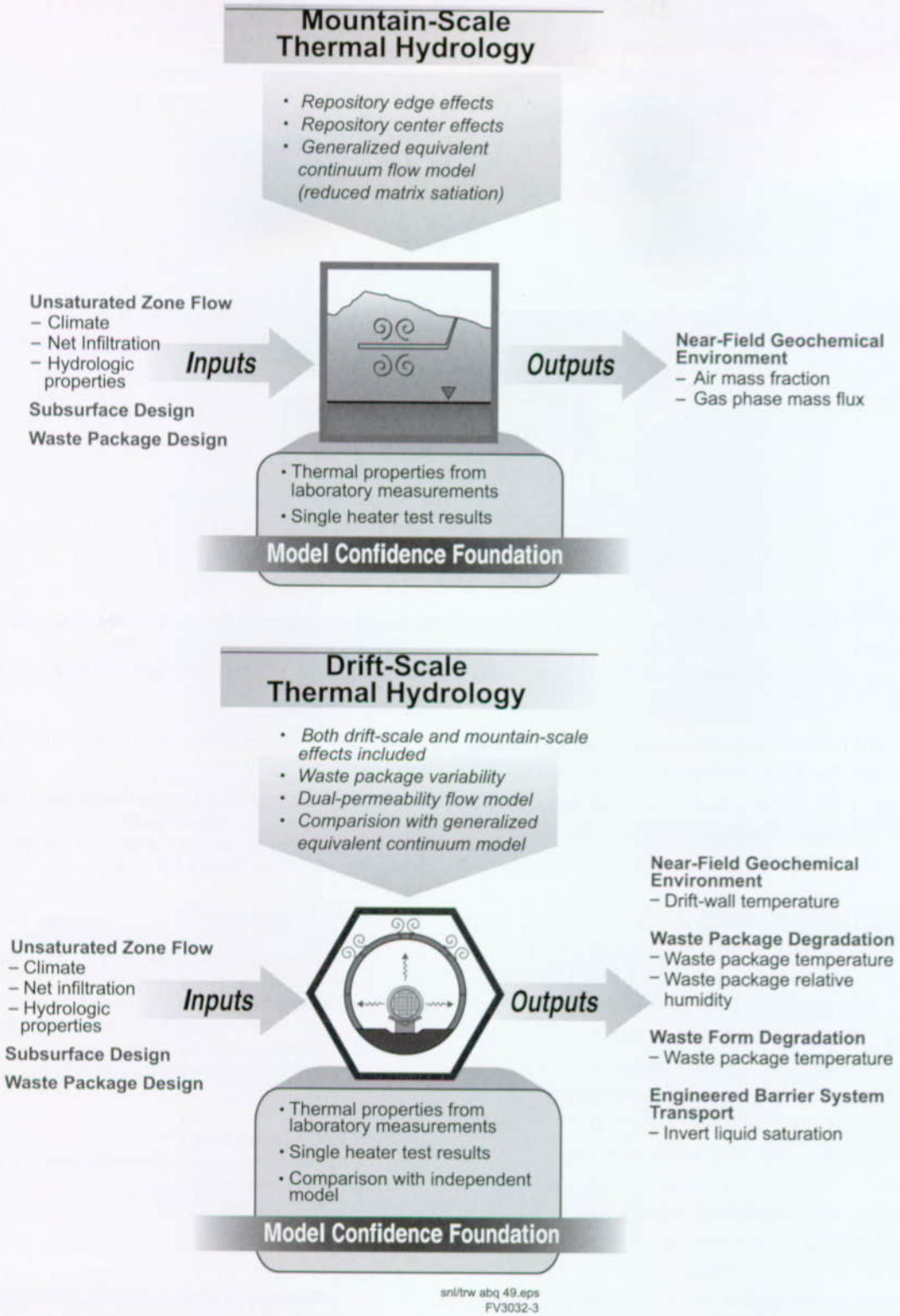

Figure 3-16. Coupling of Thermal Hydrology to Other Total System Performance Assessment for the Viaiblity Assessment Components
The "drift-scale" model is actually a multiscale abstraction that takes into account both drift-scale and mountain-scale processes.

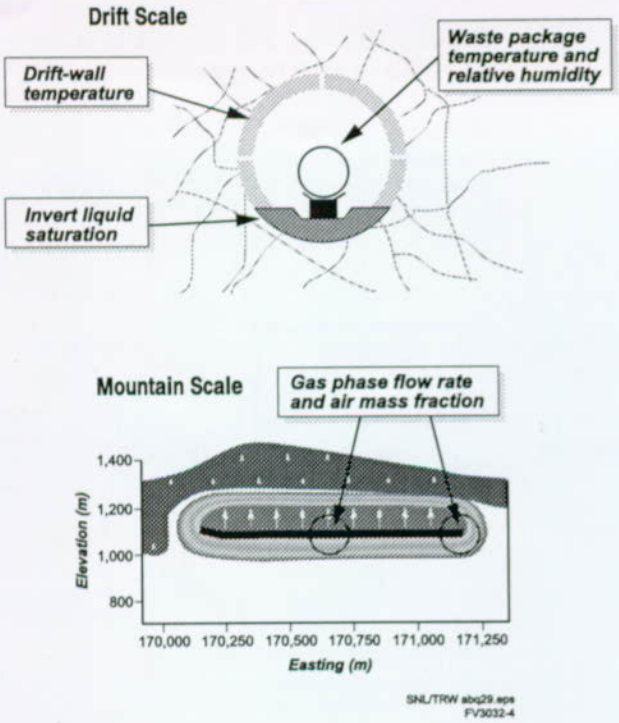

Figure 3-17. Quantities Passed to Other Total System Performance Assessment for the Viability Assessment Components
This figure shows the locations of the important parameters calculated by the mountain-scale and drift-scale models.

cooling around the repository edges or gas-phase convection. The calculations were also based on a conceptual flow model that restricted the amount of flow through fractures during the thermal period.

Thermal-hydrologic models for the TSPA-VA were improved over earlier efforts because of benefits derived from recommendations of the Thermohydrologic Modeling and Testing Program Peer Review (CRWMS M&O 1996e), the YMP thermal testing program, and faster computers. Specific improvements have been made to conceptual flow models, hydrologic and thermal property values, model dimensionality, and infiltration rates.

A key effort in formulating models for this TSPA was a workshop convened by the performance-assessment group in January 1997. Workshop participants developed a list of issues and prioritized them based on criteria for long-term repository performance (Table 3-8). Workshop participants determined that conceptual models allowing for more flow through fractures, in particular

Table 3-8. Thermal Hydrology Abstraction/Testing Workshop

THERMAL HYDROLOGY ABSTRACTION/TESTING WORKSHOP
January 21–23, 1997, Albuquerque, NM
(CRWMS M&O 1997l)

PRIORITIZATION CRITERIA
- Does the process/issue affect the magnitude, spatial distribution, or temporal variation of
  - Waste package temperature?
  - Relative humidity around a waste package?
  - Liquid water flow rate into the drift environment and onto a waste package?
  - Aqueous flow from the repository to the saturated zone?

HIGHEST PRIORITY ISSUES
- Thermal-hydrologic processes and parameters
- Mountain-scale models
- Drift-scale models
- Coupled processes

ANALYSIS PLANS
- Mountain-scale thermal-hydrologic abstraction and testing plan
- Abstracting drift-scale temperature, relative humidity, liquid saturation, and liquid-phase flux as a function of location in the repository
- Thermal-hydrologic modeling of seepage into drifts
- Coupled processes abstraction and testing plan

during the thermal periods (Figure 3-14), would be the most appropriate. The available conceptual models for increased fracture flow are the generalized equivalent-continuum model and the dual-permeability model (see Section 3.1.1.3). The dual-permeability model gives a more realistic description of a thermally driven system and ensures consistency with flow models for the unsaturated zone (see Section 3.1.1.3). More movement of water through fractures allows condensate or reflux waters mobilized by heat (and ambient percolation) to drain through fractures either back toward the drifts or through the pillars separating drifts.

The workshop participants also considered "coupled processes," or the coupled effects of temperature, hydrology, mechanics, and chemistry. When heated, the rock around the emplacement drifts will expand. This thermal expansion will cause fractures to open and close, which in turn will change the permeability and porosity of the rock and affect movement of gas and liquid. These changes will last only while the rock is heated. In addition, the thermal stresses can potentially cause rock blocks to move and new fractures to form, which again can affect permeability, porosity, and fluid flow. Unlike the simple thermal-expansion effects, these changes to the rock hydrologic properties can be permanent. All of these effects are called thermal-hydrologic-mechanical coupled processes. Heating also can cause chemical changes in the host rock, such as mineral dissolution in some regions and mineral precipitation elsewhere. Mineral dissolution and precipitation can potentially alter the hydrologic properties of the rock permanently, which would in turn alter fluid flow. These effects are referred to as thermal-hydrologic-chemical coupled processes. Based on thermal-hydrologic workshop discussions, some limited follow-up studies of coupled processes were completed.

Preliminary thermal-hydrologic-mechanical modeling (Ho and Francis 1998) was done with a one-dimensional, dual-permeability model at the mountain scale. This modeling indicated that the liquid-phase flow fields are essentially unaffected by non-permanent increases or decreases of a factor of ten in permeability. Based on this modeling, thermal-hydrologic-mechanical alteration of the flow field is considered negligible.

Preliminary thermal-hydrologic-chemical modeling (summarized in CRWMS M&O 1998i, Section 3.6.8.2; CRWMS M&O 1998c) studied silica within the fracture system in the unsaturated zone. This fully coupled thermal-hydrologic-chemical study was at the drift scale and included reactions for silica-cristobolite-quartz in the system. Changes in fracture and matrix porosity (which also affect permeability) caused by mineral dissolution and precipitation were calculated. Waste package temperature and relative-humidity time histories were not greatly affected by the reactive-transport processes included in the simulation, even though a mineral cap formed above the drifts. However, the effects of a mineral cap above the drift on seepage flow into the drift have not been fully investigated. Because of its complexity, the work that has been done so far only represents a start on addressing the uncertainties associated with thermal-hydrologic-chemical effects.

The near-field environment expert elicitation (CRWMS M&O 1998d) was established to help quantify the large uncertainties associated with thermal-hydrologic-mechanical and thermal-hydrologic-chemical processes. The panel was tasked to consider how these processes occur, both temporally and spatially, and over what range of values the hydrologic properties (for example, fracture permeability) may be influenced.

The elicitation panel examined recent YMP process models and experimental data on coupled processes from the single heater test. They considered thermal-hydrologic-mechanical and thermal-hydrologic-chemical processes, potential changes to hydraulic interactions between fractures and the rock matrix, and effects of rockfall. The panel found that fracture-permeability changes might occur in both the vertical and horizontal directions and in condensate and boiling zones. According to the experts, fracture permeability in the vertical direction can either decrease by 10 to 100 times or increase by 10 to 1,000 times, depending on location and other factors. Fracture

permeability in the horizontal direction may increase by no more than 10 times. Based on the results of the elicitation, the potential for thermally driven alteration of fracture properties (for example, permeability) falls within the range of the natural spatial variability of the system. However, an overall decrease of rock-mass permeability could result. The panel concluded that the mechanical effects would tend to be reversible upon cooling, with the possible exception of horizontal changes in permeability caused by shear stress, but that chemical effects will be more permanent. The panel indicated that the fracture-matrix interaction parameter (see Section 3.1.2.3) used in the dual-permeability models may also be affected because of chemical precipitation or dissolution. Although this effect may be permanent, the magnitude of such changes is uncertain.

Thermal-hydrologic-mechanical and thermal-hydrologic-chemical processes are not included in the base case for this TSPA. Based on the expert-elicitation results and the preliminary modeling studies, it is likely that thermal-hydrologic-mechanical effects are not significant; however, the significance of thermal-hydrologic-chemical effects is more uncertain. In addition, changes to the thermal hydrology caused by drift collapse (and the resultant filling of the drift with rockfall rubble) are not considered in this TSPA.

3.2.2 Implementation of the Performance Assessment Model

As discussed earlier, thermal-hydrologic processes occur on two important scales, drift scale and mountain scale, each passing different information to the other TSPA-VA components (Figure 3-17). The key issues discussed in Section 3.2.1 determined the form of the models developed for thermal-hydrologic analyses. Section 3.2.2.1 describes the reference design, Section 3.2.2.2 describes implementation of the drift-scale model, and Section 3.2.2.3 describes implementation of the mountain-scale model.

3.2.2.1 Repository and Waste Package Design

Thermal-hydrologic models require specific repository subsurface design and waste package design information. This information includes waste package geometry and decay heat outputs, emplacement drift geometry and layout configuration, and waste stream information including total thermal loading.

The total mass of commercial spent nuclear fuel to be emplaced at Yucca Mountain is 63,000 MTU (CRWMS M&O 1997c, p. 3-14). This mass includes several waste package types of different initial heat outputs (CRWMS M&O 1997e, pp. 45 and 55). Emplacement of about 7,650 commercial spent nuclear fuel waste packages is expected. It is not expected that additional area will be needed for emplacing wastes such as high-level-radioactive waste glass and DOE spent nuclear fuel. The waste packages containing these additional wastes will be placed between the commercial spent nuclear fuel waste packages, with a requirement of at least 1 m (3.28 ft) of separation between waste packages. The total emplaced mass of the expected 2,550 additional waste packages will be 7,000 MTU (2,333 MTU of DOE spent nuclear fuel and 4,667 MTU of high-level radioactive waste glass). These waste packages will include co-disposal waste packages (that is, two types of waste in the same waste package) and waste packages for separate disposal of DOE spent nuclear fuel. The co-disposal waste packages will contain both high-level-radioactive waste glass and DOE spent nuclear fuel; the separate-disposal waste packages will contain only DOE spent nuclear fuel.

The reference-design mass loading of 85 MTU/acre (CRWMS M&O 1997g, p. 23) includes only the amount of commercial waste; DOE spent nuclear fuel and high-level radioactive waste glass are not counted when calculating the mass loading. The reference design specifies point-loading emplacement, meaning that the waste packages are far enough apart that there is little direct thermal communication between packages. A point-loaded drift segment loaded with all three waste package

types (commercial spent nuclear fuel, co-disposal, and separate-disposal) is illustrated in Figure 3-18.

The reference repository design specifies that the emplacement drifts are to contain no backfill. The waste packages are to be placed on carbon steel supports compatible with the waste package outer-barrier composition, on top of and supported by a concrete pier on top of a concrete invert floor (concrete segments put in the bottom of the round emplacement drift to provide a level floor). The thermal-hydrologic calculations for the base case use these design conditions.

Design options are under evaluation that include use of backfill. Design options and alternative design concepts under evaluation that may enhance repository performance are discussed in Section 4.5 and Volume 2, Sections 5.3 and 8.

3.2.2.2 The Drift-Scale Model

Output from the drift-scale analyses includes waste package surface temperature and relative humidity, and drift-wall and invert-floor temperature and liquid saturation. Time histories of these quantities are used in analyses of the engineered barrier system.

Drift-scale modeling must include coupling of drift-scale processes with mountain-scale processes to properly account for effects such as faster cooling of waste packages near the edge of the repository as compared to waste packages near the repository center. A multiscale modeling and abstraction method was developed to couple drift-scale processes with mountain-scale processes. This method uses a series of four mountain-scale and drift-scale submodels to abstract the thermodynamic environment within emplacement drifts throughout the repository area (Figure 3-19). The four submodels are described in the following paragraphs.

Line-Averaged-Heat-Source, Drift-Scale, Thermal-Hydrologic Submodel. The line-averaged-heat-source, drift-scale, thermal-hydrologic submodel is a two-dimensional drift-scale model that computes average temperature and relative humidity at the drift wall and liquid saturation of the drift invert. This submodel effectively represents average thermal-hydrologic behavior at any

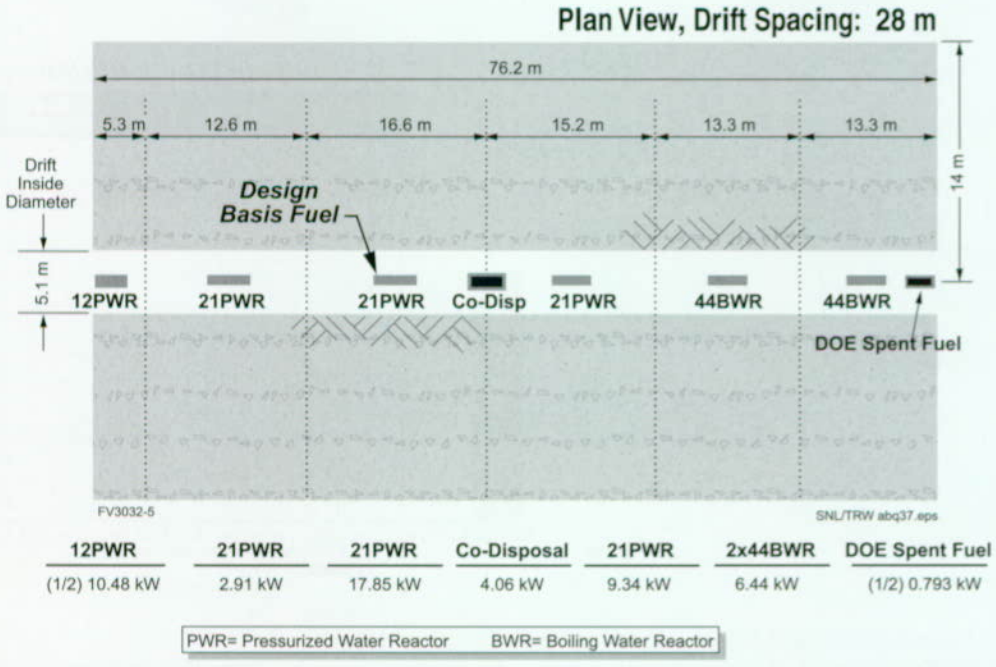

Figure 3-18. Plan View of a Typical Emplacement-Drift Segment for Drift-Scale Thermal-Hydrologic Analyses Heat output is shown for each waste package. The drifts are 28 m (92 ft) apart, center-to-center.

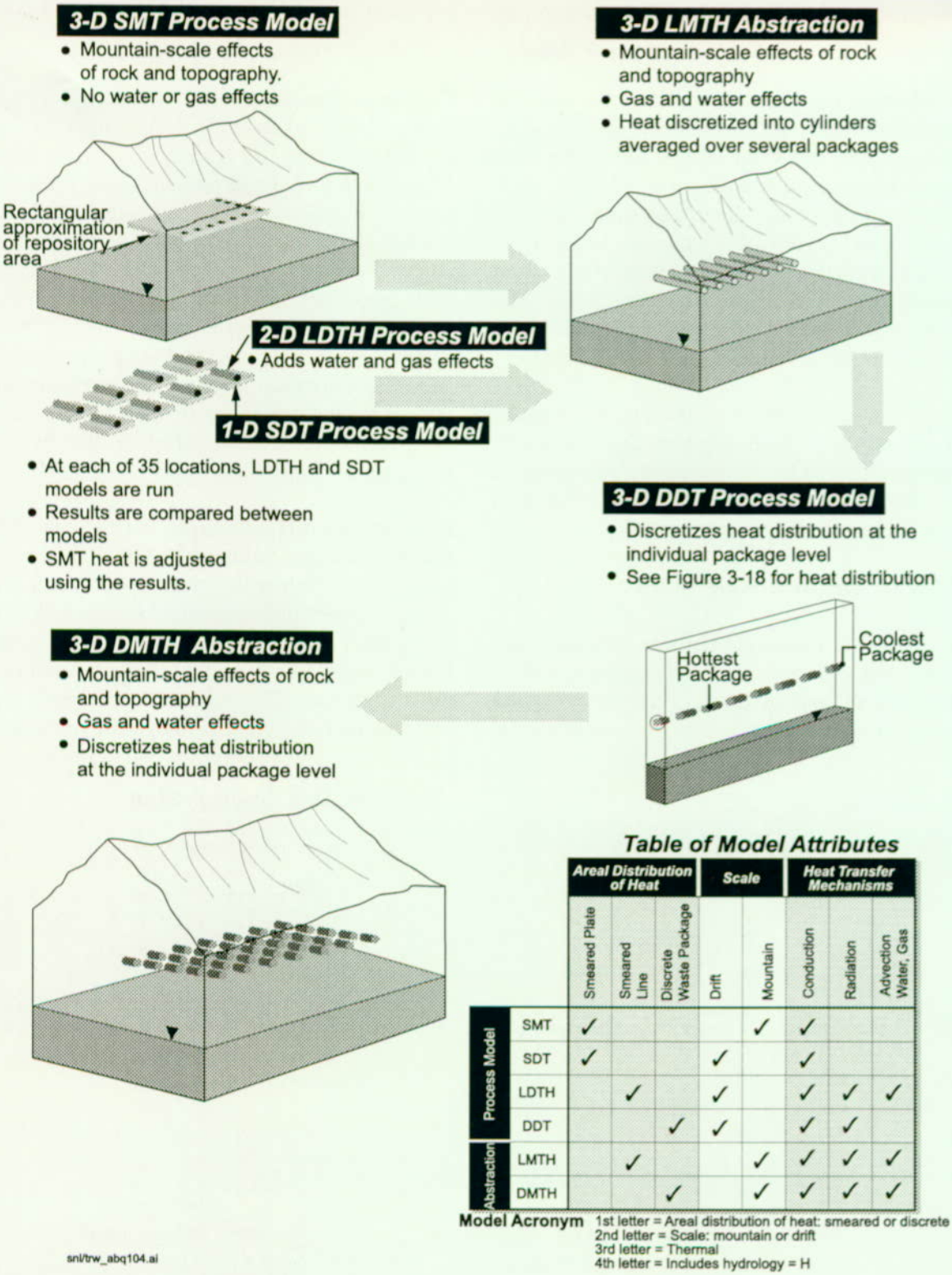

Figure 3-19. Illustration of the Multiscale Modeling and Abstraction Method
Four models at different levels of abstraction are combined to produce the final abstracted model, which then effectively includes both drift-scale and mountain-scale effects.

specific location within the repository, taking into account the location-specific thermal and hydrologic properties, boundary conditions, and percolation flux. Heat and fluid flow are modeled as dual-permeability, consistent with the mountain-scale unsaturated zone flow model (Section 3.1.1.3). Radiant heat transfer within open drifts is also modeled. This submodel addresses key issues related to modeling of fracture and matrix interactions for fluid and heat flow. It also addresses the issue of the appropriate scale of fracture properties and thermal-hydrologic processes by using hydrologic properties developed for mountain-scale flow by inversion models. Consistency with the mountain-scale unsaturated zone flow model ensures that hydrologic conditions are properly accounted for, including variability of infiltration with location and changes of infiltration with climate.

Smeared-Heat-Source, Mountain-Scale, and Smeared-Heat-Source, Drift-Scale, Thermal-Conduction Submodels. Both the smeared-heat-source, mountain-scale, thermal-conduction submodel and the smeared-heat-source, drift-scale, thermal-conduction submodel consider conduction heat transfer only. They are used to establish temperature relationships and to account for the influence of repository edges, topography, and mountain-scale variability in hydrogeologic layering. The smeared-heat-source, mountain-scale submodel is a three-dimensional model that includes the appropriate stratigraphy, topography, and repository location and extent. The smeared-heat-source, drift-scale submodel is a one-dimensional model. These two submodels address key issues related to the differences between repository center and edge locations by coupling the drift-scale submodels with the mountain-scale submodel. The coupling uses the average temperatures of repository host rock obtained from the smeared-heat-source, mountain-scale submodel, corrected for hydrology using a relationship derived from the line-averaged-heat-source, drift-scale submodel and the smeared-heat-source, drift-scale submodel. The resulting "modified" temperatures inherently include repository edge effects because they originated from a full mountain-scale model. The temperature prediction also includes the effects of the system fluid components through the temperature relationship between the two drift-scale submodels. This results in an "abstracted" drift-wall temperature that approximates the effects of the most important thermal-hydrologic processes. A similar procedure provides an abstracted relative humidity at the drift wall.

Discrete-Heat-Source, Drift-Scale, Thermal Submodel. The abstracted drift-wall quantities are further modified at the drift wall and at the waste package surface using waste-package-specific deviations computed by the discrete-heat-source, drift-scale, thermal submodel. This submodel provides temperatures and relative humidities for different waste packages along the drift. The discrete-heat-source, drift-scale submodel is a three-dimensional model of a drift segment containing eight representative waste packages of varying heat outputs (Figure 3-18). This submodel includes only conductive heat transfer, plus radiant heat transfer within open drifts. It accounts for variability in temperature and relative humidity among packages along the drifts, which is another of the key issues from the thermal-hydrologic workshop (Section 3.2.1). One limitation of the analyses is that only one type of separate-disposal waste package was modeled. The heat output listed in Figure 3-18 for the separate-disposal package is appropriate for a waste package containing N-Reactor fuel. Some types of DOE spent nuclear fuel are cooler and some are hotter. N-Reactor fuel was modeled because it represents nearly 90 percent of the total MTU of DOE spent nuclear fuel (see Section 3.5.1.5). The inconsistency of using near-field thermal conditions for N-Reactor fuel to represent all types of DOE spent nuclear fuel could affect the release calculations for the other fuel types, but the effect is moderated by the long waste package life (differences in waste package conditions are greatest at early times). In addition, the heat from the naval-spent-fuel component is represented by the 44-assembly boiling-water-reactor waste packages in the modeled drift segment. The 44-assembly boiling-water-reactor allotment in the drift segment is over-represented by about 0.8 percent to account for the naval spent nuclear fuel.

The multiscale modeling and abstraction method involves calculations at a number of repository locations. A repository-wide set of calculations for a given case involves only one computer run using the mountain-scale submodel and only one computer run using the discrete-heat-source, drift-scale, thermal submodel. However, the line-averaged-heat-source, drift-scale, thermal-hydrologic submodel and the smeared-heat-source, drift-scale, thermal submodel are run for 35 locations within the repository and for three different local heating rates. The results of these 105 submodel runs are interpolated over the repository area and as a function of local heating conditions to provide a continuous distribution of the drift-scale thermal-hydrologic variables throughout the repository area. The abstracted temperature and relative humidity are calculated for an array of 425 repository locations, giving reasonable resolution for mountain-scale topographic and stratigraphic effects.

This procedure provides too much information for the near-field TSPA components. Because resource demands increase considerably as the number of waste package groups modeled within RIP (the top-level TSPA program, see Section 2.3) increases, six repository regions were defined for modeling the near-field, as shown in Figure 3-20. The regions were selected to limit variability of net infiltration within the regions, although there is still considerable variability (see Figure 3-8). The regions also represent a range of geometric relations, with Region CC being the region most like the repository center and Region SW being most like the edge. Lastly, the regions represent the variation of hydrogeologic properties around the repository. The reference repository cuts across three hydrogeologic units, the Topopah Spring middle nonlithophysal, lower lithophysal, and lower nonlithophysal units. Region SW is mostly in the lower nonlithophysal; Regions NW, NE, CC, and SC are mostly in the lower lithophysal; and Region SE is mostly in the middle nonlithophysal.

This complex modeling process includes multiple scales (mountain and drift), multiple dimensions

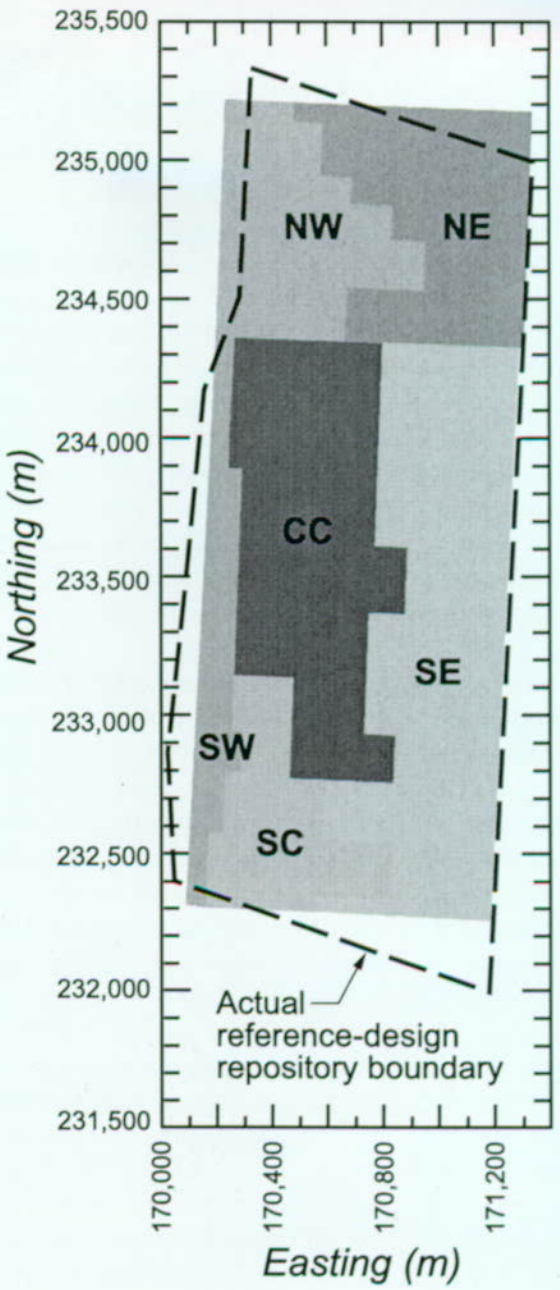

SNL/TRW abq38.eps
FV3032-7

Figure 3-20. Division of the Repository Area into Six Subregions
The dashed line shows the actual reference-design repository boundary; the solid lines show the idealization of the repository by a rectangle and the six regions used for averaging thermal-hydrologic data. Averaging data values in six zones is an enhancement over averaging data over the entire repository area.

(one-, two-, and three-dimensional models), and varying assumptions regarding the coupling of heat transfer to fluid flow (conduction only and full thermal-hydrologic). To provide greater confidence that this abstraction method adequately represents the thermal-hydrologic behavior of Yucca Mountain, an independent model was also developed. This model incorporates three-dimensional, fully coupled heat transfer and fluid flow but uses a less mechanistic conceptual flow model (generalized equivalent-continuum rather than dual-permeability) and a less sophisticated coupling between drift scale and mountain scale. It uses data from mountain-scale thermal-hydrologic models to approximate edge effects. The computational requirements of the verification model do not allow the many abstraction simulations that are required for a total-system calculation. However, this type of model provides an important check on the abstraction processes. Good agreement was found when the independent modeling approaches were compared at repository center and edge locations. This analysis addresses the key issue of tradeoffs between model dimensionalities. This comparison shows that the combination of one- or two-dimensional models with reduced complexity in heat-transfer models suffices for determining near-field responses associated with waste package heating. This simplicity provides flexibility in producing the many simulations required.

3.2.2.3 The Mountain-Scale Model

Mountain-scale thermal-hydrologic models are used to calculate quantities associated with larger scales, such as air mass fraction and gas-phase fluxes. The thermal-hydrologic multiscale modeling and abstraction method is unable to account for gas-phase advection from large-scale temperature and pressure gradients because only conduction is included in its mountain-scale submodel. At the mountain scale, gas-flow patterns from repository heating can only be realized with a fully coupled thermal-hydrologic model. The key issue addressed by this model is the movement of gas and liquid through fractures at the mountain scale. A generalized equivalent-continuum flow model was used to determine gas-phase data for the mountain. Use of this model reduces the computational requirements of the larger-scale thermal-hydrologic simulations (as compared to use of the dual-permeability model) while still allowing for sufficient mobility of liquid water in fractures.

A mountain-scale model based on east-west cross sections was used for each of the property sets and associated infiltration rates considered. The mountain-scale model includes large-scale features such as mountain topography and variability by location of the net infiltration rate at the ground surface. It also includes repository edge effects and the ability to develop large-scale fluid-flow processes such as buoyant convection, in which fluid moves in response to a density gradient. The cross sections used to calculate gas flow were taken directly from the mountain-scale unsaturated zone flow model (Section 3.1). The model includes the stratigraphy and hydrologic properties established for the unsaturated zone flow model. The mountain-scale model includes the heat output of the entire repository waste stream (scaled for a two-dimensional application) emplaced at the time of repository closure.

The smeared heat source in the mountain-scale model does not allow for important effects such as shedding of condensate between drifts and it does not capture the difference in thermal-hydrologic behavior in the drifts as compared to in the rock between drifts. Because of these limitations, the mountain-scale model probably underestimates reduction in air mass fraction in the drifts during the thermal period.

3.2.2.4 Uncertainties

Except for uncertainties associated with repository design (for example, thermal loading, the use of backfill, and waste package configurations), the thermal-hydrologic analyses introduce no new important parameter uncertainties to the analyses. The major uncertainties for thermal hydrology have to do with water and gas flow, and the thermal-hydrologic calculations use the same uncertain parameters as the ambient unsaturated zone flow component (Section 3.1). Some of the most important of these uncertainties are in hydro-

logic properties, infiltration rates, and future climate states. Examples of how these uncertainties influence thermal hydrology are shown in Section 3.2.3.

In addition to the neglect of thermal-hydrologic-chemical coupled processes, the most important limitations of the thermal-hydrologic modeling are those discussed in Section 3.1 for unsaturated zone flow, because the hydrology part of thermal hydrology shares most important issues with the ambient hydrology discussed in Section 3.1.

3.2.3 Results and Interpretation

The following selected results illustrate features of the thermal-hydrologic analyses, including effects of variability of waste package heat output and the use of different hydrologic property sets and infiltration rates.

Figure 3-21 shows the variability in average waste package temperature among the six repository regions. The early behavior, when temperature is increasing, is largely influenced by infiltration rates, initial liquid saturation of the host rock, and host-rock thermal properties. During cooldown, faster cooling of regions near the repository edge becomes increasingly noticeable with time.

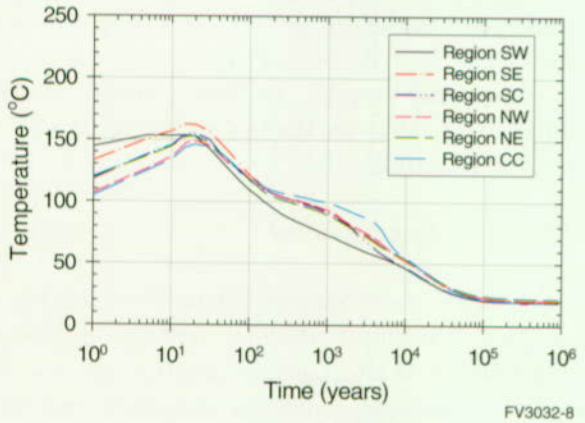

Figure 3-21. Average Waste Package Temperature History for Six Repository Regions
Average waste package temperature history for six repository regions using commercial spent nuclear fuel, long-term average climate, mean infiltration, and base case hydrologic properties.

Region SW cools off the fastest because it is along the repository edge. Region CC cools off the slowest because it is farthest from the repository edges. After 10,000 years, there is little variability among regions.

Figure 3-21 illustrates temperatures calculated for the entire period using the long-term average climate (see Section 3.1), with an average infiltration of about 40 mm/year (1.6 in./year). In reality, the climate model includes cycling between drier (present-day average infiltration of about 8 mm/year, or 0.3 in./year) and wetter (long-term average) climate states. Climate effects on thermal hydrology are included by making two sets of calculations, one with dry climate for the entire period and one with long-term average climate for the entire period. Switching from one set of calculated results to the other at the time of climate change approximates the influence of climate change on thermal-hydrologic behavior. When this approximation was tested against simulations in which infiltration was varied through time, the response to changes in infiltration was found to be fast enough to use the approximation. Results based on long-term average climate are used for illustration because this climate is in effect most of the time. Temperatures for dry climate are slightly higher because lower infiltration results in less influx of cooler infiltrating water. Only the first climate change, between 0 and 10,000 years, is relevant to thermal hydrology. By the time of the second climate change, between 80,000 years and 110,000 years, temperatures and relative humidities will have essentially returned to ambient conditions (climate-change times are summarized in Table 3-4). Although these illustrations are for commercial spent nuclear fuel waste packages, the results for high-level radioactive waste and DOE spent nuclear fuel are similar.

Figures 3-22 and 3-23 show the variability of waste package temperature and relative humidity within one of the repository regions (Region NE). This variability results primarily from the differences in heat output among waste packages and to a lesser extent from differences in infiltration and stratig-

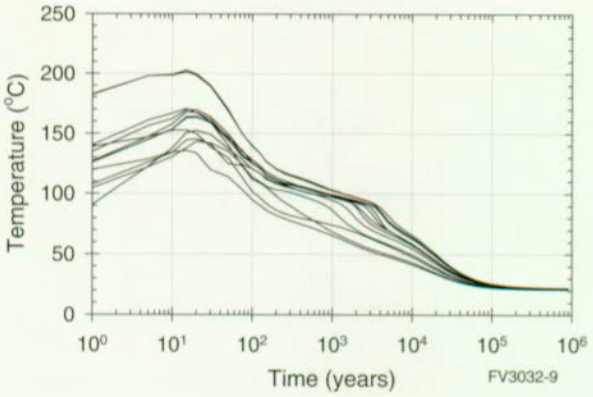

Figure 3-22. Variability of Temperature History Among Waste Packages
Variability of temperature history among waste packages in Region NE (see Figure 3-20) using commercial spent nuclear fuel, long-term average climate, mean infiltration, and base case hydrologic properties.

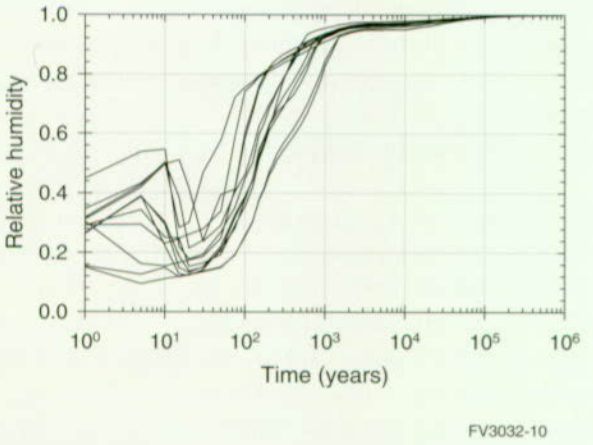

Figure 3-23. Variability of Relative-Humidity History Among Waste Packages
Variability of relative-humidity history among waste packages in Region NE (see Figure 3-20) using commercial spent nuclear fuel, long-term average climate, mean infiltration, and base case hydrologic properties.

raphy within the region. The influence of decay heat is negligible after 100,000 years.

Figure 3-24 shows how average waste package temperature is affected by the uncertainty in unsaturated zone flow incorporated into the base case. The high-infiltration cases (approximately 90 mm/year or 3.5 in./year) have cooler temperatures than the mean-infiltration (approximately 30 mm/year or 1.2 in./year) or low-infiltration (approximately 10 mm/year or 0.4 in./year) cases. This figure shows that the thermal-hydrologic variability associated with infiltration uncertainty dominates the variability associated with hydrologic-parameter uncertainty (represented here by variations in the fracture air-entry parameter α_f, which is proportional to fracture aperture).

Figure 3-25 shows how waste package temperature is affected by additional hydrologic uncertainty beyond that included in the base case. The dual-permeability/Weeps alternative flow model is described in Sections 3.1.1.3 and 3.1.3.3. The

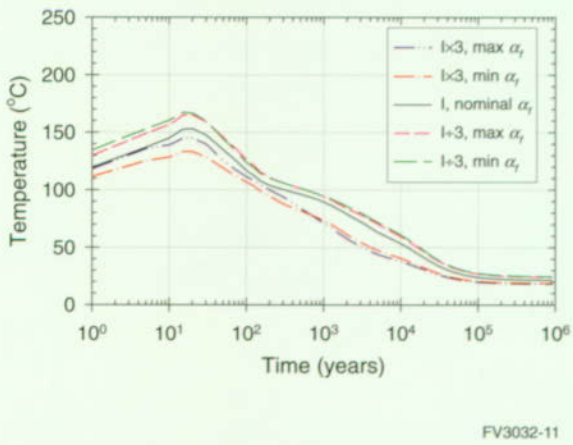

Figure 3-24. Average Waste Package Temperature History for Five Base Case Property Sets
Average waste package temperature history in Region NE (see Figure 3-20) for the five base case hydrologic-property sets using commercial spent nuclear fuel and long-term average climate. Shown are effects of variations in infiltration (I) and fracture air-entry parameter (α_f), which is an important hydrologic property.

"thermal-hydrologic" property set is different from the base case hydrologic properties primarily because of a much lower imbibition diffusivity for the rock matrix of the Topopah Spring lower nonlithophysal hydrogeologic unit, a change suggested by results of the single heater test (CRWMS M&O 1998i, Section 3.4.5). Results in Figure 3-25 are shown for Region SW because the repository is in the Topopah Spring lower nonlithophysal unit in that region, so the difference introduced by the thermal-hydrologic property set is greatest in Region SW. The figure shows that the dual-permeability/Weeps model has a greater effect on waste package temperature than the thermal-hydrologic property set does, but neither one has much effect after the first 100 years.

Figure 3-26 displays the time history of air mass fraction as obtained from the mountain-scale thermal-hydrologic model. This model provides air fractions at repository center and edge locations (Figure 3-17). The center and edge are quite different. Air mass fractions are higher at edge locations because above-boiling conditions subside more quickly as heat is lost to the surrounding unheated rock mass. When temperatures are above boiling, steam generation causes the reduction in air mass fraction as the generated steam drives away the air. The figure shows that steam generation is only strong enough to drive out the air for a few thousand years at most, and for only a few hundred years near the repository edge. The double-minimum shape of the "center" curve is a result of details of water movement near the repository. There is a pulse of condensate drainage as heat mobilizes water, then a drying period, and then a gradual rewetting as the repository cools.

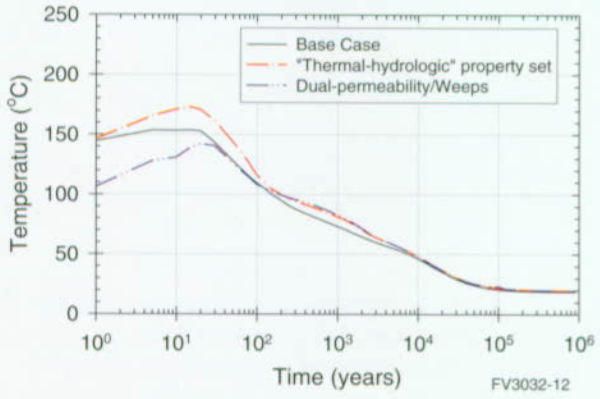

Figure 3-25. Effect of Alternative Hydrologic-Property Sets on Waste Package Temperature
Effect of alternative hydrologic-property sets on waste package temperature in region SW (see Figure 3-20) using commercial spent nuclear fuel, long-term average climate, and mean infiltration.

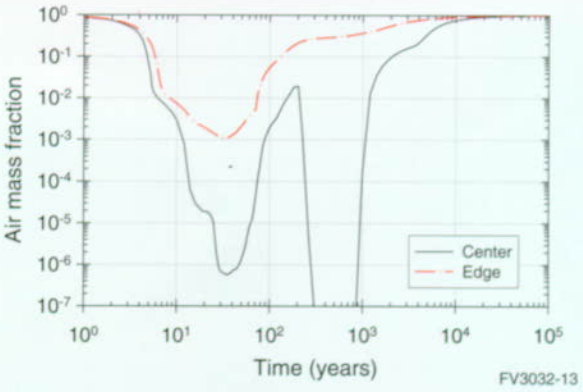

Figure 3-26. Air Mass Fraction for Center and Edge Repository Locations
Air mass fraction for center and edge repository location, from the mountain-scale thermal-hydrologic model using dry (present day) climate, mean infiltration, and base case hydrologic properties. When the air mass fraction is low, it indicates that air has been driven away from the waste packages by steam generation.

In summary, thermal-hydrologic models require quantification of processes at two different scales. The use of models at different scales requires different details and refinement to reproduce the important processes caused by emplacement of heat-generating waste in a geologic repository. Because of the complex interaction between heat and fluid flow (for example, phase-change processes), several of the models used to determine the thermal-hydrologic processes important to long-term repository performance are computationally intensive. These thermal-hydrologic models have undergone a significant evolutionary process to address key issues from the thermal-hydrology workshop (CRWMS M&O 1997l) and from recommendations made by the Thermohydrologic Modeling and Testing Program Peer Review (CRWMS M&O 1996e). This process built upon

the knowledge gained through previous TSPAs. Important concerns related to conceptual flow models, use of site-characterization data for hydrologic and thermal properties, and incorporation of results from the thermal-testing program into decisions regarding property sets were implemented in the thermal-hydrology component.

Some important issues remain unresolved, in particular the impact of thermal-hydrologic-mechanical and thermal-hydrologic-chemical coupled processes. As new site data are obtained (for example, from the drift-scale thermal test) they will be incorporated into the thermal-hydrologic models.

3.3 NEAR-FIELD GEOCHEMICAL ENVIRONMENT

The near-field geochemical environment component is a description of the changing composition of gas, water, colloids, and solids within the emplacement drifts under the perturbed conditions of the repository environment. The major changes are caused by the planned thermal loading of the system and the emplacement of large masses of materials that can react with water and gas in the system. Because the system will heat and then cool off, the system will continue to change. Not only will the thermal perturbation affect the movement of gas and water through the unsaturated system (thermal hydrology as described in Section 3.2), but it will also affect the composition of the gas and water. These fluids of altered composition may enter the drifts and react with the materials emplaced during repository construction. Most of these emplaced materials will be very different in chemical composition from the host rock. In the drifts, reactions with materials such as concrete may alter water and gas compositions before they react with the waste package and the waste forms, and along the flow paths for radionuclide transport in the unsaturated zone. The emplaced materials may also provide additional sources of colloids. These colloids from emplaced materials may be more effective in transporting radionuclides than natural colloids. Figure 3-27 is a general view of processes, phases, and design materials that are considered for the near-field geochemical environment.

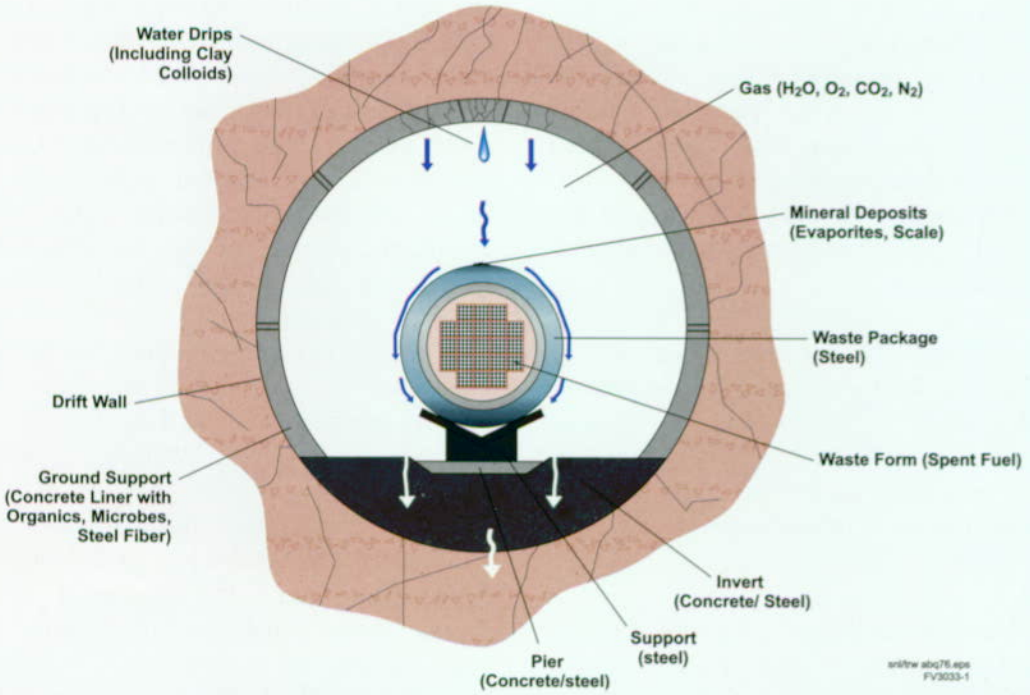

Figure 3-27. General Near-Field Geochemical Environment Conceptual Processes, Phases, and Design Material This TSPA-VA component describes changing compositions of gas, water, colloids, and solids within the potential emplacement drifts.

The geochemical modeling studies and analyses presented in this section were prepared with the view of addressing selected aspects of the NRC Key Technical Issue on Evolution of the Near-Field Environment (NRC 1997c). Specifically, the information presented is pertinent to three of the four subissues of this key technical issue, namely, effects of coupled processes on seepage, rate of release of radionuclides from breached waste packages, and radionuclide transport through engineered and natural barriers.

The most direct way the near-field geochemical environment may impact long-term performance is by changing the engineered barrier system that inhibits the supply and limits the release rate of radionuclides to the geosphere (to the unsaturated zone component for radionuclide transport, see Section 3.6). Chemical changes to the in-drift environment may affect the amounts and types of mobile radionuclides and the properties of the solids through which they are transported. The near-field geochemical environment is the set of compositional conditions under which the waste package corrodes, the waste forms dissolve and precipitate as secondary phases, the radionuclides mobilize from the waste form, and the radionuclides migrate through the engineered barriers. In addition to these primary effects within the engineered barrier system, perturbed fluids generated in the near-field geochemical environment could react with the host rock. Such alteration may change the flow pathways in the geosphere and change conditions for unsaturated zone transport.

A set of five models has been developed to represent the near-field geochemical environment. These models are:

1. The incoming gas, water, and colloids (compositions of those phases as they enter the drift)

2. The in-drift gas phase (composition of the gas phase relative to major gas sinks in the drift)

3. The in-drift water/solid chemistry (evolution of water composition reacting with major materials and the drift gas phase)

4. The in-drift colloids (stability and quantity of clay and iron-oxide colloids in the drift)

5. The in-drift microbial communities

The relationships between the models for the near-field geochemical environment, including the general flow of information from one model to another and the major components of each submodel, are shown in Figure 3-28. In some cases, these five models contain process-level calculations to represent the evolution of water, solid, and gas reactions in the system. In other cases, the models consist of "bounding" arguments for applying observed values. There are a number of submodels for the water/solids interaction model covering steel corrosion products (iron oxyhydroxides), concrete, waste form (spent nuclear fuel), and mineral precipitates from boiling

The near-field geochemical environment model has several connections with other component models. The near-field geochemical environment models take input from the unsaturated zone flow and thermal-hydrology models and provide output to the waste package corrosion model, the waste form model (degradation, radionuclide mobilization, and engineered barrier system transport), the unsaturated zone radionuclide transport model, and the criticality model. The connections and specific inputs and outputs to and from the near-field geochemical environment component are shown as a flow diagram in Figure 3-29. The interfaces are discussed in more detail below.

Unsaturated Zone Flow. The flux of water and dissolved constituents through the near-field geochemical environment is given either as the seepage flux through the drifts or as the average percolation flux at the repository horizon. Seepage flux is used for the in-drift water-solids model and the colloid model. Average percolation flux is used for the in-drift gas model because gas mobility is relatively high near the drifts and, therefore, the

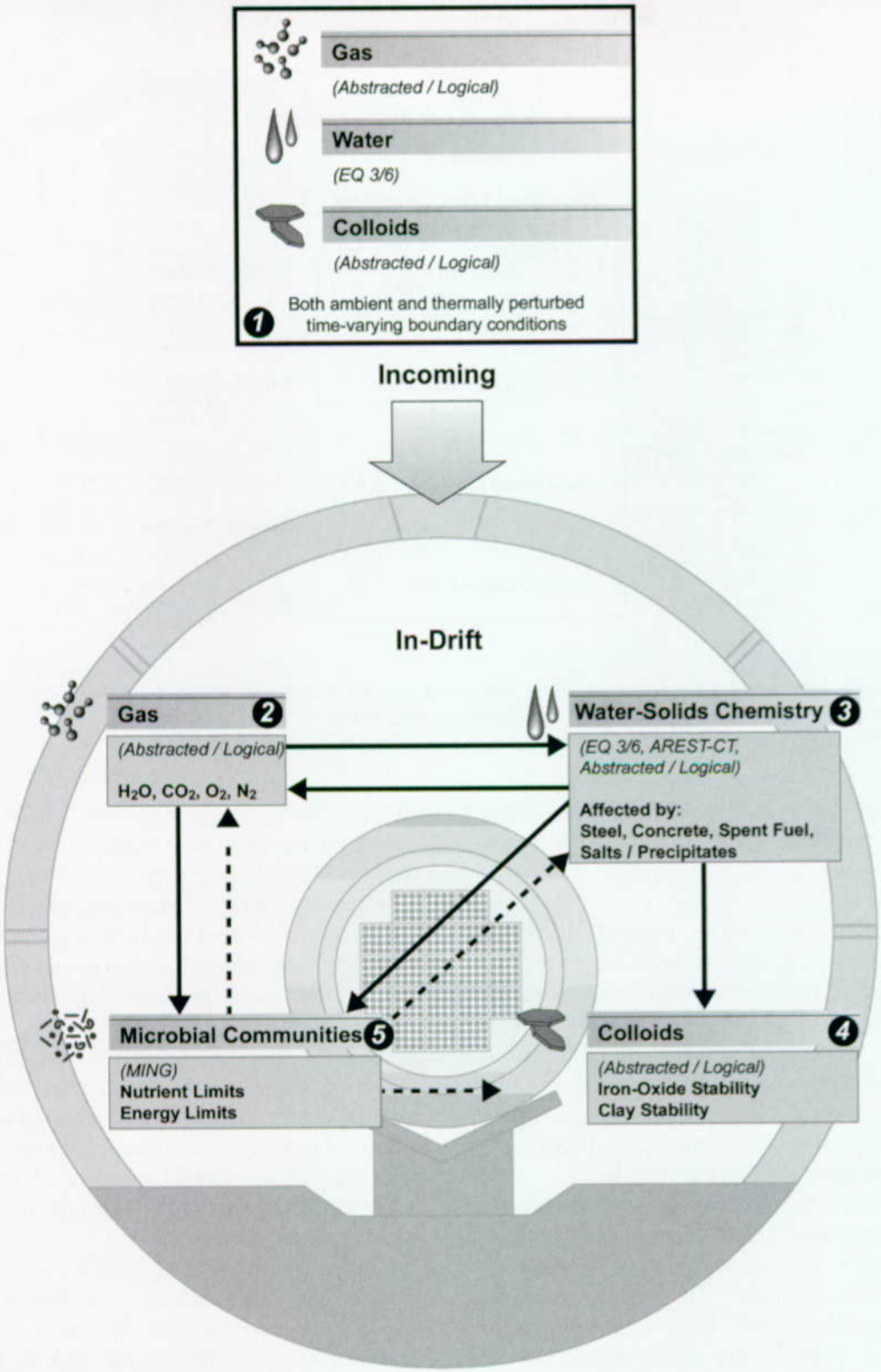

Figure 3-28. Relations Between the Five Near-Field Geochemical Environment Models
Information flow between models is shown by the arrows. Model implementations are either as abstracted/logical parameter descriptions or via computer codes (MING, EQ 3/6, and AREST-CT).

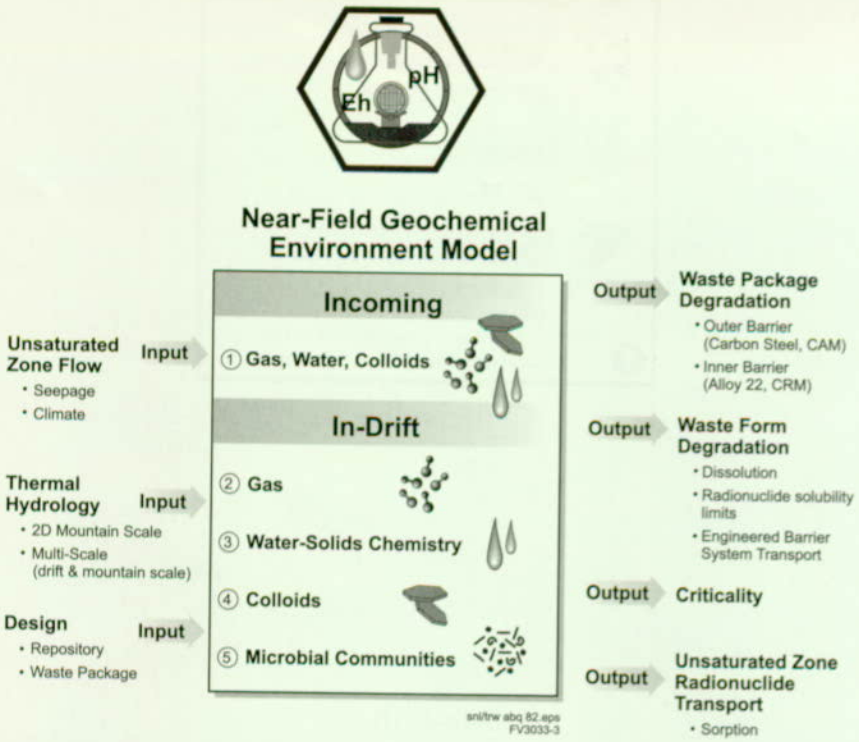

Figure 3-29. Interconnections Between Near Field Geochemical Environment Component and Other Total System Performance Assessment for the Viability Assessment Components (CAM—corrosion allowance material; CRM—corrosion resistant material)

gas composition is in equilibrium with a much greater volume of water than just the seeping water.

Thermal Hydrology. The thermal disturbance caused by repository heating provides a number of time-dependent boundary conditions for the near-field geochemical environment model, including the flux of groundwater and gas into the drift, the drift temperature, and the relative abundance of air in the gas. Thermal effects can drive changes in the fluid and gas compositions through changes to temperature-dependent phase equilibria or reaction kinetics. Such changes may also occur within the heated geosphere surrounding the engineered barrier system and change the compositions of those incoming phases. The effects of thermal perturbations may also have long-term consequences for minerals and solids within the drift because of changes in phase stabilities, reaction rates, permeabilities, and porosities.

Waste Package Degradation. The in-drift geochemistry may have impacts on corrosion of waste package barrier materials. The composition of water contacting the waste package and the bulk oxidation state within the drifts are supplied by the near-field geochemical environment model. Also, just as the waste package degradation will be affected by the composition of fluids reacting with it, the waste package materials themselves are an extensive mass of introduced materials. These materials and their solid corrosion products can change the aqueous and gas compositions in the drift, as well as provide a source of iron-oxyhydroxy colloids that may enhance migration of certain radionuclides.

Waste-Form Degradation, Mobilization, and Engineered Barrier System Transport. The degradation rates of the waste forms (including cladding) depend on the composition of the gas phase and the aqueous phase reacting with the waste form. The near-field geochemical environment component provides the compositions

of water and gas that may react with the waste forms and provides the state of materials through which radionuclide transport will occur in the engineered barrier system. The major chemical constituents of the waste form have also been evaluated for their potential to change the water chemistry from its initial composition.

Unsaturated Zone Radionuclide Transport. The overall composition of the water moving from the engineered barrier system into the unsaturated zone transport pathways of the geosphere is determined from the near-field geochemical environment component. Radionuclide transport depends on the water composition, particularly for radionuclide retardation processes, but also for potential alteration of the pathways themselves. The potential altered fluid compositions that may migrate through the unsaturated zone are used as constraints on the cases for altered unsaturated zone radionuclide transport sensitivity analyses (see Section 5.6).

Criticality. A portion of this work (Section 4.4) considers the possibility of a critical configuration of fissile material forming within the drift (near-field) environment after release from waste packages ("external" criticality), and its potential performance consequences. This external criticality is linked directly to radionuclide transport processes in the emplacement drifts and depends on the location and time-dependent chemical changes that occur there. In addition, the changes (mainly thermal) caused by a critical event could affect the chemical environment within a drift.

3.3.1 Construction of the Conceptual Models

There are several issues and coupled processes relevant to the development of near-field geochemical environment models (CRWMS M&O 1998c). Performance assessment personnel and principal investigators within the scientific program worked together to develop abstracted models of the near-field geochemical environment models. Some of the near-field geochemical environment models are based, in part, on conceptual process models developed within the *Near-Field/Altered-Zone Models Report* (CRWMS M&O 1998c). Such conceptual models are combined with time-dependent, abstracted results of the potential repository system thermal-hydrologic evolution (see Section 3.2), that were used as constraints for the near-field geochemical environment models of gas composition. This abstraction entailed using average constant values for defined periods with step changes in between them. One primary result of this is that short-term transient effects (for example, lasting less than about 100 years) are included in an average manner. This was assessed as a reasonable way to proceed for this initial model development effort because the TSPA system integration model uses time-steps of at least 100 years (CRWMS M&O 1998i, Section 4.4 and 11.1).

3.3.1.1 The Near-Field Geochemical Environment Workshop and Highest Priority Issues

A workshop about the treatment of the near-field (in-drift) geochemical environment in this TSPA was held in March 1997. The details of the workshop activities and results are documented in *Near-Field Geochemical Environment Abstraction/ Testing Workshop Results* (CRWMS M&O 1997d). A brief overview of the workshop is provided because it was the primary initiator for development of the near-field geochemical environment component for this TSPA. The criteria used at the workshop to prioritize issues, the highest priority issues, and the resulting abstraction plans are listed in Table 3-9.

At the near-field geochemical environment workshop, YMP personnel from the design, scientific programs, and performance assessment organizations delineated, discussed, and prioritized issues relevant to chemistry within emplacement drifts that might impact system performance. The two issues given the highest priority focused on evolution of design materials within the drift (that is, the in-drift water/solid chemistry). These two issues are, "the amount of water coming into the drift" and "the introduced material masses and compositions."[2] Three additional issues that were also given high priority for this topic are "aqueous

Table 3-9. Near-Field Geochemical Environment Abstraction/Testing Workshop

NEAR-FIELD GEOCHEMICAL ENVIRONMENT ABSTRACTION/TESTING WORKSHOP
March 5-7, 1997, Berkeley, CA
(CRWMS M&O 1997d)

PRIORITIZATION CRITERIA
- Does the process/issue affect the
  - Dissolved radionuclide concentration?
  - Colloidal radionuclide abundances?
  - In-drift sorption capacities?
  - In-drift porosity and permeability?

HIGHEST PRIORITY ISSUES
- Solid phases throughout the drift:
  - Volume and flux of water in drift
  - Compositions, abundances, and distribution (cement, alloys, organics, microbes, ceramics)
  - Aqueous and gas reactions on materials
  - Aqueous and gas reactions (corrosion) on waste package
  - In-drift system open or closed
- Gas phase throughout the drift:
  - Gas flux
  - Reactions with solids and microbes (excluding waste package)
  - Reactions with waste package
  - Thermal effects (water reactions)
  - Temporal heterogeneity
  - Climate effects
- Aqueous phase throughout the drift:
  - Aqueous phase reactions with major introduced materials (excluding waste package)
  - Open versus closed system
  - Aqueous phase reactions with waste package
  - Temporal evolution of aqueous phase composition
  - Perturbed water composition entering drift
  - Aqueous reactions with waste form
  - Thermal effects on aqueous phase compositions
  - Aqueous phase reactions with evaporite minerals
  - Microbial process effects on aqueous composition
  - Reversibility of radionuclide sorption onto colloids
  - Water-composition effects
  - Waste form
- Other (introduced materials in rock)
  - Temporal heterogeneity
  - Microbial processes
  - Temperature effects

ANALYSIS PLANS
- Incoming Gas, Water, and Colloids
- Gas composition evolution in the drift
- Water solid chemistry model
- Colloid-facilitated radionuclide transport
- Effects of microbial communities

and gas reactions with materials," "aqueous and gas reactions with the waste package," and "open versus closed system behavior." The gas composition issue given top priority was "gas flux into the drift." The third-highest overall prioritized issue relates to the in-drift water composition, "effects from reactions with introduced materials." Workshop participants gave high priority to two other issues related to in-drift water chemistry: "open versus closed system," and "aqueous reactions with the waste package." The highest priority issue related to in-drift colloids was assessed to be "reversibility of sorption." The issues "water composition effects" and "waste form" were also given high priority for colloids in the drift. These priorities, together with the group discussion of issues in each topic area, provided the bases for development of the component models.

The workshop itself, together with post-workshop synthesis and planning, led to the five model areas for the near-field geochemical environment:

- Incoming gas, water, and colloids (compositions of those phases as they enter the drift)
- The in-drift gas phase (composition of the gas phase relative to major gas constituent sinks in the drift)
- The in-drift water/solids chemistry (evolution of water composition reacting with major materials and the gas phase in the drift)
- The in-drift colloids (stability and quantity of clay and iron-oxide colloids)
- The in-drift microbial communities

The conceptual models for each of these areas are summarized in Sections 3.3.1.2 and 3.3.1.3. Their specific implementations for the analyses are given in Section 3.3.2.

[2] Although the waste package is a design material, it was considered separately from other potential repository-design materials for clarity because it is also a major component of the engineered barrier system.

3.3.1.2 Incoming Gas, Water, and Colloids

The near-field geochemical environment model provides values for the time-varying compositions and fluxes of gas, water, and colloids entering the drift. Changes to these variables are primarily driven by the thermal changes to the system. Reactions between the gas, water, and minerals in the rock occur as the system is heated and pore water boils. These processes change the system by changing phase stabilities or increasing rates of reaction for existing phases. The time evolution of the system was divided into two thermal regimes; a boiling regime and a cooling regime. These two regimes are further subdivided based on large changes to the gas composition (mainly within the boiling regime) or the changing temperature of the cooling system (within the cooling regime). The periods are defined to have constant chemical conditions so that the description of the near-field geochemical environment evolution consists of a set of step changes in system conditions.

Conceptual Model for Incoming Gas. In the conceptual model for incoming gas, gas composition is represented by the major gas constituents: steam (H_2O), oxygen (O_2), carbon dioxide (CO_2), and nitrogen (N_2). The primary sources of these gases and the mountain scale processes affecting their quantities are shown in Figure 3-30. Steam (or water vapor) is generated during the boiling period and affects the rate at which waste packages corrode. The other three gas constituents are components of air considered in this model.[3] Oxygen is included because of its role in metal oxidation. Carbon dioxide directly affects the pH of solutions (which affects waste form dissolution) and can strongly affect actinide complexes (increasing their dissolved concentrations). Finally, nitrogen generally comprises most of the air component of the gas and may serve as a nutrient source for microbial activity.

Because gas is less soluble at higher temperature, heating drives dissolved gases out of the water and into the gas phase. Rapid gas movement in the fractures may transport those dissolved gas constituents away from the heated water they came from and towards cooler water (that is, down the temperature gradient) where they can redissolve. This process tends to deplete the heated water and enrich the cooler water in these gas species. As the temperature of the mountain increases farther away from the repository, these gas species are remobilized and transported farther away from the drifts in a continual process of revaporization and redissolution. In the rock near the heat sources temperatures will rise above the boiling point of water, generating abundant steam, causing an overall dilution of the air component.

The major source of both oxygen and nitrogen is the atmosphere, so dilution of these two constituents by steam (from boiling) is accounted for by a direct reduction in their atmospheric partial pressures. For carbon dioxide, the system is somewhat more complex. Measurements of gas compositions from various unsaturated zone boreholes demonstrate that unsaturated zone CO_2 gas concentrations are elevated above atmospheric CO_2 partial pressures (about 350 ppmv [parts-per-million by volume]) by about a factor of three (CRWMS M&O 1998i, Section 6.2.7.2, pp. 6.2–40). The values of unsaturated zone pore-gas composition analyzed for the site indicate that the CO_2 content of pore gases tends to average about 1,000 ppmv (ibid., Section 5.3.4.2.4.6, pp. 5.3–173). These elevated values could be the result of mixing of CO_2-rich gases generated in the soil zone with the rest of the gas volume of the mountain (ibid., Section 5.3.4.2.4.6, pp. 5.3–173). Because the rock contains the mineral calcite ($CaCO_3$) and there is a non-negligible amount of dissolved carbonate in the water, these phases may act as sources of carbon dioxide that must be accounted for in the assessment of the air composition diluted by steam. However, because gas flow is much more rapid than water flow, the near-field geochemical environment model assumes that the water composition will be primarily controlled by the gas composition diluted by steam for most of the thermal period. Nevertheless, there are indica-

[3] Air does not necessarily imply atmospheric composition of these gases but is the term for the gas ingredient "other than steam" in the thermal-hydrologic models (see Section 3.2).

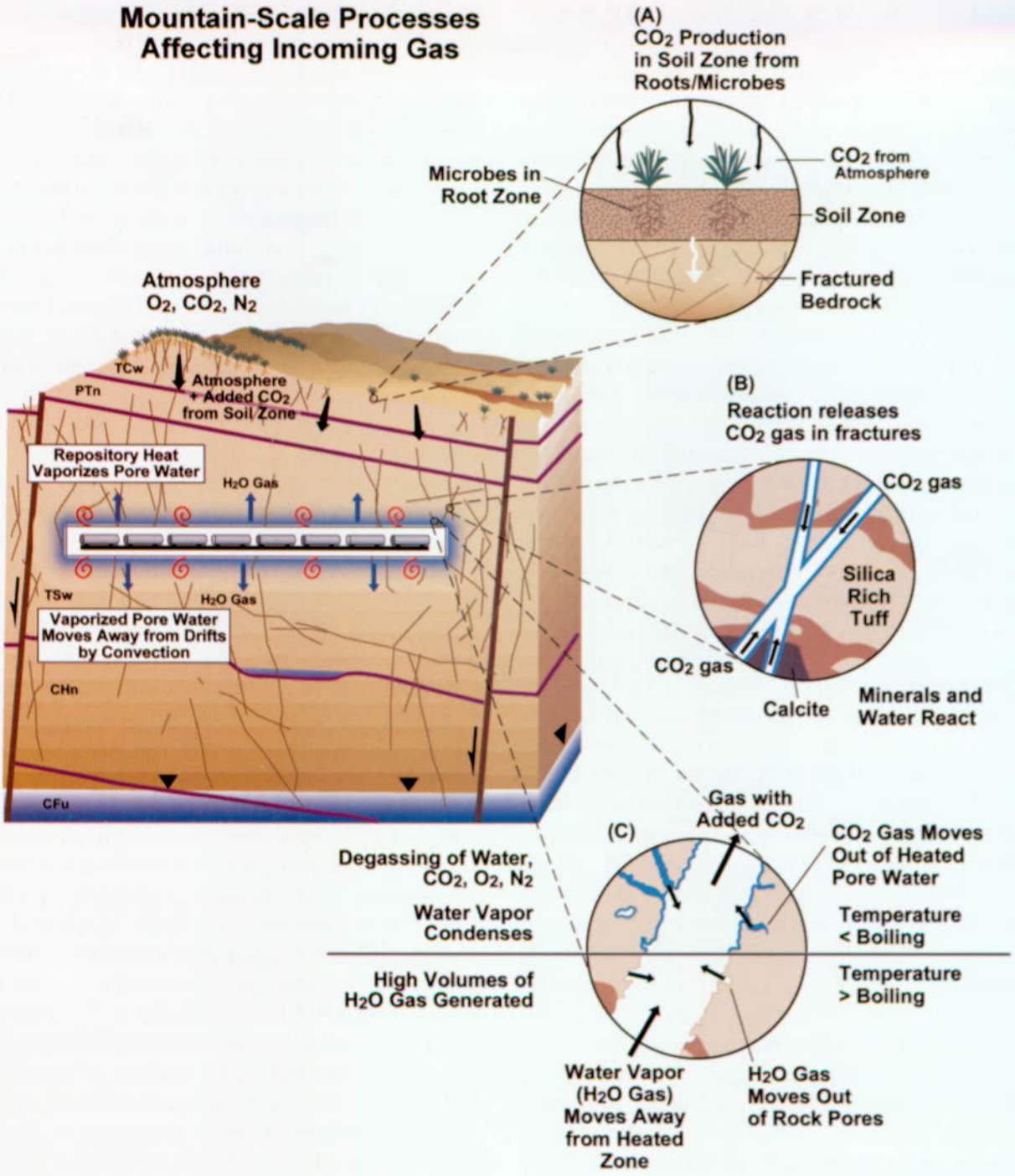

Figure 3-30. Mountain-Scale Conceptual Picture of Incoming Gas Model Processes
Incoming gas picks up added carbon dioxide content as it passes through the soil zone. Carbon dioxide gas migrating in rock fractures reacts with minerals and water in the tuff rock. Heating caused by waste packages in the repository causes water to boil, to steam, and move away from the heated area in vapor form until it reaches a cooler area where it condenses.

tions from water compositions in the single-heater test that calcite may be reacting to release carbon dioxide during the heating stage (CRWMS M&O 1998c, Section 6.2.1). In addition, the potential exists for short-term increases in the carbon dioxide content (of the air) as it is released from heated water (CRWMS M&O 1998i, Section 4.4). Therefore, a brief period with an elevated level of carbon dioxide in the air, which is then diluted by steam, was included at the start of the model to represent these potential sources of carbon dioxide.

The incoming gas model also assesses constraints on the fluxes of the gas constituents into the drift. These values are used in analyses that evaluate the potential for depletion of these constituents by reaction with the solids in the drift, and the potential effects on water/solids chemistry of those reactions (discussed below). For each of the gas constituents in the model, the cumulative gaseous flux of that chemical component into the drift is given by the product of the cumulative gas phase flux and the fraction of that constituent in the gas for a given period. In the conceptual models for the gas and water/solids chemistry in the drift, the fluxes of these gas constituents that could be derived from their dissolved counterparts in the water flux were also included. For this model, the fluxes of the dissolved gas constituents were based on the percolation flux for the drift cross-section. This water flux is larger than that given by the seepage model, which only has a fraction of the percolation flux entering the drift. Because gaseous diffusion for carbon dioxide or oxygen gas species is relatively rapid at this scale, the gas composition may be buffered by water just outside the drift. Therefore, this larger water flux should represent a more realistic bound on the masses of these gas constituents available for reaction in the drift (CRWMS M&O 1998i, Section 4.4).

Conceptual Model for Incoming Water. In the conceptual model for incoming water, water composition is represented by the major dissolved constituents and by some of the less abundant dissolved constituents that participate in some of the dominant mineral reactions within the system. The compositional components considered for the water in the model are pH, sodium (Na^+), potassium (K^+), calcium (Ca^{2+}), magnesium (Mg^{2+}), iron (Fe^{2+}, Fe^{3+}), aluminum (Al^{3+}), silica (SiO_2), chloride (Cl^-), fluoride (F^-), carbonate (CO_3^{2-}), and sulfate (SO_4^{2-}). These constituents represent the total masses of these components within the fluid, and each may be comprised of a number of different species in solution. In addition, the dissolved oxygen content is included as constrained by the oxygen fugacity (approximately the partial pressure), and this value is used to calculate the equilibrium oxidation potential (Eh) of the system. Figure 3-31 shows the major processes at the mountain scale affecting the concentrations of these constituents in the incoming water.

The composition of ambient water moving through fractures and entering the drift has been constrained by examination of the various fluid compositions observed both at the site, and near Yucca Mountain. Pore water in unsaturated tuffs appears to have higher concentrations of some constituents like sulfate and chloride (CRWMS M&O 1997d, Appendix 3 Table 1; Bodvarsson et al. 1997, Chapter 14; CRWMS M&O 1998m, Section 6.2.5 and 6.2.8) compared to the water in the saturated zone tuffs (Figure 3-31, Inset A). However, the composition migrating through the unsaturated zone fractures into the drift is assumed to be that observed within the saturated zone tuff aquifer (from well J-13, Figure 3-31, Insets B and C). This assumption is based on compositional similarities between the perched water bodies, fracture fluids collected at Ranier Mesa (a nearby mountain of unsaturated volcanic tuffs analogous to Yucca Mountain), and groundwater samples from the J-13 well (CRWMS M&O 1998c, Section 6.2 Table 6.2-1; CRWMS M&O 1998i, Section 4.4).

The processes that change ambient water composition are driven by heating of the system and are closely linked with the processes shown in Figure 3-30 for evolution of the gas composition entering the drift. In the conceptual model for the incoming water composition, the time-varying gas composition is imposed as an equilibrium constraint on the water composition at the temperature of the system because the gas transport is fast relative to

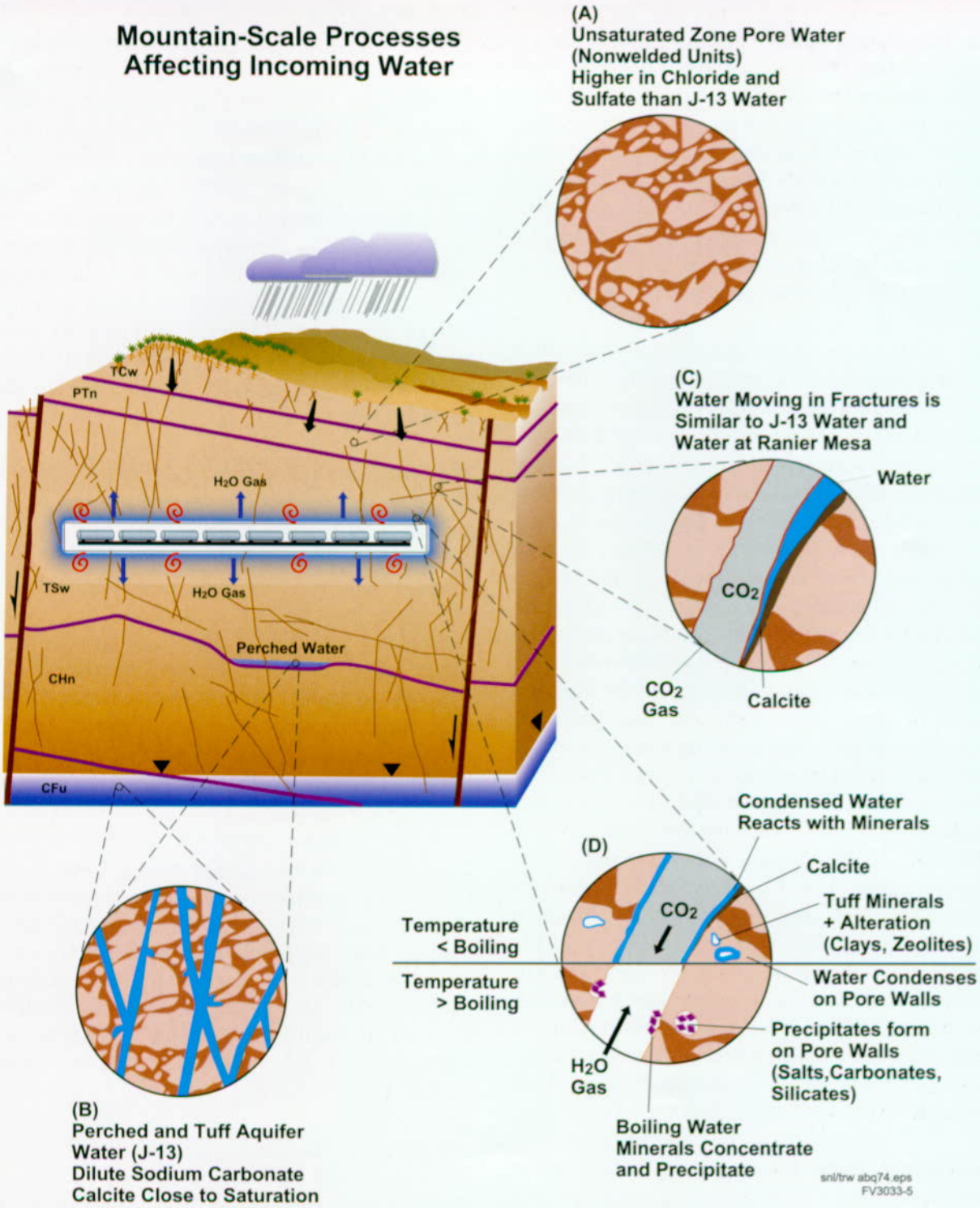

Figure 3-31. Mountain-Scale Conceptual Picture of Incoming Water Model Processes
A variety of ambient water compositions has been observed in unsaturated pores, saturated pores, and perched water. Water composition moving in fractures is similar to that in well J-13, which is used as ambient, undisturbed, water for modeling. Heating caused by waste packages in the repository causes boiling of water and increased gas movement away from the heated area. Evaporation of water in the heated zone leaves behind mineral precipitates and condensed water in the cooler zone reacts with minerals.

the water flow (that is, the changes to gas composition from the dilution by steam generation are expected to be very large compared to the other compositional changes to the gas in the geosphere and therefore these perturbed gas compositions are imposed directly (CRWMS M&O 1998i, Section 4.4). Water composition is also changed by reaction with minerals in the tuff and in the fracture linings at various temperatures (CRWMS M&O 1998c, Section 5). In addition to the heated reaction of water, gas, and minerals, the thermal change is projected to be large enough to create a boiling zone around the drifts (see Section 3.2).

The boiling process will affect water chemistry in a number of ways (Figure 3-31, Inset D). First, the gas composition changes as discussed above (Figure 3-30, Inset C). Second, many of the dissolved mineral constituents become more concentrated as the water boils (CRWMS M&O 1998c, Section 6.2). Some of these constituents concentrate to the point where solids (such as calcite and silica) precipitate and further constrain the water composition (CRWMS M&O 1998c, Section 6.2). When the water boils away completely, some of the precipitated phases are relatively soluble salts that will react later with water and steam to create concentrated salt solutions. In addition, salt will cause water to condense from steam at a lower relative humidity than salt-free systems, forming concentrated salt solutions earlier and at higher temperatures if salt is in the fractures. During the period of boiling, the reaction of water, gas, and minerals was calculated at 95°C (203°F), just below boiling (at the elevation of the proposed repository). As the system cools, the boiling front will migrate back into the drift, ending up at the surface of the waste package. The potential amount of salt buildup within a drift (as discussed below) was assumed to depend on the composition of the starting fluid and the cumulative flux of that fluid through the fractures.

Conceptual Model for Incoming Colloids. The near-field geochemical environment component also contains a conceptual model for incoming colloids. Natural colloids are minute particles (from about 1×10^{-8} m, or 100 angstroms, up to about 1×10^{-5} m, 1×10^{5} angstroms), which may be transported by the groundwater. Radionuclides can attach to these colloids and be transported through the system at a different rate than their dissolved counterparts. The colloids entering the drift are assumed to be those found in the natural system for the ambient saturated zone water. These natural colloids are a small mass of entrained particles composed of clays, silica, and iron oxyhydroxides (about 20 to 30 ng/mL—Triay et al. 1996 page 9, Table I; CRWMS M&O 1998m Section 6.3.6.1). Because the iron-oxyhydroxide colloids generated within the drift represent a much larger potential source than the incoming natural iron-oxyhydroxide colloids, the incoming colloids are represented by the clay component of the natural colloids. The amounts of the clay and iron-oxyhydroxide colloids are constrained by the ionic strength of the fluid in the drift. This relation is based on colloid concentrations in groundwaters of various ionic strengths from around the world (CRWMS M&O 1998m Section 6.3.6.1; CRWMS M&O 1998c, Section 4.4).

The models of the incoming gas, water, and colloids provide time-dependent boundary conditions for the models of chemical reactions in the drift. The processes for incoming gas, water, and colloids in the near-field geochemical environment component are shown at the drift scale as Inset A in Figures 3-32a, 3-32b, and 3-32c. Figure 3-32 delineates three generalized time frames for the physical-mechanical evolution of the materials in the drift, based in part on a more detailed description of this evolution (CRWMS M&O 1998c, Section 2.2).

3.3.1.3 Evolution of the In-Drift Chemistry

Once the model compositions of gas, water, and colloids entering the drift have been established, the chemical processes within the drift can be considered. Within the drifts, the coupling of the physical-mechanical deterioration of the introduced design materials (CRWMS M&O 1998c, Section 2.2) plays a large role in the reaction of water and materials because of changes to the flow pathways. Representations of these processes (pathways for fluid migration through the drifts

Time Frame 1 First Few 100s of Years

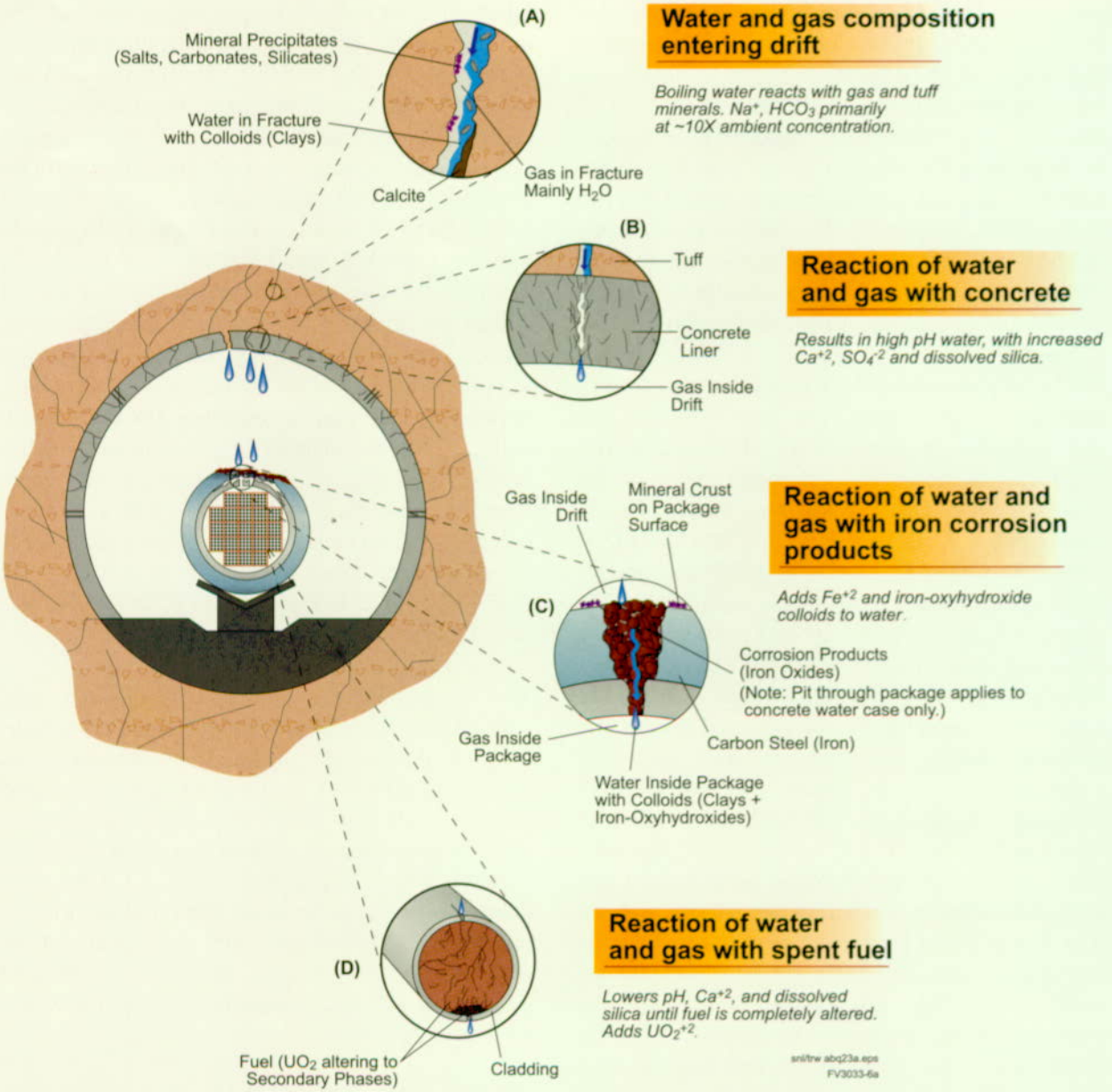

Figure 3-32a. Drift-Scale Near-Field Geochemical Environment Conceptual Processes Time Frame 1—First Few Hundred Years

Within fractures intersecting the drift (Inset A), boiling water reacts with gas and minerals, causing higher concentration sodium-bicarbonate fluid, and carries, natural colloids (primarily clays) into the drift. Water reacting with concrete (Inset B) at these conditions becomes highly alkaline (high pH). Water dripping through areas without concrete would precipitate mineral crusts directly onto the waste package (Inset C) but would not be affected by the concrete's alkaline constituents. Any water moving into the package would react with corrosion products (iron oxyhydroxides) along pitted pathways through the package (Inset C). Reaction of water with spent fuel (Inset D) decreases the pH and scavenges some other cations from the solutions while primary UO_2 is actively altered to secondary phases. At this time the waste package has not been breached in a manner that would allow a release, only areas seeing alkaline fluids and/or sale crusts are substantially corroded. Clay colloids enter the drift and iron oxyhydroxide colloids are generated from materials within the drift.

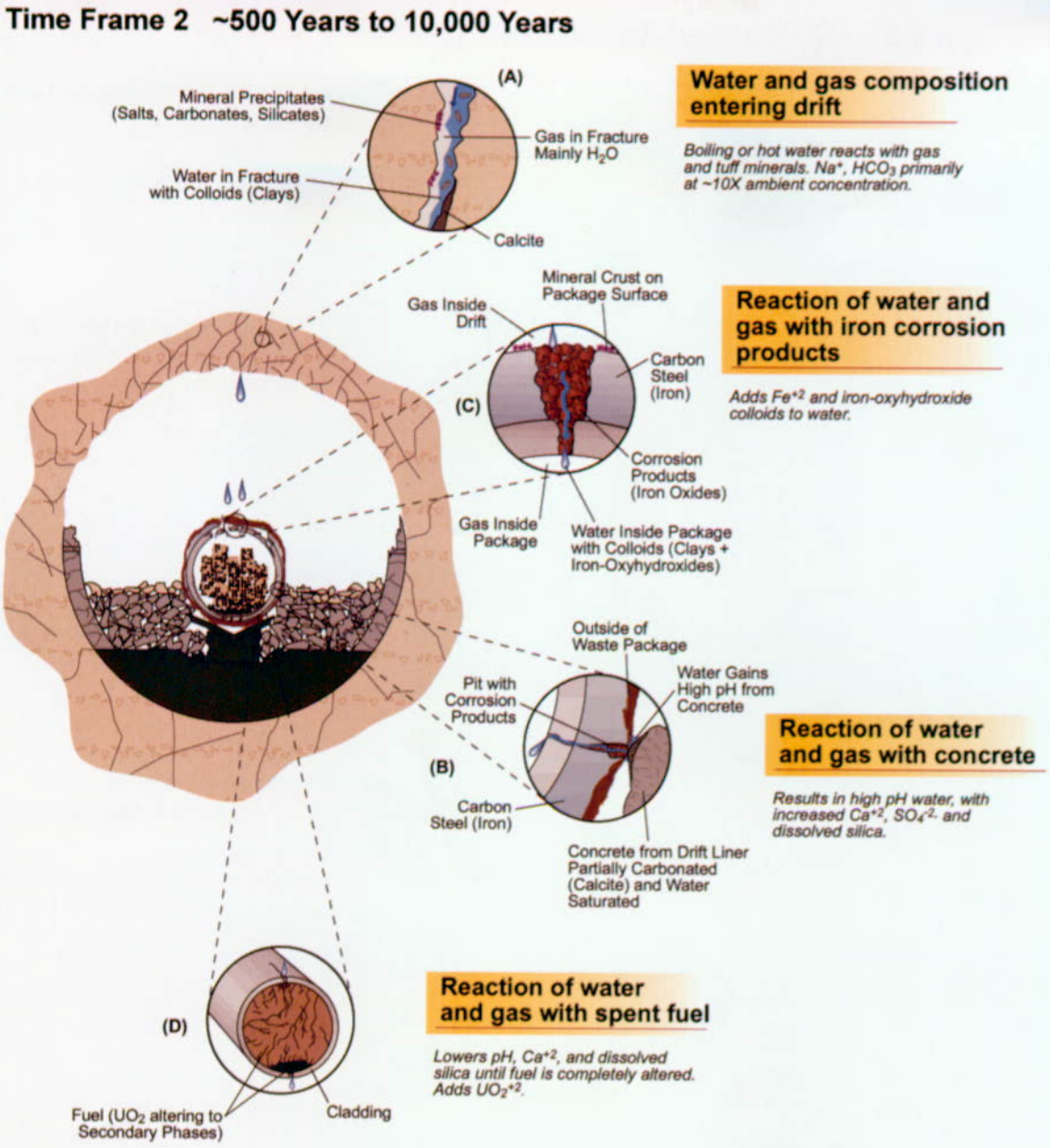

Figure 3-32b. Drift-Scale Near-Field Geochemical Environment Conceptual Processes Time Frame 2—Approximately 500 to 10,000 Years

Water at the interface of concrete blocks and the waste package surface (Inset B) is highly alkaline from reactions with the cement in the concrete. Carbonation of the cement constituents (making calcite—$CaCO_3$) is ongoing but not complete during this time frame. The process is not complete enough to neutralize the concrete's alkalinity. In the post-boiling portion of this time frame, microbial activity is able to start. At this stage the concrete drift liner is assumed to have collapsed and may be lying against the waste package wall. The waste package has corroded substantially in areas receiving drips.

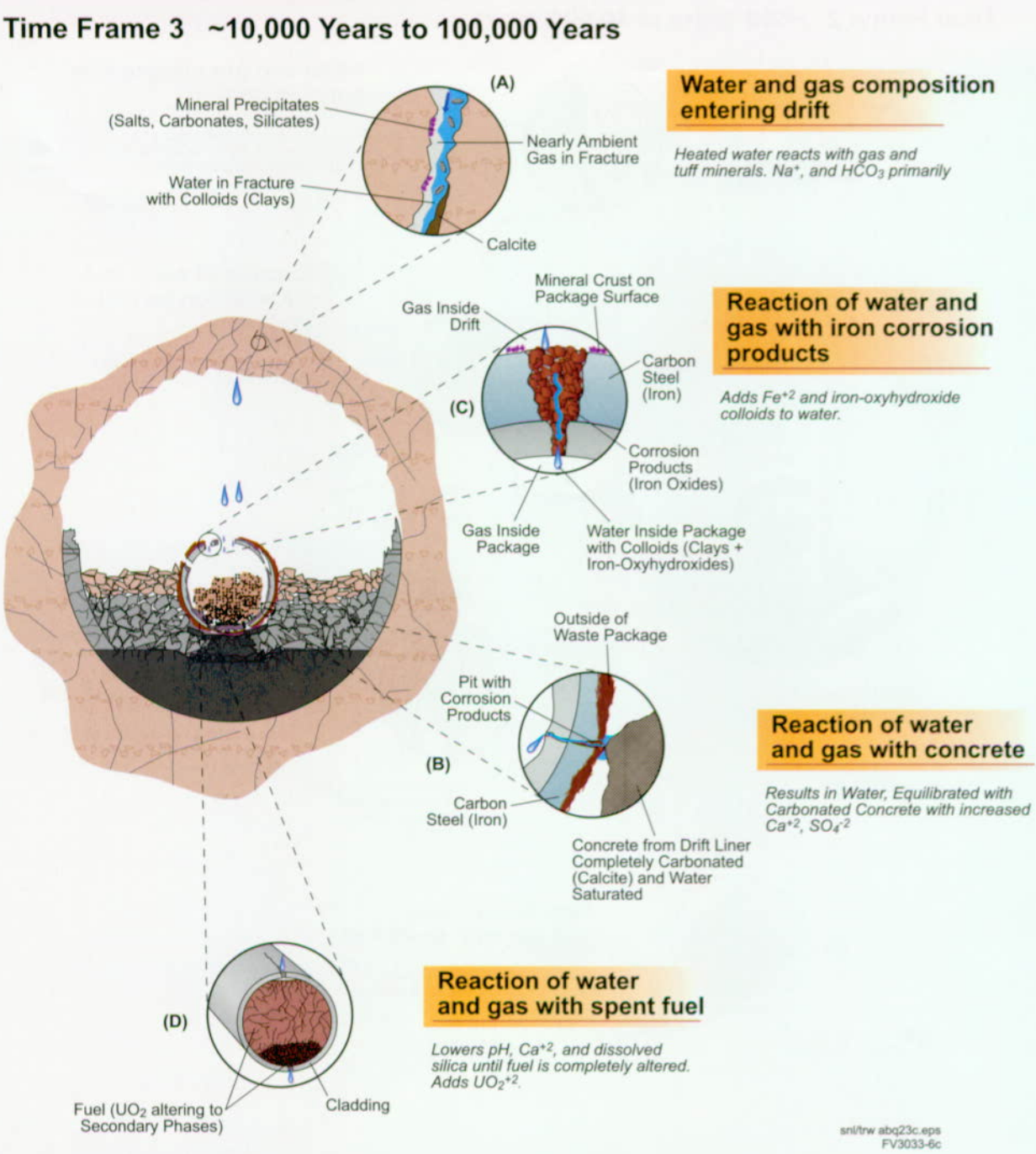

Figure 3-32c. Drift-Scale Near-Field Geochemical Environment Conceptual Processes Time Frame 3—Approximately 10,000 to 100,000 Years

Rock-fall is extensive and the liner and waste package support have fully collapsed. Water entering the drift (Inset A) is only slightly heated at the beginning of this time frame and is cooled to ambient by the end of it. Concrete becomes virtually fully neutralized by reaction with carbon dioxide at the early part of this time frame (Inset B). Corrosion pathways are lined with iron oxides that react with water entering the package (Inset C). The effects on fluid composition of reaction of the secondary uranium phases are relatively minor (Inset D). Microbial growth increases and maximizes during this stage. At this stage the concrete drift liner, support holding the package, and the invert are significantly deteriorated. The waste package is substantially breached by corrosion and radionuclides are released from the package.

and reaction with materials along those pathways) at the drift scale are shown in Figure 3-32a, 3-32b, and 3-32c. The major physical aspects of the system that change are the location and integrity of the concrete that comprises the lining and other ground support, and the integrity of the waste package and its support. While the concrete lining is still intact during the first few hundred years, any water dripping out of the rock will react with it before dripping on the waste package (Figure 3-32a). However, once the lining has collapsed, concrete-modified water is most likely to contact the waste package where concrete blocks lie against the container (Figure 3-32b and 3-32c, Inset B), or below that point. All of the boiling occurs within Time Frames 1 and 2 (Figures 3-32a and 3-32b), even for the center portions of the repository block. The system is at ambient temperatures by the end of Time Frame 3 (Figure 3-32c).

In-Drift Gas. The composition of the in-drift gas phase is assumed to be constant throughout the drift because of rapid migration of gas constituents at this scale, particularly for higher temperatures (Figures 3-32a, 3-32b, and 3-32c). However, the mass of each gas constituent available to react with the water and materials in the drifts is limited by the flux of that gas into the drift. If for a given period the amount of gas needed for a reaction exceeds the amount available because of the gas flux, the water flowing close to the drift wall can degas dissolved volatile constituents to supply the reactions taking place. However, once that reservoir of gas is exhausted, the concentration in the gas phase of the reacting gas constituent will decrease until a new equilibrium concentration is reached. This new level depends in a complex manner on reaction rates that change with compositional changes, but the capacity to use up a particular gas constituent in a given period can be assessed using mass balance relations. Steel (or iron) is the major material that will act as a sink for the oxygen in the system as it oxidizes to either hematite (Fe_2O_3) or goethite (FeO(OH)). The cement phases (portlandite and calcium-silicate hydrates) in concrete are the major sink for carbon dioxide because reaction with calcium in the cement will lead to calcite precipitation. The degree to which these reactions may affect the gas composition is discussed in Section 3.3.2.

In-Drift Water-Solids Chemistry. The model for the in-drift water-solids chemistry is comprised of a number of submodels. Some of these submodels are used quantitatively within the performance assessment analyses and others are used for conceptual scenario development for other components and analyses. A flow chart depicting the detailed relations among the submodels of the in-drift water-solids chemistry portion of the near-field geochemical environment is shown in Figure 3-33. Both the incoming water submodel and in-drift gas model feed water composition and gas constraints directly into the water-solids chemistry submodels. As shown in Figure 3-33, the calculated fluid composition is provided by one submodel and used by another submodel that represents materials "downstream" in the conceptual flow pathway through the system (Figure 3-32). The four features (submodels) of the water-solids chemistry model (corrosion products, concrete, spent nuclear fuel, and precipitates/salts) are described below, following some general conceptual discussion of reaction between water and solids in the drift.

For water that has entered the drift, model calculations were done to evaluate the reaction with the major solids in the drift, in particular with concrete and the corrosion products of the steel (represented by iron oxides). Constraints for the composition of water reacting with the waste form were derived from these models. These reactions between water and solids in the drift are assumed to occur at the conditions for gas fugacities and gas fluxes derived from the in-drift gas model. The reactions will proceed to equilibrium depending on the relative magnitude of gas sinks versus gas fluxes into the drift.

For reaction with repository design and waste package design materials in the repository, the in-drift water-solids chemistry model represents local equilibrium (water movement is slow compared to the reaction rates of the dripping water and reacting solids). This local equilibrium would correspond to reaction along permeable matrix pathways,

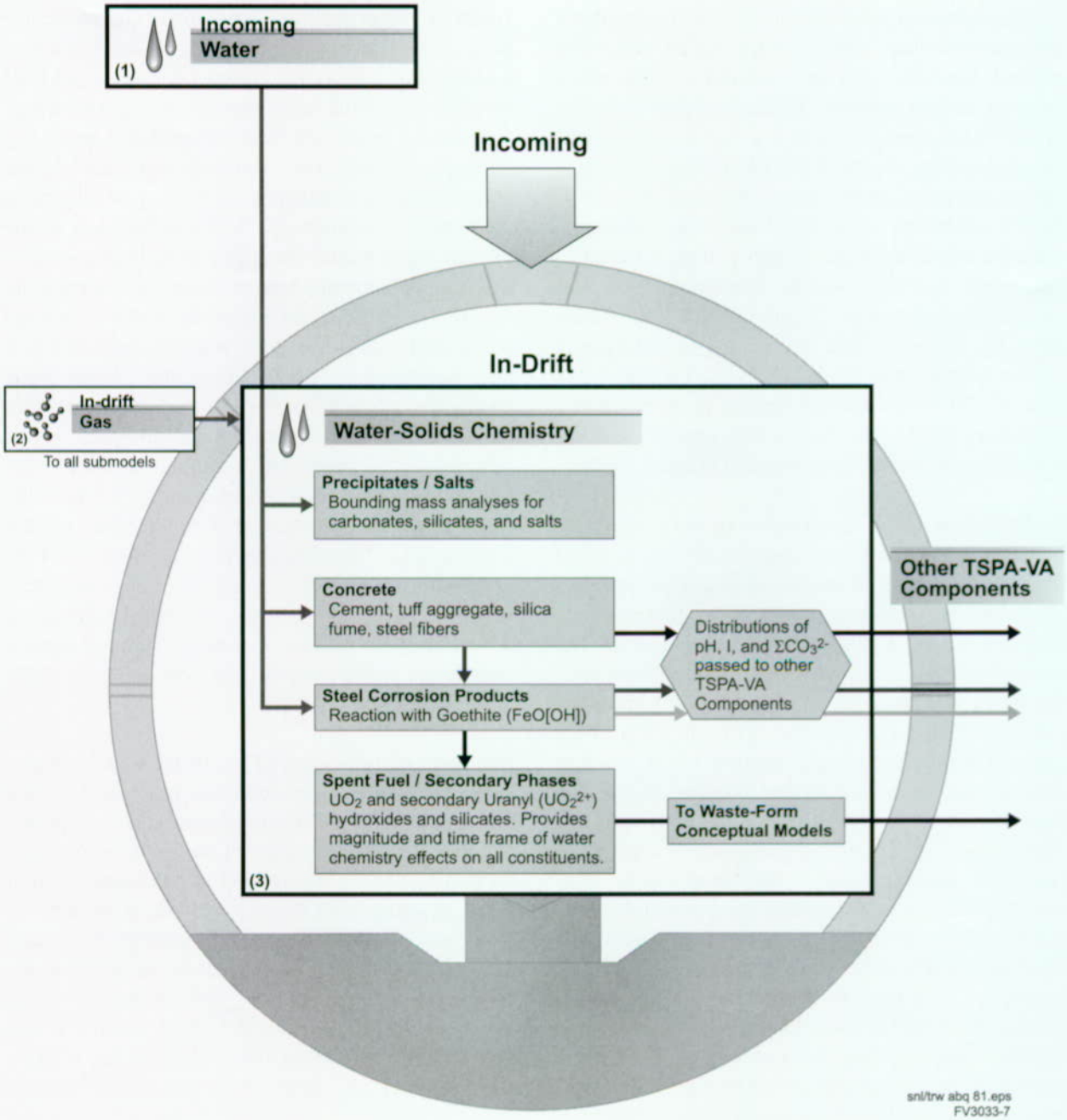

Figure 3-33. Connections Among the In-Drift Water-Solids Chemistry Sub-Models
This is a detailed depiction of Model 3 in Figure 3-28. Various conceptual pathways for water-solids reactions are shown by the arrows.

perhaps with small fractures (Figures 3-32a, 3-32b, and 3-32c, Insets B and C), but does not correspond to reaction along large, highly permeable fractures through the system. Fast flow along such pathways would result in less pronounced changes to fluid composition. Two conceptual pathways for the incoming water were defined.

Corrosion Products. In the first pathway, water does not react with concrete, but drips directly onto the waste package through gaps in the lining during early time frames (Figure 3-32a), or through the area from which the concrete lining has collapsed during later time frames (Figures 3-32b and 3-32c). Because there will likely be water-flow pathways without concrete after the drift lining collapses (CRWMS M&O 1998c, Section 2.2), the water compositions calculated for this corrosion products only pathway are used as the base case fluids. This leg of the pathway is represented by iron oxides, (goethite, FeO(OH)) because the bulk of water that gets into the waste must encounter corroded package material. The primary effect on water chemistry from this reaction is to increase the dissolved iron content of the fluid. The resulting water composition is used as the initial fluid composition for calculating the effects of reaction with spent nuclear fuel during the active alteration period and at later stages when secondary uranium phases are reacting.

Concrete. The second pathway is the concrete conceptual pathway, which was not part of the base case, but considered as a sensitivity case (see Sections 5.3, 5.4, and 5.6). As shown in Figures 3-32b and 3-32c, concrete adjacent to the waste package could provide concrete-modified fluid compositions through diffusive migration of alkaline components into the waste package. Such fluids could then affect the waste package corrosion and possibly change waste form behavior (Figure 3-32b, Inset B). Along this conceptual pathway, water will react with corrosion products after reaction with concrete.

The concrete within the potential drifts will be comprised of tuff aggregate, sand, cement, and steel fibers (CRWMS M&O 1998i, Section 4.3 and 4.4). The alkaline components of cement, in particular the calcium content, will represent a large compositional change to the system. The phases that produce high pHs are primarily portlandite ($Ca(OH)_2$) and calcium-silicate-hydrate phases formed by reaction of the silica with portlandite in the cement. Reaction of the incoming water with these constituents will continue to cause high pH in the resulting fluids until the cement phases are neutralized by carbonation via reaction with water and gas. Until the alkaline cement compounds are neutralized, water compositions may be mostly affected by reaction with the concrete. Reaction rates for this neutralization process are assumed to be relatively fast; however, availability of carbon dioxide will tend to constrain the time frame for this process. In addition, the cement contains sulfate phases that will tend to control the concentration of dissolved calcium, silica, and sulfate through mineral equilibria in a manner different from the interaction of water with tuff.

Spent Fuel. Once inside the waste package, water can react with exposed fuel. The effects of this reaction have been calculated with a model (CRWMS M&O 1998i, Chapter 6) that couples the flow rate of water through the package with the kinetics of spent nuclear fuel dissolution and the formation of secondary phases. Because the base case waste package failures occur primarily after the boiling period, this submodel for spent nuclear fuel, iron oxide reacted water shows reaction with UO_2 at two different temperatures during the cooling period. The cladding and basket materials within the package were assumed to be inert. This reactive-transport model is not part of the base case, but its effects are examined in a sensitivity study discussed in Section 5.5.

The spent nuclear fuel is conceptualized as a porous medium, with an initial porosity equal to the porosity inside a waste package. The water flux through the spent nuclear fuel is assumed to be the long-term average seepage flux through the drift (CRWMS M&O 1998i, Section 3.1), taken directly or modified for the breached area of the waste package; flow rates depend on the evolution of porosity within the system. The water drips into the top of the waste package and then reacts with

spent nuclear fuel along a 1.56-m (5.12-ft) path, after which it leaves the waste package. The transport of dissolved constituents through the system includes advection, diffusion, and dispersion in the solution. The water composition at the outlet of the system is the primary focus of this submodel for the near-field geochemical environment.

In the model, the waste form dissolves as oxidized uranyl (uranium) species with secondary uranium phases precipitating at the carbon dioxide and oxygen-gas conditions determined for the cooling periods (from the in-drift gas model). Carbonate equilibria and calcite precipitation and dissolution are included in this submodel. The uranium solids considered for precipitation are four secondary uranyl (uranium) minerals: uranophane, sodium-boltwoodite, schoepite, and soddyite. These phases are commonly observed in alteration of uranium ore deposits and in laboratory tests of spent-fuel dissolution (CRWMS M&O 1998c, Section 6.5; CRWMS M&O 1998m, Section 6.3). In addition, after conversion of UO_2 to secondary phases, the dissolution of those secondary phases occurs more slowly because they are closer to equilibrium with the fluid entering the waste package. The effects on water composition of the secondary phases are evaluated to provide a boundary on the magnitude of the entire suite of chemical changes.

Precipitates/Salts. Mineral deposits will develop as refluxed water drips through fractures and possibly onto the waste packages throughout the boiling period. The degree of boiling and evaporation of the water will cause various minerals to saturate within the solution. These precipitating minerals will change with time as the water composition changes. The major purpose of this model is to assess the magnitude of mineral precipitation and salt formation, the length of time to redissolve the soluble salts, and the amount of concentrated salt solutions from these processes. Although the amount of salt precipitation was assessed in the near-field geochemical environment component, it was not directly used (CRWMS M&O 1998i, Sections 4.4 and 4.6). The effect of salt on waste package degradation was only used indirectly (see Section 3.4). The potential effects of salt on waste package degradation are discussed briefly in Section 3.4 and in more detail in Chapter 5 of the *Total System Performance Assessment-Viability Assessment (TSPA-VA) Analyses Technical Basis Document* (CRWMS M&O 1998i), but have not been directly incorporated into the TSPA-VA analyses. The effect of solution composition and concentration on the degradation of Alloy 22 was considered in the Waste Package Degradation Expert Elicitation (CRWMS M&O 1998b) and formed part of the basis of the elicited corrosion-rate uncertainty distributions. Data on the effect of salt build-up on stress-corrosion cracking of Alloy 22 is quite limited at present, but as it becomes available between VA and LA, it will be incorporated into the waste package modeling.

Colloids in the Drift. Another consideration in the evolution of the in-drift chemistry is colloids in the drift. The in-drift colloids are comprised of both the clay colloids entering the drift (Figure 3-32 Inset A), and the iron-oxyhydroxy colloids produced within the drift from the steel components of the design materials (Figure 3-32, Inset C). Because these colloids act to sorb and transport radionuclides, the amounts of these colloids affect the amounts of radionuclides that can be transported. The concentration of these colloids depends on the ionic strength of the solution; water with higher ionic strength causes colloids to coagulate and drop out of solution (Triay et al. 1996; CRWMS M&O 1998m, Section 6.3.6). Radionuclide sorption to these colloid types and the transport of colloids through the engineered barrier system are discussed in more detail in Section 3.5.

In-Drift Microbial Communities. In-drift microbial communities are also considered as part of the in-drift chemistry. Microbial activity exists at low levels in the host rock (CRWMS M&O 1998c, Section 7). Throughout the drift, microbes will use the nutrients and available energy from chemical oxidation and reduction reactions. The nutrients and energy are present because of system heating, fluid movement, and materials emplaced in the drifts. In the repository environment, many

different microbes could grow and provide a plethora of potential chemical processes that may affect the bulk chemistry within the emplacement drifts (CRWMS M&O 1998c, Section 7). A large source of potential nutrients for microbes is the organic material in concrete ground supports. The waste package materials represent reduced metals that can be oxidized to provide energy for microbes to thrive, and the waste forms themselves contain both nutrient and energy sources for microbes.

A model was developed to assess the possible magnitude of such effects on the system's total chemistry by bounding the magnitude of development of microbial communities (CRWMS M&O 1998c, Section 7; CRWMS M&O 1998i, Sections 4.4 and 4.6). This model uses constraints on the supply rates of both the energy available from oxidation and reduction reactions in the drift and the nutrients used to build an idealized microbial composition, comprised of carbon, nitrogen, sulfur, and potassium in addition to the water components. Other constraints on microbial growth are temperature and relative humidity thresholds in the model that limit the start of microbial activity until the boiling period is over. Even though microbes could be sterilized out of the drifts during the highest temperature period, because they are present in the water-rock system they will return as water drips back into potential drifts. Microbes could also be sterilized in high radiation fields, but microbes would be reintroduced from the geosphere once the radiation field decays to lower levels. This model was not directly used in the base case, but provided first-order limits on potential microbial effects.

3.3.2 Implementation of the Near-Field Geochemical Environment Models

The input, output, and bases for the models in the near-field geochemical environment component are shown as the flow chart in Figure 3-34. The major input parameters come from the unsaturated

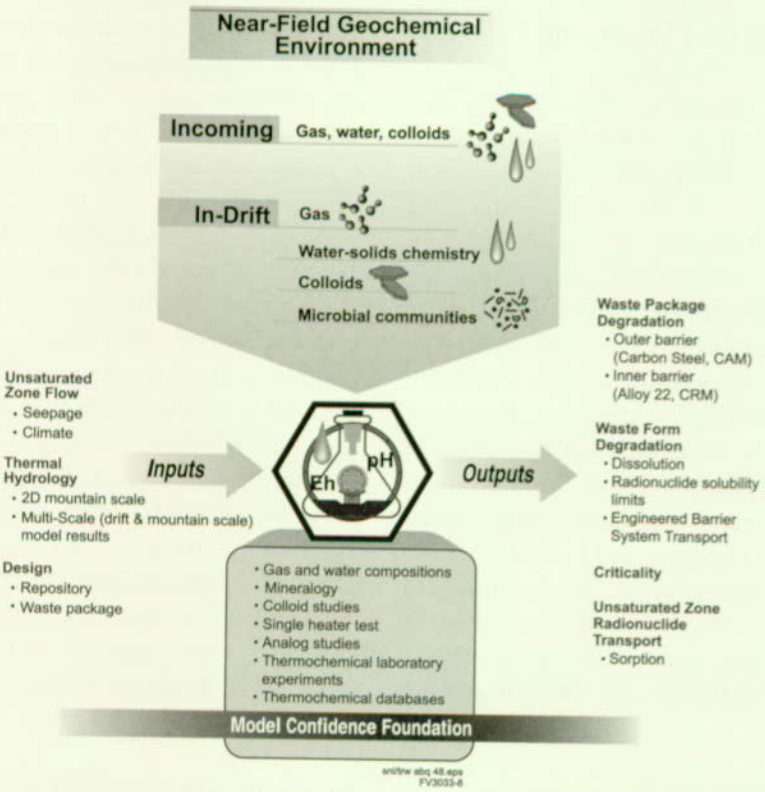

Figure 3-34. Inputs, Outputs, and Bases for the Total System Performance Assessment for the Viability Assessment Near-Field Geochemical Environment Component
The types of studies that have supplied data/concepts to constrain the models are listed. (CAM—corrosion allowance material; CRM—corrosion resistant material)

zone flow and thermal-hydrology components and from the VA design. The primary outputs of the near-field geochemical environment are water and gas compositions provided to the waste package and waste form components. Additional input for conceptual scenarios is provided to the criticality, waste form, and unsaturated zone transport component analyses. In the latter two cases, sensitivity studies were conducted based on scenario development in the near-field geochemical environment (see Section 3.3.3). The bases for the conceptual models and parameter sets defining the near-field geochemical environment models discussed in Section 3.3.1 are in five general categories: site measurements, site experiments, site analog, laboratory experiments, and data analysis and compilation (Figure 3-34). The implementation for each of the near-field geochemical environment models is discussed in this section. The connections among the near-field geochemical environment models are shown in Figure 3-35.

3.3.2.1 Incoming Gas, Water, and Colloids

The submodels of incoming gas, water, and colloids in the near-field geochemical environment component provide both the time-dependent boundary conditions for the gas, water, and colloids compositions and the cumulative fluxes of gas and water constituents entering the emplacement drift. For all the models in the near-field geochemical environment component, the abstracted evolution of system conditions is based on the thermal-hydrologic changes. However, because the total system analyses use time steps of 100 years, explicit coupling of the near-field geochemical environment evolution with the time-dependent thermal changes only captures the coarse behavior of the system. The development of the abstracted periods used in the process-level calculations for the near-field geochemical environment is discussed in the following paragraphs.

Model Implementation for Incoming Gas. The model implementation for incoming gas combines a model of the "air" composition in the mountain with the results of the thermal-hydrology calculations for gas flux. This combination determines changes to the air-mass fraction values caused by boiling water. The thermal-hydrology models evaluate a two-component gas phase (steam and air, see Section 3.2). The air portion represents the fraction of all non-condensable gas components (i.e., everything that is not steam), given by the air-mass fraction (which is 1 minus the steam fraction). The thermal-hydrologic results include the effects of boiling and gas flow on the mix of air and steam in the gas phase but none of the chemical interactions.

The two-dimensional thermal-hydrology model at the mountain scale provides both the air mass fraction and the gas flux through the drifts as continuous functions of time to 100,000 years. After that time, the system is considered to have returned to ambient conditions. These results were provided at the center and edge of a two-dimensional cross section running east to west through the middle of the repository (Section 3.2). The air-mass-fraction variations and the changes in air fluxes were used to delineate a number of periods for which gas compositions can be approximated as constant values with step changes at the transition points. For each of these periods, constant average values for air mass fraction were abstracted from the more continuous thermal-hydrologic results resulting in a stepped representation that captures the major variations that occur. Because most of the variation is caused by boiling effects during the early, higher temperature conditions (boiling regime), these earlier times are divided at a finer scale than the later periods that represent below boiling conditions (cooling regime). The thermal-hydrologic results for gas flux into the drift were used with the air mass fractions to constrain the cumulative flux of air into the drift for the defined periods. Combining these with the air composition defined for each period (as discussed below) allowed derivation of cumulative fluxes of each air constituent per meter of drift.

In general, the abstracted air mass fractions return to constant ambient values in only hundreds to a few thousand years after the boiling regime. Therefore the air mass fractions do not provide

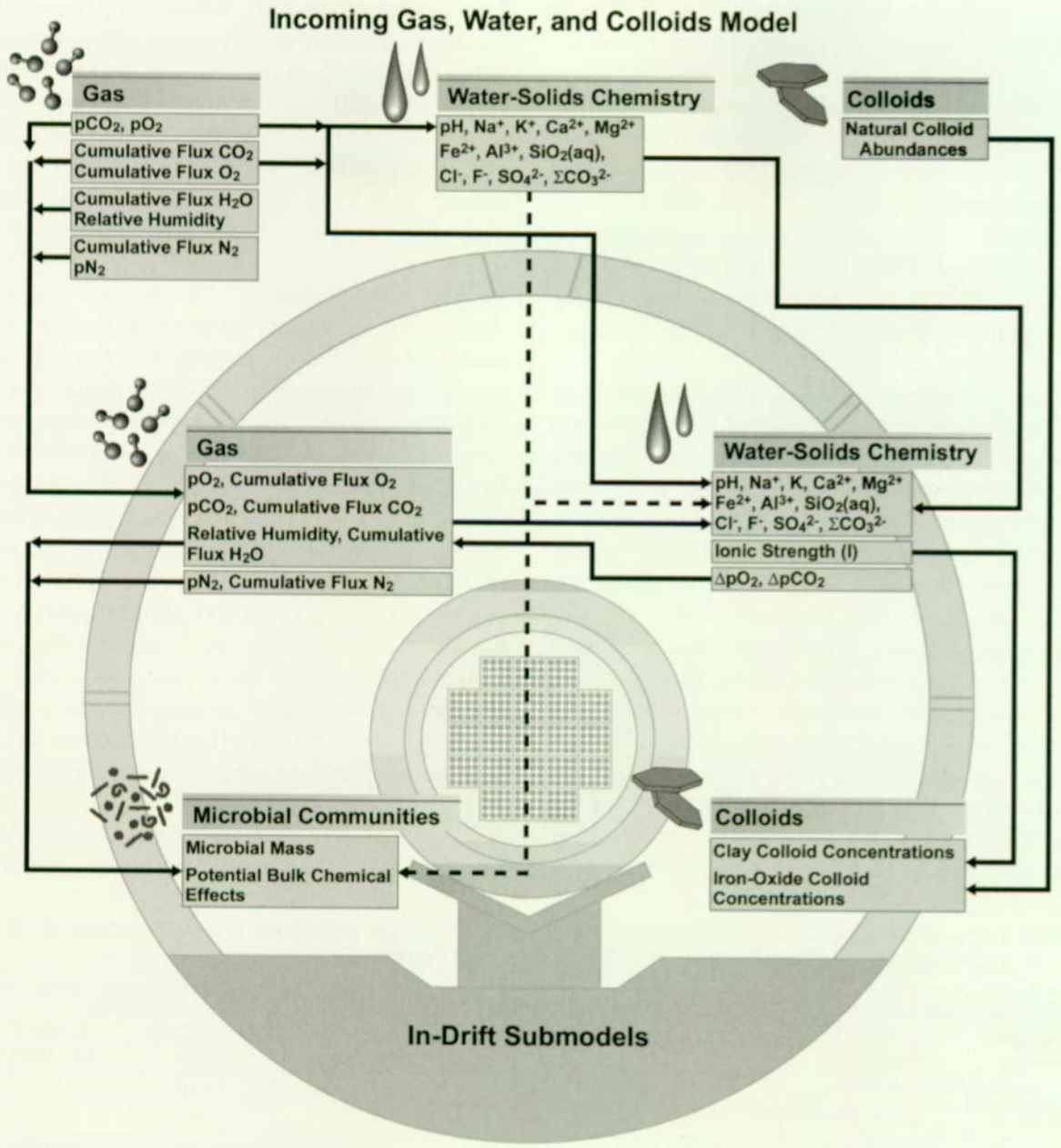

Figure 3-35. Flow Diagram Depicting the Parameter Exchanges Among all Near-Field Geochemical Environment Models
This figure provides a more detailed representation of the flow of information presented in Figure 3-28.

a useful basis for delineating abstracted periods after that point. For later times, variations in temperature were used to develop an additional set of abstracted periods representing the transition from boiling to cooling and the temperature decrease during the cooling regime. The time above boiling was defined based on the drift wall temperature because, for gas-water-rock reactions, the water boiling in the host rock is most important. During the boiling regime, any reaction of gas with fracture water was assumed to occur at 95°C (203°F), just below the boiling temperature), approximating reflux water reacting just before re-evaporation. The cooling regime was divided into temperatures of 70°C (158°F) and 30°C (86°F) to capture coarsely the intermediate- and lower-temperature conditions for reaction in the system.

The two dimensional, thermal-hydrology model at the mountain scale uses a smeared heat source and provides temperatures in the rock a small distance from the drift wall (Section 3.2). The model does not give an accurate drift wall temperature history, including the transition time to below boiling conditions. Instead, the drift-scale results of the multiscale (drift plus mountain scale) thermal-hydrologic models were used because they provided a more accurate thermal history of the drift wall. The multiscale thermal-hydrologic calculations provided average thermal evolutions for six repository regions (Section 3.2). These six regions were classified as center-like (Region CC), edge-like (Region SW), and intermediate (the other four regions) to determine how to link their average thermal evolutions with the center and edge results from the two-dimensional, mountain-scale model. The time that average drift wall temperatures are above boiling is given by drift-scale results of the multiscale (drift plus mountain scale) thermal-hydrologic model for Region CC. The abstracted periods defined for the system based on this thermal history overlap somewhat with those based on the air-mass fraction. These two sets of abstracted periods were synchronized by ensuring that the break between the boiling and cooling regimes corresponded to the end of the last boiling period as defined by air-mass fraction changes.

Because the duration of the thermal change is greatest for the central portion of the repository, the near-field geochemical environment analyses were focused on this portion of the system. For the repository center, the time-period abstractions created three boiling periods which were defined as Period A (0–200 years), Period B (200–1,000 years), and Period C (1,000–2,000 years), and three cooling periods which were defined as Period D (2,000–4,000 years), Period E (4,000–10,000 years), and Period F (10,000–100,000 years). The boiling-regime periods are assigned the same temperatures, but they have various gas constraints (air mass fractions and air fluxes). The cooling-regime periods have different temperature and gas constraints (gas fugacities and cumulative fluxes). The conditions that result from this submodel (CRWMS M&O 1998i, Section 4.5) are summarized in Table 3-10. For the repository edge areas,

Table 3-10. Abstracted Periods, Temperatures, Gas Fugacities and Cumulative Gas Fluxes (Per Meter of Drift) Used for the Near-Field Geochemical Environment Component

Boiling Regime						
Abstracted Period	**Time Years**	**Temperature °C/°F**	**CO_2 Fugacity ppmv**	**ΣCO_2 gas flux Moles/Meter**	**O_2 Fugacity ppmv**	**ΣO_2 gas flux Moles/Meter**
A	0-200	95/203	$1x10^2$	180	2×10^2	510
B	200-1,000	95/203	$1x10^{-4}$	190	$2x10^{-2}$	1000
C	1,000-2,000	95/203	$1x10^1$	270	$2x10^3$	25,000
Cooling Regime						
Abstracted Period	**Time Years**	**Temperature °C/°F**	**CO_2 Fugacity ppmv**	**ΣCO_2 gas flux Moles/Meter**	**O_2 Fugacity ppmv**	**ΣO_2 gas flux Moles/Meter**
D	2,000-4,000	70/158	$1x10^2$	810	$2x10^4$	170,000
E	4,000-10,000	70/158	$1x10^3$	2,100	$2x10^5$	530,000
F	10,000-100,000	30/86	$1x10^3$	4,500	$2x10^5$	1,200,000

ppmv—parts per million by volume

the time in the boiling regime is much shorter than it is in the central portion of the repository, and the return to ambient conditions occurs more rapidly. Because the thermal change is shorter in the edge and intermediate regions, the evolution of the near-field geochemical environment in these regions is bounded by modeling only the central portion of the repository. The TSPA-VA results are put into the general context of these periods in Section 2.4.

The incoming gas submodel defines the air composition. The model air composition description is based on the ambient pore gas (which differs from atmospheric air in carbon-dioxide content), with inclusion of a limited period of elevated carbon dioxide values for the early behavior of the heated system. This early change in carbon dioxide content reflects primarily potential mineral sources of carbon dioxide in the rock. The model of air composition is implemented only as a logical model (there is not a code that calculates the values); the values are assigned directly for the specific periods in the system evolution. The values used are atmospheric, about 20 percent oxygen and 80 percent nitrogen gases, through all periods with the partial pressure of the nitrogen gas adjusted to offset the increased carbon dioxide in certain conditions. For carbon dioxide, as discussed in Section 3.3.1, the ambient value is taken as 1,000 parts per million by volume. A value of 100,000 parts per million by volume, or 10 percent, is designated for the first 200 years (Period A) to reflect reaction of heated calcite and silica to form a calcium-silicate mineral and release carbon dioxide (Figure 3-30, Inset B). Combining the air-composition model and the abstracted air mass fractions from the thermal-hydrology model provides the incoming gas compositions within the near-field geochemical environment.

Model Implementation for Incoming Water. The model implementation for incoming water included process-level calculations using the EQ3/6 geochemical modeling code package (Wolery 1992a; 1992b; Wolery and Daveler 1992). The calculations are discussed below and details of the analyses are given in Section 4 of the *Total System Performance Assessment-Viability Assessment (TSPA-VA) Analyses Technical Basis Document* (CRWMS M&O 1998i, Section 4). For each of the abstracted periods, the conditions for gas composition and temperatures shown in Table 3-10 were used in calculations of water compositions. For each period, calculations were performed for reaction and equilibration of the heated water with the minerals and the gas phase. The two types of temperature regimes, a boiling regime and a cooling regime, were again recognized here. The additional processes considered during boiling regime calculations required a slightly different model implementation than the implementation for cooling regime calculations. The specific differences between these two implementations are detailed in the following paragraphs.

Despite some differences in the methods of calculation, the boiling and cooling regime implementations have many factors in common. Both of these implementations consider the same dissolved constituents in the aqueous phase: pH, sodium (Na^+), potassium (K^+), calcium (Ca^{2+}), magnesium (Mg^{2+}), iron (Fe^{2+}), aluminum (Al^{3+}), silica (SiO_2), chloride (Cl^-), fluoride (F^-) carbonate (CO_3^{2-}) and sulfate (SO_4^{2-}). These constituents comprise the total masses of these components within the fluid and may be represented by a number of different species in solution. In process-level calculations, initial concentrations for many of these constituents are taken from the average composition of the groundwater sampled at Well J-13 for the saturated zone tuff aquifer (CRWMS M&O 1998c, Section 6.2; CRWMS M&O 1998i, Section 4.5). In addition, the equilibrium oxidation potential of the system was constrained by the oxygen fugacity, and the total dissolved carbonate was set to equilibrium with the carbon dioxide fugacity. The total Ca^{2+} content of the solution was set to be in equilibrium with the mineral calcite, and the system pH was calculated by charge balance constraints.

Calculations for the two temperature regimes, as given in Table 3-10, differ in the mineralogical constraints on the fluid composition and in the calculation method for the final fluid composition. The cooling regime implementation is simpler; for each of the periods in the cooling regime, a single model calculation was performed

using the EQ3NR code (Wolery 1992a; 1992b). In these calculations, the average J-13 water composition was equilibrated with the gas phase and a set of minerals at the appropriate temperature. In addition to the common constraints listed in the previous paragraph, the cooling regime calculations had dissolved silica set to equilibrium with alpha-cristobalite, Al^{3+} set to equilibrium with calcium-montmorillonite, Fe^{2+} set to equilibrium with calcium-nontronite, and Mg^{2+} set to equilibrium with calcium-saponite. These mineral constraints represent the silica and clay minerals resulting from alteration of the primary phases in the tuff (CRWMS M&O 1998c, Section 5; CRWMS M&O 1998i, Section 4.5).

In the calculations for the boiling-regime fluids, the water is not simply equilibrated with the changed gas compositions and minerals. Instead, to represent some of the effects of concentration via boiling, calculations were done to evaporate 90 percent of the water, allowing mineral phases to precipitate as the solution becomes more concentrated. Equilibrated water compositions were calculated using the strategy proposed in the *Near-Field/Altered-Zone Models Report* (CRWMS M&O 1998c, Section 6.2), modified with appropriate gas compositions and temperatures for each of the three boiling regime periods in Table 3-10. Equilibration of the initial J-13 water composition was calculated at the appropriate temperature and gas conditions with dissolved silica set to alpha-cristobalite equilibrium, in addition to the common constraints listed earlier. Then, the evaporation of water was simulated at the same temperature and gas conditions using the resulting fluid from the previous calculation. Quartz, tridymite, and talc are suppressed, or prevented from precipitating for these analyses, to reflect kinetic constraints in the system (CRWMS M&O 1998c; CRWMS M&O 1998i, Section 4.5). Conservative elements that are not precipitated in minerals have their final concentrations increased to 10 times the starting J-13 concentration. However, final concentrations of elements such as Ca^{2+} are controlled by phases that precipitate during the evaporation and boiling process.

Incoming-Colloids Model. The incoming-colloids model is a qualitative assessment of the types of colloids that may enter the drift and general constraints on the amounts of those colloid types. This model provides those qualitative constraints to the in-drift colloids model, in the form of a potential source of clay colloids. The in-drift colloid model is the only source of colloid abundances that are used by the other performance-assessment models. Therefore, the implementation of the model for incoming colloids (i.e., calculated abundances of clay colloids) was handled within the model for in-drift colloids discussed in Section 3.3.2.2. In brief, this entailed the use of site measurements on naturally occurring colloids in Yucca Mountain groundwaters (Triay et al. 1996, Table I) to show that a relation universally observed for colloids is relevant for the Yucca Mountain site (CRWMS M&O 1998m, Section 6.3.6; CRWMS M&O 1998i, Section 4.5). This relationship was implemented directly within the TSPA computer program RIP (Golder Associates, Inc. 1998) in the engineered barrier system cells (CRWMS M&O 1998i, Section 6).

3.3.2.2 Evolution of the In-Drift Chemistry

Model Implementation for In-Drift Gas. The model implementation for in-drift gas used the incoming gas compositions and fluxes directly to define in-drift gas constituents through time. There are two related major assumptions underlying this model. The first is that the in-drift gas composition is not affected substantially by reaction with the in-drift solids, and the second is that gas migration and mixing in the drift is rapid enough to maintain a homogeneous gas composition throughout the environment. The second assumption is relatively robust because gaseous diffusion alone is rapid enough to ensure homogeneity on these scales. The first assumption precludes generation of local changes to the in-drift gas composition from reaction with materials that are abundant compared to the gas. However, this assumption was evaluated to be reasonable for oxygen and carbon dioxide, the two major gas constituents of interest.

The first assumption was evaluated using mass-balance calculations. For these calculations, the in-drift materials were first assessed for their ability to act as either source or sinks of oxygen and carbon dioxide, and then relative masses for the sink and the source were compared. For oxygen, the major sink was taken to be oxidation of the iron content of the steels in both waste package and ground support materials. No major sources of oxygen from in-drift materials have been identified. The large mass of calcium in the concrete that would need to be carbonated to prevent extensive development of alkaline water in the drift was used for the mass-balance assessment for carbon dioxide. A simple mass-balance calculation was performed for each of these cases in which the cumulative flux of the constituent was compared with the mass that potentially could be removed by the material. Results of both the mass-balance and reaction-path analyses are presented in Section 3.3.3.

In-Drift Water-Solids Chemistry. For model implementation of in-drift, water-solids chemistry, the incoming water composition is used as the starting composition for reaction. In most cases, the reaction of this initial fluid with in-drift materials, including spent nuclear fuel, was evaluated at the temperature and gas conditions of the appropriate abstracted period (Table 3-10).

Corrosion Products. These analyses were implemented to simulate the equilibration of the incoming water with goethite, FeO(OH). This oxidized-iron phase was used to represent the corrosion products of the iron in steel (CRWMS M&O 1998i, Section 4.5). The calculations were done for each period at the appropriate temperature and gas composition as given in Table 3-10, with the initial dissolved concentrations specified as those from the incoming water composition except for the total dissolved iron constraint which was set to equilibrium with goethite. The output results are discussed in Section 3.3.3 and represent the base case for water that may enter the waste package. The resulting water compositions are used in the base case analyses and provided to the spent-fuel submodel as shown in Figure 3-33.

Concrete. The model calculations to evaluate the geochemical effects of concrete on the water composition were performed as reaction-path calculations using the EQ6 code (Wolery 1992a; Wolery and Daveler 1992). These calculations were performed as titration calculations where mineral constituents in the concrete progressively react with the incoming water compositions at the gas constraints and temperature conditions given in Table 3-10. The carbon dioxide and oxygen gas concentrations were specified initially but, as the reaction progressed, the gas composition could change in response to the water-mineral reactions. This flexibility was provided to evaluate whether available carbon dioxide could neutralize concrete alkalinity (high pH).

Design information on the concrete compositions was used to define reactant materials for these analyses (CRWMS M&O 1998i, Sections 4.3, 4.5). The concrete consists of cement, coarse and fine tuff aggregate, and steel fiber (iron) (CRWMS M&O 1998c, Sections 6.3, 7.2; CRWMS M&O 1998i, Section 4.5). The cement and tuff consist of multiple phases. The mineral assemblage used for the cement is for a relatively young cement that has not undergone much chemical or thermal alteration. This mineral assemblage consists of ettringite, calcium-silicate hydrate, brucite, hydrogarnet, and portlandite, with the relative amounts calculated based on the oxide composition (CRWMS M&O 1998i, Sections 4.3, 4.5). Both the coarse and fine aggregate are composed of Topopah Spring tuff and were represented by a normative modal mineral assemblage consisting predominantly of alkali feldspar, alpha-cristobalite and quartz (CRWMS M&O 1998c, Section 6.3; CRWMS M&O 1998i, Sections 4.3, 4.5). These minerals reacted with the incoming water composition at relative rates assigned to represent relatively fast dissolution of the cement phases and slower dissolution of the tuff aggregate phases and steel fiber.

Results of the analyses for water reaction with concrete are given in Section 3.3.3. Because the concrete lining is expected to collapse within the first few hundred years (see Section 3.3.1), concrete-modified water is not used in the base

case. The collapse of the concrete lining would remove it from much of the potential pathways of dripping water above waste containers. However, because the collapsed concrete mass will still be available to react with water on the lower portion of the waste package for a long time, these water compositions are evaluated in a sensitivity study (see Section 5.3). In addition, the possibility that these fluids could migrate through the unsaturated zone, causing large changes to radionuclide sorption, is examined in Section 5.6.

Spent Fuel. Because the spent nuclear fuel represents a large material mass, its capacity to affect the bulk fluid composition was evaluated for the near-field geochemical environment. The tool used for these analyses is the general reactive-transport code AREST-CT (Chen et al. 1995; 1996; 1997a; 1997b; Chen 1998). Using this program, this evaluation considers both equilibrium and kinetically controlled chemical reactions between solid phases, aqueous solutions, and gas under flowing conditions.

These analyses were done to reflect conditions within either Period E or Period F (Table 3-10) for both active alteration of spent-fuel to secondary phases, and subsequent dissolution and alteration of the secondary phases to a tertiary set of uranium minerals. These periods were chosen because only a few base case waste packages fail before 4,000 years (Section 3.4). For these calculations, both the oxygen and carbon dioxide fugacities were set to their ambient compositions (Table 3-10). The spent nuclear fuel is represented as a one-dimensional porous medium with various specific surface areas (CRWMS M&O 1998i, Section 4.4).

The chemical system is a subset of the water composition reacted with corrosion products and consists of the components pH, sodium (Na^+), calcium (Ca^{2+}), silica (SiO_2), chloride (Cl^-), and carbonate (CO_3^{2-}), with the addition of the spent nuclear fuel components uranium (UO_2^{2+}) and neptunium (NpO_2^+). These constituents comprise the total masses of these components within the fluid and may be represented by a number of different species in solution. The kinetic rate of the spent nuclear fuel dissolution reaction was constrained by the rate model based on observations for UO_2 dissolution rates (CRWMS M&O 1998i, Section 4.4). Besides the UO_2 dissolution reaction, the simulation also considered the kinetically controlled precipitation of four secondary uranium (UO_2^{2+}) mineral reactions. The concentration of neptunium that may enter a secondary uranium phase was also constrained by data from dissolution testing of secondary phases developing within waste under dripping water conditions (CRWMS M&O 1998i, Section 4.4).

Four simulations were carried out to evaluate the effects of water composition during the active period of primary waste form alteration and subsequent effects of secondary-phase dissolution. The four simulations were carried out at 70°C (158°F) and 30°C (86°F) with two different percentages of cladding failure (two different amounts of spent nuclear fuel available to react with water; 1 percent and 100 percent). The bulk composition of the water at the end of the one-dimensional pathway was assumed to be the resulting water composition for consideration in the near-field geochemical environment. These results for spent nuclear fuel effects on water composition are discussed in Section 3.3.3. The results of the evolutions of the waste form and secondary uranium phases, and the release and retention of neptunium by these phases, are discussed more fully in Section 3.5.

Precipitates and Salts. This submodel was used to evaluate a set of bounding analyses of the mass and timing of precipitated minerals build up on the waste package surface and the capacity for generation of highly concentrated brines during the boiling period. These analyses were not used directly within the calculations but were used to assess the need for future work in this area (CRWMS M&O 1998i, Section 4.6).

Model Implementation for In-Drift Colloids. The model implementation for in-drift colloids calculated colloid concentrations as a function of ionic strength based on a statistical fit of measured colloid concentrations. This statistical fit of measured colloid concentrations was calculated for particles greater than 100 nm in groundwaters of

various ionic strengths from around the world (CRWMS M&O 1998m, Section 6.3.6; CRWMS M&O 1998i, Section 4.4). Although colloids smaller than 100 nm exist, the available data to constrain the colloid abundance relation are most accurate for the greater than 100 nm colloids (CRWMS M&O 1998m, Section 6.3.6.1; CRWMS M&O 1998i, Section 4.4). This relation may therefore not include an amount of colloids that potentially could account for about 10–40 percent of colloidally transported radionuclides (CRWMS M&O 1998i, Section 4.4). The colloid abundance relation and its associated uncertainty were implemented directly as part of the waste form engineered barrier system source-term cells.

For each of the abstracted periods, the ionic strength of fluids calculated from the submodel for the in-drift water-solids chemistry was used with this relationship to assess the stability and concentration of the suspended colloids reacting with the waste form. Other than this connection, the in-drift colloid model is relatively independent of the other near-field geochemical environment submodels (Figure 3-35). The amounts of iron-oxyhydroxide and clay colloids were assessed by this method directly within the system integration program RIP (CRWMS M&O 1998i, Section 4.5). They are used as input to the colloid sorption and transport model for plutonium, which is discussed within Section 5.5 and the *Total System Performance Assessment-Viability Assessment (TSPA-VA) Analyses Technical Basis Document* (CRWMS M&O 1998i, Section 6).

Model Implementation for In-Drift Microbial Communities. The model implementation for in-drift microbial communities was intended to be a bounding assessment on the masses of produced microbes. The model is implemented with a code (Ehrhorn and Jolley 1998; CRWMS M&O 1998i, Sections 4.4, 4.6) for microbial impacts to the near-field geochemistry and uses an idealized approach to assess the biomass production. At each time step, the analysis determines whether biomass production is limited based on the available energy in the system or the nutrient supply for microbes. The microbial production for that time step is the lower of the two values. The production rate and the cumulative biomass can then be tracked for the time of the analysis to determine the biomass yield and system limitations. These analyses were not used directly within the calculations but were used to assess the need for potential future work in this area (CRWMS M&O 1998i, Section 4.6).

3.3.2.3 Major Uncertainties Within the Models

This section provides a general discussion of sources of uncertainties in the near-field geochemical environment models that are described in greater detail in the *Total System Performance Assessment-Viability Assessment (TSPA-VA) Analyses Technical Basis Document* (CRWMS M&O 1998i, Sections 4.4–4.6). Much of the uncertainty for the near-field geochemical environment stems from conceptual model uncertainties. This is particularly true for models of in-drift materials that use thermochemical data (equilibrium and kinetic parameters). The coupling among geochemical effects and physical processes in real systems cannot be incorporated comprehensively into the current near-field geochemical environment submodels. The inability to represent this coupling is another large contributor to conceptual uncertainty in these models; this is particularly the case for the evolution of the gas composition in this system. Thermal-hydrologic processes interact strongly to drive gas flow and generation of certain gas constituents. However, reactions among the gas, water, and minerals occurring simultaneously in this flowing system are only coupled in a limited manner in the near-field geochemical environment component. Limited representation of coupling is also true for the models of concrete effects that do not explicitly evaluate system flow or address permeability changes of the concrete caused by mechanical evolution or precipitation of alteration phases.

Further conceptual uncertainty is related to the inability to observe processes for geologic time spans, which introduces uncertainty about the appropriate time scale for applying those processes. Observations of analogs provide some insight, particularly into the state that a system has

evolved to over geologic time. However, only portions of the system can be observed generally (usually only the solids), and chemical and flow conditions must be inferred to extract quantitative information from the analogs. Applying observations of analogs to another system that may not be governed by the same conditions is another source of conceptual uncertainty.

Part of the conceptual uncertainty for coupled processes stems from limitations of the modeling tools applied to these types of systems. In general, a tradeoff must be made between tools that allow evaluation of a more comprehensive chemical system and those that allow an idealized geochemistry to be coupled to the thermal-hydrology. Uncertainty in the mathematics of the model, or representational uncertainty, is generally relatively small for the geochemical aspects of the near-field geochemical environment submodels in comparison to the conceptual uncertainties. However, computer codes that provide a representation more closely coupled to the hydrology of the system, tend to have larger mathematical or numerical uncertainties.

Parameter uncertainty may be large for models using thermochemical data if well constrained measurements are not available or are not available for the conditions needed (e.g., higher temperature). Lack of data for the appropriate species in a system is a type of conceptual uncertainty because the chemical processes involving those species cannot be included in the model.

The general approach to the large amount of conceptual uncertainty in the geochemical system is to separate the major potential contributors to water compositional changes into various subsystem models (e.g., gas phase, concrete, and microbes). These separate models can be used individually to assess the relative capacities of these processes to alter compositions of various chemical phases at various times. Such uncoupled models facilitate identification of the processes that may control the bulk chemistry for various time frames. Then, the dominant processes can be assigned to the appropriate time frames, or the models that need to be coupled can be identified.

A first level of coupling can be achieved by identifying conceptual scenarios that link the various processes along a pathway for water reaction. These pathways can be examined both with and without a particular subsystem model included as a means to bound the conceptual uncertainty in that subsystem model. For example, modeling scenarios for the in-drift water-solids chemistry with and without concrete capture the major portion of the conceptual uncertainty in the effects of concrete ground support. This approach does not encompass all sources of conceptual uncertainties because they also exist within each model, for example, the local equilibrium assumption in the water-solids submodel. These additional submodel conceptual uncertainties, together with parameter and representational uncertainties, are reflected in the parameter output distributions generated by the various submodels for each scenario (e.g., concreted versus no-concrete) analyzed in the TSPA-VA.

3.3.3 Results and Interpretation

The results of the near-field geochemical model analyses are presented in sections that follow. The focus is on results that provide quantitative inputs either for other TSPA-VA component models or for the TSPA model, and are therefore incorporated into the system-level performance assessment results (e.g., see Sections 3.4 and 5.3). Other analyses conducted in this near-field geochemical environment component of the TSPA-VA provide preliminary constraints on the potential magnitude of additional issues having large uncertainties. The results of those analyses are used to evaluate the potential need for incorporation of those additional processes into system-level assessments. Such analyses also provide a basis for planning and directing process-level and performance-assessment-level investigations and model enhancements to be used in future analyses of performance. All of the results discussed below are described in detail in the *Total System Performance Assessment-Viability Assessment (TSPA-VA) Analyses Technical Basis Document* (CRWMS M&O 1998i, Sections 4.5, 4.6).

3.3.3.1 Gas Compositions

Time variation in gas composition (carbon dioxide and oxygen) provided by submodels of the near-field geochemical environment component are shown in Figure 3-36. These gas compositions apply to the entire region near the drift, within and outside the drift. During the boiling period (0-2,000 years for the center portion of the modeled repository), these gas components are diluted by steam generation. A relatively large decrease in the levels of these gases can be seen from 200 to 1,000 years, which corresponds to the peak boiling conditions. Although there are several smaller changes after 1,000 years, the model values of carbon dioxide and oxygen fugacities return to ambient levels at around 4,000 years. The reduction in oxygen content may provide some benefit to any degradation processes dependent on oxidation (waste package, cladding, or waste form). However, because this reduction occurs primarily at conditions above boiling, no waste package degradation would be expected (see Section 3.4). For the corresponding edge areas, the return to ambient gas composition occurs around 1,000 years. On the 100,000-year time scale shown in Figure 3-36, the effects of gas composition are relatively short lived.

A simple bounding, mass-balance calculation was used to evaluate the likelihood of depletion of oxygen during package corrosion producing reducing conditions for waste form reactions. To decrease the oxygen fugacity to a reducing

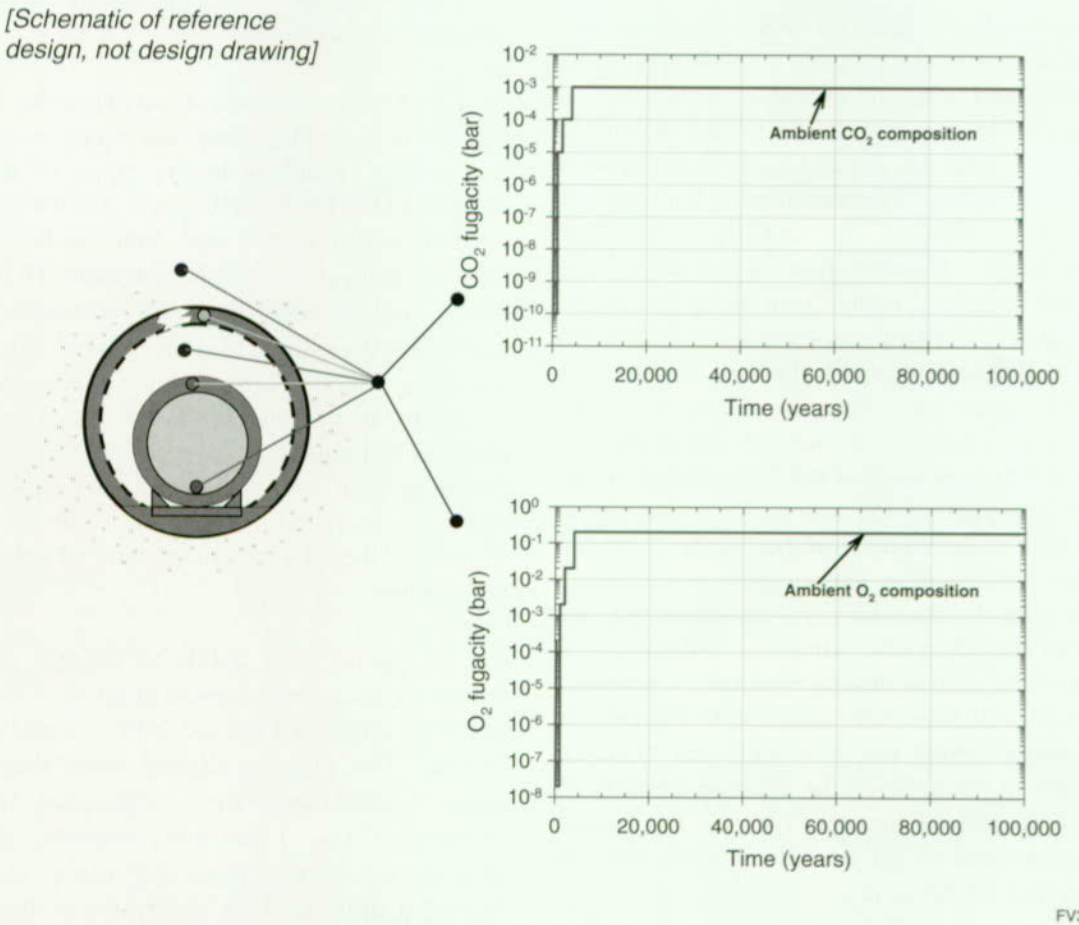

Figure 3-36. Near-Field Geochemical Environment Gas Composition Results for Carbon Dioxide and Oxygen from Time of Waste Emplacement to 100,000 Years

As indicated by reference to the schematic of a drift cross-section and waste package. These gas compositions apply to the entire region within and near the drift, including inside of the waste package.

condition (reduced by at least two orders of magnitude), the waste packages must be able to use effectively all of the oxygen as it is supplied. The cumulative mass flux of oxygen from both the gas and water flux indicates that oxygen levels may be low during the peak boiling period (out to about 1,000 years). By 4,000 years the cumulative oxygen gas flux is up to about 1.7×10^5 moles of oxygen gas per meter of drift, or about 450 percent of the oxygen gas needed for full oxidation. At 100,000 years, about seven times that mass of oxygen has been fluxed through the drifts. Therefore, reducing conditions in the drift do not appear very likely as a result of this mechanism.

A mass-balance analysis also assessed whether the amount of carbon dioxide entering the drifts was sufficient to completely carbonate the cement.

This mass-balance analysis was based on the assumption that all the calcium in the cement must bond with carbonate to prevent an increase in alkalinity. The cumulative mass flux of carbon dioxide from both the gas and water flux provides about 51,300 moles of carbon dioxide per meter of tunnel fluxed through the drift over the first 100,000 years. Most of this carbon dioxide is supplied as dissolved materials in the groundwater. At 10,000 years, only about 4,200 moles of carbon dioxide have passed through the drift, and the gas and water fluxes contribute about equally to this mass. To form calcite, one mole of carbon dioxide is needed for every mole of calcium. Based on the mass of concrete in the tunnel, there are about 20,000 total moles of calcium per meter of tunnel. Therefore, there is more than twice as much carbon dioxide than is necessary to carbonate all the cement in 100,000 years. However, only about 20 percent of the carbon dioxide needed to carbonate the cement will have been supplied to the drift in 10,000 years. Other reactions will need to play a major role in neutralizing the alkaline capacity of the large masses of concrete planned for ground support, or alkaline fluids will be likely over at least the first 10,000 years.

3.3.3.2 Water Compositions

Figures 3-37a, 3-37b, and 3-37c show water composition results for the near-field geochemical environment through the first 100,000 years for pH, total dissolved carbonate, (ΣCO_3^{2-}), and ionic strength (I), respectively. In the figures, different modeled results apply to the different regions, both within and outside the drift. During the boiling period, (0–2,000 years for the center portion of the modeled repository), pH values are near 10 for both incoming water and water that has reacted with iron oxides. Later, the pH values drop. The total dissolved carbonate (ΣCO_3^{2-}) values show a large decrease until about 1,000 years. This decrease is caused mainly by changes to gas compositions as shown in Figure 3-36. The ionic strength of these fluids is about 10 times higher until about 2,000 years, primarily because of concentration by boiling.

By 10,000 years, the calculated pH values are near 8 for both incoming water and water reacted with iron oxides, which is in the range of measured ambient pH at the site. However, for the water that reacted with concrete and iron oxides, the pH values remain close to 11 for the entire 10,000-year period, and the total dissolved carbonate (ΣCO_3^{2-}) and ionic strength values are lower than for the incoming fluid. These lower values are caused primarily from interaction of water with the alkaline and sulfate components of cement in the concrete; even with additional reactions that bind calcium included, such as silicate-mineral formation, the alkaline components of the concrete still influence water pH.

For the period from 10,000 to 100,000 years, pH values are projected to be about midway between 7 and 8 for water that reacted with concrete and iron oxides. This range is slightly lower than for the cases without concrete. The total dissolved carbonate (ΣCO_3^{2-}) and ionic strength values are also slightly lower. These differences also result from the different bulk chemistry in the system with concrete, with the calcium content of the solids and fluid playing a primary role.

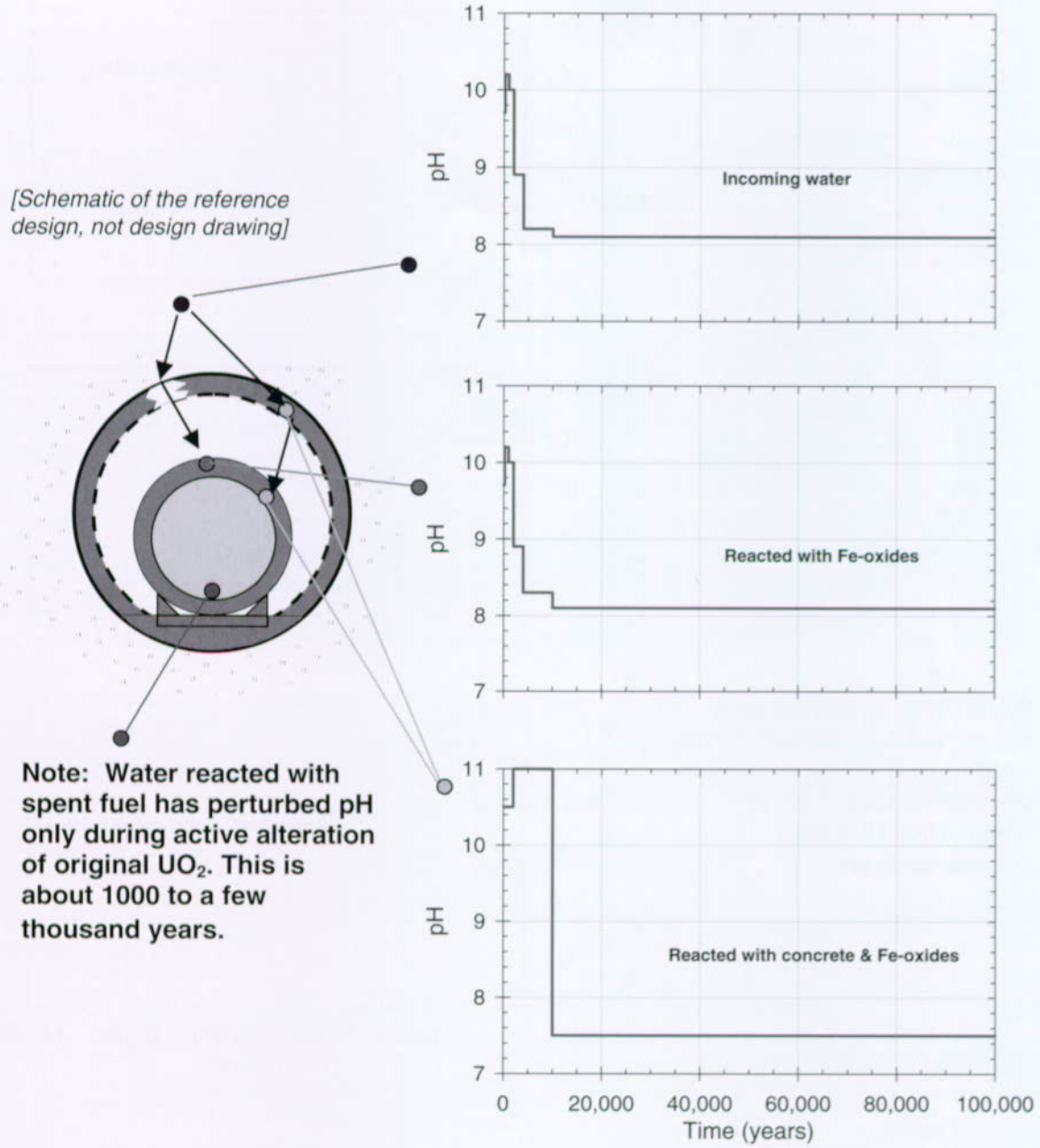

Figure 3-37a. Near-Field Geochemical Environment Water Composition Results, pH Values, for the Time Frame from Time of Waste Emplacement to 100,000 Years
The region where the results of each plot applies is indicated by reference to a schematic of a drift cross-section with a waste package.

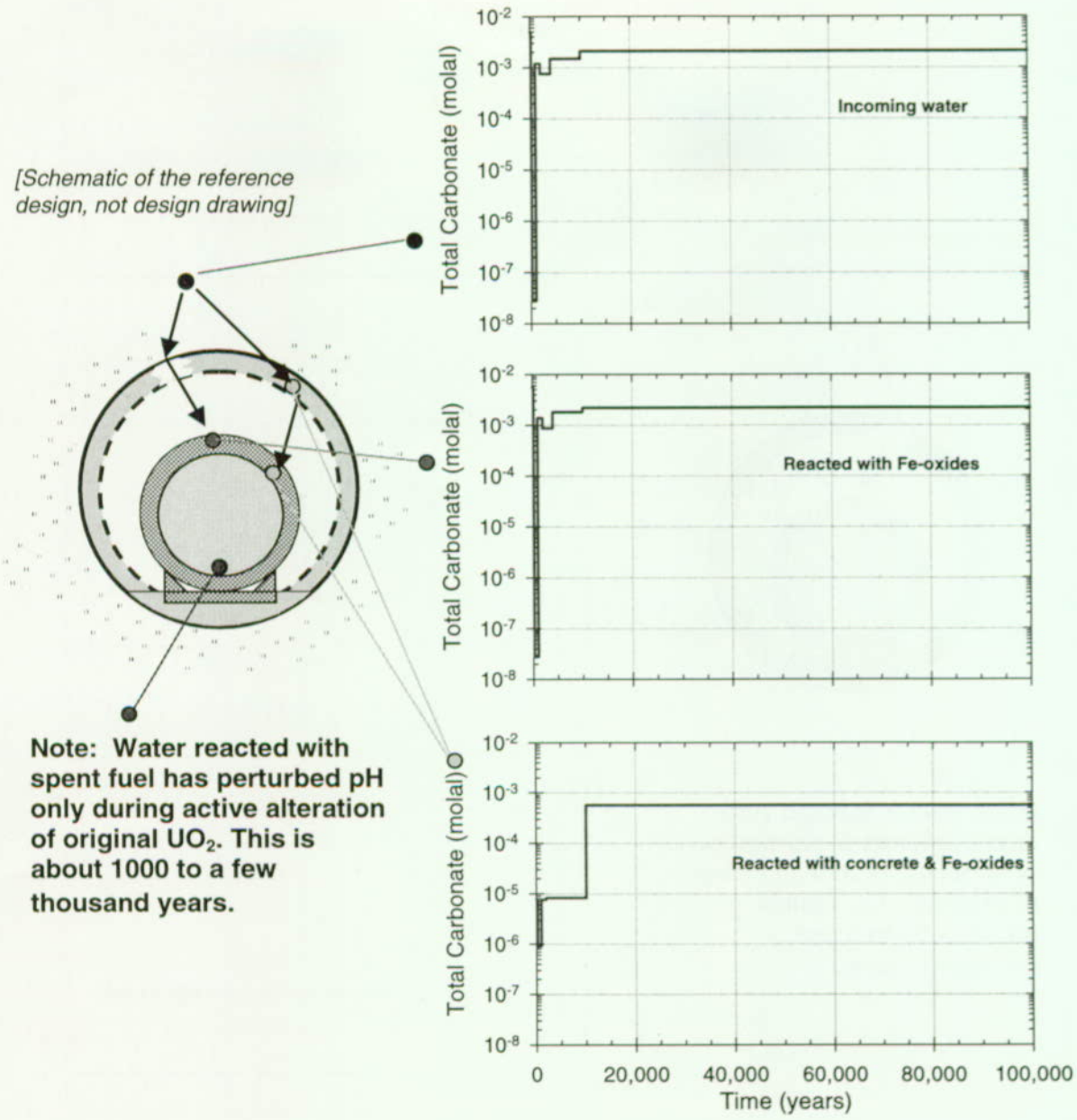

Figure 3-37b. Near-Field Geochemical Environment Water Composition Results, Total Dissolved Carbonate Values (ΣCO_3^{2-}), for the Time Frame from Time of Waste Emplacement to 100,000 Years
The region where the results of each plot applies is indicated by reference to a schematic of a drift cross-section with a waste package.

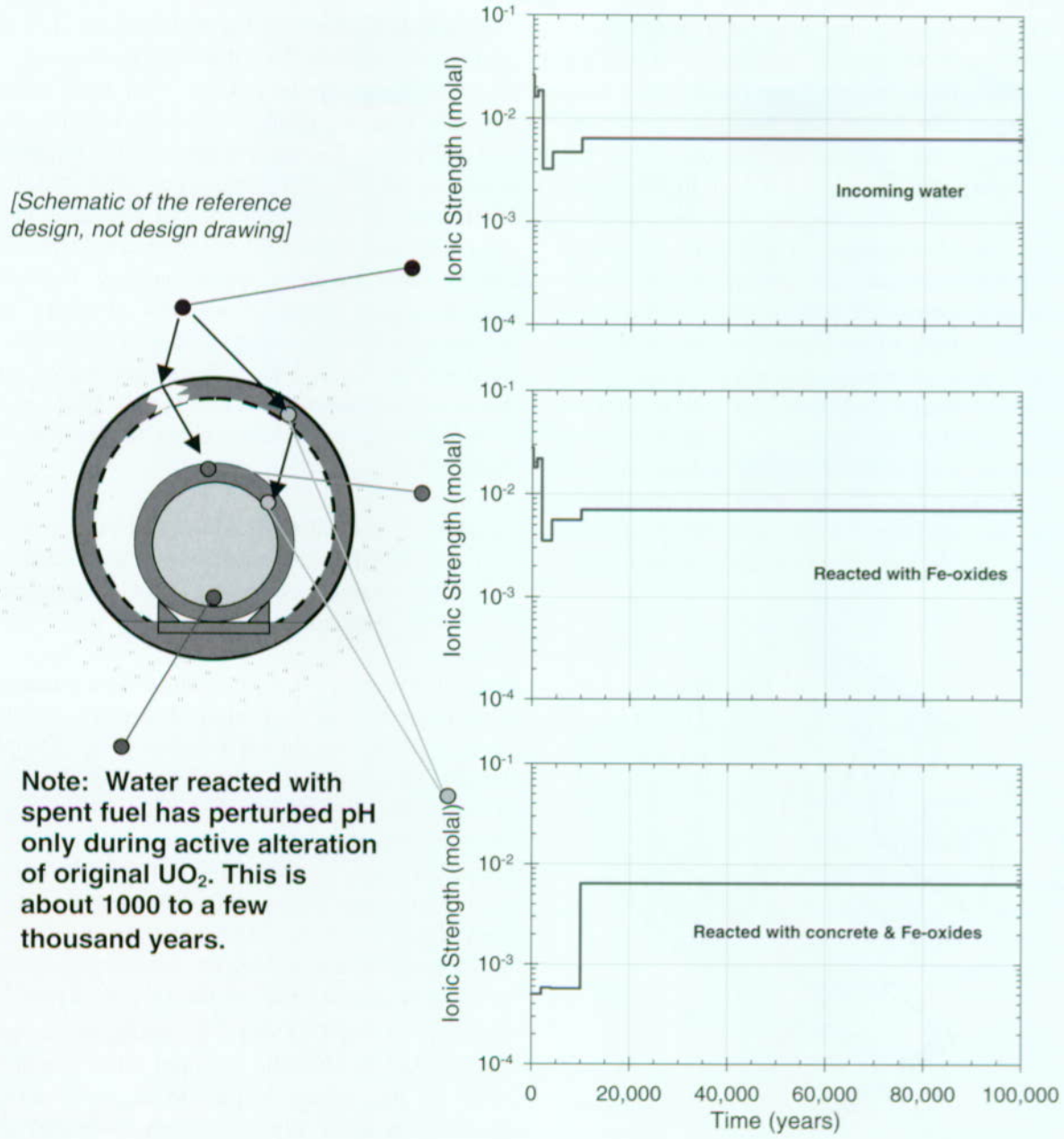

Figure 3-37c. Near-Field Geochemical Environment Water Composition Results, Ionic Strength Values, for the Time Frame from Time of Waste Emplacement to 100,000 Years
The region where the results of each plot applies is indicated by reference to a schematic of a drift cross-section with a waste package.

The model values shown for gas compositions in Figure 3-36, and for water compositions in Figures 3-37a–3-37c, were assumed to represent the expected values of those parameters. However, because processes in the near-field geochemical environment have a large amount of associated uncertainty, these deterministic results were also used to generate probability distributions for the base case. The uncertainties assessed for the model results (see Section 3.3.2 of this volume; CRWMS M&O 1998i, Section 4.5) were used to construct the distributions, which were defined as log normal for dissolved constituents (this corresponds to a normal pH distribution). Figure 3-38 shows an example of the inputs from the near-field geochemical environment component showing the probability density functions for pH conditions within the drift at various times. These probability distributions are used to explicitly include some of the uncertainty in the modeled pH conditions within the analyses. The probability density functions are shown at the final time of their applicability to the system. For example, the probability density function shown at 100,000 years is applicable from 10,000 years to 100,000 years

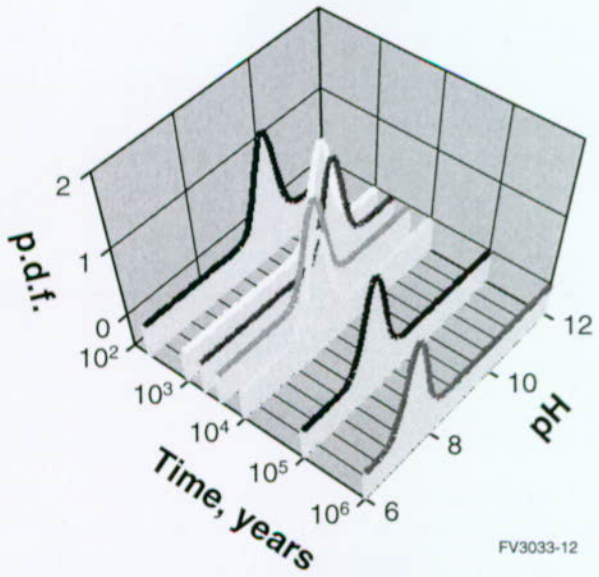

Figure 3-38. Example of Input to the Total System Performance Assessment for the Viability Assessment from the Near-Field Geochemical Environment Component Showing Distributions of pH for Incoming Water Reacted with Iron-Oxides Distributions are shown as probability density functions. (p.d.f.—probability density functions)

The expected values for the distributions (i.e., the peaks) are given by the results shown in Figure 3-37 for water reacted with iron oxides, together with ambient site values applied after 100,000 years. The uncertainties reflect a standard deviation of 0.3 pH units (i.e., one order of magnitude on either side of the expected value should capture 99 percent of the uncertainty). The use of these data for waste package corrosion models, waste form dissolution models, and unsaturated zone transport models is detailed in Sections 3.4, 3.5, and 3.6, respectively, with discussion of the results of those applications in the form of sensitivity studies given in Sections 5.3 through 5.6.

3.3.3.3 Consideration of Spent Fuel Alteration and Secondary Phase Effects on Near-Field Geochemical Environment

One set of results for simulations of water reacting with spent nuclear fuel within the waste package over 5,000 years is shown in Figure 3-39. The plot depicts the evolution of pH for fluid that has reacted with spent nuclear fuel. The water composition effects are shown during the active primary alteration stage at early times in which UO_2 is converted to the first set of secondary phases. At both higher (70°C, or 158°F) and lower (30°C, or 86°F) temperatures, the water chemistry is affected to a larger extent if all of the fuel is exposed to reaction.[4] At 70°C (158°F), the ability of the spent nuclear fuel to alter the pH (and other characteristics of the water) begins to decrease almost immediately and is almost entirely dissipated after about 2,000 years. The calculation predicts that exposed spent nuclear fuel will be consumed in about 2,000 years, converted to the major secondary phase, schoepite. Once the exposed spent nuclear fuel is converted to schoepite, the water composition tends to revert to the incoming

[4] The initial pH at of water entering the waste package is about 8.2.

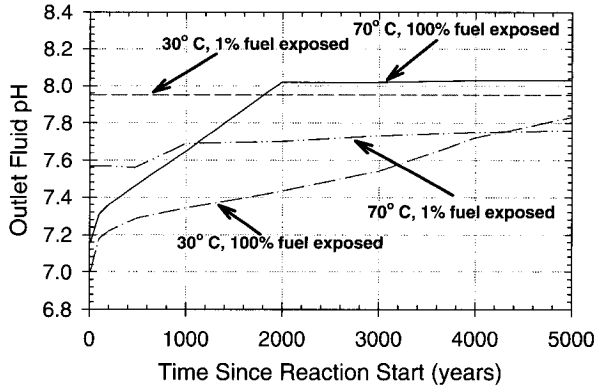

Figure 3-39. Results of Simulations for Primary Spent Fuel Reacting with Water to Form Secondary Alteration Phases
The plot depicts the evolution of pH of fluid that has reacted with spent nuclear fuel at both higher (70°C) (158°F) and lower (30°C) (86°F) temperatures, as well as for small amounts of exposed fuel (cladding failure = 1 percent) and completely exposed spent nuclear fuel (100 percent cladding failure).

composition. This conversion takes longer at 30°C (86°F), because the reaction rates are lower than at 70°C (158°F).

Additional analyses that specifically included neptunium in the secondary phases indicate that the pH of incoming water is changed by less than about two tenths of a unit during secondary phase dissolution. Although the dissolved calcium content decreases greatly, only small (about 10 percent) changes occur for dissolved carbonate and silica, and for ionic strength. These small effects indicate that the behavior of the secondary phases may be primarily controlled by the composition of the fluid entering the waste package. Because the major effects on fluid composition from spent nuclear fuel reaction appear either large but relatively short lived or minor for many constituents (depending on temperature and percentage of exposed fuel), the only aspect of the performance assessment that was modified to address these effects was the waste form component itself. This modification was accomplished in a sensitivity analysis by using the alteration rate of secondary uranium phases to assess the concentration of neptunium in the resulting fluids. These analyses are discussed in detail in Section 3.5, and the performance assessment sensitivity results are presented in Section 5.5.

3.3.3.4 Colloid Amounts

The relation derived for colloid abundance as a function of ionic strength was used directly within the system integration program RIP (CRWMS M&O 1998i, Sections 4.4, 4.5). External to the system code, the relation was used to generate colloid amounts for values of ionic strength to ensure that the fit coefficients reproduce the data used and produce reasonable values for the amounts of clay and iron-oxyhydroxy colloids in the drift. A couple of examples are provided here. Using the relation indicates that an ionic strength of about 3×10^{-2} molal (boiling regime) corresponds to a colloid concentration of about 8×10^{-6} mg/mL, and ionic strength of 5×10^{-3} molal (cooling regime and ambient) corresponds to about 6×10^{-5} mg/mL. These values correspond to about 1×10^{6} and 7×10^{6} particles per milliliter, respectively (CRWMS M&O 1998i, Section 4.5). The performance-assessment-level results of the colloid model for release at the edge of the engineered barrier system, at the water table, and at the accessible environment are discussed in Sections 5.5, 5.6, and 5.7, respectively.

3.4 WASTE PACKAGE DEGRADATION

The waste package is a significant component in the overall performance of the repository system. Until the waste package is breached, it provides environmental isolation of the radionuclides in the waste forms within the waste package. As the waste package ultimately degrades with time, it will still provide substantial containment and will delay radionuclide releases to the rest of the engineered barrier system.

The waste package degradation modeling studies and analyses presented in this section were prepared with the view of addressing selected aspects of the NRC Key Technical Issue on Container Life and Source Term (NRC 1998b). Specifically, the information presented is pertinent to one of the four subissues of this key technical

issue consisting of effects of corrosion on the lifetime of the containers and the release of radionuclides to the near-field environment.

Waste package failure occurs when the waste package is breached by at least one perforation, allowing gaseous or aqueous release of radionuclides. Failure or first breach of the waste package may occur through perforations created by localized corrosion of the corrosion-resistant inner barrier. However, high performance, corrosion-resistant alloys such as the candidate inner barrier material are expected to undergo degradation mainly through general corrosion processes (CRWMS M&O 1998b). An additional small fraction of waste packages may fail prematurely, experience "juvenile failures," caused by processes other than corrosion including material imperfections, manufacturing defects, handling effects, and rockfall.

Evaluating waste package degradation is an important component of TSPA because the waste package must fail before any dissolution and release of the waste form can occur. Important aspects of the evaluation of waste package degradation include determining the processes that cause degradation and finding an appropriate approach for evaluating degradation over long simulated periods.

The current design for the reference waste package is discussed in detail in Volume 2, Section 5.1.2. In summary, the reference design calls for a multi-barrier system consisting of a 10-cm (4-in.) outer barrier and a 2-cm (0.8-in.) inner barrier. The outer barrier is composed of corrosion-allowance material and is intended to provide structural strength and initial corrosion resistance; the inner barrier is composed of a corrosion-resistant material and is intended to withstand the environmental conditions within the drift. Carbon steel (Alloy A516) (ASTM 1990) is the reference material for the corrosion-allowance outer barrier, and nickel-base Alloy 22 is the reference material for the corrosion-resistant inner barrier (CRWMS M&O 1998l). The waste package characteristics are shown in Figure 3-40. The waste packages will

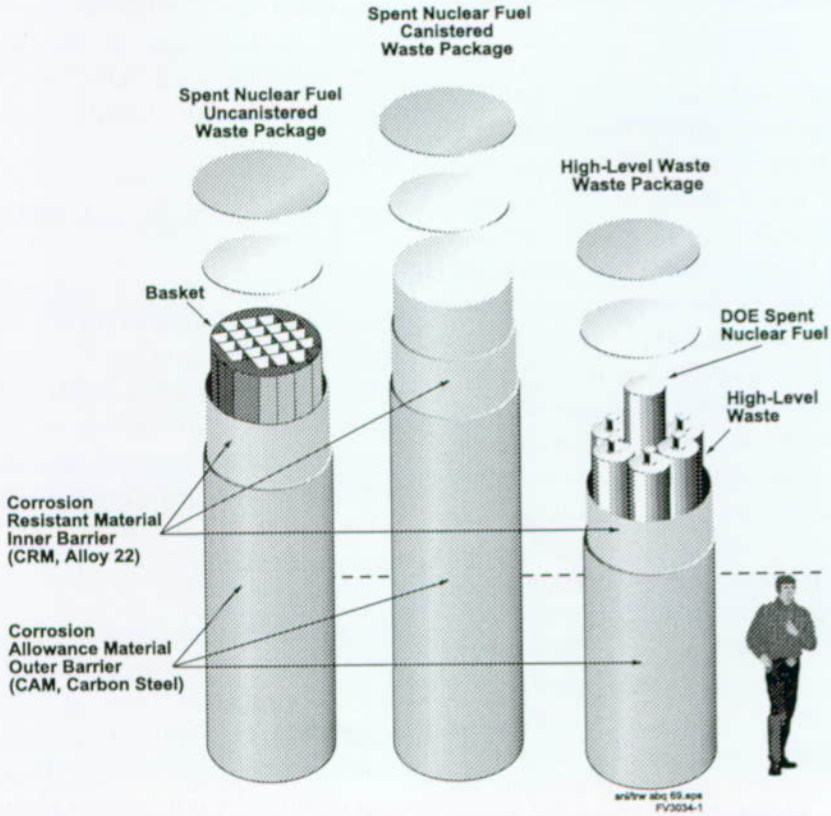

Figure 3-40. Waste Package Reference Design

be emplaced in the engineered barrier system on carbon-steel support assemblies located on concrete segments put in the bottom of the round emplacement drift to provide a level floor, as shown in Figure 3-41.

Most waste packages are expected to be exposed to high temperature, humid air conditions for a period after emplacement (see Section 3.2). These conditions will result in slow degradation of the waste packages. A small fraction of the waste packages may be emplaced in drifts with fractures that periodically drip water. Water may drip on these packages after emplacement. The dripping rate, frequency of drip periods, and water chemistry, especially pH and chloride concentration, will significantly contribute to waste package degradation.

Waste package degradation is shown schematically in Figure 3-42. Outer barrier corrosion is followed by corrosion of the inner barrier, leading to penetration of the waste package. This penetration allows either vapor or liquid water to enter the waste package and begin degrading and mobilizing the waste form inside the waste package (see Section 3.5).

The degradation rate of the waste package depends on many things, including the waste package materials and the thermal-chemical-hydrologic regime close to the emplacement drifts. Important parameters of this regime are temperature, relative humidity, and those related to dripping effects and chemical and redox conditions. Analysis of waste package degradation requires information from all of these areas. In particular, waste package design defines the shape and materials used in the degradation and lifetime analyses. Thermal-hydrologic modeling defines the dripping conditions, temperature, and relative humidity input for the analyses. Near-field geochemical modeling provides the basis for the chemical conditions used in the analyses. In overall system modeling, information about waste package failure affects the modeling of waste form degradation and, ultimately, radionuclide transport from the breached waste package.

The detailed modeling of the carbon-steel waste package supports was not conducted for the TSPA-

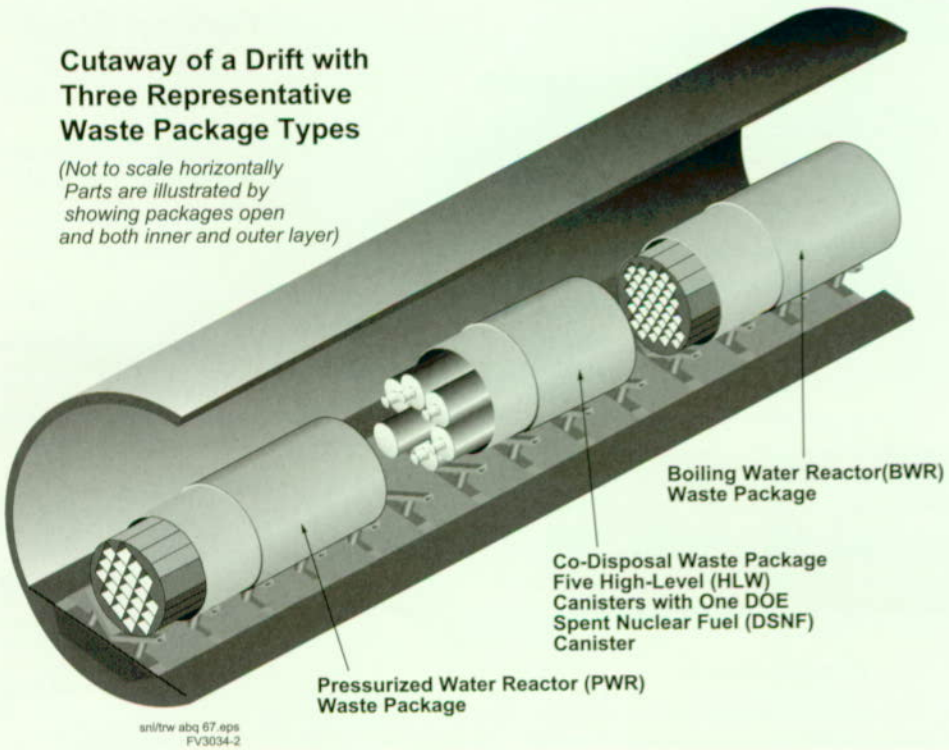

Figure 3-41. Engineered Barrier System Reference Design

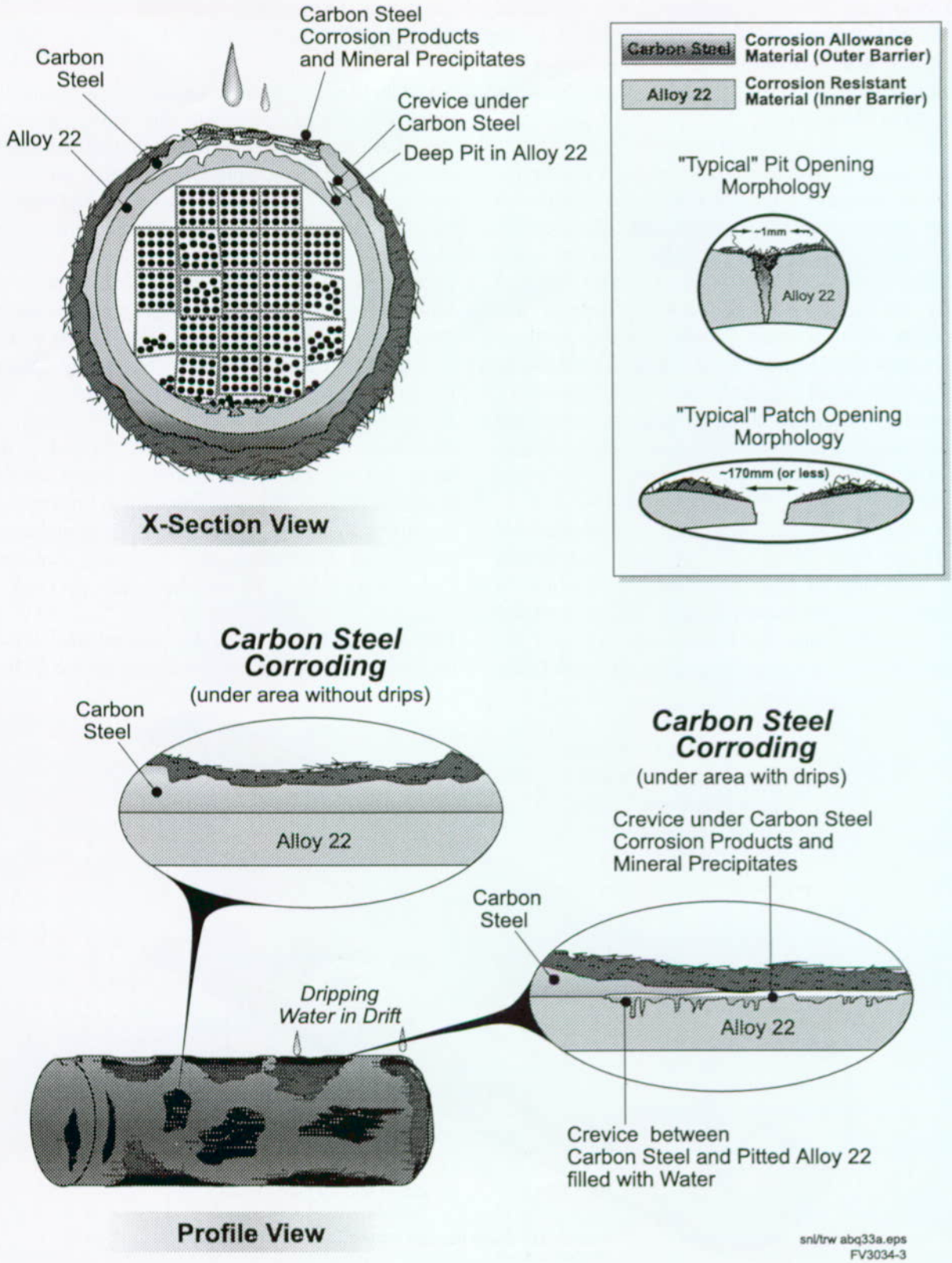

Figure 3-42. Waste Package Degradation Schematic

VA. The degradation of the supports with time, their potential contribution to wicking moisture from the invert to the waste package, their potential role as a trap for salts from evaporating water could lead to different waste package lifetimes and transport characteristics. However, due to the expected short lifetime of the supports relative to the repository lifetime, these effects were considered to be inconsequential.

The remainder of this section deals with construction of the conceptual model for waste package degradation, followed by a discussion of implementation of the waste package degradation model in the performance assessment model, and evaluation of some of the key aspects of waste package degradation relative to performance. Additional information on the waste package component can be found in Chapter 5 of the *Total System Performance Assessment-Viability Assessment (TSPA-VA) Analyses Technical Basis Document* (CRWMS M&O 1998i).

3.4.1 Construction of the Conceptual Model

The conceptual model for waste package degradation incorporates the important modes of corrosion of both the outer and inner waste package barriers. Several corrosion modes are evaluated for the variety of environments expected in the repository. Figure 3-43 is a summary of the conceptual model used for waste package degradation. The figure identifies the conceptual model input and output, degradation modes considered, and bases for the model. Figure 3-44 shows the degradation modes and thresholds included and the logic flow for the waste package degradation model discussed in detail in Section 3.4-2. As discussed below, the base case conceptual model was developed based on the information from the expert elicitation results (CRWMS M&O 1998b).

Juvenile failures and degradation of corrosion-allowance and corrosion-resistant material are included in the base case. Degradation modes that impact waste package lifetime, those included as well as those not included in the base case model, are discussed in Section 3.4.1.2.

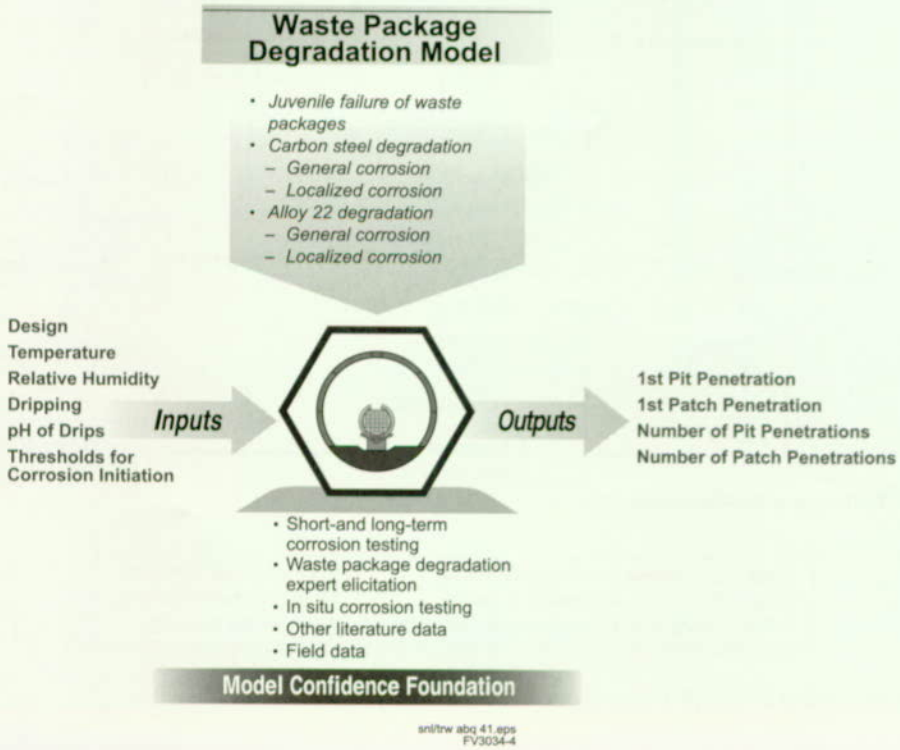

Figure 3-43. Waste Package Degradation Information Flow

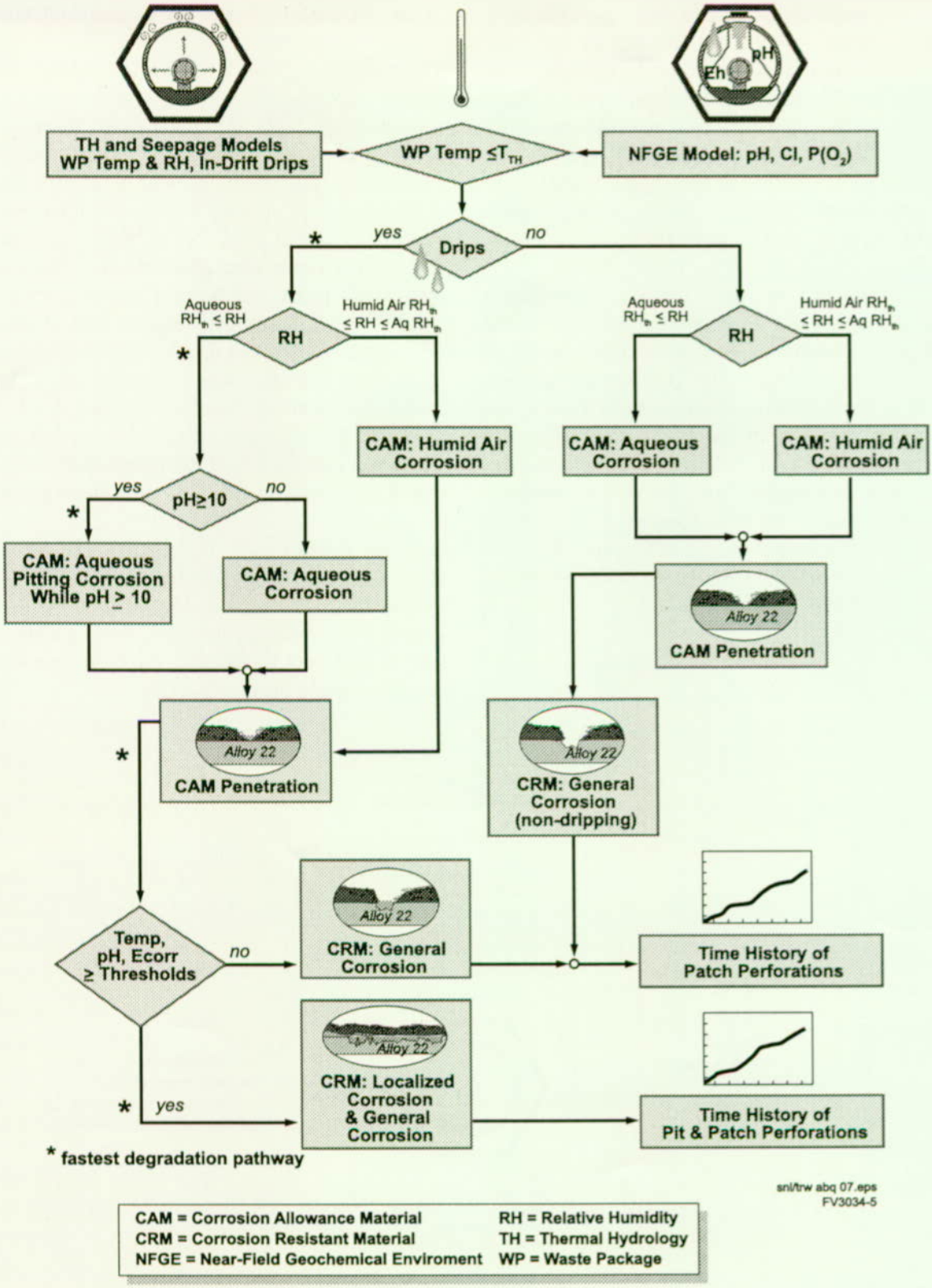

Figure 3-44. Waste Package Degradation Model Logic Diagram

The waste package degradation abstraction and testing workshop was held in early 1997 and focused on the project capabilities to evaluate the degradation modes of the waste package. A summary of the prioritization criteria, high priority issues relative to those criteria, and analysis plans from the workshop is presented in Table 3-11.

Table 3-11. Waste Package Degradation Abstraction/ Testing Workshop

Waste Package Degradation Abstraction/Testing Workshop
January 8-10, 1997, Las Vegas, Nevada
(CRWMS M&O 1997h)

PRIORITIZATION CRITERIA

How significantly does the process/issue affect

- The time of waste package failure?
- The rate of failure of waste packages?
- The rate of waste package perforations and thus the rate of radionuclide release from the waste package?

HIGHEST PRIORITY ISSUES

- Carbon-steel outer barrier corrosion and salt-scale deposit effect:
  - Refluxing and concentration of electrolyte (Cl^-, pH, etc.)
  - Microbiological
  - Temperature dependence on corrosion
  - Model of salt buildup
  - Critical relative humidity (transition from dry oxidation to humid-air corrosion)
  - Critical relative humidity (transition from humid-air to aqueous corrosion)
  - Aqueous corrosion
  - Flow rate and episodicity of water
  - General corrosion in humid-air environment
- Nickel-based material inner-barrier corrosion:
  - Aqueous corrosion
  - Crevice corrosion (geometry, etc.)
  - Cathodic (or galvanic) protection
  - Choice of waste package materials
  - Barrier interface environment
- Galvanic coupling effect:
  - Barrier materials (alloy choice)
  - Water chemistry versus time
  - Threshold for galvanic protection cessation
  - Crevice corrosion (including welds)
  - Electrode area ratio
  - Ionic conductivity at interface
  - Fabrication process (contact effectiveness)
  - Water-contact mode inside container and outside container
- Microbiologically influenced corrosion
  - Water variability
  - Amount of nutrients
  - Susceptibility of inner barrier
- Preferential weld susceptibility
- Container material (microconstituents)
- Rockfall, premature failure, and structural failure
- Timing of rockfall

ANALYSIS PLANS

- Carbon-steel outer-barrier corrosion
- Corrosion-resistant inner-barrier corrosion
- Microbiologically influenced corrosion
- Effects of variability in near-field conditions, manufacturing, and materials on waste package degradation

3.4.1.1 Waste Package Degradation Expert Elicitation

Data on corrosion of the candidate materials and their process models are being developed in conjunction with the comprehensive corrosion testing programs at Lawrence Livermore National Laboratory (McCright 1998). However, long-term test data are not yet available under expected repository conditions and, as a result, the models for waste package performance contain large uncertainties. An expert elicitation was conducted to develop additional information and models that are needed for evaluating waste package degradation for the TSPA-VA (CRWMS M&O 1998b). The major goal of the expert elicitation was to quantify the uncertainties involved in assessing degradation modes for the waste package, including uncertainty in both the models used to represent the degradation modes and the parameter values used in those models. The process followed the procedures and approaches for eliciting expert judgments that have been formalized in documents such as DOE guidance for the formal use of expert judgment by the YMP (DOE 1995 p. 1) and the NRC branch technical position on the use of expert elicitation in the high-level radioactive waste program (Kotra et al. 1996 pp. 3, 4, 7). The assessments and probability distributions that resulted from the expert elicitation provide a reasonable aggregate representation of the knowledge and uncertainties about issues in evaluating waste package degradation. For details of the ranges of values and opinions, see the expert elicitation report (CRWMS M&O 1998b).

During the elicitation, the experts provided an overview of the modes for waste package degradation in the repository, taking into consideration possible evolution of the exposure conditions in the emplacement drifts. Then the experts evaluated the parameters of various important degradation modes and corrosion models for the corrosion-allowance material and the corrosion-resistant material forming the outer and inner barriers. The

information from the elicitation was used to develop the base case model for waste package degradation. Experts also evaluated the parameters of the corrosion processes and models that are components of the base case waste package degradation model discussed above. The following parameters were evaluated by the expert panel:

- The temperature threshold for starting corrosion of the corrosion-allowance material.
- Relative humidity thresholds for starting corrosion of the corrosion-allowance material by humid air and water.
- Roughness factors (see Section 3.4.1.6) for corrosion of corrosion-allowance material by humid air and neutral-pH water.
- Parameters for models that simulate pitting of corrosion-allowance material in alkaline conditions (pH greater than or equal to 10).
- Density of pits in corrosion-allowance material in alkaline conditions.
- General corrosion rate of corrosion-resistant material as a function of temperature under nondripping conditions.
- Three local exposure conditions on corrosion-resistant material under dripping conditions (pH of 3–10 and moderately oxidizing, acidic and moderately oxidizing, and acidic and highly oxidizing) and the probability of their occurrence. Note: These conditions are for in-crevice chemistry, not bulk chemistry as discussed in section 3.3.
- General corrosion rate of corrosion-resistant material as a function of temperature for each of three local exposure conditions.
- Probability of initiating pitting, and crevice corrosion rate of corrosion-resistant material as a function of temperature for each of three local exposure conditions.
- Density of pits in corrosion-resistant material.

In addition to evaluating these parameters, the expert panel also evaluated uncertainties in the parameter values.

3.4.1.2 Model Input and Output

The inputs to the modeling of waste package degradation include waste package design and expected environment, including the near-field geochemical environment, dripping conditions, and temperature and relative humidity. Additional information from corrosion data from short- and long-term testing of the reference and similar materials and expert elicitation results provided the basis for both input and confidence in the model.

The output from the modeling of waste package degradation is a time dependent quantitative assessment of waste package degradation and failure. The output is the time to initial breach for each of the waste packages, either a small hole, or pit, made by localized corrosion or a large opening, or patch, formed by general corrosion, and the subsequent perforation of the waste packages. The time of the initial breach corresponds to the start of waste form degradation inside the breached waste package. The perforated or opened area on the waste package provides the opening through which radionuclide transport out of the package can occur. The number of waste package failures plotted as a function of time (failure distribution) provides a time-dependent description of waste package failures. Additional output from the model include the uncertainty and spatial variability of the degradation information both on a package and at different repository locations.

3.4.1.3 Modeled Degradation Modes

The conceptual model incorporates significant degradation modes associated with waste package lifetime. Many factors influence the ways that corrosion can affect candidate materials. These include metallurgical factors (alloy composition and alloy microstructure); physical factors (temperature, relative humidity, and mode of water contact); chemical factors (pH and concentration of

aggressive species such as chloride, sulfate, nitrate, and carbonate); and mechanical factors such as stress (McCright 1998).

Degradation modes for the candidate barrier materials that are potentially important in the near-field repository environment at Yucca Mountain are identified by McCright (1998) as general corrosion; pitting corrosion; crevice corrosion; stress corrosion cracking; galvanically enhanced corrosion; microbiologically influenced corrosion; radiation-induced corrosion; corrosion in welded materials; and low-temperature oxidation.

Some of the unincorporated degradation modes are discussed later in this section. Degradation modes not analyzed in the base case for this TSPA that may negatively affect performance include late-time structural failure, microbiologically induced corrosion (see Section 3.4.1.7); stress corrosion cracking of Alloy 22, especially on closure welds (see Section 3.4.1.7), and hydrogen embrittlement of Alloy 22. Also, the potential for migration of molybdenum to grain boundaries exists, especially in those areas with high temperatures (e.g., weld areas). This can lead to additional stress, cracking, and generally poor corrosion resistance.

3.4.1.4 Early Waste Package Failure (Juvenile Failure)

With the large number of waste packages to be manufactured and emplaced in the potential repository, there is the potential for degradation modes or factors other than the anticipated corrosion degradation to cause failure of the waste packages at relatively early time. These degradation modes or factors could include materials defects, human-induced factors (manufacturing including welding, handling and transportation), placement on active displacement faults, shifts during emplacement, rockfalls, shaking of waste packages by seismic activity, etc. Early failure from such processes or factors is called juvenile failure. Quantification of waste package juvenile failure is highly uncertain. The analyses for this TSPA attempt to include this potential failure mode based on information gained from available sources.

The initial analyses of juvenile failure included assessment of weld failures, discussed below. Other factors that could contribute to juvenile failure were incorporated into the probability of juvenile failure by expanding the range of failures. In an early study related to a nuclear waste program, the probability of a waste package being initially perforated was assessed based on data for simple pressure vessel components (Doubt 1984 p.7). Based on failure data among about 20,000 pressure vessels that were examined, a failure rate of 8.5×10^{-4} per vessel (17 out of 20,000) was estimated. That is, about 1 in 1,000 among a heterogeneous mixture of high-quality pressure vessels can be expected to fail early because of an undetected critical defect. The analysis was to suggest an upper limit to the probability of early waste package perforation, caused by undetected defects. Doubt (1984) indicated that in a large population of geometrically simple waste disposal containers subjected to highly standardized inspection procedures, the proportion containing critical undetected defects should be much lower. In a recent analysis for the potential repository, assuming independence between inner and outer barrier weld failures, a probability of 5.8×10^{-6} through-wall defects per waste package was estimated (CRWMS M&O 1997q). Based on approximately 10,500 total waste packages and the estimated frequency of waste package through-wall defects, the probability that there will be one waste package with a through-wall manufacturing defect in the potential repository was estimated to be 6.3×10^{-2}. This indicates less than one waste package potentially fails by weld failures in the expected case. The model used for this TSPA assumes one package failure for the expected case (10^{-4}) with a range of one to ten packages potentially failing. The failure time is assumed to be 1,000 years.

3.4.1.5 General Corrosion

General corrosion normally causes a relatively uniform thinning of materials without significant localized corrosion. The carbon steel (Alloy A516) outer barrier would be affected mostly by this corrosion mode; however, exposure of carbon steel to alkaline water (i.e., caused by the presence

of concrete) could reduce its resistance to corrosion, allowing the steel surface to be corroded locally with high-aspect ratio pitting (Marsh et al. 1988). This type of pit is a deep pit with a small diameter pit mouth.

The general corrosion rate of carbon steel in water is also strongly affected by temperature, with maximum corrosion rates at temperatures of about 60° to 80° C (140° to 176°F) (Figure 3-45). Such behavior is commonly observed in corrosion processes governed by the reduction of dissolved oxygen. An increase in temperature enhances both mobility or diffusivity of oxygen molecules and reaction rates, but at the same time decreases the solubility of oxygen gas. The net mass transport of oxygen increases with temperature until it reaches a maximum where the oxygen concentration begins to decrease. In other words, the corrosion rate reaches a maximum and then decreases with further increase in temperature (Boden 1994, p. 2:18).

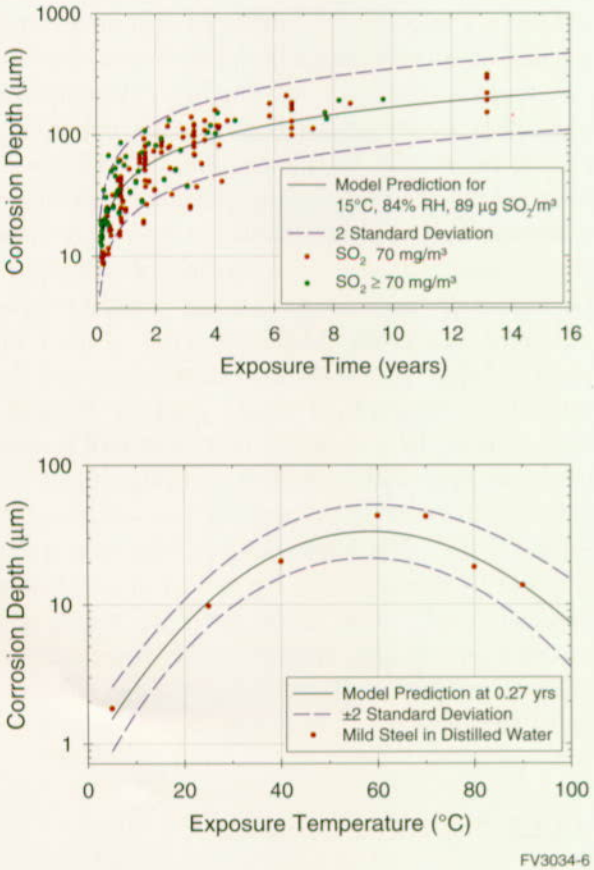

Figure 3-45. Corrosion Allowance Material Corrosion Rates and Data
Corrosion data are given for general corrosion in humid air and aqueous corrosion (in the presence of liquid water such as from drips). Corrosion allowance material is composed of carbon steel and is the material of the outer waste package layer.

Alloys such as Alloy 22 with a high nickel, chromium, and molybdenum content are not expected to undergo localized corrosion under repository conditions. Consequently, the mechanism for degradation of these alloys is expected to be significant general passive corrosion and is expected to proceed at very low rates (CRWMS M&O 1998b). The factors affecting degradation of Alloy 22 include temperature, salt concentration (sodium and ferric chloride), and pH.

3.4.1.6 Localized Corrosion

Localized corrosion, or pitting and crevice corrosion, is induced by local variations in the electrochemical potential or driving force for corrosion on a micro-scale over small regions. Variations in electrochemical potential may be caused by localized irregularities in the structure and composition of usually protective passive films on metal surfaces and in the electrolyte composition of the solution that contacts the metal (McCright 1998; Henshall 1992; Henshall et al. 1993). Complex electrochemical processes associated with these factors strongly influence the initiation of pitting and pit growth processes. In general, metal pitting is caused by complicated interactions among many factors and appears to be random. As a result, stochastic approaches have been used in waste package degradation modeling to represent and quantify localized corrosion processes.

In neutral pH water, local variations of the depth of general corrosion of carbon steel are commonly represented with a roughness factor, that is defined as the ratio of the local general corrosion depth to the average general corrosion depth considered over the entire sample surface at a given exposure time. A roughness factor was used in modeling local variations of the general corrosion of carbon steel. However, when in contact with alkaline pH

water, carbon steel could undergo pitting corrosion with high-aspect ratio pits. A pit growth law was suggested for modeling pitting corrosion of carbon steel in alkaline water (CRWMS M&O 1998b). However, the one-year test results in concentrated repository-groundwater conditions in which the test solutions are maintained at approximately a pH of 9.7, showed no such pitting corrosion for the carbon steel samples (McCright 1998).

If the carbon steel outer barrier is penetrated, a number of factors determine the probability that localized corrosion of the inner barrier will begin. These factors include the availability of water and its pH, temperature, and chloride ions, ferric ions, and dissolved oxygen content which affect the corrosion potential of the material. The probability that localized corrosion of the inner barrier will begin is essentially the probability that an aggressive environment will exist relative to these factors. The availability of water to initiate localized corrosion of the inner barrier will vary depending on whether water drips onto the waste package. When the outer barrier is penetrated, crevices could form under the following conditions: between the inner barrier and the uncorroded carbon steel, or under a thick layer of material from the corrosion of carbon steel. For this reason, crevice corrosion of the inner barrier is considered a more probable process than pitting, and this process can begin at lower temperatures than pitting. For example, crevice corrosion may begin if the temperature is between 80° and 100°C (176° and 212°F) when the outer barrier fails. Once begun, crevice corrosion will grow similar to corrosion described by the pit growth law. If the temperature is below the threshold, no exposed site would initiate crevice corrosion, and the inner barrier can be assumed immune to localized corrosion. Under these conditions, the inner barrier will only experience general corrosion. The conditions required for crevice corrosion are necessary to sustain the process, as well. The data used to develop the localized corrosion model of the corrosion-resistant material include 38 experimental observations of Alloy 22.

3.4.1.7 Other Degradation Modes for Waste Packages

Several processes have not been included in the model for waste package degradation. These processes include dry oxidation, galvanic protection, stress corrosion cracking, microbiologically influenced corrosion, radiation-induced corrosion, and late-time structural failure. These processes are briefly discussed below.

Dry Oxidation. At the moderately elevated temperatures expected at the waste package surface in the repository, the corrosion-allowance material may be degraded by dry oxidation. A previous study concluded that the impact of oxidizing the candidate barrier materials under repository conditions is insignificant (Henshall 1997; CRWMS M&O 1998b). Because of this, the dry oxidation process is not included in the base case model.

Galvanic Coupling. Galvanic coupling of the inner and outer barriers may be an important process in the waste package degradation. Galvanic protection of the inner barrier may occur because of interaction between the outer and inner barriers. However, the panelists of the *Waste Package Degradation Expert Elicitation* (CRWMS M&O 1998b) noted that, while there could be galvanic protection of the inner barrier as the outer barrier is penetrated, the effect will be small and of short duration relative to the time scale of interest for repository performance. Thus, this effect is not incorporated in the base case. A recent analysis (Farmer and McCright 1998) showed that the galvanic coupling keeps the crevice solution chemistry from being extremely acidic and aggressive, conditions that are observed in crevices of single material nickel-based alloy. There is a potential for enhanced corrosion of carbon steel if it is single material coupled galvanically to Alloy 22 but this essentially protects the Alloy 22. Another potentially adverse effect from the galvanic coupling is hydrogen embrittlement of Alloy 22 from the production of hydrogen at the cathodic sites of the Alloy 22 surface and hydride phase formation in the alloy. This process is not included in the base case model, and is potentially non-conservative.

Stress Corrosion Cracking. This is a crack propagation process caused by the combined and synergistic interaction of mechanical stress and corrosion reactions. Recent bounding analyses using linear elastic fracture mechanics (McCright 1998) showed that, except for very high aspect ratio, the critical crack size for stress corrosion cracking is always larger than the thickness of both the barriers for the stresses (245 MPa for carbon steel and 410 MPa for Alloy 22) and aspect ratios that are considered. The expected stress in the design basis metals is expected to be (McCright 1998) much lower than the stress range studied here; therefore, there would be no stress corrosion cracking in the design basis metals (carbon steel and Alloy 22). Because of potential technical difficulties associated with relieving stresses in the closure welds of the double-walled waste package, stress corrosion cracking of the closure welds could be a potential degradation mode. Another potential degradation mode is the development of wedging stresses on the corrosion-resistant material. This may occur because of accumulation of corrosion-allowance material corrosion products in the gap between the inner and outer barriers, when the corrosion-allowance material is breached at early times and a substantial thickness of the corrosion-allowance material remains. Because of the low probability of occurrence, this process is not included in the base model.

Microbiologically Influenced Corrosion. This is caused by the metabolic activity of microorganisms. Microbiologically influenced corrosion may occur throughout the life of the repository, especially after the near-field temperature of the repository cools down. Microbial metabolism produces corrosive chemicals. Although 300-series stainless steels are known to be susceptible to microbiologically influenced corrosion, the nickel-based alloys such as Alloy 22 seem to be immune to this type of corrosion (CRWMS M&O 1998b). The panelists of the *Waste Package Degradation Expert Elicitation* (CRWMS M&O 1998b) discussed various aspects of potential microbial activity and microbiologically influenced corrosion in the repository. The experts generally agreed that, until the repository has cooled to temperatures below 100°C (212°F) and relative humidity is above 60 percent, microbiologically influenced corrosion would not occur. Also, significant microbiologically influenced corrosion was deemed unlikely if there is no dripping onto the waste package. The panelists concluded that the importance of microbiologically influenced corrosion is to increase pit and crevice density and the probability that localized corrosion will start, rather than to affect the rate once corrosion has begun is low. Further, they noted that Alloy 22 has not been associated with documented cases of microbiologically influenced corrosion. Thus, this process is not included in the base model.

Radiolysis-Induced Corrosion. This is another potentially important degradation process for waste packages in the repository. If irradiated by gamma radiation, fixed nitrogen may exist in the liquid phase as nitrite and nitrate ions that are corrosive to metals. Nitrogen fixation in water, as used here, is a process to transform nitrogen gas to a stable (fixed) form in water. The total amount of nitrite and nitrate that can be formed in a liquid phase is limited by the gamma radiation dose rate and the volume of irradiated air. If a thin film of water on the waste package container in contact with a relatively thicker air space is irradiated, there can be a significant concentration of nitrate in the relatively small amount of water in the film (Van Konynenburg et al. 1995 p. 8, vol. 3). This process is not included in the base model because the thickness of the waste package reduces the gamma flux, therefore reducing the amount of radiolysis to negligible levels.

Structural Failure. Sometime after closure of the repository and significant degradation of the concrete linings, rocks are expected to fall in the emplacement drift. A degrading waste package hit by falling rocks will experience a dynamic load initially. The degrading waste package will experience a static load from the weight of the rocks remaining on the waste package, the waste package itself and the waste inside. After a certain degree of degradation, the waste package will lose structural stability. A recent analysis reported results for the thinning of waste packages and how thinning relates to structural failure (CRWMS M&O 1996a). The structural analyses in the report provide a basis for determining the structural capabilities of waste package containment barriers

at various levels of uniform thinning degradation. The analysis results indicate that if the thickness of the carbon steel outer barrier and an inner barrier of Alloy 625 (a nickel-based alloy with lower molybdenum content than Alloy 22) is reduced, the waste package maintains containment even when the entire outer barrier and more than half of the inner barrier have been removed because of corrosion. That is, 9.5 mm of the original 20 mm remains. The analysis assumed no support from the basket assembly inside the waste package. While the analyses were conducted using Alloy 625 as the inner barrier, the results should also be valid for the Alloy 22 inner barrier. This degradation mode is not included in the base model.

3.4.2 Implementation of Waste Package Degradation Model

The waste package degradation model includes both juvenile failures (as described in Section 3.4.1.4) and degradation with time according to corrosion processes. The range of probability of juvenile failures is based on the analysis of weld failures but is expanded to cover other potential conditions that may lead to early failure. The evaluation of waste package degradation with time is incorporated into a computer code that is based on a probabilistic approach (CRWMS M&O 1998j; Lee et al. 1997). The code has the capability for modeling various designs, waste package materials, and degradation mechanisms. Figure 3-46 shows the degradation models and thresholds included and the logic flow for the model. The model tracks waste package degradation by first defining the environmental inputs to the system, then checking for dripping and pH conditions, followed by degradation of the corrosion-allowance material and the corrosion-resistant material. The model simulates degradation of both the corrosion-allowance material and the corrosion-resistant material because of general and localized, or pitting corrosion. The model divides the waste package into discrete corrosion patches for general corrosion. The corrosion patches are 310 cm^2 (48 in^2) regions in which corrosion properties are assumed to be homogeneous.

Several environmental parameters affect degradation of the corrosion-allowance material:

- Relative humidity. The threshold at which relative humidity initiates corrosion is based on the distributions developed from the *Waste Package Degradation Expert Elicitation* (CRWMS M&O 1998b). This relative humidity threshold was used for all waste packages, even those in dripping conditions, to initiate humid air corrosion. For dripping conditions, aqueous corrosion was initiated after relative humidity reached a certain threshold (85–100 percent relative humidity).

- Temperature. The temperature at the waste package surface must be below a threshold temperature that represents the boiling point for corrosion to initiate. No dry oxidation corrosion is included in these analyses.

- Dripping conditions. Dripping conditions are assumed for a certain fraction of the waste packages based on water seepage into the drift (see Section 3.1 for discussion of the seepage model). If water drips onto a waste package, it is assumed to be 100 percent wet from the dripping. The sensitivity of the analysis to changes in these conditions is discussed in Section 5.4.

- pH of incoming water. The pH of the incoming water in the base case does not change because of interaction with concrete because the concrete lining is assumed to have fallen in at an early time and is not important over the performance period (see Section 3.3 for discussion of the development of the pH values as a function of time). The sensitivity of the analysis to changes in this parameter is discussed in Section 5.4.

- Other drift conditions not included in the base case. Other geochemical parameters are not included in the base case analyses of waste package degradation, because of modeling constraints. However, omitting chloride concentration is potentially not

conservative, while omitting oxygen partial pressure is probably conservative in terms of system performance.

The model for degradation of corrosion-resistant material was developed from existing data with significant input from the panelists of the *Waste Package Degradation Expert Elicitation* (CRWMS M&O 1998b). Figure 3-46 shows the elicited general corrosion rates for the corrosion-resistant material along with the data for degradation of Alloy 22. Data about variability and uncertainty were also elicited from the panel (CRWMS M&O 1998b). The base case definition assumes that uncertainty and variability are evenly divided in determining the general corrosion rates for the corrosion-resistant material under dripping conditions.

A temperature threshold is used for initiation of localized corrosion of Alloy 22 after the outer barrier is breached. The threshold for an Alloy 22 patch is sampled from a uniform distribution between 100° and 80°C (212° and 176°F) when a patch of corrosion-allowance material fails. Three local (in crevice) exposure conditions (not bulk near-field chemistry) on the inner barrier defined in the *Waste Package Degradation Expert Elicitation Project* (CRWMS M&O 1998b) are represented in the following model:

- 84 percent of the area that is dripped on is assumed to be in moderately oxidizing conditions, with pH of 3 to 10 and 340 mV standard hydrogen electrode

- 13 percent of the area that is dripped on is assumed to be in acidic and moderately oxidizing conditions, pH of 2.5 and 340 mV standard hydrogen electrode

- 3 percent of the area that is dripped on is assumed to be in acidic and highly oxidizing conditions, pH of 2.5 and 640 mV standard hydrogen electrode

These are the local environments the expert panel felt were representative of potential conditions in crevices on the waste package, not bulk pH values.

The experts provided cumulative distribution functions of general corrosion rates for corrosion-resistant material at three temperatures (25°, 50°, and 100°C; or 77°, 122°, and 212°F) for each local exposure condition (a total of nine cumulative distribution functions for corrosion rates).

The elicited cumulative distribution functions (indicating the spread in general corrosion rate values) of corrosion rates for the corrosion resistant material included both uncertainty and variability. There is uncertainty in the rates because of lack of extensive experimental information on the rates. There is variability in the rates because of the range of environments and material conditions that will be present in the repository (package to package variability) and on a package (patch to patch variability). The uncertainty and variability in corrosion rates was split up for dripping and no-dripping general corrosion conditions, as well as for the localized corrosion conditions to attempt to bound the effect of these parameters. The variability in the corrosion rates was further split up between package to package and patch to patch variability to attempt to bound the effect of these parameters. The full discussion of the approach to uncertainty/variability allocation is found in Chapter 5 of the *Total System Performance Assessment-Viability Assessment (TSPA-VA) Analyses Technical Basis Document* (CRWMS M&O 1998i).

The primary stochastic parameters used in the model are the following (CRWMS M&O 1998j):

1. Fraction of variability assigned to waste package to waste package and patch to patch.

2. The roughness factor multiplier for corrosion-allowance material is a bounded normal distribution with a mean equal to 1.5, standard deviation equal to 0.25, lower bound equal to 1, and upper bound equal to 1×10^6 (in other words, no upper bound).

3. In the high pH model for corrosion-allowance material, $D = Bt^n$, where D = pit depth, B = pit depth when time is 1, t =

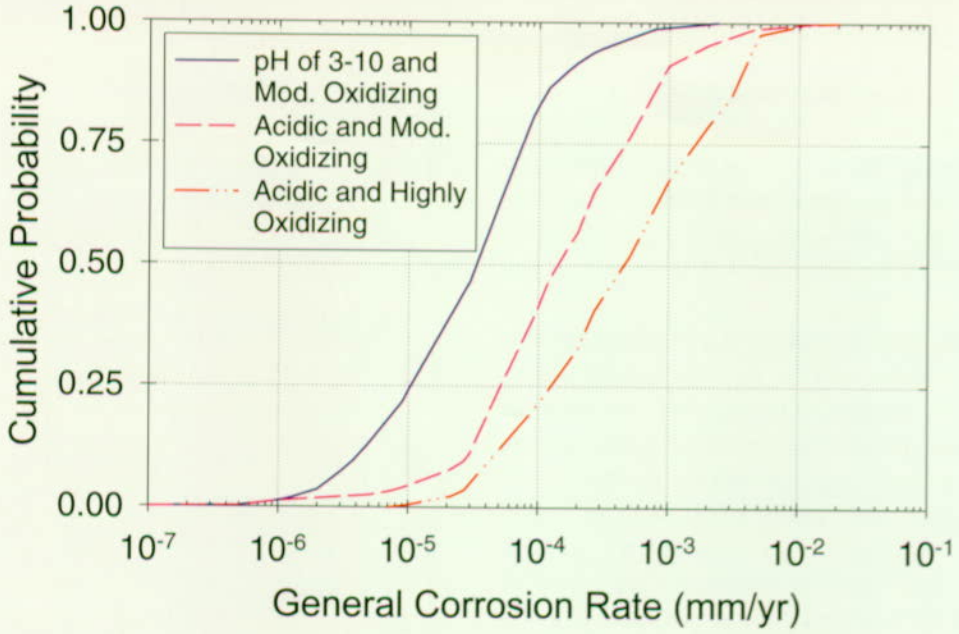

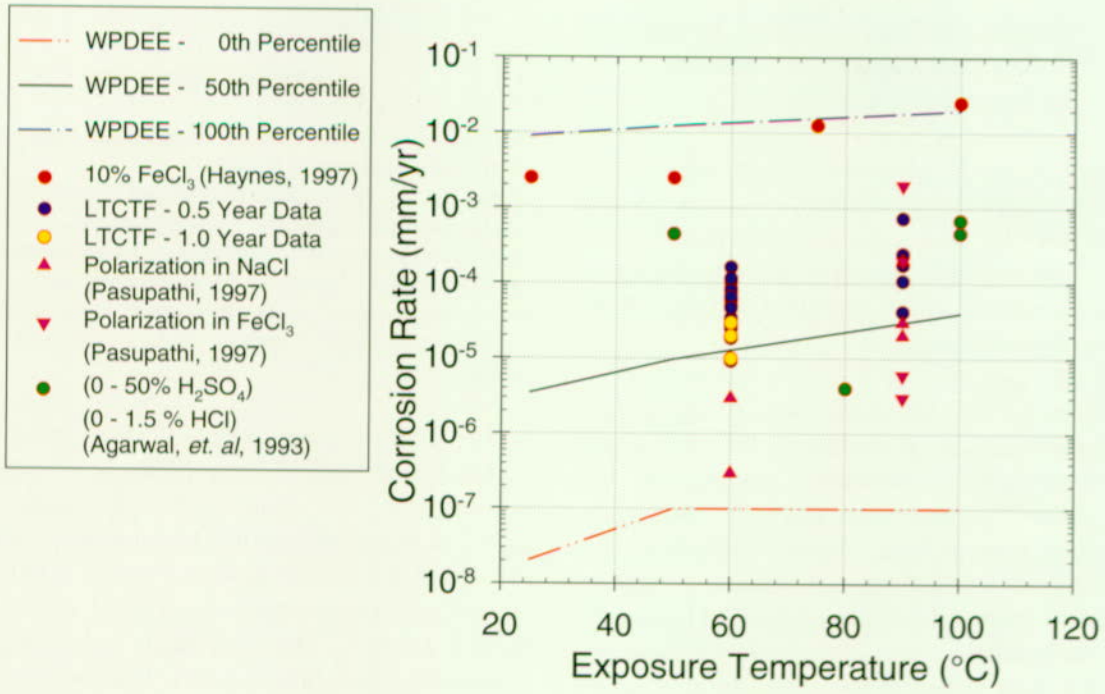

Figure 3-46. Abstracted General Corrosion Rate Distributions of Alloy 22
Abstracted general corrosion rate distributions for the corrosion-resistant material for three different local exposure conditions at 100°C, and the comparison of the abstraction with the literature data for varying exposure conditions at different temperatures.

time, and n is between 0 and 1, B and n have cumulative distribution functions.

4. Drip and no drip conditions for general corrosion of the corrosion-resistant material, three cumulative distribution functions at three user-defined temperatures (25°, 50°, and 100°C; or 77°, 122°, and 212°F).

The results are provided as input to the total system performance analyses in the form of lookup tables. The tables contain cumulative distribution functions that represent the first breach time distribution for the waste package and the variation with time of the average number of pit and patch penetrations per failed waste package. These distributions are used to determine the time at which waste form degradation occurs and radionuclide release begins, and the effective area through which release can occur.

3.4.3 Results and Interpretation: Evaluation of Key Issues and Importance to Performance

The results of using the waste package degradation model to estimate performance of the waste package for the base case are presented in this section. These results point out the importance of various parameters in the modeling and the effects of some of the assumptions.

The results of using the waste package degradation model to estimate performance of the waste package provide a quantitative analysis of the initial failure of the waste packages and their degradation through time. Figure 3-47 shows the failure curves for the various aspects of failure when water drips on waste packages. The breach curve for corrosion-allowance material indicates when the first penetrations occur in the outer-barrier material. These breaches start at approximately 1,000 years and continue until the corrosion-allowance material fails for all packages at approximately 6,000 years. This curve for corrosion-allowance material shows that breaching occurs significantly before the simulated failure of the corrosion-resistant material. The first-breach

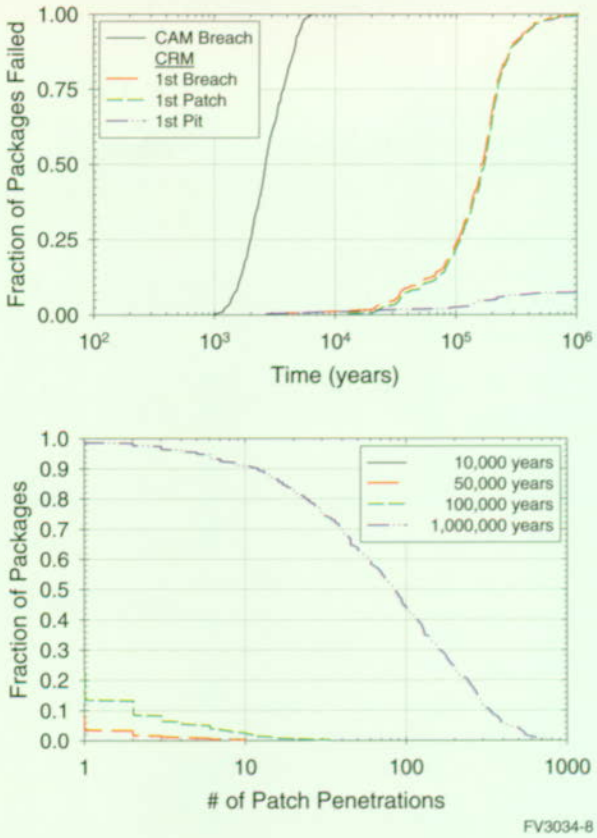

Figure 3-47. Waste Package Degradation History of Packages Exposed to Drips
The top figure shows the failure rate history of packages for a period of 1 million years and the bottom figure shows the number of patch penetrations at different time periods. (CAM—corrosion-allowance material [waste package outer layer]; CRM—corrosion-resistant material [waste package inner layer])

curve indicates the time of first penetration completely through a waste package, whether it is because of a pit or a patch. This curve is primarily from patch failures, with a few initial pit penetrations, and shows that failures start at 3,000 years. All waste packages that are dripped on fail by 1 million years. The first-patch curve basically follows the first-breach curve because not many packages fail through pitting. The overall degradation of the waste package through patch failure is shown in Figure 3-47. At 1 million years, 50 percent of the packages that are dripped on have approximately 80 patch perforations.

The base case analyses incorporate both dripping and nondripping conditions. The effect of these

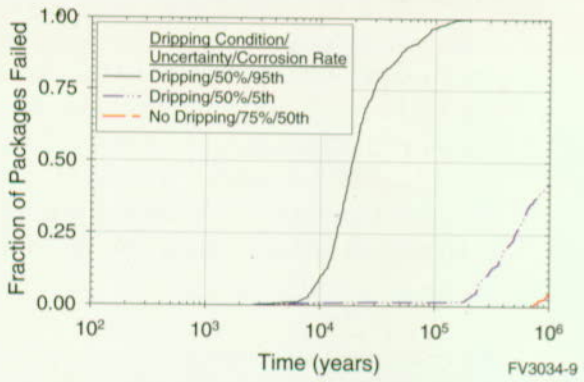

Figure 3-48. Dripping Versus No-Dripping Effect on Waste Package Degradation
Exposure to dripping accelerates failure of packages.

two drift environments on waste package degradation is shown in Figure 3-48. The waste packages that are dripped on have a higher percentage of failures and fail much earlier than the waste packages that are only exposed to humid air conditions within the drift.

The waste packages will be exposed to different dripping environments within the drifts. The effect of alternate dripping environments is shown in Figure 3-49. The waste package failures are higher for the wetter climates, because of the effect of dripping on Alloy 22 corrosion. All of these dripping scenarios are included in the base case.

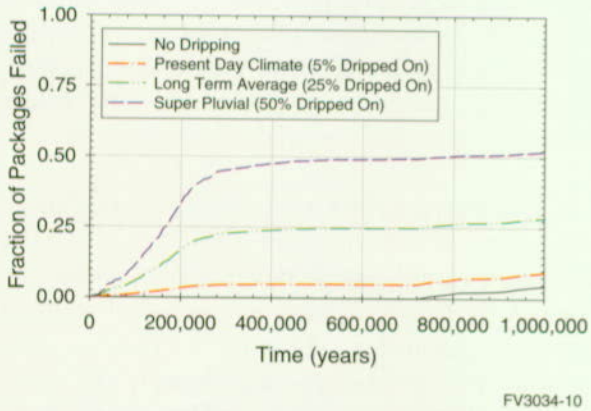

Figure 3-49. Effect of Alternative Dripping Scenarios on Waste Package Degradation
This figure shows fraction of packages failed for three dripping scenarios including present-day climate, long-term-average climate, and superpluvial climate as well as a no-dripping comparison.

The impact of waste package performance on the overall system is potentially quite significant. The overall corrosion rate for corrosion-resistant material and the number of waste packages that get wet are significant determinants to the overall release of radionuclides from the system. A sensitivity analysis shows that system performance is highly dependent on the corrosion rate for corrosion-resistant material.

Based on previous results from the waste package degradation computer code and conceptual understanding of corrosion degradation processes for waste packages, a ranked list of potentially important parameters for evaluating waste package degradation was developed. The ranking looks at parameters that affect waste package failure, including first penetration of the waste package and the number of pit and patch penetrations that directly affect radionuclide releases from the waste packages. The ranking is as follows:

1. Allocation of the model variance, especially for corrosion-resistant material, to uncertainty and variability of waste package degradation

2. Local chemical and electrochemical exposure conditions for corrosion-resistant material

3. General corrosion rate for corrosion-resistant material under dripping conditions

4. Initiation threshold for localized corrosion of corrosion-resistant material

5. Localized corrosion rate for corrosion-resistant material

Other potentially important model parameters follow:

- Surface area of a waste package that is wetted under drips

- Allocation of the total variability to waste package-to-waste package and patch-to-patch variability

- Roughness factor for corrosion-allowance material

The overall strength of the model is that a significant amount of data has been reviewed to determine corrosion rates for corrosion-allowance material. The primary weakness of the model is the overall reliance on expert elicitation rather than on long-term test data of corrosion rates for corrosion-resistant material. These rates significantly affect overall system performance but are based on limited data for environments unlike those expected at Yucca Mountain.

The model provides highly uncertain analyses of corrosion of corrosion-resistant material because data are so limited. Providing additional defense of these analyses for the LA will require laboratory testing data for general and localized corrosion of Alloy 22 and for stress corrosion cracking, as well as further process model development.

3.5 WASTE FORM ALTERATION, RADIONUCLIDE MOBILIZATION, AND TRANSPORT THROUGH THE ENGINEERED BARRIER SYSTEM

The waste forms emplaced in the repository will initially be contained in and protected by the waste packages. Location of the waste forms in the overall repository system is shown in Figure 2-2. The major processes effective in this part of the repository system are identified in Figure 3-50. After degradation and failure of the waste packages, spent nuclear fuel assemblies and high-level radioactive waste canisters will be exposed to the drift environment including air, water vapor and, possibly, dripping water. After waste package failure, radionuclides are not available for release and transport until three things have occurred:

1. Failure of the fuel cladding, (the tubular material surrounding the fuel matrix), or high-level radioactive waste canister. (Note: The extra performance provided by the canisters is not accounted for in TSPA-VA.)

2. Degradation of the solid waste form

3. Mobilization of radionuclides into aqueous solution, aqueous colloidal suspension, (interaction with particles 0.001 to 1 micron in size through sorption and other chemical mechanisms), or gaseous form, (Note: No gaseous transport was considered in TSPA-VA because it was not a significant release mode in previous TSPAs.)

Mobile radionuclides are transported out of the degraded waste package and through the engineered barrier system to the unsaturated zone. Transport occurs through one of two mechanisms:

- Movement of dissolved or colloidal material because of random molecular, or thermal, motion along continuous water pathways within the waste package (diffusive transport)

- Movement of dissolved or colloidal material because of the bulk flow of a fluid, which in this case is water, through the waste form and waste package (advective transport)

Waste form degradation and radionuclide mobilization depend on the initial waste form type and amount, the initial design of the system and the processes occurring in the drift environment. Thermal history and package lifetime determine the temperature of the waste forms when they are exposed to degrading processes. Composition of the gas phase and aqueous chemistry of incoming water, along with the waste temperature, control the rates of waste form degradation and the nature of mobilized products available for transport.

The engineered barrier system is comprised of all components of the repository within the drifts. The analysis of transport of radionuclides within the engineered barrier system requires definition of numerous parameters and models. This transport is influenced by waste package degradation; waste form degradation, including cladding degradation; the thermal-hydrologic and chemical environment; and design of the engineered barrier system. Radionuclides released from the engineered barrier system enter the natural system for transport through the unsaturated and saturated zones to the

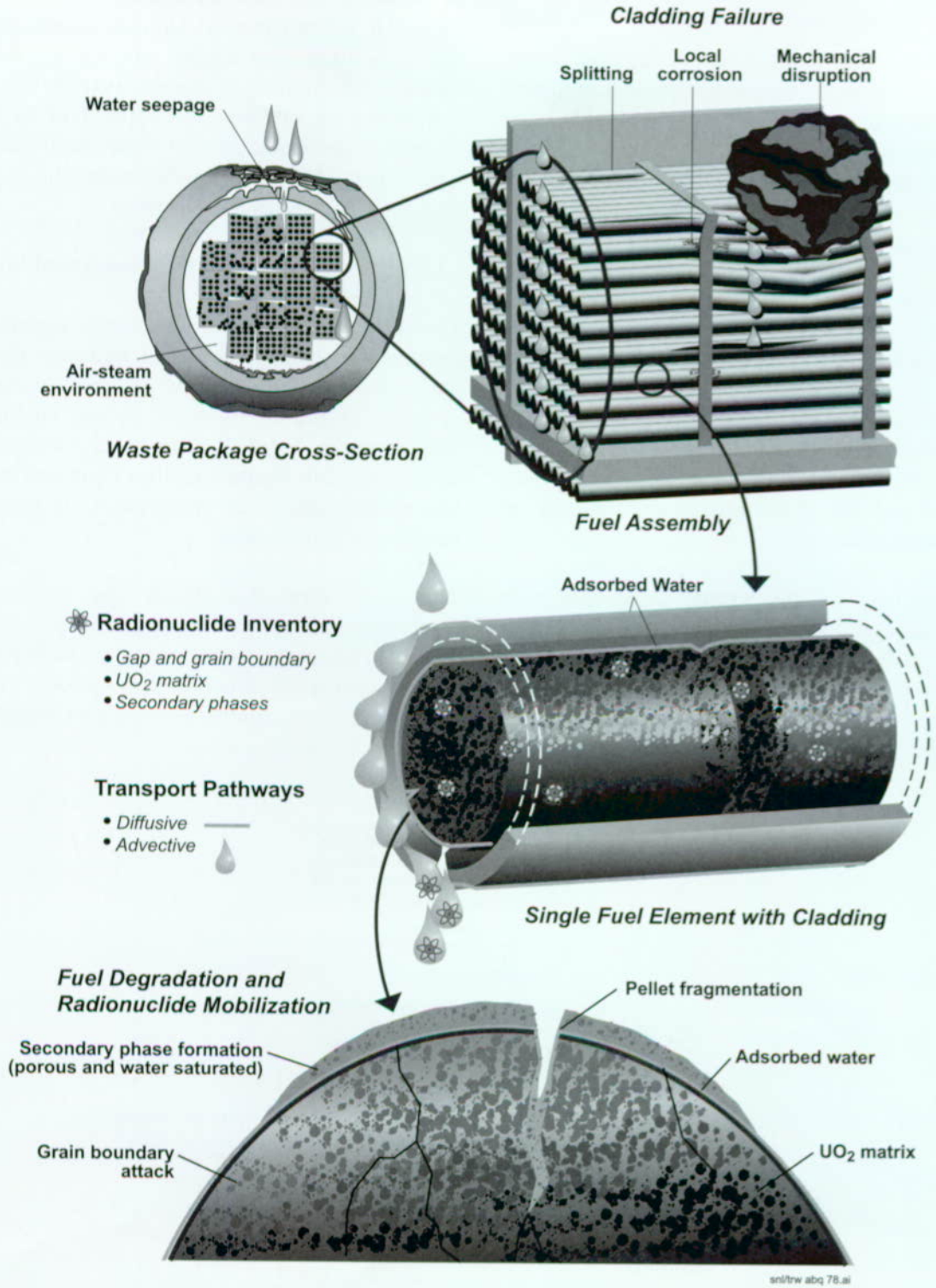

Figure 3-50. Schematic of Waste Form/Waste Package/Engineered Barrier System

accessible environment where overall repository performance is measured.

The waste form degradation and engineered-barrier-release modeling studies presented in this section were prepared with the view of addressing selected aspects of the NRC Key Technical Issues on Container Life and Source Term (NRC 1998b), Evolution of the Near-Field Environment (NRC 1997c), and Total System Performance Assessment and Integration (NRC 1998a). Specifically, the information presented is pertinent to the container life and source term subissue on contribution of spent nuclear fuel resistance to degradation towards controlling radionuclide releases to the near-field environment, the near-field environment subissue on effects of coupled processes on rate of release of radionuclides from breached waste packages and the TSPA integration subissue on model abstraction.

The remainder of this section deals first with construction of the conceptual model for waste form degradation, radionuclide mobilization, and transport through the engineered barrier system. This is followed by a discussion of the implementation of the engineered barrier system model in the performance assessment model, and the evaluation of some of the key aspects of the subsystem relative to performance. Additional information on the waste form degradation, radionuclide mobilization, and engineered barrier system transport component can be found in Chapter 6 of the *Total System Performance System Assessment-Viability Assessment (TSPA-VA) Analyses Technical Basis Document* (CRWMS M&O 1998i).

3.5.1 Construction of the Conceptual Model

The conceptual model for waste form degradation, radionuclide mobilization, and transport through the engineered barrier system incorporates the key processes expected to occur in the engineered barrier system. Figure 3-51 provides a summary of this model. The figure identifies input and output, key components of the model, and the bases for confidence in the model.

The waste form degradation and mobilization abstraction/testing workshop was held in February 1997 and focused on the key issues for this topic. The prioritization criteria, high priority issues relative to those criteria, and analysis plans from

Figure 3-51. Waste Form Degradation/Mobilization/Engineered Barrier System Conceptual Model

the workshop are presented in a summary in Table 3-12.

An expert elicitation was conducted to consider issues, including processes, parameter ranges, alternative models and uncertainties, related to waste form degradation and radionuclide mobilization and transport through the engineered barrier system. A six-member panel was selected to represent a range of expertise. Members were from both from within and outside of the YMP. Results from this elicitation were not available for the TSPA-VA base case, but preliminary input influenced both construction of the base case and some of the sensitivity analyses. Issues considered, preliminary suggestions from the elicitation panel, and advice incorporated in the TSPA-VA include the following:

- Exposed, wet, and active surface areas—The experts suggested several approaches to bounding values, with the TSPA representation being on the conservative side.

- Cladding degradation—The experts expressed concern about assuming the cladding provides waste isolation benefits because of the large uncertainties and limited available data. The panelists suggested several long-term degradation modes that were incorporated into the TSPA.

- Dissolution rate for spent nuclear fuel—The experts suggested several alternative approaches, but the results would effectively be consistent with the model currently being used for the TSPA.

- Radionuclide solubilities—The experts gave a range of opinions on radionuclide solubilities, with substantial support for conservative bounds.

- Secondary-phase retention of radionuclides—The topic of secondary phase evolution and retention of radionuclides created a variety of input, with support for pursuing this credit for sensitivity studies and for licensing.

- Rapid-release fractions—The experts suggested revision of rapid-release fractions, but doing so would not cause significant change in release rates for the TSPA-VA analysis.

- Dissolution rate for high-level radioactive waste—The panelists suggested additional sophistication in the dissolution model, but the TSPA model was found to be acceptable in providing a usable bound.

- Colloid formation—The panelists supported including colloidal mobilization processes

Table 3-12. Waste Form Degradation and Radionuclide Mobilization Abstraction/Testing Workshop

Waste Form Degradation and Radionuclide Mobilization Abstraction/Testing Workshop
February 19-21, 1997, Livermore, CA
(CRWMS M&O 1997o)

Prioritization Criteria
Does the process/issue affect the
- Radionuclide concentration at the waste form?
- Mass release rate of radionuclides from the engineered barrier system?
- Time and spatial variability in mass release rate?
- Form of radionuclides entering the unsaturated zone for transport?

Highest Priority Issues
- Spent nuclear fuel:
  - Dissolution rate
  - Time dependent evolution of solution and alteration layer
  - Representation of evolution of the near-field
  - Exposed spent nuclear fuel surface area
  - Cladding degradation model
- High-level radioactive waste (glass) and other wastes
  - Time dependent evolution of solution and alteration layer
  - Vapor hydration
  - Evolution of near-field environment
  - Dissolution rate
- Solubilities and engineered barrier system transport:
  - Physical processes—water contact mode
  - Mobilization—colloids
  - Chemical processes—mobilization—fluid dependence
  - Physical processes—transport paths
  - Chemical processes—mobilization—solid dependence

Analysis Plans
- Cladding and canister credit
- Spent nuclear fuel dissolution
- Spent nuclear fuel dissolution water chemistry and precipitated phases
- High-level radioactive waste glass degradation and release
- Solubility limits
- Engineered barrier system transport and release

and discussed several approaches for providing bounds guided by the limited data.

The results of the expert elicitation are documented in the *Waste Form Expert Elicitation* (CRWMS M&O 1998k).

3.5.1.1 Input

The important input to the waste form degradation and mobilization models include the following:

- The inventory of radionuclides
- Thermal-hydrologic modeling results: temperature at the waste package surface, relative humidity at the waste package surface, and liquid saturation in the invert
- Results from waste package degradation
- Results from cladding degradation
- Water ingress to the system
- Amount of exposed fuel surface area caused by cladding degradation
- Near-field geochemical conditions

The following are key inputs to the transport model for the engineered barrier system:

- Parameters relating to mobilization of radionuclides from the waste form
- Flux and chemistry of the water moving through the system
- Retardation in and permeability of the engineered barrier system materials, for example, the waste package and the invert, or emplacement drift flooring

3.5.1.2 Output

The output from the modeling of waste form degradation, radionuclide mobilization, and engineered barrier system transport is a release of radionuclides from the engineered barrier system into the geosphere. These releases are in both aqueous and gaseous form (although TSPA-VA does not model gaseous release), along with a colloidal fraction.

3.5.1.3 Components of the Models

The components of the models include the following:

- The initial inventory
- Degradation of the cladding on commercial spent nuclear fuel
- Dissolution rates for the waste forms
- Solubility constraints on radionuclide mobilization
- Formation of colloids and secondary mineral phases
- Flow and diffusion of radionuclides through the system and sorption within the system

3.5.1.4 Bases for Confidence in the Model

The model is based on a substantial amount of data in some cases, and reliance on expert elicitation in others. In particular, the waste inventory and the dissolution rates are based on data and testing that have been in progress for over 14 years. Values for radionuclide solubility have been obtained from a combination of testing and expert evaluation. The cladding model is based on evaluation of cladding degradation processes, zirconium experiments, and literature data. Colloid parameters are based on a range of laboratory experiments and field observations. Sorption parameters are based on both site-specific data and expert elicitation. For the TSPA-VA, natural analogs have been used to corroborate dominant processes related to waste form degradation and engineered barrier system transport.

Several issues pertaining to the engineered barrier system have not been fully evaluated. These issues include the effects of lining and tunnel collapse on engineered barrier system transport and thermal-mechanical effects on the engineered barrier system.

3.5.1.5 Inventory

The following waste forms are to be included in the potential Yucca Mountain Repository:

- Commercial spent nuclear fuel; irradiated uranium dioxide pellets encased in cladding
- High-level radioactive waste; canistered borosilicate glass waste
- DOE spent nuclear fuel; primarily canistered irradiated uranium encased in cladding
- Plutonium waste forms; mixed oxide spent nuclear fuel and canistered ceramic waste forms

The waste form for commercial spent nuclear fuel to be emplaced in the repository is comprised of 63,000 MTHM from both pressurized water reactor and boiling water reactor commercial reactors. The high-level radioactive waste is comprised of canisters of glass from four sources:

- Hanford Site
- Savannah River Site
- West Valley
- Idaho National Engineering and Environmental Laboratory

The canisters of glass contribute 4,667 MTHM equivalent to the repository. Each source of high-level radioactive waste was assumed to contribute the same MTHM percentage (46 percent) of their total high-level radioactive waste to the repository, because the total inventory (10,110 MTHM is well over the repository allocation of 4,667 MTHM. The DOE spent nuclear fuel consists of over 250 different types of spent nuclear fuel (Duguid et al. 1997, p. A-2) and will contribute 2,333 MTHM to the total repository (Table 3-13). The major contributor to this waste form is the N-Reactor fuel currently stored at the Hanford Site. This waste form also includes 65 MTHM of naval spent nuclear fuel. The 50 metric tons of plutonium is assumed to be disposed in a combination of mixed-oxide fuel and ceramic waste forms.

There are over 200 radionuclides in the waste inventory. However, for evaluation of postclosure performance, the number of radionuclides considered can be reduced based on several characteristics of the radionuclides:

- Decay of radionuclides with short half-lives
- Sorption characteristics
- Low biosphere dose conversion factors

The inventory that is used in the analysis is crucial in defining which radionuclides are released from the system and their concentrations. Based on these considerations and previous TSPA results (Wilson et al. 1994; Andrews et al. 1994), a limited number of dominant radionuclides were chosen for analysis. The inventory for the nine radionuclides included in the base case inventory for each of the three waste forms is presented in Table 3-14. The inventory includes ingrowth of radionuclides because of the decay of parent radionuclides that are not included in the analyzed inventory. For example, all of the americium-241 and plutonium-241 in the waste is assumed to decay to neptunium-237 when the waste is emplaced to determine the initial inventory of neptunium-237. Radionuclide decay of the nine radionuclides is accounted for during the analysis, but daughter product ingrowth has been incorporated into the initial inventory. Also a simplified approach is used that adjusts the radionuclide source term to compensate for the production of the radionuclides neptunium-237, uranium-234, and protactinium-231. In the case of neptunium-237 and uranium-234, where the parents of concern have a shorter half-life, it was assumed that the parents had decayed to the isotopes of interest at the start of the simulation. However, for protactinium-231 the half life is much shorter that of the parent, uranium-235. To allow for the neglect of decay, it was assumed that the protactinium was, at all time, in secular equilibrium with the uranium parent, that is, for every curie of uranium in the waste form there was a curie of protactinium. A portion of the inventory is expected to be in the void space between the fuel and the cladding, allowing for rapid release of

Table 3-13. U.S. Department of Energy Spent Nuclear Fuel Categories, Typical Spent Fuel in Each Category, and Metric Tons Heavy Metal in Each Category

Category	Typical Spent Fuel	MTHM
1. Uranium metal	N-Reactor	1979.88
2. Uranium-Zirconium alloy	Heavy Water Component Test Reactor	0.04
3. Uranium-Molybdenum alloy	Enrico Fermi Reactor	3.51
4. Uranium oxide	Commercial Pressurized Water Reactor	92.06
5. Uranium oxide (disrupted clad)	Three Mile Island core debris	81.18
6. Uranium-Aluminum alloy	Advanced Test Reactor	8.15
7. Uranium silicide	Foreign Research Reactor-Materials Test Reactor	10.78
8. Uranium-Thorium carbide (high integrity)	Fort St. Vrain	23.01
9. Uranium-Thorium carbide (low integrity)	Peach Bottom	1.55
10. Uranium-Thorium carbide (non-graphite)	Fast Flux Test Facility carbide	0.14
11. Mixed oxide	Fast Flux Test Facility oxide	11.49
12. Uranium-Thorium oxide	Shippingport Light Water Breeder Reactor	46.30
13. Uranium-Zirconium hydride	Training Research Isotope-General Atomic	1.89
14 Sodium-bonded[a]	Will be treated prior to disposal	
15. Naval spent nuclear fuel	Naval Nuclear Propulsion Uranium Based with Zircaloy Cladding	63.00[b]
16. Miscellaneous	Not specified	10.01
Total[c]		2332.99

Source: CRWMS M&O 1998i, Section 6.

[a]Sodium-bonded spent nuclear fuel was not analyzed.

[b]At the time of publication of this document, the intent is to allow 65 MTHM of naval fuel into the repository; however, at the time the TSPA-VA analyses were completed, the direction was to only emplace 63 MTHM (CRWMS M&O correspondence, Robert W. Andrews, Duke Engineering & Services, Las Vegas, Nevada from E.P. Stroup of Lockheed Martin Idaho Technologies Company, Idaho Falls, ID, May 4, 1998). Therefore, all of the TSPA-VA analyses have been completed with the assumption of 63 MTHM of naval fuel. The difference between these two numbers would have a negligible effect on the outcome of the analyses.

[c]The total amount of DOE spent nuclear fuel is approximately 2,496 MTHM which was reduced by about 7 percent to reach 2,333 MTHM.

Table 3-14. Inventories for Various Waste Forms

Radionuclide	Waste Package Type			Half-Life (Years)
	Commercial Spent Nuclear Fuel (Ci/pkg)	High-Level Radioactive Waste (Ci/pkg)	DOE Spent Nuclear Fuel (Ci/pkg)	
Carbon-14	11.7	0	0.31	5.73×10^3
Iodine-129	0.29	0.0000417	0.00567	1.57×10^7
Neptunium-237	11.4	0.735	0.153	2.14×10^6
Protactinium-231	5.08[b]	0.0364*	0.661*	3.30×10^4
Plutonium-239	3050	24.3	115	2.41×10^4
Plutonium-242	17	0.02	0.114	3.87×10^5
Selenium-79	3.72	0.286	0.0885	6.50×10^4
Technetium-99	118	29.5	2.55	2.13×10^5
Uranium-234	21.1	0.898	0.541	2.45×10^5

Source: (CRWMS M&O 1998i)

*gm/waste package

Note: These inventories are for 30-year old fuel.

these radionuclides when the cladding fails (CRWMS M&O 1998i, Chapter 6).

The waste form inventory was abstracted to allow appropriate analyses. Figure 3-52 shows the abstraction of the inventory. This abstraction allows representation of the inventory as three separate waste forms in the total system analyses.

3.5.1.6 Cladding

The evaluation of cladding degradation includes the processes expected to affect the cladding over long periods of time. The analysis assumes a small fraction, 0.1 percent, of the commercial spent nuclear fuel rods to have failed from reactor operations. This is actually two times higher than data reported by the Electric Power Research Institute (EPRI 1997, p. 4-1). A small fraction, 1.15 percent, of the commercial spent nuclear fuel waste has stainless steel cladding. This cladding is assumed to fail immediately after the waste package fails because of rapid corrosion of stainless steel relative to the time scale being considered. Additional mechanisms in the cladding model include creep failure, which is primarily only an issue at high temperatures, and general and localized corrosion failure. Another long-term failure mechanism for fuel rods is mechanical disruption. After the waste package has lost structural integrity, mechanical loads caused by rocks falling from the drift walls and ceiling and disruption of the fuel support structure may break the fuel rods (CRWMS M&O 1998a, p. 45).

3.5.1.7 Dissolution Rates

The dissolution rate of the waste forms is another aspect of the system that requires analysis because this process provides the rate at which the radionuclides are made available for mobilization and release. Because the three major waste forms analyzed in TSPA-VA have different characteristics, it is essential to have a unique dissolution model for each waste form.

The dissolution rate for commercial spent nuclear fuel is a parametric equation that has been fitted to high flow-rate experimental data on commercial spent nuclear fuel and uranium oxide. This fit provides dependence on temperature, pH, total carbonate ($[CO_3]_T$), burnup, and oxygen potential. The rate is expressed in mass dissolved from a given surface area in a given time. The effective surface area is derived from experimental observations and accounts for fracturing of fuel pellets and some grain boundary activity. The dissolution rate is used as a conservative upper bound for the availability of radionuclides to mobilize. This dissolution rate does not account for solubility limits or retention of radionuclides in secondary phases that may form (see Section 3.5.1.8).

The model developed for high-level radioactive waste dissolution is based on or is consistent with several types of tests that are used to define the processes, fit rate parameters, or confirm general behavior. The forward reaction rate parameter used in the model is developed from data from laboratory tests that monitor a single flow across fuel material. The saturation term comes from chemical kinetic theory and is consistent with the results of static tests. The temperature effect is based on single pass flow through tests performed from 25° to 70°C (77° to 158°F) and is consistent with static tests done at temperatures up to 250°C (482°F). The evolution of secondary phases and dissolution rates under low flow conditions is consistent with low flow rate drip tests and vapor hydration tests.

The DOE spent nuclear fuel included in the repository is comprised primarily of N-Reactor fuel. In the base case a surrogate is used for the DOE spent nuclear fuel that is composed of 2,333 MTHM with a radionuclide inventory that is a weighted average of Categories 1, 4, 5, 6, 8, and 11 (as defined in Table 3-13). These categories were found to contribute significantly to dose from all DOE spent nuclear fuel (Duguid et al. 1997). A reasonable dissolution-rate model for this surrogate waste form is the metallic fuel model. The uranium metal fuel radionuclide release rate is expected to be very close to the uranium matrix dissolution or corrosion rate. The dissolution rate model was developed by fitting a response surface to the available data. When the repository temperature is below 100°C (212°F), water was assumed

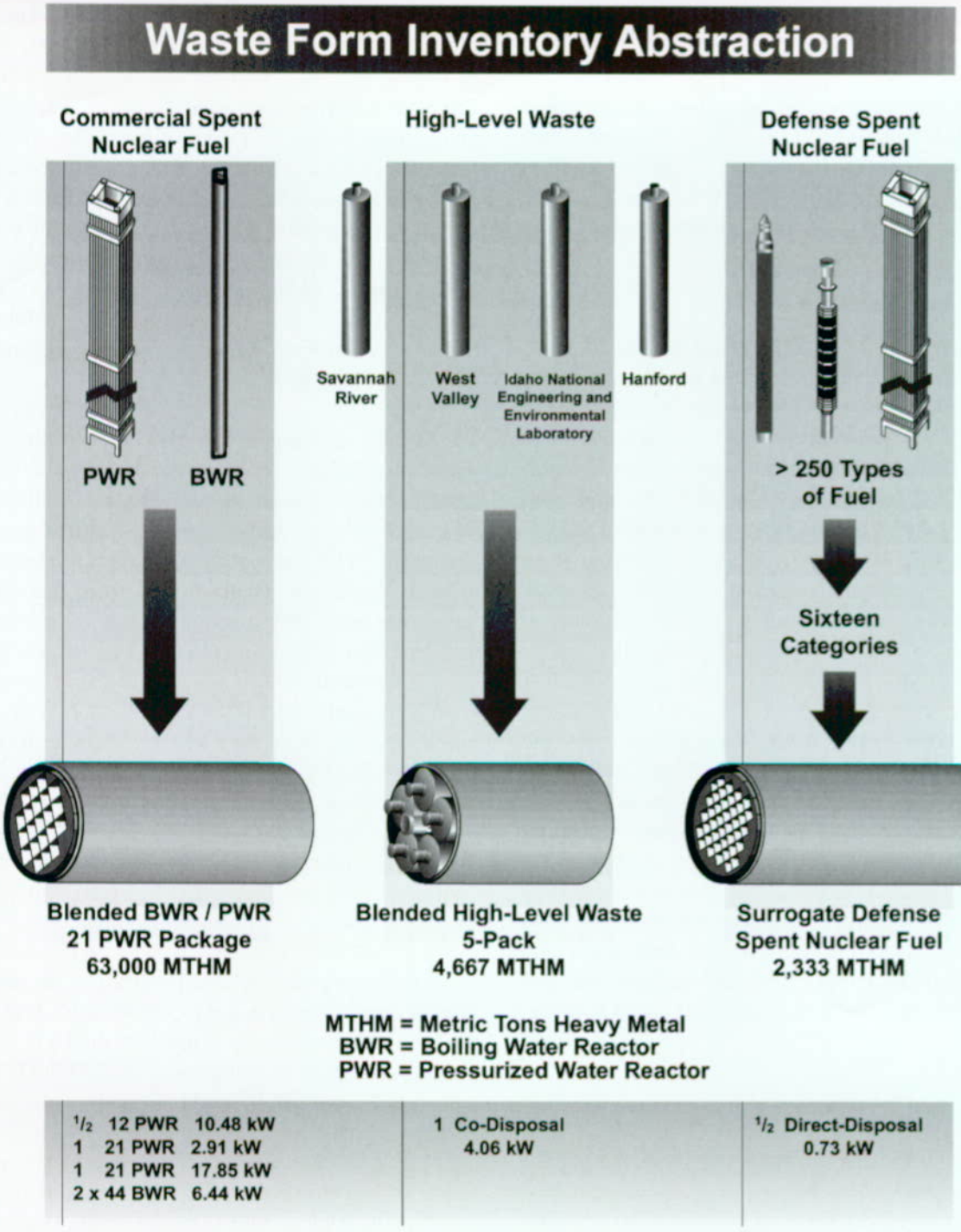

Figure 3-52. Inventory Abstraction

to be present on the waste form (wet oxic conditions) and humid air conditions are assumed for all other times.

3.5.1.8 Solubility Limits

The concentration of each radionuclide mobilized from the waste form cannot exceed the radionuclide solubility limit, unless suspended colloids are included. The solubility-limit model is a hybrid of solubility-limit distributions determined by expert elicitation (Wilson et al. 1994, pp. 9-1–9-11), previous assessments (EPRI 1992; Golder Associates 1993), and a reassessment of measured neptunium concentrations (CRWMS M&O 1997v; CRWMS M&O 1998c). Including the observed concentration for neptunium from waste form dissolution studies in the model is an initial attempt to incorporate the effect of secondary precipitation phases into the evaluation of release from the waste form. Some of the elicited solubility constraints (americium, neptunium, plutonium) were also described as functions of temperature and pH (CRWMS M&O 1995). The neptunium solubility constraints currently range from a minimum value just below the maximum values based on spent-fuel drip tests (Finn et al. 1995) to a maximum value that encompasses the minimum values developed through the expert elicitation (CRWMS M&O 1998i). Additional work will refine this uncertainty in the future. Along the transport pathways through the engineered barrier system, the radionuclide concentrations are checked against the solubility limit. Table 3-15 lists the solubility distributions used in TSPA-VA analysis.

3.5.1.9 Colloids

Colloids may be important to performance for two reasons: they may increase the release of radionu-

Table 3-15. Solubility Limit Distributions

RN	Distribution Type	Distribution Variable	Minimum Value g/m^3 & [mol/L]	Maximum Value g/m^3 & [mol/L]	Mean or Peak g/m^3 & [mol/L]	C.V.	Source
C	---	---	---	---	1.2e4 [1.0]	---	Project Elicitation
I	---	---	---	---	1.27e5 [1.0]	---	Project Elicitation
Np	beta	log (Concen.)	log(1.2e-2) [log(5e-8)]	log(2.4e+1) [log(1.0e-4)]	log(3.4e-1) [log(1.4e-6)]	1.20 [0.099]	CRWMS M&O 1998i
Pa	uniform	log(Concen.)	log(2.3e-5) [log(1.0e-10)]	log(2.3) [log(1.0e-5)]	log(7.3e-3) [log(3.2e-8)]	---	Project Elicitation
Pu	uniform	Concen.	2.4e-3 [1.0e-8]	2.4e-1 [1.0e-6]	1.2e-1 [5.1e-7]	---	Project Elicitation*
Se	triangular	log(Concen.)	log(7.9e+2) [log(1.0e-2)]	log(5.5e+5) [log(7.0)]	log(7.9e+3) [log(1.0e-1)]	---	Golder Associates 1993, EPRI 1992
Tc	triangular	log(Concen.)	log(3.5e-2) [log(3.6e-7)]	log(9.9e+5) [log(1.0e+1)]	log(1.0e+2) [log(1.0e-3)]	---	Golder Associates 1993, EPRI 1992
U	beta	log(Concen.)	log(2.4e-3) [log(1.0e-8)]	log(2.4e+3) [log(1.0e-2)]	log(7.6) [log(3.2e-5)]	1.02 [0.2]	Project Elicitation

log–refers everywhere in the table to the base 10 logarithm.

RN–radionuclide

Mean or Peak–The values listed are the arithmetic mean for all distributions *except* log triangular distributions where the values listed correspond to the peak of the distributions. *NOTE*: For any distribution of log (concen.), the value of the mean is *not equivalent* to the log (mean) for the corresponding distribution of concentration.

C.V.–Coefficient of Variation, which equals the absolute value of the ratio of the Standard Deviation to the Mean. Values given only for log beta distributions.

e+ represents positive power(s) of ten

e- represents negative power(s) of ten

*–indicates modifications to original source information

Project Elicitation–Conducted at Sandia National Laboratory on April 13, 1993.

clides from the waste package, and they may increase the transport velocity of radionuclides. When a radionuclide concentration is solubility limited, transport as mobile colloids increases the release of the radionuclide from the waste package. The transport velocity of radionuclides attached to colloids may be faster than that of dissolved radionuclides because colloids may travel in the faster parts of the flow paths, and colloids may sorb to host rock less than dissolved radionuclides.

While many radionuclides have the potential for colloidal transport, this initial colloid analysis focused on plutonium. Plutonium is a major part of the waste inventory, has low solubility and high sorption onto host rock, and is the radionuclide most likely to be affected by colloidal transport. As more data are obtained, colloidal transport of additional radionuclides will be investigated.

Many types of colloids are expected to be present in the Yucca Mountain repository system, but only four types were chosen for explicit modeling: clay, iron corrosion products, spent nuclear fuel colloids, and glass waste colloids. The spent nuclear fuel and glass waste colloid types refer to all colloids that are produced during the degradation of the waste forms containing these waste types. The four colloid types were chosen because they may be present in significant concentrations and have enough attached plutonium to affect repository performance. The effect, however, will depend on the transport properties of the colloids, for example, velocity, filtration, and sorption, and the reversibility of the plutonium attachment to colloids.

For this initial modeling of colloids, transport was assumed to be unretarded through the fracture continuum. The reversibility of plutonium attachment to colloids has been investigated at Los Alamos National Laboratory. Their studies of sorption/desorption of plutonium (IV) and plutonium (V) on hematite, geothite, and clay show fast attachment and slow detachment. Therefore, sorption of dissolved plutonium onto the major near-field and far-field colloids is expected to be reversible on the time scale of transport to the accessible environment (hundreds to millions of years). The reversibility of attachment to waste form colloids, however, has not been determined. Co-precipitation, in particular, has the potential to create colloids having radionuclides encapsulated by stable minerals. Workers at Argonne National Laboratory have observed radionuclide-containing phosphate minerals co-precipitated with clays in their glass dissolution experiments for high-level radioactive waste. These colloids may be able to move large distances without giving up their radionuclides. It is not clear what fraction of waste form colloids may have irreversibly attached radionuclides. Experiments are planned to address this issue.

3.5.2 Implementation of the Waste Form Degradation and Mobilization Model

The various components of the waste form degradation and mobilization model are included in the TSPA analyses as abstractions from the observed data or expert elicitation. This section discusses the major models included in the analyses: cladding, waste form dissolution, solubility, colloids, and engineered barrier system transport.

3.5.2.1 Cladding Model Abstraction

Most of the commercial spent nuclear fuel is encased in Zircaloy cladding that isolates it from the environment. Models were developed to describe cladding degradation from creep, corrosion, and mechanical failure, or rockfalls. The model assumed cladding was failed at the time of emplacement in the repository for the stainless-steel-clad fuel (1.15 percent of inventory; CRWMS M&O 1998a, p. 30) and for fuel with defective cladding from reactor operation (0.1 percent; EPRI 1997, p. 4-1). The latter type of failure is termed "juvenile" cladding failure. Both creep and delayed hydride cracking, a process where hydrides facilitate cracking of the cladding, were modeled, but neither contributes significantly to the amount of fuel available for dissolution. Hydride embrittlement was also evaluated. If the assumption is made that the waste package failed after 100 years (during high temperature period), the amount of hydrogen taken up from the cladding corrosion is less than 50 ppm. This level of uptake of hydrogen is expected to have negligible effect on the cladding fracture toughness. For instance,

Kreyns et al. (1997, p. 766) showed that the fracture toughness decreased from 42 MPa-$m^{0.5}$ to 8 MPa-$m^{0.5}$ as the hydrogen content increased from zero to 4,000 ppm, a hydrogen uptake value much higher than is expected for the cladding.

One cause of cladding already being failed when it arrives at the repository is the type of cladding used in early fuel designs. Fuel design for commercial reactors has been evolving. Eight of the earlier reactors used stainless steel cladding, but no operating reactor currently uses this type of cladding. This type of fuel represents a total of 723 MTU, 1.15 percent of the estimated 63,000 metric tons of commercial fuel to be placed in the repository. Because the stainless steel cladding is expected to corrode rapidly relative to Zircaloy, this fraction of the fuel is likely to be exposed for dissolution when the waste package fails.

The failure rate for commercial fuel that is clad in Zircaloy has improved with time. Reactor cores prior to 1985 had an individual fuel rod or pin failure rate from 0.02 percent to 0.07 percent (EPRI 1997, p. 4-1). The pin failure rate has decreased to the current rate of 0.006–0.03 percent, (EPRI 1997, p. 4-2) with an average pin failure rate for both time periods of 0.01–0.05 percent. Occasionally, a specific core will have a higher failure rate, with the highest reported rate being 0.4 percent. For this analysis, the pin failure rate is intended to represent a conservative average, and not the extreme damage to a single core or assembly. The analysis assume an average of 0.1 percent of all pins are damaged to some degree. This is approximately twice the rate of failures in EPRI (1997, p. 4-1).

In the early stages of postclosure (first 50 years), the cladding could be damaged by creep or strain failure if the temperature (and, therefore, cladding stress) is high enough. This failure mode leads to a pinhole or hairline crack. This type of failure is not predicted to occur for pins in the average waste package and does not significantly contribute to the source term.

The fraction of fuel exposed for dissolution is used directly in the RIP computer program that integrates the components of the repository system. The type of pin damage from reactor operation can be characterized as follows (EPRI 1997, pp. 4-3,):

- Pinhole and hairline cracks 80–90 percent
- Intermediate condition 0–20 percent
- Severe damage 0.04–0.9 percent

The fuel damaged by creep failure has either a pinhole or a hairline crack, exposing a very limited amount of fuel. The fuel temperatures are too low to produce U_3O_8 and cladding unzipping, or tearing open. Therefore, only a limited amount of fuel is exposed for dissolution. The analysis assumes that the exposed fuel from juvenile failures, 0.1 percent of total fuel, has no cladding and is available for dissolution. This amount is added to the amount of fuel exposed because of the failure of stainless steel cladding, yielding a total of 1.25 percent of commercial fuel available for dissolution when the waste package fails. This approach is potentially non-conservative because it spreads the release over a larger area than if all stainless steel clad fuel was packaged together. The overall effect on performance however is negligible because of the mixing in the unsaturated zone.

Zirconium corrosion has been studied since 1946 when commercial grades became available. Rothman (1984, p. 11) compared the oxidation rates for Zircaloy, an alloy of zirconium, assessed by six different authors and predicts corrosion amounts that vary from 4 to 53 microns for cladding exposed for 10,000 years at 180°C (356°F). Rothman assumed (for both the pressurized-water reactor and the boiling-water reactor) that fuel was 10 years old, loaded to 44 kW/acre, 3.3 kW/package. Cladding temperatures start out at about 330°C (626°F) and cool to about 100°C (212°F) in about 1,000 years. The water used was J-13. All of the corrosion rate models use a temperature dependency that predicts near zero corrosion rates at long-term repository temperatures. Using recent correlations by four different authors, Einziger (1994, p. 556) for dry oxidation, VanSwam and Shann (1991, p. 771) for wet oxidation, Hillner et al. (1998, p. 6) for the most recent naval spent nuclear fuel wet correlation, and Hillner et al. (1998, p. 23 eg. 6) for this

widely used EPRI sponsored model, an analysis of the hottest pin in an average waste package exposed to the temperature history predicted at YMP gives corrosion depth from 1 to 5 microns if the waste package is assumed to have a breach at emplacement. The hottest pin in the hottest waste package would have from 38 to 93 microns of oxidation depending on the correlation used and again assuming that the waste package had a breach at emplacement. If the hottest waste package stays sealed for 50 years and then is breached, the hot pin cladding will oxidize to a depth of 2–10 microns. Such depths are small compared to the cladding thickness, which is typically 570 microns.

Yau and Webster (1987, pp. 707-708) reviewed the aqueous corrosion of Zircaloy in various chemical environments. While it is corrosion resistant in typical environmental conditions, Zircaloy is susceptible to corrosion by fluoride ions (greater than 100 ppm and pH dependent); hydrofluoric acid; and aqua regia, which is a mixture of nitric and hydrochloric acids. Yau and Webster (1987, pp. 709, 717) reported that Zircaloy is resistant to crevice corrosion, which is corrosion facilitated by conditions in a crevice between two pieces of metal. If the Zircaloy oxide layer is removed, Zircaloy is susceptible to galvanic corrosion if coupled to a more noble metal, either platinum, gold, graphite, titanium, or silver. It has a corrosion rate of 18 microns per year in a 3.5 percent boiling sodium chloride solution containing 500 ppm of copper ions at a pH equal to 5; however, there was no observed corrosion at a pH equal to 6 (Yau and Webster 1987, p. 717, Table 13). Zircaloy is susceptible to pitting from ferric chloride ions. Ferric chloride pitting requires ferric ions, and the pH must be less than 3. Current analysis of the water chemistry inside the waste package predicts that the pH is above 7.0. However, the chemistry within the waste package, hence the long term performance of Zircaloy cladding, is not well understood and has considerable uncertainty. Stress corrosion cracking has been observed in fuel pin locations that have high local stresses from pellet interactions. Such interactions are not expected after reactor discharge when the pellet contracts from the cladding.

Corrosion of Zircaloy was modeled using the waste package degradation computer code. This model assumes corrosion occurs after 100,000 years. Experimental results are available for corrosion of Zircaloy and high-nickel alloys such as Alloy 22, (other types of material used for cladding), under very severe conditions of hot, concentrated acids. Corrosion rates for the Zircaloy tend to be from ten to many thousands of times slower than the high-nickel alloys such as Alloy 22 under extreme acid conditions.

The Zircaloy corrosion model calculated the fraction of cladding patches that are 75 percent corroded using the Alloy 22 general corrosion model with the corrosion rate decreased by a factor of 10 (upper limit) and 1,000 (lower limit). For each realization, corrosion of the Zircaloy starts at the first penetration of the waste package, and the fuel area exposed (fraction of failed patches) is calculated as a function of time. Fuel exposure is initiated at about 30,000 years after the first patch penetrates the waste package. After one million years, the amount of fuel that could be exposed with this model ranges from 0.3 percent to 40 percent.

Rockfall onto the fuel after a waste package has experienced general corrosion causes mechanical failure. The assumed sequence of events leading to mechanical failure is the following:

- Rocks fall onto the upper surface of the waste package.
- The inner supports of the waste package fail and the fuel falls to the bottom of the waste package.
- Rocks fall 20 cm (8 in.) from the top of the waste package to the top of the fuel.

A separate statistical analysis of Zircaloy mechanical failure caused by falling rocks predicts that 0.2 percent to 11 percent of the fuel is exposed by this mechanism over 1 million years (CRWMS M&O 1998a, p. VIII-9). Mechanical failures are expected to begin to occur at 100,000 years as the loss of waste package integrity becomes significant. The failure rate is assumed to continue

linearly on a logarithmic time scale to 1 million years.

3.5.2.2 Dissolution Rates

Commercial Spent Nuclear Fuel Dissolution. The dissolution of spent nuclear fuel and radionuclide release are not thermodynamic equilibrium processes, so the development of a dissolution rate model uses concepts from nonequilibrium thermodynamics. The objective is to derive an equation for the dissolution rate consistent with quasi-static thermodynamic processes and laboratory data. Currently, detailed knowledge is not available for the sequence of chemical and electrochemical reaction steps to describe the dissolution process over the range of spent nuclear fuel inventory, potential water chemistries, and temperatures. The current approach is to obtain an experimental database of dissolution rates for a subset of specific spent nuclear fuels over a range of controlled, aggressive water chemistries and temperatures. These data are then used to evaluate empirical parameters in a rate law to describe the dissolution rate of spent nuclear fuel (Stout and Leider, 1997, p. 3.4.2-1).

The test data for dissolution response were best represented by a model, in the form of a rate law as a product polynomial of the bulk water chemistry concentrations and temperature. This follows the form of the Butler-Volmer equation, which is commonly used in correlation of corrosion and electrochemical rate data. In the above approach, thermodynamic nonequilibrium was assumed for the dissolution process. By substituting the traditional chemical potentials that include a logarithmic dependence on activities or concentrations for the chemical potential changes in the Butler-Volmer-like model form, the classic chemical kinetic rate law was derived.

Burnup was represented as a concentration term as well, because it is proportional to the aggregated production and concentration of fission products. For regression purposes, the model was linearized by taking logarithms of each term, and fitting that equation, and allowing cross and quadratic terms to explain interactions and nonlinearities. This model describes features of the chemical dissolution processes far from thermodynamic equilibrium and provides a reasonably good fit to the available data. Depending on the terms and coefficients in the model, extrapolation outside the measured independent variable space could cause large prediction errors. The TSPA-VA model does not extrapolate outside the range of measured values.

High-Level Radioactive Waste Dissolution. Experimental and modeling work on aqueous alteration of borosilicate glass shows that the most important parameters in predicting glass alteration rates are temperature, exposed surface area, solution pH, and dissolved silica concentration in solution (O'Connell et al. 1997, p. 2; Bourcier et al. 1994). Long-term dissolution models for borosilicate glass employ a rate equation that includes these parameters and is consistent with transition state theory. The rate equation indicates that the dissolution rate will slow down as the dissolution process of the borosilicate glass adds to the silica in solution. As the glass dissolves, secondary phases begin to precipitate. A fraction of the silica contained in the glass will be trapped in the secondary phases. Thus only a fraction of silica in altered glass actually dissolves in the solution. That fraction depends on the types and amounts of alteration minerals that form during the glass alteration process.

The experimental data for several glass compositions show that even when the solution is saturated with silica after a long period of time, there persists a residual dissolution rate, as evidenced by the continuously increasing concentrations of certain highly soluble elements of the glass composition (Grambow 1987, pp. 34-37). This requires an additional parameter to the rate equation which accounts for this residual reaction rate under silica saturated conditions. The TSPA-VA analyses do not include any performance credit for the stainless steel canister for the glass waste form. The analyses assume failure of the canister after waste package failure.

3.5.2.3 Solubility Limits

The waste form dissolution model initially provides calculated upper and lower boundary values on the aqueous concentration of radionu-

clides in groundwater that has reacted with the waste form. Subsequently, these values are filtered by comparing them with solubility-limited values that are sampled from either a distribution of solubility limits for radionuclide-bearing minerals or a functional form for the solubility limit for each radionuclide considered. If the sampled solubility-limited value is lower for the given radionuclide than its derived concentration from the waste form dissolution model, then the aqueous concentration is set to the solubility-limited value and the difference in mass is calculated to precipitate out of solution. These solubility-limited values place constraints on the aqueous concentration of the particular radionuclide element considered, with each isotope of that element present in proportion to its isotopic abundance.

3.5.2.4 Colloids

Colloids are particles that are small enough to become suspended and transported in a liquid. Based on experiments and observations to date, plutonium attachment to colloids can vary from relatively fast and reversible to effectively irreversible. However, the necessary parameter values for modeling plutonium attachment to colloids are not available. In addition, the performance assessment computer codes for modeling radionuclide transport currently cannot accommodate the complexity needed for these calculations. Instead, plutonium attachment to colloids has been modeled using the two extremes: instantaneously reversible attachment and totally irreversible attachment as shown in Figure 3-53. Partitioning of plutonium into these two categories is treated as a sampled parameter.

The reversible model assumes instantaneous equilibrium between dissolved radionuclides and colloid particles and was available within the RIP code for use in the near-field and the FEHM code for use in the far-field. The RIP model defines the amount of radionuclide mobilized in colloidal form as the product of the dissolved radionuclide concentration, the dissolved-colloid sorption partitioning coefficient (K_d), and the colloid concentration. The colloid concentration was calculated as a function of the ionic strength of the fluids as described in Section 3.3.3.4. The FEHM model combines the K_d and colloid concentration parameters into a single parameter; the aqueous-colloid partitioning coefficient, K_c. The parameter ranges used in the calculations are summarized in Table 3-16.

The irreversible model was also included in the calculation to capture the possibility of a fraction of the radionuclides moving rapidly through the transport system irreversibly attached to colloids. At the Benham nuclear test site at the Nevada Test Site, rapid transport of colloid-associated plutonium may have occurred (Thompson et al. 1998, pp. 13, 18). At 1.3 km (0.8 mile) from the blast site, 1×10^{-14} *M* colloid-associated plutonium was detected 30 years after the blast. It is not clear what fraction of the transport was caused by transport on colloids, injection through fractures at the time of the blast, or transport as dissolved plutonium. However, fracture injections have not been observed to extend beyond a few hundred meters and dissolved plutonium is expected to sorb strongly to the fracture surfaces. In fracture systems, colloids that are repelled from the host material walls may move even faster than nonsorbing dissolved species because they remain in the faster flowing portions of the flow paths. This behavior was seen in a fraction of specially designed colloids pumped through 32 m (105 ft) of fractured tuff near Yucca Mountain (CRWMS M&O 1997f). These observations suggest that some small fraction of colloid-associated plutonium may travel relatively quickly through water-filled fractures, but these observations do not adequately define the uncertainty in this process.

Table 3-16. Parameters Used in Reversible Attachment Model

	K_d(mL/g)	Effective K_c
Near-field colloids		
Clay	**10^3 - 10^5**	*~10^{-5} - 10^{-2}*
Iron oxyhydroxy colloids	**10^4 - 10^6**	*~10^{-4} - 10^{-1}*
Spent fuel waste form colloids	*10^2- 10^8*	**10^{-5} - 1**
Glass waste form colloids	*10^2- 10^9*	**10^{-5} - 10**
Far-field colloids		**10^{-5} - 10**

Notes:
bold: as input
italic: effective value in calculation

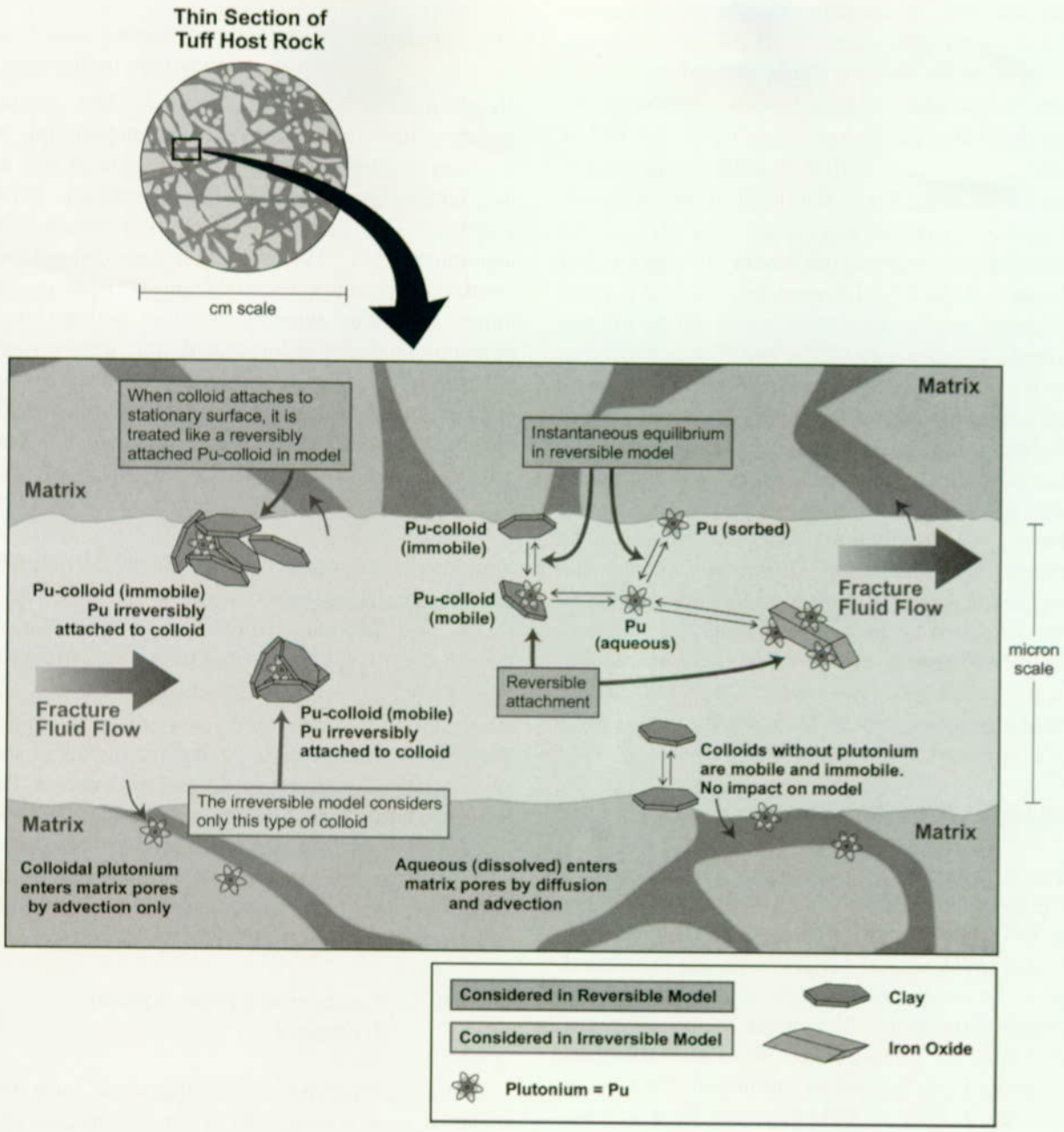

Figure 3-53. Colloidal Plutonium Transport

Specifics of colloid properties such as surface charge, size distribution, and stability in expected groundwaters, and of the transport and filtration properties in the pathways within the fractured tuff, and are not adequately known for accurate prediction at this time. These observations, however, were used to guide the selection of a large range for sensitivity studies. Based on the expected value plutonium solubility of 5×10^{-7} *M* and the observed 1×10^{-14} *M* colloidal plutonium concentration 1.3 km (0.8 mile) from the blast site, DOE has estimated that about 1×10^{-7} of the plutonium has attached irreversibly to colloids and also moved quickly. Because this estimate is quite uncertain and because the applicability of this estimate to transport within the Yucca mountain site is unknown, a three order of magnitude range was added to either side of this estimate. While this fraction includes effects from both source term and transport, it was implemented into the calculations at the interface between the engineered barrier system and the natural barrier system. The "irreversible plutonium" mass flux from the engineered barrier system to the unsaturated zone was calculated as the "reversible plutonium" mass flux times this irreversible plutonium fraction. Once passed to far-field, the "irreversible plutonium" was treated as a nonsorbing, slowly diffusing tracer.

3.5.2.5 Secondary Phase Analyses

Laboratory experiments (Wronkiewicz et al. 1992, p. 125) and field observations (Pearcy et al. 1994, pp. 713, 716, 718, 722, 724) demonstrate that when nuclear spent nuclear fuel is contacted by groundwater, it starts to dissolve and forms uranyl (uranium) minerals. The major secondary phases are schoepite, uranophane, Na-boltwoodite, and soddyite. Both theoretical prediction (Burns et al. 1997, pp. 1, 3–5, 8) and laboratory measurements (Buck et al. 1998, pp. 87, 91–93) indicate that neptunium would be incorporated into the structure of secondary phases during dissolution of spent nuclear fuel. Therefore, neptunium release would be controlled by the dissolution rate of secondary phases. Based on this concept, a computer model has been built to calculate the release rate of neptunium using a reactive-transport simulator (Chen et al. 1995, p. 8–24; 1996, pp. 1051–1052).

The simulations start with schoepite, which is allowed to dissolve and precipitate uranophane, Na-boltwoodite[5], and soddyite. The model assumes that the molar ratio of neptunium to uranium in schoepite is 0.0016, the same as that in the initial spent nuclear fuel inventory (with americium-241 and plutonium-241 grouped with neptunium-237). Two scenarios were considered: all of the neptunium released from schoepite dissolution goes into aqueous solution; and released neptunium is also incorporated into uranophane, Na-boltwoodite, and soddyite with the same uranium to neptunium ratio. Simulations with different temperature (30° and 70°C, or 86° and 158°F) and different cladding failure (1 percent and 11 percent) were carried out.

Simulated neptunium concentration at the bottoms of waste packages ranges from 1×10^{-9} to 1×10^{-6} mol/kg of solution. Based on the simulation results, a log-uniform distribution ranging from 1×10^{-9} to 1×10^{-6} mol/kg with a expected value of $1 \times 10^{-7.5}$ mol/kg was proposed for a sensitivity study. This effort was the first attempt at including the attenuation of neptunium release because of the incorporation of neptunium in secondary phases. The lower limit of these simulations is consistent with the drip tests conducted at Argonne National Laboratory that reported neptunium concentrations of 10^{-9} mol/kg (Finn et al. 1995, pp.65, 67).

3.5.2.6 Engineered Barrier System Transport

Radionuclide transport out of the waste form and waste package, through the invert system, and into the unsaturated zone is dependent on several events. The waste package must degrade, providing a path out of the waste package. The waste form must also degrade to allow radionuclide release. The primary transport medium is

[5] Unlike Argonne National Laboratory's drip tests, no Na-boltwoodite was seen in the simulations. It is believed to be caused by the inaccuracy in the thermodynamic data of Na-boltwoodite.

water, as previously discussed. Either a water film or moving water is necessary for radionuclide transport out of the waste package and through the remainder of the engineered barrier system. Gaseous releases were not analyzed in TSPA-VA.

The waste packages that are emplaced in repository areas with dripping water will degrade more rapidly. Also, radionuclide releases from degraded waste packages will be more rapid in repository areas with dripping water. If water is not dripping on a waste package, then a water film on a waste form and waste package can cause diffusive release, but this process is significantly slower than release caused by water moving through the waste package.

Transport through the invert can also occur because of advection and/or diffusion. Retardation in the concrete invert slows the transport. No degradation or reduction of permeability of the invert is modeled in these analyses.

3.5.3 Results and Interpretation: Evaluation of Issues Important to Performance

The model for waste form degradation, radionuclide mobilization, and transport through the engineered barrier system is an important part of the overall performance analysis of the repository system. The rate at which the waste forms degrade and the quantity of radionuclides that can be mobilized and moved out of the waste packages and through the engineered barrier system into the unsaturated zone provide the magnitude of release from the engineered barrier system. This release is reduced by decay and transport characteristics of the natural barrier system before reaching the accessible environment.

3.5.3.1 Cladding Degradation

Several mechanisms can cause cladding degradation, as previously described. The resulting exposed surface area of the waste forms through time is shown in Figure 3-54. The two main causes of cladding degradation in the TSPA-VA analyses are mechanical failure and corrosion failure. These mechanisms are expected to be present, but the magnitude and timing of their effect on cladding

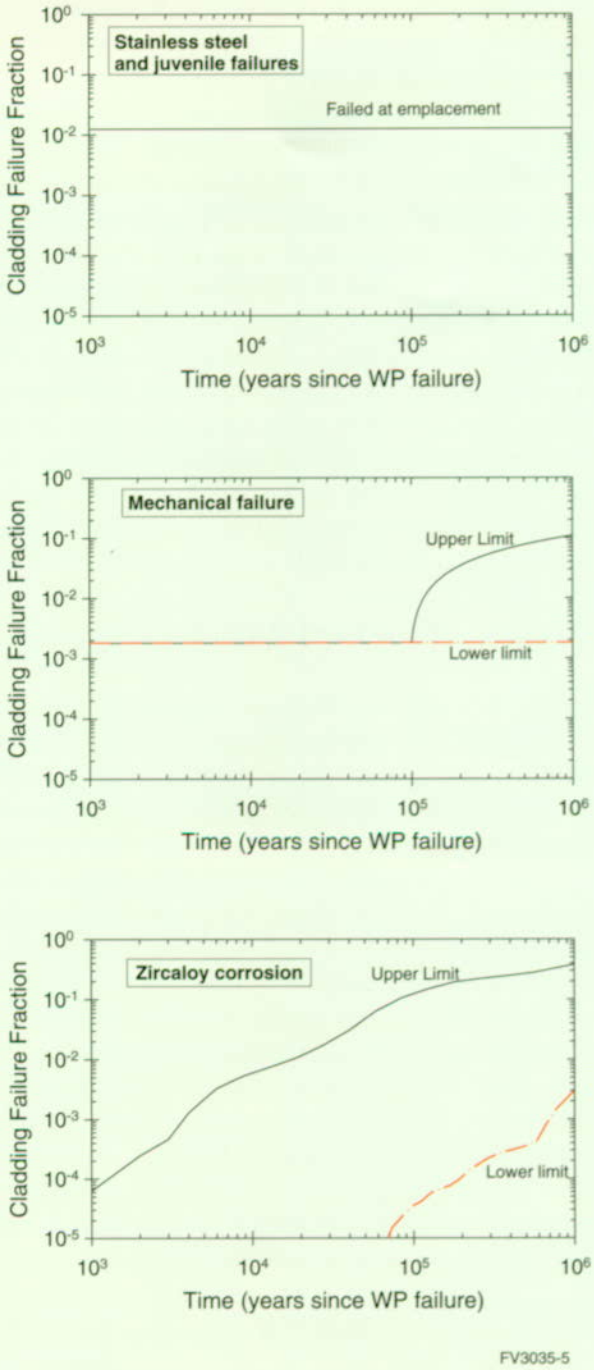

Figure 3-54. Fraction of Commercial Spent Nuclear Fuel Surface Area Exposed as a Function of Time
Fraction of commercial spent nuclear fuel surface area exposed as a function of time for the TSPA-VA base case, for several different failure mechanisms (see text). (WP—waste package)

degradation is uncertain. Section 5.5 provides sensitivity analyses of the effect of cladding on repository performance. Both the maximum and minimum values of exposed surface area through time are shown in Figure 3-54. Sampling between the maximum and minimum values using a log-uniform distribution is performed within the repository integration computer program. Before 60,000 years, the stainless steel clad fuel in breached waste packages and in defective waste packages will be available for dissolution when the waste package is breached. At about 100,000 years, waste packages that fail through both mechanical failure and corrosion will begin to expose more fuel for dissolution. At one million years, about 31 percent of the spent nuclear fuel in failed waste packages will be available for dissolution in the base case cladding model.

3.5.3.2 Waste Form Degradation

Under repository conditions, degradation of the commercial spent nuclear fuel occurs within a few thousand years, while degradation of the high-level radioactive glass waste form occurs over a period of 8,000 to 10,000 years. Thus, the degradation rates of both waste forms are not identified as key parameters in controlling long-term repository performance. This lack of importance of degradation rate could change if retention in less soluble secondary phases is considered, as is observed in dissolution tests at low flow rates that are currently underway. Another aspect of this is the radioactive decay of the initial inventory through time. Figure 3-55 presents the decay as a function of time to show the key long-lived radionuclides, especially neptunium, and the other important radionuclides initially present in the inventory.

3.5.3.3 Doses from DOE Spent Nuclear Fuel

The DOE spent nuclear fuel is comprised of multiple waste form types with unique characteristics. The base case uses a surrogate for the many different types of waste in the DOE spent nuclear fuel inventory. A comparison of the surrogate DOE spent nuclear fuel to the spent nuclear fuel total is presented in Section 5.5.7.

3.5.3.4 Releases from Plutonium Waste Forms, High-Level Radioactive Waste, and the Commercial Spent Nuclear Fuel Waste Form

The comparison of releases from the plutonium waste form with the high-level radioactive waste and commercial spent nuclear fuel waste forms is also presented in Section 5.5.

3.5.3.5 Releases from Naval Spent Nuclear Fuel

One of the types of DOE-owned spent nuclear fuel to be disposed of in the potential repository is naval spent nuclear fuel. There will be approximately 65 MTHM of naval spent nuclear fuel. Because naval nuclear fuel is designed and built to meet demanding warship operating requirements, naval spent nuclear fuel cladding would outperform commercial spent nuclear fuel cladding in a repository environment. Through the repository environmental impact statement (EIS) data collection effort, the Naval Nuclear Propulsion Program provided values for the extremely small expected releases from naval spent nuclear fuel waste packages (Beckett 1998, Attachment A, p. 2).

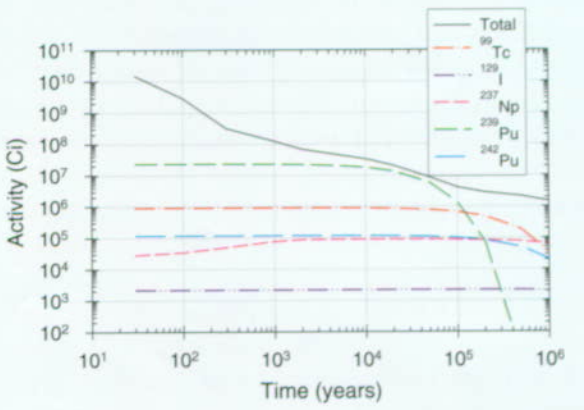

FV3035-6

Figure 3-55. Activity as a Function of Time
The reduction of activity for the total and some of the key radionuclides affecting the performance of the system is shown.

3.5.3.6 Remaining Uncertainties in Engineered Barrier System Analyses

There are several remaining areas in the analysis of the engineered barrier system that are not fully analyzed in the TSPA:

- The invert is assumed not to degrade with time but to retain the same transport characteristics of concrete for the duration of the analyses. However, the chemistry of the invert will probably change as the system is heated during the thermal period. Heating may alter the transport characteristics of the invert. Likewise, the invert sorption characteristics are not well known and are under study. The impact of more complex invert analysis on overall system performances is not expected to be significant because of the small transport length involved relative to the total transport length.

- The base case does not fully account for rock falling into the drift at later times, which is an expected condition. The cladding model attempts to evaluate some effect of rockfall on the cladding, but the rest of the analyses do not incorporate rockfall at later times. Rockfall may alter the thermal-hydrologic characteristics and enhance waste package degradation. Its effect on overall performance is uncertain.

- The effect of the secondary phases on subsequent radionuclide transport is not fully analyzed in the TSPA. Neither the dissolution rate of the secondary phase nor the identity of radionuclides that will become fixed in the secondary phases has been well characterized. This process could have the effect of delaying radionuclide releases, which may prove improved overall system performance.

- The amount of seepage into the waste package and onto the waste form has been previously discussed and is a significant factor in releases from the engineered barrier system. How much water actually enters the waste package once it is breached is highly uncertain. The TSPA-VA analyses are conservative in this area.

- Diffusive transport out of a locally failed fuel rod is not explicitly considered and could significantly reduce release rates.

3.6 UNSATURATED ZONE TRANSPORT

As described in Volume 1, the repository is located in Yucca Mountain in the unsaturated zone, about midway between the ground surface and the regional water table. In the unsaturated zone, available voids in the rock, in the form of rock matrix pores and fractures, are filled partially with water and partially with air. The regional water table is the top of the saturated zone, below which the rock voids are fully saturated with water. Water movement is primarily downward through the unsaturated zone at Yucca Mountain, with possible lateral flow in certain regions such as perched water. The sequence of hydrogeologic units, their hydrologic and geochemical characteristics, and the imposed infiltration flux control radionuclide transport in the unsaturated zone. The unsaturated zone transport component of the TSPA evaluates the migration of radionuclides from their introduction at the edge of the engineered barrier system to the water table (Figure 3-56). Definitions of technical terms used in Volume 3 are available in the VA glossary.

The unsaturated zone transport modeling studies and analyses presented in this section were prepared with the view of addressing selected aspects of the NRC Key Technical Issues on Unsaturated and Saturated Flow under Isothermal Conditions (NRC 1997e; 1997f) and Total System Performance Assessment and Integration (NRC 1998a). Specifically, the information presented is pertinent to the unsaturated zone flow and transport under isothermal conditions subissue on the groundwater percolation through the repository horizon and the ambient flow conditions in the saturated zone, and the TSPA integration subissue on model abstraction.

Yucca Mountain was formed from a sequence of volcanic ash flows and ash falls that created a

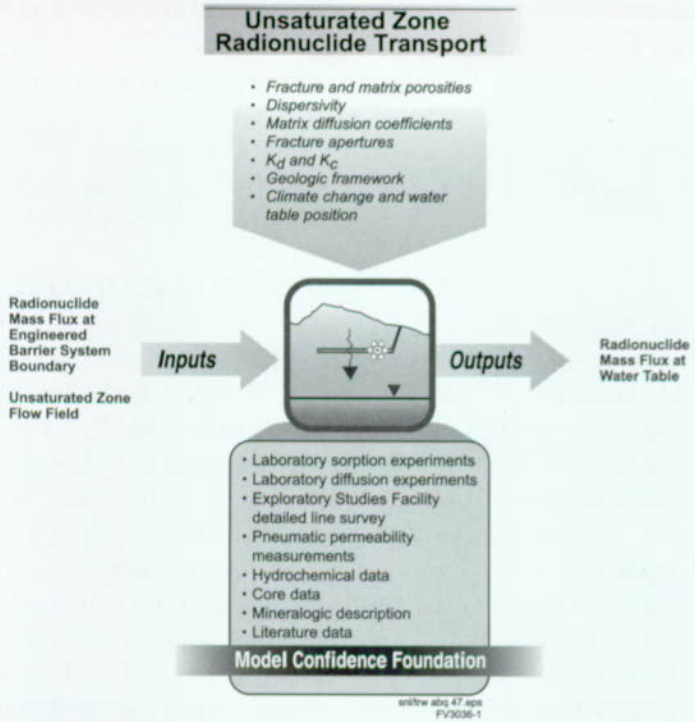

Figure 3-56. Coupling of Unsaturated Zone Radionuclide Transport to Other Total System Performance Assessment for the Viability Assessment Components

lithostratigraphic sequence of welded and nonwelded tuffs (Sawyer et al. 1994), as shown in Figure 3-57. The welded tuffs, formed by massive ash flows, are dense, brittle rocks with relatively low matrix porosity and a high fracture density. The nonwelded tuffs, formed from smaller ash flows and ash falls, are a more porous and elastic rock having relatively high matrix porosity and lower fracture density. The nonwelded tuffs can have either high or low matrix permeabilities depending primarily on the degree of alteration of the rock minerals into zeolites. Zeolitic units are common in the lower portions of the unsaturated zone and have matrix permeabilities similar to those in the welded tuffs. Nonwelded tuffs that have not been altered to zeolite, such as the nonwelded vitric tuffs, have much larger matrix permeabilities. Hydrogeologic stratigraphy of the unsaturated zone at Yucca Mountain is illustrated in Figure 3-57. The Calico Hills nonwelded unit may be further divided into vitric and zeolitic units.

An important characteristic of both the welded tuffs and nonwelded zeolitic tuffs is the difference in permeability between the fractures and the matrix. The fractures typically have permeabilities that are several orders of magnitude larger than the matrix permeabilities, and fracture porosities that are orders of magnitude smaller than the matrix porosities. The differences are important characteristics of these tuffs because the high permeability, low porosity fractures can provide a much more rapid transport pathway to the water table than the matrix. On the other hand, the unaltered, or nonwelded, tuffs have larger matrix permeabilities that are of the same order of magnitude as the fracture permeabilities. These tuffs play an important role in the hydrologic behavior of the unsaturated zone because fracture flow is strongly attenuated, transport velocities are much slower, and contact of dissolved materials with the rock matrix is enhanced.

Perched water has been observed in some boreholes penetrating the repository, mainly in the northern area of the repository and along the western border of the Ghost Dance fault (see Figure 3-57). Perched water is a localized saturated zone that lies above unsaturated rock and the regional water table and typically forms on top of hydrogeologic units that have relatively low permeability. When present, perched water is

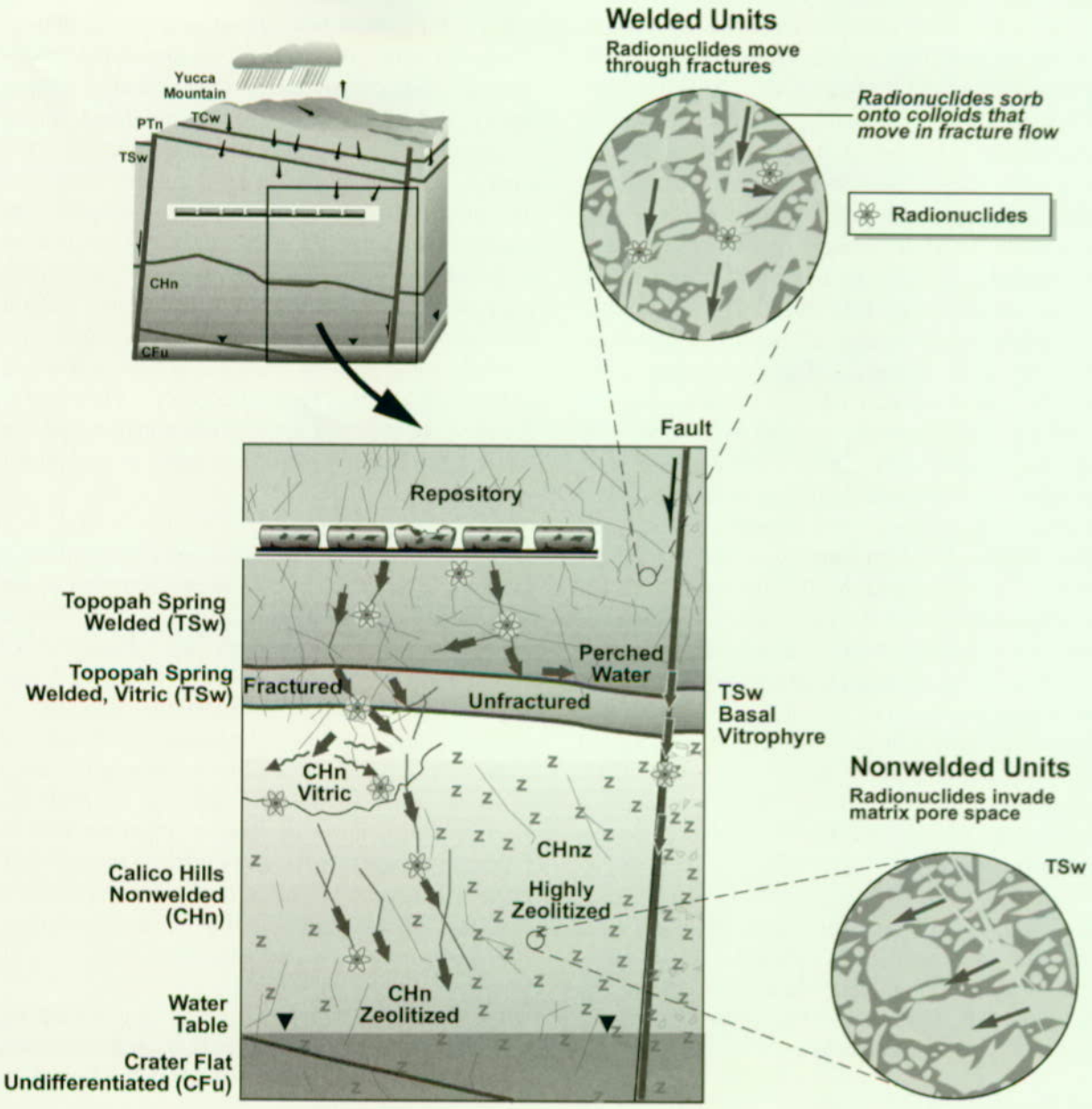

Figure 3-57. Conceptual East-West Hydrogeologic Section Through the Unsaturated Zone
Conceptual east-west hydrogeologic section through the unsaturated zone at Yucca Mountain and process diagram for unsaturated zone radionuclide transport.

typically found at the base of the Topopah Spring welded unit and in areas of the Calico Hills zeolitic unit. These perched water bodies are believed to have formed by alteration of minerals in fractures to low permeability minerals that effectively block flow through the fractures (Bodvarsson et al. 1997, Section 13.5 pp. 13-13 and 13-14). This blockage of fracture flow will lead to lateral diversion of radionuclide transport if the percolation flux is sufficiently large. See Section 3.1 for additional information on unsaturated zone flow. Under nominal and most disruptive scenarios, transport of radionuclides through the unsaturated zone is one of several processes that impede the release of radioactive waste to the accessible environment after repository closure. The radioactive waste may migrate in unsaturated zone groundwater as a dissolved molecular species or associated with particles called colloids. Colloids are fine particles, between 0.001 and 1 micron that can interact with radionuclides through sorption and other chemical mechanisms, and are potentially mobile. Colloids reduce the interaction of the aqueous species with the rock matrix and enhance advective transport of the radionuclides, which is described below. Colloid interaction with radionuclides may be described in terms of reversible and irreversible interactions. Reversible interactions allow the radionuclide to detach from the colloid. For irreversible interactions, the radionuclide is attached to the colloid for the duration of the transport process.

Five processes affect the movement of dissolved or colloidal radionuclides: advection, diffusion, dispersion, sorption, and radioactive decay (de Marsily 1986, Chap. 10) (Figure 3-57). These processes are described below.

Advection is the movement of dissolved or colloidal material because of the bulk flow of a fluid, which in this case is water. This key transport mechanism can readily carry radionuclides through the approximately 300 m (984 ft) of unsaturated rock between the potential repository and the water table. Advection is also an important mechanism for radionuclide movement between fractures and rock matrix. In many of the hydrogeologic units, advection through fractures is expected to dominate transport behavior, primarily because the expected flow rates through these systems exceed the matrix flow capacity under a unit gravitational gradient. Advection through fractures is fast because of high permeability and low porosity, with few opportunities for radionuclides to contact rock matrix. A few of the hydrogeologic units have much larger matrix permeability and are expected to capture most of the fracture flow by advection from the fractures to the matrix, causing much slower transport velocities and closer contact of the radionuclides with the matrix. Advective transport pathways result from and therefore follow the flow pathways, which are predominately downward. However, lateral diversion is expected along hydrogeologic unit contacts having strong contrasts in rock properties, particularly in areas of perched water. Flow that is diverted laterally ultimately finds a pathway to the water table through more permeable zones, which may be faults.

Diffusion is the movement of dissolved or colloidal material because of random thermal motion at the molecular scale. Diffusion results in mass flux at the continuum scale when the dissolved or colloidal material is nonuniformly distributed, that is, exhibits concentration gradients. It is not an effective mechanism for transport between the repository and the water table because of the large distance involved (about 300 m, or 984 ft). However, diffusion can play an important role in radionuclide exchange between fractures and rock matrix. Diffusion from fractures to the rock matrix can slow the advance of radionuclides undergoing advective transport through fractures.

Dispersion is a transport mechanism caused by localized variations in the radionuclide transport velocity due to localized variations in the flow field and molecular diffusion. These variations cause dispersion of the radionuclides both along and transverse to the average flow direction. Variations in both the magnitude and direction of the radionuclide velocity contribute to the overall dispersion. The dispersion resulting from variations in the flow field, under certain limiting conditions, can act in a manner analogous to diffusion, in which mass flux is proportional to the concentration gradient. Dispersion is most important where concentration gradients are the largest—near the front of a propa-

gating plume or along the lateral edges of the concentration field. Dispersion smears sharp concentration gradients and can reduce the breakthrough time, or arrival time at a specific point, for low concentration levels of an advancing concentration front.

Sorption is a general term for describing a combination of chemical interactions between the dissolved radionuclides and the solid phases, that is, either the immobile rock matrix or colloids. Any given sorptive interaction is caused by a set of specific chemical interactions such as surface adsorption, precipitation, and ion exchange. However, the sorption approach does not require identifying the specific underlying interactions. Instead, batch sorption experiments are used to identify the overall partitioning between the aqueous and solid phase, characterized as a sorption or distribution coefficient (K_d). The strength of the sorptive behavior is a function of the chemical element, the rock type involved in the interaction, and the geochemical conditions of the water contacting the rock. Sorption reduces the rate of advance of a concentration front in advective and diffusive transport, and amplifies the effects of diffusive flux of radionuclides from the fractures to the rock matrix through its influence on the concentration gradient. In this context, sorption acts to retard the movement of solutes. The sorption coefficient, K_d, is generally combined with other terms in transport equations to give a retardation coefficient. This coefficient expresses the increase in effective pore volume that is provided by partitioning between the aqueous and the solid phases.

Radioactive decay is a process that affects the concentration of radionuclides during transport through the unsaturated zone. For simple decay, the radionuclide concentration decreases exponentially with time, creating decay products that are stable. Chain-decay adds another layer of complexity because of the ingrowth of new radionuclides created from the decay of a parent radionuclide. One aspect of potential significance with respect to chain-decay is that daughter products may have significantly different sorption behavior than the parent radionuclide, thus affecting transport.

To reach the accessible environment, radionuclides must traverse the unsaturated zone to water table, and then migrate through the saturated zone. An exception to this would be radionuclides that partition into the gas phase in the unsaturated zone, and therefore may potentially escape the unsaturated zone at the ground surface. Very few radionuclides are expected to be able to move in the gas phase. These radionuclides are carbon-14 (as CO_2) and perhaps chlorine-36 and iodine-129 (as Cl_2 and I_2, respectively). Even if these radionuclides do manage to transport in the gas phase, the dose consequences for such releases are expected to be inconsequential (National Research Council 1995). Therefore, gas-phase radionuclide transport in not modeled in the TSPA.

Because radionuclide movement is almost exclusively in water, radionuclides tend to migrate with the unsaturated zone flow, which is mainly vertical. After movement through the unsaturated zone, radionuclide transport is primarily horizontal through the saturated zone to the location where repository performance is measured. The primary role of the unsaturated zone (below the engineered barrier system) for performance is to delay radionuclide movement. If the delay is long enough that a given radionuclide will decay considerably, then the unsaturated zone can have a large effect on decreasing the dose from that radionuclide at the accessible environment. The amount of delay strongly depends on the climate (infiltration) and sorptive interaction between the radionuclide and the rock matrix in the unsaturated zone.

3.6.1 Construction of the Conceptual Model

The conceptual model for radionuclide transport in the unsaturated zone is a combination of conceptual models for the processes described in the previous section: unsaturated zone flow, or advection; diffusion; dispersion; sorption; colloid-facilitated transport; and radioactive decay (Figure 3-57).

The primary vehicle for formulating the conceptual models for these processes was the workshop on unsaturated zone radionuclide transport held in Albuquerque, New Mexico, on February 5-7, 1997 (CRWMS M&O 1997p). The workshop addressed the attributes of radionuclide transport within the unsaturated zone that may impact the long-term performance of a geologic repository at Yucca Mountain. Issues related to unsaturated zone radionuclide transport were reviewed and prioritized. Methods to capture the key processes in performance assessment models were discussed and problem formulations were proposed (see Table 3-17).

The results of the workshop led to investigations of the following subjects:

- Fracture/matrix interaction and sensitivities
- Transient flow and transport
- Colloid-facilitated radionuclide transport
- The linear sorption model relative to more complex geochemical interaction models
- The effects of dispersion and fine-scale heterogeneity

The results of these investigations formed part of the basis for the unsaturated zone radionuclide transport model discussed below.

3.6.1.1 Unsaturated Zone Flow Model

The detailed geometry of fractures and matrix pore spaces at Yucca Mountain is far too complex to be modeled explicitly. Nevertheless, it is important to capture the larger-scale spatial variability, such as differences between welded and nonwelded hydrogeologic units, and the differences in fracture and matrix properties at the local scale. To show this variability, a dual-permeability model is used for fractured rock. In the dual-permeability model, the fractures and matrix are distinct interacting continua that coexist at every point in the modeling domain. Each continuum is assigned its own hydrologic properties such as permeability and porosity, which may also vary spatially. In general, the fractures are modeled as a highly permeable continuum having low porosity; the matrix is modeled as a much less permeable continuum having higher porosity. The dual-permeability model offers a bimodal approximation to the true spectrum of fracture and matrix properties. More importantly, the dual-permeability model can capture the effects of fast pathways for radionu-

Table 3-17. Unsaturated Zone Radionuclide Transport Abstraction/Testing Workshop

UNSATURATED ZONE RADIONUCLIDE TRANSPORT ABSTRACTION/TESTING WORKSHOP
February 5-7, 1997, Albuquerque, NM
(CRWMS M&O 1997p)

PRIORITIZATION CRITERIA
- Does the process/issue affect the
  - Radionuclide concentration?
  - Radionuclide velocity?
  - Water flux?
  - Spatial and temporal distribution of travel times to the water table?

HIGHEST PRIORITY ISSUES
- Physical transport processes:
  - What conceptual model should be used for fracture/matrix interactions?
  - How should long-term transient flow be included in unsaturated zone radionuclide transport modeling?
  - What range and dependencies should be used for the fracture/matrix interaction parameter?
- Chemical interactions and repository-perturbed environment:
  - Is the minimum K_d approach an appropriate modeling approach for unsaturated zone radionuclide transport?
  - Are colloids expected to play an important role in unsaturated zone radionuclide transport?
  - Is thermal-chemical alteration of existing minerals expected to be important for unsaturated zone radionuclide transport?
- Heterogeneity:
  - Is lateral diversion of radionuclide pathways expected to be important for unsaturated zone radionuclide transport?
  - Is a more detailed stratigraphy below the repository expected to be important for unsaturated zone radionuclide transport?
  - Are areal variations in abundance and composition of zeolites expected to be important for unsaturated zone radionuclide transport?
- Model calibration:
  - What are the criteria and methods for model calibration?

ANALYSIS PLANS
- Fracture/matrix interaction
- Transient flow and transport
- Colloid-facilitated radionuclide transport
- Sorption models for radionuclide transport
- Effects of dispersion and fine-scale heterogeneity on radionuclide transport

clide transport from the repository to the water table. This feature is an important improvement over single-continuum models (Robinson et al. 1996, Section 9.5.3; Robinson et al. 1995, Section 8.3).

The conceptual model for unsaturated zone transport is strongly tied to the conceptual model for unsaturated zone flow. As described above, advective transport because of flow is the main transport mechanism that can move radionuclides from the repository to the water table. Conceptual models for unsaturated zone flow are commonly based on a continuum relationship, known as Darcy's law, which relates volumetric flow rate and the gradient of hydraulic potential. In the case of fractured, porous rock such as the volcanic rock that constitutes Yucca Mountain, these continuum relationships are extended to embrace two coexisting continua, fractures and rock matrix, that interact according to the same constitutive relationships that govern flow in a single continuum.

From the standpoint of unsaturated zone transport, the need for explicit and separate representation of fracture and matrix flow arises because of the extreme disparity in transport velocities that can occur in the two continua. Travel times for radionuclides transported to the water table exclusively in fractures are expected to be about 10,000 times faster than travel times for radionuclides moving exclusively in the matrix. In addition, the transport velocities in the fractures may be sufficiently rapid that radionuclide concentrations in the fractures are in disequilibrium with concentrations in the matrix. For example, a high concentration of radionuclides entering fractures at the repository may penetrate the entire unsaturated zone before establishing a uniform, equilibrated concentration in the rock matrix. Therefore, a mechanistic and dynamic model of transport through the fractures and matrix, as well as exchange between the fractures and matrix, is needed to represent the system.

The dual-permeability model provides the necessary level of detail to capture the important differences between transport through fractures and matrix. There are other possible approaches to modeling flow in fractures and matrix rock. However, these other models, such as the equivalent continuum model, do not recognize the important dynamic coupling between fractures and matrix. For these reasons, the flow and transport models for the unsaturated zone are based on dual permeability.

In general, flow in the unsaturated zone is time dependent or transient. One mechanism responsible for this time dependence is the time variations in the infiltration flux at the surface. The time variation of the infiltration flux may be approximated as occurring over short intervals characterized by changes in weather, resulting in episodic transient flows, or over much longer time periods corresponding to climate changes. Existing information concerning episodic transient flow seems to indicate that it may not be able to frequently penetrate through the unsaturated zone to the level of the repository because fracture flow tends to be absorbed by the matrix of the Paintbrush nonwelded hydrogeologic unit. This information also suggests that episodic transient flow appears to be localized in preferential pathways associated with through-going faults that breach the Paintbrush nonwelded unit (Robinson et al. 1997; p 6–15). Episodic transient flow propagating through fractures tends to be absorbed by the Paintbrush nonwelded unit, resulting in much slower drainage of the episodic flow events in hydrogeologic units at and below the repository level (Robinson et al.. 1997, Section 6.13). Simulation results indicated that transport is not too different under episodic transient flow as compared with steady flow (CRWMS M&O 1998i, Section 7.6). Simulations show instances where breakthrough is faster for the steady flow case as compared to the episodic transient flow case (given the same average flow) and also the reverse. The reasons for this behavior are not understood. Therefore, the total quantity of water able to penetrate the unsaturated zone in the fracture system without interacting with matrix may, in fact, be larger for steady flow than for transient pulses, given the same average infiltration flux (CRWMS M&O 1998i, Section 7.6). For these reasons, episodic transient flows have not been incorporated into the TSPA-VA calculations. Changes in unsaturated flow because of longer-term changes in climate have a more pronounced influence on unsaturated zone flow than episodic transient flow. Sustained changes in infiltration

associated with climate change ultimately impact the entire flow field in the unsaturated zone. The actual transient period during which the unsaturated zone flow responds to a climate change, however, has been found to be less significant (Robinson et al. 1997, Section 8.11, pp. 8-47 and 8-48; CRWMS M&O 1998i, Section 7.4). The reason is that the change in flow in the fractures, which dominates the flux in most hydrogeologic units, responds relatively quickly to a change in infiltration. Therefore, the quasi-steady flow model was used to estimate the effects of climate change on radionuclide transport. In this model, infiltration rate is assumed to change abruptly when climate changes from one steady flow field to another. Transport calculations simply re-start when climate changes with radionuclides that were present in the unsaturated zone at the end of the previous climate included as an initial condition for the next climate. A distributed source of radionuclides throughout the unsaturated zone is derived from transport calculations using the flow field for the previous climate, and a new steady flow field is selected based on the new climate.

In addition to the change in the unsaturated zone flow field, the location of the water table is also assumed to change abruptly at the time of climate change. The three climate states—present day, long-term average, and superpluvial (see Section 3.1)—have successively higher water table elevations in response to the increasing infiltration. If the water table rises with the climate change, the radionuclides in the unsaturated zone between the previous and new water table elevations are immediately available for saturated zone transport. Water table elevations change by 80 m (262 ft) from present-day to long-term-average climates and by 120 m (394 ft) from present-day to superpluvial climates.

The flow field is expected to be mainly downward over large scales. However, local flow field variations are expected to be three-dimensional. The importance of these variations lies primarily in the kinds of rock units and fracture characteristics that dominate along the three-dimensional flow paths. A secondary consideration is that three-dimensional flow paths from the repository to the water table will necessarily be longer than strictly vertical flow paths. Three-dimensional flow patterns are expected along rock unit contacts with contrasting properties, particularly in zones where these contrasts are believed to be features that create perched water (see Figure 3-57). To capture these effects, the flow and transport calculations are performed in three dimensions. Spatial variability is captured in the three-dimensional relationships of the hydrogeologic units and structural features, for example, faults, and in the variations in hydrogeologic and transport properties assigned to the hydrogeologic units.

3.6.1.2 Matrix Diffusion Model

Matrix diffusion is one mechanism (the other is advection) that transports radionuclides between the fracture and matrix continua. Bulk diffusive flux occurs when concentration gradients are present because diffusion is driven by random molecular motion. In addition, matrix diffusion is a function of temperature, radionuclide mass, atomic or molecular dimension, and charge, as well as the matrix pore structure and water saturation. The temperature variations are expected to be small over the time period for radionuclide releases to the unsaturated zone. The effects of pore structure and water saturation have been shown to depend primarily on the volumetric water content of the rock (Los Alamos National Laboratory 1997, pp. VI-5 and VI-6). For rock in the unsaturated zone, the water content is relatively uniform spatially. Therefore, as a simplification, variations in the matrix diffusion coefficient are assumed to be primarily dependent upon the radionuclide type, that is, mass, size, complexation, and charge. In this case, measurements indicate that the primary difference is between cationic and anionic radionuclides (Triay et al. 1997, Section VI, pp. 189–198). Anionic radionuclides have lower matrix diffusion coefficients than cationic radionuclides, that is, they are transported more slowly by diffusion. Lower coefficients for anionic radionuclides are believed to be a result of size and charge exclusion from a portion of the pore structure. The surfaces of the pore minerals are generally negatively charged under the chemical conditions of the undisturbed environment.

In general, the direction of radionuclide transport by matrix diffusion between the fracture continuum and the matrix continuum depends on the direction of the concentration gradient. However, the most important influence of matrix diffusion is expected to be on radionuclide transport through fractures. The distance between an average radionuclide in the fractures and the matrix is small compared with the distance between an average radionuclide in the matrix from the fractures. This proximity is a result of the fracture and matrix geometry, where the ratio of fracture aperture to fracture spacing is small. Also, diffusive penetration of the matrix is proportional to the square root of the fracture transport time. Because of relatively fast transport through fractures, most radionuclides diffusing from fractures into the matrix do not penetrate far relative to the fracture spacing. For this reason, the effects of fracture spacing on matrix diffusion are expected to be negligible, and the effects of finite fracture spacing may be ignored. Similarly, because of the relatively small fraction of matrix affected by matrix diffusion, that is, diffusive movement from fractures into the matrix is relatively slow, an approximate representation can be made for fracture transport, including matrix diffusion, separately from the advection of radionuclides through the matrix. This is done in the transport model by having separate, noninteracting matrix regions for diffusive exchange with transport in the fracture continuum and for transport in the matrix continuum.

3.6.1.3 Sorption Model

Numerous rock-water chemical interactions may influence radionuclide transport:

- Ion adsorption: metal cations sticking to mineral surfaces due to London-van der Waals forces and hydrogen bonding
- Ion exchange: substitution of an aqueous cation for the cation in a mineral structure
- Surface complexation: coordination of an aqueous cation with a deprotonized metal hydroxide at the mineral surface
- Precipitation: generation of a bulk solid phase

The nature and strength of these rock-water interactions are highly dependent on the chemical composition of both the aqueous and solid phases. The conceptual model used to capture all these interactions and sensitivities is the minimum K_d model. This model bounds the distribution of radionuclides between the mobile, or dissolved in the aqueous phase, and immobile, attached to the solid phase, radionuclides using a linear, infinite-capacity partitioning model. In this model, the sorbed, or immobile, concentration is equal to the aqueous concentration times the partitioning coefficient (K_d). Because of the numerous mechanisms and dependencies known to influence sorption, using a linear partitioning model with a single coefficient provides only a minimum bound for K_d, and hence the immobilized fraction.[6]

The range of pore-water compositions of the matrix of the undisturbed, that is, pre-repository, unsaturated zone is expected to overlap the combined range of groundwater compositions for the tuffaceous aquifer and the deeper carbonate aquifer (Meijer 1992, pp. 18–19). Therefore, sorption behavior investigated under this range of conditions is used to bound sorption in the unsaturated zone (Triay et al. 1997, p. 173). Under the assumptions of the model, the minimum K_d approach is conservative for radionuclide transport, except in the case of colloid-facilitated transport, which is discussed in Section 3.5 and is further discussed in Section 3.6.1.4.

The surfaces of fractures, often lined with minerals that differ from the bulk of the rock matrix, may be capable of sorbing many of the radionuclides (Triay et al. 1997, p. 173). However, there has been limited characterization of the distributions of

[6] Minimum bound means that the K_d used in the model represents the smallest reasonable ratio of radionuclides attached to the solid phase versus the aqueous phase. This assumption is conservative because it implies maximum transport of radionuclides in the aqueous phase.

the fracture-lining minerals and sorptive interactions with these minerals. For these reasons, it is conservatively assumed that there is no sorptive interaction with the fracture surfaces, and sorptive interactions are only possible for radionuclides in the matrix continuum.

Sorption is known to be sensitive to rock mineralogy and texture because these characteristics affect the types and available areas of different mineral surfaces. Although many different mineral types are present in Yucca Mountain, three basic rock types have been identified as having distinct sorptive interactions with the different elements of the waste form. These rock types are devitrified tuff, vitric tuff, and zeolitic tuff. Sorption coefficients for all radionuclides are specified for each of these rock types in the TSPA conceptual model.

Many of the investigated radionuclides are sorbed most strongly by the zeolitic tuff (CRWMS M&O 1998i, Table 7.5-1). Zeolitic tuff is primarily composed of clinoptilolite, and usually includes opal-CT (cristobalite - tridymite), quartz, and feldspar. Vitric tuffs, primarily composed of glass and feldspar, are generally less sorptive than zeolitic or devitrified tuffs. Devitrified tuff, also known as welded tuff, is primarily composed of alkali feldspar and tridymite. However, the importance of sorption in the different rock types is not only a function of the sorptive strength, K_d, but also the degree of exposure the radionuclides have with the rock matrix during transport through the unsaturated zone. The relative amount of radionuclide transport through the matrix is a strong function of the matrix permeability, where radionuclide transport is favored through a matrix with higher permeability. The vitric tuff is typically much more permeable than the devitrified or zeolitic tuffs, providing greater radionuclide contact with the vitric matrix.

Variations of geochemical conditions in time and space will affect the characteristics of radionuclide-rock interactions. Geochemical variability may be separated into two broad categories. One type of variability may be attributed to natural processes of the undisturbed environment that are observed in water samples from different locations. The method for determining the appropriate minimum K_d is based on the range of geochemical conditions representative of this natural variability. Sensitivity studies suggest that future natural variations in geochemical conditions because of climate change will have little influence on radionuclide transport (Robinson et al. 1997, p. 11-48). A second type of variability is caused by the thermal-chemical interactions of the repository with the geochemical/mineralogical environment, disturbed environmental conditions. Although sensitivity studies indicate that transient thermal effects have little influence on radionuclide transport (Robinson et al. 1997, pp. 11-48 and 11-49), potential longer-term effects on geochemical and mineralogical conditions require further investigation (CRWMS M&O 1998i, Section 7.7).

3.6.1.4 Colloid-Facilitated Transport Model

Colloids are potentially mobile in water flowing through the unsaturated zone. Colloids, because they are small solids, can interact with radionuclides through sorption mechanisms. Unlike sorption of radionuclides to the rock matrix, however, radionuclides sorbed on colloids are potentially mobile. Therefore, colloids can facilitate radionuclide transport through the unsaturated zone at a faster rate than the aqueous phase alone. Another form of colloidal radionuclide movement occurs when the radionuclide is an integral component of the colloid structure (see Section 3.5). In this case, the radionuclide is irreversibly bound to the colloid, as compared to the typically reversible sorption mechanism.

The transport equation of any aqueous radionuclide through fractures is expressed in terms of the previously mentioned processes of advection, sorption on fracture surfaces, if included, matrix diffusion, dispersion, and radioactive decay. If the radionuclide is sorbed on colloids, then additional terms are needed in the equation to describe the advection, sorption, dispersion, and decay of the radionuclides on colloids. Colloid particles themselves are not expected to experience any significant matrix diffusion because of the very low diffusion coefficients associated with colloids. It is assumed that sorption of radionuclides on

colloids may be approximated using the K_d conceptual model described above for sorption, except that the conservative bound now is the maximum K_d. A maximum K_d for sorption on the colloidal minerals is a conservative bound because more of the radionuclides are placed on the colloids. Advective radionuclide transport through the fractures is enhanced by reduced matrix diffusion and matrix sorption. Given a steady, uniform concentration of colloids and the K_d model for sorption, the ratio of the radionuclide mass in colloidal and aqueous form is a constant value (K_c). Both the linear nature of the transport equations for aqueous and colloidal forms and the linear partitioning of the aqueous and colloidal concentrations allow simplification of the transport equation. The mathematical transport model for aqueous and colloidal radionuclides may be reduced to a single equation in terms of the aqueous radionuclide concentration (Robinson, et al. 1997, Section 8.10). Additionally, no new terms appear in this transport equation, as compared with strict aqueous transport. Therefore, the new transport equation for reversibly sorbed aqueous-colloidal transport has the same structure as that for strict aqueous transport. The difference is that the transport coefficients now include information concerning the colloidal partitioning.

Colloids may not be able to move through the rock matrix, particularly the welded and zeolitic rock types, because of colloid size relative to the matrix pore size. However, movement through the more permeable, nonwelded vitric rock in the Calico Hills may be possible. Advective, aqueous-phase transport of radionuclides between fractures and matrix is only a strong feature of the flow field in this higher-permeability unit. As an approximation to simplify the transport model, colloids are also allowed to move by advection with the aqueous-phase radionuclides between the fractures and matrix. However, colloids are not allowed to exchange between fractures and matrix through matrix diffusion (CRWMS M&O, 1998i, Section 7.4.5.1).

In some cases, radionuclides may be an integral part of the colloid structure itself, which can be approximated by an irreversible sorption model. To model the transport of these irreversibly sorbed radionuclides, the transport model described above for reversibly sorbed, colloid-facilitated transport is modified to account only for transport processes that affect colloids. In other words, for this portion of the radionuclide mass, interaction with the aqueous phase and immobile rock phase is neglected. With this simplification, colloid transport is mathematically analogous to aqueous radionuclide transport with no matrix diffusion and no sorption (CRWMS M&O, 1998i, Section 7.4.5.2).

3.6.1.5 Dispersion Model

Dispersion is included in the transport conceptual model using a standard relationship based on Fick's law between mass flux and concentration gradient. The dispersion coefficient in the Fickian relationship is expressed as the product of the mixing length scale, or dispersivity, and the average linear velocity. Dispersion is independently represented in both the fracture and matrix continua. However, longitudinal dispersion is not expected to play an important role in the unsaturated zone transport. The repository emplacement area is very broad relative to the distance to the water table, and this geometrical arrangement tends to suppress longitudinal dispersion effects. Longitudinal dispersion becomes secondary to the explicitly modeled variations in transport velocities across the potential repository because of variations in infiltration. Also, the explicitly modeled variations in transport velocity caused by the fracture/matrix system also tend to dominate dispersion. Lateral dispersion may play a more important role, but is limited by the relatively short transport path from the repository to the water table compared with the size of the source.

3.6.1.6 Chain-Decay Model

Radioactive decay is modeled using simple exponential decay. For the base case, neptunium-237, uranium-234, and protactinium-231 are the only radionuclides significantly affected more than a few percent by the neglect of the chain-decay processes. Consideration of chain decay causes transport calculations to be more complex because

daughter radionuclides are created during transport of the parent isotope. The creation of progeny could be modeled in a complex calculation as a distributed source term throughout the modeling domain. However, the unsaturated zone transport model does not directly consider chain decay and progeny ingrowth. As discussed in Section 3.5.1.5, the effects of progeny ingrowth are included in the determination of the radionuclide inventory present. Therefore, the effects of chain decay and progeny ingrowth on unsaturated zone transport are approximately included through these adjustments to the radionuclide inventory. The accuracy of this approximation is affected by the relative degree of sorption for the parent radionuclides as compared with the daughter products. In most cases, the parent radionuclides are at least as sorptive as the daughter products. Therefore, the approximation is conservative.

3.6.2 Implementation of the Performance Assessment Model

This section outlines the methods used to implement the models described in Section 3.6.1 for total system performance assessment calculations. The description of this implementation includes the mathematical models used, the connections with other TSPA models, and the basic data used to define model parameters.

3.6.2.1 Finite Element Heat and Mass Particle Tracking

The conceptual model described above has been implemented using a modified method for tracking the transport of particles. This modified method is used in the general-purpose, multi-phase flow and transport code FEHM (Zyvoloski et al. 1995). Particle tracking using FEHM is a cell-based approach in which particles move from cell to cell in a numerical grid. The finite-difference grid described below that computes the flow field also defines the cells. The movement from one cell to another requires a way to compute how long the particle will reside in the current cell and to select the next cell the particle will enter. The cell-to-cell routing is performed with sufficient time resolution that the next cell the particle will occupy is always an adjacent cell. The selection of the adjacent cell is based on a mass-flux-weighted probability among adjacent cells that can have an outflow from the current cell, that is, particles cannot move into adjacent cells that are flowing into the current cell. The time that a particle will reside in a given cell is based on probabilistic distributions of residence time derived from mathematical models of the transport process (Robinson et al. 1997, Chapter 4, pp. 4-1, 4-6, and 4-7). Because the properties within a given cell are uniform, the mathematical development of residence time distributions may be carried out either analytically or semi-analytically, making the residence time calculations computationally efficient.

The particle tracking method is limited to transport conditions in which advection dominates dispersion, in the sense that the spread of an initially sharp concentration front is small compared with the distance that the front has advanced. This limitation is due to the nature of dispersive processes in which there is a finite probability for a particle to move into cells other than those adjacent to the current cell. Similarly, the assumption that cell-to-cell transfer is proportional to water flux also becomes inaccurate for dispersive-dominated transport. Advective-dominated transport is the expected condition in the unsaturated zone.

3.6.2.2 Linkage with Other Models

Radionuclide transport calculations for the three-dimensional, dual permeability model are directly coupled, that is, dynamically linked, with the computer program for total system integration (Golder Associates, Inc. 1998, Section 2.3.2). RIP provides the source term for radionuclide transport calculations in the unsaturated zone, that is, the radionuclide releases from the engineered barrier system as described in Section 3.5. Also, the FEHM particle tracker receives flow fields from an external flow calculation (see Section 3.1) and provides radionuclide mass flux values at the water table to the transport model for the saturated zone (see Section 3.7 and Figure 4-10).

For unsaturated zone transport, RIP directly accesses the FEHM particle tracker module (Robinson et al. 1997, Chapter 4, pp. 4-1 to 4-16)

to perform three-dimensional, site-scale transport calculations. The unsaturated zone flow fields required by the FEHM module are accessed separately by the program, as described below. For every simulation time step in RIP (for example, 100 years), source term radionuclide mass flux information is passed from the engineered barrier system cells to the FEHM module. The repository is divided into six regions in an attempt to capture the spatial variation for infiltration over the potential repository block (see Section 3.2.2.2). The radionuclide releases from a given region of the repository are assumed to be well mixed with the unsaturated zone flow through that region. The FEHM module then moves the particles as far as they would travel during that time step, based on the steady state velocity field in the fractures and matrix of the unsaturated zone rock units. The FEHM module sends back to RIP the amount of mass flux that leaves the unsaturated zone model domain in FEHM (i.e., the mass to be passed to the saturated zone model, which is the mass that enters the water table). The amount of radionuclide mass in the fractures is passed separately from that in the matrix so that intermediate results can be plotted. The two masses are mixed in a RIP code mixing cell, and the results are passed to the convolution integral function for the saturated zone[7]. The FEHM module also passes back the average fracture and matrix liquid fluxes in the six water table regions of the saturated zone model (see Figure 4-10).

For the TSPA, FEHM calculates transport dynamically. However, the flow fields used in the transport calculations are pre-generated with TOUGH2, a computer code that simulates three-dimensional flow of water and heat in porous and fractured media (Pruess 1991; Bodvarsson et al. 1997). The use of pre-generated flow fields implies the assumption of quasi-steady flow. There is a library of flow fields corresponding to the uncertainty in the unsaturated zone flow parameters and infiltration rate (see Section 3.1). For each realization, a different flow field is used based on a random sampling of infiltration rate and key hydrogeologic parameters that are uncertain. Also, for each sampled flow field corresponding to present day climatic conditions, there are two corresponding flow fields that have a higher boundary condition at the surface for infiltration flux based on two future climate scenarios, long-term average and superpluvial. A detailed discussion of the unsaturated zone flow field, climate states, and generation methods is given in Section 3.1.

Based on the description of waste package groupings in Section 3.2.2.2, the radionuclide source term for the unsaturated zone transport model is divided into six distinct regions based on heterogeneity of infiltration flux. Therefore, there are six distinct sets of engineered barrier system cells in the computer program (see Section 4.1) that supply six distinct areas of the three-dimensional, unsaturated zone domain in the FEHM particle tracker. Radionuclide release within each of the six regions is spatially uniform over the common grid structure of the TOUGH2 flow code and FEHM particle tracker. The outflow of the unsaturated zone FEHM particle tracker is also divided into six distinct regions at the water table, based in part on the lithology of the geologic units intersecting the water table. These regions provide a coarse discretization of the radionuclide mass flux from the unsaturated zone as input to the saturated zone transport model. The six regions at the water table are unrelated to the six regions at the repository horizon. As mentioned above, fracture and matrix mass fluxes from these six distinct water table regions are supplied to six RIP mixing cells and then used for computation of saturated zone transport with the saturated zone convolution integral described in Section 3.7.2. Both solute and colloid mass are tracked throughout the models.

3.6.2.3 Parameter Inputs

The unsaturated zone transport model requires several parameter inputs to quantify the magni-

[7] For multi-realization simulations, RIP also passes an index parameter to FEHM that points to a row in a table of 100 realizations of the transport parameters in the unsaturated zone that are uncertain. The specific stochastic parameters that comprise these 100 vectors are discussed in Section 4.1.

tudes of matrix diffusion, sorption, dispersion, fracture aperture, and the aqueous-colloid partitioning coefficient. Because these parameter values have varying degrees of uncertainty, a probability distribution is identified for each parameter value that may be used in stochastic performance assessment calculations. The following descriptions summarize the data sources used to establish these parameter distributions (see Table 3-18).

Sorption K_ds have been quantified using results of batch sorption experiments for different radionuclides and rock types (Triay et al. 1997, Sections VA and VB, pp. 1-8). The results from batch sorption experiments were compared with those from experiments with crushed rock and whole rock columns for neptunium, plutonium, technetium, and selenium. The batch sorption technique provided conservative estimates for K_d. Of the eight elements considered in the base case, three elements have little or no sorption: technetium, iodine, and carbon. These elements are modeled using a K_d of zero (ibid, p. 174). Of the remaining five elements, neptunium, uranium, and selenium have small but nonzero K_ds, with expected values less than or equal to 7 mL/g (ibid, p. 174). Only protactinium and plutonium have expected values of K_d greater than 10 mL/g (ibid, p. 174). As discussed for the conceptual model, sorption is identified for devitrified, vitric, and zeolitic rock types. Probability distributions for the K_ds, representing uncertainties in the parameter values, were identified through expert judgment (CRWMS M&O 1998i, Section 7.4). The assignment of K_d values were made on the assumption that their values are uncorrelated.

Matrix diffusion coefficients have been quantified in laboratory experiments for different radionuclides and rock types (Triay et al. 1997, p. 181). Anionic radionuclides have somewhat smaller

Table 3-18. Parameter Values Used for Unsaturated Zone Radionuclide Transport in Total System Performance Assessment for the Viability Assessment

Parameter Description	Distribution
K_d of ^{14}C in all units (mL/g)	0
K_d of ^{129}I in all units (mL/g)	0
K_d of ^{237}Np in devitrified units (mL/g)	Beta; mean = 1.0, COV = 0.3, min = 0, max = 6.0
K_d of ^{237}Np in vitrified units (mL/g)	Beta; mean =1.0, COV = 1.0, min = 0, max = 15.0
K_d of ^{237}Np in zeolitic units (mL/g)	Beta; mean = 4.0, COV = 0.25, min = 0, max =12.0
K_d of ^{231}Pa in devitrified units (mL/g)	Uniform; min = 0, max = 100
K_d of ^{231}Pa in vitrified units (mL/g)	Uniform; min = 0, max = 100
K_d of ^{231}Pa in zeolitic units (mL/g)	Uniform; min = 0, max = 100
K_d of ^{239Pu} and ^{242}Pu in devitrifed units (mL/g)	Beta; mean = 100, COV = 0.25, min = 20, max = 200
K_d of ^{239}Pu and ^{242}Pu in vitrifed units (mL/g)	Beta; mean = 100, COV = 0.25, min = 50, max = 200
K_d of ^{239}Pu and ^{242}Pu in zeolitic units (mL/g)	Beta; mean = 100, COV = 0.25, min = 30, max = 200
K_d of ^{79}Se in devitrified units (mL/g)	Beta; mean = 3, COV = 1.0, min = 0, max = 30
K_d of ^{79}Se in vitrified units (mL/g)	Beta; mean = 3, COV = 1.0, min = 0, max = 20
K_d of ^{79}Se in zeolitic units (mL/g)	Beta; mean = 2, COV = 1.0, min = 0, max = 15
K_d of ^{99}Tc in all units (mL/g)	0
K_d of ^{234}U in devitrified units (mL/g)	Beta; mean = 2.0, COV = 0.3, min = 0, max = 4.0
K_d of ^{234}U in vitrified units (mL/g)	Beta; mean = 1, COV = 0.3, min = 0, max = 3.0
K_d of ^{234}U in zeolitic units (mL/g)	Beta; mean = 7, COV = 1.0, min = 0, max = 30.0
Diffusion Coefficient (m^2/s) of ^{237}Np, ^{239}Pu, ^{242}Pu, ^{234}U, ^{231}Pa	Beta; mean = 1.6×10^{-10}, COV = 0.3125, min = 0, max = 1.0×10^{-9}
Diffusion Coefficient (m^2/s) of ^{99}Tc, ^{14}C, ^{129}I, ^{79}Se	Beta; mean = 3.2×10^{-11}, COV = 0.3125, min = 0, max = 1.0×10^{-9}
K_c of ^{239}Pu and ^{242}Pu in all units	Log uniform; min = 1×10^{-5}, max = 10
Dispersivity (m) of both fracture and matrix units	Normal; mean = 20, SD = 5.0
Aperture (m) of fractures in all units	Log normal; geometric mean =1×10^{-4}, geometric SD = 3.16

matrix diffusion coefficients than cationic radionuclides. At least for technetium, the lower diffusion rate may be caused by its exclusion from some matrix pores because of the larger ion size and negative charge of the pertechnetate anion TcO_4^-, the predominant aqueous species of technetium for present-day conditions, as compared with tritium, for example. Matrix diffusion of sorbing, cationic radionuclides is estimated using the matrix diffusion coefficient for tritium. As discussed for the conceptual model, matrix diffusion is assumed to be a function of radionuclide type, although variations in matrix diffusion coefficients are expected with changes in bulk water content. These variations were estimated from the range of bulk water content in the unsaturated zone and a previously determined relationship between the matrix diffusion coefficient and bulk water content (Los Alamos National Laboratory 1997, pp. VI-5 and VI-6). These variations form the basis for the uncertainty range in matrix diffusion coefficients (CRWMS M&O 1998i, Section 7.4).

Dispersion coefficients are commonly modeled as a product of transport velocity and a mixing length scale called dispersivity. Dispersivity is a property of the flow geometry that is determined by the structure of the fracture paths, for dispersion in the fracture continuum, or pore structure, for the matrix continuum. There are no measured data at Yucca Mountain that can be directly applied to determining dispersivity in the unsaturated zone. However, a value of 20 m (66 ft) over the approximately 300 m (984 ft) of unsaturated zone travel distance is consistent with the dispersivity versus scale correlation of Neuman (1990). The base case distribution for dispersivity was selected to be normal with a mean of 20 m (66 ft) and a standard deviation of 5 m (16 ft), which captures a range of 7.5–32.5 m (25-107 ft) within the 99 percent probability limits. This dispersivity distribution applies to transport for both the fracture and matrix continua, but values for fracture and matrix are sampled independently for TSPA calculations. Sensitivity studies indicate that radionuclide transport in the unsaturated zone is insensitive to dispersivities over a range from 0 to 75 m (0–246 ft) (CRWMS M&O 1998i, Section 7.4).

One concern for implementation of a numerical transport model is numerical dispersion. Numerical dispersion is an artifact of numerical solution algorithms and has no physical basis. It is a function of spatial-grid size and time-step size. The effects of numerical dispersion on transport solutions are similar in character to physical dispersion. The particle tracking technique used here for unsaturated zone transport is formulated specifically to reduce numerical dispersion. For flow parallel to the grid, numerical dispersion is expected to be zero (Goode and Shapiro 1991). Benchmark tests have shown the accuracy of this technique for systems with low physical dispersion (Robinson et al. 1997, Section 4.6.1).

Fracture aperture plays a role in calculations of residence time distributions for matrix diffusion. Matrix diffusion between fractures and matrix is enhanced for fractures with smaller aperture. Fracture aperture is equivalent to the fracture volume per unit area of fracture/matrix contact. Hydraulic fracture apertures derived by Bodvarsson et al. (1997) mostly lie between about 100 to 200 microns, with some ranging up to 500 microns (Bodvarsson et al. 1997, Table 7.12). Therefore, as a first approximation a log-normal distribution is used with a geometric mean of 100 microns and a geometric standard deviation of 3.16, that is, a two standard deviation width is a factor of 10. (Specifically, this means that the ratio of the value one standard deviation above the mean to that value one standard deviation below the mean is 10.)

3.6.3 Results and Interpretations

This section presents results of the unsaturated zone transport model in terms of travel times and transport pathways, and sensitivities of the results to the conceptual model for unsaturated zone flow, matrix diffusion, and the sorptive characteristics of different rock types. A summary of the findings based on analyses of the unsaturated zone transport subsystem is provided, along with recommendations for additional work prior to LA.

3.6.3.1 Results for the Unsaturated Zone Transport Model

Simulations using the unsaturated zone transport model were performed to investigate the travel times and transport pathways from the various repository regions to the water table. The simulations used 100,000 particles released from each node in the repository to develop a travel time distribution for transport to the water table. The simulations were also used to identify the center of mass at the water table for releases from each repository node. This information indicates transport pathways through the unsaturated zone. The results presented here are for expected infiltration under long-term average climate, which averages about 40 mm/year (1.6 in./year) over the repository block. The long-term average climate is expected during about 90 percent of the postclosure time period.

Figure 3-58 shows the contour plots of the repository region; color represents travel time to the water table. These calculations were done using hypothetical nonsorbing, non-diffusing particles to focus on the advective transport processes. Two plots are presented. Figure 3-58a shows the times for 0.1 percent of the released mass to arrive at the water table as a function of location within the repository. Figure 3-58b shows the times for 50 percent of the released mass to arrive at the water table. The general trend is for the travel time to increase from northeast to southwest through the repository. The shorter travel times in the northeast (less than 50 years for 0.1 percent; less than 200 years for 50 percent) are attributed to transport dominated by the fracture continuum.

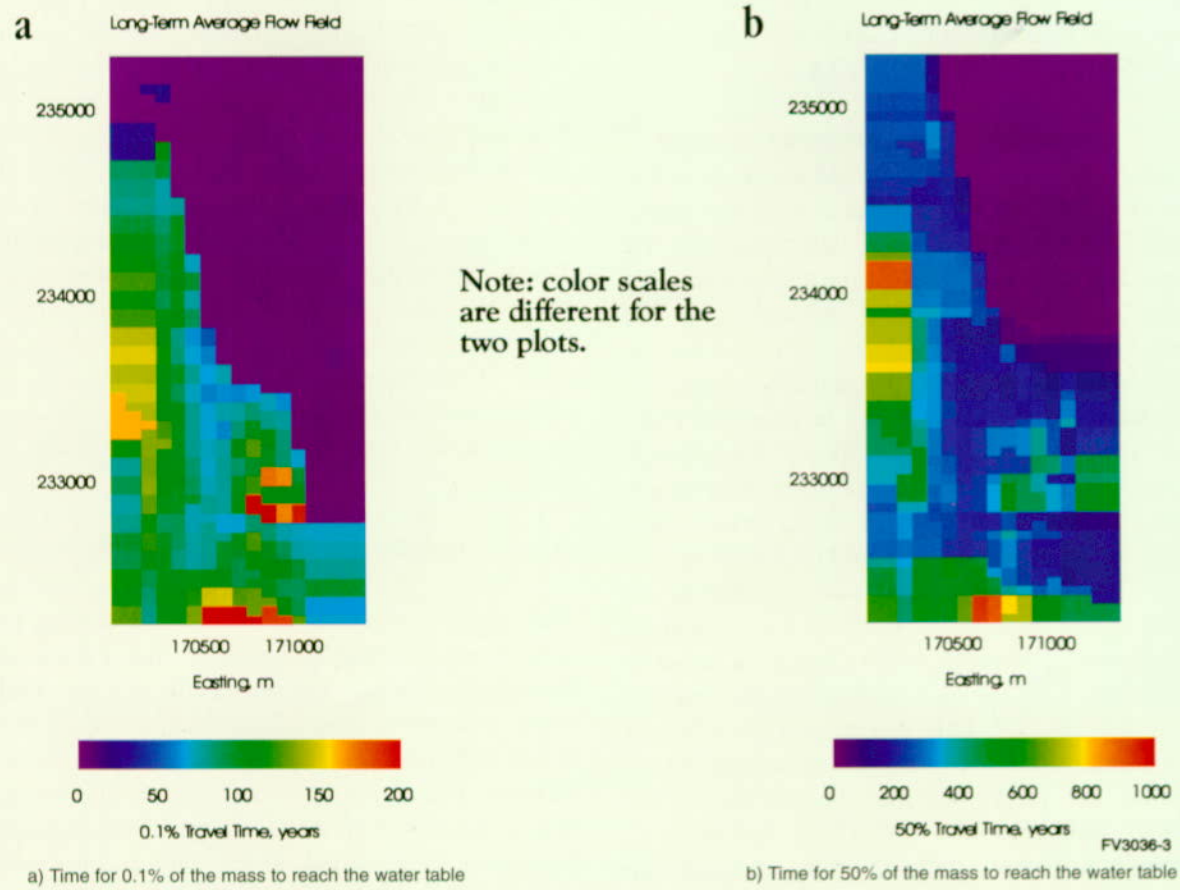

Figure 3-58. Color Contour Plot Showing Travel Times from the Repository to the Water Table for Hypothetical Nonsorbing, Nondiffusing Tracer Particles
(100,000 particles per grid cell)
Using the base case parameter set, long-term average climate and mean infiltration.

The northeast section is a zone in which site characterization studies have commonly found perched water along the basal vitrophyre of the Topopah Spring welded unit and upper zeolitic units in the Calico Hills nonwelded unit. The flow model has been calibrated to reproduce observations of perched water. This calibration was achieved by severely reducing fracture permeabilities in zones immediately underlying zones of observed perched water. This reduction in fracture permeability leads to lateral diversion of the flow through more permeable fracture pathways around the perched water. Further east, the diverted water eventually returns to flow pathways that are mainly vertical, either along the Ghost Dance fault or other fracture pathways. Another factor influencing travel times is the uneven distribution of infiltration over the repository block. Infiltration models predict higher infiltration rates in the northeast than in the southwest (CRWMS M&O 1998i, Chapter 2).

Figure 3-59 is a similar plot to Figure 3-58, but in this case the travel times are for particles having the transport characteristics of plutonium. In the base case, plutonium is assumed to interact with colloids both reversibly and irreversibly. Irreversible sorptive interaction with colloids causes particles to act as nonsorbing and nondiffusing, causing the travel times as shown in Figure 3-58. Reversible sorptive interaction with colloids causes different magnitudes and patterns for travel times. Similar qualitative trends in travel time are shown in Figure 3-59a as in Figure 3-58a (both for

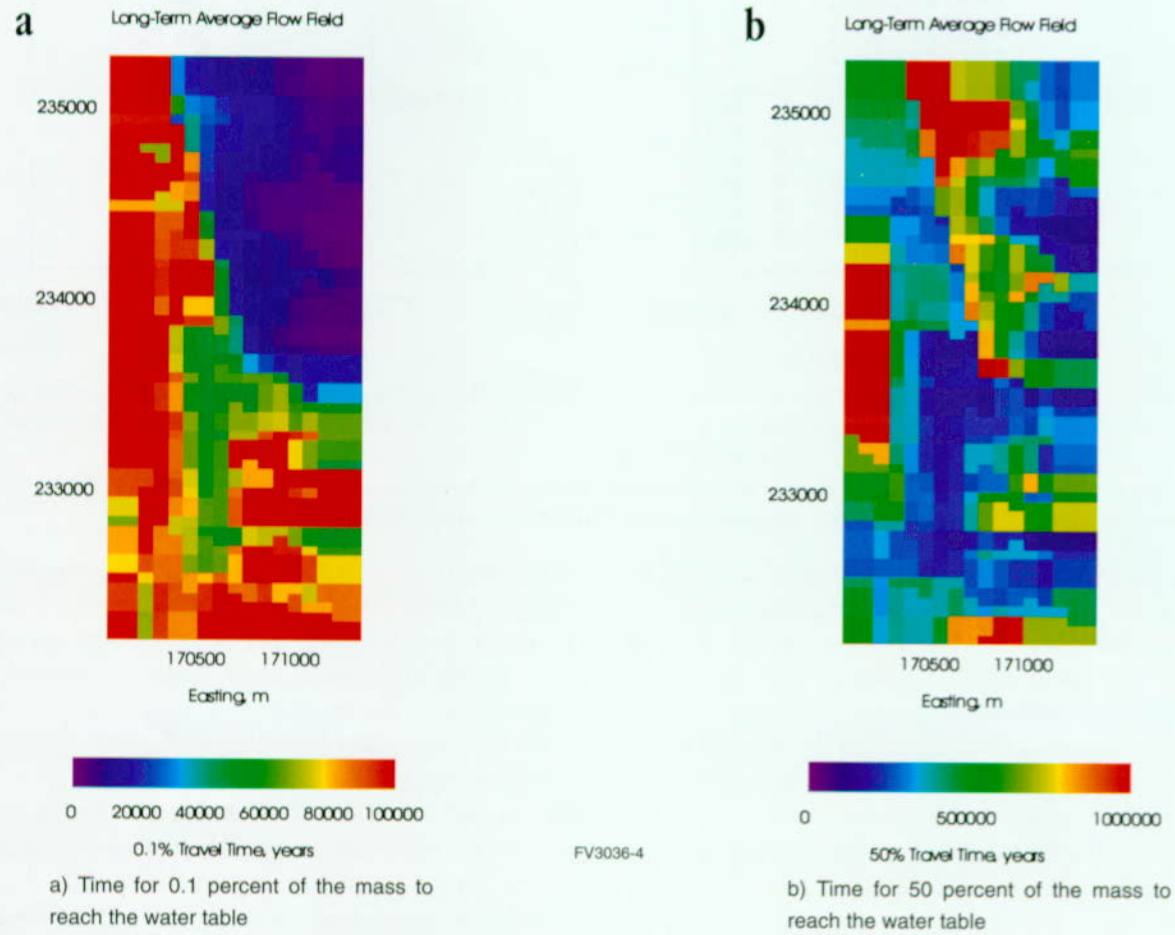

a) Time for 0.1 percent of the mass to reach the water table

b) Time for 50 percent of the mass to reach the water table

Figure 3-59. Color Contour Plot Showing Travel Times from the Repository to the Water Table for Hypothetical Tracer Particles Having the Characteristics of Plutonium
(100,000 particles per grid cell)
Using the base case parameter set; long-term average climate and mean infiltration.

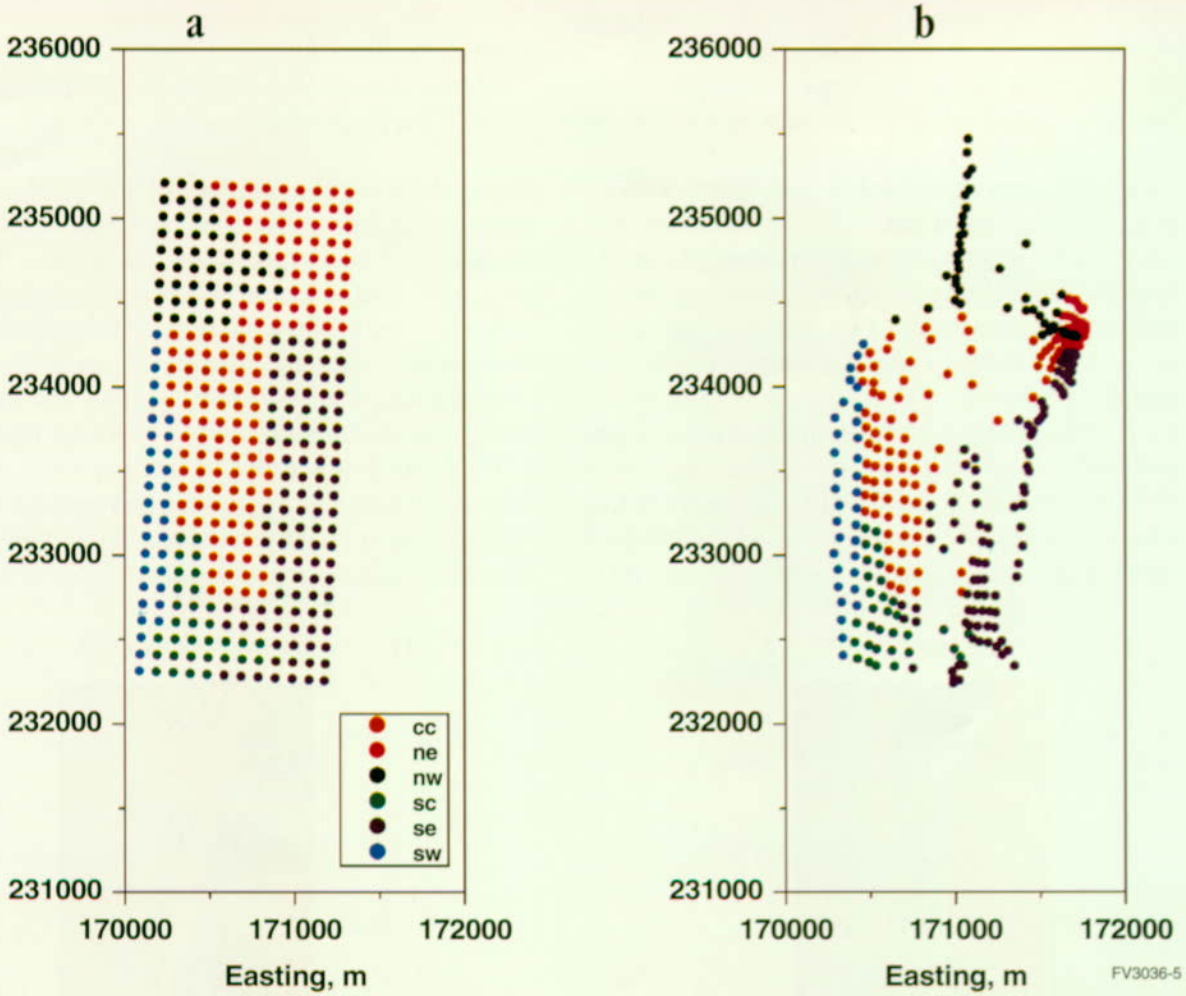

a) Release locations with the colors denoting the repository sub-domains

b) Computed center of mass of releases at the water table for each of the release

Figure 3-60. Average Locations for Hypothetical Releases from each Repository Grid Cell at the Water Table Using the base case parameter set; long-term average climate and mean infiltration.

0.1 percent recovered mass). However, the magnitudes of the travel times are much larger for the plutonium case. Travel times approach 100,000 years for plutonium, compared with maximum travel times that are less than 200 years for the passive tracer. Travel times for 50 percent of the released plutonium are in excess of 100,000 years, and some exceed one million years. Also, the spatial trends in travel time have changed and are much less distinct.

Figure 3-60a shows the origin points of particle releases from the repository. These points have been color coded so that releases from the six zones (cc ≡ central; ne ≡ northeast; nw ≡ northwest; sc ≡ south central; se ≡ southeast; sw ≡ southwest) can be identified at the water table in Figure 3-60b. The colored dots in Figure 3-60b represent the center of mass of each of the releases upon arrival at the water table. Lateral diversion of releases from the northern portions of the repository is the most prominent feature. Some diversion is also seen from the southeast portion of the repository. The somewhat abrupt termination of lateral diversion eastward is attributed to the Ghost Dance fault (see Figure 3-1). The linear pattern of releases at the water table originating from the northwest portion of the repository (black dots) may result from the dip of the hydrogeologic units intercepting the water table or alternatively, a high-permeability feature is interrupting lateral diversion. Transport pathways from the southwest,

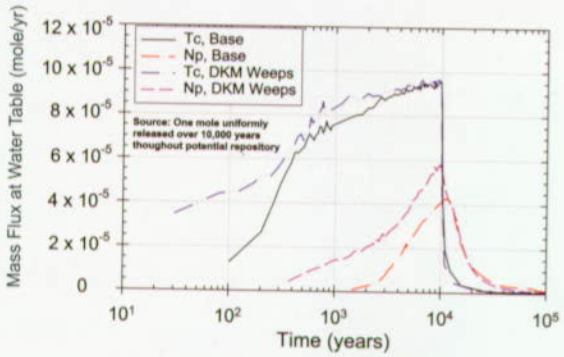

a) Mass flux at the water table

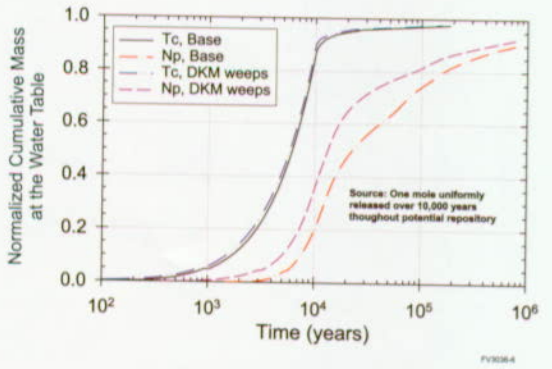

b) Cumulative mass recovered at the water table

Figure 3-61. Comparison of the Effects of Unsaturated Zone Flow Fields on Technetium and Neptunium Transport: Base Case Versus DKM Weeps Flow Models
Using the base case parameter set; long-term average climate with mean infiltration.

south central, and central-central regions are more nearly vertical.

3.6.3.2 Influence of the Unsaturated Zone Flow Model

The use of alternative flow models for radionuclide transport in the unsaturated zone is shown in Figure 3-61 (see Section 3.1). In this simulation, one mole each of technetium and neptunium were released uniformly over the repository region for a period of 10,000 years. The calculations were performed for the mean infiltration under long-term-average climate. Technetium is assumed not to sorb, whereas neptunium has limited sorptive interaction with the different rock types. The mean flow field for the base case, and the dual-permeability/Weeps model using mean permeability (see Section 3.1) are compared in Figure 3-61. The dual-permeability/Weeps model reduces flow interaction between fractures and matrix compared with the base case flow field. Figure 3-61a shows mass flux at the water table, and Figure 3-61b shows cumulative mass arrival. The primary difference in these flow fields is due to differences in the fracture/matrix coupling strength. This factor, discussed in Section 3.1, affects the magnitude of advective exchange between the fractures and the matrix. The dual permeability model with Weeps modeling reduces the amount of fracture/matrix exchange, causing transport behavior that has a greater tendency to be dominated by fracture flow. In Figure 3-61a, mass flux increases over time until 10,000 years, when the source is depleted. These results indicate that higher concentrations of technetium and neptunium arrive sooner for the flow field derived using the dual permeability model with Weeps. However, Figure 3-61b shows that the cumulative mass of technetium recovered at the water table is relatively insensitive to the different flow fields. Some differences are seen in the cumulative recovery of neptunium at the water table. Reduced fracture/matrix contact in the dual permeability model with Weeps modeling results in faster neptunium movement to the water table, although the differences are not large. Radionuclide decay is not modeled in this calculation.

3.6.3.3 Influence of Matrix Diffusion

Matrix diffusion is another mechanism that allows radionuclides moving through fractures to enter the matrix. In the simulation, one mole each of technetium and neptunium are released uniformly over the repository region for a period of 10,000 years. The calculations were performed using the mean flow field for the base case and mean infiltration for the long-term average climate. Figures 3-62a and 3-62b show the effects of matrix diffusion on the transport of technetium and neptunium in which, as before, technetium is nonsorbing and neptunium moderately sorbing. The mass flux plot in Figure 3-62a shows that early releases arrive at the water table sooner without matrix diffusion, that is, for $D_m = 10^{-30}$ m²/s (this very low value has been used to represent zero

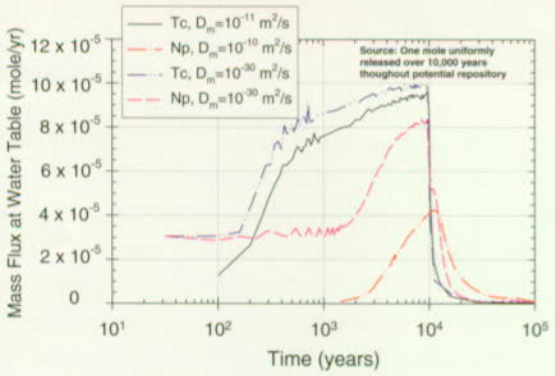

a) Mass flux at the water table

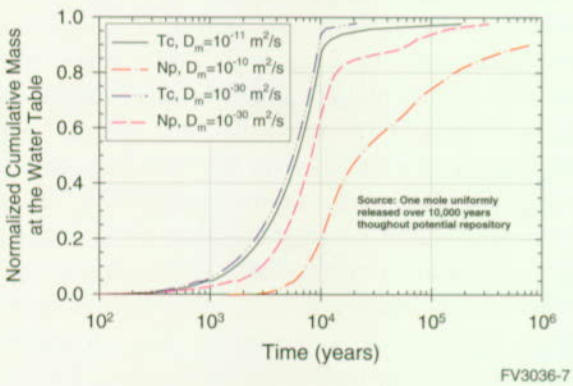

b) Cumulative mass recovered at the water table

Figure 3-62. Comparison of the Effects of Matrix Diffusion on Technetium and Neptunium Transport
Using the base case parameter set; long-term average climate with mean infiltration.

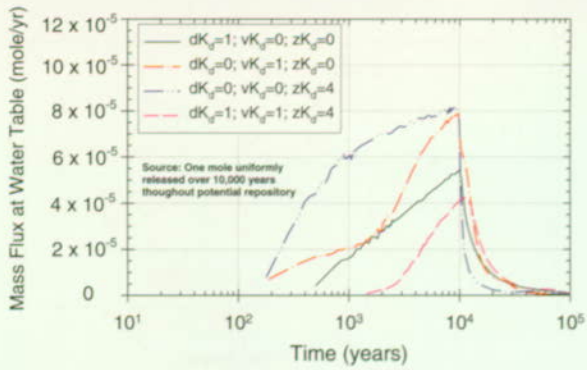

a) Mass flux at the water table

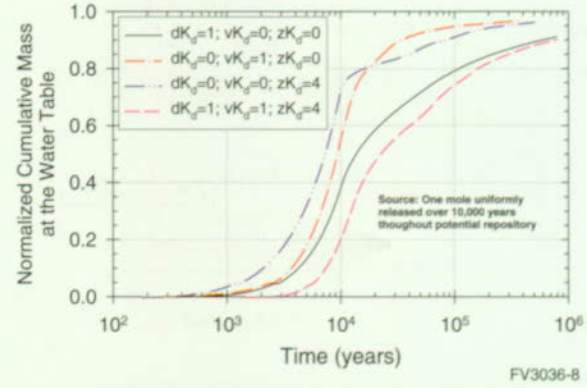

b) Cumulative mass recovered at the water table

Figure 3-63. Comparison of the Influence of Sorption on Devitrified, Vitric, and Zeolitic Rock on Neptunium Transport
Using the base case parameter set; long-term average climate with mean infiltration; dK_d = sorption coefficient on devitrified rock; vK_d = sorption coefficient on vitric rock; zK_d = sorption coefficient on zeolitic rock, all in mL/g.

matrix diffusion). Differences in mass flux and in cumulative mass recovered are much larger for neptunium than technetium. These results suggest that matrix diffusion has little affect on nonsorbing radionuclides but is more important for sorbing radionuclides, because of sorption sites in the matrix which are accessed by matrix diffusion.

3.6.3.4 Influence of Rock Type

Differences in hydrogeologic and geochemical properties between the devitrified, vitric, and zeolitic rock types suggest that they may not affect transport in the same way. For this simulation, one mole of neptunium is released uniformly over the repository region for a period of 10,000 years. As before, the calculations were performed using the mean flow field for the base case and mean infiltration for the long-term average climate. The K_ds for neptunium sorption on the different rock types are 1 mL/g for devitrified rock, 1 mL/g for vitric rock, and 4 mL/g for zeolitic rock. Three transport calculations were conducted with sorption "turned on" in one layer only, that is, K_ds were equal to zero in the other layers, to see the influence of each individual rock type. A final calculation was done using all the base case K_ds "turned on." The results are shown in Figures 3-63a and 3-63b for the radionuclide mass flux and cumulative mass arrival, respectively, at the water table.

The conclusion based on this sensitivity calculation is that the Topopah Spring welded unit (with

sorption parameter dK_d, where the leading "*d*" stands for the devitrified rock type) is the most important unit in delaying radionuclide arrival at the water table. Flow through the Topopah Spring welded unit is nearly vertical throughout the repository domain, and this flow pattern causes longer residence times during transport through the fractures, allowing greater interaction with the matrix. On the other hand, large portions of the Calico Hills unit are bypassed because of lateral diversion. Therefore, in many areas the flux that does pass through the Calico Hills is relatively focused and residence times in these fracture pathways are short, leading to poor interaction with the matrix. The Calico Hills vitric unit generally has the next largest effect on radionuclide retardation because of high matrix permeability that attenuates fracture flow and causes greater radionuclide contact with the matrix.

3.6.3.5 Summary and Conclusions

Calculations for radionuclide transport in the unsaturated zone use a modified form of the particle tracking method implemented in the FEHM flow and transport code. This transport code is dynamically linked with RIP. The transport model uses a dual-permeability approach for computing radionuclide transport in a fracture/matrix system. For the particle tracking transport calculations, three-dimensional, steady flow fields in the unsaturated zone are computed using TOUGH2, the code platform of the unsaturated zone flow model. Changes in infiltration because of climate change are treated using a quasi-steady flow approximation. The transport model includes the effects of fracture/matrix interaction due to advective and diffusive exchange between the fracture and matrix continua. The effects of radionuclide sorption on the rock matrix are addressed using a bounding, minimum-K_d modeling approach, but fracture sorption is not included. The effects of colloids on plutonium transport are included in two forms—reversibly sorbed to colloids and irreversibly bound in the colloid structure.

The results of investigations into radionuclide transport through the unsaturated zone lead to the following conclusions:

1. Under the dominant long-term average climate, releases of nonsorbing or weakly sorbing radionuclides from the northern portion of the repository have short travel times, only a few years, because of fracture-dominated transport.

2. Under the dominant long-term average climate, releases of nonsorbing or weakly sorbing radionuclides from the southern portion of the repository may have much longer travel times (hundreds of years).

3. For most of the mass of strongly sorbing radionuclides, such as plutonium, arrival at the water table is delayed tens to hundreds of thousands of years. Radionuclides that reversibly sorb onto colloids are also delayed; however, irreversibly bound radionuclides may behave as nonsorbing radionuclides.

4. Matrix diffusion has little effect on transport of nonsorbing radionuclides. However, combining matrix diffusion with sorption significantly retards radionuclides compared with sorption and no matrix diffusion.

5. The Topopah Spring welded unit is the primary barrier to radionuclide transport in the unsaturated zone because of slower fracture transport in this unit compared with the Calico Hills zeolitic unit, and its greater thickness and continuity compared with the Calico Hills vitric unit.

6. Alternative flow models like the dual-permeability model with Weeps modeling, which have smaller coupling strengths for effective fracture/matrix contact area, increase fracture-dominated transport, particularly for sorbing radionuclides. However, the magnitude of this effect is not large for weakly sorbing radionuclides.

3.7 SATURATED ZONE FLOW AND TRANSPORT

The saturated zone at Yucca Mountain is the region beneath the ground surface where rock pores and fractures are completely saturated with groundwater. The upper boundary of the saturated zone is called the water table. The repository is located in the unsaturated zone, which is above the saturated zone. The flow-and-transport component of the TSPA for the saturated zone evaluates the migration of radionuclides from their introduction at the water table below the repository to the release point to the biosphere (Figure 3-64). This component of the analysis is coupled with the transport calculations for the unsaturated zone that describe the movement of contaminants in downward percolating groundwater from the repository to the water table. This input to the saturated zone flow-and-transport calculations is the spatial and temporal distributions of simulated mass flux at the water table. The saturated zone results are linked to the biosphere analysis by the simulated time history, or system response as a function of time, of radionuclide concentration in groundwater produced from a hypothetical well. The geosphere/biosphere interface is assumed to be located 20 km (12 miles) from the repository (Figure 3-65). Radionuclide concentrations in the hypothetical well water are used in the biosphere component to calculate radiation dose rates received by the public.

The saturated zone modeling studies and sensitivity analyses presented in this chapter were prepared with the view of addressing selected aspects of the NRC Key Technical Issues on Unsaturated and Saturated Flow under Isothermal Conditions (NRC 1997e; 1997f) and Total System Performance Assessment and Integration (NRC 1998a). Specifically, the information presented is pertinent to the unsaturated and saturated flow under isothermal conditions subissue on groundwater percolation through the repository horizon,

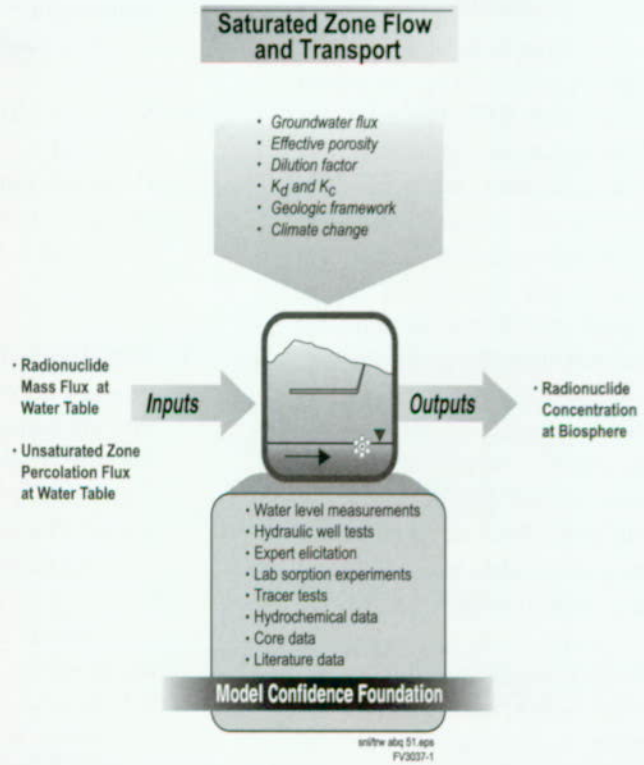

Figure 3-64. Summary of Inputs and Outputs for the Saturated Zone Flow and Transport Component of the Total System Performance Assessment for the Viability Assessment Analysis
Site characterization information that forms the basis of saturated zone flow and transport modeling is also indicated.

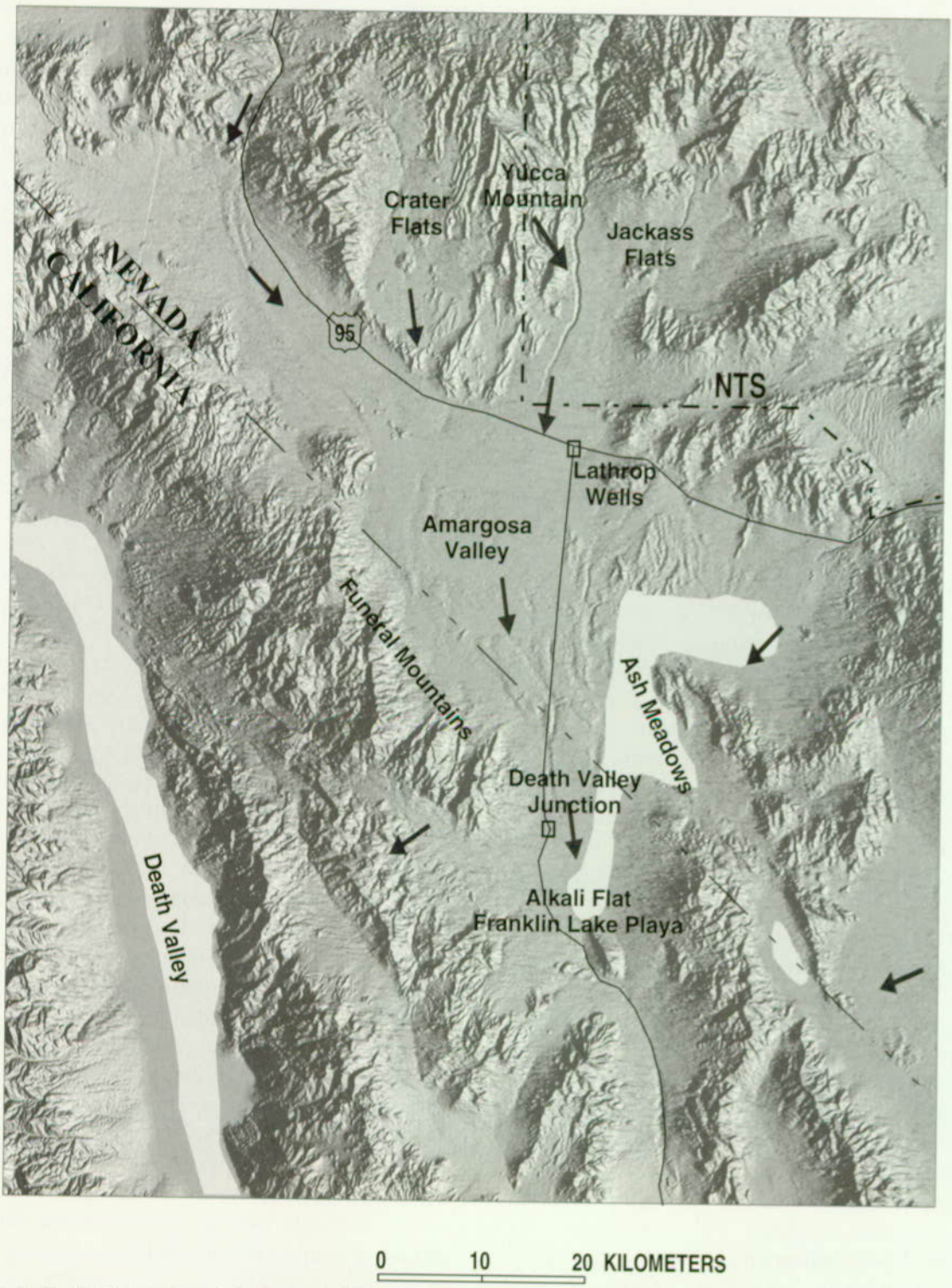

Figure 3-65. Regional Map of the Saturated Zone Flow System
Arrows indicate general directions of groundwater flow in the saturated zone on a regional scale. Lighter area (Ash Meadows, Alkali Flat, Death Valley) indicates major areas of groundwater discharge by a combination of spring discharge and evapotranspiration by plants.

ambient flow conditions in the saturated zone, and the TSPA integration subissue on model abstraction.

3.7.1 Construction of the Conceptual Model

This section describes the conceptual model of the flow-and-transport processes in the saturated zone that are relevant to radionuclide migration from the repository and shows how the model has been applied. Model application includes using judgment provided by panelists of an expert elicitation on processes in the saturated zone. Information from observations of the saturated zone system that forms the basis of the conceptual model is also summarized.

3.7.1.1 Conceptualization of Saturated Zone Flow and Transport Processes

Groundwater flow in the saturated zone below and directly downgradient of the repository at Yucca Mountain occurs in fractured, porous volcanic rocks at relatively shallow depths beneath the water table and in fractured carbonate rocks of Paleozoic age at much greater depths. At distances greater than about 10–20 km (6–12 miles) downgradient from the repository where the volcanic rocks thin and disappear under alluvium, groundwater flows either through the alluvium or the deep Paleozoic carbonates. Based on measured water levels in wells, the groundwater flow is generally to the southeast near the repository, with a transition toward the south and southwest farther south of the repository, as shown in Figure 3-65 (D'Agnese et al. 1997a, pp. 64 and 67). Groundwater that has flowed beneath Yucca Mountain is probably captured at pumping wells 20 km (12 miles) or more to the south in the Amargosa Valley under present conditions. Under predevelopment conditions (before pumping in the Amargosa Valley) and for the current climatic state, natural discharge of groundwater from beneath Yucca Mountain probably occurs further south at Franklin Lake Playa (Czarnecki 1990, p. 1-12), although spring discharge in Death Valley is a possibility (D'Agnese et al. 1997a, pp. 64 and 69). Under past wetter climatic conditions, groundwater discharge occurred at locations nearer to Yucca Mountain than Franklin Lake Playa.

Radionuclides migrating from the repository must be transported approximately 300 m (1,000 ft) downward by groundwater in the unsaturated zone to the water table, where they enter the saturated zone. Radionuclides are then carried downstream in the groundwater system. At 20 km (12 miles), the radionuclides reach the hypothetical water well located near the Amargosa Valley, where they could become a source of contamination in the biosphere (see Figure 3-66).

Important processes that must be considered in describing radionuclide travel time in the saturated zone include advection, transport by moving water; matrix diffusion, diffusion of contaminants into the rock pores; and sorption, capture of particles on rock surfaces by chemical processes (see Figure 3-66). The fractured, porous media of the volcanic units consist of an interconnected network of fractures and matrix material. The effective porosity is the porosity for the combination of fractures and matrix pores through which the radionuclides are carried. Effective porosity affects how fast the contaminants travel. Effective porosities are greater in porous media (e.g., alluvium) than in fractured media (e.g., volcanic tuffs), where contaminant movement is thought to occur primarily through the fractures. Because of the smaller effective porosity, travel times tend to be shorter in the fractured media than in the porous media. Matrix diffusion is the movement of dissolved radionuclides from groundwater flowing in fractures into the relatively immobile pore water of the matrix due to differences in concentration. Diffusion occurs at a small scale, probably not more than a few centimeters into the rock from fractures, and slows radionuclide movement by providing additional solute storage in the matrix pores. Geochemical retardation, through sorption of radionuclides on mineral grains, slows radionuclide migration in groundwater in both fractured and porous media. Processes such as sorption and matrix diffusion increase the residence time for certain radionuclides and allow reduction of dose by radioactive decay.

The most important process that influences radionuclide concentration in the saturated zone is dilution from hydrodynamic dispersion. Radionuclides are expected to move through the unsat-

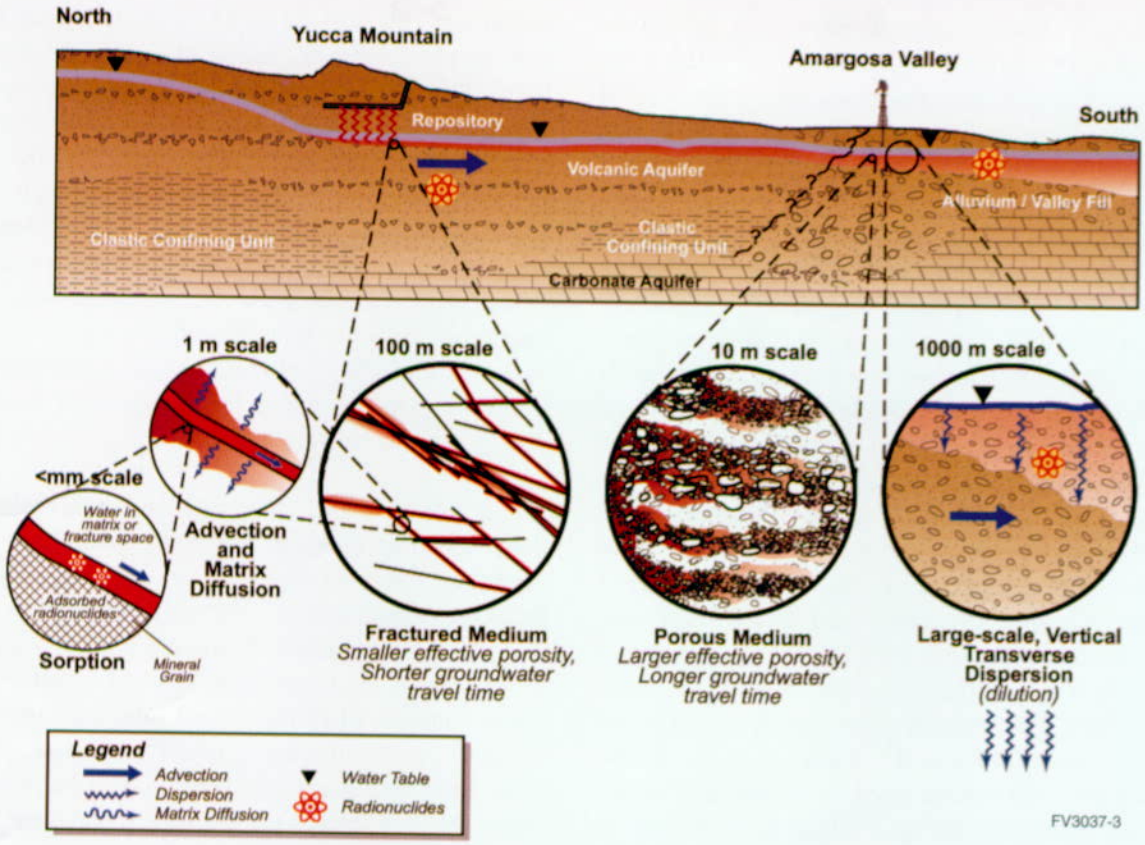

Figure 3-66. Conceptual Model of the Saturated Zone Groundwater Flow System and Processes Relevant to Performance of the Potential Repository at Yucca Mountain
Processes that affect radionuclide travel times in the saturated zone from beneath Yucca Mountain to potential pumping wells include advection, matrix diffusion and sorption. Processes that affect the concentration of radionuclides in groundwater include transverse dispersion of the contaminant plume and radioactive decay.

urated zone below the repository and enter the saturated zone in a well-defined plume, that is, as a flow system distinguishable from the surrounding flow because of differences in chemistry, temperature, concentration, or other parameters. Transverse dispersion, or horizontal and vertical spreading of the plume perpendicular to the travel path, causes dilution of radionuclide concentration. Longitudinal dispersion, or horizontal spreading in the direction of groundwater flow, decreases radionuclide concentrations if the source is varying with time. Transient changes in the direction of groundwater flow may contribute to apparent transverse dispersion and dilution. Transience in the saturated zone flow system could result from climatic variations over long time periods or from focused recharge on shorter time scales. Processes that cause dilution of radionuclides contribute directly to the attenuation of radiological dose by reducing radionuclide concentrations in groundwater.

3.7.1.2 Saturated Zone Flow and Transport Data

Numerous observations and scientific studies have provided both regional-scale and near-site knowledge about the saturated zone groundwater system at Yucca Mountain. Much of the information in the following summary is taken from the synthesis report of Luckey et al. (1996), from Czarnecki et al. (1997), and from D'Agnese et al. (1997a).

The saturated zone flow system at Yucca Mountain is part of the Alkali Flat-Furnace Creek groundwater subbasin of the larger Death Valley groundwater flow system. Groundwater flows regionally from recharge areas at higher elevations in mountain ranges, most significantly, the Spring Mountains and Pahute Mesa, toward natural discharge areas at springs. Groundwater also

discharges through evapotranspiration at playas (see Figure 3-65). Significant quantities of groundwater are also currently being discharged from the regional saturated zone system by pumping in areas such as the Amargosa Valley.

Measurements of water levels in wells near Yucca Mountain indicate that north of the site is a region of possible large hydraulic gradient, potentially 150 m/km (790 ft/mile). An alternative interpretation is that the higher apparent heads in wells north of the site are the result of perched water. West of the site is a region of moderate hydraulic gradient, corresponding to a 45-m (150-ft) increase in water table elevation. Water level data indicate a small horizontal hydraulic gradient (0.1 to 0.3 m/km or 0.5 to 1.6 ft/mile) immediately southeast of the site. Groundwater flow from the repository site for a distance of 5 to 8 km (3 to 5 miles) is apparently to the southeast toward Fortymile Wash. From there, the apparent direction of groundwater flow for about 20 km (12 miles) is to the south-southwest. Hydraulic head is a measure of the driving potential for groundwater flow that is inferred from water level measurements in wells. Near the Yucca Mountain site, hydraulic head in the deeper volcanic units and in the Paleozoic carbonate aquifer, based on one well, are generally higher than in the shallower saturated zone, indicating the potential for groundwater to flow upward. Variations in temperature and heat flow measured in boreholes in the saturated zone suggest significant redistribution of heat by vertical groundwater movement in some areas. These observations suggest that there is (an imperfect) confining unit separating the shallow volcanic flow system from the deeper flow system.

Variations in water table elevations have been directly monitored for a few decades and inferred from geological and geochemical data over hundreds of thousands of years. Water level fluctuations in most wells have been small—on the order of a few decimeters—primarily in response to barometric variations and earth tides. Variations have been greater in the Amargosa Valley area because of pumping. Highly transient and longer-term variations in hydraulic head of a few meters to a few decimeters have been observed following earthquakes. Significantly higher water table elevations (80–120 m or 260–390 ft higher than current elevations) at Yucca Mountain have been inferred from the locations of nearby paleospring deposits and from geochemical and mineralogical evidence from the unsaturated zone at the site. Higher water table elevations in the geologic past were apparently associated with wetter climatic conditions. From the perspective of performance assessment calculations, fluctuations of this magnitude in water table elevations suggest potentially significant alteration of radionuclide transport path lengths in the unsaturated zone on geologic time scales.

The aquifer in volcanic rocks has been hydraulically tested at many of the wells near the Yucca Mountain site, although there are no borehole data between approximately 10 and 20 km (6 and 12 miles) downgradient of the repository. Most of the available data are from single borehole tests using constant discharge, fluid injection, pressure injection, and radioactive tracer methods. From these tests, estimates of hydraulic conductivity (a factor that determines the amount of water that can flow through a material) in the fractured volcanic rocks of the saturated zone generally range over three orders of magnitude, depending on the depth and the particular hydrogeologic unit. The apparent hydraulic conductivity values determined from multiple borehole hydraulic tests at the C-hole complex tend to be much higher, by about two orders of magnitude, than the values from single-borehole tests for the same intervals (Geldon 1996, p. 59). The C-hole complex is located approximately 2.5 km (1.6 miles) to the southeast of the repository. Multiple-borehole hydraulic tests generally yield results that are more representative of large-scale hydraulic conductivity of the aquifer, suggesting that the single-borehole tests elsewhere at the site may have significantly underestimated the effective hydraulic conductivity (and thus the groundwater flow velocity) at those locations. Thus, results from the multiple-borehole tests were used in the saturated zone flow modeling for TSPA-VA. Surveys of flow in the deeper wells in the saturated zone near Yucca Mountain indicate that groundwater production in most of the wells occurred in a few discrete intervals within the volcanic units. For performance assessment calculations, these results

suggest that most groundwater flow in the fractured volcanic units is through only a small fraction of the saturated thickness.

Forced-gradient, cross-hole tracer tests conducted at the C-hole complex have provided data on in situ transport of the non-radioactive surrogate solutes and synthetic colloids in fractured, porous volcanic tuffs in the saturated zone (CRWMS M&O 1997f; Geldon et al. 1997, p. Background-2). These tests have been interpreted to indicate that the tracers diffused from fractures into the rock matrix and that sorption occurred. Test results that indicate relatively high flow porosity suggest that flow may have occurred in both fractures and the rock matrix during the tracer tests. There was relatively good agreement between tracer-test results and laboratory measurements of sorption coefficients (K_d) for transport of lithium. Lower recovery of microspheres, a uniformly sized surrogate colloid with a neutral surface charge, suggests significant filtration over the 30-m (100-ft) transport distance. For the TSPA analyses, these results support accounting for matrix diffusion in fractured volcanic units and using laboratory measurements of the sorption coefficient parameter for sorbing radionuclides.

Groundwater sampling from fractured volcanic tuff in the saturated zone near the Benham underground nuclear test site on Pahute Mesa suggests that colloid-facilitated transport of plutonium in the saturated zone may be relatively rapid (Thompson et al. 1998, p. vii). Although some component of transport may have been associated with the underground nuclear test, low concentrations of plutonium, associated with colloidal material in groundwater samples, indicate transport in the saturated zone of at least 1,300 m (4,300 ft) in 28 years (Thompson et al. 1998, p. 13). For the TSPA, this observation was used to develop an alternative conceptual model for colloid-facilitated transport of plutonium (Section 3.7.2.2).

3.7.1.3 Saturated Zone Flow and Transport Modeling

Analyses of groundwater flow and radionuclide transport in the saturated zone use numerical modeling results at different scales for site characterization and TSPA calculations. The regional-scale flow model (D'Agnese et al. 1997a) encompasses a large portion of southern Nevada and parts of eastern California. The regional-scale model was designed to use natural system boundaries so that estimates of groundwater flux through the model are constrained. The estimate of groundwater flux through the saturated zone flow system is based on the system's overall water budget. The regional-scale model has also been used to estimate the influence of climate change on changes to groundwater flux and flow direction in the saturated zone flow system (D'Agnese et al. 1997b).

A smaller-scale TSPA three-dimensional flow model for groundwater flow was developed to determine the flowpath from the repository footprint, or outline, at the water table to a distance 20 km (12 miles) downgradient, the approximate distance to the nearest domestic extraction of groundwater. Based on the simulation, the hydrogeologic units that were present along the contaminant travel path were determined as well as the percentage of the flowpath occupied by each unit. The travel distance through each hydrogeologic unit provided by this analysis was used to define the travel-path characteristics in the saturated zone for the TSPA one-dimensional transport, base case analysis (see Section 3.7.2).

The TSPA three-dimensional flow model used for this analysis incorporated an area of about 20 km × 36 km (12 miles × 22 miles) to a depth of 950 m (3,100 ft) below the water table. The model grid was a uniform orthogonal mesh with 500-m × 500-m × 50-m (1,600-ft × 1,600-ft × 160-ft) elements. The hydrogeologic framework in the model was based on a refined version of the regional geologic framework model used by D'Agnese et al. (1997a, p. 29-35). Seventeen different hydrogeologic units were represented in the model. Two linear, vertical features with low permeabilities to the west and north of Yucca Mountain were included to simulate the moderate and large hydraulic-gradient regions, respectively.

Flow was modeled as steady state through a single-continuum, porous medium. Focused recharge

along Fortymile Wash, consistent with USGS measurements, was included as a specified flux. Specified-pressure boundary conditions were applied to the lateral boundaries based on the interpolation of measured values of hydraulic head. Groundwater flow was not allowed to occur across the bottom boundary of the model. Permeability was assumed to be uniform within hydrogeologic units in the model domain, and average isothermal conditions were applied in the three-dimensional flow model for the saturated zone.

The TSPA three-dimensional model was calibrated by an iterative procedure, and the simulated hydraulic heads were compared with measured head values in the model domain. There was good agreement between the simulation results and most of the well measurements, particularly in the area downgradient of the repository. The differences between simulated and measured hydraulic head values were less than 5 m (16 ft) for shallow wells downgradient of the repository, within a 10 km (6 miles) distance. The direction of groundwater movement in this flow model is consistent with the conceptual model of the system and is evident in the plot of simulated particle paths shown in Figure 3-67.

Particle tracking in the simulated flow field of the TSPA three-dimensional flow model was used to estimate the flowpath lengths in the saturated zone through each of the hydrostratigraphic units downstream from the repository. In the model simulations, a swarm of particles was released at the water table and evenly distributed across the repository footprint. Flowpath lengths within the units were then tabulated. Flow was significant in four of the hydrostratigraphic units, and the resulting information was incorporated into the one-dimensional transport simulations used in the TSPA analyses (Section 3.7.2).

3.7.1.4 Saturated Zone Workshop and Expert Elicitation

To help understand how to best model saturated zone flow and transport for TSPA-VA, a workshop was held in Denver, Colorado (Table 3-19). The goal of the workshop was to bring together a number of experts in order to define issues related to the saturated zone that were important to repository performance, in particular, issues concerning transport travel times and dilution. The issues were then evaluated to determine if they were sufficiently well understood and accounted for in the modeling. If not, analysis plans were developed to address the issue. Some analyses had an indirect effect on TSPA-VA; for example, the study of how structural controls, such as faults, influenced flow and transport aided in the development of, but did not explicitly produce, a distribution for effective porosity. Other analyses were specifically directed toward TSPA-VA modeling; for example, the convolution integral method (Section 3.7.2) was developed and tested as part of this effort. The analysis plan concerning climate directly led to modeling that derived the groundwater fluxes used in TSPA-VA for future climates.

In addition to the workshop, an expert elicitation was conducted to provide guidance for the saturated zone component of TSPA-VA. Five panelists participated in the expert elicitation to assess the uncertainty in conceptual models of processes and specific parameter values relevant to the saturated zone. The elicitation process consisted of the following:

- Written and oral presentation of data to the experts by researchers from the YMP
- Exchange of opinions and assessments among the panel members
- Formal interviews with the individual experts to elicit assessments of key issues

The experts expressed their general opinions about the appropriate conceptual models for flow and transport in the saturated zone and provided probabilistic distributions for some key parameters (CRWMS M&O 1998g, pp. 1-1 to 1-7).

The experts generally agreed that groundwater in the saturated zone flows from beneath the repository to the southeast and south primarily through fractured volcanic tuffs of the middle volcanic aquifer and the valley fill alluvium. Some panel members suggested that sorptive characteristics of

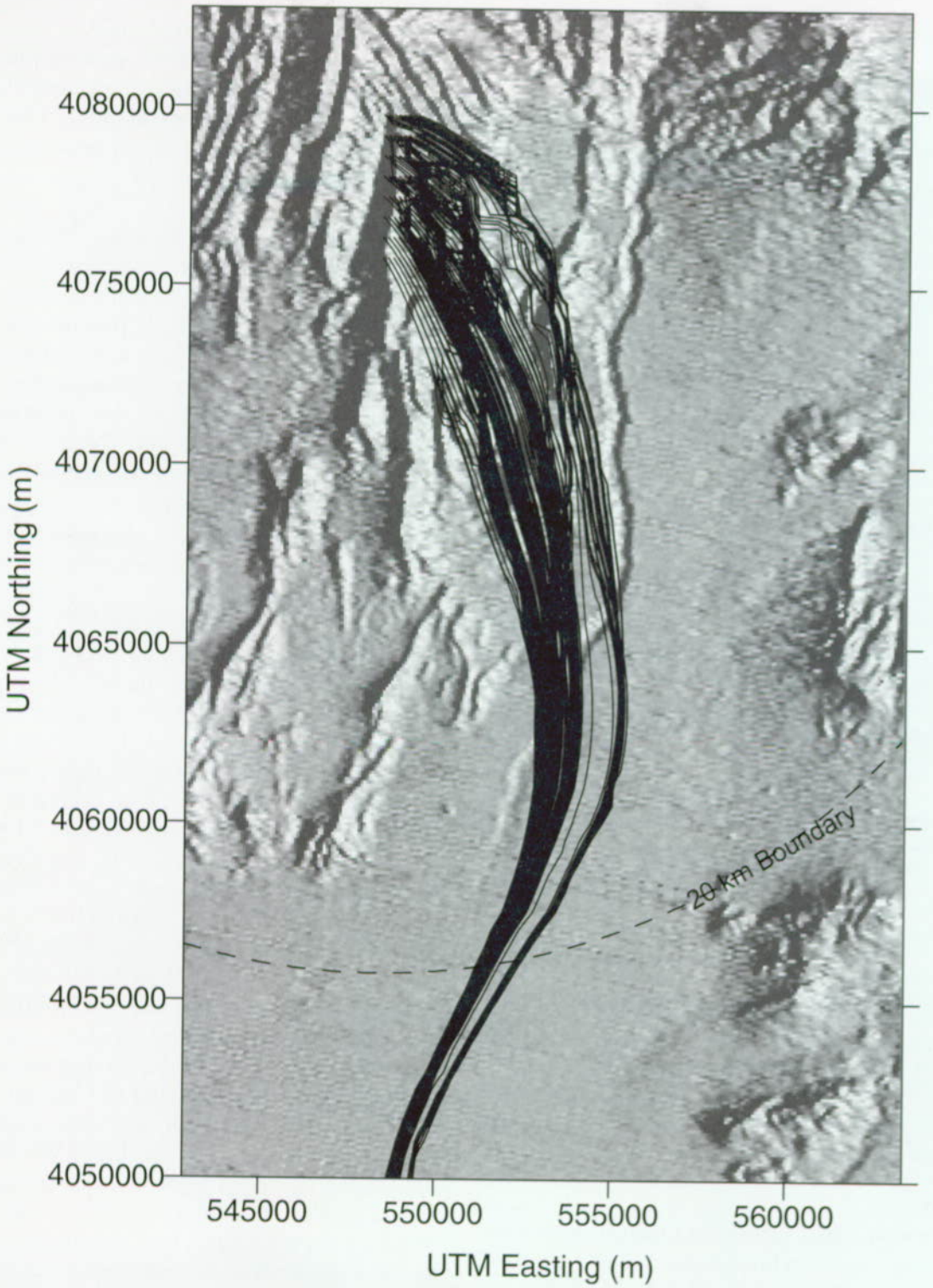

Figure 3-67. Simulated Particle Paths from the Total System Performance Assessment for the Viability Assessment Three-Dimensional Flow Model for the Saturated Zone
The simulated pathlines are superimposed on a shaded relief map of the surface topography. The transport model results shown are for a hypothetical release of a nonsorbing radionuclide at 10,000 years following the introduction of a source evenly distributed over the footprint of the repository.

Table 3-19. Saturated Zone Flow and Transport Abstraction/Testing Workshop

SATURATED ZONE FLOW AND TRANSPORT ABSTRACTION/TESTING WORKSHOP
April 1-3, 1997, Denver, CO
(CRWMS M&O 1997s)

PRIORITIZATION CRITERIA

- Does the process/issue affect the
  - Peak radionuclide concentration at 5 km from the repository?
  - Peak radionuclide concentration at 30 km from the repository?
  - Time to first arrival (1% of peak)?
  - Spatial distribution of the plume (both horizontal and vertical)?
  - Spatial distribution of groundwater flux (e.g., dilution at the unsaturated zone-unsaturated zone interface)?

HIGHEST PRIORITY ISSUES

- Conceptual models of saturated zone flow:
  - Regional discharge
  - Regional recharge
  - Vertical flow
  - Alternative conceptual models
- Conceptual models of saturated zone geology:
  - Channelization in vertical features
  - Properties of faults
  - Channelization in stratigraphic features
  - Distribution of zeolites
  - Fracture network connectivity
- Transport processes and parameters
  - Dispersivity
  - Matrix diffusion (effective porosity)
  - Matrix sorption
  - Fracture sorption
- Coupling to other components of TSPA
  - Climate change
  - Unsaturated zone and saturated zone coupling
  - Thermal and chemical plume
  - Well withdrawal scenarios

ANALYSIS PLANS

- Sensitivity study on uncertainties in site-scale saturated zone transport parameters and models
- Coupling unsaturated and saturated zone models
- The effects of large-scale channelization on effective transport parameters
- Determination of effective field-scale transport parameters using C-Wells testing results
- Past, present, and future saturated zone fluxes
- Geologic structure and processes affecting flow channelization

the alluvium could significantly contribute to retardation of some radionuclides. They expected faults and fracture zones to have important impacts on flow in the volcanic units. The panel members offered alternative hypotheses for the large hydraulic gradient north of Yucca Mountain, and there was disagreement regarding the importance of this feature to repository performance. The panel members did agree that any major transient change in the large hydraulic gradient is unlikely. The panel members generally concurred with interpretations of geochemical and paleospring data indicating water table rises of 80–120 m (260–390 ft) beneath the repository in response to past climatic variations.

For transport of contaminants in the saturated zone, the experts emphasized the limitations of processes that would cause dilution of contaminant concentrations. The experts believe that transport is by movement in vertically thin plumes through flow tubes beneath the repository. Dilution of contaminants occurs by vertical transverse dispersion and transient fluctuations in the direction of the hydraulic gradient. The experts generally rejected a mixed tank model in which contaminated flow from the unsaturated zone mixes on a large scale with uncontaminated groundwater in the saturated zone.

The dilution-factor distribution suggested by the experts was used to reduce the maximum concentration in the saturated zone at the source beneath the repository to the concentration in the groundwater approximately 20 km (12 miles) downgradient from the repository. The aggregate uncertainty in this parameter ranges from 1 to 100, with a median value of about 10. This range of values for dilution in the saturated zone represents a significant departure from previous TSPA analyses for Yucca Mountain (for example, CRWMS M&O 1995, pp. 7–23 and 7–25; Wilson et al. 1994, p. 11–35) in which effective values of dilution were typically orders of magnitude higher. The expert elicitation provided a median value for specific discharge in the saturated zone (0.6 m/year or 2 ft/year) that was used in the one-dimensional transport simulations for the TSPA-VA. Finally, the experts discussed what the effective porosity should be, that is, the fraction of the bulk volume of the aquifer that carries flow and solute transport. Some of the panel members believed that effective porosity for radionuclide transport in fractured volcanic rocks in the saturated zone could be as low as conservative estimates of fracture porosity, implying little diffusive interaction with the rock matrix. Consequently, the uncertainty distribution for effective porosity in fractured volcanic units

used in the TSPA-VA analyses has a maximum value equivalent to the average matrix porosity and a value of 1×10^{-5} at its lower end.

3.7.2 Implementation of the Performance Assessment Model

For the TSPA, a hierarchy of models was used to simulate the transport of radionuclides in the saturated zone. Explicit, three-dimensional modeling was not used to simulate radionuclide concentrations because it can generate numerical dispersion, which artificially lowers concentration. Three-dimensional modeling was used only to determine flow paths. One-dimensional transport modeling was used, based on the flow paths from the three-dimensional modeling, to determine concentration breakthrough curves at a distance of 20 km (12 miles) for unit releases of radionuclides. Then, within the TSPA calculations, the convolution integral technique described in Section 3.7.2.3 was used to combine the breakthrough curves with the time-varying radionuclide sources from the unsaturated zone. Finally, the radionuclide concentrations were divided at 20 km (12 miles) by the dilution factor, which was sampled from the distribution suggested by the expert elicitation process described above. These final radionuclide concentrations, corresponding to groundwater contamination in a hypothetical well, were used to calculate dose in the biosphere model. No additional dilution in the pumping well was considered in the analysis (Section 5.8.2 addresses issues related to dilution from well pumping).

3.7.2.1 One-Dimensional Flow and Transport Modeling

A diagrammatic representation of the conceptual model for saturated zone transport is shown in Figure 3-68. Simulations of radionuclide transport in the saturated zone for the TSPA calculations were performed with six one-dimensional flow tubes using FEHMN (Zyvoloski et al. 1995), a computer code for simulating heat and mass

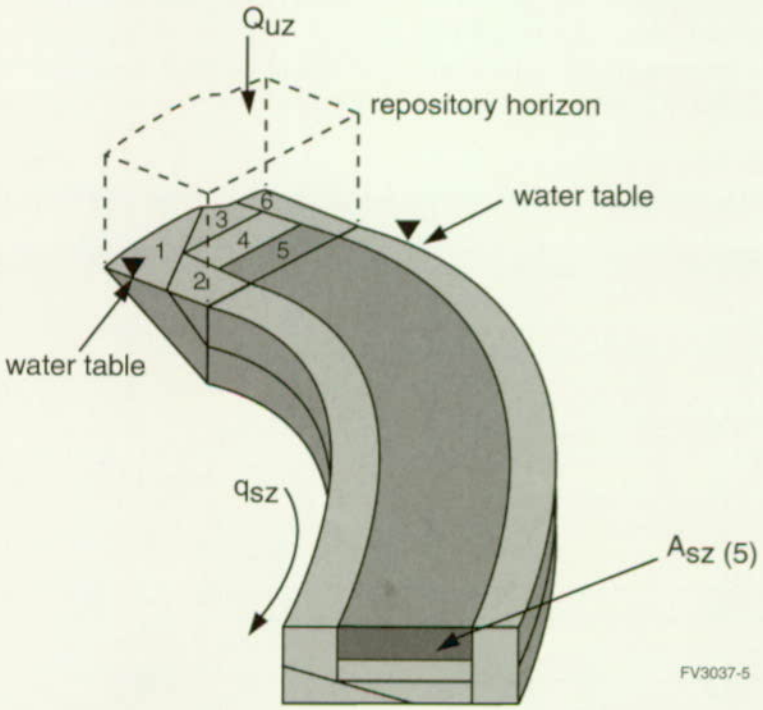

Figure 3-68. Schematic Diagram of the Conceptual Basis of the Total System Performance Assessment for the Viability Assessment One-Dimensional Transport Model for the Saturated Zone from Below the Repository to 20 km (12 miles) South

The six source subregions at the water table beneath the repository correspond to the six streamtubes in the saturated zone. The cross-sectional area of each streamtube (for example, $A_{sz}(5)$) is proportional to the volumetric groundwater flux through that streamtube. The specific discharge for groundwater in the saturated zone is q_{sz}.

transfer with finite elements. Streamtubes are taken from a concept in classical fluid dynamics that is used to visualize and estimate the behavior of the elements of a flow system. Each of the six streamtubes is a continuation of a groundwater flow path from the repository in the unsaturated zone. Note that the six source subregions at the water table shown in Figure 3-68 were used to divide radionuclide mass and groundwater flow among the streamtubes. The shapes of these subregions were defined to capture potential variability in radionuclide releases (e.g., edge versus center of the repository) and to capture geologic variability (e.g., presence of welded Bullfrog tuff at the water table in source subregion 1). The volumetric flux of groundwater through each streamtube (Q_{UZ}) was determined at the water table from flow simulations using the site-scale flow model developed by Bodvarsson et al. (1997) for the unsaturated zone (see Section 3.1). Transport simulations with the one-dimensional streamtube approach implicitly assume complete mixing of the radionuclide mass in the volumetric groundwater flux specified for each streamtube. The specific discharge within the streamtubes in the saturated zone (q_{SZ}) was 0.6 m/year (2 ft/year) for current climatic conditions. The streamtubes are 20 km (12 miles) long, with a regular grid spacing in the tubes of 5 m (16 ft). The four hydrostratigraphic units in the streamtubes are the middle volcanic aquifer, the upper volcanic aquifer, the middle volcanic confining unit, and the alluvium/valley fill. The lengths of these units within the streamtubes were defined by modeling particle transport using the TSPA three-dimensional flow model for the saturated zone described in Section 3.7.1.3.

3.7.2.2 Model Parameter Uncertainty

Uncertainty in radionuclide transport through the saturated zone was incorporated into the analysis by varying key transport parameters. The stochastic parameters used in the one-dimensional transport simulations were effective porosity in the volcanic units and the alluvium unit; distribution coefficients (K_ds) for sorbing radionuclides in the volcanic and alluvial units; the ratio of the radionuclide mass in aqueous and colloidal forms (K_c) for colloid-facilitated transport of plutonium; longitudinal dispersivity; the fraction of flowpath through the alluvium; and the dilution factor (Table 3-20).

A broad range of uncertainty in effective porosity for fractured volcanic units was employed in the

Table 3-20. Stochastic Parameters for Saturated Zone Flow and Transport

Parameter	Distribution Type	Distribution Statistics [Bounds]
Dilution Factor	CDF	Median=10, [1., 100.] (Section 3.7.1.4)
Effective Porosity (Alluvium)	Truncated Normal	Mean=0.25, SD=0.075 [0., 1.0]
Effective Porosity (Upper Volcanic Aquifer)	Log Triangular	[1e-5, 0.02, 0.16]
Effective Porosity (Middle Volcanic Aquifer)	Log Triangular	[1e-5, 0.02, 0.23]
Effective Porosity (Middle Volcanic Confining Unit)	Log Triangular	[1e-5, 0.02, 0.30]
Effective Porosity [Pu] (Volcanic Units)	Log Uniform	[1e-5, 1e-3]
K_d [Np] (Alluvium) (mL/g)	Uniform	[5., 15.]
K_d [Np] (Volcanic Units) (mL/g)	Beta (Approx. Exp.)	Mean=1.5, SD=1.3, [0., 15.]
K_d [Pa] (Alluvium) (mL/g)	Uniform	[0., 550.]
K_d [Pa] (Volcanic Units) (mL/g)	Uniform	[0., 100.]
K_d [Se] (Alluvium) (mL/g)	Uniform	[0., 150.]
K_d [Se] Volcanic Units) (mL/g)	Beta (Approx. Exp.)	Mean=2.0, SD=1.7, [0., 15.]
K_d [U] (Alluvium) (mL/g)	Uniform	[5., 15.]
K_d [U] (Volcanic Units) (mL/g)	Uniform	[0., 4.]
K_c [Pu] (All Units)	Log uniform	[1e-5, 10.]
Longitudinal Dispersivity (All Units) (m)	Log normal	Logmean=2.0, LogSD=0.753
Fraction Of Flowpath in Alluvium	CDF	[0., 0.3] (See Text)

CDF–cumulative distribution function
SD–standard deviation
Approx. Exp.–Approximate Exponential

TSPA-VA analyses to reflect uncertainty in the underlying processes affecting contaminant travel times in the saturated zone. The effective porosity is the fraction of the bulk rock volume that is available for storage of dissolved radionuclides during transport in the saturated zone. The effective porosity approach is a simplified representation of the system that includes the influences of molecular diffusion from fractures into matrix pore water and the spacing between fractures with flowing groundwater. The effective porosity approach also implies potential limited access of contaminants to the sorptive capacity of the rock matrix, an effect accounted for in the TSPA-VA simulations.

Colloid-facilitated transport of plutonium in the saturated zone was simulated using a conceptual model based on both equilibrium, reversible sorption of plutonium onto colloids and the potential for irreversible sorption of plutonium onto some colloidal particles (see Section 3.5). These two components of plutonium transport were included in the analysis. A large fraction of the plutonium mass was simulated to move through the saturated zone assuming chemical equilibrium among dissolved plutonium, plutonium sorbed onto colloids, and plutonium sorbed onto the aquifer material. This conceptual model uses the partition coefficient (K_c) to define the distribution of plutonium sorbed on colloids relative to the aqueous concentration of plutonium. The values of K_c were correlated in the saturated zone and unsaturated zone components of the TSPA-VA probabilistic calculations. A small fraction of the plutonium mass was simulated to be irreversibly attached onto colloids and transported relatively rapidly in the saturated zone, without significant retardation. This small fraction was defined to be consistent with the reduction in plutonium concentration inferred at the Benham site (Sections 3.5.2.4 and 3.6.1.4). The fraction of irreversibly sorbed plutonium used in the calculations implicitly considers partitioning of plutonium at the source and filtration during transport. Because attenuation of irreversible colloid-facilitated transport was implicitly included in characterization of the source term, filtration of colloids was not explicitly included in the saturated zone transport model. Colloid transport occurred only within the fracture porosity of the volcanic units, so the uncertainty distribution of effective porosity for colloids varied only over the estimated range of fracture porosity.

The stochastic parameters in the probabilistic analyses for saturated zone-flow and transport are summarized in Table 3-20. The dilution factor was applied to radionuclide concentrations to implicitly account for transverse dispersion out of the one-dimensional streamtubes. The uncertainty distribution for the dilution factor was a product of the expert elicitation described in Section 3.7.1. The travel distance through the alluvium/valley fill unit was varied from 0 to 6.0 km (0 to 3.7 miles), with a 10 percent probability that no alluvium is present along the 20 km (12 miles) of travel path for radionuclides in the saturated zone. The uncertainty in the fraction of the flowpath in alluvium was included to account for uncertainty in the flow system, which was not explicitly evaluated with the TSPA three-dimensional flow model.

3.7.2.3 Integration of Transport Modeling with Total System Performance Assessment Calculations

The convolution integral method was used in the TSPA calculations to determine the radionuclide concentration in the outlets of the six streamtubes, 20 km (12 miles) downgradient of the repository as a function of the transient radionuclide mass flux at the water table beneath the repository. This computationally efficient method combines information about the unit response of the system, as simulated by the TSPA one-dimensional transport modeling, with the radionuclide source history to calculate transient system behavior, as shown in Figure 3-69. The most important assumptions of the convolution method are linear system behavior (i.e., doubling mass input results in doubling of concentration) and steady-state flow conditions in the saturated zone.

The effects of climate change on radionuclide transport in the saturated zone were incorporated into the analysis by assuming instantaneous change from one steady-state flow condition to another steady-state condition in the saturated zone.

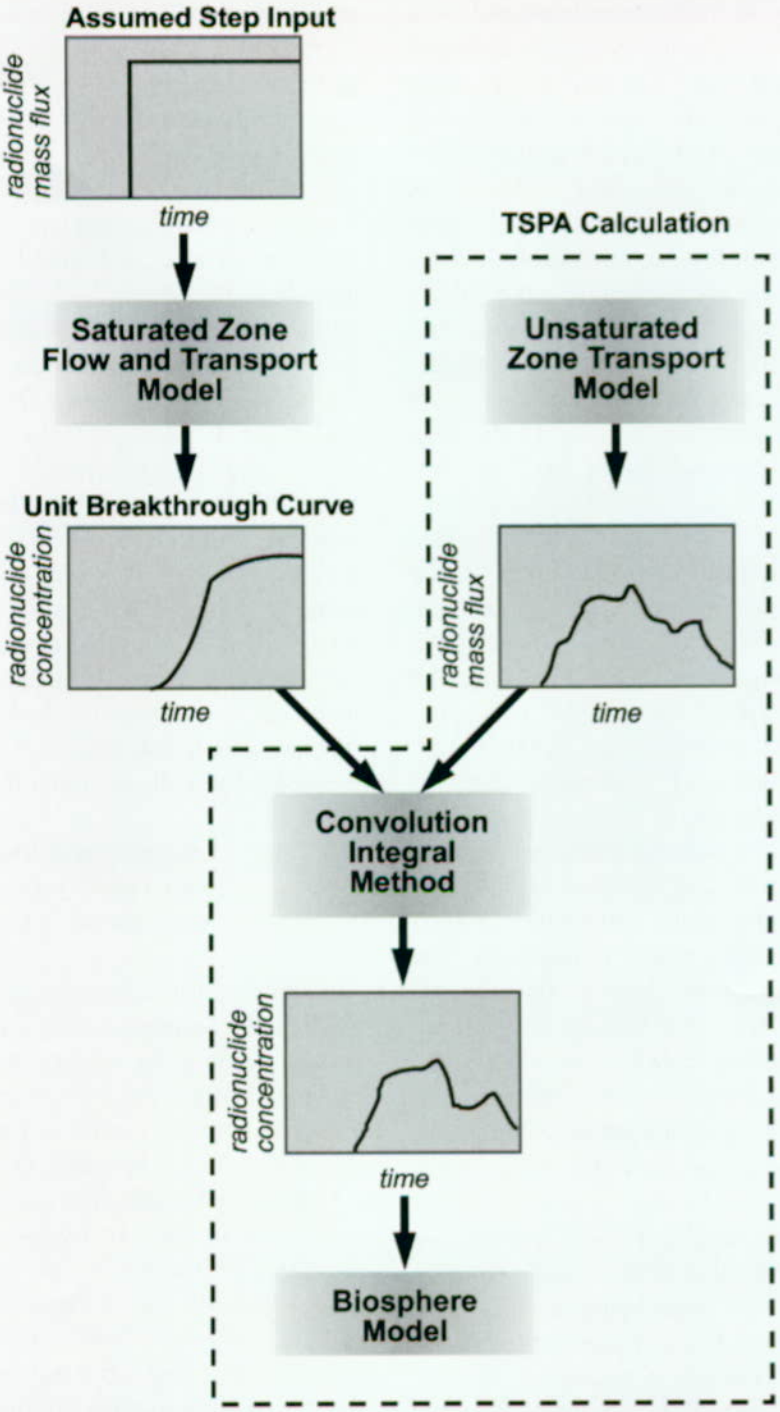

Figure 3-69. Flow Chart for Utilization of the Convolution Integral Method in Saturated Zone Flow and Transport Calculations in Total System Performance Assessment for the Viability Assessment
As illustrated in this flowchart, information on radionuclide travel times and concentrations in the saturated zone (contained in the unit breakthrough curve) is combined with information on radionuclide mass flux at the water table beneath the repository by the convolution integral method to calculate the radionuclide concentration history at 20 km (12 miles) downstream from the repository. The nature of the unit breakthrough curve varies significantly among Monte Carlo realizations (see Figure 3-71) to reflect uncertainty in the transport characteristics of the saturated zone.

Changes in climate state were assumed to affect the magnitude of groundwater flux through the saturated zone system but have a negligible impact on flowpaths. These effects were incorporated into the convolution method by scaling the velocity of radionuclide breakthrough curves proportionally to the change in saturated zone specific discharge. Also, the concentrations of the radionuclide breakthrough curves were scaled proportionally to the change in volumetric flux from the unsaturated zone into the streamtubes. The regional-scale flow model for the saturated zone provided estimates of the relative change in specific discharge in the saturated zone for future climate states (as summarized in e-mail message from Pat Tucci, 12/11/97; D'Agnese et al. 1997b). The site-scale flow model for the unsaturated zone (Bodvarsson et al. 1997) provided estimates of changes in volumetric flux through the repository horizon. These estimates are summarized in Table 3-21. Radioactive decay was also applied to radionuclide concentrations calculated with the convolution integral computer program. Ingrowth of radionuclide daughter products was not included in the saturated-zone transport calculations, but the inventory at the repository was adjusted to account for progeny ingrowth (Section 3.5.1.5).

Table 3-21. Climatic Alterations to Saturated Zone Flow

Climate State	Saturated Zone Specific Discharge (q_{SZ}) (m/year)	Volumetric Flux Through Repository Horizon (Q_{UZ}) (m^3/year)
Dry (Present)	0.6	26,900
Long-Term Average	2.3	146,300
Superpluvial	3.7	395,000

The radionuclide concentrations in the six streamtubes were decreased by the dilution factor and then summed to obtain an estimate of the maximum concentration in the saturated zone at 20 km (12 miles) from the repository. For this approximation it is assumed that, in a conceptual sense, implicit spreading of radionuclide mass from individual streamtubes via dilution causes six plumes that essentially overlap. At each time step, the maximum estimated concentration was compared to the maximum undiluted concentration at the source in the saturated zone. The maximum estimated concentration was not allowed to exceed the maximum undiluted concentration in any individual streamtube at the source (Section 5.7.3 contains an evaluation of methods for combining flow tubes).

3.7.3 Results and Interpretation

For the TSPA-VA, the results of the flow and transport analysis for the saturated zone are the radionuclide concentration histories at the geosphere/biosphere interface, which is a well head located 20 km (12 miles) downgradient in the Amargosa Valley region. These concentrations are directly proportional to the radiation dose rate calculated for possible future inhabitants.

A steady boundary condition for unit radionuclide mass flux was applied at the inlet of each streamtube for the TSPA one-dimensional transport simulations. The resulting unit breakthrough curves of concentration formed the basis for calculating radionuclide concentrations using the convolution integral method. The breakthrough curves for unit concentration for the nine radionuclides at 20 km (12 miles) from the repository are shown in Figure 3-70. These curves were generated using the expected parameter values. Differences in the arrival times of different radionuclides are because of variations in sorption among the radionuclides. Differences in the maximum concentration among radionuclides are because of radioactive decay during transport through the saturated zone system. To include parameter uncertainty in the TSPA, 100 breakthrough curves were simulated for each radionuclide by sampling parameter values from their respective probability distributions (see Section 3.7.2, Table 3-20). The impact of uncertainty in the one-dimensional transport simulations for the saturated zone is illustrated in Figure 3-71. This figure shows the unit breakthrough curves for technetium-99 concentrations for all 100 realizations used in the base case analyses. Travel times for the nonsorbing technetium-99 vary from a few hundred years to about 4,000 years; maximum concentrations, primarily influenced by the dilution factor, vary over two orders of magnitude among these simulations. The uncertainty in longitudinal dispersion is shown by variations in the slopes of the breakthrough curves in Figure 3-71.

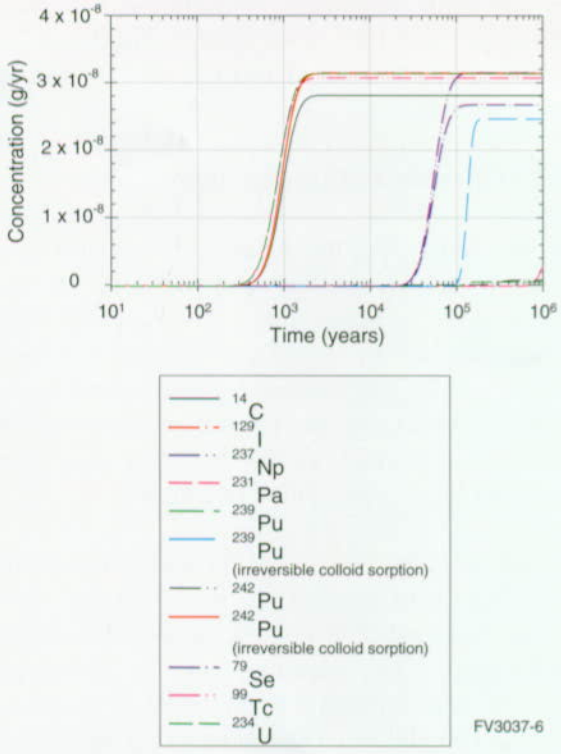

Figure 3-70. Unit Radionuclide Concentration Breakthrough Curves from the Total System Performance Assessment One-Dimensional Transport Modeling for the Saturated Zone at a Distance of 20 km (12 miles) for all Modeled Radionuclides
The radionuclide concentration breakthrough curves are shown for the expected parameter value case from source subregion 1 at the water table under dry climatic conditions, assuming a source mass flux of 1 g/year for each radionuclide spread over source subregion 1.

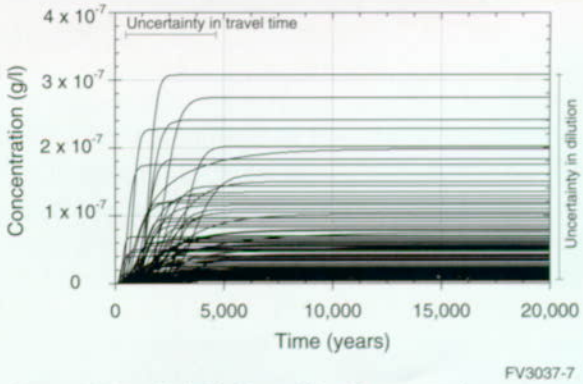

Figure 3-71. Unit Radionuclide Concentration Breakthrough Curves from the Total System Performance Assessment One-Dimensional Transport Modeling for the Saturated Zone at a Distance of 20 km (12 miles) for Technetium-99
The radionuclide concentration breakthrough curves are shown from source subregion 1 at the water table under dry climatic conditions, assuming a source mass flux of 1 g/year spread over source subregion 1. The uncertainty bars indicate the range of variability in the important characteristics of the saturated zone system in the TSPA-VA analyses.

Radionuclide migration through the saturated zone affects total system performance in two ways. First, the saturated zone may function as a mechanism for significant delay in releasing radionuclides to the biosphere. Second, there may be significant dilution of radionuclide concentrations that occurs during transport in the saturated zone. Both impacts are functions of the distance between the repository and the point of release to the biosphere, which is assumed for the TSPA-VA to be 20 km (12 miles) from the repository.

Delays in radionuclide migration caused by processes in the saturated zone are potentially important to repository performance if the travel time for a radionuclide through the saturated zone system is long in comparison to its half life. For example, in the expected-value case shown in Figure 3-70, the maximum concentrations of plutonium-239 (equilibrium colloid sorption) and selenium-79 are significantly attenuated relative to the other radionuclides because of radioactive decay. Delay in radionuclide migration in the saturated zone may also be significant if the travel time through the system is long relative to the time period of concern. For example, the travel time of unretarded radionuclides such as technetium-99 (see Figure 3-71) may be relevant to repository performance in a 10,000-year time frame. However, the delay in radionuclide release from the saturated zone for a period of 100,000 years for unretarded radionuclides would be insignificant. Retardation in the saturated zone for most of the radionuclides that experience sorption is highly uncertain, particularly with regard to sorption characteristics of the alluvium/valley fill material.

The dilution of radionuclide concentrations in the saturated zone is handled in a straightforward manner in the TSPA-VA calculations through the dilution-factor parameter. Although there is significant uncertainty in this parameter and complexity in the underlying processes that lead to dilution, the relationship between the dilution factor and

radiation dose rate is a simple linear function for a steady radionuclide source from the unsaturated zone. Transient peaks in the radionuclide concentration at the source in the saturated zone are also attenuated by longitudinal dispersion during transport in the saturated zone.

3.8 BIOSPHERE

The biosphere is that part of the earth where all living organisms reside, including all components of the environment, such as soil, water, and air. Of interest is how a potential high-level radioactive waste repository at Yucca Mountain could affect the biosphere. In particular, it is important to know how radionuclides move through the biosphere and how they might eventually impact the human inhabitants of the region. The primary measure of the repository performance is the annual dose of radiation that would be received by an individual living in the region.

The biosphere scenario adopted for the base case assumes a reference person who is living 20 km (12 miles) from a potential repository at Yucca Mountain, in the Amargosa Valley region. The 20-km (12-mile) distance is not a regulatory boundary, as no performance regulation presently exists for a repository at Yucca Mountain; it was selected for TSPA-VA because it marks the closest present-day habitation to Yucca Mountain. People living in the community of Amargosa Valley are considered to be the group of people most likely to be affected by radioactive releases (the critical group), because of their proximity to Yucca Mountain, and because the Amargosa valley region is hydraulically down-gradient from the potential repository site (Luckey et al. 1996, p. 14). The reference person is intended to be representative of this group: an adult who lives year-round at this location, uses a well as the primary water source, and otherwise has habits, such as the consumption of local foods, that are similar to those of inhabitants of the region. Because changes in human activities over millennia are beyond current capabilities to predict, the present-day reference person is also assumed to be typical of future inhabitants.

A survey was conducted of inhabitants residing within an 80-km (50-mile) grid centered on Yucca Mountain to collect information for several programs, with a primary emphasis on biosphere modeling. Over one thousand interviews were completed for the survey, including 43 percent of the households in the Amargosa Valley. The survey collected dietary and lifestyle information on adults and was used to define the food consumption of the reference person.

Incorporation of the biosphere into the TSPA-VA calculations involved two steps. The first step was creating a model of the reference person and the biosphere pathways that might direct radionuclides to that person. The model was implemented in an accepted computer program for predicting radiation dose, GENII-S (Leigh et al. 1993). Model parameters were quantified using the regional survey, other site-specific data, and data from accepted national and international sources. The model uses a unit concentration of a radionuclide in water as the input, and produces a biosphere dose conversion factor for that radionuclide as the output. The biosphere dose conversion factor includes the effects of various pathways through the environment (e.g., irrigation and uptake of a contaminant by vegetables, then ingestion by the reference person), as well as various pathways through the reference person (e.g., the fraction of the contaminant that is taken up by the reference person, where it is accumulated in the body, and its retention time).

The second step required calculating radionuclide concentrations in the groundwater and multiplying them by the appropriate biosphere dose conversion factors. The end product of these calculations is prediction of the annual radiation dose to the reference person, the primary performance measure for TSPA-VA.

An overview of how the biosphere component fits in TSPA-VA is depicted in Figure 3-72.

In addition to the biosphere scenario considered for the base case, comparative analyses were performed to examine the impact of several assumptions. In addition to a typical Amargosa Valley adult resident, two other types of inhabitants

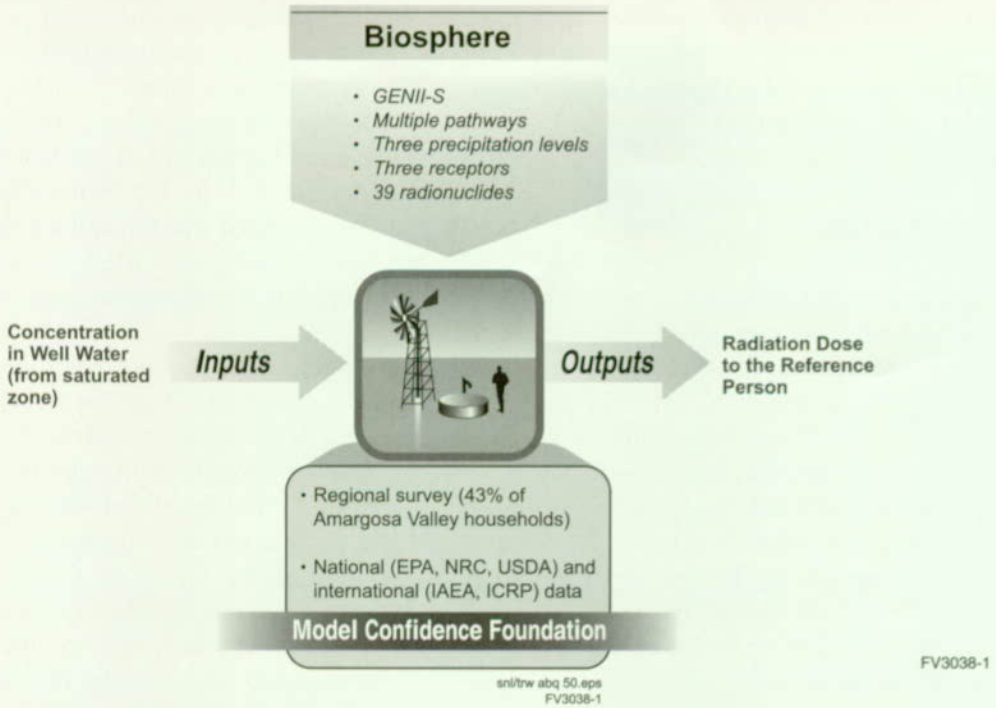

Figure 3-72. Overview of the Modeling Process Employed in the Biosphere Component of Total System Performance Assessment for the Viability Assessment

were considered. One was a subsistence farmer who takes all drinking water from a local well and only consumes locally produced foodstuffs. The other was a resident farmer whose food consumption is 50 percent locally grown but who still gets all drinking water from the well. Also, scenarios involving climate change and a volcanic eruption (Section 4.4.2) at Yucca Mountain were considered.

The biosphere pathway/dose modeling studies and analyses presented in this section were prepared with the view of addressing selected aspects of the NRC Key Technical Issues on Total System Performance Assessment and Integration (NRC 1998a) and Unsaturated and Saturated Flow under Isothermal Conditions (NRC 1997e; 1997f). Specifically, the information presented is pertinent to the TSPA integration subissue on model abstraction and on the unsaturated and saturated zone flow and transport subissue of ambient flow conditions in the saturated zone as those conditions affect evaluations of dilution caused by pumping.

3.8.1 Construction of the Conceptual Model

Yucca Mountain lies in a semi-arid, sparsely populated region between the Great Basin and the Mojave Deserts in southern Nevada. The local vegetation is primarily desert scrub and grasses. The mean annual precipitation in the area is about 170 mm/year (6.7 in./year) and the mean annual temperature is about 16°C (61°F). The nearest community in the direction of flow of groundwater is Amargosa Valley (Figure 3-73), an area of approximately 500 miles^2 defined as a tax district by the Nye County commissioners in the early 1980s. Within this district the closest inhabitants to Yucca Mountain are approximately 20 km (12 miles) south at the intersection of US 95 and Nevada State Route 373, in the location known as Lathrop Wells. There are about eight inhabitants at this location. The closest agricultural area and where the majority of the people live is the Amargosa Farms area located approximately 30 km (20 miles) to the south of Yucca Mountain. The Amargosa Farms area is a triangle of land bounded by the Amargosa Farm Road to the north, Nevada State Route 373 to the east, and the California border running from the northwest to the

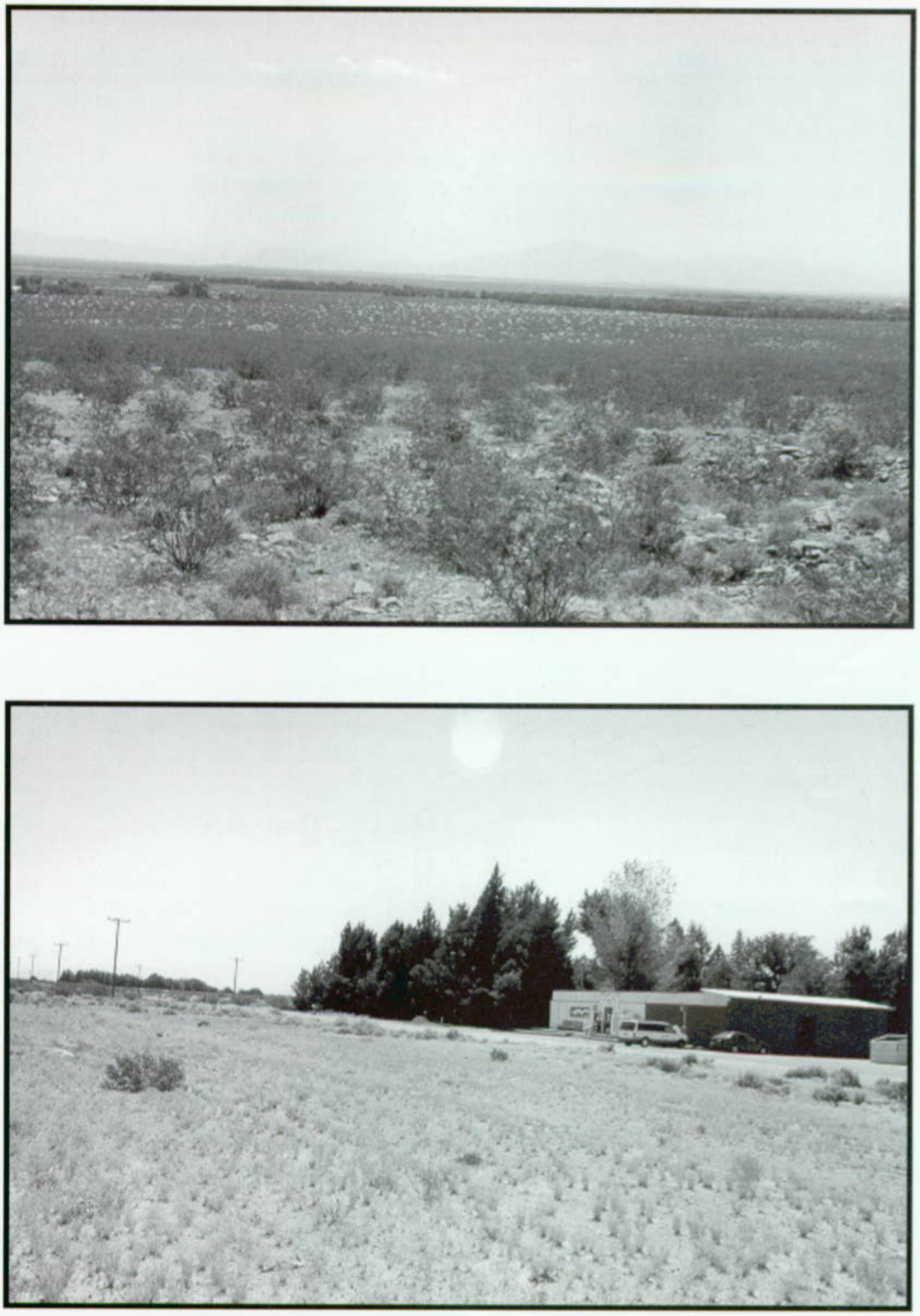

Figure 3-73. Present-Day Biosphere in the Amargosa Valley
The upper photograph shows a view of the Amargosa Valley looking eastward from the edge of the Funeral Mountains. The lower picture is the general store in the community.

southeast. The next community in the direction of groundwater flow is across the California state line in Inyo County. The community known as Death Valley Junction is about 60 km (40 miles) south of Yucca Mountain and has a permanent population of less than 10. Evaluation of water flow and wind patterns suggests that any contamination from a repository at Yucca Mountain could spread south and east into this region.

The Amargosa Valley region is primarily rural agrarian in nature (Figure 3-74). Agriculture is mainly directed toward growing livestock feed, for example, alfalfa; however, gardening and animal husbandry are common. Water for household uses, agriculture, horticulture, and animal husbandry is primarily acquired from local wells. Although sparsely populated, the Amargosa Valley region does support a population of 1,270 in approximately 450 households (CRWMS M&O 1997k, Section 2.4; CRWMS M&O 1997i). Commercial agriculture in the Amargosa Valley farming triangle area includes a relatively large dairy that operates with approximately 4,500 milk cows and employs approximately 50 people, a garlic farm that produces about 2,000 lbs. of garlic per year, and a catfish farm that sustains approximately 15,000 catfish. The area contains approximately 1,800 acres planted in alfalfa, 30 acres in oats, 80 acres in pistachios, and 10 acres in grapes. There is a general store, community center, senior center, library, medical clinic, elementary school, restaurant, hotel-casino, and a motel.

To help understand how to best model the biosphere for TSPA-VA, a workshop was held in Las Vegas, Nevada (Table 3-22). The workshop primarily reinforced the modeling strategy that was initially developed for the YMP—to investigate the radiological effects on a "reference person" (the person likely to be exposed to radionuclides released from a repository at Yucca Mountain) living near Amargosa Valley. Analyses were defined that would direct the modeling more toward the goals of TSPA-VA, especially in defining the habits of the reference person that would be modeled and the climates that would be modeled. No expert elicitation was conducted for the biosphere component of TSPA-VA.

Table 3-22. Biosphere Abstraction/Testing Workshop

BIOSPHERE ABSTRACTION/TESTING WORKSHOP
June 2–3, 1997, Las Vegas, NV
(CRWMS M&O 1997a)

PRIORITIZATION CRITERIA
- To what extent does the issue/process affect the following:
  - Individual dose?
  - Population dose?
  - The range or uncertainty in the resultant biosphere dose conversion factor?

HIGHEST PRIORITY ISSUES
- Critical group:
  - Extrapolation of present habits to the future
  - Location of critical group
  - Habits of critical group
- Biosphere pathways:
  - Which radionuclides
  - Soil build up
  - Climate change effects as it impacts pathways only
- Geo-biosphere interface—present and future:
  - Location and definition of bio/geosphere interface
  - Climate change effects as it impacts interface only
  - Important radionuclides transferred by disruptive events

ANALYSIS PLANS
- Critical group definition
  - Biosphere pathways variability
  - Climate

3.8.1.1 Model Basis

The strategy used to conceptualize the Amargosa Valley environment for the TSPA-VA biosphere component was to be consistent with similar activities being pursued by the international scientific community. In this regard, guidance was taken from the National Research Council (National Research Council 1995) and the Biosphere Model Validation Study II Steering Committee (BIOMOVS II 1994). The steering committee established a reference biosphere working group to develop consensus on an approach to evaluating long-term effects of radioactive-waste disposal systems (BIOMOVS II 1996). In developing the model basis for the biosphere component of TSPA-VA, the recommended methodology for biosphere analysis and the list of features, events, and processes developed by the international participants of the steering committee and the working group were used. The TSPA-VA biosphere component focuses on an individual—the

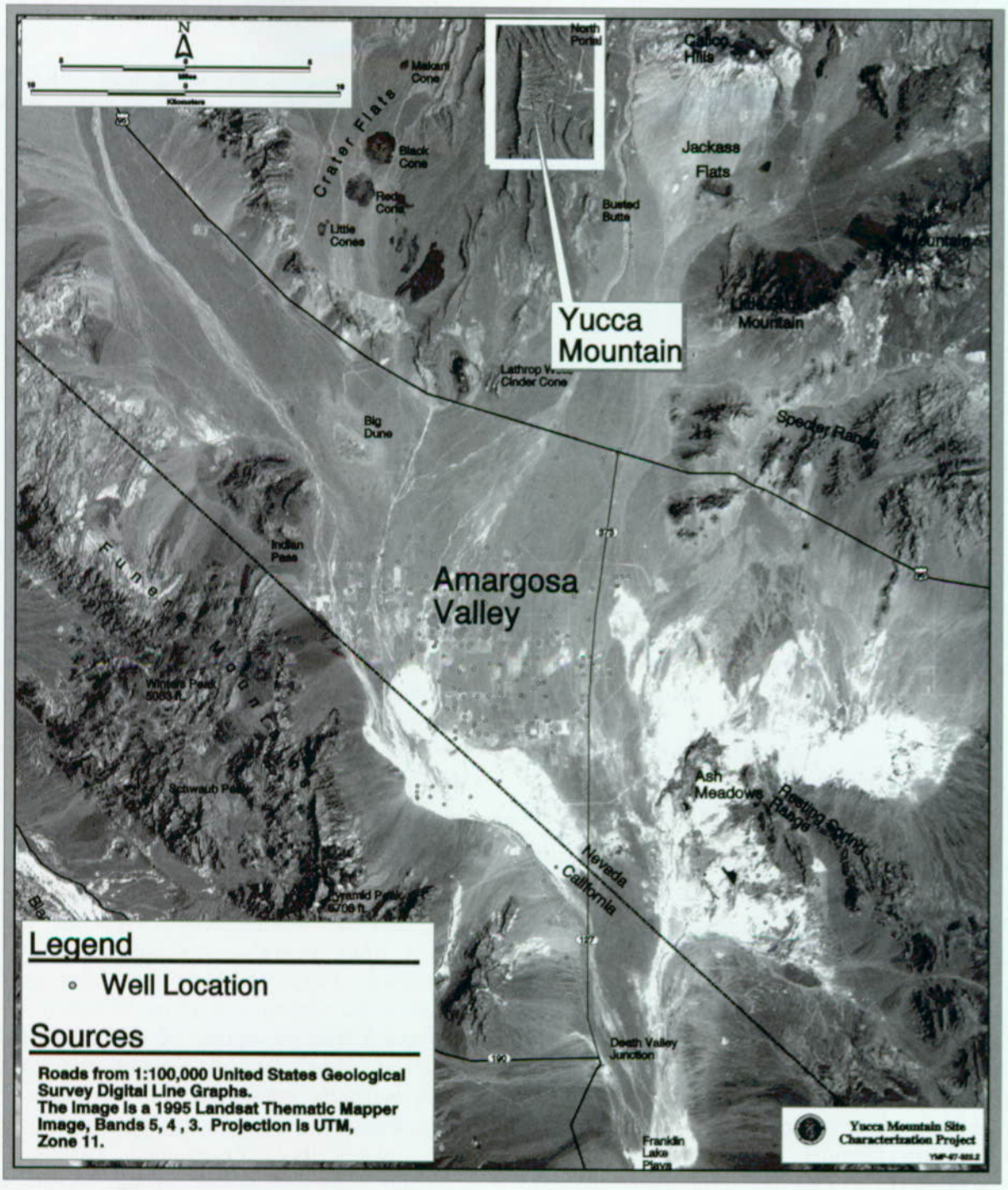

Figure 3-74. Satellite Image Showing the Yucca Mountain Area Including the Amargosa Valley Area
Amargosa Valley is the nearest populated area to Yucca Mountain that would be affected by radionuclide release and subsequent transport by groundwater from the repository.

reference person—living in an Amargosa Valley environment that might change over time. Consistent with guidance from the National Research Council (National Research Council 1995, p. 52), this reference person is defined as the average member of the "critical group," where the critical group is composed of those individuals expected to receive the highest doses as a result of the discharges of radionuclides from a repository. Because predicting future human technologies, lifestyles, and activities are beyond this TSPA effort, it is assumed that the present-day inhabitants of the region are similar to future inhabitants. This assumption has been accepted in similar international efforts at biosphere modeling, and is preferable to developing a model for a future society.

Climate conditions could become wetter in the future, so two other climates were considered: a long-term average climate, which is colder and wetter than the present climate; and a superpluvial climate, which is much colder and wetter than the present (Section 3.1). The mean annual precipitation rate for the long-term average climate is estimated to be about twice the present-day rate; the mean annual precipitation rate for the superpluvial is estimated to be about three times the present-day rate. The major impact of these different climates on the reference person is to reduce the amount of well water required for irrigation. Other climate effects, for example, a rise in the water table and the appearance of springs, seeps, or other surface water, are not directly considered (although by assuming no dilution in the well withdrawal, the end result would be the same as if the water came from a spring).

The reference person is an adult; children are not considered in TSPA-VA. The closest distance people presently live to Yucca Mountain is just over 20 km (12 miles). In this area, groundwater depth is approximately 100 m (328 ft). Closer to Yucca Mountain, groundwater is at a depth of greater than 200 m (656 ft), which imposes economic constraints on agricultural uses of land. The reference person lives year-round on a farm or in a similar domicile. The person has a garden and livestock and access to locally grown food. The person consumes locally grown food in types and amounts typical of present-day inhabitants. The person takes all water for agriculture and domestic uses from wells.

Except for releases associated with volcanism (Section 3.8.3.3), the assumption is that contaminated well water is the only way that radionuclides from the repository can reach the reference person. It is also assumed that the reference person takes all water from a well at the point of the highest concentration of radionuclides at the distance under consideration. A further assumption is that no dilution of the contaminated water occurs during pumping of the well. (Section 5.8.1 contains an investigation of the effects of some of these assumptions.)

3.8.1.2 Pathways

Radiation dose to the reference person occurs via exposure pathways. A pathway is the route taken by a contaminant through the biosphere from its source until it interacts with a human. For example, one pathway is from well water to soil via irrigation, from soil to dust via resuspension, from dust to human lungs via inhalation. Exposure pathways fall in three principal categories: ingestion pathways, inhalation pathways, and external exposure pathways (Figure 3-75).

Primary ingestion pathways include the consumption of drinking water, the consumption of locally produced crops irrigated with contaminated water, and the consumption of meat and dairy products from livestock given contaminated water and fodder. Major uncertain or variable factors that affect the ingestion pathways include the leaf interception fraction, uptake of radionuclides by plants and animals, and the amounts of contaminated foodstuffs consumed. In the biosphere model, livestock and poultry are sustained only by locally grown feed, for example, pasture and seasonally harvested alfalfa. These animals are exposed to the groundwater-derived radionuclides by watering and by consuming radionuclides present in the plant tissues. Alfalfa is the predominant crop produced in the Amargosa Valley and alfalfa and forage grasses comprise a major proportion of Nye County agricultural land

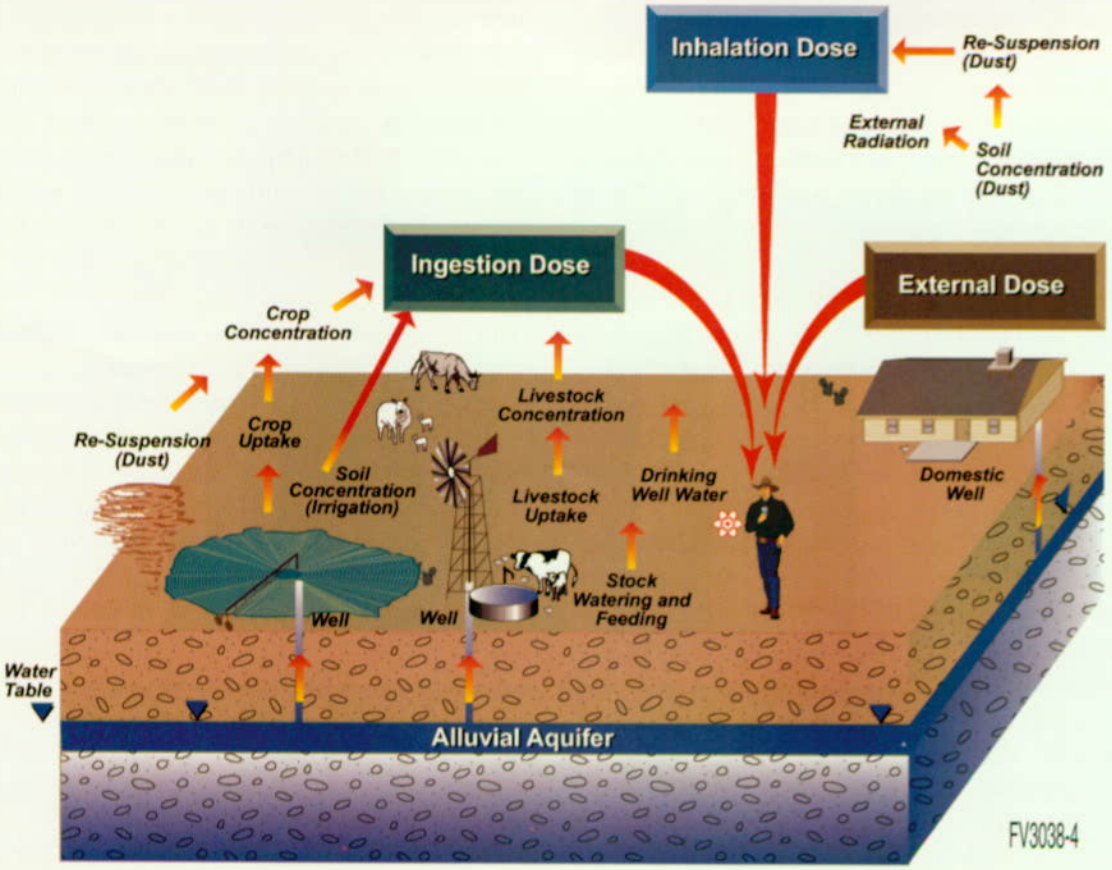

Figure 3-75. Illustration of the Biosphere Modeling Components and Pathways Contributing to Three Major Dose Categories to Humans
The categories are the ingestion of contaminated food and water, the inhalation of contaminants, and the direct exposure to contaminated soil.

(LaPlante and Poor 1997, p. 2-6). Another ingestion pathway is the inadvertent ingestion of contaminated soil, such as while eating vegetables.

The inhalation pathways involves breathing dust during outdoor activities such as farming and recreation. Uncertainty in the parameters describing this pathway results from difficulties establishing quantities of radionuclides associated with the suspended particles as well as the quantities of material inhaled by residents in the Amargosa Valley. Some of the factors that affect dust resuspension are the density and mineralogical composition of the soil particles and their effects on radionuclide binding, changes in binding and retention of the sorbed radionuclides through time, and the amount of time residents spend outdoors.

The external exposure pathway results from proximity to a radiation source that is external to the body. This pathway is also called "ground shine" when the contaminants are on the ground; but the pathway includes submersion when the contaminants are in the atmosphere, or immersion when in water. Again, there is uncertainty in the dose from this pathway due to differing habits, such as time spent outdoors, time working irrigated crops, or time bathing/showering.

3.8.1.3 Regional Survey

A survey of people living in the area was completed in 1997. Among other reasons, the survey was designed to permit an accurate representation of dietary patterns and lifestyle characteristics of residents within the 80-km (50-mile) radiological monitoring grid surrounding Yucca

Mountain. The survey was focused on the Amargosa Valley region, but included Beatty, Indian Springs, and Pahrump (Figure 3-76). Of special interest was the proportion of locally grown foodstuff that was consumed by local residents, that is, irrigated with the potentially contaminated groundwater, and details of what food types were eaten on a regular basis.

An initial small-scale survey was conducted in January and February 1997 to facilitate the process of defining the requirements for a more comprehensive survey. Using the knowledge gained from the initial survey, questionnaire design and interviewing procedures were established, and a full-scale sample survey was conducted in the spring of 1997. The full survey included an inverse gradient sample design to provide for more comprehensive survey representation of the inhabitants closer to Yucca Mountain. It was estimated that 13,000 adults reside in the survey area, with 900 adults (7 percent) residing in the Amargosa Valley. The fraction of households contacted over the entire survey area was 16 percent. This fraction ranges from 43 percent in Amargosa Valley to 11 percent in Pahrump (Table 3-23).

Table 3-23. Adults Surveyed for the Food and Water Consumption Model

Community	Households		
	Number Surveyed	Total Number	Percent Surveyed
Amargosa Valley	195	452	43
Beatty	250	751	33
Indian Springs	65	529	12
Pahrump	569	4,993	11
Total	1,079	6,725	16

The survey was conducted within the context of federal guidelines on minimizing respondent burden (Paperwork Reduction Act of 1995, as amended). As was the case for the pilot survey, the comprehensive survey questionnaire design followed the principles developed by the U.S. Office of Management and Budget (OMB 1983a; OMB 1983b). Underlying the entire project were Dillman's (1978) total design method principles and interviewing standards promulgated by the Institute for Social Research, University of Michigan (Guenzel et al. 1983), to maintain high response rates and accuracy. To ensure accuracy, the survey aimed at minimizing sample error and non-sampling error (Andersen et al. 1979, pp. 1-14). The survey included Spanish language interviews to accommodate respondents whose primary language is Spanish. Measures were taken to compensate for subjects who were difficult to interview. Additionally, demographic information was used to compensate for any gender bias that may have arisen (Dillman 1978, p. 248).

The biosphere modeling required estimates of annual consumption of selected foods in terms of weight. Although it was not feasible to collect this type of information directly through the survey, it was feasible to collect frequency information on food consumption. Therefore, data taken from tables compiled through national surveys on food intake (U.S. Department of Agriculture 1993, pp. 18–29) were combined with information from the survey to produce estimates of annual quantities, in kilograms, of the various food groups consumed (CRWMS M&O 1998i, Section 9.4.4.2). The percentage of survey respondents consuming well water and locally produced food from Amargosa Valley and the remainder of the survey area are shown in Figure 3-77. Estimates of the annual quantities of the various food groups are shown in Figure 3-78.

In general, a higher percentage of locally produced food is consumed by residents in the Amargosa Valley than residents in the remainder of the survey area. Well water is consumed by nearly 88 percent of Amargosa Valley residents while 79 percent did so in the remainder of the survey area. Nearly 80 percent of the survey respondents reported consuming locally produced food of some type over the past year in the Amargosa Valley, while only about 57 percent did so in the remainder of the survey area. Thus Amargosa Valley residents have food consumption habits that make them more susceptible to radionuclide intake through the ingestion pathway than their immediate neighbors, supporting their designation as a likely population that includes the critical group.

The survey data were stratified into six subsets to evaluate each group for their appropriateness to represent the three potential reference persons (Section 3.8.3.2)—a statistically average person, a

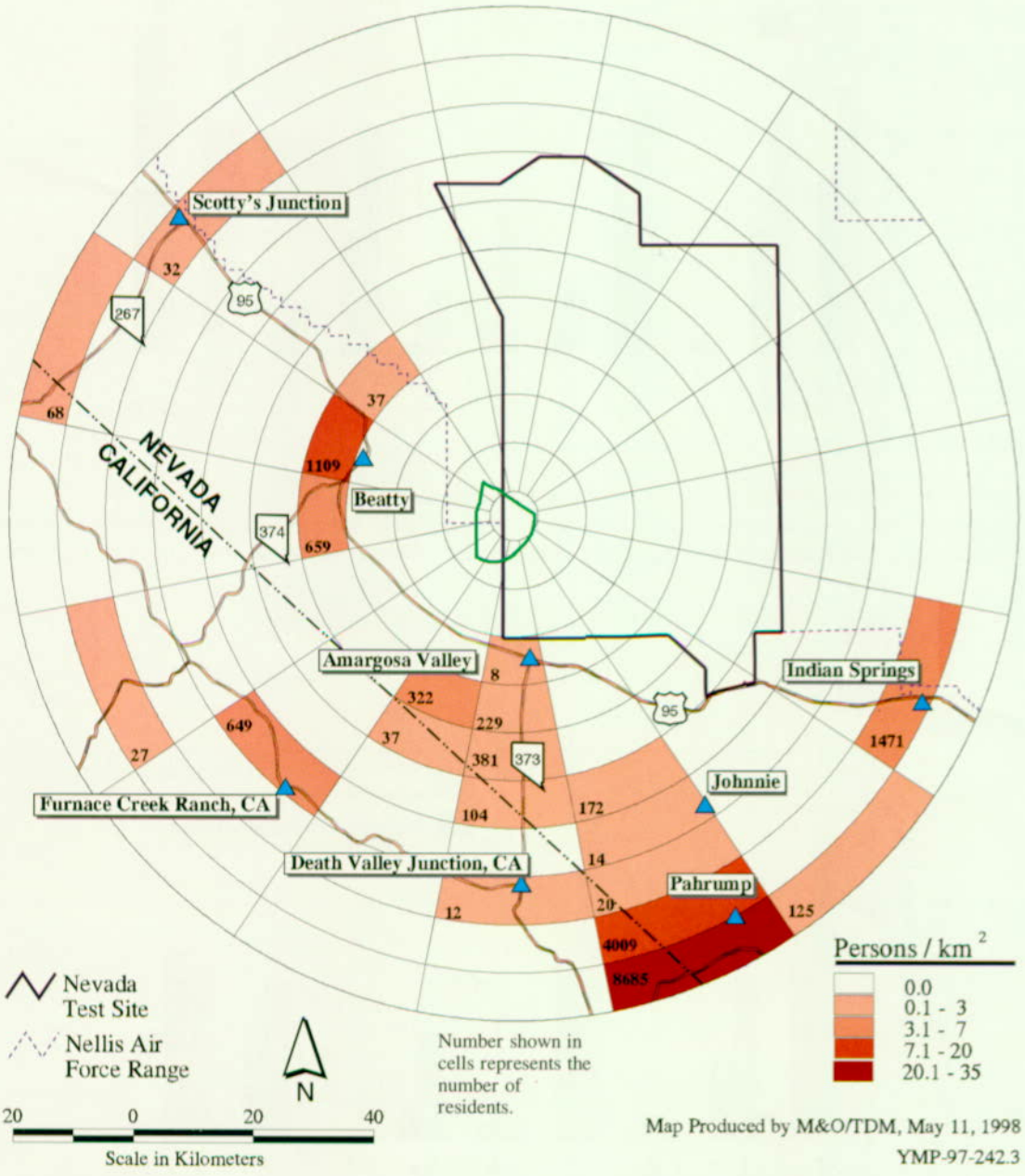

Figure 3-76. Map Showing the Number of Permanent Inhabitants Included in the Biosphere Modeling Work Group's Regional Food and Water Consumption Survey
A larger percentage of people were surveyed in the Amargosa Valley because of proximity to the potential repository.

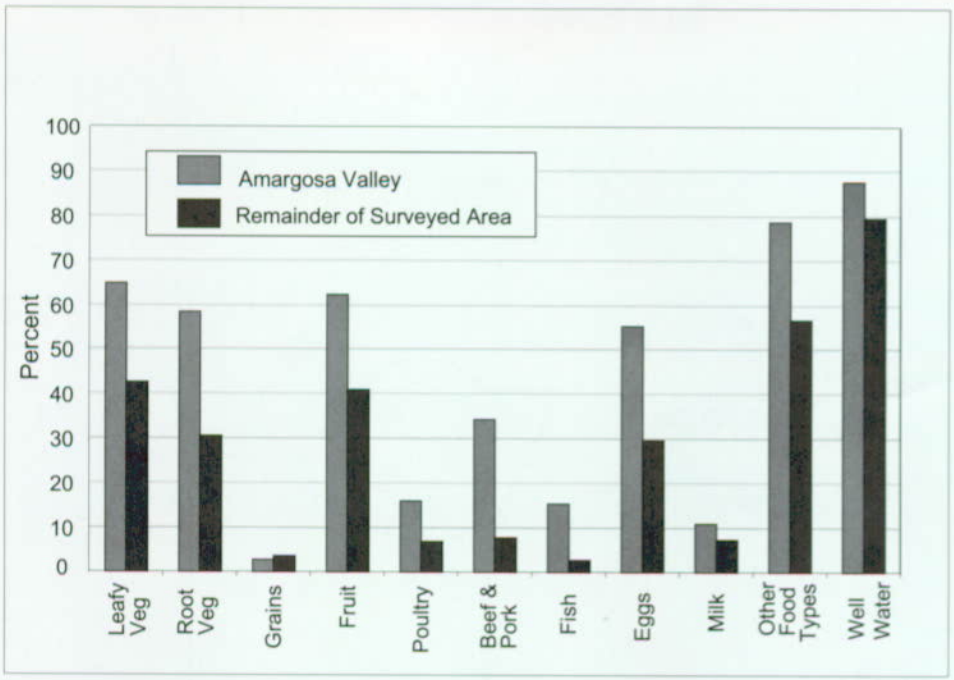

Figure 3-77. The Biosphere Regional Food and Water Consumption Survey
The survey found that a higher percentage of Amargosa Valley residents consume locally produced foods (with the exception of grain) and well water than those in the remainder of the survey area which included Pahrump and Beatty.

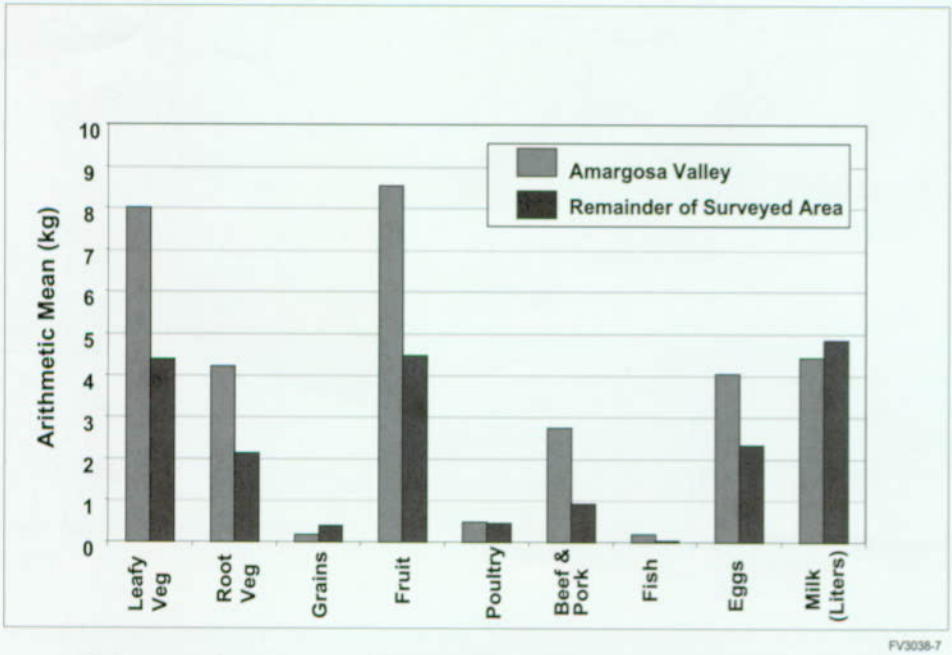

Well water: **Amargosa residents consumed 684 liters.**
Remainder of surveyed area consumed 646 liters.

Figure 3-78. Quantities of Locally Produced Food and Well Water Consumed by Amargosa Valley Residents
Survey data show that Amargosa Valley residents annually consume substantially greater quantities (kg) of locally produced food and well water than the residents in the remainder of the survey area.

Table 3-24. Receptor Types Considered in the Total System Performance Assessment Biosphere Modeling Effort (CRWMS M&O 1998i, Ch. 9)

Biosphere Modeling Receptor	Regional Survey Data Subset Correlate	Comments
Subsistence Farmer: Consumes only locally produced food and tap water. Adult spends large amount of time (about 17 hours/day) outdoors engaged in activities required to maintain subsistence. [Represents upper limit of contamination exposure]	Total survey subsistence resident adult	Survey data set for Amargosa Valley subsistence resident adult was deemed too small of a population to yield statistically meaningful interpretations for parameter development.
Residential Farmer: Relative to the subsistence farmer, this receptor consumes half the quantity of locally produced food, (but the same quantity of water) and spends less than half as much time engaged in outdoor activities and about 10 hours/day on weekdays and 5 hours/day on weekends outside Amargosa Valley.	None	This receptor is intended to represent the "median" level of exposure risk relative to the subsistence farmer and the average Amargosa Valley resident.
Average Amargosa Valley Resident: Adult living the average lifestyle of an Amargosa Valley resident. Consumes some locally produced food, almost as much tap water as the other two receptors (about 1.8 L/day versus 2.4 L/day), and spends about 10 hours/day outdoors on weekdays.	Amargosa Valley total population resident adult	Survey data set for Amargosa Valley total population resident adult was sufficiently large to yield statistically meaningful interpretations for parameter development. Because of its proximity to Yucca Mountain, this data subset was deemed more appropriate than the total survey area total population resident adult data set.

resident farmer, and a subsistence farmer (Table 3-24). No person interviewed in Amargosa Valley completely fit the description of a subsistence farmer; consequently, the data from the total survey area for subsistence residents were used to represent a subsistence farmer for the sensitivity studies. Also, none of the survey data subsets were considered to be representative of the resident farmer. The residential farmer was thought to be more representative of a member of the critical group currently residing in Amargosa Valley. For the TSPA-VA base case, the average person was selected as the reference person, again to be consistent with guidance from the National Research Council (National Research Council 1995, p. 52).

3.8.2 Implementation of the Performance Assessment Model

The complexity of the biosphere conceptual model requires a computer program to analyze all the factors. For performance assessment, the biosphere is only one of many component models, and a complex biosphere model is inappropriate for direct inclusion into the TSPA-VA calculations. Therefore, a two-phased approach was used. First, a complex computer model of the biosphere was used to generate biosphere dose conversion factors for each radionuclide of interest. Second, the annual dose from each radionuclide was calculated by forming the product of the biosphere dose conversion factor and the radionuclide concentration in groundwater as predicted by the TSPA computer program. The total annual dose to the reference person was then compiled as the sum of the individual annual doses from all radionuclides.

A biosphere dose conversion factor is a multiplier that converts radionuclide concentration in the groundwater at the well into an annual dose received by a human. To accurately predict the annual dose, the model used for generating the biosphere dose conversion factor must take into account all significant features, events, and processes involved. The model takes into account the pathways taken by radionuclides from a source (in the base case, well water) to and within a human (pathways and radiation dose within a human are approximated using a dose conversion factor). While the TSPA base case considers only nine radionuclides (Section 3.5.1.5), biosphere dose conversion factors were calculated for a unit concentration of 1 pCi/L for 39 radionuclides, including the nine in the base case. The biosphere dose conversion factors were generated by performing multiple evaluations of the biosphere model using input parameters sampled from

defined distributions and are, therefore, statistical distributions.

The approach followed in generating the biosphere dose conversion factors comprised a rigorous process (CRWMS M&O 1996d, pp. 13-14). The initial step was to determine an appropriate computer program. Computer programs that have been used in the United States regulatory environment for dose assessment purposes were evaluated. Each program was compared with capability criteria established by the Yucca Mountain Site Characterization Project (CRWMS M&O 1998i, Section 9.2.2.1). GENII-S (Leigh et al., 1993) was the most comprehensive program and included a stochastic modeling capability, and therefore, was selected as the modeling tool for this effort (CRWMS M&O 1996d).

An interaction matrix was developed to identify the features of the biosphere and the events and processes by which radionuclides move from one feature to another (CRWMS M&O 1998i, Table 9-1). Using the interaction matrix, important elements of the biosphere and pathways between these elements were defined. These elements are presented in Figure 3-75. Most of the parameters used by the model define the characteristics of these elements and the pathways.

Although many of the input parameters were derived from local site-specific data obtained through the Yucca Mountain regional survey and weather data, many input parameters were also taken from other published sources (LaPlante and Poor 1997; International Atomic Energy Agency 1994). The input parameters employed in the biosphere modeling realizations are detailed in the *Total System Performance Assessment-Viability Assessment (TSPA-VA) Analyses Technical Basis Document* (CRWMS M&O 1998i, Table 9-3). Some of the important uncertain parameters (that is, parameters defined with probability distributions) that were used in the model are outlined in Table 3-25.

The ingestion pathway involves plant and animal uptake factors, irrigation rates, the amounts and

Table 3-25. Selected Uncertain Parameters Used in the Biosphere Modeling
(Source data are found in DTNM09806MW DGENII.000 and are non-Q)

Uncertain Parameter	Distribution
Soil-to-Plant Transfer Scale Factor	Log normal (0.117, 8.51)*
Animal Uptake Scale Factor	Log normal (0.117, 8.51)*
Inhalation Exposure (hr/year)—Amargosa Valley	Triangular (3248, 3869, 4217)
Inhalation Exposure—Mass Load (g/m^3)	Log normal (2.40E-6, 1.54E-4)
Home Irrigation Rate (in./year)—Current Precipitation Regime	Uniform (46, 96)
Crop Re-suspension Factor (/m)	Log normal (5.89E-7, 1.70E-4)*
Crop Interception Fraction (-)	Triangular (0.06, 0.4, 1.0)
Drinking Water Consumption (L/year)—Amargosa Valley	Triangular (0, 683.8, 1487.5)
Leafy Vegetable Grow Time (days)	Triangular (45, 67, 75)
Leafy Vegetables Irrigation Rate (in./year)—Current Precipitation	Triangular (25, 36, 66)
Leafy Vegetables Irrigation Time (month/year)	Triangular (2, 3, 4.9)
Leafy Vegetables Yield (kg/m^2)	Uniform (1.8, 2.6)
Leafy Vegetables Consumption Rate (kg/year)—Amargosa Valley	Log uniform (0.035, 59.68)
Other Vegetables Consumption Rate (kg/year)—Amargosa Valley	Log uniform (0.0045, 38.01)
Fruit Consumption Rate (kg/year)—Amargosa Valley	Log uniform (0.001, 97.69)
Grain Consumption Rate (kg/year)—Amargosa Valley	Log uniform (1.0E-31, 12.33)
Beef Consumption Rate (kg/year)—Amargosa Valley	Log uniform (2.0E-7, 53.11)
Poultry Consumption Rate (kg/year)—Amargosa Valley	Log uniform (5.0E-9, 10.50)
Milk Consumption Rate (L/year)—Amargosa Valley	Log uniform (5.0E-12, 136.03)
Eggs Consumption Rate (kg/year)—Amargosa Valley	Log uniform (0.009, 33.34)

* Truncated Log normal Distribution -- Values Represent: Min. (0.1 percentile), Max. (99.9 percentile)

Note: The log normal distributions are actually truncated distributions, parameterized by the 0.1 and 99.9 percentile values, and not the typical mean and standard deviation.

types of foodstuffs that are consumed by the reference person, etc. The consumption rates for drinking water, vegetables, fruit, grain, beef, poultry, milk, and eggs were estimated from the results of the survey. The soil-to-plant transfer factor represents the activity concentration (Ci/kg, dry weight) ratios between the soil and the edible parts of plants. This factor determines the amount of radioactive material accumulated in plants from soil. Similarly, the animal food transfer coefficient is the ratio of activity concentration in animal product (Ci/kg) to the daily activity intake rate (Ci/day). The coefficient determines the amount of radioactive material in edible animal products resulting from the ingestion of contaminated feed. Data on the transfer factors for local food types are limited; therefore, generic food transfer factors were taken from the International Atomic Energy Agency (International Atomic Energy Agency 1994, Chapter 6).

Inhalation exposure is influenced by two factors: the mass concentration of particles of such size that they can enter and be retained by the lungs and the duration of the exposure. Inhalation exposure, as well as direct external exposure, is dependent on the amount of time the reference person spends outdoors. The external/inhalation exposure mass load is the amount of material, dust for example, in a given volume of outside air. The home irrigation rate is the water application rate to lawns. Although not shown in Table 3-25, irrigation rates change with the different climates modeled and decrease with increasing precipitation.

Not all uncertainty in parameters is reflected in the values and distributions assigned. For example, the soil-to-plant uptake parameter, although defined by a distribution, does not reflect the soil properties of the area surrounding Yucca Mountain, but rather a more generalized temperate soil (International Atomic Energy Agency 1994). A recently completed study of the soils in the Amargosa Valley and the area north extending to Yucca Mountain reported exclusively alkaline soils (CRWMS M&O 1997i, Table 2, p. 8). Soils with naturally high pH, including many of the calcareous soils of the western United States, are associated with deficiencies of high-valance metal cations—iron, manganese, zinc, copper—for agronomic and agricultural production (Brady 1984, Section 11.4, p. 371). Given that many of the radionuclides of concern are metallic cations, the soil-to-plant uptake factors used in TSPA-VA might overestimate the actual amount of radionuclides transferred to plants.

As is usual practice for radiological compliance evaluations, dose conversion factors (not to be confused with the biosphere dose conversion factors) used in the biosphere model were assigned constant values and, therefore, do not appear in Table 3-25. A dose conversion factor converts an amount of a radionuclide into a radiation dose, taking into account such effects as the uptake of a radionuclide by the body, the residence time for a radionuclide in the body, and where a radionuclide is concentrated in the body. There are separate dose conversion factors for ingestion, inhalation, and direct external exposure. The values used in the biosphere modeling were derived using the methodology from the International Commission on Radiological Protection 30 (ICRP 1978) and are similar to those specified by EPA.

The final result of the complex biosphere modeling is the biosphere dose conversion factor. To calculate the radiation dose incurred by the reference person in the TSPA-VA, a biosphere dose conversion factor for a given radionuclide is sampled from its distribution, and the sampled biosphere dose conversion factor is multiplied by the concentration of that radionuclide at the biosphere/geosphere interface. The result is the annual dose rate that the reference person receives from that radionuclide at a given time. The biosphere dose conversion factors are completely correlated in the TSPA-VA calculations; that is, if a large biosphere dose conversion factor is sampled for one radionuclide, then large biosphere dose conversion factors are sampled for all radionuclides. During a TSPA-VA calculation, at appropriate sample times, the climate is allowed to change and biosphere dose conversion factors are changed to the precipitation regime associated with this climate. The sum of the dose rates for all radionuclides is the total annual dose rate at that time. The maximum total dose rate over all times

in a TSPA realization is the peak dose rate—the end product of the TSPA-VA calculation.

3.8.3 Results and Interpretation

For each radionuclide, the GENII-S biosphere model performed 130 evaluations to generate a distribution of the biosphere dose conversion factor. Each of the 130 values was sorted into bins and used to construct a histogram. A log-normal distribution was fit to the output and a test for goodness-of-fit indicated that there is no reason to reject the hypothesis that these distributions were log-normal. Log-normal distribution approximations of the biosphere dose conversion factors were used in the TSPA-VA calculations to simplify the parameter sampling. Figure 3-79 presents the histogram and log-normal distribution for the biosphere dose conversion factor for neptunium-237

Analysis of the results of the biosphere modeling shows that the most important pathway in the calculation of the biosphere dose conversion factors is typically the drinking-water-ingestion pathway. The next most important pathway is the leafy-vegetable-ingestion pathway. All other pathways generally affect the biosphere dose conversion factors at a relatively insignificant level. The fractional contribution to the biosphere dose conversion factors from the drinking-water-ingestion pathway for three radionuclides that have an important impact on the TSPA-VA base case results (Sections 4.2 and 4.3) are as follows: 57 percent for technetium-99, 44 percent for iodine-129, and 64 percent for neptunium-237. The fractional contribution from the leafy-vegetable-ingestion pathway are as follows: 37 percent for technetium-99, 21 percent for iodine-129, and 31 percent for neptunium-237. The only other important pathway for these radionuclides is the meat-ingestion pathway for iodine-129, which contributes 26 percent of the iodine biosphere dose conversion factor. These numbers were generated with a deterministic calculation that used the expected values of all parameters and considered the average Amargosa Valley resident and the current climate.

The following two sections present analyses to examine parameters and assumptions that are important to the GENII-S biosphere modeling.

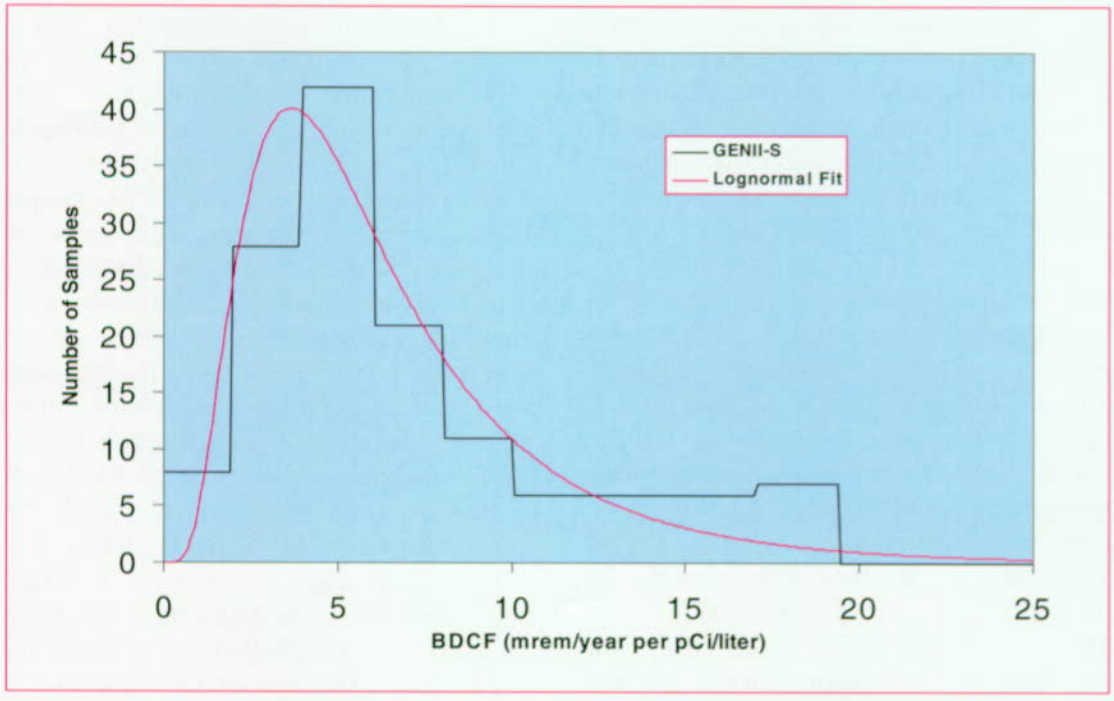

Figure 3-79. Histogram of the Biosphere Dose Conversion Factor for Neptunium-237

The last section contains a description of the biosphere modeling and assumptions used in the assessment of the impact of volcanism on repository performance (Section 4.4). Sensitivity analyses that look at the impact of parameters and assumptions on the complete TSPA-VA base case calculations are discussed in Section 5.8.

3.8.3.1 Biosphere Probabilistic Results

The stochastic biosphere modeling shows that for a given radionuclide the biosphere dose conversion factors can vary by about a factor of three above and below the mean value, giving a range of approximately one order of magnitude. Figure 3-79 shows the distribution predicted by GENII-S, with a mean of 6.6 mrem/year per pCi/liter, and the log-normal distribution used to approximate it. It is useful to understand which input parameters are most responsible for this variance in the output. Rank regression is a technique employed to assess the relationship between the model input and the output. The partial correlation coefficient is a measure of how much the calculated biosphere dose conversion factor is correlated with a given sampled parameter. Forty-six variables were evaluated in the parametric sensitivity study. Depending on which radionuclides were considered, typically less than 10 independent variables accounted for more than 90 percent of the variance of the model output. Table 3-26 summarizes the results of sensitivity analysis for technetium-99, iodine-129, and neptunium-237. Only the parameters with partial correlation coefficients greater than 0.2 are included in the table, which is approximately the level of insignificance in the analysis; the results of the biosphere modeling are even less sensitive to other parameters, such as the inhalation and external exposure parameters.

Of the uncertain or variable parameters that most affect the calculation of the biosphere dose conversion factors, the leafy-vegetable and drinking-water consumption rates are the most important. That is, changes in these two parameters typically produce the largest changes in the biosphere dose conversion factor. That these two parameters are identified by the analysis is not unexpected, because the probability distributions used to define them have relatively large variances, and because the drinking-water and leafy-vegetable pathways were identified as the major contributors to the dose rate (Section 3.8.3). Iodine-129 differs somewhat from technetium-99 and neptunium-237 in that iodine is more easily concentrated in animals and, thus, the beef consumption rate, and to a certain extent the milk consumption rate, are important to its biosphere dose conversion factor.

Parameters that are identified as the next in importance are the crop-interception fraction and the crop resuspension factor. The crop-interception

Table 3-26. Sensitivity Analysis for the Three Most Important Radionuclides for the Base Case Scenario

Radionuclide	Parameter	Partial Correlation Coefficient
Tc-99	Leafy vegetable consumption rate	0.87
	Drinking water consumption rate	0.77
	Crop interception rate	0.29
	Root vegetable consumption rate	0.26
	Eggs yield	0.20
I-129	Leafy vegetable consumption rate	0.62
	Beef consumption rate	0.52
	Drinking water consumption rate	0.46
	Milk consumption rate	0.26
	Crop resumption rate	0.25
	Grain irrigation rate	0.22
	Animal uptake scale factor	0.20
Np-237	Leafy vegetable consumption rate	0.84
	Drinking water consumption rate	0.77
	Crop interception rate	0.31
	Root vegetable consumption rate	0.23
	Eggs yield	0.22

fraction is the fraction of contamination from rainfall, irrigation, or aerosol deposition that is intercepted by and adheres to the plant surface. The crop resuspension factor describes the amount of contaminated dust that settles on the plant surface and can then be resuspended into the air. The adsorbed contaminants are then available for ingestion by foraging livestock and poultry, or direct ingestion by humans. Processes that contribute to these parameters are wind, and overhead irrigation, which is becoming more common in the region.

The least important parameters shown in Table 3-26 are the root-vegetable consumption rate, the eggs yield, the grain irrigation rate, and the animal-uptake scale factor. Although the partial correlation coefficients for these parameters are relatively insignificant, it is important to note that they still rank highly among the 46 parameters defined with probability distributions. The results of this sensitivity analysis can be used to identify the factors driving uncertainty of the model output and determine where attention and resources should be focused in the future (Section 6.5.1.11).

3.8.3.2 Biosphere Comparative Analyses

Several additional calculations were performed to evaluate some of the more important assumptions made in the biosphere modeling on the biosphere dose conversion factor calculations. Of particular interest is how the assumption of an average consumption rate of locally produced foodstuffs influenced the results. Also of interest is the effect of climate on the results.

To examine the effect of consumption rates, three different types of reference persons were defined: the average Amargosa Valley resident (the base case reference person), a resident farmer, and a subsistence farmer, each with defined characteristics (Table 3-24). The significance of the amount of local food and well water consumed on the biosphere dose conversion factors is presented in Figure 3-80. The figure shows that the magnitude

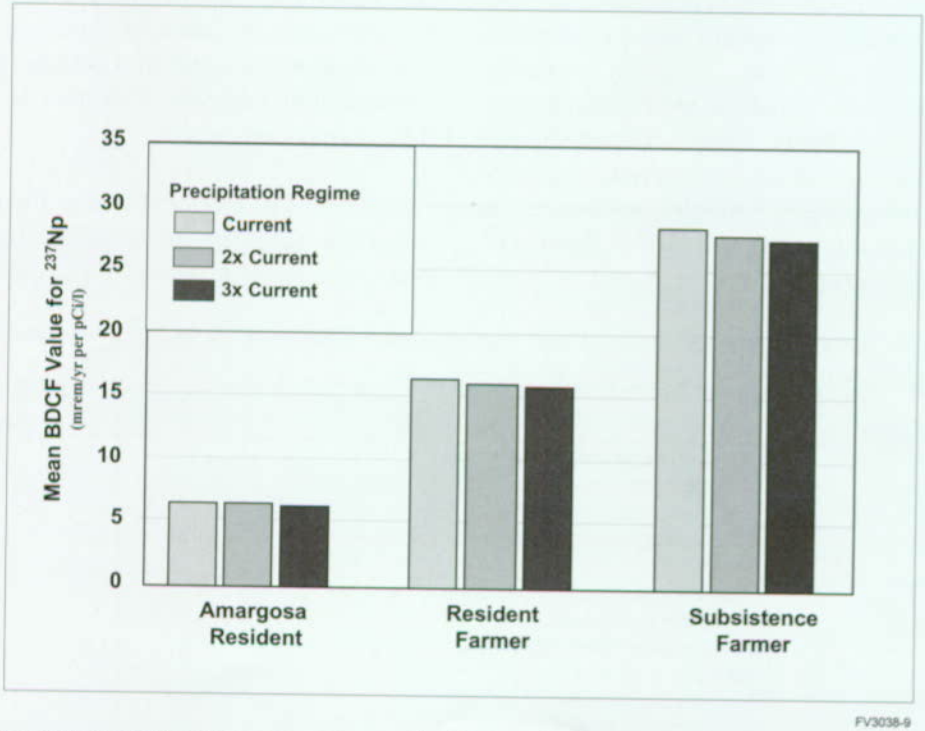

Figure 3-80. Comparison of Biosphere Dose Conversion Factors for Neptunium-237 as a Function of Receptor and Precipitation Regime
The biosphere dose conversion factors generated for the subsistence farmer are approximately 5–6 times greater than those calculated for the average current Amargosa Valley resident. However, the biosphere dose conversion factors do not vary notably among the three precipitation regimes modeled. (BDCF—Biosphere Dose Conversion Factors)

of biosphere dose conversion factor for a given isotope increases with the increased consumption of locally grown food (CRWMS M&O 1998i, Section 9.7.3.1). In general, a subsistence farmer could receive a radiation dose from neptunium-237 approximately five times greater and a resident farmer could receive a dose three times greater than that received by an average inhabitant of the region, respectively. However, these factors are dependent on the radionuclide; for iodine-129, a subsistence farmer would incur a radiation dose rate approximately 10 times greater than an average Amargosa Valley resident.

Also shown in Figure 3-80 is the change in climate, which is modeled only by the change in irrigation rates and has little effect on the biosphere dose conversion factors. For each unit of increase in precipitation, where a unit is the present-day mean annual precipitation, calculated biosphere dose conversion factors were reduced by about two percent. The decrease in dose rate results because the increase in precipitation allows a reduction in irrigation, and thus less contamination to soil and plants. The decrease in dose rate is small because the major pathway—drinking water—is unaffected by an increase in precipitation. Also, most of the precipitation increase is expected to occur in the winter when crops are not produced. The two-percent change is inconsequential in comparison to the approximate order-of-magnitude spread of the biosphere dose conversion factor distributions (CRWMS M&O 1998i, Table 9-22). Data gathered from a survey conducted in late 1997 in Lincoln County, Nevada, are presently being analyzed in order to determine the eating habits of residents in a cooler and wetter environment similar to that anticipated in the future at Yucca Mountain. The impact of this effect will be addressed as a sensitivity study when the data from Lincoln County are analyzed.

3.8.3.3 Biosphere Scenarios Associated with Volcanic Activity

As part of an assessment of the effects of disruptive events on a potential repository at Yucca Mountain (Section 4.4), two biosphere scenarios related to volcanic activity were modeled. The two biosphere scenarios for volcanism were as follows: the reference person is living in the vicinity when the eruption occurs and inhales air containing particles of contaminated ash, and the reference person returns to the region soon after the eruption and lives on and farms the contaminated volcanic soil. The biosphere model used to evaluate the volcanic scenarios involved the same biosphere-pathways model and reference-person parameters as developed for the base case, except that for Scenario 2 contaminated volcanic ash was assumed to be mixed into the upper 15-cm (6-in) of soil.

In the first scenario, the dose rate is primarily from inhalation; the dose rate from exposure by submersion in the ash cloud is very small in comparison to the dose rate from inhalation. In this scenario, the biosphere dose conversion factors were calculated for unit concentrations of the radionuclides in air and one hour of exposure. To determine the dose rate from these biosphere dose conversion factors, the quantity of radionuclides expelled by the event is calculated, then the radionuclides are distributed in an appropriate volume of air. Exposure time (in hours) is estimated. The dose rate is then determined by the product of the radionuclide concentration, the biosphere dose conversion factors for inhalation and submersion, and the assumed time of exposure.

In the second scenario, it is assumed that the ash from the eruption contributes its activity to the upper 15 cm (6 in) of the ground surface because this depth encompasses the root zone of most agricultural plants. For these calculations, the groundwater is assumed not to be contaminated because this factor has already been taken into account in the base case biosphere-dose-conversion-factor calculations. As with the base case, the biosphere dose conversion factors include the ingestion, inhalation, and external exposure pathways. Also, as with the base case, the dominant pathway is the ingestion of contaminated foods. To determine the dose rate in a TSPA calculation, it is necessary to determine the amount of radionuclides expelled by a volcanic event and the area over which the radionuclides are dispersed. These two parameters allow the concentration of radionuclide in the soil to be calculated. The concentration of radionuclides in the soil is then

multiplied by the volcanic biosphere dose conversion factors to give the annual dose.

Within the time frame allowed for completion of the TSPA-VA, only the dose rate associated with exposure to contaminated ash after the assumed volcanic event (Scenario 2) was calculated (Section 4.4.2). The dose rate associated with inhalation and external exposure during the volcanic event itself (Scenario 1) will be addressed in additional studies if it is deemed that volcanic activity requires further consideration.

4. BASE CASE DEFINITION AND RESULTS

The previous sections in this volume have shown the complexity of the repository system, both the engineered and natural barriers, and the resulting need to break the system into various components in order to analyze repository performance. Section 2 described the specific components or subsystems used in the TSPA-VA models (Figure 2-2), the rationale for choosing these specific components (how they correlate to specific physical-chemical processes and to location within the overall system, and how they are coupled to one another), and the specific methodology used to incorporate and analyze these components in the overall total system performance model (Figure 2-13). Section 3 gave detailed descriptions of each of the key component models: the conceptual basis of these models as determined by experimental data, how to implement these conceptual models into the overall TSPA analyses (including model abstractions or simplifications that are necessary in some instances), the range of uncertainty underlying these component models and their corresponding data, and finally some key results of the component models, that is, how well the models fit available data and how the range of uncertainty in available data leads to a range of predictions of key model output parameters (e.g., groundwater flux).

Having shown in previous sections the necessity of breaking the total system into components and the details of modeling each component, it is now appropriate to describe the results of recombining all the component models into one integral total system performance model, specifically the predictions of this overall model with respect to both total system performance (i.e., dose rate at the accessible environment) and to subsystem performance of the various components (e.g., performance of the saturated zone by itself). A key point is that the assessments will be based on the calculated source term, that is, the predicted radionuclide releases from the repository as the waste packages and waste forms degrade with time. This is a bit different from some of the results in Section 3 (e.g., Sections 3.6 and 3.7), which were based on an idealized source term.

The phrase "base case" has already been defined in more general terms in Section 2.3.3 as it relates to uncertainty. However, in this section "base case" is defined more specifically as it relates to the various component models of the TSPA-VA, that is, which parameter ranges and models are used to define the TSPA-VA base case. The phrase "base case" might also be termed the "baseline" case, where baseline is used in the sense of "likely" rather than as "initial," implying that the "base case" encompasses some of the possible uncertainty regarding predictions of system performance, but not all. For example, consider the fourth type of uncertainty listed in Section 2.3.3.3 regarding features, events, and processes: uncertainty about future events. The TSPA-VA base case encompasses some uncertainty related to climate-change events, but no uncertainty related to volcanism events. Or consider the second type, conceptual model uncertainty. The TSPA-VA base case does not include the DKM/Weeps model discussed in Section 3.1, but does include the DKM model. These are a couple of examples of how the base case represents a narrowed range of uncertainty in comparison to the entire space of possible outcomes. It represents a judgement. However, because of the still remaining uncertainty in all of the component models and future scenarios (features, events, processes), the base case necessarily encompasses multiple outcomes (i.e., realizations) for the future repository behavior. The intent of Section 4 is to quantify the range of possible outcomes of overall system behavior for the TSPA-VA base case and to describe the key parameters of the component models that are most responsible for the performance variation across this range of system behavior (Section 4.3). Before describing this entire range of overall base case behavior, that is, the probability distribution of dose in the biosphere at 20 km (12 miles) downgradient of the repository, a single realization of repository behavior is examined to illustrate in detail how the behavior of the various components influences both the behavior of the dose and the behavior of other components (Section 4.2). This will lead to a more thorough understanding of why the repository behaves as it does and what can be done to develop a more robust (i.e., an inherently safer) system through either better engineering in the drifts or better characterization of the natural system. This

single realization is the realization that chooses the expected value of all the stochastic input parameters.

System behavior outside of the range of the base case is also discussed in this section, and in Section 5, including:

- Effects on the system behavior from unanticipated, or low-likelihood, disruptive events such as volcanism (Section 4.4)
- Alternative design options for the repository and waste packages (Section 4.5)
- Less likely conceptual models for various components (Volume 5)

4.1 BASE CASE DESCRIPTION

Figures 2-11 through 2-13 illustrated how the base case component models described in Section 3 are coupled together and what information is passed through the couplings. A detailed description of the base case includes two features: the specific parameter values used within the component-model "boxes" in Figure 2-13, and the specific information and form of that information passed through the arrows that couple the boxes. Uncertain ranges of parameters used within and between the boxes for the TSPA-VA base case have been described in detail in the component sections of Section 3. The purpose of Section 4.1 is to provide a concise summary of these base case parameter values and models as used in TSPA-VA.[1]

The TSPA-VA base case is predicated on the reference repository and waste package design described in detail in Volume 2, and summarized in Section 3.2.2.1 of Volume 3. Variations in this design and their effect on performance are described in Section 4.5 but are not considered in Sections 4.2 through 4.4.

4.1.1 Climate

As explained in Section 3.1.2.1, future climate changes in the TSPA-VA base case are assumed to alternate between three states: present-day or dry climate, long-term average climate (about twice the dry-climate precipitation), and superpluvial climate (about three times the dry-climate precipitation). For the expected-value simulation described in Section 4.2, this sequence of alternating climate states, including the durations of each climate state, is shown in Figure 4-1. As summarized in Table 3-4, the length of the first dry climate, or current climate, is sampled uniformly between 0 and 10,000 years, with an expected value of 5,000 years, which was the value used for the expected-value base case calculation (Section 4.2). The length of subsequent dry climates is sampled uniformly between 0 and 20,000 years, with an average of 10,000 years. The duration of long-term average climates is sampled uniformly between 80,000 and 100,000 years, with an average of 90,000 years, which is the value used for the expected-value base case calculation. The duration of the superpluvial climates is sampled similarly to dry climates, from 0 to 20,000 years. Dry and long-term average climates alternate from the time of repository closure until the long-term average climate that spans the 250,000-year mark. For the expected-value case, the last 10,000 years of that long-term average period is replaced by 10,000 years of superpluvial climate. Then the climate model returns to alternating dry and long-term average climates until the long-term average climate that spans the time of 400,000 years after the first superpluvial. The end of that long-term average climate is again replaced by a superpluvial, and then back to dry, followed by alternating long-term average and dry climates. For the expected-value base case simulation shown in Figure 4-1, about 90 percent of the time is spent in the long-term average climate.

[1] A complete listing of all model parameters is beyond the scope of this document. The complete listing is found in the various chapters of the *Total System Performance Assessment-Viability Assessment (TSPA-VA) Analyses Technical Basis Document* (CRWMS M&O 1998i).

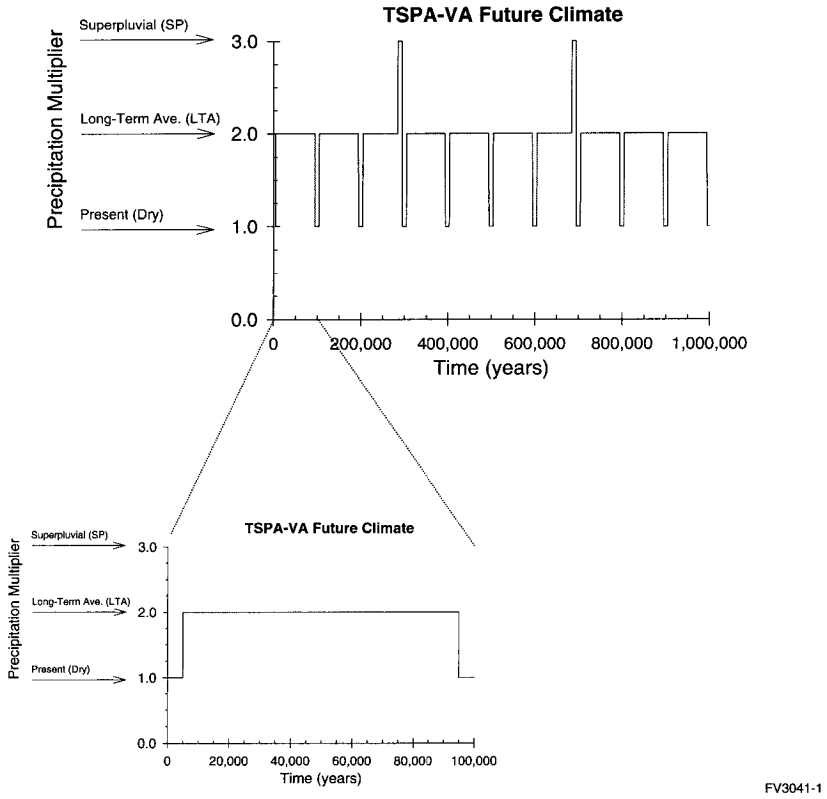

Figure 4-1. Climate History for the Expected-Value Realization of the Total System Performance Assessment for the Viability Assessment Base Case at Two Different Time Scales
For other realizations, the duration of the various climate states is different, since these durations are stochastic parameters.

4.1.2 Unsaturated Zone Flow and Infiltration

Unsaturated zone flow uses three calibrated hydrogeologic property sets for present-day conditions, resulting in three calibrated steady-state flow fields: the "base infiltration" case with mean fracture alpha, which represents the best estimate of current infiltration conditions; the "base infiltration × 3" case with maximum fracture alpha, which represents a pessimistic (very wet) estimate for current infiltration; and the "base infiltration ÷ 3" case with minimum fracture alpha, which represents the most optimistic (driest) estimate for current conditions.[2] To derive flow fields for the other climate states, these three calibrated property sets were used in the TOUGH2 computer code to attain steady states at boundary conditions representing precipitation in the two wetter climates. For the base case, there were 3 × 3 steady-state flow fields accessed by the RIP computer program. All nine resulting flow fields are three-dimensional, with vectors for fracture and matrix flux and for fracture-matrix interflux at each of the approximately 40,000 grid points (actually 80,000 since there are two continua-fracture and matrix).[3]

[2] Originally there were five calibrated hydrogeologic property sets for present-day climate conditions: the three mentioned plus a "base infiltration × 3" case with minimum fracture alpha and a "base infiltration ÷ 3" case with maximum fracture alpha (see Section 3.1). These latter two were dropped from the TSPA-VA base case because of similarities to the other "base infiltration × 3" and "base infiltration ÷ 3" cases.

[3] The unsaturated zone transport model requires only the vectors from the repository horizon down to the water table.

The water table level changes with climate, rising by 80 m (262 ft) from dry to long-term average climate and another 40 m (131 ft) from long-term average to superpluvial climate.

Figure 4-2 illustrates how the flow fields are used throughout the climate history. The figure indicates that infiltration is heterogeneous over the model domain and, therefore, the percolation at the repository horizon is heterogeneous. This heterogeneity is taken into account in the unsaturated zone transport model, which directly uses the three-dimensional flow fields. The repository area in this figure is the area in the center where the grid-block discretization is much greater. The exploratory studies facility is also shown by areas of greater discretization. (The actual repository does not cover the entire area of greater discretization but only about the northernmost 80 percent of that area.) Also shown on the figure is the approximate average infiltration over the repository area for the three climate states.

4.1.3 Drift Scale Seepage

Liquid seepage into the drifts in the model is based on numerous simulations of a three-dimensional, heterogeneous, fracture continuum surrounding the drifts, as described in the *Total System Performance Assessment-Viability Assessment (TSPA-VA) Analyses Technical Basis Document* (CRWMS M&O 1998i). The simulations use many different infiltration rates and nine different property sets (Table 3-6) that represent nine combinations of fracture permeability and fracture alpha. The results were statistically weighted and represented as two stochastic response surfaces (Figure 3-13) of seepage fraction, (i.e., the fraction of packages in the drifts that have seeps dripping on them), and seepage flux per package (in m^3/ year). These two

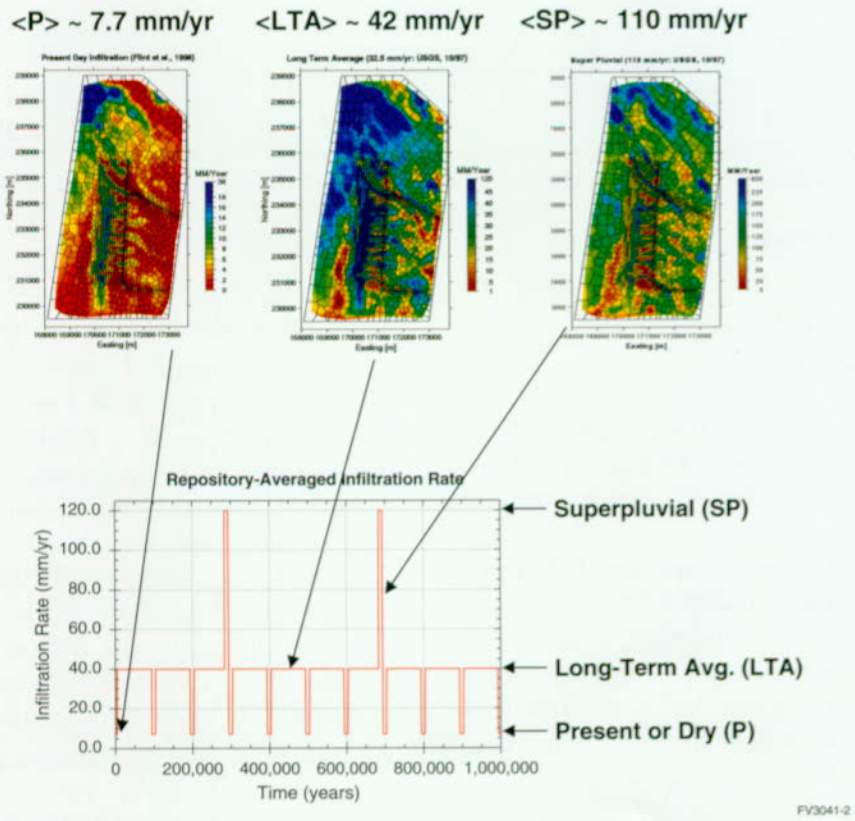

Figure 4-2. Infiltration History for the Expected-Value Realization of the Total System Performance Assessment for the Viability Assessment Base Case
This figure shows the infiltration map for the unsaturated zone flow model in the three different climate states, and the average infiltration over the repository horizon during these climate states.

response surfaces are a function of percolation flux: when the climate changes, different values for seepage fraction and seepage flux are used based on the new percolation flux. For the base case, the seepage flux and seepage fraction were given perfect positive correlation, that is, the same random number was sampled for these two parameters. Also, the same random number was used in all climate states, meaning that although seepage changes with climate state (because percolation flux changes), the different seepage values used in different climate states have the same probability. The seepage fraction and seepage flux histories (along with the corresponding response surfaces) are shown in Figure 4-3. The repository horizon was divided into six discrete regions based on infiltration and thermal-hydrologic response. Each region used a separate value of seepage flux and seepage fraction over the entire region. These values were based on the average percolation flux over each region as determined from the histogram over all grid blocks in the region. The average percolation flux was taken from the steady-state values of percolation predicted by the unsaturated zone flow model. This discretization is illustrated in Figure 4-4.

The seepage flux and fraction used in the TSPA-VA base case are for ambient percolation conditions, that is, unperturbed by the thermal pulse. This is justified because the large changes to seepage from waste heat occur at times earlier than

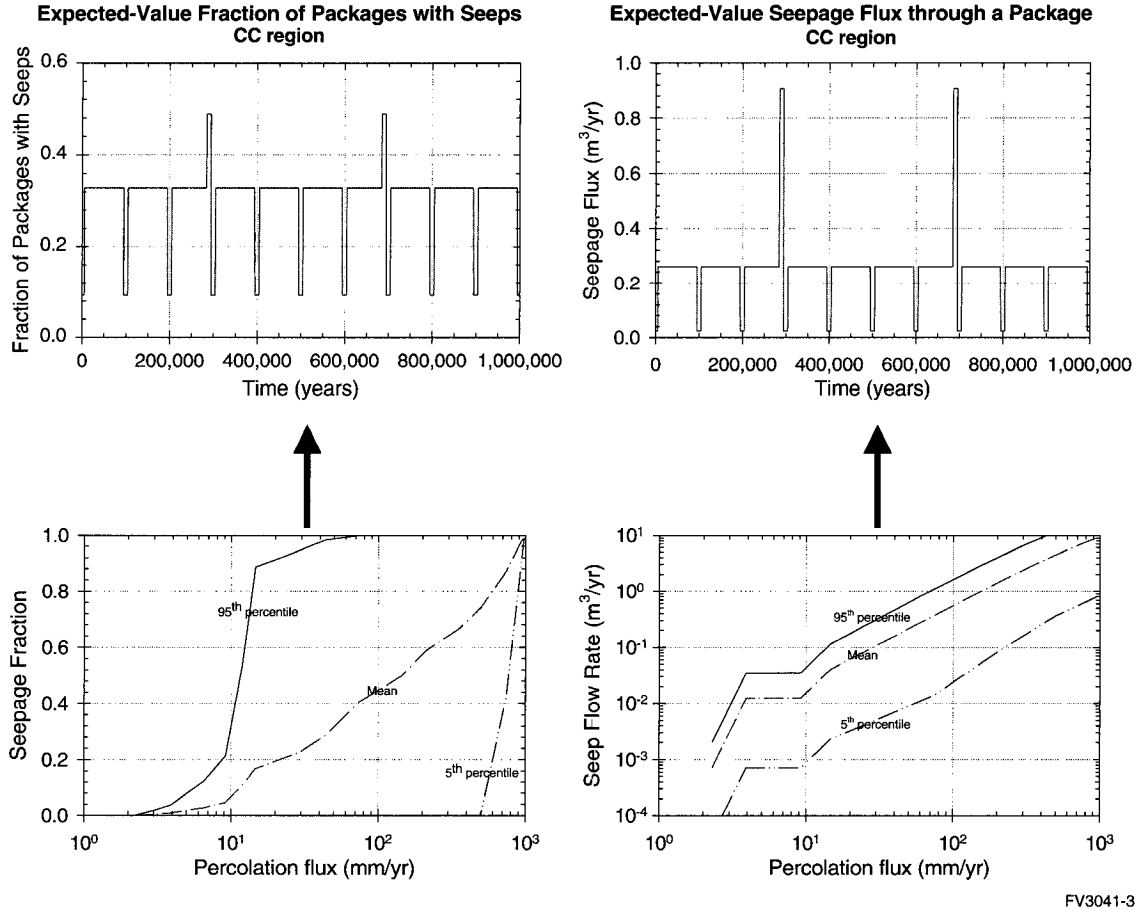

Figure 4-3. Total System Performance Assessment for the Viability Assessment Base Case Drift-Scale Seepage Model

This figure shows the 1 million-year expected-value histories of seepage flux into the drift and fraction of packages in a given region that encounter seeps (seepage fraction). Also shown is the probabilistic distribution used to predict seepage flux and seepage fraction based on percolation flux at the repository horizon in any of the six regions (see Figure 3-8 for an illustration of the six regions).

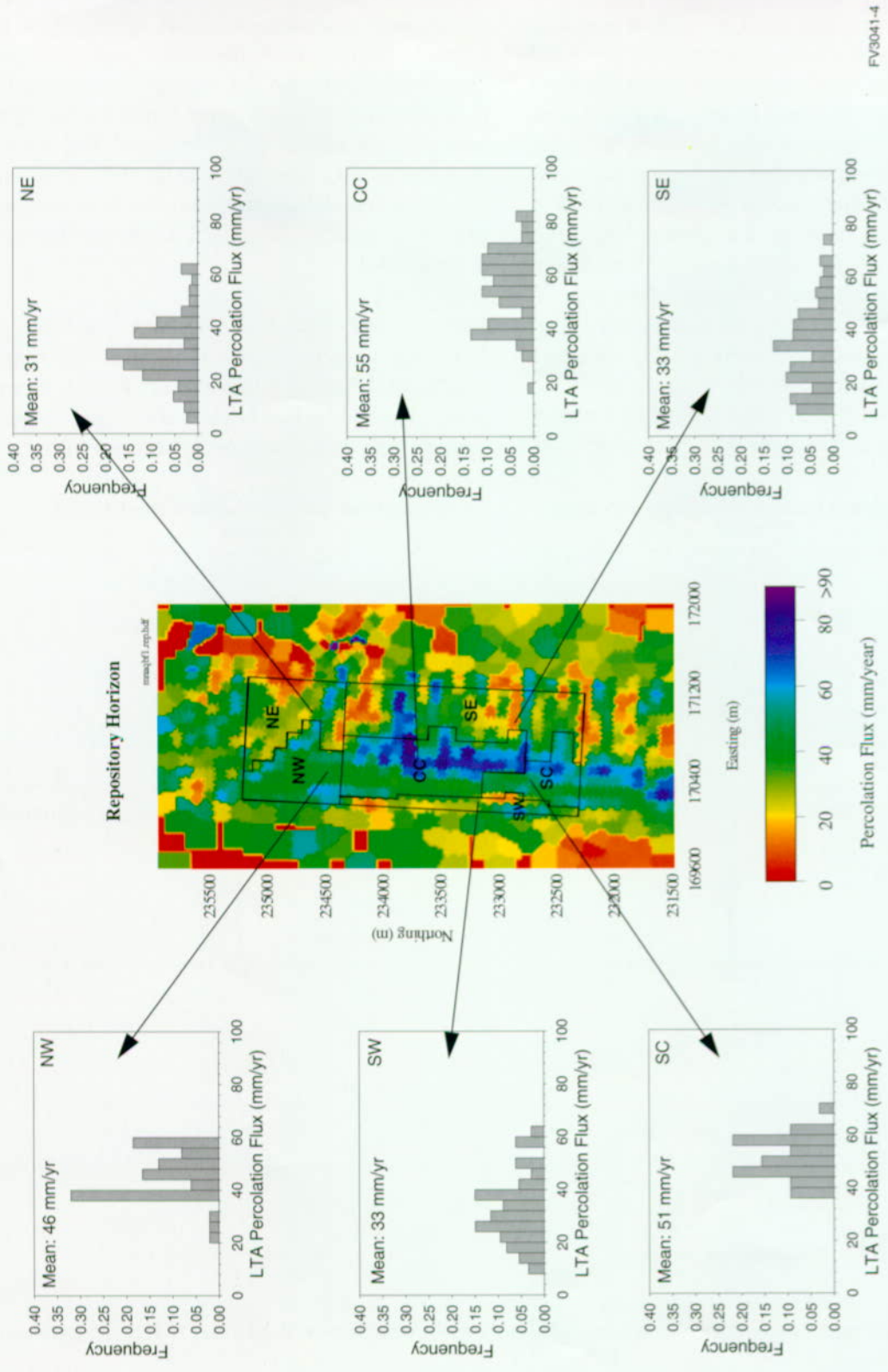

Figure 4-4. Total System Performance Assessment for the Viability Assessment Base Case Percolation Flux at the Repository Level for the "Base Infiltration" Flow Field During the Long-Term-Average Climate
Shown are the six waste package regions, including the histogram (spatial frequency distribution) of fluxes in each region derived from the unsaturated zone flow model and the spatially averaged percolation flux in each region. LTA means long-term average.

the first package failures, and so have no effect. This is discussed in the *Total System Performance Assessment-Viability Assessment (TSPA-VA) Analyses Technical Basis Document* (CRWMS M&O 1998i).

4.1.4 Drift Scale Thermal Hydrology

In the base case, the results of drift-scale, thermal-hydrologic modeling are as follows:

- Waste package surface temperature (T_{wp}) and relative humidity at the waste package surface (RH_{wp}) for seven different package types and heat outputs within six discrete spatial regions of the repository, which is used by the waste package degradation model to represent some of the package-to-package variability within each region[4]

- Average waste form temperature (T_{wf}) and liquid saturation in the invert (S_l) in each of the six regions, which is used by the waste form degradation model[5]

- Average drift-wall temperature (T_{dw}), relative humidity at the drift wall (RH_d), and liquid saturation in the invert (S_l) in the central-central region, which is used by the near-field geochemical models

Each of these results is generated separately for the three different unsaturated zone flow fields: "base infiltration × 3, with maximum fracture alpha" case, "base infiltration, with mean fracture alpha" case, and "base infiltration ÷ 3, with minimum fracture alpha" case. Waste package degradation histories are then generated for each of these unsaturated zone flow scenarios and fed into the RIP computer program. Also, waste form degradation within the RIP program uses all three flow field results. However, near-field geochemistry only uses average drift wall temperature (T_{dw}), relative humidity, and liquid saturation in the invert (S_l) for the "base infiltration with mean fracture alpha" flow field. The waste package degradation model produces different results only for packages that are dripped on versus those that are not. Otherwise, the same package degradation history is used for each inventory type (commercial spent nuclear fuel, DOE spent nuclear fuel, and high-level radioactive waste). Figure 4-5 shows the package-to-package variability in waste package surface temperature (T_{wp}) and relative humidity at the waste package surface (RH_{wp}) in the northeast region predicted by the drift-scale thermal-hydrologic modeling. The details of which waste packages correspond to the curves in this plot are described in the *Total System Performance Assessment-Viability Assessment (TSPA-VA) Analyses Technical Basis Document* (CRWMS M&O 1998i).

4.1.5 Repository Scale Thermal Hydrology

Thermal-hydrology models at the scale of the entire repository were only used in two places in the base case:

- As three-dimensional, conduction-only models that fed the abstraction methodology for drift-scale thermal-hydrologic parameters (see Section 3.2)

- As two-dimensional, thermal-hydrologic models (over an east-west cross section running through about the center of the repository) that provided air mass fraction and gas flux to the near-field geochemical environment models

In both cases, the hydrogeologic property set came from the "base infiltration" flow field from the unsaturated zone flow model (see Section 3.1). For the first set of models (three-dimensional,

[4] Actually, after numerous simulations of waste package degradation in the six discrete repository regions (see Sections 3.2 and 3.4), the failure histories were determined to be similar enough to only warrant further simulations in one of the six regions. The northeast region was conservatively chosen because it had the most variability (although only marginally so), implying slightly earlier package failures, and the package-failure history for this region was used for all the package groups in the RIP program.

[5] In this case, the results for all six regions (rather than just the northeast region) are used in the RIP model.

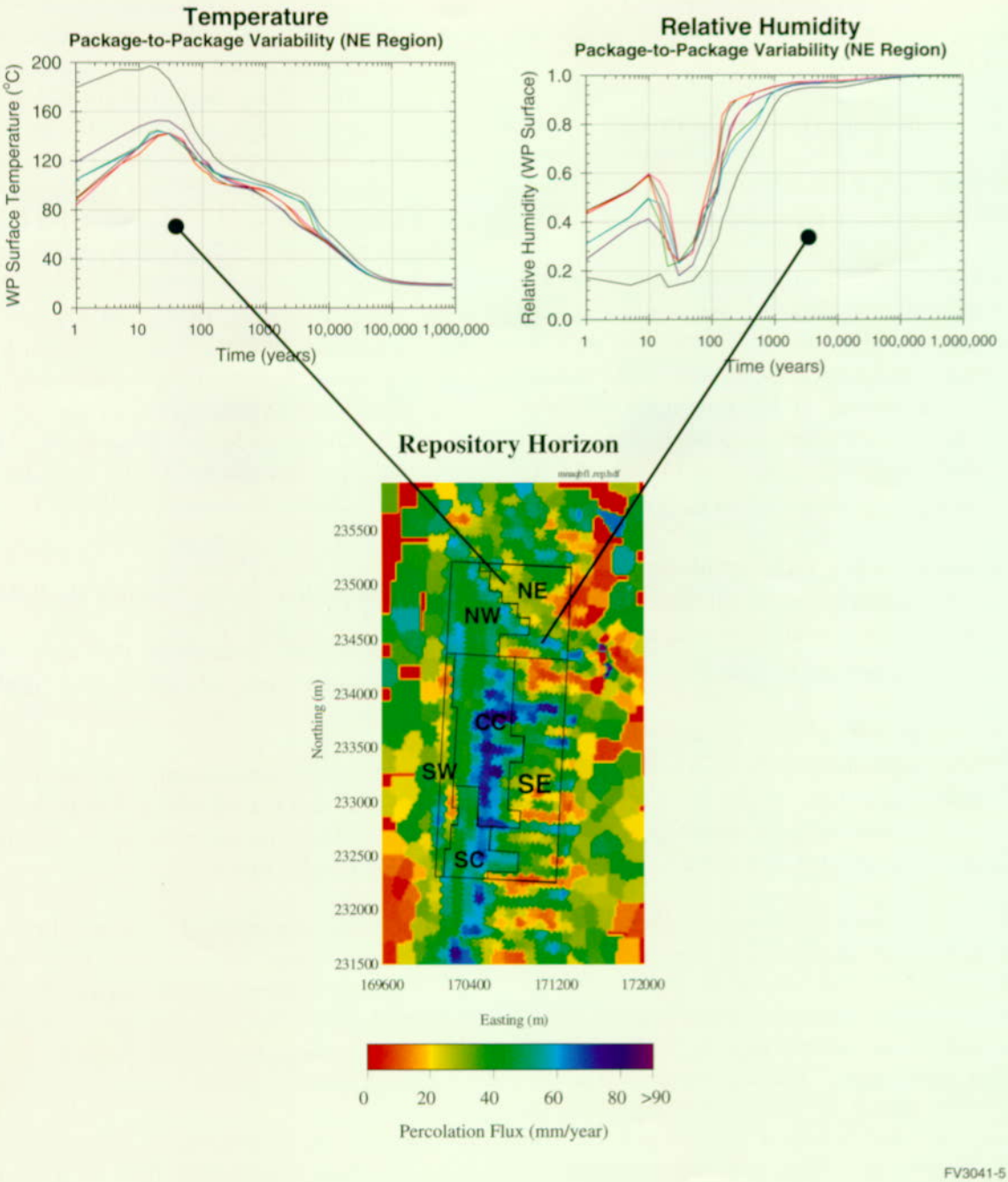

Figure 4-5. Variability of Total System Performance Assessment for the Viability Assessment Base Case, Drift-Scale, Thermal-Hydrologic Parameters (Temperature and Relative Humidity) in the Northeast Region at the Repository Horizon

These plots are for the "base infiltration" flow field using the long-term-average climate. Variability results from spatial variability in infiltration flux, thermal-hydrologic properties, and heat loading of the packages. (The abbreviation "WP" means waste package.)

conduction-only), the climate state was irrelevant, since hydrology was not modeled. For the second set of models (two-dimensional, thermal-hydrology), only the long-term average climate was used. This was appropriate because it is assumed that this climate exists approximately 90 percent of the time.

4.1.6 Near-Field Geochemical Environment

For the base case analyses, the near-field geochemical environment is represented by time-dependent distributions of the gas and water compositions that interact with the waste package and waste form inside the drift. The parameters supplied to the RIP analyses are the oxygen fugacity (fO_2),[6] the solution pH, the total dissolved carbonate (ΣCO_3^{2-}), and the ionic strength (I) of the water. Figure 4-6 shows time histories of these four chemical composition parameters as used by the RIP program for the TSPA-VA base case, derived from the various near-field geochemical models and supplied in tabular form to RIP. The first three parameters are used for waste form degradation modeling and the last one for colloidal transport in the engineered barrier system. These four parameters are derived from considering a more comprehensive 13-component chemical system. The values represent the time-dependent composition of water entering the drift and reacting with iron-oxide corrosion products, as opposed to water that has reacted with concrete. (Concrete-modified water is the subject of a sensitivity analysis considered in Section 5.)

It is clear from Figure 4-6 that these four composition time histories are not smooth functions; they are a series of steps. This step—change approximation is based on a simplified representation of the thermal history derived from various thermal-hydrologic models. The temperature, gas flux, and air mass-fraction histories from these thermal-hydrologic models were approximated as a sequence of steady states, which allowed the near-field environment to be modeled as a sequence of constant-composition states. This is the way all numerical models work—approximations of continuous functions with a series of discrete values. In the case of the near-field environment, the width of the discrete time periods was rather large. For each of these discrete time periods, often referred to as "abstracted" time periods, a batch calculation is performed with a geochemical simulator (EQ3/6; Wolery 1992a) to determine the appropriate chemical composition of the groundwater during that time period based on the temperature and air mass fraction from the thermal-hydrology models and on the incoming composition of the groundwater reacted with iron oxides. The base case values and abstracted time periods represent the thermal history of the "central" portion of the repository, as opposed to the "edge" portion. The values and time periods were generated using both the air-mass fractions and gas fluxes from the two-dimensional, mountain-scale, thermal-hydrologic results for the center portion of the two-dimensional cross section and the average drift-wall temperature history of the central-central region for the "base case infiltration" history, derived from three-dimensional drift-scale thermal-hydrologic modeling.[7] The central-central region was chosen because the excursions from ambient conditions, in particular the period of boiling, are largest for this region and will bound[8] the effects at the edge portions of the repository where the excursions occur for shorter time periods.[9]

4.1.7 Waste Package Degradation

Because modeling every distinct waste package is not computationally efficient, waste packages are grouped according to their inventory (commercial spent nuclear fuel, DOE spent nuclear fuel, and high-level radioactive waste) and environment.

[6] For an ideal gas, oxygen fugacity is the same as oxygen partial pressure, which is about 0.2 atmospheres at sea level.

[7] More details of the rather complicated set of models used to derive the near-field geochemical parameters are given in Section 3.3 and also in the *Total System Performance Assessment-Viability Assessment (TSPA-VA) Analyses Technical Basis Document* (CRWMS M&O 1998i).

[8] "Bound" is always used in the sense of "conservative" (i.e., "bounding" models always predict higher doses).

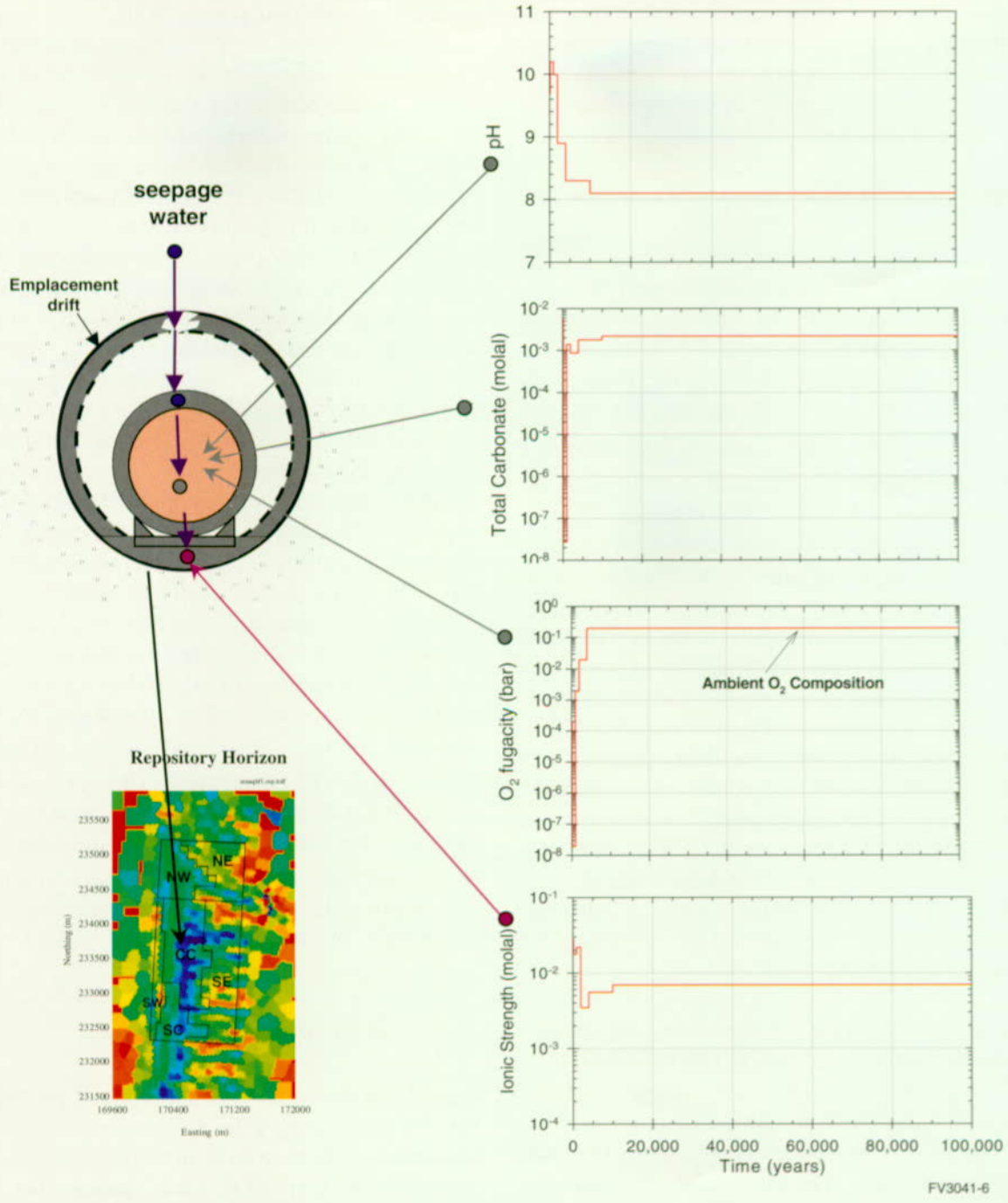

Figure 4-6. Time Histories of the Near-Field Geochemical Parameters
Histories are for pH, Total dissolved carbonates, oxygen fugacity, and infiltration used at various locations in the TSPA-VA base case, based on the expected-value climate history shown in Figure 4-1. These near-field geochemical time histories are based on the central-central (CC) region but are applied to all six waste package regions.

Packages are grouped into four environments based on dripping conditions:

- Packages dripped on during the dry climate and throughout the simulation time
- Packages that are not dripped on during the dry climate but will be in all other conditions (long-term average and superpluvial)
- Packages that are dripped on only during the superpluvial climate
- Packages that are never dripped on[10]

Although seepage behavior through the packages is different for each of these four groups, only two waste package failure histories are used: packages that are always dripped on and packages that are never dripped on. The *Total System Performance Assessment-Viability Assessment (TSPA-VA) Analyses Technical Basis Document* (CRWMS M&O 1998i) has supporting analyses to show why degradation of the corrosion allowance material and the corrosion resistant material is sufficiently modeled with only these two conditions. As explained in a footnote in Section 4.2.2, the packages that are never dripped on and the packages dripped on only during the superpluvial climate are modeled with the no-drip failure history from the WAPDEG computer code, and the other two groups are modeled with the always-drip failure history. The packages are also grouped according to the six regions shown in Figure 4-4, which yields different seepage fluxes in different regions, and therefore different rates of radionuclide transport out of the waste packages and through the engineered barrier system. However, as mentioned in a footnote in Section 4.1.4, the same waste package failure histories are used regardless of region, based on the responses in the northeast region.

The waste package degradation analysis for the base case includes a set of nine cases to represent a range of the uncertainty in the median high-nickel alloy (Alloy 22) corrosion rate and the variability of the Alloy 22 corrosion rate among waste packages and patches. Uncertainty and variability are represented by splitting the total variance of the general corrosion rate for Alloy 22 into three different variability and uncertainty combinations: 75 percent variability and 25 percent uncertainty, 50 percent variability and 50 percent uncertainty, and 25 percent variability and 75 percent uncertainty. For each of the variability-uncertainty splits, the median general corrosion rate is sampled from the 5th, 50th and 95th percentiles of the uncertainty variance, respectively. The expected-value base case is the 50 percent variability and 50 percent uncertainty split and the median corrosion rate at the 50th percentile of the uncertainty variance.

In addition to corrosion degradation of waste packages, the base case includes the effect of early or "juvenile" waste package failures by noncorrosion processes such as materials defects, seismic activity, and human-induced factors, such as welding, handling, and transportation. In the base case, juvenile failure is assumed to cause a single patch opening in a commercial spent nuclear fuel package in a dripping environment, in the southeast region. The expected-value base case assumes a single juvenile failure at 1,000 years. The probabilistic base case uses a log-uniform distribution for juvenile failures from

---

[9] The multi-scale thermal-hydrology models described in Section 3.2 indicate that much of the repository functions as though it is center-like in thermal-hydrologic behavior; however, there is a gradual transition to edge-like behavior as the repository edges are approached. The major difference between the center and edge portions is that shorter abstracted time periods are appropriate for the boiling regime in the edge region as compared to the central portion of the repository. This difference is also true for the two wetter climate states because of the increased cooling capacity of the system.

[10] It is important to realize that packages never move from one environmental group to another, that is, packages that are "dripped on" are dripped on for the entire simulation history and packages that are "never dripped on" are never dripped on for the entire simulation history.

0.001 percent to 0.1 percent, all occurring at 1,000 years after closure.

Figure 4-7 shows the cumulative package penetrations by corrosion, through either pits, patches, or breaches (pits plus patches), for the base case (50/50 split on uncertainty/variability). The figure also shows the time history of average pit area per package and average patch area per package. Because of their much larger area, patches are far more important than pits in causing releases from the packages. Also, all patches and pits are assumed to encounter seeping water at all times.

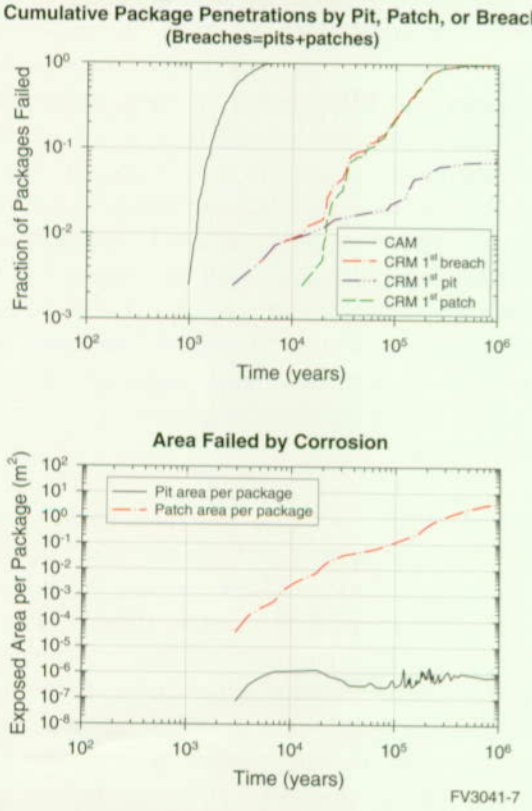

Figure 4-7. Total System Performance Assessment for the Viability Assessment Base Case Waste Package Degradation Histories
Shows cumulative package penetrations by pit, patch, or breach. Also shows growth of average patch area and average pit area per waste package. (CAM—corrosion allowance material [the outer waste package layer made of carbon steel]; CRM—corrosion resistant material [the inner waste package layer made of Alloy 22])

4.1.8 Cladding Degradation

Several mechanisms for cladding degradation of commercial spent nuclear fuel[11] are included in the base case:

- Creep (strain) failure at high temperatures with simultaneous exposure to oxygen
- Juvenile cladding failures (packages emplaced in the repository with cladding already failed)
- Total failure of stainless-steel-clad fuel rods
- Mechanical failure of cladding because of structural failure of the waste package, due to rockfall, corrosion, or seismic events after closure
- Long-term corrosion failure

Juvenile and creep failures combined with failure of the stainless steel cladding is defined at a constant rate of 1.25 percent, beginning at the time of any waste package failure and continuing indefinitely. Most of this is due to the stainless-steel failure. Long-term mechanical failure is initiated with package failure and is defined as a distribution with an expected value of 0.18 percent at 100,000 years after package failure and 2.62 percent at 1 million years after package failure. Long-term corrosion failure is also initiated with package failure, with an expected value of 1.51 percent at 100,000 years after package failure and 7.75 percent at 1 million years after package failure (see Figure 3-54).

[11] In TSPA-VA, cladding on DOE spent nuclear fuel elements is assumed to have failed before emplacement. This is a conservative assumption intended to provide a bound on the maximum possible impact of DOE spent nuclear fuel on repository performance. In reality, not all DOE spent nuclear fuels have faulty cladding (e.g., about 50 percent of N-reactor cladding is intact, as well as 100 percent of naval spent nuclear fuel).

4.1.9 Waste Form Degradation and Mobilization

In the base case, waste form degradation is modeled within the RIP program by defining the dissolution rate equations for fuel exposed by package and cladding degradation. The dissolution rate for commercial spent nuclear fuel is a function of the temperature (T), total dissolved carbonate, oxygen fugacity, and pH of the water contacting the waste form. There is also some uncertainty in the dissolution rate model associated with the equation used to fit the experimental data, and this is a stochastic parameter in the base case. Figure 4-8 shows the commercial spent nuclear fuel dissolution rate as a function of temperature, pH, and total dissolved carbonate. Oxygen fugacity is assumed at atmospheric conditions for these plots. Within the RIP program, the input variables, temperature, total dissolved carbonate, oxygen fugacity, and pH are passed to an external routine, and the dissolution rate is calculated at every time step. The average temperature on the waste package surface is used for the six different repository regions, as calculated by the drift-scale, thermal-hydrology model. This assumption is appropriate because at the time the waste packages begin to fail, the difference between the interior and surface temperatures of the waste package will be small.

The glass dissolution rate is a function of the waste package surface temperature and the pH of the incoming water, and also has a similar stochastic parameter related to uncertainty in the regression fit of the experimental data. A metallic dissolution rate is used for the DOE spent nuclear fuel, which is modeled using a surrogate radionuclide inventory composed mostly of N-Reactor fuel. (The differences in the dissolution rates for the commercial spent nuclear fuel, DOE spent nuclear fuel, and high-level radioactive waste fuels are shown in Figure 4-17.) The specific surface area for commercial spent nuclear fuel is about 0.004 m^2/g, which causes exposed commercial spent nuclear fuel to dissolve in about 1,000 years if the entire surface area is 100 percent wet, which is the assumption for the TSPA-VA. For high-level radioactive waste, the specific surface area is 5.7×10^{-5} m^2/g and for DOE spent nuclear fuel it is 7.0×10^{-5} m^2/g.

4.1.10 Transport in the Engineered Barrier System

Transport in the engineered barrier system is modeled within the RIP program using a series of mixing cells coupled by advective and diffusive "connections" (Figure 4-9). The waste package and the waste form together are represented as a single cell pathway. The concrete invert below the

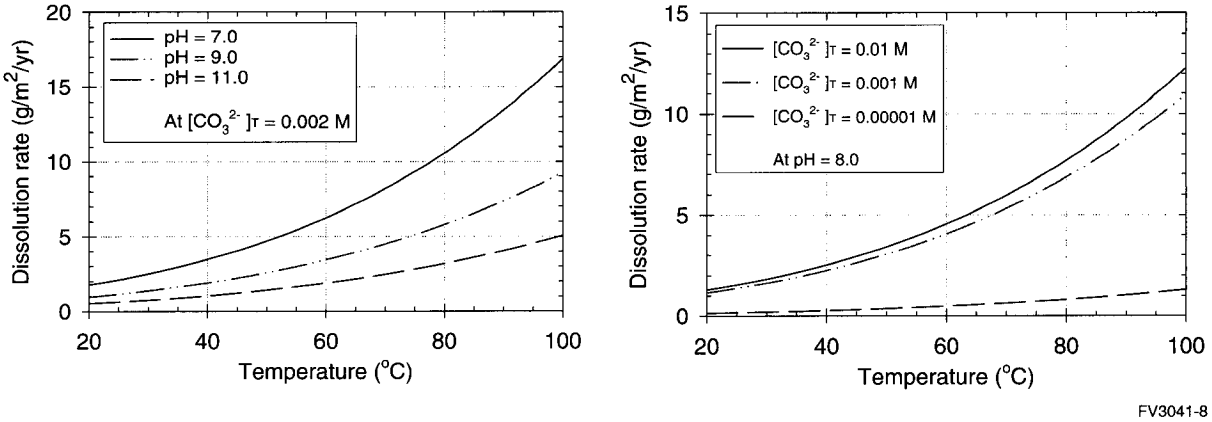

Figure 4-8. Commercial Spent Nuclear Fuel Degradation Rate
Rates are for the TSPA-VA base case as a function of temperature, pH, and total dissolved carbonate in the water contacting the waste form assumes an oxygen fugacity equal to 0.2 atmospheres. (*M*—molar)

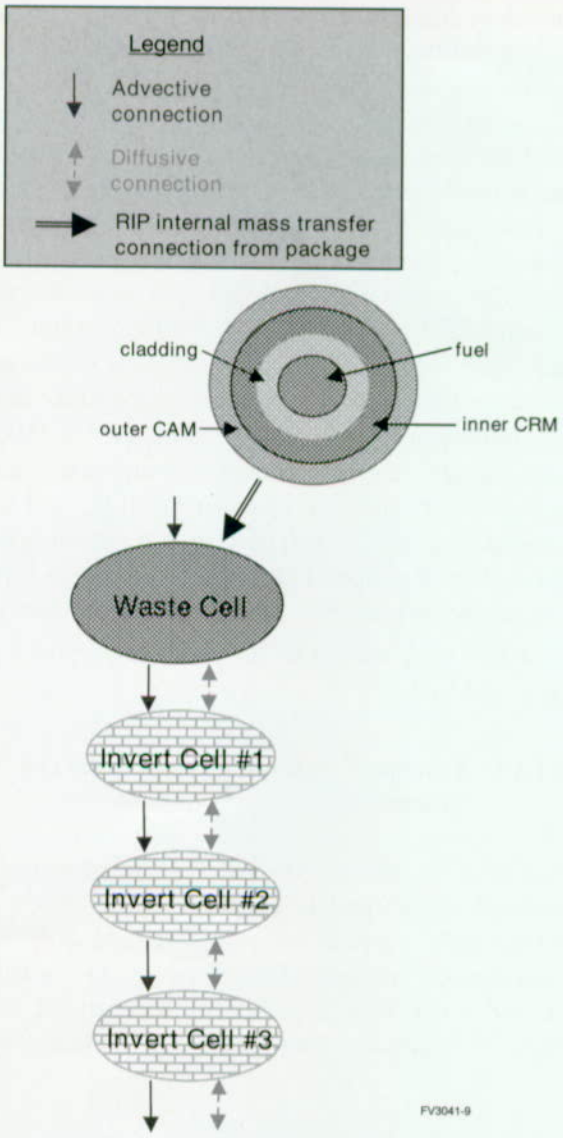

Figure 4-9. Configuration of Cells in the RIP Program for Engineered Barrier System Transport in the Total System Performance Assessment for the Viability Assessment Base Case
(CAM—corrosion allowance material [the outer waste package layer made of carbon steel]; CRM—corrosion resistant material [the waste package layer made of Alloy 22])

package is assumed to be shaped as a semi-circle around the package and is discretized into three cell pathways to decrease the numerical dispersion. The waste-package/waste-form cell pathway is coupled to the first invert cell pathway through an advective connection to represent water seepage through the failed waste package into the invert, and with two diffusive connections for separately modeling the diffusive mass transfer through the pit perforations and patch perforations of a failed waste package. The volumetric flux through the waste package was calculated by scaling the seepage flux into the drift with the available surface area arising from patch and pit failures (see Figure 4-7).[12] The pit perforations and the patch openings also define the area for diffusion.

Volumetric flux through the invert cells is not the same as the reduced flux through the packages but is equal to seepage into the drift. Diffusion through the invert is calculated for a concrete material with 10 percent porosity and 99.8 percent water saturation[13] using an equation for diffusion in a partially saturated medium (Conca 1990; Conca and Wright 1992). The concrete invert also sorbs some of the radionuclides, based on the following sorption coefficients (K_ds) (see Chapter 6 of the *Total System Performance Assessment-Viability Assessment (TSPA-VA) Analyses Technical Basis Document* [CRWMS M&O 1998i]):

- Neptunium K_d is uniform from 0 to 200 mL/g; expected value is 100
- Protactinium K_d is uniform from 0 to 100 mL/g; expected value is 50
- Plutonium K_d is uniform from 0 to 1,200 mL/g; expected value is 600
- Uranium K_d is uniform from 0 to 100 mL/g; expected value is 50

Colloid-facilitated mobilization and transport of radionuclides in the engineered barrier system is modeled for plutonium-239 and plutonium-242, assuming fast reversible attachment. There are four types of colloids in the engineered barrier

[12] The surface area available for seepage was increased by a "seepage collection factor" to account for the focusing of water dripping on the waste package. This factor was sampled uniformly from 1 to 10, with a mean of 5.5.

[13] The liquid saturation is actually a function of time, as determined by drift-scale, thermal-hydrologic modeling, but it returns to 99.8 percent (that is, ambient saturation) by the time the packages begin to fail.

system: two natural types, iron-oxides and clays; and two types based on fuel degradation, spent nuclear fuel colloids and glass waste colloids. The expected-value colloid partition coefficients (K_cs) for these four types are as follows (see Chapter 6 of the *Total System Performance Assessment-Viability Assessment (TSPA-VA) Analyses Technical Basis Document* [CRWMS M&O 1998i]):

- 0.24 for iron-oxides
- 0.024 for clays
- 0.087 for spent nuclear fuel particles
- 0.72 for glass particles

A small fraction of the total mobilized plutonium, that is, the plutonium in both the aqueous and reversibly sorbed colloid phases, is assumed to sorb irreversibly to colloids at the edge of the engineered barrier system to account for the fraction observed at various nuclear waste sites, for example, the very small amount observed at the Nevada Test Site from the Benham nuclear blast. This fraction is sampled log-uniformly in the range of 1×10^{-4} to 1×10^{-10}, with a value of 1×10^{-7} for the expected-value case.[14] The basis for this range is discussed in Chapter 6 of the *Total System Performance Assessment-Viability Assessment (TSPA-VA) Analyses Technical Basis Document* (CRWMS M&O 1998i).

For radionuclides with a very high solubility in the pore water seeping through the packages, the radionuclide mass dissolved at each time step is swept away in the next time step, that is, the carrying capacity of the water is very high. Low solubility radionuclides re-precipitate and are only removed slowly as a linear function of the seepage flux through the package. This effect is most important for neptunium-237, plutonium-239, plutonium-242, and uranium-234. The solubilities used in TSPA-VA are about the same as in the 1995 TSPA, except for neptunium-237, (CRWMS M&O 1995) and are listed in Table 3-15. The most important solubility value is for neptunium-237, which is 0.34 g/m^3 or 1.43×10^{-6} *M* for the expected-value realization shown in Section 4.2.[15] The volume of water available for mobilization of waste at any time step (i.e., for computing solubility) is equal to the volume of water in the pores of the "rind", which is the in growing shell of altered fuel being changed into other minerals through contact with gases and liquids that have entered the degraded waste package. This water volume is based on a porosity of 40 percent and a water saturation of 100 percent in the rind. The rind volume itself is linearly proportional to the fuel rod volume times the fuel dissolution rate (a constant with units of year^{-1}) times the time since first water contact.

4.1.11 Unsaturated Zone Transport

The unsaturated zone transport model for the base case is based on the unsaturated zone flow model. The transport model uses the same three flow fields described above and the same climate states. As with unsaturated zone flow, a dual-permeability model is assumed, and transport is modeled with the FEHM particle tracker in three dimensions. Therefore, transport is assumed to occur in two continua, with fracture-matrix interflow based on the steady-state flow fields generated by the TOUGH2 computer code. The FEHM particle tracker transports particles on the same dual-permeability TOUGH2 spatial grid as used in the flow model. When the climate shifts, a new TOUGH2 flow field is provided from the run-time file directory, and the particles are assumed to be instantly traveling with the new velocities. When the water table elevation rises, the particles in the "lost" vertical distance corresponding to this rise are instantly released in that timestep to the water table. When the water table elevation falls, there is a brief time when there are no particles in this new vertical distance.

[14] Actually, the exponent is sampled uniformly in the range of -10 to -4, which yields a mean of -7.

[15] Section 5.5.4 and Figure 5-34 discuss the solubility range for neptunium-237 used in TSPA-VA. The mean and upper and lower limits of this range have been reduced by about a factor of 100 from the 1995 TSPA based on new interpretations of experimental data. This is discussed in detail in Chapter 6 of the *Total System Performance Assessment-Viability Assessment (TSPA-VA) Analyses Technical Basis Document* (CRWMS M&O 1998i).

Sorption based on experimental data is assumed for the radionuclides (see Section 3.6). As discussed in Section 4.2, sorption is important for three key radionuclides in the unsaturated zone; neptunium-237, plutonium-239, and plutonium-242. The sorption coefficient (K_d) value for neptunium-237 is 1.0 mL/g in the vitric and devitrified tuff units and 4.0 mL/g in the zeolitic units. For the two plutonium species, the K_d is 100 mL/g in all units. Matrix diffusion is assumed for all radionuclides but, as shown in Section 5.6, has little effect on the dose rates. The assumed matrix-diffusion coefficient has a mean of 3.2×10^{-11} m^2/s for carbon-14, technetium-99, iodine-129, and selenium-79 and 1.6×10^{-10} m^2/s for neptunium-237, plutonium-239, plutonium-242, uranium-234, and protactinium-231. The expected value for the dispersivity used in the unsaturated zone model is 20 m in all three directions. Figure 4-10 shows an overlay of the source-term discretization at the top of the unsaturated zone model and the discretization of the output at the water table. Between the top and bottom, particles are free to move in any direction. The travel time during the long-term average climate is illustrated for a pulse release for three key radionuclides; technetium-99, neptunium-237, and plutonium-242.

4.1.12 Saturated Zone Flow and Transport

Figure 4-11 is a combination of several figures from Section 3.7 that illustrate the base case model for saturated zone flow and transport. A coarsely discretized (500 m in the x and y directions and 50 m in the z direction), three-dimensional numerical model is first used to simulate flow in the saturated zone. The model determines the general plume direction and flowpath length in the tuff and alluvium, based on the revised geologic framework model for lithostratigraphy (see Section 3.7). Radionuclide transport in the saturated zone is then modeled with six one-dimensional streamtubes placed along the general plume direction determined from the three-dimensional model. The six regions at the water table in Figure 4-11 are used to determine total volumetric flux from the unsaturated zone into each of six one-dimensional streamtube models in the saturated zone. The average specific discharge in the dry climate is assumed to be 0.6 m/year in all six of the streamtubes, based on the results of the saturated zone expert elicitation panel (CRWMS M&O 1998g). The streamtube models are run with the FEHM computer code, assuming an effective continuum, that is, the permeability is approximately equal to the fracture permeability but the porosity is approximately equal to the matrix porosity. The six streamtubes are used to develop unit breakthrough curves based on a constant concentration source. The breakthrough curves are scaled by the area of the streamtubes, which is proportional to the volumetric unsaturated zone flow into each streamtube, to get the correct concentration in each streamtube. The unit breakthrough curves are convolved at each time step with the actual RIP source term during run time. A dilution factor to simulate transverse dispersion is applied to the concentration curves for each 20-km streamtube, based on a probability distribution determined from the saturated zone expert elicitation panel. The same dilution factor (see Figure 4-11) is applied to all radionuclides, all streamtubes, at all time scales. The actual saturated zone concentration used to compute dose rate is essentially a function of the dilution factor; for high dilution factors, effective diffusive mixing among streamtubes is assumed and the six concentrations are added. For low dilution factors, no mixing is assumed and the maximum concentration streamtube is used. (See Figure 4-19 for a plot of the effective dilution factor used. See the end of Section 4.2.1 for a more detailed summary of the basis for either using the summed concentrations or the maximum concentration.) For the TSPA-VA base case, the values used for the various stochastic saturated zone model parameters are listed in Table 3-20.

4.1.13 Biosphere Transport

The final dose rate is calculated within RIP by multiplying a biosphere dose conversion factor by the saturated zone concentration discussed above. Water having a concentration equivalent to the saturated zone concentration is assumed to be drawn from a well 20 km (12 miles) downgradient from the repository. The water is then used as drinking and irrigation water for an "average" adult living in Amargosa Valley (see third row of

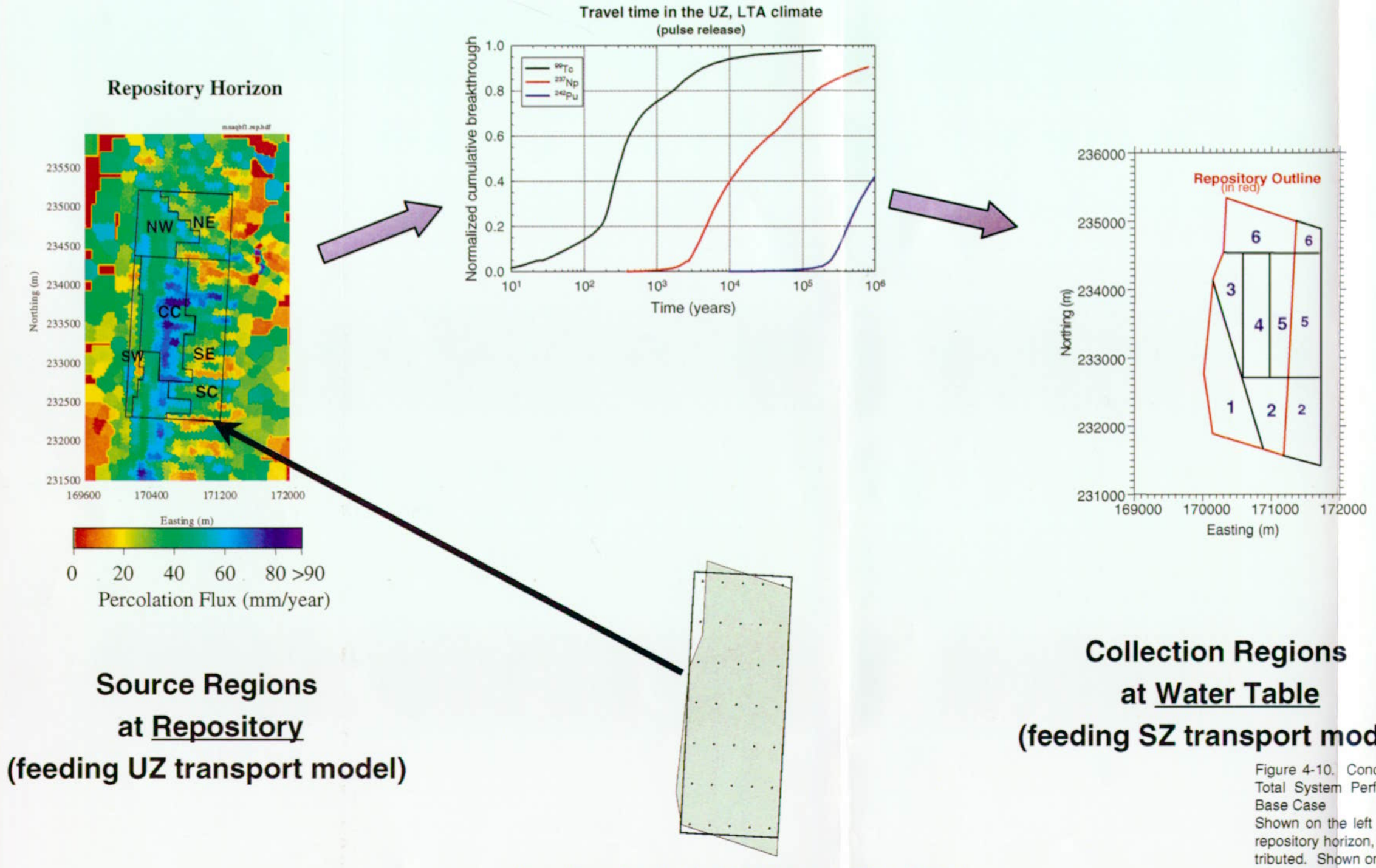

FV3041-10

Figure 4-10. Conceptualization of Unsaturated Zone Transport for the Total System Performance Assessment for the Viability Assessment Base Case
Shown on the left are the six waste package or source regions at the repository horizon, within which radionuclide releases are uniformly distributed. Shown on the right are the six "collection" regions at the water table, which define the area and volume flux of the six one-dimensional streamtube models for saturated zone transport. Also shown are breakthrough curves tor technetium-99, neptunium-237, and plutonium-242 transport through the unsaturated zone in the long-term average climate for a pulse source. (The small overlay shows how nearly the six regions at the repository horizon approximate the actual repository layout.) Maps showing six regions can be compared by comparing coordinate grids. (UZ—unsaturated zone; SZ—saturated zone; LTA—long-term average)

INTENTIONALLY LEFT BLANK

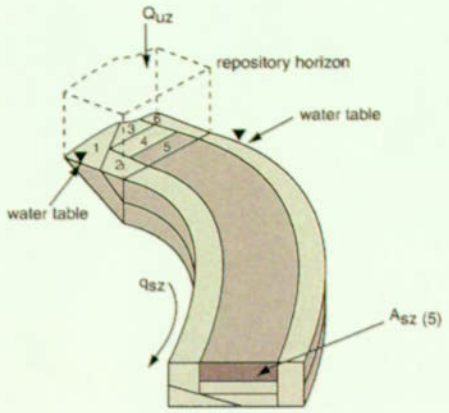

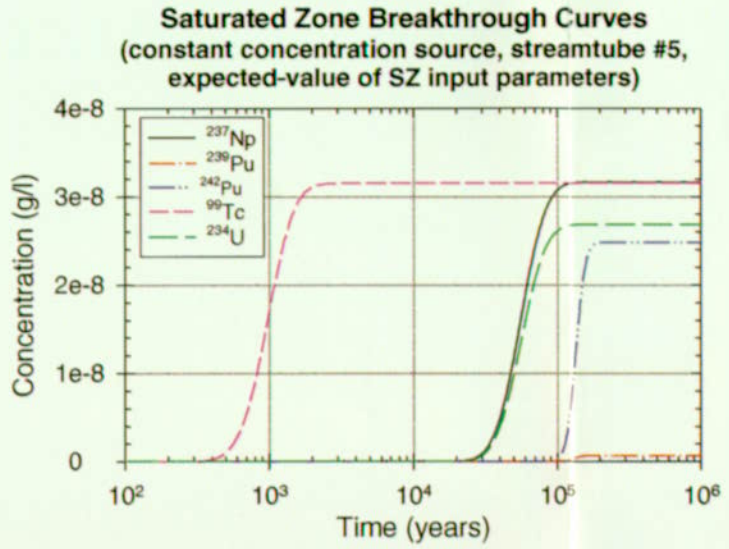

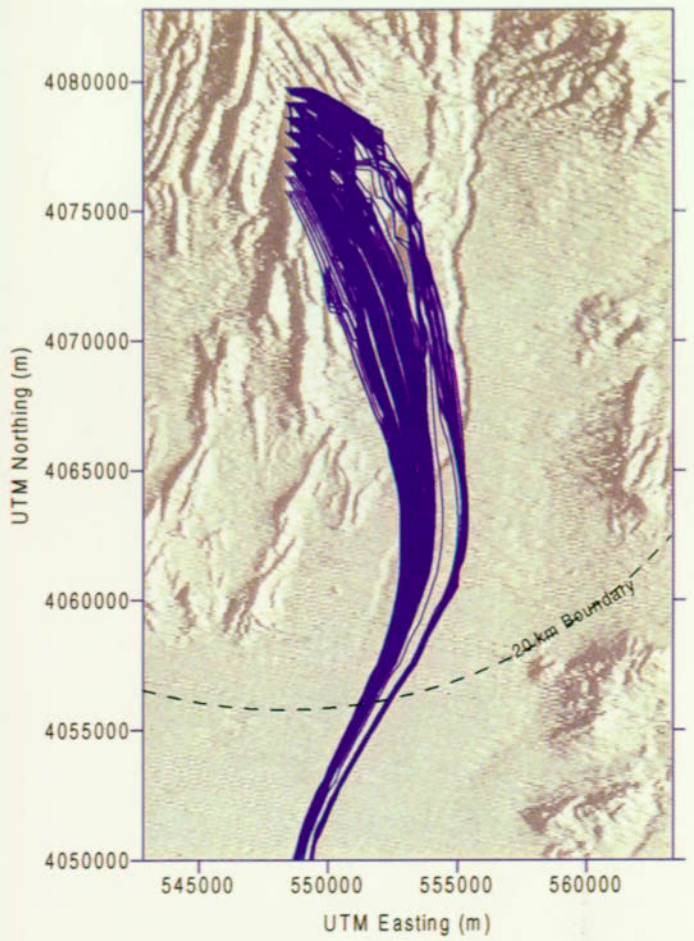

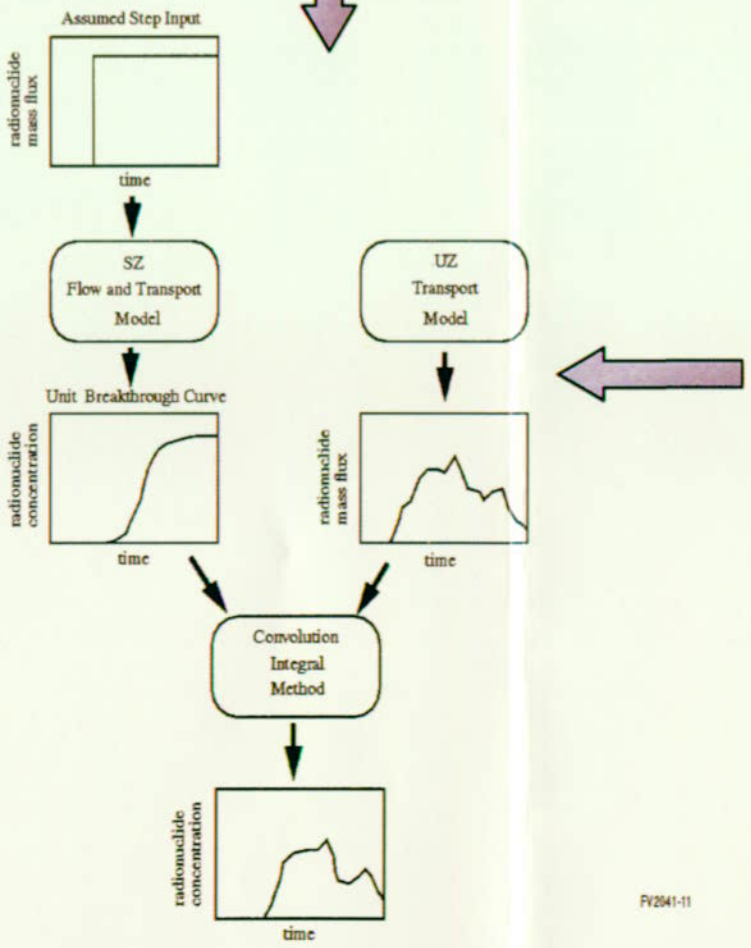

FV2641-11

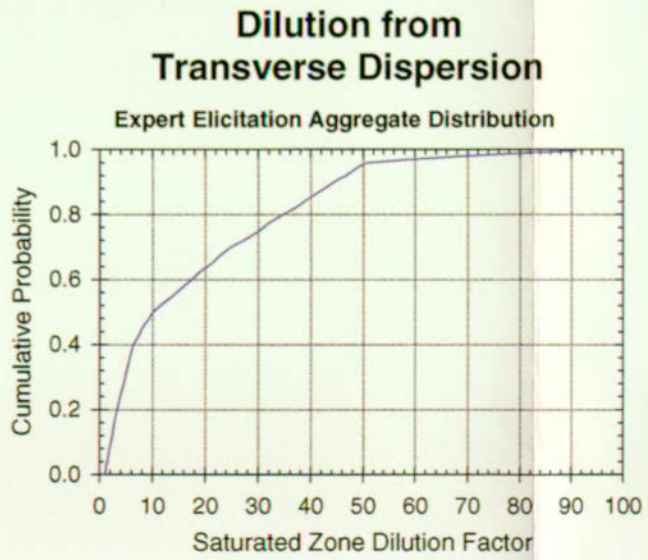

Figure 4-11. Conceptualization of Saturated Zone Transport for the Total System Performance Assessment for the Viability Assessment Base Case

In the lower left is a plan view of the particle pathlines predicted by the three-dimensional flow model. In the upper left is a diagram of the six one-dimensional streamtubes, showing how each is associated with one of the six water table regions depicted in Figure 4-10. To the right of the streamtubes is a plot of 20-km (12 miles) breakthrough curves in the saturated zone for a constant concentration at the beginning of streamtube #5, for five key radionuclides. In the lower middle is the flow chart for the convolution integral method, which combines the breakthrough curves with the mass release from the unsaturated zone. In the lower right is the dilution-factor cumulative distribution function applied to the concentration at 20 km (12 miles). (SZ—saturated zone)

INTENTIONALLY LEFT BLANK

Table 3-24). The dose rate to the individual (millirems per year) for a given radionuclide is the product of the biosphere dose conversion factor and the saturated zone concentration. Section 3.8 discussed the parameters used in the biosphere modeling. The expected-value biosphere dose conversion factors for the nine radionuclides considered in the TSPA-VA base case, under long-term average climatic conditions, are as follows:[16]

- Carbon-14 = 1.23×10^7 (mrem/year)/(g/m^3)
- Iodine-129 = 8.24×10^4 (mrem/year)/(g/m^3)
- Neptunium-237 = 4.60×10^6 (mrem/year)/(g/m^3)
- Protactinium-231 = 6.56×10^8 (mrem/year)/(g/m^3)
- Plutonium-239 = 2.72×10^8 (mrem/year)/(g/m^3)
- Plutonium-242 = 1.56×10^7 (mrem/year)/(g/m^3)
- Selenium-79 = 9.30×10^5 (mrem/year)/(g/m^3)
- Technetium-99 = 5.29×10^4 (mrem/year)/(g/m^3)
- Uranium-234 = 2.22×10^6 (mrem/year)/(g/m^3)

4.2 DETERMINISTIC RESULTS OF THE TOTAL SYSTEM PERFORMANCE ASSESSMENT BASE CASE

The single realization described in this section is the outcome of sampling all uncertain input parameters in the TSPA-VA component models at the expected value of their ranges (i.e., at their mean or average value). The intent is to illustrate how total system behavior (i.e., individual dose rate) is influenced by the various component or subsystem models and parameters. The method is to compare time history plots of key subsystem parameters (e.g., waste package failure history) with the time history plots of both dose rate and release rate at various system boundaries (e.g., the bottom boundary of the unsaturated zone—the water table).

Figure 4-12 illustrates the dose rate versus time from all biosphere dose pathways to an average adult (see Section 3.8) residing 20-km (12-miles) downgradient of the repository, for the expected-value simulation. The three graphs in this figure correspond to three different time frames:

- The first 10,000 years after repository closure
- The first 100,000 years after repository closure
- The first 1 million years after repository closure, which is the likely maximum geologically stable time period according to the National Research Council panel on Yucca Mountain performance standards (National Research Council 1995, p. 72)

The shape and timing of various dose histories in these plots is explained in subsequent figures in this section. Key points about the three plots in Figure 4-12 are the following:

1. Within the first 10,000 years, the only radionuclides to reach the biosphere are the nonsorbing radionuclides with high inventories, technetium-99 and iodine-129, and the total peak dose rate is about 0.04 mrem/year.
2. Within the first 100,000 years, the weakly sorbing radionuclide neptunium-237 begins to dominate doses in the biosphere at about

[16] Justification for the use of only these nine radionuclides is presented in Chapter 6, Appendix C of the *Total System Performance Assessment-Viability Assessment (TSPA-VA) Analyses Technical Basis Document* (CRWMS M&O 1998i).

INTENTIONALLY LEFT BLANK

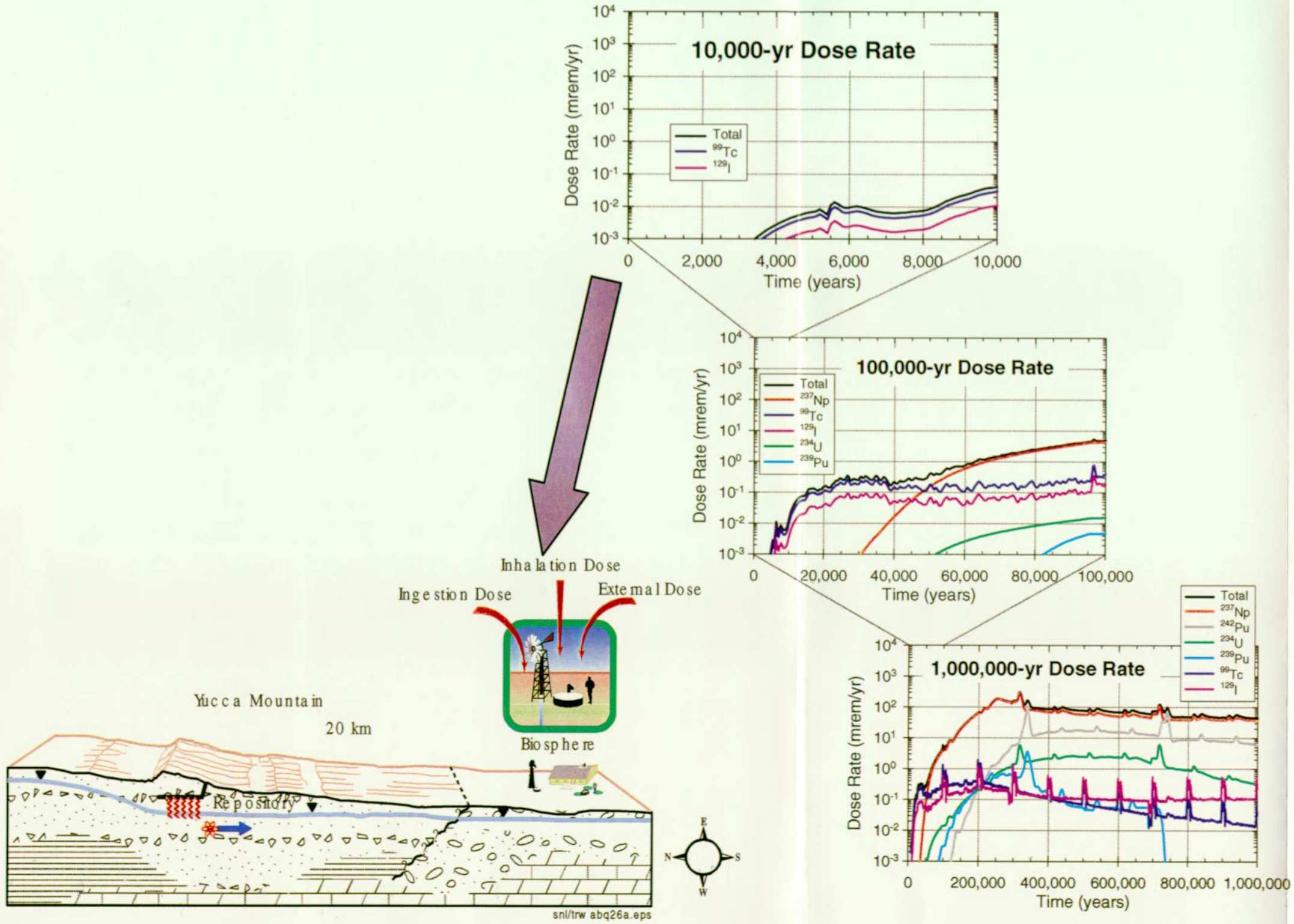

Figure 4-12. Dose Rate to an "Average" Individual Withdrawing Water from a Well Penetrating the Maximum Plume Concentration in the Saturated Zone 20 km (12 miles) Downgradient from the Repository
This figure shows the most important radionuclides in different time periods: technetium-99 and iodine-129 within the first 10,000 years; technetium-99 and neptunium-237 within the first 100,000 years; and neptunium-237 and plutonium-242 within the first 1 million years.

INTENTIONALLY LEFT BLANK

50,000 years, with the total dose rate reaching about 5 mrem/year.

3. Within the first 1 million years, neptunium-237 continues to be the major contributor to peak dose rate, which reaches a maximum of about 300 mrem/year at about 300,000 years after closure of the repository, just following the first climatic superpluvial period.[17] The radionuclide plutonium-242 is also important during the 1 million-year time frame and has two peaks at about 320,000 years and 720,000 years, closely following the two superpluvial periods. There are regularly spaced spikes in all the dose rate curves (more pronounced for nonsorbing radionuclides such as technetium-99 and iodine-129) corresponding to the assumed climate model for the expected-value base case simulation, as shown in Figure 4-1. As described below, these spikes are a result of assumed abrupt changes in water table elevation and seepage through the packages.

4.2.1 Ten-Thousand-Year Dose Rates

Within the first 10,000 years after closure, technetium-99 and iodine-129 are the dominant radionuclides to reach the biosphere. Relatively large inventories of technetium-99 and iodine-129 are emplaced in the commercial spent nuclear fuel packages. Following are three important qualities of these two radionuclides:

- High solubility in the Yucca Mountain pore water seeping into the waste packages,[18] which allows rapid release from the waste packages and the engineered barrier system compared to releases of the actinide elements, that is, uranium, neptunium, curium, and americium

- Negligible sorption onto the tuff rock matrix in the natural barriers, which allows relatively rapid transport through the natural system compared to other, more chemically reactive, elements[19]

- Relatively slow decay compared to the 10,000-year time span[20]

Because both technetium-99 and iodine-129 behave similarly with respect to these three key attributes, only the movement of technetium-99 needs to be tracked through the system to explain the behavior of both ions, and the behavior of the total dose rate within 10,000 years.

---

[17] This dose rate is comparable to the annual mean background radiation in the United States from natural sources (NCRP 1987, p. 149; National Research Council 1990, p. 19). The dose rate shown in Figure 4-12 reaches a peak after the superpluvial period (see Figure 4-1) because of a sorption delay affecting neptunium-237 transport in the saturated zone. Also, as discussed in Chapter 6, Appendix C of the *Total System Performance Assessment-Viability Assessment (TSPA-VA) Analyses Technical Basis Document* (CRWMS M&O 1998i), the predicted total dose rate of 300 mrem/year would perhaps increase by 15 to 20 percent if the daughter products of neptunium-237 (uranium-233 and thorium-229) had been included in the model.

[18] The composition of the water seeping into the waste packages may be altered from ambient (i.e., pre-repository) conditions because of thermal-chemical processes, including evaporation and recirculation during the early high-temperature period and chemical reaction with the emplaced in-drift, waste package, and waste form materials. Thus, the use of ambient pore-water solubility in the radionuclide mobilization model in TSPA-VA is an approximation. See the *Total System Performance Assessment-Viability Assessment (TSPA-VA) Analyses Technical Basis Document* (CRWMS M&O 1998i) for clarification of this modeling assumption.

[19] Both technetium and iodine are assumed to be dissolved in the pore water in their anionic, oxidized forms as pertechnetate (TcO_4^-) and iodide (I^-). Under ambient or chemically unaltered conditions in Yucca Mountain, anions have a low affinity for sorption onto the volcanic tuff rocks, which implies that they can travel more rapidly through the unsaturated zone than other radionuclides that are in a cationic, or positively charged, state in the oxidized groundwater. Furthermore, pertechnetate and iodide have a lower potential for incorporation into minerals via precipitation than some other elements, such as the actinide elements, particularly under oxidizing conditions.

[20] Technetium-99 has a half life of about 213,000 years and iodine-129 about 15,700,000 years.

Figures 4-13 through 4-15, discussed in detail in this section, show the primary causes for the shape and timing of the 10,000-year dose rate graphs for technetium-99 and iodine-129. Two primary sets of plots are shown:

- Time histories of activity release and radionuclide concentrations at the downgradient boundaries of various parts of the natural and engineered barriers (e.g., engineered barrier system, unsaturated zone, and saturated zone)

- Time histories of key subsystem parameters

Figure 4-13 shows the performance of the engineered barrier system. It is evident from Figure 4-13 that the initial releases of technetium-99 (and also iodine-129 and carbon-14) from the waste packages and the engineered barrier system are caused by the first package failure at 1,000 years, which is an assumed juvenile, or early, failure arising from possible manufacturing defects, rockfall, or seismic activity. This failure is assumed to occur in the southeast repository region, the largest in area of the six regions (see Figure 4-4). The small initial peak and oscillation in release from the engineered barrier system in the southeast region at about 1,000 years is caused by the initial gap fraction release from the single juvenile-failure package. The gap fraction is the 2 percent of the total technetium-99 inventory residing in very soluble form in the gap between the fuel matrix and the cladding.

After the initial juvenile failure at 1,000 years, the first corrosion failures occur at about 4,100 years and 4,200 years (the first one in the southeast region and second one in the central-central region), indicated by the bar heights equal to 1 in the histogram plot of package failures. After that, more packages fail by corrosion in all the various regions starting at 5,000 years. Besides this waste package failure history, the other key event influencing performance in the 10,000-year time frame is the abrupt climatic change from current dry conditions to the relatively wetter long-term average climate, occurring at 5,000 years in this expected-value realization. This climatic change is evident in both the waste package and engineered barrier system mass-release graphs and causes the abrupt peak in releases at 5,100 years. However, this mass-release peak originates almost solely from the single juvenile-failure package and not from the two corrosion-failed packages.[21] For example, the advective/diffusive release plot shows that the two corrosion-failed packages at 4,100 and 4,200 years have a negligible influence on either total[22] advective or total diffusive mass-release curves prior to the climate change at 5,000 years.[23]

This lack of influence is a result of the very small initial patch area per package, shown graphically in Figure 4-13. This small area means a low diffusive flux out of the corrosion-failed packages and a low seepage flux into the corrosion-failed packages. The latter causes low advective releases during the dry climate (Figure 4-13).[24] (The seepage flux

[21] The juvenile-failure package has the same clad failure fraction initially (about 1.25 percent) as the corrosion-failed packages.

[22] "Total" as used here means the total releases from all waste packages in the entire repository.

[23] During the dry climate in the first 5,000 years, the technetium-99 releases from advection and diffusion are about the same from the juvenile-failure package and add up to the total release curve from the engineered barrier system. Later, in the 100,000-year and 1 million year time frames (see Figures 4-16 and 4-21), diffusion dominates over advection by about a factor of 10 for technetium-99 releases during the dry climate periods. This is because technetium-99 is not released by advection from the package at nearly as high a rate during the dry climate compared to the long-term average climate. Therefore, a higher concentration of technetium-99 builds up in the waste package during the dry climate, producing a much higher concentration gradient from the inside to the outside of the package. This concentration gradient is the force that produces diffusive releases. However, at very early times, from 1,000 to 5,000 years, the patch area on the single juvenile-failure package is too small to allow diffusive releases to dominate advective releases (compared to the larger patch area available on corrosion-failed packages at later times).

[24] On the seepage flux plot, the red line indicates the average seepage flux through the packages, averaged over all six repository regions. The six gray lines (hard to see individually because they overlap) are the seepages into the six individual regions. Similarly, for the seepage into the drift, the blue line represents an areal average over the regions.

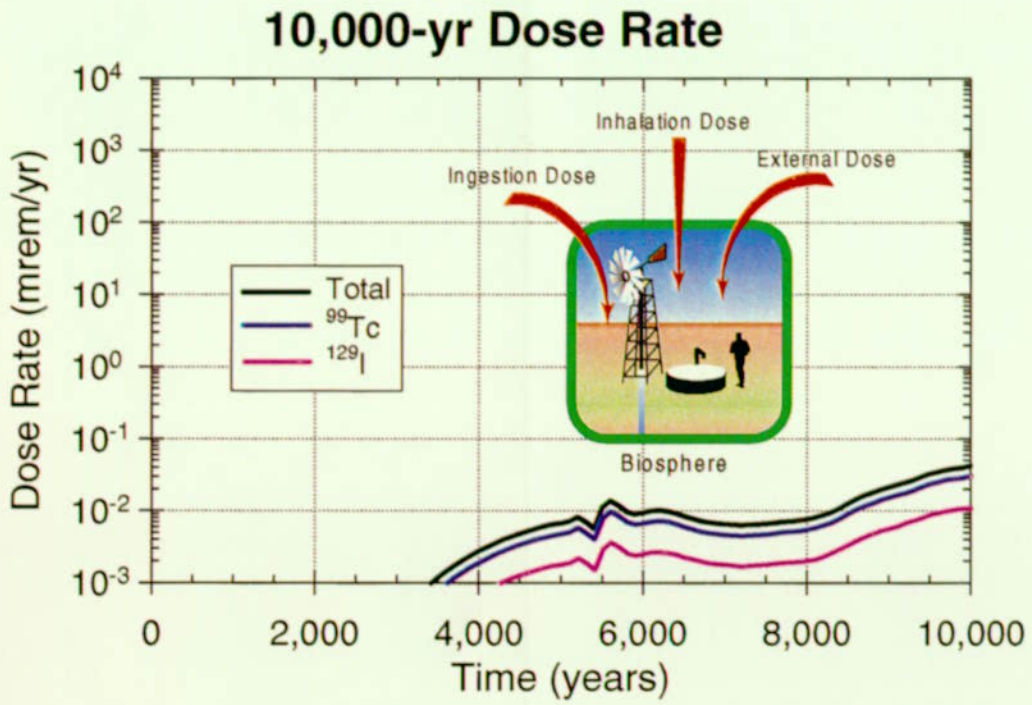

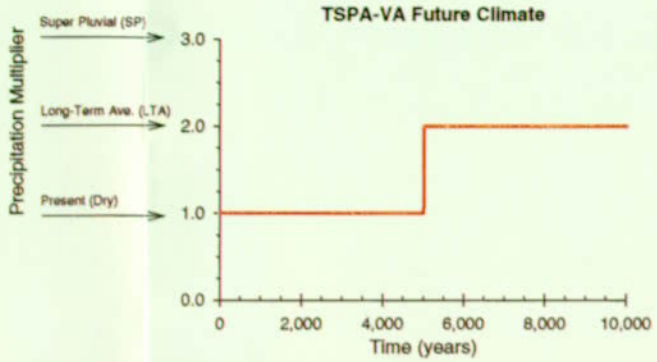

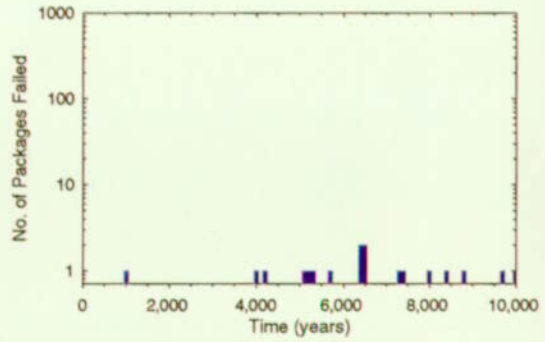

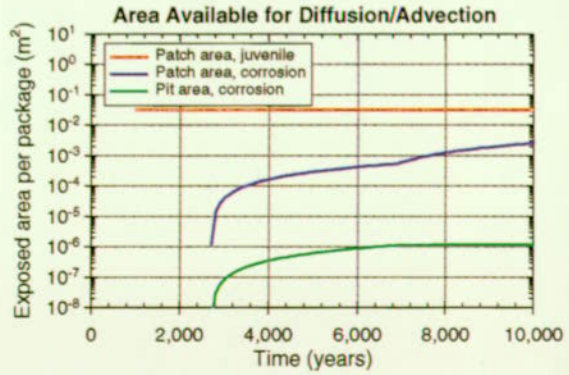

both ^{99}Tc and ^{129}I

no sorption → fast transport

high solubility → fast EBS release

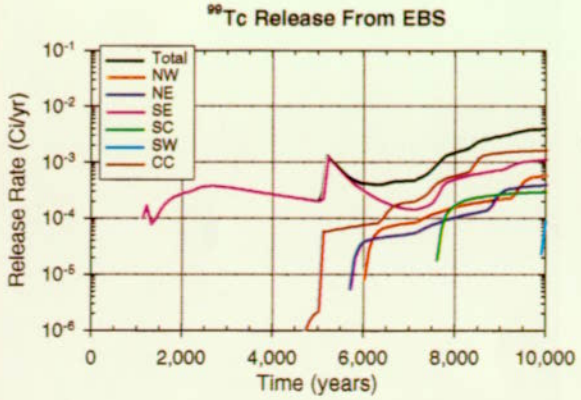

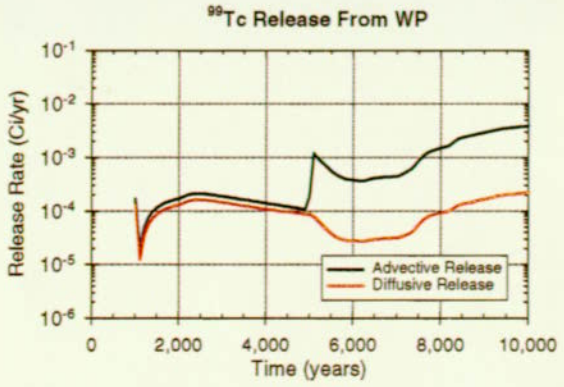

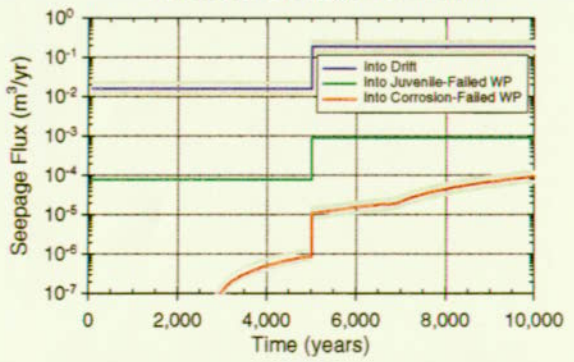

Figure 4-13. Effects of Climate Change, Seepage Flux, and Waste Package Degradation on Engineered Barrier System Releases and Dose Rates in the First 10,000 Years After Waste Emplacement
(EBS—engineered barrier system; WP—waste package)

INTENTIONALLY LEFT BLANK

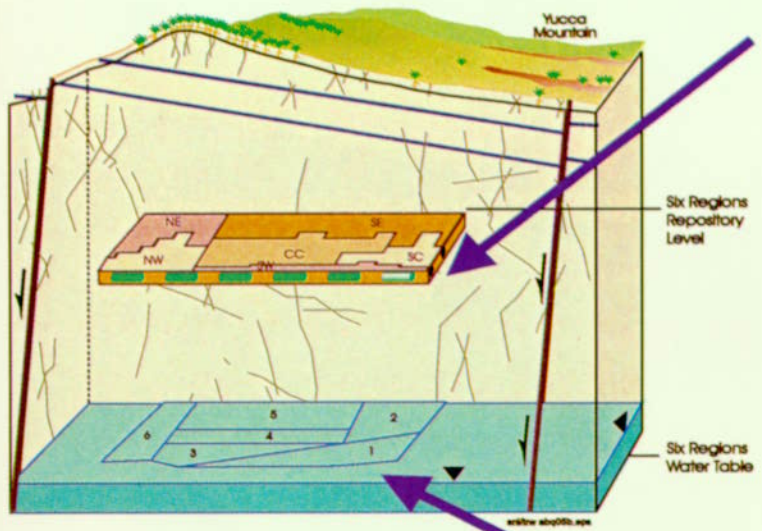

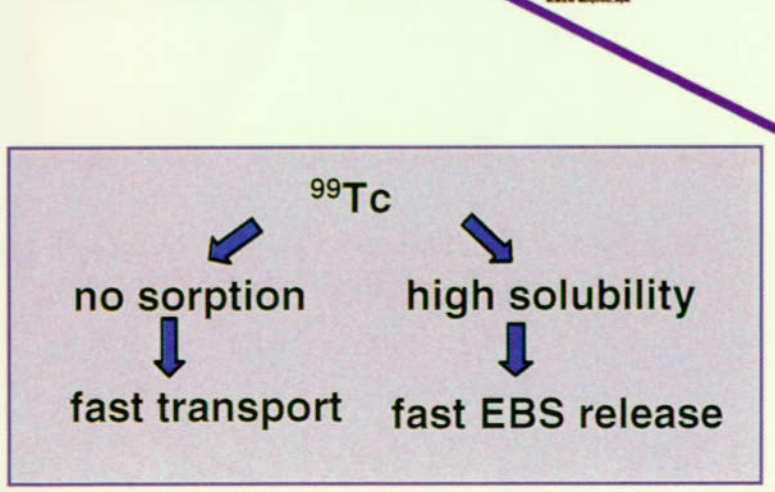

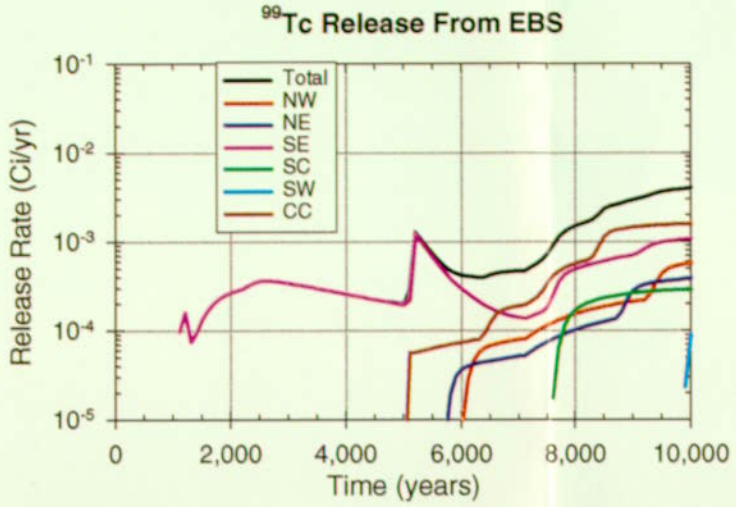

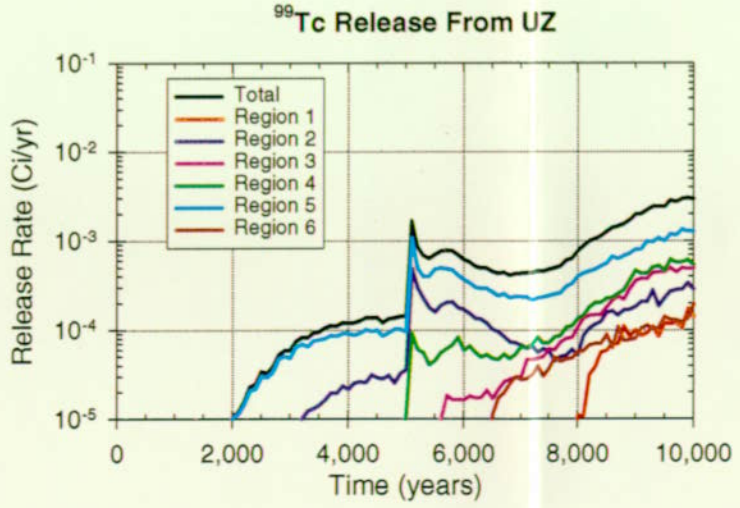

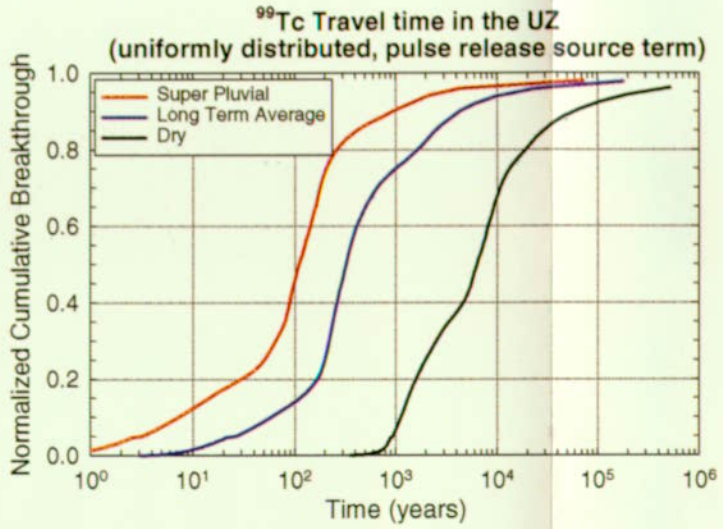

Figure 4-14. Performance of the Unsaturated Zone with Respect to Technetium-99 During the First 10,000 Years After Waste Emplacement
Shown is the effect of different climate states, the engineered barrier system released from various repository regions, and the unsaturated zone releases to the various water table regions. (UZ—unsaturated zone; EBS—engineered barrier system)

INTENTIONALLY LEFT BLANK

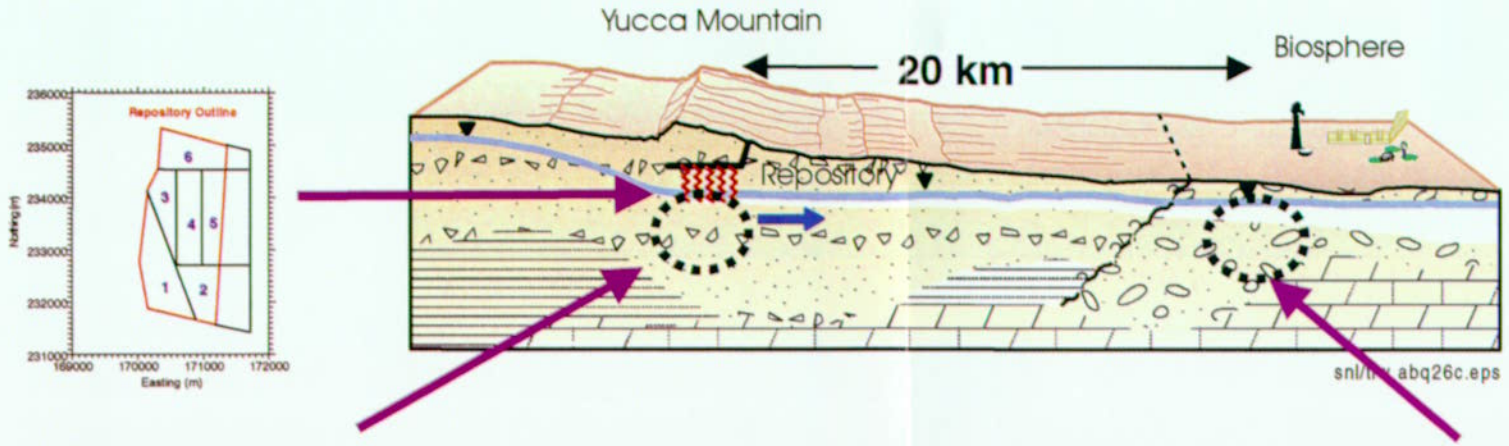

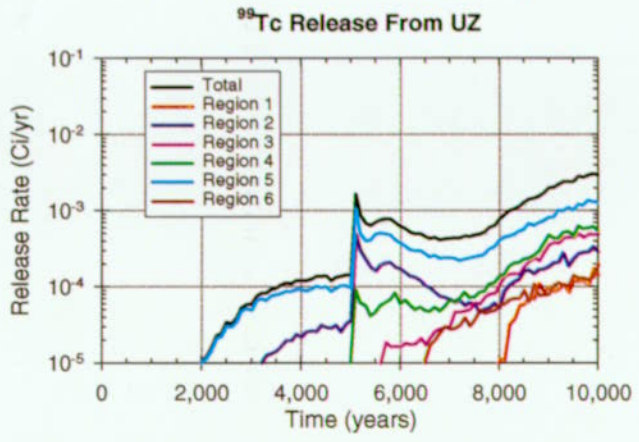

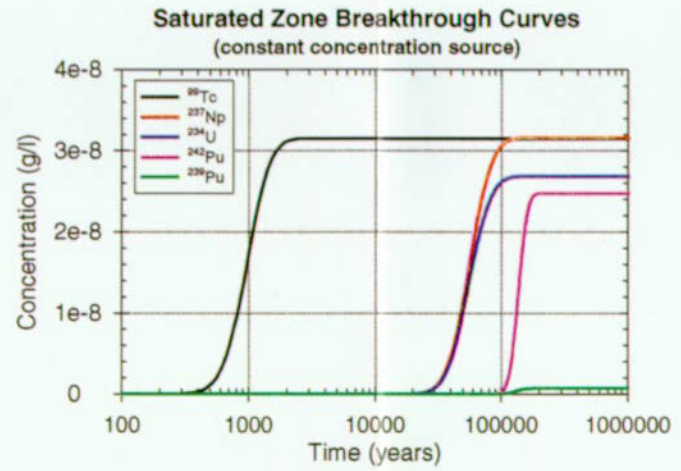

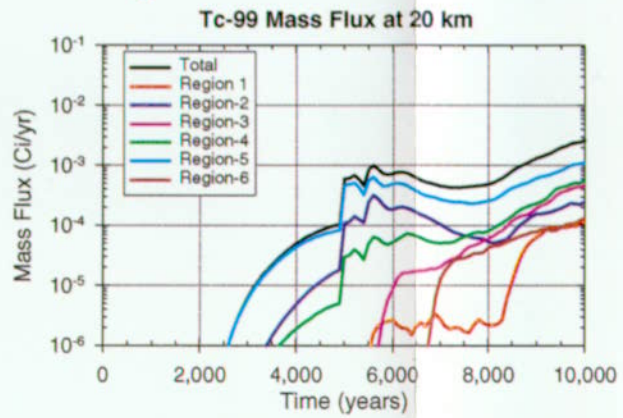

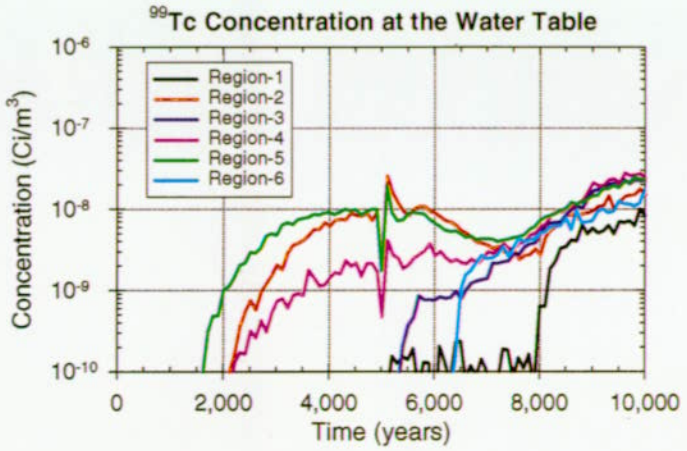

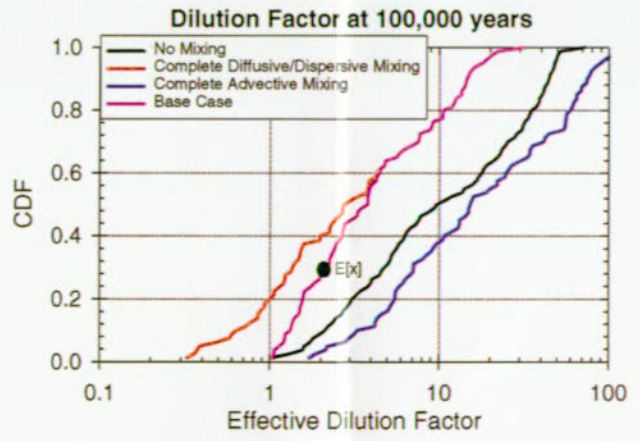

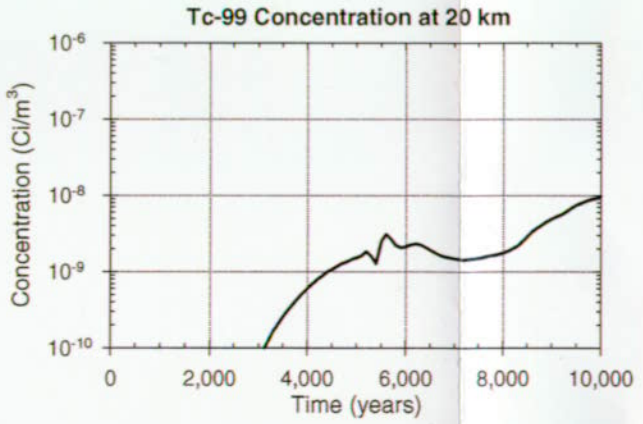

Figure 4-15. Performance of the Saturated Zone with Respect to Technetium-99 During the First 10,000 Years After Waste Emplacement
Shown are concentration and releases in six stream tubes (each associated with one of six regions at the water table level) and the impact of dilution in the saturated zone. Shown in the upper left corner are the six water table regions. (UZ—unsaturated zone; CDF—cumulative distribution function)

INTENTIONALLY LEFT BLANK

into the drift is the same for both the juvenile package and the corrosion packages, but the seepage into and through the packages is different because of the different patch area.) The single juvenile-failure package was conservatively assumed to have a larger failed area (0.031 m^2, which stays constant with time) than the initial corroded patch area per package for the corrosion failed packages. The patch area on corrosion failed packages eventually equals the failed area of the juvenile failure package at about 30,000 years.

At 5,000 years, the climate becomes wetter and the seepage flux through both the juvenile-failure package and the corrosion-failed packages abruptly increases, as shown on the plot of seepage flux. This increase produces a burst of technetium-99 release from the repository at 5,000 years, shown by the peak in the technetium-99 advection curve. The diffusive release curve drops off during the long-term average climate because the removal of technetium-99 by advection decreases the concentration in the waste package. The burst in technetium-99 release at 5,000 years is caused almost solely by the greater flushing of the juvenile failure package, with only a negligible contribution from the corrosion-failed packages. The contribution from the corrosion-failed packages is very small because the patch area and seepage flux are low enough that the solubility limit for technetium-99 becomes important for those packages.

Figure 4-13 has shown the major factors controlling the 10,000-year repository performance. These factors are related to the engineered barrier system, primarily waste package performance and seepage. Some additional contribution to performance is gained within the natural geologic setting, that is, the barriers of the unsaturated and saturated zones, but primarily only during the dry climate up to 5,000 years. This additional performance is caused by delay in transport because of slow liquid flow through the 300 m of unsaturated zone between the repository and the water table. It is also caused by the relatively long (20 km, or 12 miles) travel distance in the saturated zone—from the repository footprint at the water table to the water withdrawal location. On the other hand, in the long-term average climate, the delay because of travel time in the unsaturated zone is greatly reduced by the higher overall infiltration flux, from an average of about 7 mm/year to an average of 40 mm/year. The delay is also influenced by the increase in proportion of the unsaturated zone travel path associated with fracture flow and the much greater proportion of fracture flow (compared to matrix flow). The delay during the long-term average climate is only about 300 years, based on the 50 percent point of the breakthrough curve.

Figure 4-14 shows the effect of the unsaturated zone on technetium-99 activity releases. The fast transport of nonsorbing radionuclides is apparent. However, comparing the total activity release from the engineered barrier system with the total activity release from the bottom of the unsaturated zone does not provide a measure of the technetium-99 travel time through the unsaturated zone because the engineered barrier system releases have only been occurring over a 4,000-year period prior to the switch to long-term average climate. Thus, the full time needed for completely traversing the 300 m of unsaturated zone during a dry climate is not realized before the switch to long-term average climate. This fact is shown in the pulse-release, breakthrough-curve plot shown in Figure 4-14 for the three climate states. The 50 percent point on the breakthrough curves requires about 6,000 years in the dry climate and 300 years in the long-term average climate. Another point with regard to these activity release plots is that the sharp peak in the total unsaturated zone release curve at 5,100 years is *not* caused by the transport of the sharp peak in the total engineered barrier system release curve. Rather, it is caused by a rapid (modeled as instantaneous) 80-m rise in the water table when the climate changes from dry to long-term average. This rise causes an instantaneous burst of technetium-99 into the saturated zone from the 80 m of unsaturated zone pore water, which produces the activity-release peak at the base of the unsaturated zone.[25]

Examination of the engineered barrier system release plot in Figure 4-14 also reveals that during the period from 5,000 to 10,000 years, packages

have failed by corrosion in all six repository regions. The failures can be seen in the curves for the six individual regions as they begin to appear at various times corresponding to initial corrosion failures of packages in the various regions. The southwest region, being the smallest and driest region, has the longest delay in initial failures, with the release curve appearing just before 10,000 years.

Further comparison of the engineered barrier system release plot with the unsaturated zone release plots reveals some of the behavior of the unsaturated zone between the repository and the water table. The initial juvenile failure of a waste package has occurred in the southeast repository region, which approximately overlies regions 2, 4, and 5 at the water table (see Figure 4-4). Therefore, during the period of release from the juvenile-failure package (1,000 to 5,000 years), the radionuclide mass arrives at the water table only in saturated zone regions 2, 4, and 5. This arrival location is also because of the generally south-easterly direction of lateral diversion in the unsaturated zone as described in Sections 3.1 and 3.6.

Similarly to the unsaturated zone, the saturated zone provides its best performance during the dry climate periods that occur approximately every 90,000 years on average (see Section 3.1). During these dry periods, the delay in the saturated zone for nonsorbing radionuclides such as technetium-99 and iodine-129 is about 1,000 years (Figure 3-72). During the long-term average climate, the delay is equal only to 1000/5.44 = 184 years, where 5.44 is the flux multiplier used for the long-term average climate relative to the dry climate (Section 3.7).[26] The performance of the saturated zone during the first 10,000 years after closure is illustrated in Figure 4-15, which compares activity releases at the base of the unsaturated zone, or entry to the saturated zone, to activity releases at the end of the saturated zone, at 20 km (12 miles). Seeing the time delay in either the dry or long-term average climate from these two activity release figures is difficult. However, comparing the temporal location of the water-table-rise peak on the unsaturated zone release figure with the location on the saturated zone release figure indicates that the peak is delayed by at least the expected 200-year travel time in the long-term average climate. In the dry climate, all that can be compared is the temporal location of a specific value of the activity release rate (e.g., the 10^{-4} Ci/year rate). This location is at about 3,600 years on the unsaturated zone release plot and about 4,700 years on the saturated zone release plot, which demonstrates the approximate 1,000-year delay during the dry climate (shown in Figure 4-15 by the technetium-99 breakthrough curve, for a constant-concentration source).

The other key feature of saturated zone performance is the dilution it provides because of plume dispersion. This dilution is illustrated on Figure 4-15 by the two concentration plots, one at the beginning of the saturated zone for the six regions, or streamtubes, and one at the end where a single concentration value is chosen for determining dose rate. An explanation of the choice for saturated zone concentration has already been given in Section 3.7.2.3. Here the explanation is briefly summarized with the plot of effective dilution factor shown in Figure 4-15. In particular, the dilution factor range of 1 to 100 was based on the *Saturated Zone Expert Elicitation* (CRWMS M&O 1998g), which assumed a plume dimension of approximately the size of each of the streamtubes in the TSPA-VA saturated zone model. In reality, there are six saturated zone streamtubes adjacent to one another. Therefore, at high dilution factors within the 1-to-100 range, the radionuclides will overlap and mix by diffusion, which can be approximated by adding the concentrations in the six streamtubes to determine a concentration to use for calculating dose. This is the appropriate scenario for the expected value case, which assumes a dilution factor of 10 in each individual streamtube. In this case, the diffusional mixing method results in an effective dilution factor of

[25] The sharp peak in the engineered barrier system curve at 5,200 years is transported through the unsaturated zone and appears in the unsaturated zone release curves as a subdued peak at about 5,600 years.

[26] The superpluvial climate flux multiplier is 14.7.

only four, as shown by comparing the concentration plots at the beginning and end of the saturated zone. The cumulative distribution function plot for the effective dilution factor can also be examined, and it shows that the median probability of 0.5 corresponds to a dilution factor of four. (This median value is the median of a 100-realization run [see Section 4.3], so this dilution factor is not exactly the same as the expected-value run being described in this section, though it is nearly the same.) For low dilution factors, the saturated zone model chooses the maximum of the six streamtubes because this is effectively the case of no or very little mixing between the streamtubes. For the expected-value run, this choice would cause a dilution of 10; however, as previously mentioned, a value of 10 is high enough to invoke the diffusive mixing scenario. For completeness, the effective dilution plot also shows the case of advective mixing of the six streamtubes, which means averaging the concentration of all six streamtubes, and corresponds to the scenario of a well intersecting all six streamtubes and then having their waters mixed in the wellbore.

A final summary point about the 10,000-year dose rates is that only nonsorbing radionuclides such as technetium-99 and iodine-129 reach the biosphere because most of the other radionuclides react to some degree with the tuffaceous rocks in the geosphere. These radionuclides are delayed enough by these reactions that they do not reach the biosphere during the first 10,000 years after repository closure.

4.2.2 One-Hundred-Thousand Year Dose Rates

Within the first 100,000 years after closure, technetium-99 and neptunium-237 are the dominant radionuclides to reach the biosphere; technetium-99 dominates dose rates up until about 50,000 years, after which neptunium-237 finally reaches the biosphere and dominates thereafter. There are relatively large inventories of both radionuclides in the commercial spent nuclear fuel packages. The three important qualities about technetium-99 were pointed out in the previous section: high solubility in Yucca Mountain porewater, no sorption on the volcanic tuffs, and relatively slow decay. Following are three key qualities about neptunium-237:

- Relative low solubility in the porewater seeping into the waste packages,[27] implying that neptunium-237 mass release from failed waste packages is "solubility-limited" until the failed inventory is nearly depleted. In other words, the neptunium-237 release rate from the packages will be linearly proportional to the liquid flow rate through the failed packages.

- Weak, but nonzero, sorption onto the tuff rock matrix in the natural barriers, which means a lower transport rate through the unsaturated and saturated zone than for technetium-99 (about a factor of 20 to 80 times slower in the rock matrix, but the same through fractures). However, the neptunium-237 transport rate is still relatively rapid compared to more chemically reactive elements.[28]

- Relatively slow decay compared to the 100,000-year time span.[29]

In the following discussion, mainly the behavior of these two key radionuclides, technetium-99 and neptunium-237, is tracked, but the behavior of plutonium-239 is also discussed. There is also a large inventory of plutonium-239, but the radionuclide has a much higher sorption than neptunium, implying much slower transport through rock

[27] As with technetium-99, the solubility used for neptunium-237 is the "ambient" solubility in pre-repository pore water.

[28] Because the pore waters are assumed to be oxidizing, neptunium is thought to be present in ionic form mainly in the Np^{+5} oxidation state, as the NpO_2^+ ion at ambient pH levels (below 8).

[29] Neptunium-237 has a half life of about 2,140,000 years.

matrix. However, because plutonium-239 has been observed in colloidal form in recent measurements at the Nevada Test Site, caused by rapid migration in the groundwater away from underground nuclear test detonations, it is important to consider its possible future behavior at Yucca Mountain.[30]

Figures 4-16 through 4-20, discussed in detail in this section, show the primary causes for the shape and timing of the 100,000-year technetium-99 and neptunium-237 dose rate graphs. As in the previous section, two primary sets of plots are displayed: time histories of activity release or concentration at the downgradient boundary of various parts of the natural and engineered barriers (i.e., engineered barrier system, unsaturated zone, and saturated zone); and time histories of key subsystem parameters. Figure 4-16 portrays the 100,000-year performance of the engineered barrier system. Similarly to the 10,000-year performance, the key factors are climate change and waste package failure history. Consider first the waste package and engineered barrier system releases of technetium-99 and also its dose rate in the biosphere. All three of these time histories mirror the jagged nature of the instantaneous waste package failure history. This instantaneous failure curve is a histogram of package failures, with the interval size being equal to the time step size of 333 years.[31] Ten or 11 packages are about the most that fail (by patch penetration) in any 333-year period. The reason that the release-rate curves and dose curve for technetium-99 mirror the package failure rate is that technetium-99 is not solubility limited at the values of seepage flux flowing through the packages after 10,000 years. Therefore, technetium-99 is flushed very rapidly from a failed package. As package inventories become available for release via the failure histogram, their inventories of technetium-99 are almost instantaneously released, which causes this mirroring of releases with package failures.

The releases of neptunium-237 are different from technetium-99 releases because of neptunium-237's low solubility. Low solubility causes the shape of the neptunium-237 release curve to be relatively smooth and controlled by two features: the flow rate of water through the packages and the cumulative amount of failed packages or inventory. The cause and effect of the first feature, seepage flux, is evident when the climate changes from long-term average to dry at 95,000 years. When the dry climate is reestablished, advective releases of neptunium-237 are dramatically reduced because of the linear proportionality between flow rate and mass release for radionuclides that have reached their solubility limit in the water seeping through the waste packages. Furthermore, the neptunium-237 diffusive releases do not abruptly change with the switch from long-term average climate to dry climate at 95,000 years because the accompanying change in seepage flux does not change the neptunium-237 concentration in the packages, which is the driving force behind diffusion.[32] In the dry climate, the technetium-99 advective release rate also drops by about the same factor as the neptunium-237 release rate. The lower release rate gives the appearance that technetium-99 is also solubility limited. However, this is not the case, as shown by the significant increase in diffusive releases for technetium-99 during the dry climate. The explanation for this phenomenon is found in the "seepage fraction" plot shown in Figure 4-16, which shows the fraction of all packages that are exposed to seeps in each of the six repository regions, plus the average over the regions. This average fraction drops from about 0.27 to 0.045 with the switch to dry climate; however, the packages keep failing at about the same rate during the dry climate,[33] continually exposing technetium-99 inventory to contact with water, but in this case stagnant or nonflowing water. Because of the very high solubility of technetium-99 (0.34 g/m^3 or 1.43×10^{-6} *M* for this expected-value realization), the concentration of

[30] Plutonium-239 has a relatively short half life of about 24,000 years.

[31] If divided by the total number of packages, this instantaneous failure history becomes a probability density function (pdf) for waste package failure as a function of time.

[32] This, in fact, is the key point about reaching a solubility limit: that the amount of water or water flow present does not alter the concentration (mass/volume) of the radionuclide in solution.

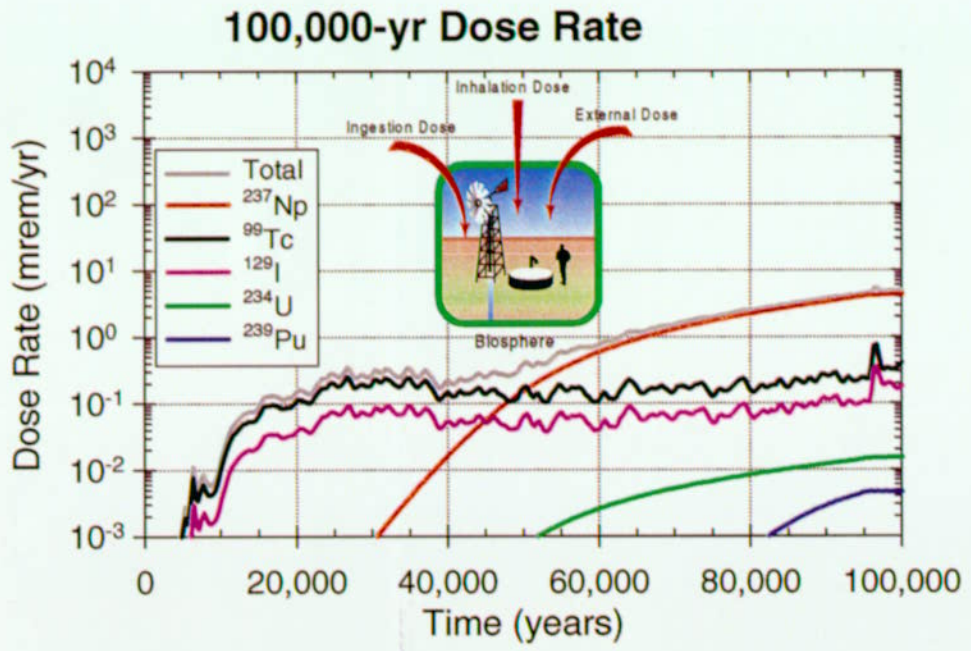

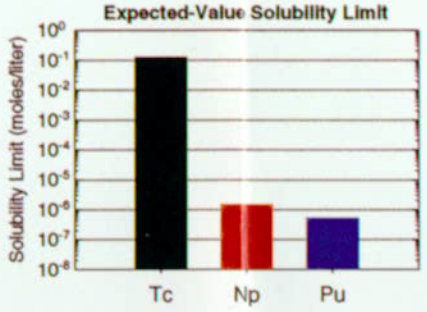

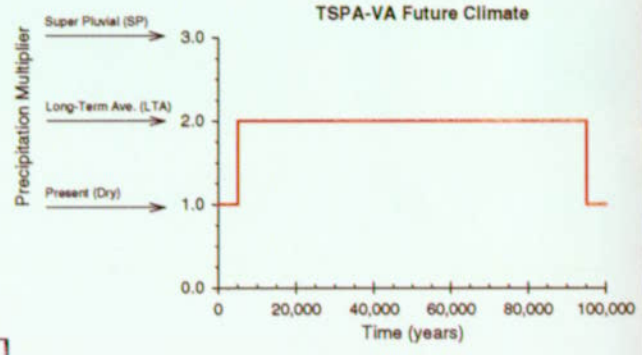

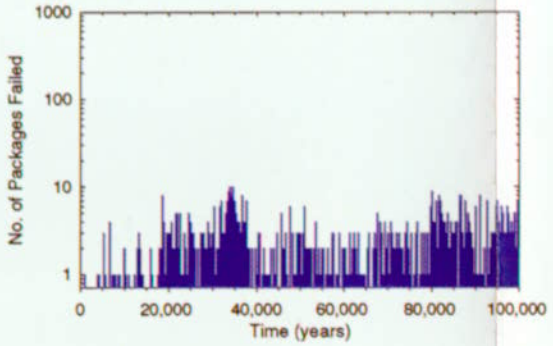

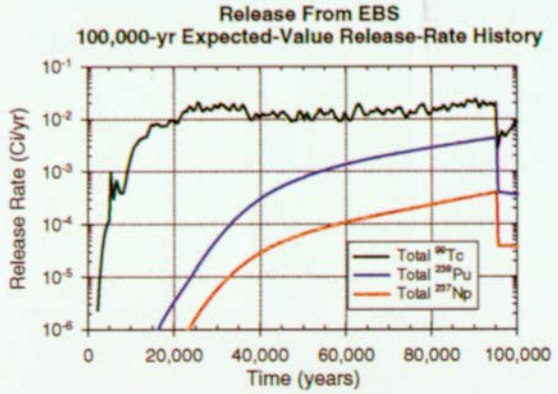

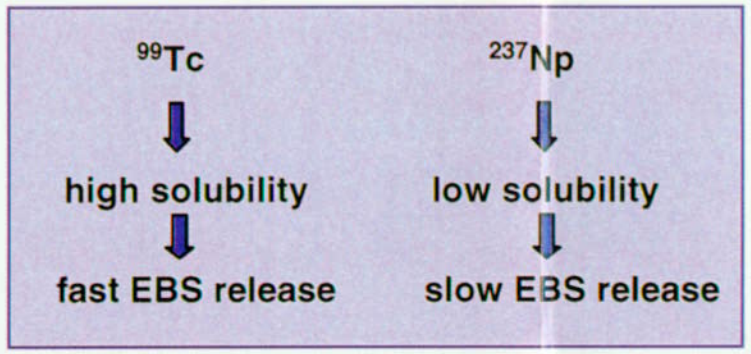

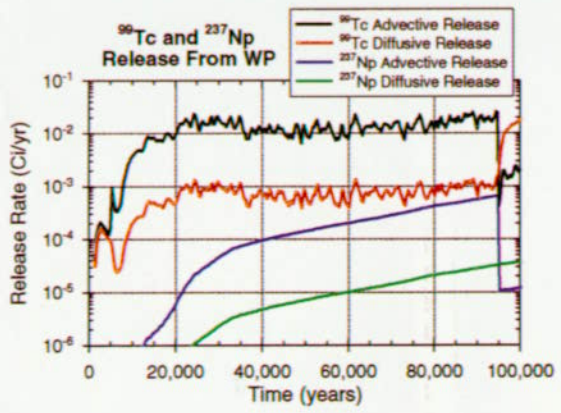

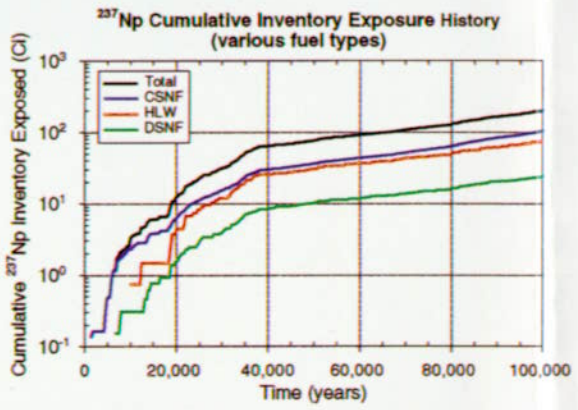

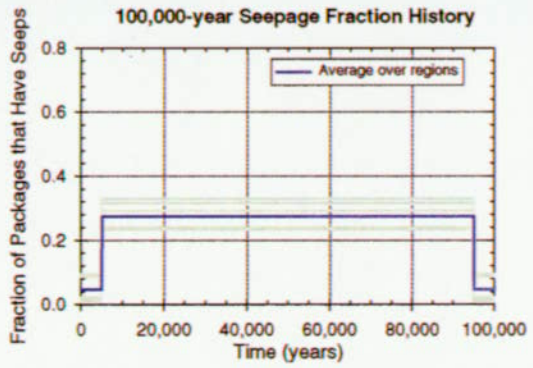

Figure 4-16. Effects of Climate Change, Seepage Flux, and Waste Package Degradation on Engineered Barrier System Releases and Dose Rates in the First 100,000 Years After Waste Emplacement
For the 100,000-year seepage flux plot the patch area curve uses the right-hand axis and other two curves use the left-hand axis.
(EBS—engineered barrier system; WP—waste package; CSNF—commercial spent nuclear fuel; HLW—high-level radioactive waste; DSNF—DOE spent nuclear fuel)

INTENTIONALLY LEFT BLANK

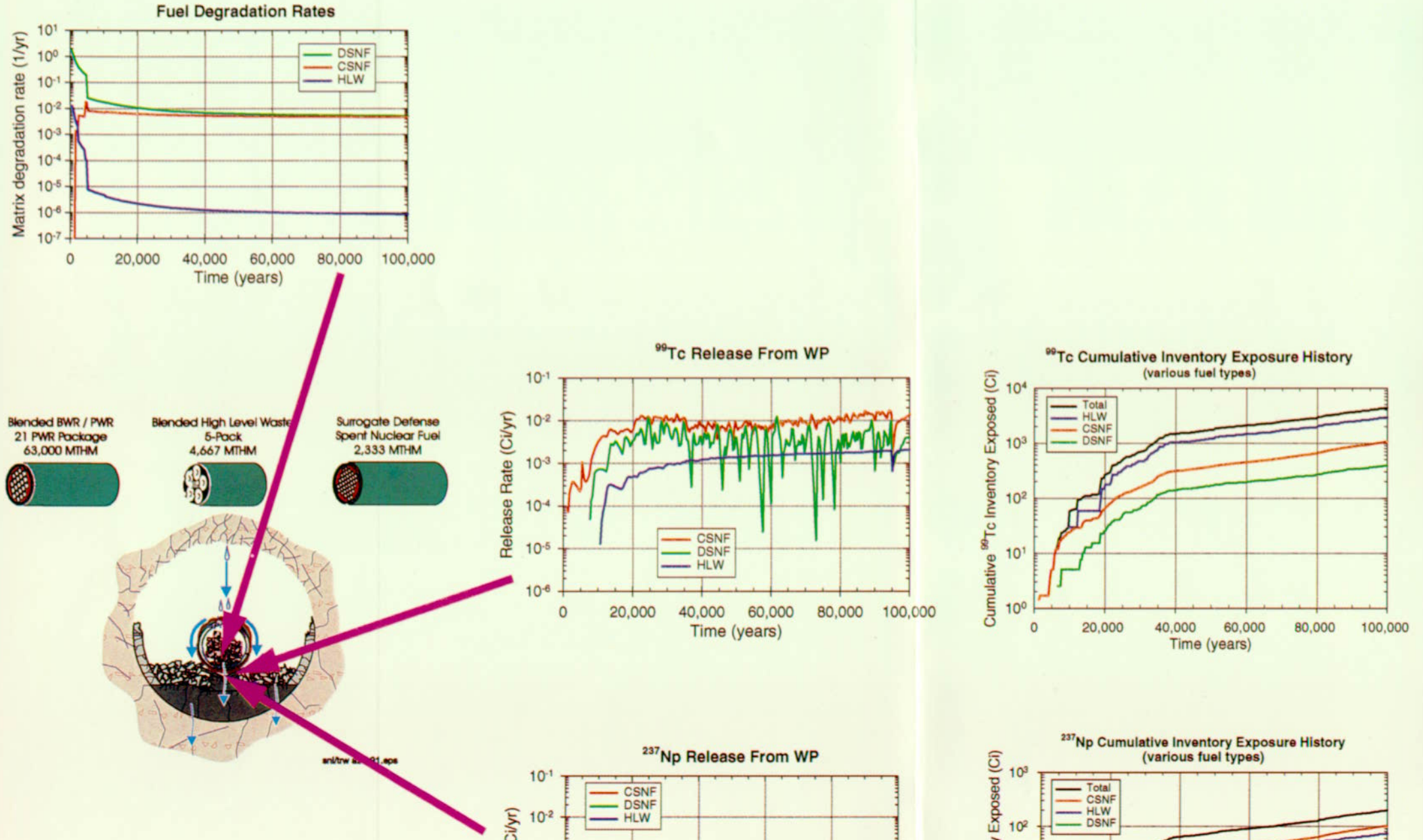

Figure 4-17. Effects of Matrix Degradation Rate and Inventory Exposure Rate on the Releases of the Three Different Fuel Types: Commercial Spent Nuclear Fuel, U.S. Department of Energy Spent Nuclear Fuel, and High-Level Radioactive Waste (WP—waste package; CSNF—commercial spent nuclear fuel; DSNF—DOE spent nuclear fuel; HLW—high-level radioactive waste)

INTENTIONALLY LEFT BLANK

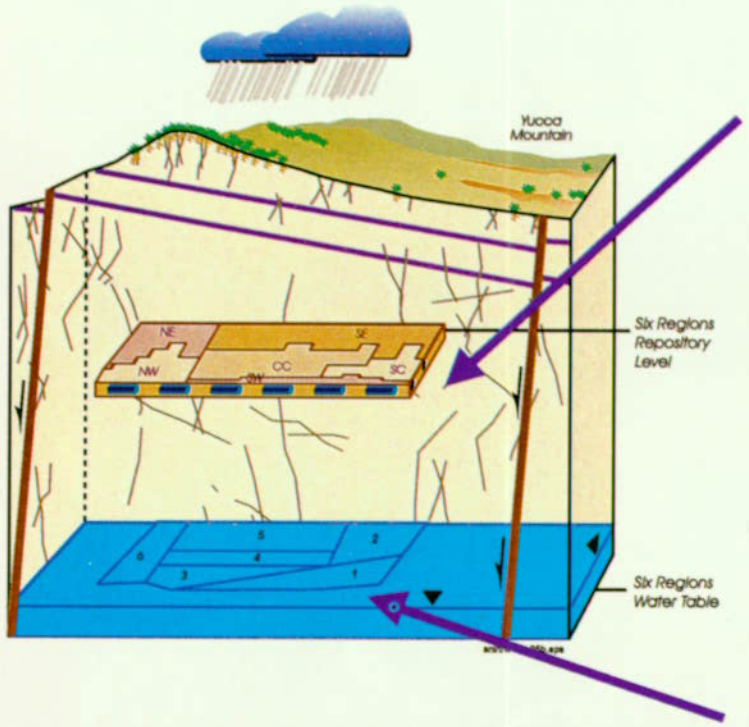

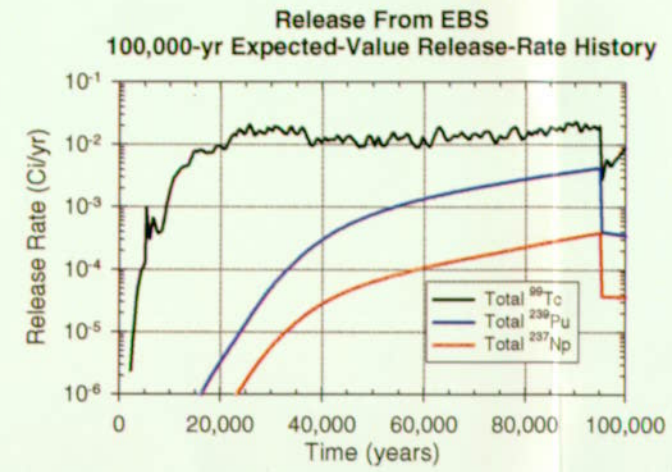

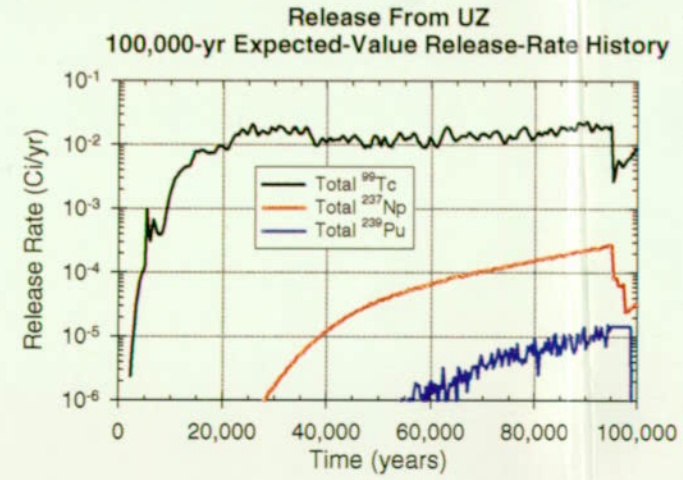

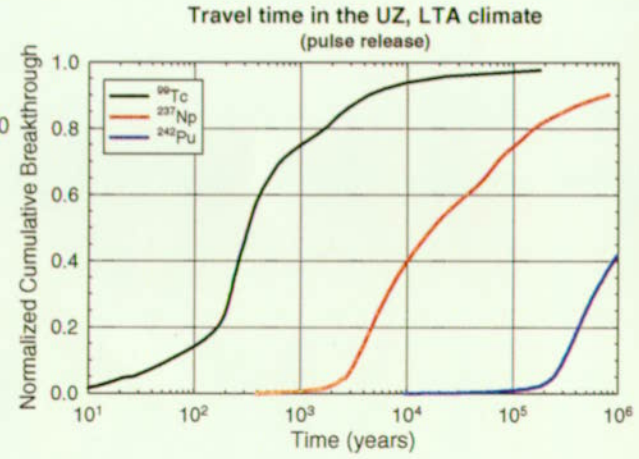

^{99}Tc	^{237}Np	^{239}Pu
⇓	⇓	⇓
no sorption	Weak sorption	strong sorption
⇓	⇓	⇓
fast transport	moderate transport	slow transport

FV3042-7

Figure 4-18. Performance of the Unsaturated Zone During the First 100,000 Years After Waste Emplacement with Respect to Technetium-99, Neptunium-237, and Plutonium-239
Shown is the importance of sorption in the unsaturated zone. (EBS—engineered barrier system; LTA—long term average; UZ—unsaturated zone)

INTENTIONALLY LEFT BLANK

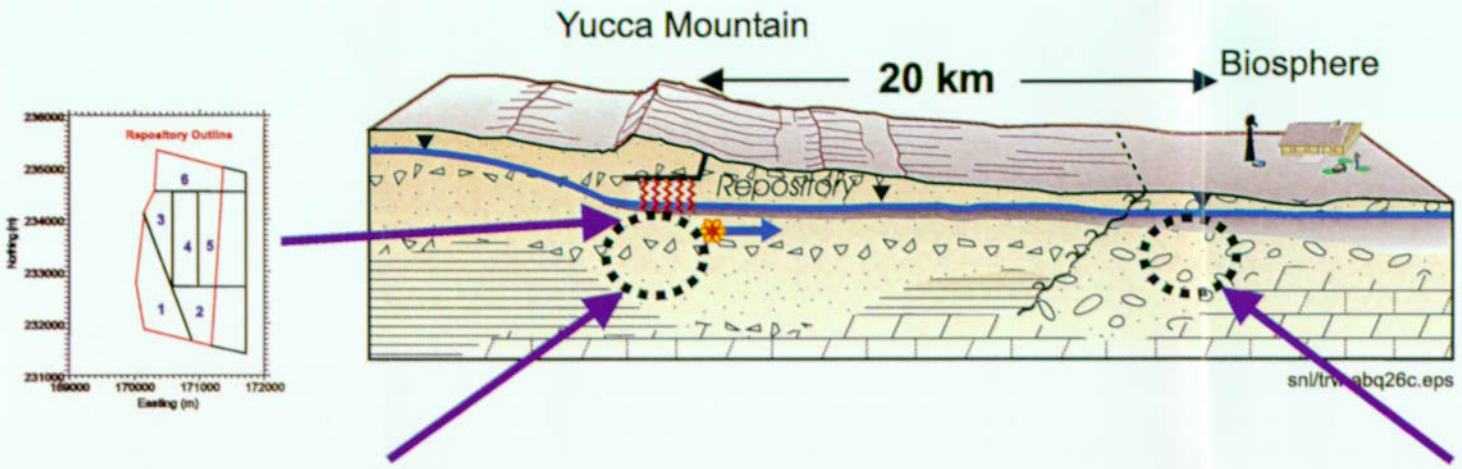

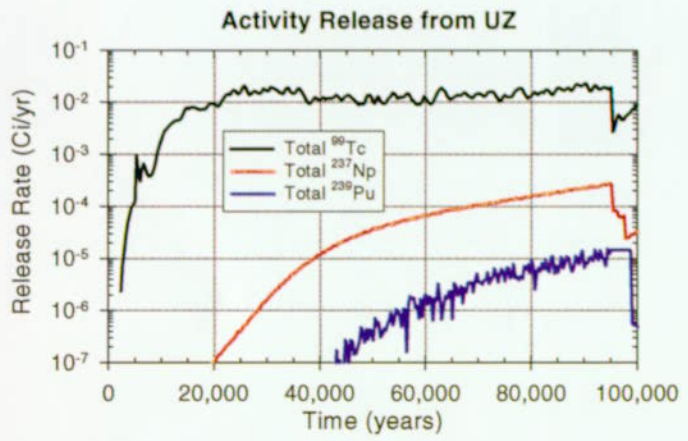

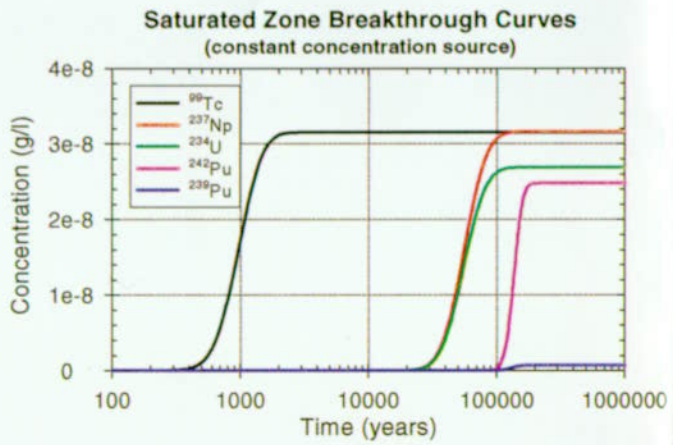

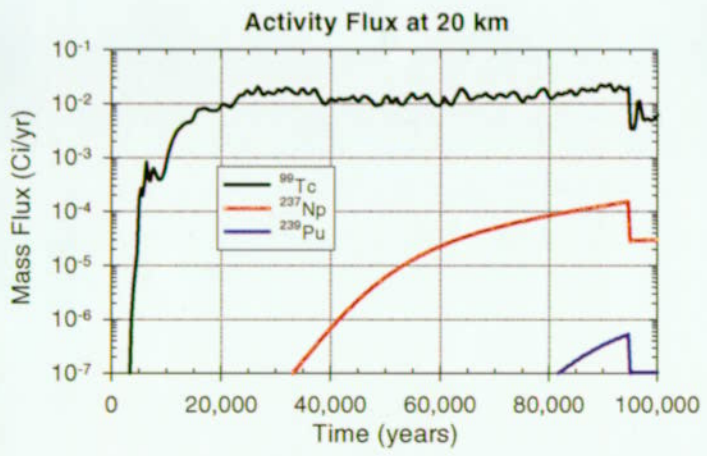

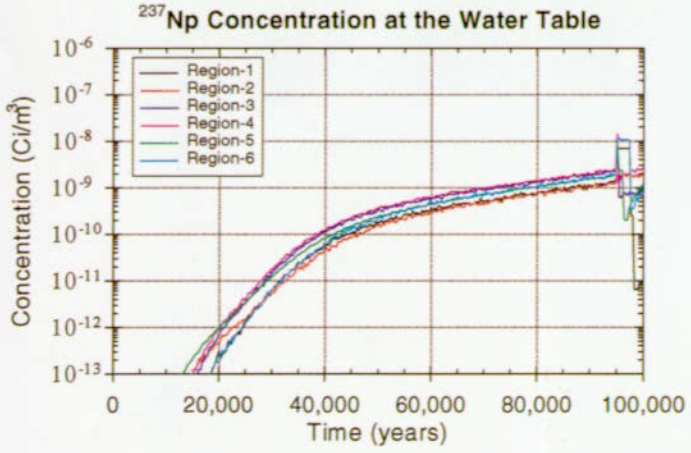

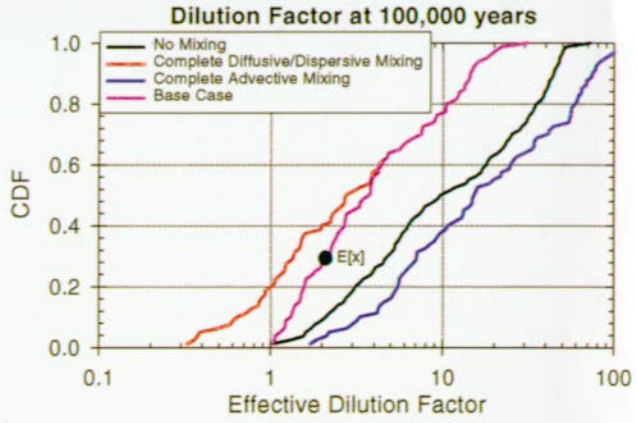

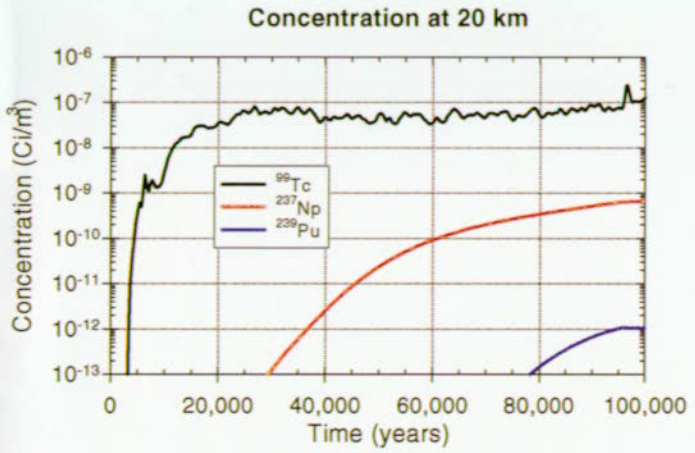

Figure 4-19. Performance of the Saturated Zone During the First 100,000 Years After Waste Emplacement with Respect to Technetium-99, Neptunium-237, and Plutonium-239
Shown is the importance of sorption and dilution in the saturated zone. (UZ—unsaturated zone; CDF—cumulative distribution function)

INTENTIONALLY LEFT BLANK

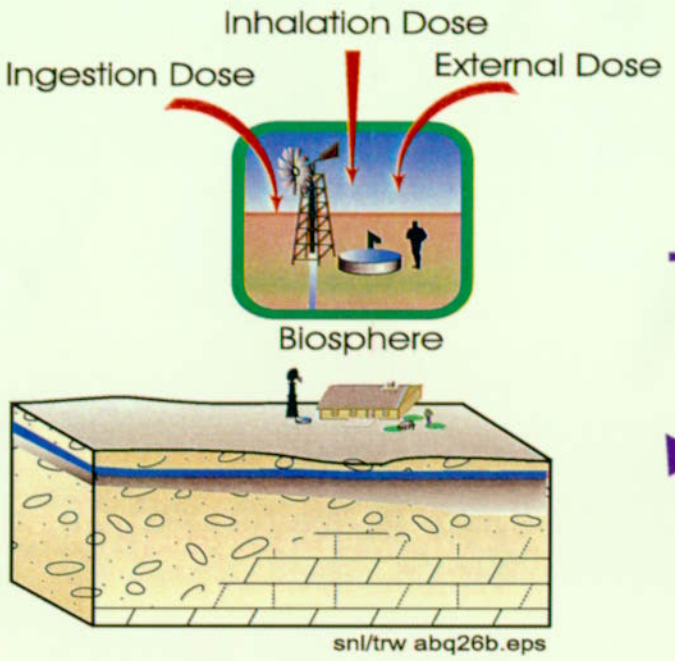

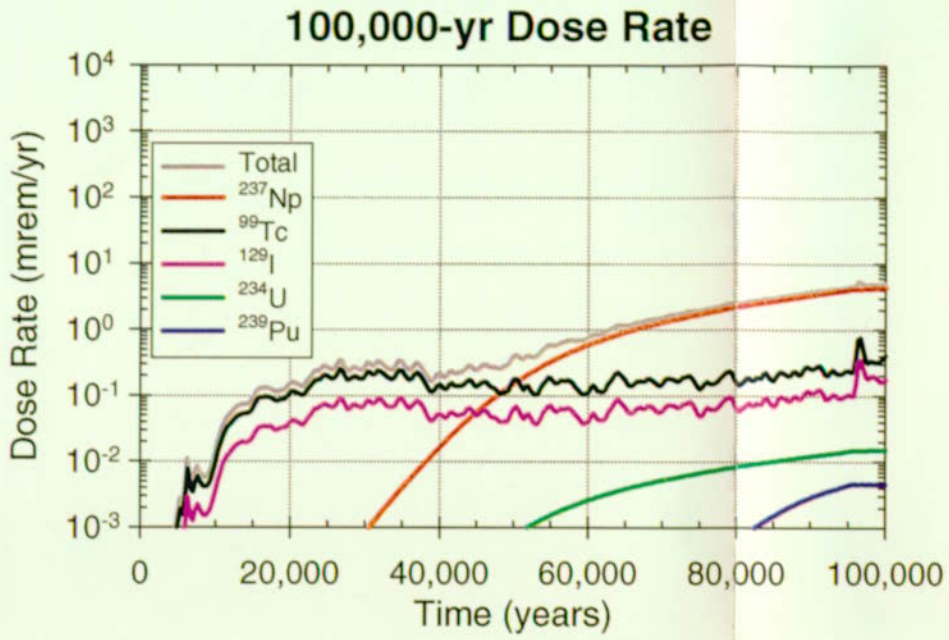

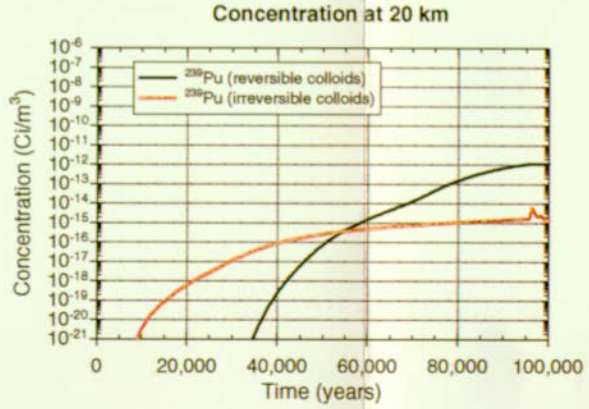

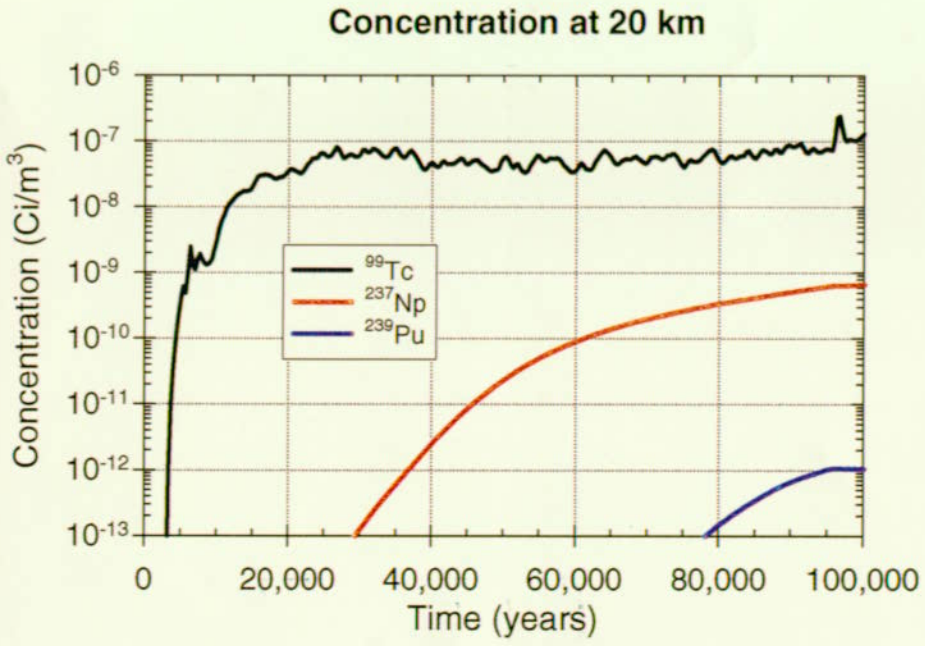

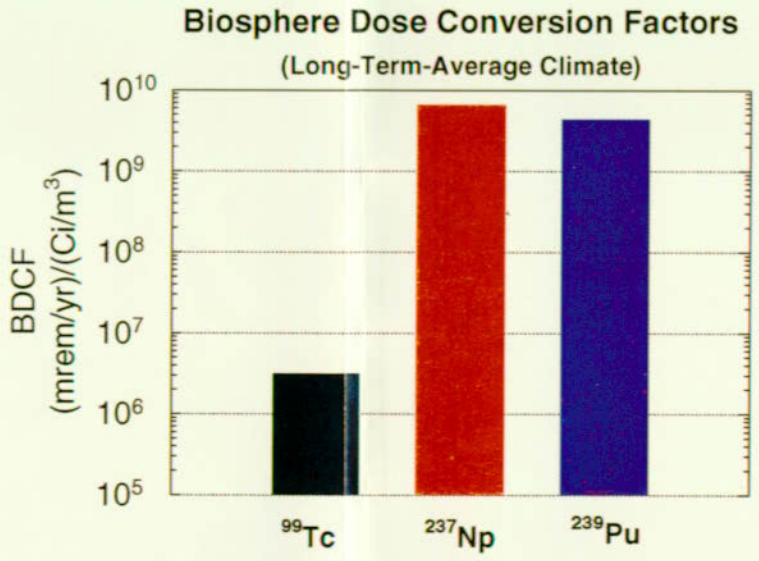

FV3042-9

Figure 4-20. Importance of Biosphere Dose Conversion Factors in the First 100,000 Years After Waste Emplacement Also shown is the impact of colloidal transport of irreversibly sorbed plutonium-239. (BDCF—biosphere dose conversion factors)

INTENTIONALLY LEFT BLANK

technetium-99 is very high in these failed packages because flowing water is not removing the inventory. A much higher concentration gradient is created between the inside and outside of the packages, causing a much higher diffusive mass release. As discussed in the next section regarding 1 million-year releases, when the climate goes back from dry to long-term average a burst of technetium-99 is released. This burst represents the technetium-99 that has built up during the long-term average climate within the fraction of packages that are not dripped on during the dry period, even though they have failed by corrosion. When this incremental fraction of packages (about 0.225) is suddenly dripped on again during the new long-term average climate, all of the technetium-99 is abruptly transported away. This technetium-99 available for rapid transport has accumulated during the dry climate because the commercial spent nuclear fuel degradation rate is very high. All of the technetium-99 available from this degradation is present in a highly soluble form that can dissolve at a very high concentration in the newly available flowing water during the long-term average climate.

The second factor controlling the neptunium-237 release is the cumulative amount of failed inventory, shown in Figure 4-16 for the three inventory types: commercial spent nuclear fuel, DOE spent nuclear fuel, and high-level radioactive waste. For the latter two, the cumulative failed-inventory curve is found by multiplying the cumulative failed-package curve by the inventory per package.[34] However, for commercial spent nuclear fuel there is a second barrier to consider: the Zircaloy fuel cladding.[35] During the first 100,000 years, this cladding is considered to be very robust in the base case, expected-value realization. At most only about 3 percent of the cladding will fail by various mechanisms by 100,000 years (see Section 3.5), meaning that to obtain the cumulative exposed inventory in commercial spent nuclear fuel, the cumulative package-failure history must be multiplied by both the neptunium-237 inventory per package and by the clad failure fraction.[36] In Figure 4-16 the neptunium-237 cumulative inventory-exposed history has the same shape as both the waste package and engineered barrier system release histories. On the other hand, the seepage flux into the packages also has the same steadily increasing curve (ignoring the climate change at 95,000 years), which is caused by the steadily growing patch area curve. It appears as if either

[33] The fact that packages keep failing at the same rate during the dry climate is a conservative assumption. Within the RIP model, there are four environmental package groupings: packages that are never dripped on (55 percent of all packages, in the expected-value base case); packages that are dripped on during all climates (4.5 percent); packages that are dripped on only during the long-term average and superpluvial climates (22.5 percent); and packages that are dripped on only during the superpluvial climates (18 percent). However, only two of these groupings are represented in the waste package degradation model: packages that are dripped on from time zero to 1 million years, and packages that are never dripped on. It is thus a conservative assumption (i.e., erring on the side of maximum releases) to assume that the long-term average fraction of packages (i.e., the fraction that is dripped on during long-term average and superpluvial climates) has the same failure rate during the long-term average climate and the dry climate. On the other hand, a somewhat nonconservative assumption is that the superpluvial fraction of packages fails according to the non-seep failure curve. This assumption is used because these packages are not dripped on at all until at least 250,000 years after repository closure.

[34] The average neptunium-237 inventory per package is 11.4 Ci per package for commercial spent nuclear fuel, 0.735 Ci per package for high-level radioactive waste, and 0.153 Ci per package for DOE spent nuclear fuel.

[35] Some of the inventory of DOE spent nuclear fuel has intact cladding (such as naval fuel and about 50 percent of N-Reactor fuel); however, it is conservatively assumed in TSPA-VA that all the DOE spent nuclear fuel cladding with the exception of naval spent nuclear fuel is failed at emplacement. This assumption is made in order to bound the effect of DOE spent nuclear fuel on repository performance. The performance of naval spent nuclear fuel cladding is discussed in Sections 3.5.3.5. and 5.5.5.

[36] This maximum fraction of 3 percent clad failure over 100,000 years is a combination of creep failure, stainless-steel-rod failure, Zircaloy corrosion failure, and mechanical failure (see Section 4.1.8).

the seepage curve or the cumulative inventory curve could be responsible for the shape of the neptunium-237 release curve. However, the latter is responsible because the seepage is already high enough to have reached the solubility limit, as demonstrated in the discussion above regarding the advective and diffusive release curves. The steadily increasing cumulative inventory curve means that more packages, seepage, and inventory are becoming available with time for transport of more neptunium-237 away from the entire repository.

Figure 4-17 shows the performance of the waste package and engineered barrier system for the three inventory types: commercial spent nuclear fuel, DOE spent nuclear fuel, and high-level radioactive waste. One implication from this figure, especially when the technetium-99 cumulative inventory exposure curves are compared, is that the exposed DOE spent nuclear fuel inventory is nearly as large as the commercial spent nuclear fuel inventory at 100,000 years—the ratio of DOE inventory to commercial inventory is about 0.4.[37] Also, this ratio is roughly maintained when translated to releases from the waste packages, because the dissolution rates for DOE spent nuclear fuel and commercial spent nuclear fuel are comparable for most of the 100,000 years, as shown in Figure 4-17. In contrast, the exposed technetium-99 high-level radioactive waste inventory is about twice as much as the exposed commercial spent nuclear fuel inventory. However, the technetium-99 high-level-waste activity released is about five times lower than the commercial-spent-nuclear-fuel activity released because the high-level-waste degradation rate is lower than the commercial and DOE spent nuclear fuel degradation rates. The exposed neptunium-237 inventory and its activity released from the engineered barrier system has a similar relationship to that of technetium-99 because of fuel degradation rate.

Returning to Figure 4-16, another point about the engineered barrier system behavior is the plutonium-239 release curve. The radionuclide plutonium-239 is another actinide that is solubility limited in ambient Yucca Mountain pore waters. Therefore, its release behavior from the waste package and engineered barrier system should be similar to neptunium-237, which is exactly the behavior shown in Figure 4-16. However, as discussed in Section 3.5, colloidal transport of plutonium-239 is also included in the TSPA-VA model, so the shape of the engineered barrier system release curve for plutonium-239 might be expected to be different from the neptunium-237 release curve. It is not different because in the TSPA-VA model the fraction of *irreversible* colloids (unaffected by interaction with rock matrix or fractures anywhere in the system) is at most only 1×10^{-4} times the concentration of reversible colloids (and only 1×10^{-7} for the expected-value base case realization being described here—see Section 4.1.10). Furthermore, since the *reversible* colloid concentration is linearly proportional to the dissolved aqueous concentration (see Section 3.5), it is necessarily true that the shape of the plutonium-239 release curve is the same with or without colloids. Also, for the expected-value base case the proportionality factor, K_c (the ratio of plutonium mass on colloids to plutonium mass dissolved in the aqueous phase), is only about 0.33, so the plutonium-239 release curve must be dominated by

[37] Roughly, the total technetium-99 commercial spent nuclear fuel inventory can be computed from the product of the number of commercial spent nuclear fuel packages (7,760) times the cladding fraction (at most only 0.03 of the cladding fails during the first 100,000 years) times the technetium-99 inventory per package (118 Ci). The product equals 27,470 exposed Ci. Similarly for the technetium-99 DOE spent nuclear fuel inventory: 2,546 DOE spent nuclear fuel packages times technetium-99 inventory per package (2.55 Ci) equals 6,492 exposed Ci. The TSPA-VA model conservatively assumes no intact cladding on the DOE spent nuclear fuel. Therefore, the ratio of DOE spent nuclear fuel to commercial spent nuclear fuel inventory is about 0.24. (Actually, the number of packages used in this computation should be the number of failed packages at a given time. Because the commercial and DOE spent nuclear fuel fail at about the same rate, the ratio of the inventories can, instead, be computed from the ratio of the total emplaced packages. Also, the 3 percent clad fraction used in this example is only an approximation and changes with time during the 100,000 years, growing from 1.25 percent at initial package failure to about 3 percent 100,000 years after package failure.)

dissolved plutonium-239, not colloidal plutonium-239.

Figure 4-16 also shows the performance of the engineered barrier system, specifically the concrete invert. Although a pulse-release breakthrough curve is not shown, a comparison of total neptunium-237 releases from the engineered barrier system with advective neptunium-237 releases from the waste package indicates that there is a transport delay of neptunium-237 in the invert. The neptunium-237 distribution coefficient (K_d) in the invert is about 100 mL/g (and the plutonium K_d is about 600 mL/g). This K_d for neptunium makes invert travel time in the dry climate very slow (on the order of 100,000 years through the 1 m of invert), while in the long-term average climate the travel time is about 7,500 years. Therefore, because there is a climate change at 5,000 years after closure, the effective travel time of neptunium-237 through the invert is about (5,000 + 7,500 =) 12,500 years. (The neptunium moves only a negligible distance during the 5,000 years of dry climate).

Figure 4-18 shows the performance of the unsaturated zone base case model over the 100,000-year time span, during which the long-term average climate predominates. In Sections 3.1 and 4.1, the unsaturated zone expected-value long-term average base case was explained as having an average of about 40 mm/year percolation through the unsaturated zone at the repository horizon. Part of this flow is diverted laterally by the perched-water zone beneath the northern portions of the repository. The net effect of the diversion, and also sorption of the radionuclides onto the rock matrix, is shown in the unsaturated zone activity-release plot in Figure 4-18. This plot represents the summed activity release over all six regions at the water table for the three indicated radionuclides. Comparison of the engineered barrier system and unsaturated zone release rates shows that the unsaturated zone has little delaying effect on the transport of the nonsorbing technetium-99. For the weakly sorbing neptunium-237, the unsaturated zone appears to delay its movement by about several thousand years. For the strongly sorbing plutonium-239, the unsaturated zone delays its releases by tens of thousands of years.[38] (Using the 50 percent point on the pulse-release breakthrough curves as the metric to gauge travel time, technetium-99 delay is 300 years, neptunium-237 delay is 20,000 years, and plutonium-242 delay is apparently greater than 1 million years. Plutonium-242 breakthrough is shown in the plot because plutonium-239 has a very short half-life of 24,000 years, while plutonium-242 has a half-life of about 387,000 years. However, even with this half-life, the 50-percent-breakthrough metric is in error because the normalization factor for the plot is the initial number of particles, many of which have decayed before traversing the entire unsaturated zone. The exact amount of error can only be determined by simulating plutonium-242 or plutonium-239 transport without decay, that is, taking into account sorption, but not decay.)

Figure 4-19 shows the performance of the saturated zone over the 100,000-year time span for this expected-value base case realization. Shown are two sets of plots; release rate graphs at both the base of the unsaturated zone and the 20-km (12-mile) distance in the saturated zone, and concentration plots at the water table beneath the repository and at the 20-km (12-mile) distance. Also shown again (see Figure 4-15) are the saturated zone generic breakthrough curves and the dilution-factor cumulative distribution functions. The saturated zone demonstrates similar behavior to the unsaturated zone for the three radionuclides; technetium-99 is only slightly delayed, neptunium-237 is moderately delayed, and plutonium-239 is strongly delayed. Based on the breakthrough curves shown, the delay of the 50 percent concentration point is about 50,000 years for neptunium-237 and about 110,000 years for plutonium-239. Finally, as with the 10,000-year technetium-99 transport discussed in Section 4.2.1, neptunium-237 transport through the six streamtubes similarly

[38] The plutonium-239 release curve is erratic at the base of the unsaturated zone. This nonphysical behavior is caused by the discrete nature of the particle tracking model when releases are very low, resulting in the observance of individual particles passing out of the domain.

experiences an effective dilution factor of about four when sampled in a well-withdrawal scenario at 20 km (12 miles).

Figure 4-20 illustrates how the relative concentrations of the three radionuclides in the groundwater translate to relatively different doses as a result of the disparate biosphere dose conversion factors. In particular, the biosphere dose conversion factors (mrem/year/Ci/m^3) of neptunium-237 and plutonium-239 are about 1,000 times higher than the technetium-99 biosphere dose conversion factor. This implies that although the neptunium-237 activity concentration in the groundwater (Ci/m^3) is much lower than technetium-99, its dose rate is about 10 times higher because of larger impact on the human body.[39] Similarly, although the plutonium-239 activity concentration in the saturated zone is very low at 100,000 years (1×10^{-12} Ci/m^3 or 0.001 pCi/L), its dose reaches several millirem per year because of its relatively high biosphere dose conversion factor.

The final plot in Figure 4-20 shows the small effect of including a model for irreversible sorption of plutonium-239 onto colloids, where the ratio of the irreversible fraction to the reversible fraction is 1×10^{-7} in the base case expected-value realization. This model accounts for the early breakthrough of plutonium colloids observed in the Benham test. The scale on this plot is not low enough to show the first breakthrough of these irreversible colloids at the 20-km (12-mile) boundary. However, examining the modeling results shows a first breakthrough at about 1,500 years, which represents the very fast fracture transport through the natural system of the releases from the juvenile-failure package that fails at 1,000 years.

4.2.3 One-Million-Year Dose Rates

Within the first 1 million years after closure, technetium-99 and neptunium-237 are the dominant radionuclides to reach the biosphere; technetium-99 dominates dose rates up until about 50,000 years, after which neptunium-237 reaches the biosphere in appreciable amounts and dominates thereafter. After a long period of delay in the natural barriers, plutonium-242 finally appears at the biosphere in appreciable amounts beginning at about 200,000 years and then remains as the second most important radionuclide, after neptunium-237, for the remainder of the 1 million-year period. In the two superpluvial periods that occur, plutonium-242 has a relatively sharp peak that contributes about the same as neptunium-237 to the total peak dose during those climatic periods. There are relatively large inventories of all three radionuclides (technetium-99, neptunium-237, and plutonium-242) in the commercial spent nuclear fuel packages. The key qualities of technetium-99 and neptunium-237 have already been discussed at the beginning of Sections 4.2.1 and 4.2.2. For the 1 million-year performance period, their behavior is again used to explain the performance of the repository system and subsystems. In addition, the behavior of the rather long-lived plutonium-242 is used to explain the behavior of strongly sorbing radionuclides during the 1-million-year period.[40]

Figures 4-21 through 4-25, discussed in detail in this section, show the primary causes for the shape and timing of the 1-million-year dose rate graphs. Figure 4-21 shows the 1-million-year performance of the engineered barrier system. Again, the key factors are climate change and waste package failure history. In contrast to the 10,000-year and 100,000-year time spans, however, an additional parameter is necessary to explain the shape of the curves after 200,000 years: cladding failure rate. This parameter is discussed in detail below.

---

[39] The mass concentrations (g/m^3) for technetium-99 and neptunium-237 are actually much closer to each other than are their activity concentrations, about 7×10^{-6} g/m^3 and 1×10^{-6} g/m3 respectively; however, the specific activity (Ci/g) of neptunium-237 is much lower than that of technetium-99.

[40] Plutonium-242 has a half life of about 387,000 years.

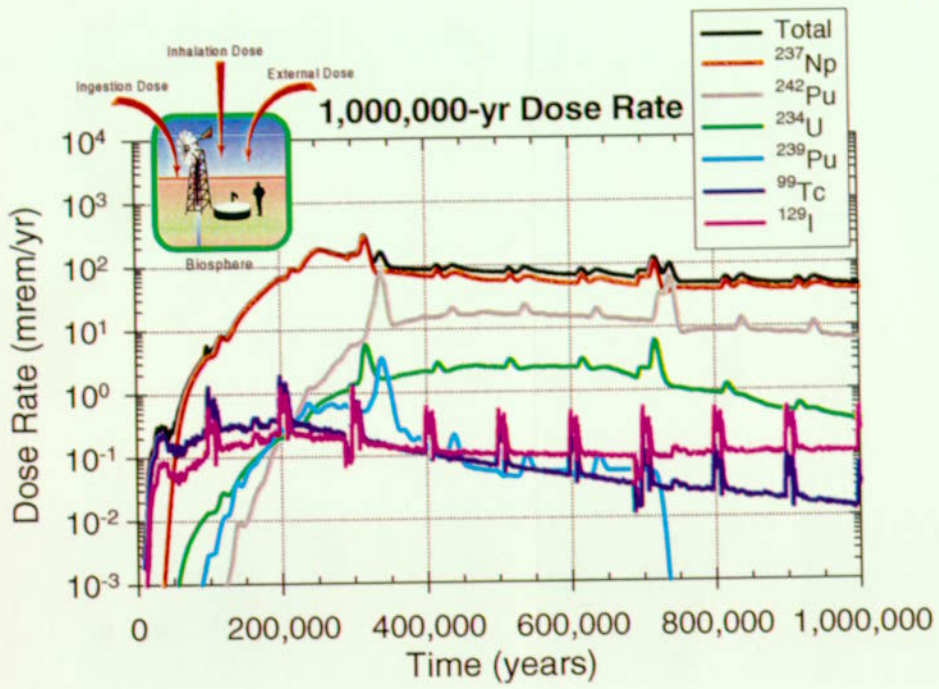

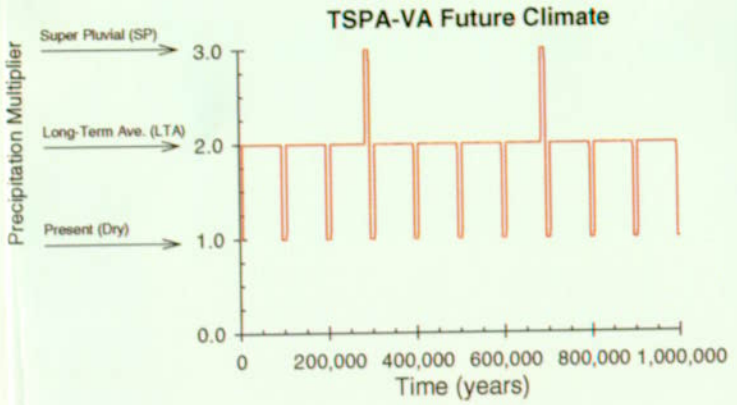

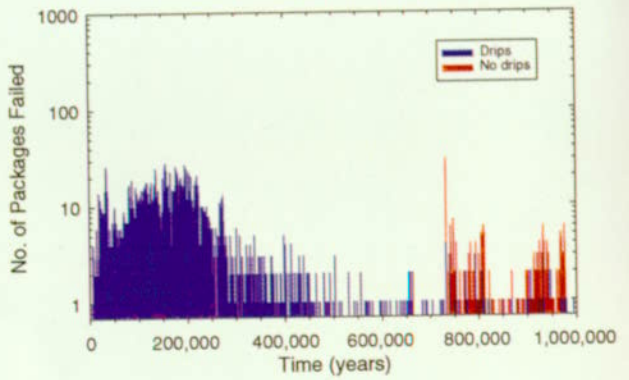

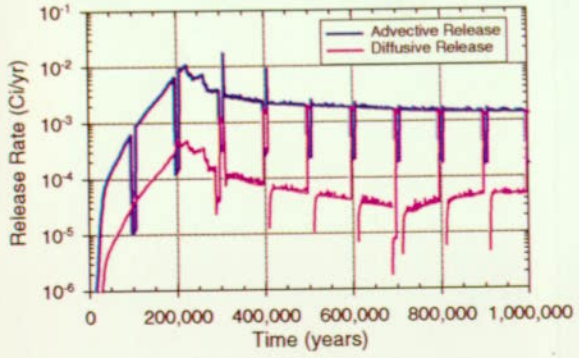

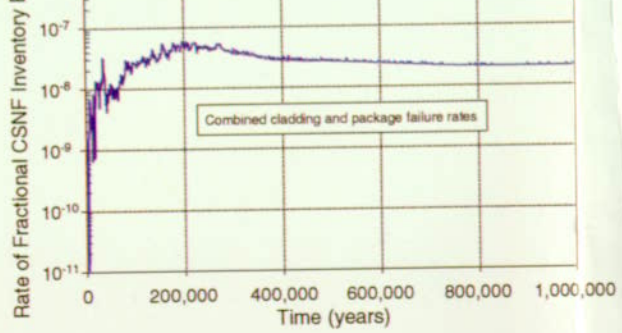

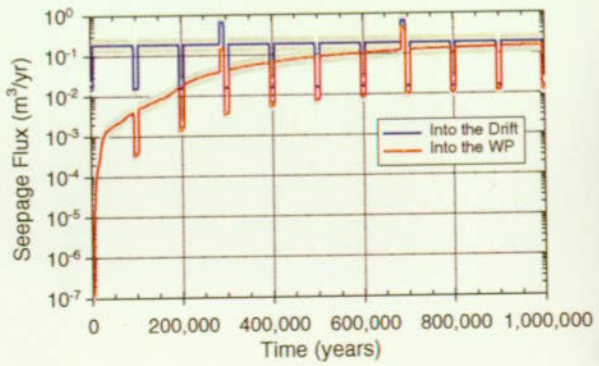

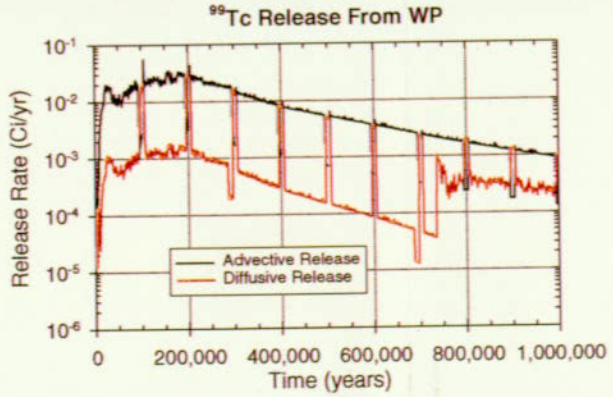

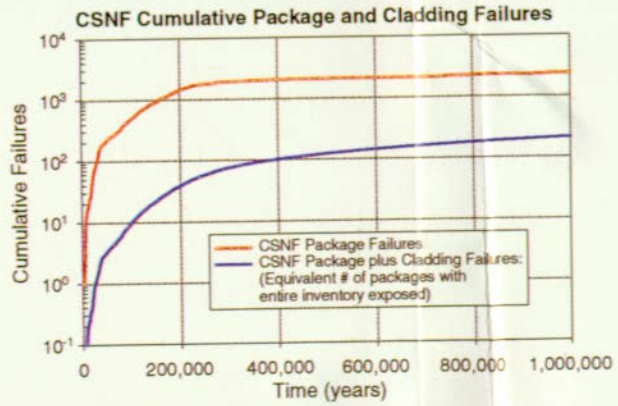

Figure 4-21. Effects of Climate Change, Seepage Flux, Waste Package Degradation, and Cladding Degradation on Waste Package Releases and Dose Rates in the First 1 Million Years After Waste Emplacement
(CSNF—commercial spent nuclear fuel; WP—waste package)

INTENTIONALLY LEFT BLANK

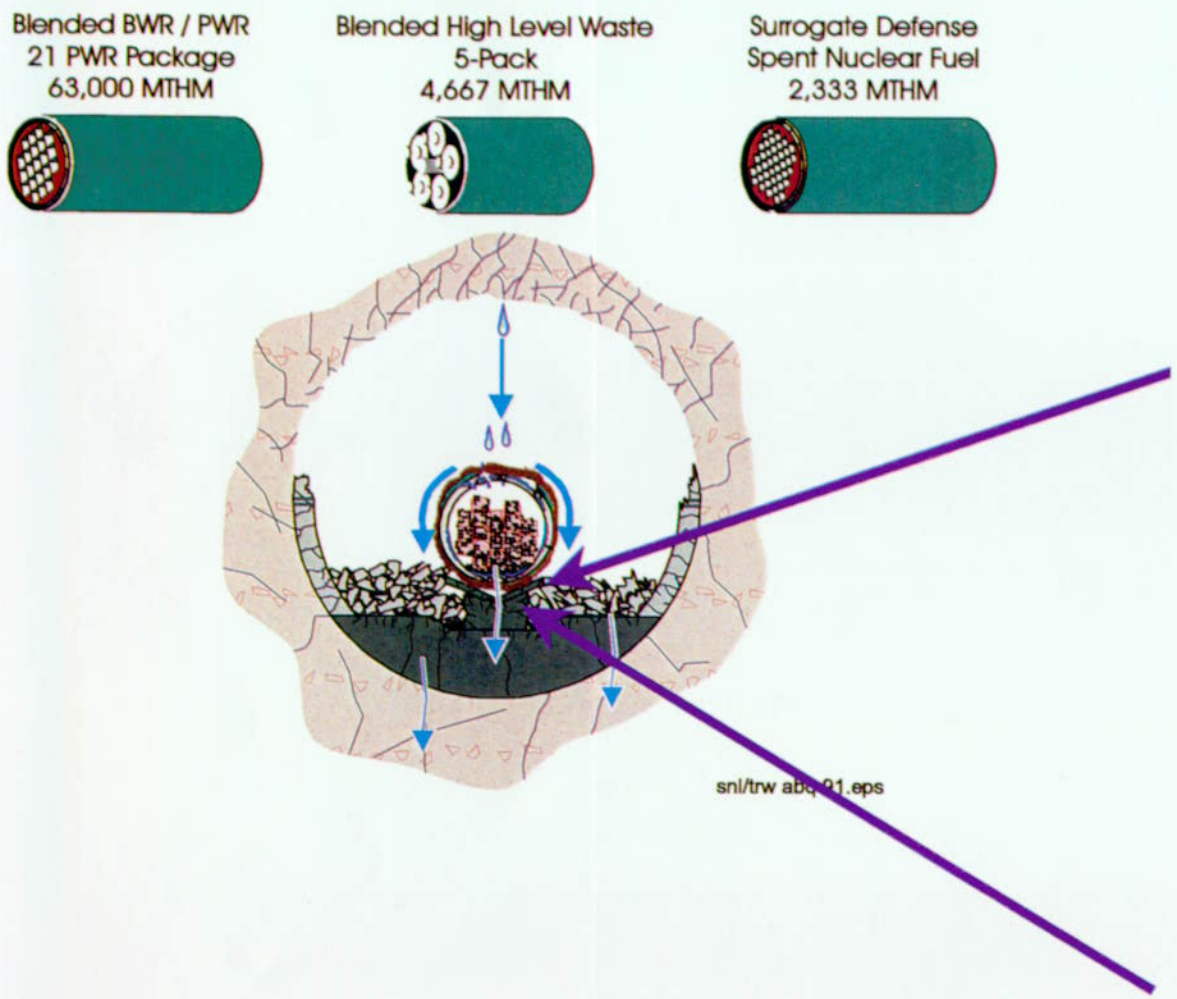

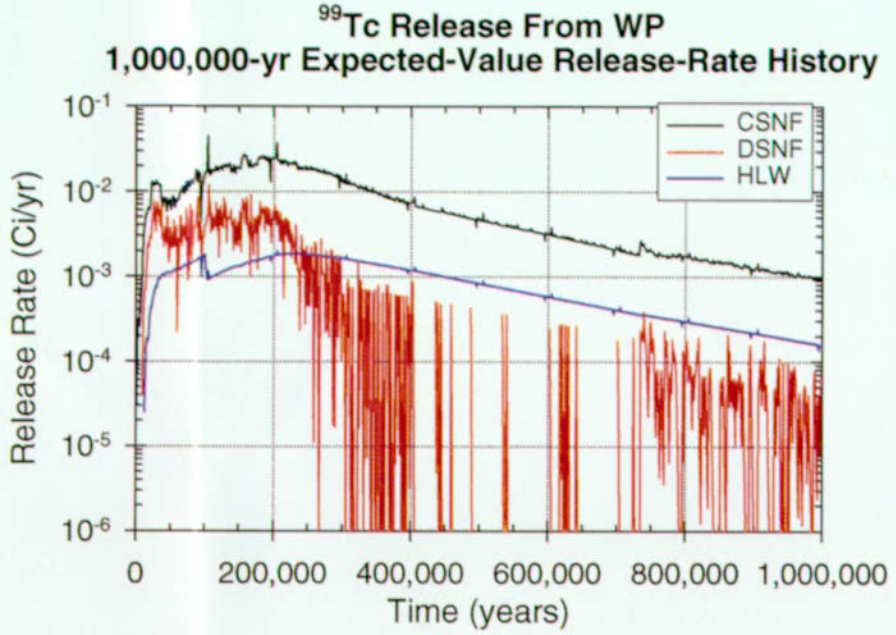

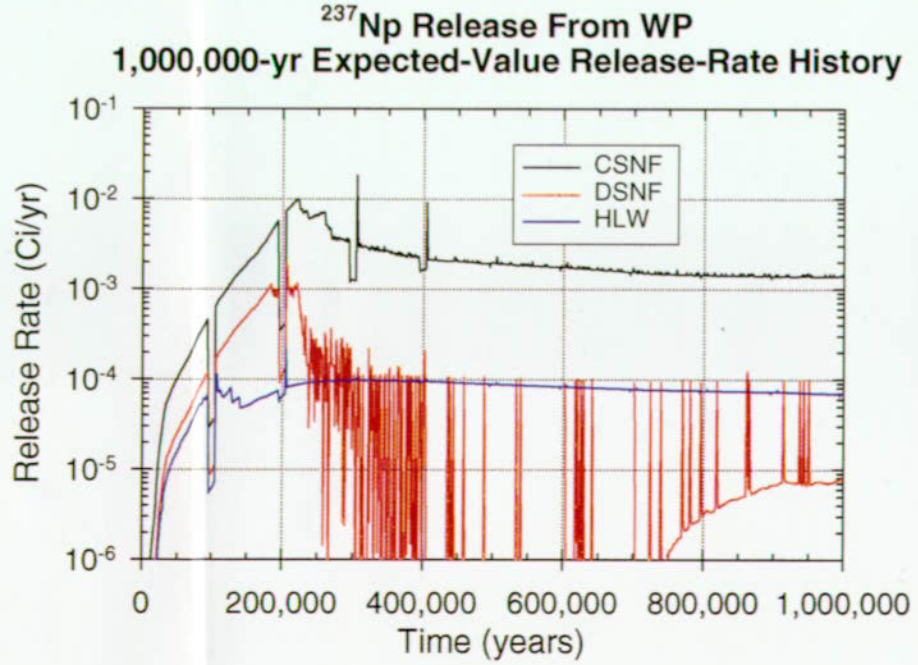

Figure 4-22. Waste Package Releases During 1 Million Years After Waste Emplacement for the Three Inventory Types: Commercial Spent Nuclear Fuel, U.S. Department of Energy Spent Nuclear Fuel, and High-Level Radioactive Waste
(WP—waste package; CSNF—commercial spent nuclear fuel; DSNF—DOE spent nuclear fuel; HLW—high-level radioactive waste)

INTENTIONALLY LEFT BLANK

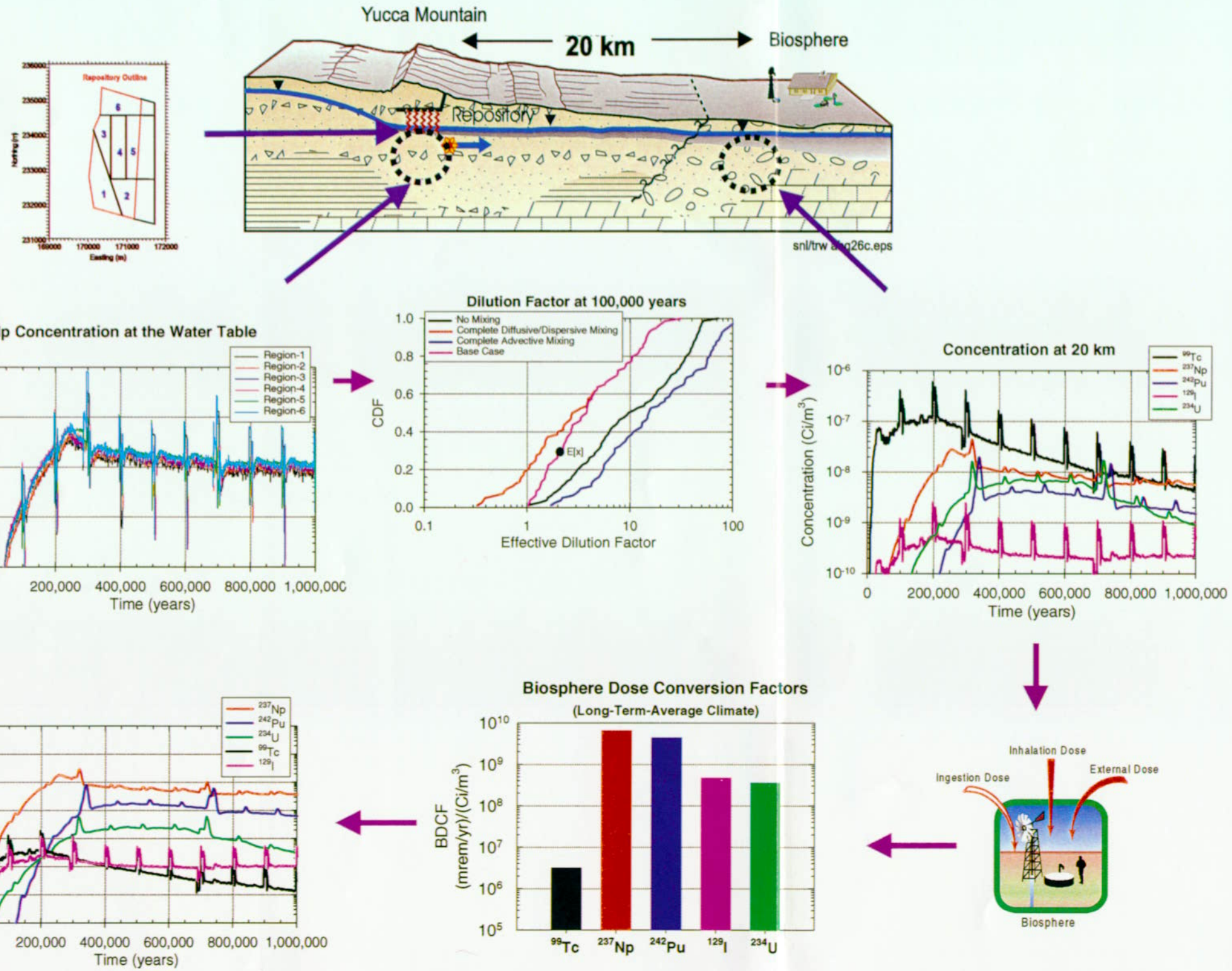

Figure 4-23. Effects of Saturated Zone Dilution and Biosphere Dose Conversion Factors on 1 Million Year Dose Rates
The insert at upper left shows the six water table regions.
(BDCF—biosphere dose conversion factors)

INTENTIONALLY LEFT BLANK

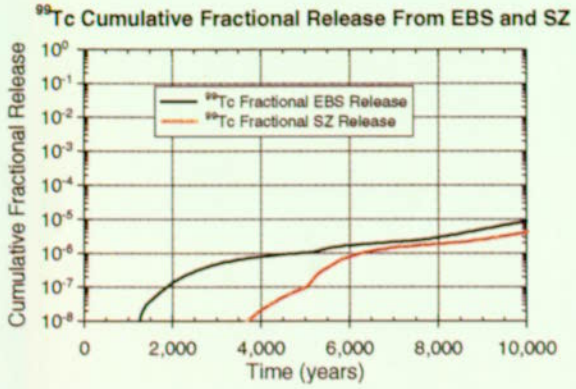

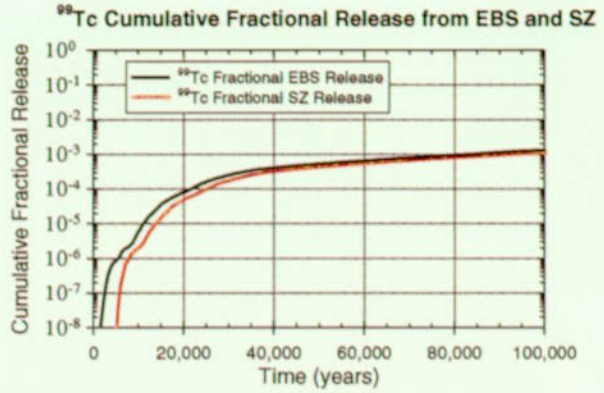

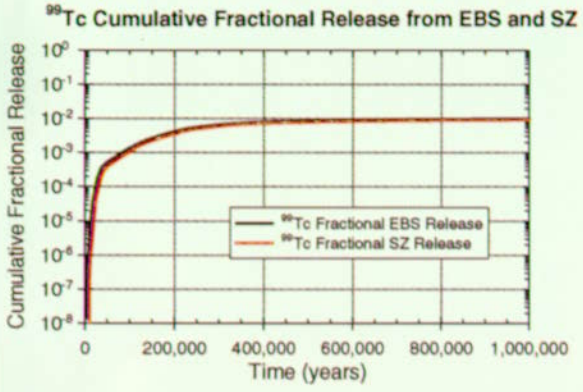

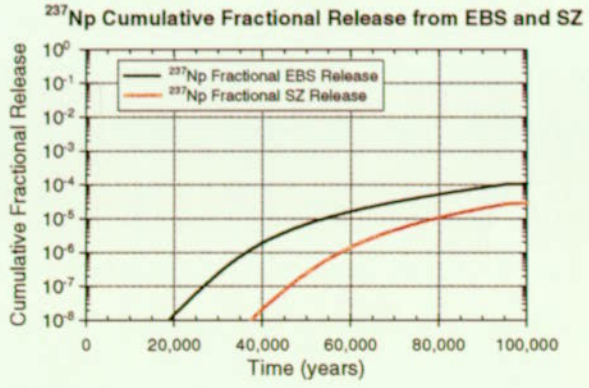

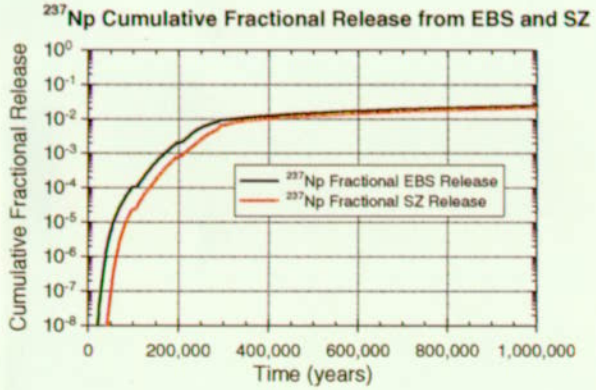

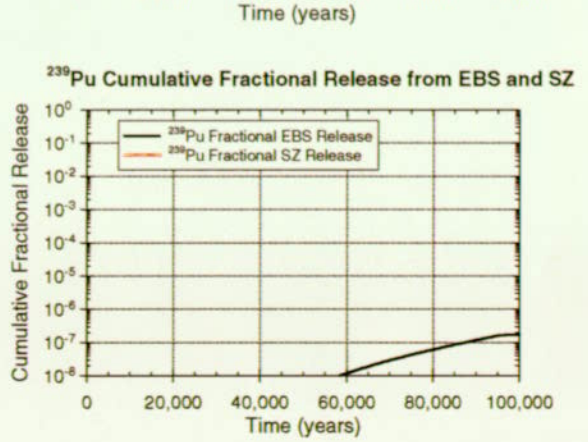

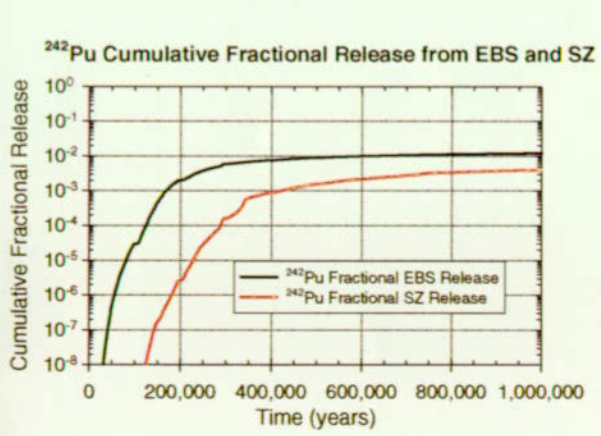

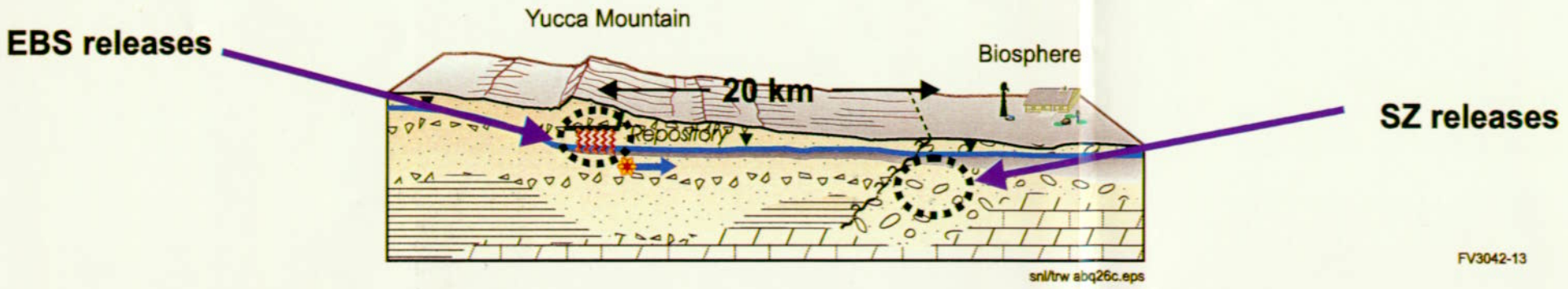

FV3042-13

Figure 4-24. Cumulative Fractional Inventory Releases of Technetium-99, Neptunium-237, Plutonium-239, and Plutonium-242 from the Engineered Barrier System and the 20-km Saturated Zone Boundary, Normalized to the Initial Inventory
Shown are the effects of sorption and decay of radionuclides. (EBS—engineered barrier system; SZ—saturated zone)

INTENTIONALLY LEFT BLANK

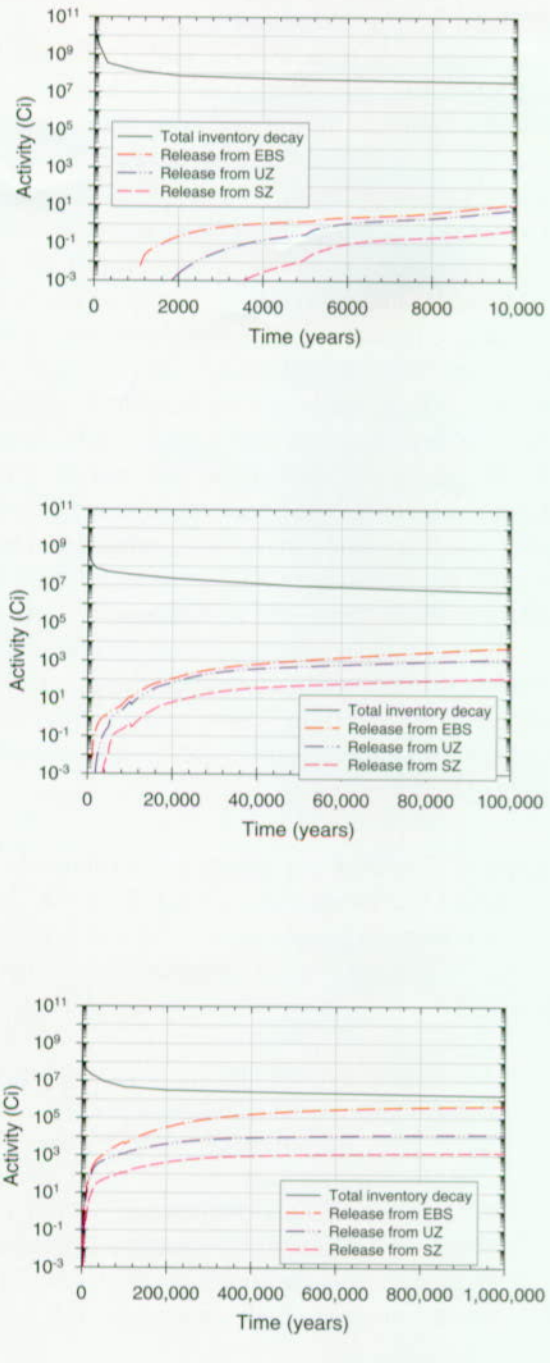

Figure 4-25. Plots of Cumulative Inventory Released from Different Boundaries of the Repository System Along with the Inventory Decay Curve over a Period of 1 Million Years
(EBS—engineered barrier system; UZ—unsaturated zone; SZ—saturated zone)

As in the 100,000-year time span, the jaggedness of the instantaneous package-failure history explains the jagged appearance of the graphs for technetium-99 waste package releases and biosphere dose rates—for the same identical reason, namely, that technetium-99 is a "release-rate-limited" radionuclide. That is, the radionuclide has such a high solubility that its release is limited by the rate at which packages fail, not the rate at which water moves it out of the packages. The instantaneous package failure history shown in Figure 4-21 is a histogram of package failures, with the interval size being equal to the time step size of 1,000 years. Because this time step is larger than for the 100,000-year simulation, some of the peaks on the histogram are larger than the 100,000-year package-failure histogram in Figure 4-16. Instead of 10 packages being the maximum in any interval, there are up to 30 or more in an interval.

Another feature of the waste package failure history is the failure of the no-drip packages beginning at about 730,000 years. This is the group of packages discussed earlier that are never dripped on; about 55 percent of the total packages in the repository. Because they are never dripped on, their corrosion rate is much lower than for dripped-on packages and, therefore, they do not begin to fail until a very long time after emplacement. Even when they do fail, there is no flowing water to sweep out the inventory, so the only release mechanism is diffusive transport. This effect is shown on the technetium-99 diffusive release curve and slightly evident on the neptunium-237 release curve; however, the effect of these no-drip packages is barely discernible on the dose rate curve in the biosphere.

As with the 100,000-year time histories discussed in Section 4.2.2, neptunium-237 releases are different from technetium-99 releases because of neptunium-237's low solubility, at least for the first 200,000 years. However, after 200,000 years neptunium-237 actually switches from being a solubility-limited radionuclide to being a release-rate limited radionuclide—limited by the cladding failure rate. A number of the plots on Figure 4-21 explain this effect. First, after about 200,000 years

the seepage flux through the packages is very high—high enough to sweep out all of the released neptunium-237, even though it has a very low solubility in the flowing water. Second, the commercial spent nuclear fuel cumulative package-failure curve flattens out at about 200,000 years, showing that very few additional commercial spent nuclear fuel packages fail for the remainder of the 1 million years. However, the combined commercial spent nuclear fuel cumulative package-cladding failure curve (the integrated or "convolved" product of package failures with cladding failures) continues to increase after 200,000 years, indicating that more inventory is being exposed. However, the rate at which this cumulative package-cladding failure curve increases is declining with time after 200,000 years. This effect is evident on the instantaneous "commercial spent nuclear fuel inventory exposure rate" curve, which represents the rate at which inventory is exposed to transport as a function of time (where the inventory is represented as a fraction of the entire repository inventory).[41] This inventory exposure curve exactly mirrors the shape of the neptunium-237 advective release curve between 200,000 years and 1 million years, and also the shape of the neptunium-237 dose rate curve. This implies that neptunium-237 is no longer solubility limited after about 200,000 years, but is "cladding release rate" limited. In other words, the release rate or exposure rate of neptunium-237 by failing cladding is slow enough and the seepage flux is high enough that the low solubility of neptunium-237 no longer limits its release from the waste package. This effect is also shown on the diffusive release curve for neptunium-237, which looks very much like the technetium-99 diffusive release curve after 200,000 years. In particular, during the dry climate states, the diffusion releases of both neptunium-237 and technetium-99 attain the same rate as the long-term average advective release rate. This is because the concentrations of both radionuclides build up during the dry climate (i.e., neither were solubility limited during the long-term average climate, so both of their concentrations in the waste packages build up during the dry climate, causing an increased diffusive flux). On the neptunium-237 release plot, this behavior is evident in the dry climate states after 200,000 years. However, in the two dry climate states before 200,000 years, neptunium-237 is solubility limited and its diffusive release curve shows no abrupt changes when the dry climate is established. Also, before 200,000 years, the neptunium-237 release curve shows a sharper rise and peak than the commercial spent nuclear fuel inventory exposure curve because the neptunium-237 release follows the package-failure cumulative distribution function up until that point. The technetium-99 release rate curves also follow the commercial spent nuclear fuel inventory exposure curve at all times, as is expected for a radionuclide that is not solubility limited.[42]

Figure 4-22 shows the relative contributions to engineered barrier system releases from the three main inventory types over the 1 million-year time frame. Following are the important points about these plots:

- DOE spent nuclear fuel is the second highest contributor to neptunium-237 and technetium-99 releases during the first 200,000 years. Commercial spent nuclear fuel is the highest contributor. After that time, the DOE spent nuclear fuel inventory begins to run out because very few DOE spent nuclear fuel packages fail after

[41] This inventory exposure rate curve is the derivative of the cumulative package-cladding failure curve normalized to (i.e., divided by) the total number of commercial spent nuclear fuel packages.

[42] An unusual feature of the neptunium-237 diffusive release curve is the series of gaps that appear in the curve each time the climate switches from dry to long-term average, and also when the climate switches from long-term average to the second superpluvial at about 730,000 years. The gaps are caused by the negative diffusion rate at these points, which cannot be plotted on a log scale. Apparently, when an abrupt change to a wetter climate occurs, neptunium-237 is rapidly flushed from the waste package, causing near zero concentration in the waste package and allowing "backwards" diffusion from the invert into the package. Although not shown in this document, the comparable advective and diffusive releases from the engineered barrier system do not exhibit these negative diffusion rates.

200,000 years. (Individual package failure is readily discernible on the plot.)

- High-level radioactive waste never contributes very much to neptunium-237 and technetium-99 releases compared to commercial spent nuclear fuel.

For performance over the 1-million-year period, the unsaturated zone is of very little consequence, so no figures are shown for it. On the other hand, the saturated zone is important because of dilution, which proves to be the second most important uncertainty (see Section 4.3).[43] Figure 4-23 shows how dilution in the saturated zone affects concentration, specifically neptunium-237, and how the biosphere dose conversion factors for the various radionuclides are used to convert saturated zone concentrations to dose rates.

4.2.4 Cumulative Activity Releases from the Repository and the Engineered Barrier System

Another way of examining repository performance is by looking at cumulative activity release (Curies) versus time at the edge of the engineered barrier system compared to the cumulative activity release in the saturated zone at 20 km (12 miles). First, this method is another means of comparing natural system performance with engineered system performance. Second, the method illustrates the large fraction of the total radioactivity that is actually retained in the repository system at various times. The expected differences in the engineered barrier system and saturated zone cumulative release curves are because of retardation (sorption) and decay. If radionuclides did not decay, eventually the engineered barrier system and saturated zone cumulative curves would become equal. Figure 4-24 shows cumulative fractional activity releases of technetium-99, neptunium-237, plutonium-239, and plutonium-242 at these two spatial locations for the time frames of 10,000 years, 100,000 years, and 1 million years. Cumulative fractional release for any radionuclide at a given spatial location and a given time is defined as the cumulative activity that has traveled past that spatial location divided by the initial inventory emplaced for that radionuclide. In the 10,000-year time frame, nearly all the technetium-99 radioactivity is retained in the repository—less than 0.001 percent has been released from either the engineered barrier system or the saturated zone.[44] After 100,000 years, less than 0.2 percent of the technetium-99 has been released from the repository system (saturated zone at 20 km, or 12 miles) and less than 0.02 percent of the neptunium-237 has been released. The amount of plutonium-239 released beyond 20 km (12 miles) in the saturated zone does not appear on this graph but is slightly less than 1×10^{-9} percent. At 1 million years, about 1 percent of the technetium-99, 2 percent of the neptunium-237, and 0.4 percent of the plutonium-242 activities have reached the 20-km (12-mile) boundary. Much of the 99 percent of the technetium-99 that is never released is a result of radioactive decay throughout the repository system.

Figure 4-25 is another way to show cumulative inventory released. It plots the absolute, rather than the fractional inventory, released (i.e., the release curves are not scaled to the initial inventory). Also, it shows total inventory released rather than individual radionuclides. Total releases from three system boundaries are shown: edge of the engineered barrier system, base of the unsaturated zone, and 20 km (12 miles) downgradient in the saturated zone. By way of comparison the total inventory decay curve is also shown. This curve is the activity versus time for all the emplaced inventory if it were never mobilized by water or gas, that is, if it were always isolated. Figure 4-25 demonstrates that by 10,000 years the inventory that has escaped from the engineered barrier system is less than 0.0001 percent of the total isolated inventory. In other words, 99.9999 percent of the inventory remains in the engineered barrier system up until 10,000 years after closure.

[43] The neptunium-237 biosphere dose conversion factor is the third most important uncertainty in the 1 million-year time frame.

[44] The percent of neptunium-237, plutonium-239, and plutonium-242 released is negligible.

At 100,000 years the plots indicate that 0.1 percent of the inventory has escaped the engineered barrier system and 99.9 percent remains isolated in the drifts. At 1 million years about one-half of the inventory has escaped the engineered barrier system, but 99.9 percent remains contained in the entire repository system—within the natural and engineered barriers, that is, it has not passed beyond the 20-km (12-mile) "boundary." [45]

4.2.5 Summary

The purpose of Section 4.2 has been to demonstrate the influence of the various subsystem and component processes on the overall system performance. The illustrative realization used for this purpose is the "expected-value" realization, that is, the realization that chooses the expected value of all input parameters. The behavior of this realization cannot necessarily be considered to represent the overall mean behavior of the repository, as determined by multiple realization simulations, because of the nonlinear behavior of the models and processes. However, as will be seen in Section 4.3, this expected-value realization does lie near the central tendency of the overall probability distribution—generally somewhere between the median and the mean.

Based on the analysis in Section 4.2, nonsorbing radionuclides, such as technetium-99, dominate peak dose rates at "early" times, perhaps up to 50,000 years after repository closure. After that, the weakly sorbing neptunium-237 controls peak dose rates, with some additional contribution from plutonium-242.

During the first 10,000 years after repository closure, the key factors controlling repository behavior are the failure of the single juvenile (or early) failed package and the few (about 17) corrosion-failed packages, and the climate change at 5,000 years. The main factor affecting releases from the waste packages is the seepage of water into the waste packages, which is controlled by the corroded pit and patch area. During this time frame the seepage flux into the corrosion-failure packages is low enough that technetium-99 releases become solubility-limited in those packages. During this 10,000-year span after closure, travel time in the unsaturated zone and saturated zone during the dry climate state is also long enough to enhance performance.

During the first 100,000 years after repository closure, the major factors controlling performance are the instantaneous waste package failure rate (controls technetium-99 releases), the cumulative waste package and cladding failures (controls neptunium-237 releases), the fraction of packages encountering seeps, and the seepage rate into the packages. The seepage rate is important because neptunium release is solubility limited, so the absolute amount of neptunium-237 escaping any package is linearly proportional to the seepage flowing through the package.

During the first 1 million years after repository closure, the major factors controlling performance are the combined cumulative package and cladding failures, and the superpluvial climate change. The latter causes the peak in the total and neptunium dose-rate curves at about 300,000 years.

Dilution in the saturated zone is important at all time frames, but because of conservative assumptions about its magnitude, it does not play as large a role as in previous TSPAs (for example, see CRWMS M&O 1995). Also, sorption in the unsaturated and saturated zones is important for all of

[45] The curve in Figure 4-25 that is labeled "release from EBS" represents a total over the 39 major radionuclides modeled (see Chapter 6 of the *Total System Performance Assessment-Viability Assessment (TSPA-VA) Analyses Technical Basis Document* [CRWMS M&O 1998i]). The curve labeled "release from UZ" represents the total over the nine radionuclides discussed in this document. However, as shown in Chapter 6 of *Total System Performance Assessment- Viability Assessment (TSPA-VA) Analyses Technical Basis Document* (CRWMS M&O 1998i) the total releases from the 39 radionuclides at the base of the unsaturated zone are essentially identical to the releases from the nine radionuclides. The curve labeled "release from SZ" is also the release from the 9 radionuclides and would be expected to be identical to the 39 radionuclides.

the strongly sorbing radionuclides, such as plutonium, and provides a very long delay (up to hundreds of thousands of years) in transport to the 20-km (12-mile) boundary.

Commercial spent nuclear fuel dominates technetium and neptunium releases, but DOE spent nuclear fuel releases are not insignificant and comprise about 25 percent of the total.

4.3 PROBABILISTIC RESULTS OF THE BASE CASE

For the TSPA-VA, a probabilistic approach is used for assessing the long-term performance of the Yucca Mountain repository. This approach uses a linked system of deterministic models to represent the repository and its associated geologic system, and a Monte Carlo technique to propagate parameter uncertainty through to the calculation of peak radiation dose rates at the specified location 20 km (12 miles) from the repository. A full analysis includes the following:

1. Selecting imprecisely known model input parameters to be sampled

2. Constructing probability distribution functions for each of these parameters, incorporating available data and subjective information to capture uncertainty

3. Generating a sample set by selecting a parameter value from each distribution

4. Calculating outcomes for the sample set

Steps 3 and 4 are repeated many times to produce a distribution of peak dose rates that represents the spectrum of repository performance. The distribution of peak dose rates is normally presented as a CCDF that gives the probability of exceeding a given peak dose rate. The range or spread of peak dose rates represents the amount of uncertainty in the results. In addition to quantifying uncertainty in the results of the performance assessment, another important component of the probabilistic approach used in the TSPA is the sensitivity analysis. Sensitivity analysis is used to identify the relative importance of uncertain input parameters to the calculated uncertainty in repository performance. This information is useful for selecting and assigning priorities to future modeling, site characterization, and design activities so that uncertainty in estimates of long-term performance may be decreased.

This section summarizes the probabilistic results obtained from the base case Monte Carlo simulations. Results are presented in Sections 4.3.1 and 4.3.2. Section 4.3.1 focuses on the calculated peak dose rates to a human located 20 km (12 miles) from the repository. Dose rates are presented in the form of CCDFs for three periods: 10,000 years, 100,000 years, and 1 million years. Factors are also discussed that cause uncertainty in the calculated peak dose rates. Auxiliary results are provided about which radionuclides contribute most to dose and the range in times at which peak dose rates occur. In Section 4.3.2, the contributions of individual parameters to uncertainty in peak dose rates are discussed. Uncertain parameters that are most important to subsystems, such as radionuclide releases from the engineered barrier system or from the unsaturated zone, can also be analyzed, and one example is briefly discussed. For more information on the methods used for probabilistic analysis, see Section 11.3 of the *Total System Performance Assessment-Viability Assessment (TSPA-VA) Analyses Technical Basis Document* (CRWMS M&O 1998i).

4.3.1 Uncertainty Analysis

In this section, uncertainty results of the Monte Carlo simulations are reported for three periods: 10,000 years, 100,000 years, and 1 million years. The following is a brief description of how the probabilistic results are obtained.

The TSPA results can be symbolically represented by a simple function of the form

$$\text{Dose Rate} = f(x_1, x_2, \ldots, x_{nc}, s_1, s_2, \ldots, s_{nu}, t),$$

where dose rate represents the dose rate to a human at the 20-km boundary as a function of time t.

The variables x_1, x_2, ..., x_{nc} are precisely known input parameters such as the acceleration of gravity and the density of water, and nc is the number of such inputs. Variables s_1, s_2, ..., s_{nu} are imprecisely known or uncertain parameters such as corrosion rate and waste form dissolution rate, and nu is the number of such parameters. In the TSPA-VA base case, nc = 1,006 and nu = 177. Note that the 1,006 certain parameters and 177 uncertain parameters include only those that are used within RIP; many additional parameters are used in the various component models such as TOUGH2 and WAPDEG. A description of the uncertain parameters is provided in Chapter 11, Appendix A of CRWMS M&O 1998i. The imprecisely known inputs are the parameters that cause uncertainty in the performance assessment results.

The uncertainty in parameters s_1, s_2, ..., s_{nu} is characterized by a sequence of probability distributions

$$D_1, D_2, ..., D_{nu},$$

where D_j is the probability distribution for variable z_j. In some cases, the definitions of these distributions are also accompanied by specifications of correlations that further define the relations between the s_j. For the TSPA-VA base case, the seepage parameters for different repository subregions are correlated, seepage and net infiltration for different climate states are correlated, and biosphere dose-conversion factors for different radionuclides are correlated (see Sections 3.1.2.2, 3.1.2.4, and 3.8.2).

Once distributions D_j are specified, the next step is to determine the uncertainty in the performance assessment results that arises from uncertainty in s_1, s_2, ..., s_{nu}. First, a sample

$$S_k = [s_{k1}, s_{k2}, ..., s_{k,nu}], k = 1, ..., nu,$$

is generated from the specified distributions D_1, D_2, ..., D_{nu}, where nk is the size of the sample, or number of realizations. In the TSPA-VA, this sample is generated using Latin Hypercube sampling and the sample size is nk = 100 for most simulations (see Section 4.3.1.2). A performance assessment calculation is then conducted for each sample S_k, with all precisely known input parameters $x_1, x_2, ..., x_{nc}$ held fixed at their known values. The performance assessment calculations yield a series of curves that show how the dose rate changes with time. These curves are referred to as dose-rate time histories and can be represented symbolically as

$$(\text{Dose Rate})_k = f(x_1, x_2, ..., x_{nc}, s_{k1}, s_{k2}, ..., s_{k,nu}, t), \quad k = 1,2, ..., 100,$$

where each $(\text{Dose Rate})_k$, k = 1,2, ..., 100, is the result of a complete calculation of all the linked TSPA components.

Once the dose-rate history for each realization is obtained, the peak dose rate that occurred during the simulation period for each realization is determined by taking the highest point on each dose-rate history curve. Once a peak dose rate is obtained for each realization, the next step is to graphically represent the results in the form of a CCDF, which shows the probability that a dose rate is greater than a given value and is constructed by first ordering the peak dose rates from smallest to largest values, with a probability of 1/nk = 1/100 assigned to each peak dose rate. The probability that a dose rate is greater than a specified dose rate is determined by summing the probabilities associated with all dose rates larger than the specified one. Representative dose-rate time histories for the 100,000-year simulation period are presented next, along with distributions of peak dose rates for the 10,000-, 100,000-, and 1-million-year simulation periods.

4.3.1.1 Uncertainty Analysis Results

Dose-rate histories for the 100,000-year simulation period are presented at the top of Figure 4-26. As noted in the figure caption, 20 realizations in the 100,000-year simulation period did not produce a dose. Also, in the 10,000-year simulation period, 27 realizations have zero dose, but in the 1-million-year simulation all realizations produced a dose. For illustration, four selected realizations are

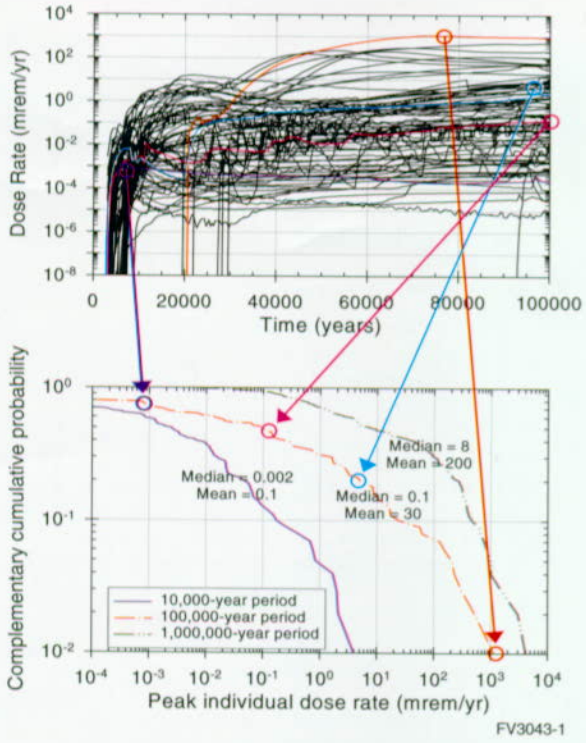

Figure 4-26. Base Case Distribution of Peak Dose Rates for Three Periods and Their Relation to Dose-Rate Time Histories
Twenty dose-rate histories do not appear on the top plot because they have no computed dose for the first 100,000 years.

highlighted; they will be discussed in more detail later in this section. Figure 4-26 shows that the majority of dose rates tend to rise quickly between 3,000 and 10,000 years. A few realizations begin to produce doses in the 20,000- to 30,000-year time interval, with one realization not having any dose until after 90,000 years. In general, four types of behavior through time are shown:

- After the initial steep rise, many of the realizations show a steady increase in dose rate with time that continues throughout the simulation period. This type of behavior reflects significant numbers of waste package failures over time because of corrosion in combination with relatively large fraction of waste packages contacted by seeps.

- Other realizations reach their peak early and their dose rate gradually decreases with time over the simulation period. This type of behavior reflects the impact of juvenile waste package failures, a lower number of waste package failures because of corrosion, and a lower fraction of waste packages contacted by seeps.

- In some realizations, the dose rate remains relatively flat with time after the initial rise. This behavior is caused by juvenile failures in combination with a small number of corrosion-induced waste package failures that are spread over the simulation period.

- In some realizations, dose rate tends to alternately increase and decrease throughout the simulation period. This behavior is primarily caused by a combination of low seepage fraction and discrete waste package failures well separated in time, with a waste package failure roughly coinciding with each dose-rate peak on the history curve.

The distributions of peak dose rates to an individual located at 20 km (12 miles) from the repository are presented at the bottom of Figure 4-26 for the 10,000-, 100,000-, and 1 million-year simulation periods. Peak dose rate is defined as the maximum dose rate that occurs for a given curve during the entire simulation period. This definition is illustrated by indicating the maxima of the four selected realizations and showing where they fall on the 100,000-year CCDF. All realizations are weighted equally, so the lowest probability shown on the curves is 1/100. The median and mean peak-dose-rate values are also shown for each simulation period. The figure shows that peak dose rates continue to increase as time increases. However, the 100,000-year curve shows about a factor of 100 increase in dose rates over the 10,000-year curve, whereas the 1-million-year curve shows only a factor of five to ten increase in dose rates over the 100,000-year curve. The time histories for the 10,000-year and

1-million-year periods are shown for reference in Figure 4-27.

Time histories of some statistical measures of the peak-dose-rate distribution are shown in Figure 4-28. To generate these plots, the statistical measures were calculated from the 100 dose-rate values at each time step in the analyses. For example, the average of the 100 dose rates was calculated and plotted as the "mean" curve and the fifth lowest dose rate among the 100 realizations was determined and plotted as the "5th percentile" curve. Note that in the 10,000- and 100,000-year simulation periods the 5th-percentile dose rate is zero and therefore is not plotted. The mean dose rate in all three periods is much higher than the median value, indicating that the mean values tend to be dominated by a few low-probability high dose rates.

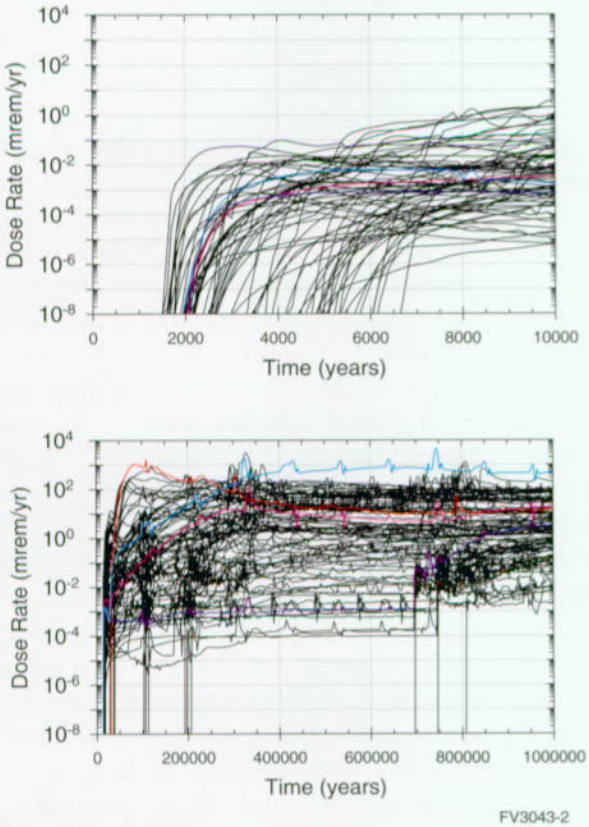

Figure 4-27. Dose-Rate Time Histories for 10,000- and 1-Million-Year Periods
Twenty-seven dose-rate histories do not appear on the top plot because they have no computed dose for the first 10,000 years.

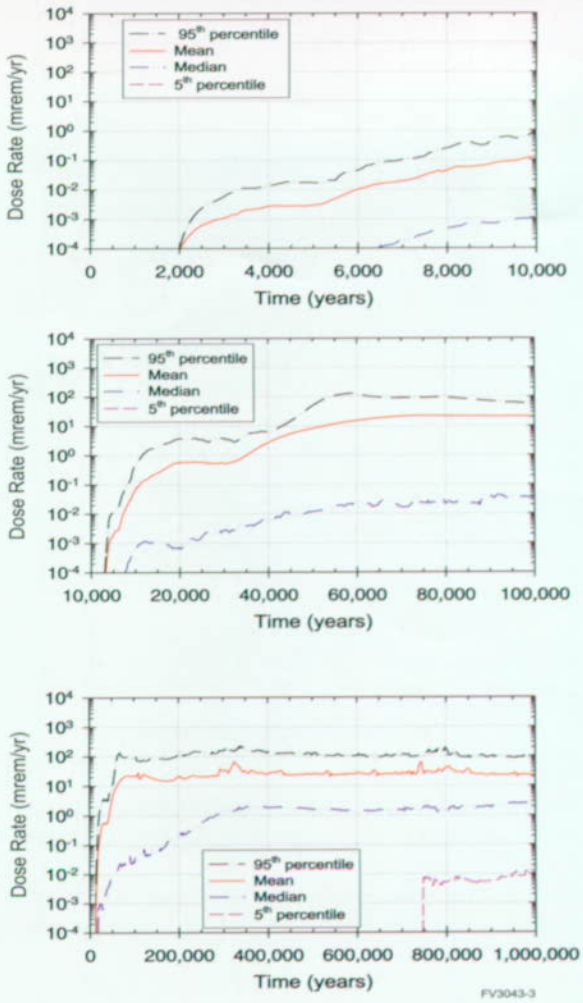

Figure 4-28. Time Variation of Statistical Descriptors of the Calculated Dose-Rate Distribution
Shown are time histories for mean and median dose rate, plus the 5th and 95th percentiles of the dose-rate distribution. The fifth-percentile curve is missing from the top two plots because the fifth-percentile dose rate is zero for those periods.

Figure 4-29 presents the average radionuclide contribution to the peak dose rate. Average contributions are determined by calculating the relative individual radionuclide contributions to the peak dose rate for each realization and averaging the relative contributions across all realizations. In the 10,000-year simulation period (see the top of Figure 4-29), contributions to peak dose rate are dominated by technetium-99 and iodine-129, with a small contribution from carbon-14. In addition, 27 percent of the realizations have zero calculated

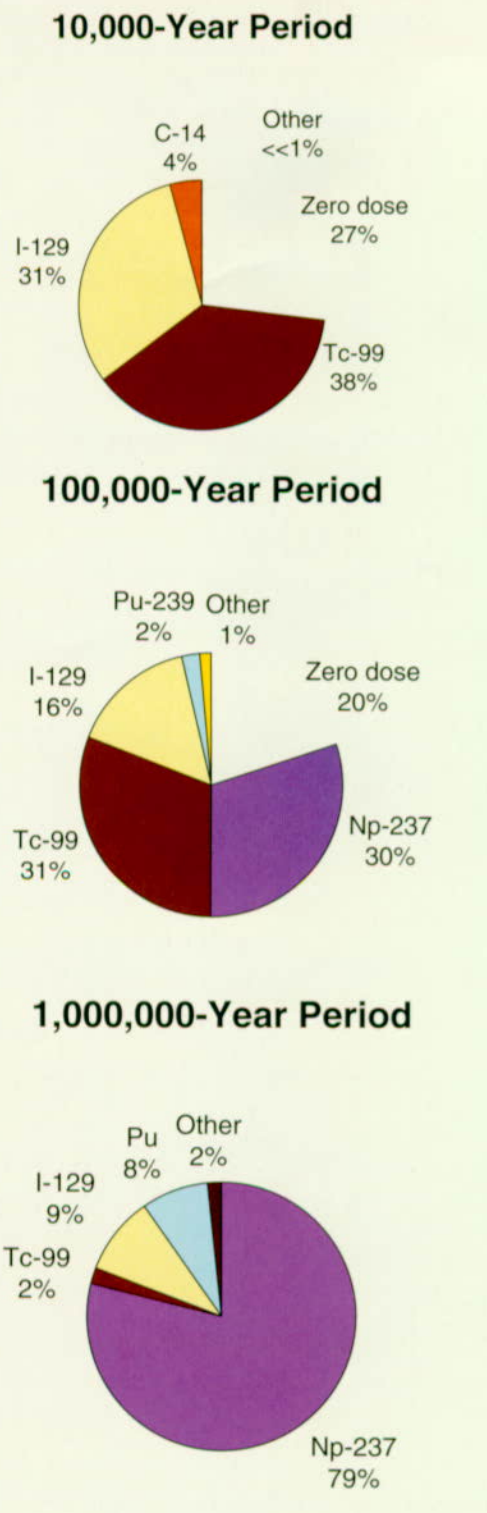

Figure 4-29. Average Contribution to Peak Dose Rate of Different Radionuclides for Three Periods Note that for the earlier two time periods many realizations have no computed dose.

dose. In the 100,000-year period (see the middle chart), contributions to peak dose rate are dominated by technetium-99, neptunium-237, and iodine-129, with 20 percent of the realizations having zero dose. Two percent of the realizations are dominated by plutonium-239. Over 1 million years (see the bottom chart), most peak dose rates are dominated by neptunium-237, with a small number being dominated by iodine-129, plutonium-239, or plutonium-242 (plutonium-239 and plutonium-242 are lumped together in the chart); technetium-99 makes a small contribution to the peak dose rate but is never dominant in any realization.

In general, technetium-99 and iodine-129 are significant contributors to dose because of the following characteristics:

- Large inventories
- Long half-lives (although technetium-99 starts to decay significantly after 100,000 years)
- Highly soluble
- Unretarded during transport

Carbon-14 has a large inventory, is highly soluble, and is unretarded during transport, but its half-life is so short (5,700 years) that it is a significant contributor only for the 10,000-year period. Neptunium-237 has a large inventory and long half-life; however, it is released more slowly from the waste and travels more slowly because of retardation by adsorption. As a consequence, neptunium-237 is not a significant contributor to dose until after 10,000 years. Plutonium (represented by plutonium-239 and plutonium-242) has a very large inventory but normally is released very slowly from the waste because of low solubility and travels very slowly because of high adsorption. These two factors can both potentially be reversed because of colloidal mobilization and transport. With the models and assumptions in the TSPA-VA base case, plutonium is very mobile in colloidal form a small percent of the time. Plutonium-239 has the greater inventory, but it has a half-life of

only 24,000 years so it is only important for the first 100,000 years or so.

The timing of the peak dose rates varies for each of the three simulation periods. Figure 4-30 presents scatter plots of the peak dose rate and the time at which peak dose rate occurs for each simulation period. In the plots, each symbol represents a single realization. The scatter plot of 10,000-year peak-dose times (see the top of Figure 4-30) shows that doses do not occur before 3,000 years and that peak dose rates are spread relatively uniformly throughout the remaining 7,000 years. Realizations having later peak times tend to have more waste packages in contact with seeps and therefore more corrosion failures. Juvenile waste package failures may lead to early releases, whereas later releases and doses are generally controlled by waste package failures that occur because of corrosion. Later-peak-dose realizations also tend to have lower net infiltration and, therefore, longer unsaturated zone travel times. Thirty-one realizations reach an apparent peak dose rate at 10,000 years, as indicated by the numerous symbols along the vertical line at 10,000 years; these realizations have not reached a true peak and will continue to increase if the simulation time is extended.

As shown in the middle plot of Figure 4-30, the peak-dose times in the 100,000-year period are clustered in two areas, with few points in between. Before 30,000 years, 16 percent of the realizations have their peak dose rate, and 56 percent of the realizations have their peak after 70,000 years, plus 20 percent have zero dose for the whole period. Many of the early peak dose rates, and especially those before 10,000 years, have only juvenile waste package failures and no corrosion failures for the first 100,000 years. The peak dose rates before 10,000 years are all very low, less than 0.1 mrem/year. For the 100,000-year period, peak-dose times are influenced by the number of packages in contact with seepage water and by waste package corrosion rate. Peak-dose times again tend to increase as both the number of packages in contact with seepage increases and the number of package failures increases. The two are closely related. However, percolation flux through the unsaturated zone and the resulting effect on travel time have less of an influence on peak-dose

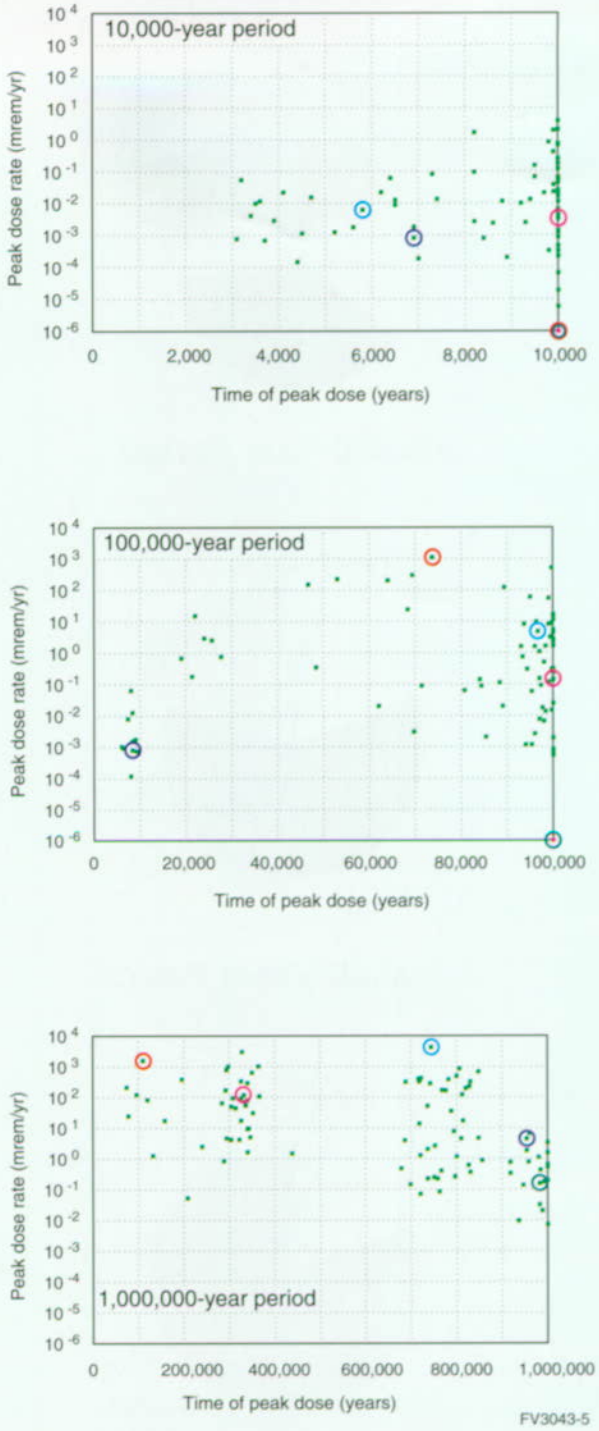

Figure 4-30. Peak Dose Rate Versus Time of Peak Dose Rate for Three Periods
Pink dots at the bottom indicate realizations with zero dose (which are off the scale of the log plot). The colored circles refer to the selected realizations highlighted in Figures 4-26 and 4-27.

time in this longer simulation period. Again, several realizations reach an apparent peak dose rate at 100,000 years, indicating that these realizations have not reached an actual peak during the 100,000-year simulation period.

The clustering of peak dose rates in particular time periods is even more pronounced in the 1-million-year simulation, as shown in the bottom plot of Figure 4-30, with 39 percent of the peaks occurring prior to 400,000 years and 57 percent occurring after 700,000 years. This behavior is mainly because of the climate model, with most of the peak dose rates associated with superpluvial climates. The figure shows two distinct clusters of points: one cluster at about 330,000 years and the other cluster at about 780,000 years. These times correspond to the two superpluvial climates, with the scatter in peak-dose time largely because of the scatter in the sampled time of the superpluvial climates.

The effect of climate changes can be seen clearly in the 1-million-year dose-rate history curves (Figure 4-27, bottom), in the regularly spaced spikes on the curves. These spikes are caused by the climate changes that occur roughly every 100,000 years. The most extreme climate changes occur at the superpluvials, which happen at approximately 300,000 years and 700,000 years. The spikes at those times are larger than the other climate-change spikes, leading to the predominance of those times in the peak-time scatter plot (Figure 4-30, bottom). The climate history for one of the realizations is shown in Figure 4-31, to show that the spikes in the dose-rate curves line up with the times of climate changes. However, the climate changes are at slightly different times in different realizations.

As for the 10,000-year and 100,000-year periods, waste package corrosion rate and seepage fraction influence peak-dose times, but here the relationship is reversed, with higher corrosion rates and more seepage tending to produce earlier peak dose rates. This difference can be explained as follows. Waste package failures and dose rates are still increasing at 100,000 years in most realizations; realizations with higher waste package

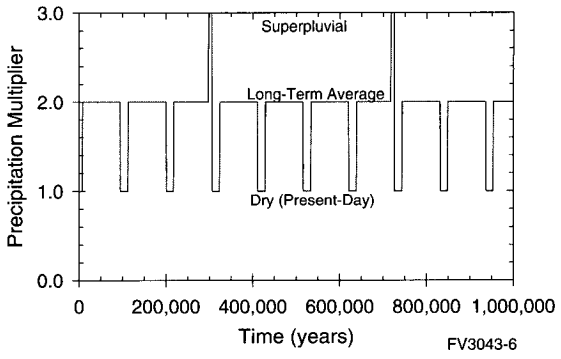

Figure 4-31. Climate History for One Realization
The others look similar. Most of the peak dose rates occur at one of the two superpluvial climates.

failure rates, influenced both by nickel-base Alloy 22 corrosion rate and the fraction of waste packages contacted by seeps, tend to have dose rates increasing faster as well, so their 100,000-year peak is at the end of the period. Those realizations then tend to have their 1-million-year peak dose rates at the earlier superpluvial. However, realizations with low corrosion-failure rates because of low sampled Alloy 22 corrosion rate or low seepage fraction, tend to have their 10,000-year and 100,000-year peak dose rates early because of juvenile waste package failures. These realizations then achieve their 1-million-year peak dose rates late in the period (or even after 1 million years), after they finally have significant numbers of corrosion-failed waste packages.

To further illustrate some of the key processes that affect calculated dose rates and their peak times, five realizations were selected for more detailed discussion. The five realizations were chosen to have a spread of peak dose rates and peak-dose times and, therefore, a variety of different behaviors. The selected realizations are indicated with different colors in Figure 4-30, and their time histories are highlighted with the same colors in Figures 4-26 and 4-27.

Additional information is given in Figure 4-32, which shows the number of failed waste packages over time for the selected realizations. In Figure 4-32, the pink and blue realizations have one juvenile waste package failure, the cyan realization has two juvenile failures, and the red

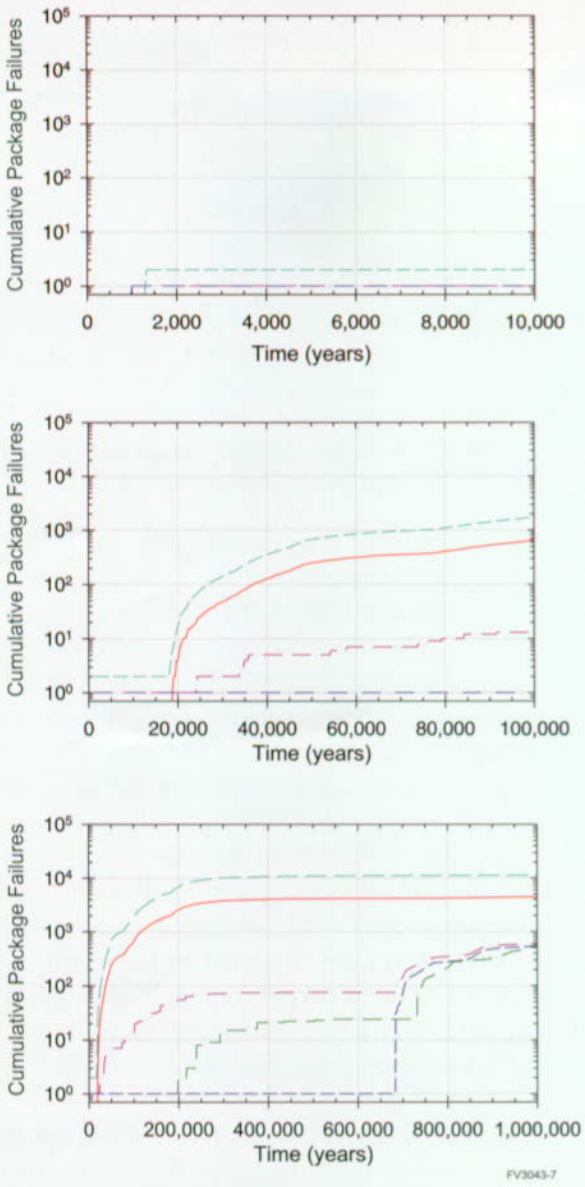

Figure 4-32. Number of Failed Waste Packages over Time for the Selected Realizations
The realizations were chosen to have a spread of peak dose rates and peak dose times and, therefore, a variety of different behaviors.

and dark green realizations have no juvenile failures. The dark green realization has no waste package failures for nearly 200,000 years. The blue realization has no additional waste package failures other than one juvenile failure for almost 700,000 years. The pink realization has a relatively small number of additional failures, and the red and cyan realizations have many corrosion failures. These numbers of waste package failures are strongly reflected in the relative dose rates in Figure 4-26. The blue realization has a low dose rate throughout the entire 100,000-year period, the pink realization is higher, and the red and cyan realizations are higher yet. However, the number of waste package failures is not the only determinant of dose, because the red realization has the highest dose rate even though the cyan realization has more waste package failures. The primary reason that the red realization has such a high peak dose rate even though it does not have the greatest number of waste package failures is that it is one of the realizations with highly mobile plutonium colloids; 97 percent of its peak dose rate is from plutonium-239. The significant falloff in dose rate after 100,000 years in that realization (Figure 4-27, bottom) is because of plutonium-239 decay.

Figure 4-32 shows that many realizations have an increase of waste package failures starting at about 700,000 years. In fact, the red and cyan realizations have a similar increase in the number of failures but it cannot be seen on the log scale because they already have so many waste package failures. The explanation for this behavior is that around 700,000 years the waste packages with no seeps dripping on them start failing. Until that time, only waste packages contacted by seeps have failed. Because the waste packages failing after 700,000 years are dry, the failures are not reflected in significantly increased dose rates in some cases (Figure 4-27, bottom). Dry waste packages have lower rates of release (diffusive only) than wet ones (diffusive plus advective). The fraction of waste packages contacted by seeps is reflected directly in the waste package failure curves. For example, the cyan realization has a seepage fraction for the long-term-average climate of 95 percent, which allows almost all of the waste packages to fail within 300,000 years. The number of failed packages is over 10,000. The red realization has a seepage fraction for the long-term-average climate of about 36 percent, so only about a third of the waste packages fail before 300,000 years in that realization. The other three selected realizations all have seepage fraction less than one percent for the long-term-average climate, so less than one percent of the waste packages fail in those realizations, until the dry ones start failing at late times.

4.3.1.2 Precision of the Base Case Complementary Cumulative Distribution Functions

The number of realizations to use in a Monte Carlo simulation is a significant issue in terms of reliable analyses and proper allocation of resources. Therefore, the number of runs required to reliably predict peak dose rates was examined. To verify whether 100 realizations are sufficient, the 10,000-year and 100,000-year base case simulations were repeated with 1,000 and 300 realizations, respectively. The resulting distributions of peak individual dose rates are compared with the 100-realization base case results in Figure 4-33—the distributions for each time period nearly overlay. The 100-realization distributions do not go below a probability of 0.01 because each predicted dose rate has a probability of occurrence of 1/100, or 0.01. Similarly, the 1,000- and 300-realization distributions display minimum probabilities of 0.001 and 0.003, respectively. In Figure 4-33, peak dose rates do continue to increase as probability decreases. Increased dose rates at these low probabilities are caused by combinations of extreme uncertain-parameter values that are sampled from the tails of the parameter probability distributions. However, 100 realizations appear to provide a good compromise between cost and precision.

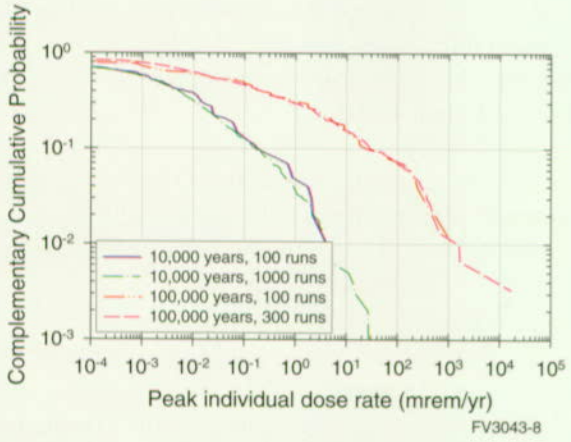

Figure 4-33. Comparison of Peak Dose Rate Distributions Determined from Simulations with Different Numbers of Realizations
The distributions are found to be quite similar, indicating reasonable stability with respect to number of realizations.

4.3.2 Sensitivity Analysis

The primary objective of sensitivity analysis is to identify those uncertain parameters that have a strong influence on the repository performance measures and to quantify the strength of their influence. The simplest tool for sensitivity analysis is the scatter plot, which is a plot of sampled numerical values of an uncertain variable, or independent variable, used in the computations versus the calculated results such as peak dose rate, or dependent variable. If little or no relationship exists between an independent-dependent variable pair, their scatter plot will resemble a random distribution of points. However, if a notable relationship exists between them, the plotted points will cluster and exhibit a recognizable form.

Scatter plots are valuable for identifying a relationship between variables, but they do not quantify the intensity of that relationship. Multiple linear regression modeling is used to quantify relationships between dependent and independent variables. By using a regression model, it is possible to identify variables that contribute most to the calculated uncertainty in the peak dose rates. A good discussion of multiple linear regression modeling and other sensitivity-analysis techniques, and their application to the performance assessment of the Waste Isolation Pilot Plant, is given by Helton (1993).

For the TSPA-VA, the primary technique for regression modeling is stepwise linear regression. In the stepwise approach, a sequence of regression models is constructed starting with a single selected input parameter, and including one additional input variable at each successive step until all significant input variables have been included in the model. This approach avoids having to treat all of the independent uncertain variables simultaneously in a single model.

A measure of goodness of fit of a linear-regression model is provided by the coefficient of multiple determination, R^2. An R^2 value near 1 indicates a good fit, meaning that the model is accounting for most of the uncertainty in the performance measure being analyzed. To avoid poor linear fits with

nonlinear data, regression analyses were performed on rank-transformed data. By rank-transformed data it is meant that the actual data values of both outputs and inputs are replaced with their corresponding ranks; that is, the smallest value for a given variable is assigned the value of 1, and the next largest value is assigned a value of 2, and so on up to the largest value.

Two importance indicators are used in the TSPA-VA sensitivity analysis, partial rank correlation coefficient and R^2-loss. Both of these indicators are outputs from stepwise regression modeling. The partial rank correlation coefficient for a particular input variable measures the correlation between the output and the selected input variable, after the linear influences of the other variables in regression have been eliminated (Helton 1993, p. 352). The square of a partial rank correlation coefficient also represents the gain in R^2 of the regression model, expressed as a fraction of the currently unexplained uncertainty, as the selected variable is brought into regression (RamaRao et al. 1998). Partial rank correlation coefficients are also useful because their sign (+ or −) indicates whether the selected input variable has a positive or negative effect on the performance measure. The second importance indicator used, R^2–loss, represents the loss in R^2 of the current n–variable regression model, if the variable of concern is dropped from the regression model, creating a model with n–1 variables, where n is the total number of variables in the final regression model. Therefore, a high value of R^2–loss indicates that the removed variable is important.

Parameter rankings are based on R^2-loss values that were computed by stepwise rank regression analysis. All parameters with an R^2-loss greater than or equal to 0.04 are reported. Partial rank correlation coefficients are also provided to indicate if a parameter has a negative or positive effect on the performance measure in question. A negative effect on a performance measure indicates that as the uncertain input parameter increases, the performance measure decreases. In contrast, if an input parameter has a positive effect, the performance measure increases as the input parameter increases.

4.3.2.1 Sensitivity Analysis Results

Sensitivity-analysis results are presented for 10,000-year peak dose rates at the top of Figure 4-34. Parameters most important to uncertainty in peak dose rates are depicted in bar-chart form with the most important parameter represented by the largest bar, the next most important variable represented by the next largest bar and so on. The important variables are as follows:

1. Fraction of waste packages contacted by seepage water
   (R^2–loss = 0.18; partial rank correlation coefficient = 0.68)

2. Mean corrosion rate of Alloy 22
   (R^2–loss = 0.13; partial rank correlation coefficient = 0.62)

3. Number of juvenile waste package failures
   (R^2–loss = 0.11; partial rank correlation coefficient = 0.60)

4. Saturated zone dilution factor
   (R^2–loss = 0.04; partial rank correlation coefficient = –0.42)

The regression model from which these results are drawn has a total of ten input variables with a total R^2 of approximately 0.80. While a higher R^2 would be desirable, it is considered adequate for the purpose of inferring the importance of the dominant input variables.

Regression results for the 100,000-year peak dose rates are presented next, in the middle chart of Figure 4-34. The important variables are as follows:

1. Fraction of waste packages contacted by seepage water
   (R^2-loss = 0.29; partial rank correlation coefficient = 0.77)

2. Mean corrosion rate of Alloy 22
   (R^2-loss = 0.20; partial rank correlation coefficient = 0.70)

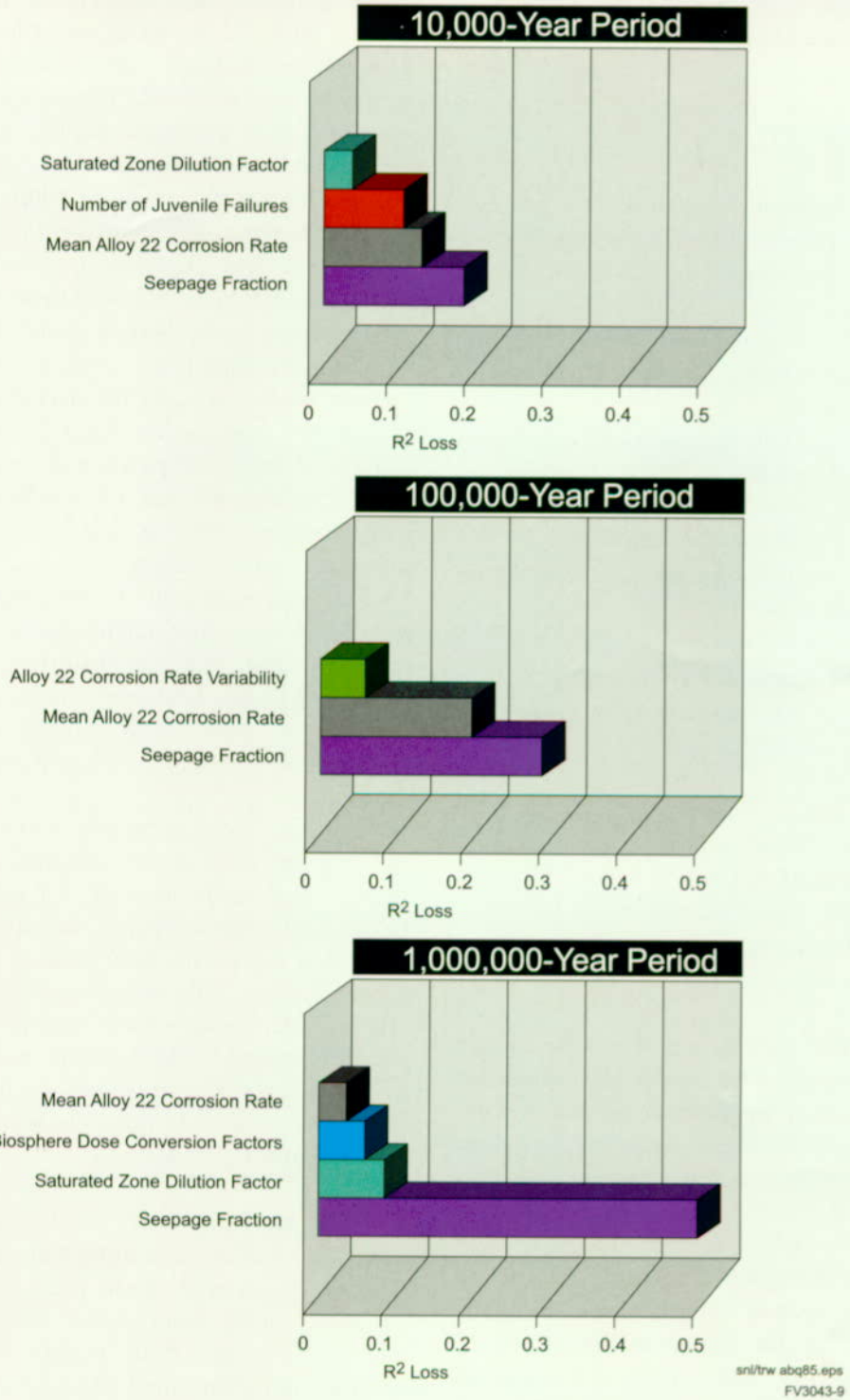

Figure 4-34. Most Important Parameters from Stepwise Regression Analysis for Three Periods
These charts show the relative importance of various parameters to the calculated uncertainty in peak dose rate for the three time periods. Importance of an individual parameter is shown by R^2-loss, the reduction in goodness of the regression fit when the parameter is left out of the calculation, as described in the text.

3. Variability of the Alloy 22 corrosion rate (R^2-loss = 0.06; partial rank correlation coefficient = 0.49)

The regression model for this case also has ten variables and an R^2 of 0.80.

Peak-dose-rate regression results for a 1 million-year period are presented in the bottom chart of Figure 4-34. The important variables are as follows:

1. Fraction of waste packages contacted by seepage water (R^2-loss = 0.51; partial rank correlation coefficient = 0.86)

2. Saturated zone dilution factor (R^2-loss = 0.09; partial rank correlation coefficient = –0.56)

3. Biosphere dose-conversion factors (R^2-loss = 0.07; partial rank correlation coefficient = 0.51)

4. Mean corrosion rate of Alloy 22 (R^2-loss = 0.04; partial rank correlation coefficient = 0.41)

The regression model for this case has ten variables and a final R^2 of 0.82.

For peak dose rates, the fraction of waste packages contacted by seepage water is the most important parameter in each of the three simulation periods, and its effect becomes more dominant over time. The positive effect indicated for this variable by its positive partial rank correlation coefficient happens because an increase in the number of waste packages contacted by water leads to an increase in radionuclide releases from the repository. The reason for the great importance of seepage fraction is two-fold. First, it has a direct effect on the number of waste packages that fail, as discussed in Section 4.3.1.1; and second, it has a very large uncertainty (see Figure 3-13). Other parameters either have less impact on dose rate or less uncertainty.

The second most important variable in the 10,000-year and 100,000-year cases is the mean corrosion rate for Alloy 22, the inner barrier in the reference-design waste package. The positive effect for this parameter arises because increasing the Alloy 22 corrosion rate produces earlier waste package failures and, therefore, more of the waste packages fail and release radionuclides within 10,000 years or 100,000 years. The corrosion rate for Alloy 22, however, is less important in the 1-million-year simulation period as indicated by its relatively low R^2-loss value in the bottom chart of Figure 4-34. This reduced importance is because the majority of the wet waste packages fail during the 1-million-year period, even for low Alloy 22 corrosion rates; failures of dry waste packages are only starting to be a factor near the end of the million-year period (see the discussion in Section 4.3.1.1). As a consequence, waste package parameters appear to become less important in this longer simulation period because the quantities of radionuclides released from the repository are primarily controlled by the inventory, the fraction of waste packages in contact with seepage water, and the seepage flow rate into the waste packages.

The second most important variable in the 1-million-year case is the saturated zone dilution factor. This factor accounts for the reduction in radionuclide concentrations caused by transverse dispersion that occurs during transport through the saturated zone. The negative effect indicated for this variable (partial rank correlation coefficient = –0.56) is caused by the fact that, as dilution during transport increases, peak radionuclide concentrations at the 20-km (12-mile) distance decrease and, consequently, doses decrease.

The next most important variables in the 10,000-year and 100,000-year simulation periods are the number of juvenile waste package failures and variability in the inner-barrier Alloy 22 corrosion rate, respectively. Both of these waste package variables have a positive effect on peak dose rates because, as noted previously for increased Alloy 22 corrosion rates, they lead to earlier waste package failures and, therefore, increased radionuclide releases from the repository during the given time period. The third most important variable for

the 1-million-year simulation period is the biosphere dose-conversion factor. Note that the biosphere dose-conversion factors for all radionuclides were correlated for the TSPA base case; that is, they are all either low or high together, rather than allowing one radionuclide to be high while another is low (see Section 3.8.2).

Examination of scatter plots provides an additional way to visualize the effects of uncertain variables on peak dose rates. Two important parameters discussed above are fraction of waste packages contacted by seepage water and Alloy 22 mean corrosion rate. Scatter plots for these two parameters are shown in Figures 4-35 and 4-36 for the 100,000-year simulation period.

Although there is a lot of scatter in the values, a pattern of higher dose rates for higher parameter values is clearly discernible in both scatter plots. As suggested by the regression-analysis results discussed above, the relationship between fraction of waste packages contacted by seepage water and peak dose rate is even more well defined for the 1-million-year simulation period, as shown in Figure 4-37. This strong relationship is reflected in the high R^2-loss value of 0.51 as compared to the

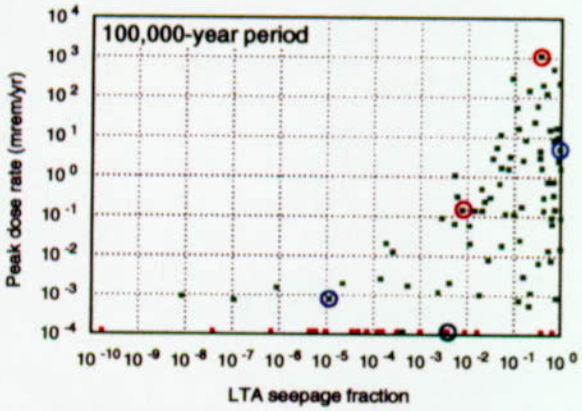

Figure 4-35. Scatter Plot of Seepage Fraction over 100,000 Years
Scatter plot of seepage fraction (fraction of waste packages contacted by seeps) for the long-term-average climate against peak dose rate for a 100,000-year period. Pink dots at the bottom indicate realizations with zero dose (which are off the scale of the log plot). The colored circles refer to the selected realizations highlighted in Figures 4-26 and 4-27.

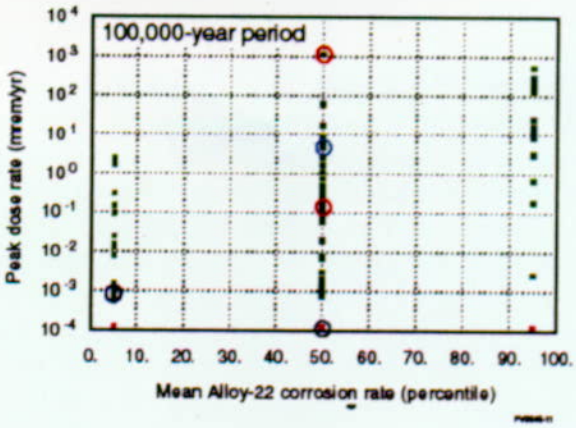

Figure 4-36. Scatter Plot of Mean Alloy 22 Corrosion Rate over 100,000 Years
Scatter plot of mean Alloy 22 corrosion (in terms of percentile from the uncertainty distribution) against peak dose rate for a 100,000-year period. Pink dots at the bottom indicate realizations with zero dose (which are off the scale of the log plot). The colored circles refer to the selected realizations highlighted in Figures 4-26 and 4-27.

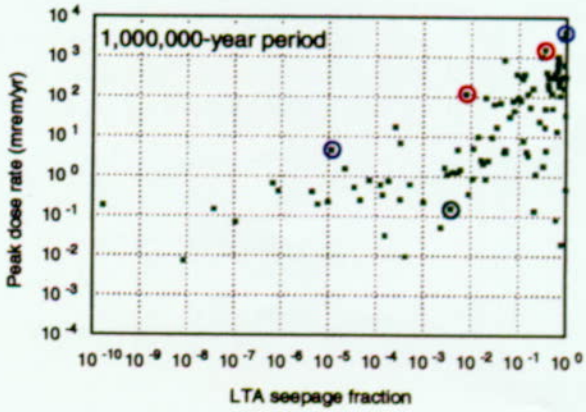

FV3043-12

Figure 4-37. Scatter Plot of Seepage Fraction over 1 Million Years
Scatter plot of seepage fraction (fraction of waste packages contacted by seeps) for the long-term-average climate against peak dose rate for a 1 million year period. The colored circles refer to the selected realizations highlighted in Figures 4-26 and 4-27.

R^2-loss value of 0.29 in the 100,000-year simulation period.

Dose rates are actually time-dependent quantities. As described in Section 4.3.1, a peak dose rate represents the highest dose rate that occurred during the simulation period for a given realization. The sensitivity analysis results presented thus far are for the peak dose rate only and, therefore, do not give explicit information about how parameter importance changes with time, although some insight is gained about changes with time by considering three different periods. To examine more directly how parameter importance changes with time, regression analyses were performed on dose rates at selected simulation times. The resulting values of partial rank correlation coefficients plotted as a function of time are presented in Figure 4-38. This figure shows that the number of juvenile waste package failures is the dominant variable at early times. However, over the long term, the importance of early releases decreases as more waste packages fail. The fraction of waste packages contacted by seepage water begins to increase in importance at around 5,000 years and becomes the dominant variable after approximately 8,000 years. The Alloy 22 corrosion rate also begins to increase in importance at around 5,000 years and remains important throughout the 1-million-year time period, with its importance decreasing somewhat after 400,000 years. Biosphere dose-conversion factors increase greatly in importance at late times.

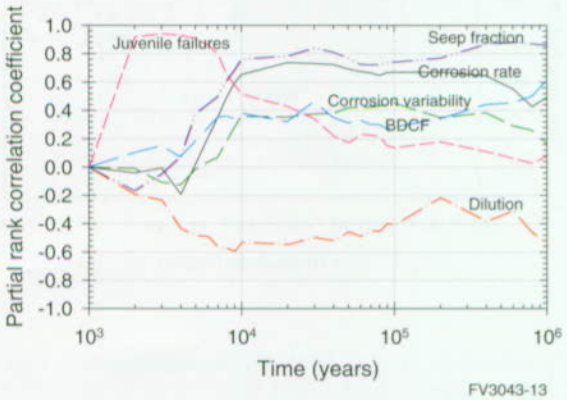

Figure 4-38. Partial Rank Correlation Coefficient as a Function of Time for Six Uncertain Parameters
This figure illustrates another way to show the change of importance of parameters through time from that shown in Figure 40-34. (BDCF—biosphere dose conversion factor)

The saturated zone dilution factor appears in the time-dependent regression model with a negative partial rank correlation coefficient because of its role in reducing radionuclide concentrations and dose rates. Some of the other variables also have small negative partial rank correlation coefficients before 5,000 years. These small negative values are probably spurious (that is, arising simply because of chance correlations among the randomly sampled variables) because they correspond to R^2-loss values smaller than 0.005 and because it is unlikely that these variables have a negative effect on dose rate. Note that the values plotted in Figure 4-38 do not correspond to the values listed earlier because the ones in the figure are for correlations with dose rate at particular times, whereas the earlier ones were for correlations with the peak dose rate over a period of time.

Regression analyses have also been performed for intermediate performance measures, including radionuclide releases from the engineered barrier system to the unsaturated zone and from the unsaturated zone to the saturated zone. These performance measures are also time-dependent and can be presented in the same way that the time-dependent dose rates were presented. Analyzing intermediate performance measures is useful for isolating individual components of the total system and assessing the importance of variables among the smaller corresponding set of uncertain parameters. As an example, results are presented for releases from the engineered barrier system to the unsaturated zone in Table 4-1. Results for releases from the unsaturated zone to the saturated zone are similar because they are not strongly influenced by uncertain unsaturated zone transport parameters. The results shown are for the specific simulation time of 1 million years. Again, the dominant variable is the fraction of waste packages contacted by seepage water. The second and fourth variables, the number of cladding failures because of corrosion and the fraction of plutonium colloids transported with irreversible sorption, did not appear to have a significant effect on dose rate but

Table 4-1. Importance Ranking of Inputs for Engineered Barrier System Releases at 1 Million Years

Rank	Variable	R^2-loss	Partial Rank Correlation Coefficient
1	Fraction of waste packages contacted by seepage water	0.45	0.84
2	Number of cladding failures because of corrosion	0.07	0.52
3	Alloy 22 mean corrosion rate	0.06	0.51
4	Fraction of plutonium colloids transported with irreversible sorption	0.04	0.43

Regression Model: Input variables = 11, $R^2 = 0.82$

are important to releases from the engineered barrier system.

4.3.2.2 Impact of Parameter Uncertainty Ranges on Sensitivity Analyses

Sensitivity analyses based on linear regression must be carefully interpreted. A regression-based sensitivity analysis will not give an uncertain variable a high importance ranking if its sample input values do not produce a relatively wide range of calculated output values. In other words, a parameter will not be assigned a high importance ranking unless it accounts for a large fraction of the variance in the output measure being analyzed. Therefore, the magnitude of peak dose rate may be strongly affected by a certain parameter, but if the range of uncertainty associated with that parameter is relatively small, the parameter may not be found to be important. As an example, neptunium solubility was not found to be an important variable in the above analysis, but because neptunium-237 often dominates the calculated dose rates (see Figure 4-29) neptunium solubility clearly does significantly influence total peak dose rate. The reason neptunium solubility did not appear as an important variable in the regression-based sensitivity analysis is largely due to the wide uncertainty ranges associated with seepage fraction and waste package corrosion.

One approach to understanding the effects of parameters that have very wide uncertainty ranges is to perform sensitivity analyses in steps. That is, perform an initial regression analysis, such as the one presented in Section 4.3.2.1, and identify important uncertain parameters. Then, assign single values, such as mean or median values, to some or all of the important uncertain parameters identified in the first step and repeat the analysis. By assigning single values to uncertain parameters identified in the first step, important parameters with less uncertainty may be identified in the second step.

This type of phased approach to sensitivity analysis was conducted for the TSPA-VA base case. For the secondary sensitivity analysis, the "expected" values (see Sections 2.3.3.3, 4.1, and 4.2) were used for the following:

1. Infiltration and mountain-scale unsaturated zone flow
2. Seepage fraction (fraction of waste packages contacted by seepage) and seep flow rate
3. Alloy 22 mean corrosion rate and variability

As for the base case analysis, 100 realizations were simulated for each of three periods: 10,000 years, 100,000 years, and 1 million years. For all parameters other than those being held fixed, the same sample values as for the base case were used. The distributions of peak dose rates for an individual located at 20 km (12 miles) from the repository are given in Figure 4-39. Comparison with the base case distributions in Figure 4-26 shows that the modified-parameter case has a much narrower spread of peak dose rates as expected, since uncertainty in seepage fraction, corrosion rate, and infiltration are not present. Note that in the base case many realizations had no calculated dose for the

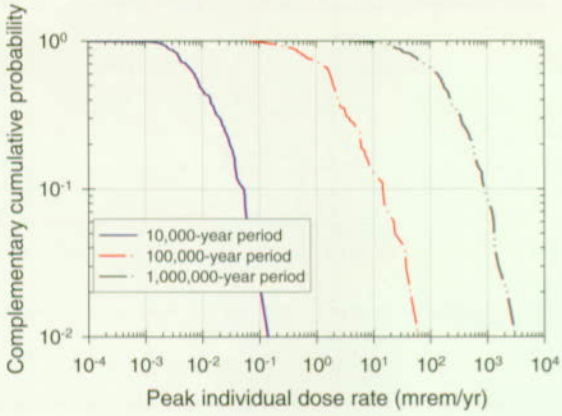

Figure 4-39. Distribution of Peak Dose Rates for Three Time Periods for the Modified-Parameter Case

Because some of the most important parameters were held fixed in this case, the spread of peak doses is much less than in the base case (Figure 4-26).

first 100,000 years, but in the modified-parameter case all realizations produced a dose within the first 10,000 years. Note that if this process of assigning expected values to important variables and conducting simulations were repeated a number of times, the distribution of peak dose rates would continue to narrow and converge towards the expected-value dose rate.

Regression-based sensitivity-analysis results are presented in Figure 4-40. Parameters most important to uncertainty in peak dose rates are depicted in bar-chart form with the most important parameter represented by the largest bar, the next most important variable represented by the next largest bar and so on. Saturated zone dilution factor and biosphere dose-conversion factors appeared on the base case bar chart (Figure 4-34), but in this analysis they account for more of the uncertainty because the most important parameters in the base case are held constant. In addition, a number of parameters are listed in Figure 4-40 that were not revealed as contributing significantly to the base case peak-dose uncertainty. The new parameters are the solubilities of technetium (for 10,000 years) and neptunium (for 100,000 years), the seepage collection factor (for 10,000 years and 100,000 years), the fraction of the saturated zone transport path in alluvium (for 100,000 years and 1 million years), the fractions of Zircaloy cladding failing because of corrosion and mechanical stresses (for 1 million years), and the saturated zone longitudinal dispersivity (for 1 million years).

The effects of these parameters on doses are straightforward. An increase in solubility can lead to faster dissolution and an increase in radionuclide releases from the repository. The seepage collection factor is used to adjust the amount of seepage water that gets into waste packages and contacts waste (see Sections 5.5.1 and 5.4.3); higher values of this factor lead to higher releases for solubility-limited radionuclides. The fraction of the saturated zone transport path in alluvium affects doses because of significantly higher radionuclide sorption in alluvium relative to the volcanic units, so that more transport through alluvium can lead to lower doses. The two cladding-failure parameters help determine the amount of commercial spent nuclear fuel exposed to water; higher values mean more waste exposed and thus the potential for higher releases and higher doses. (Note, however, that their effect is time-dependent, with most of the corrosion and mechanical cladding failures occurring after 100,000 years; see Section 3.5.2.1.) Lastly, longitudinal dispersivity in the saturated zone affects doses because higher dispersivity implies more spreading during transport and therefore lower concentrations and lower doses. Note that transverse dispersion has much greater potential for lowering doses than does longitudinal dispersion; transverse dispersion is accounted for in the analyses by means of the saturated zone dilution factor (see Section 3.7.2).

4.3.3 Summary

The Monte Carlo method is used to propagate parameter uncertainty through to the uncertainty in peak dose rate to an individual. The uncertainty in calculated peak dose rates is quantified by the CCDF. The range or spread of peak dose rates in each distribution represents the amount of uncertainty in the results. Some statistics of the calculated peak dose rates for each base case simulation period are summarized in Table 4-2.

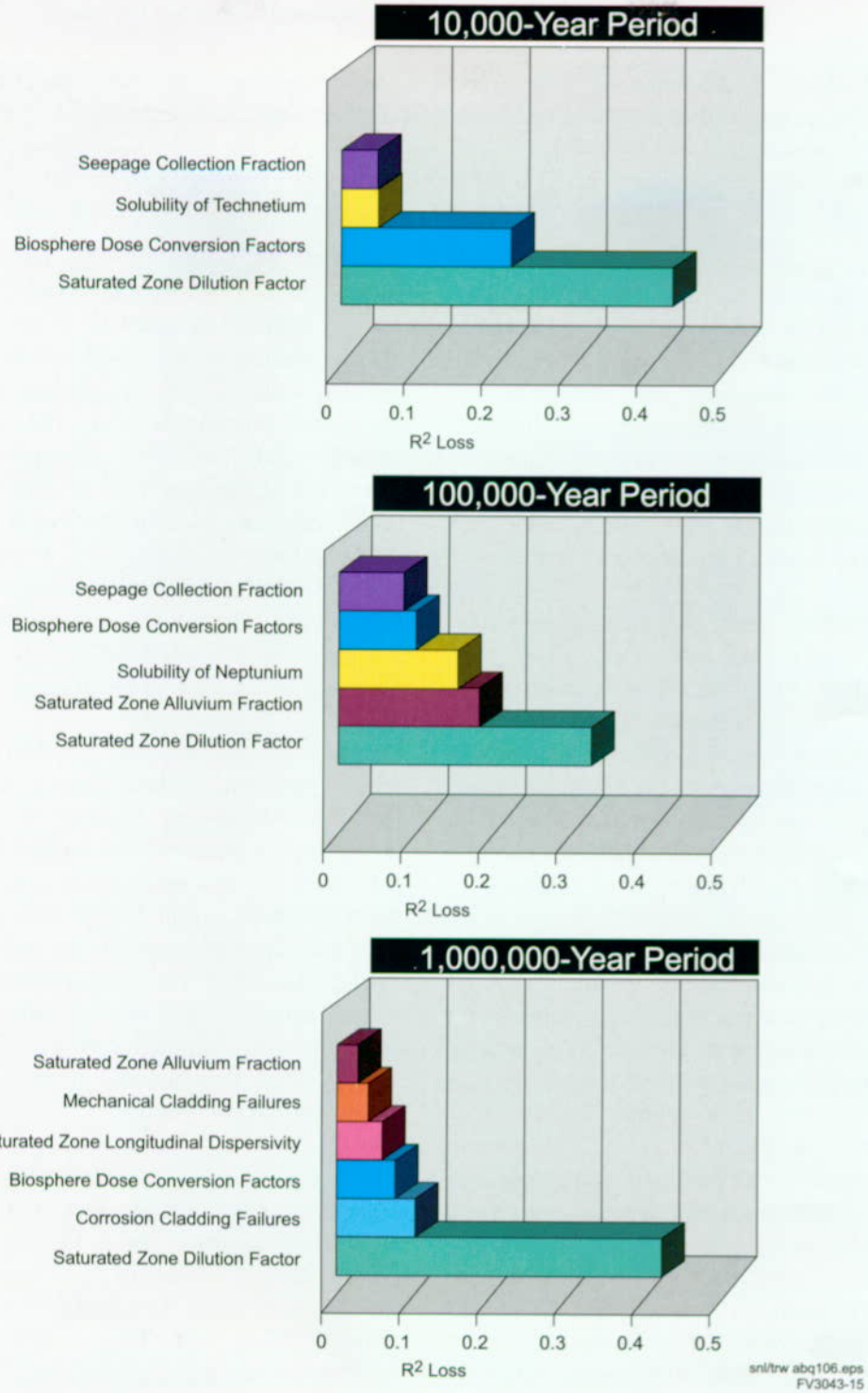

Figure 4-40. Most Important Parameters from Stepwise Regression Analysis for the Modified-Parameter Case

These charts show the relative importance of various parameters to the calculated uncertainty in peak dose rate when some of the most important parameters are held fixed. Importance of an individual parameter is shown by R^2-loss, the reduction in goodness of the regression fit when the parameter is left out of the calculation.

Table 4-2. Summary of Calculated Peak Dose Rates at 20 km (12 miles)

Simulation Period (years)	5th Percentile (mrem/year)	Mean (mrem/year)	50th Percentile (mrem/year)	95th Percentile (mrem/year)	Coefficient of Variation
10,000	0	0.1	0.002	0.8	3.8
100,000	0	30	0.09	200	4.4
1,000,000	0.07	200	8	1,000	2.8

As shown, the peak dose rates are found to increase substantially with increasing simulation time. However, the coefficient of variation, or standard deviation divided by mean, indicates that relative uncertainty in the calculated dose rates does not increase appreciably in the longer simulation periods (that is, uncertainty in dose rate increases and average dose rate increases, but their ratio does not). Thus, uncertainty in peak dose rate does not increase without bound with increased time.

The times at which peak dose rates occur were examined and found to be influenced by a number of factors, including the fraction of waste packages contacted by seepage water, Alloy 22 corrosion rate, net infiltration rate, juvenile waste package failures, and seepage flux into the waste packages. Very early dose-rate peaks are associated with juvenile waste package failures, and late dose-rate peaks are associated with superpluvial climates.

The sensitivity-analysis results indicate that the uncertainty in calculated peak dose rates in all three simulation periods is primarily dominated by the fraction of packages in contact with seepage water. Waste package corrosion rate is also an important contributor to uncertainty in peak dose rates. In particular, the mean Alloy 22 corrosion rate is an important contributor to uncertainty, but to a lesser extent than the fraction of waste packages contacted by seepage water, particularly in the 1-million-year period. In the 1-million-year simulation, the saturated zone dilution factor and biosphere dose-conversion factors were found to be more important than the mean Alloy 22 corrosion rate.

4.4 EFFECTS OF DISRUPTIVE EVENTS

Previous work has identified potentially disruptive events that might affect long-term repository performance (DOE 1988, Section 8.3.5.13; Barnard et al. 1992, Chapters 6 and 7; Wilson et al. 1994, Chapters 16 and 17). The four disruptive events considered for TSPA are basaltic igneous activity, seismic activity, nuclear criticality, and inadvertent human intrusion. The methods used to identify and select the disruptive events are described in the first part of this section. How these events are used in this TSPA is discussed in the remainder of the section. Chapter 10 of the *Total System Performance Assessment-Viability Assessment (TSPA-VA) Analyses Technical Basis Document* (CRWMS M&O 1998i) discusses the details of the disruptive-events analyses.

Disruptive events are considered to have probabilities of less than 1 (their chances of occurring are less than 100 percent over the life of the repository), in contrast to the expected events and processes (for example, waste package corrosion, thermal effects, groundwater flow and transport). Generally, disruptive events are rare (volcanoes or earthquakes) and have identifiable starting and ending times, in contrast to continuous processes like corrosion. Although criticality does not have a sudden onset, it is included here as an example of an off-normal condition.

The disruptive event modeling studies and analyses presented in this section were prepared with the view of addressing various subissues of the NRC Key Technical Issues on Igneous Activity (NRC 1998d), Structural Deformation and Seismicity (NRC 1997d), and Total System Performance Assessment and Integration (NRC 1998a). Specifically, the information presented is pertinent to the igneous activity subissue on consequences of igneous activity within the repository setting, the structural deformation and seismicity subissue on seismic motion, and the TSPA integration subissue on model abstraction.

4.4.1 Initial Selection of Important Issues

In previous TSPAs, DOE has used generalized event trees for constructing disruptive scenarios (Wilson et al. 1994, Section 3.2). This approach has created a detailed understanding of the processes that could contribute to increased radionuclide releases following a disruptive event. The approach taken in past TSPAs was not intended, however, to demonstrate that these analyses comprehensively analyzed all disruptive scenarios. Therefore, for this TSPA, DOE has begun a scenario development method that will document all features, events, and processes in the analysis. Implementation of this scenario development method is incomplete for this TSPA, partly because new information must be considered as it becomes available.

The ultimate criterion for inclusion of disturbed scenarios in TSPA analyses is whether they are likely to have a significant impact on performance of the repository system over the period of regulatory concern. The criteria for considering inclusion of disturbed scenarios in TSPA analyses are

- Probability–Is the probability of the event occurring large enough that it could affect the chances that performance of the repository would suffer?
- Consequence–Are the potential consequences of the disturbance of sufficient magnitude that repository performance could be adversely impacted?
- Regulatory–Are there regulatory requirements that mandate consideration of disturbances (or specifically exclude certain disturbances)?

To date, basaltic igneous activity, seismic activity, and nuclear criticality have been identified as the disruptive features, events, and processes to be used in scenario construction, based on evaluations using the generalized event trees (Barr et al. 1993; Barr et al. 1996; CRWMS M&O 1997b). Human intrusion has also been investigated, but the method of inclusion in the TSPA for the potential licensing analyses is uncertain, pending clarification of regulatory requirements. Other disruptive events, such as meteorite impact or erosion, have been eliminated using the three criteria listed above. Section 10.2 of the *Total System Performance Assessment-Viability Assessment (TSPA-VA) Analyses Technical Basis Document* (CRWMS M&O 1998i) discusses scenario development in detail.

4.4.2 Igneous Activity

Basaltic igneous activity includes volcanic eruptions and intrusive or extrusive events (in which molten igneous material is cooled within the earth or on the earth's surface, respectively). Volcanoes can potentially disperse radionuclides from waste packages directly into the atmosphere, where they can reach nearby populations. Igneous intrusions that penetrate the repository but do not reach the surface could potentially destroy waste packages and make the radioactive contents more readily available for transport by groundwater. Intrusions that occur in the Yucca Mountain region could potentially alter the transport of contaminants in groundwater. These scenarios have been investigated in prior TSPA analyses (Barnard et al. 1992, Chapter 7; Wilson et al. 1994, Chapter 17). The consequences of igneous activity were found to contribute less than one percent to overall repository performance measures (to either releases or doses). However, the probability of occurrence of igneous activity as estimated by the *Probabilistic Volcanic Hazard Analysis* (CRWMS M&O 1996c) is greater than the lower limit of 1×10^{-8} per year adopted by DOE as the level of concern (NRC 1995, page 3-5).

The *Probabilistic Volcanic Hazard Analysis* (CRWMS M&O 1996c) was conducted to assess the probability of disruption of the proposed repository by a volcanic event and to quantify the uncertainties associated with this assessment. The evaluations of members of a ten-person expert panel were elicited to ensure that a wide range of approaches was considered in the hazard analysis. The results of the individual elicitations were combined to develop an integrated assessment of

the volcanic hazard that reflects the diversity of alternative scientific interpretations. The assessment focused on the volcanic *hazard* at the site expressed as the probability of disruption of the repository. It provides input to an assessment of volcanic risk, which expresses the probability of increased radionuclide release because of volcanic disruption.

The possible volcanic hazard to the repository is magma feeding a dike or surface eruption. The basic elements that need to be assessed to define the hazard are the spatial distribution and the recurrence rates of future volcanic events in the region. Spatial models represent the future locations of volcanic activity. Temporal models define the frequency of occurrence of volcanic activity and, therefore, the probability of occurrence. Results of the study indicate that spatial issues are more important than temporal issues.

Based on the results of the *Probabilistic Volcanic Hazard Analysis* (CRWMS M&O 1996c), a volcanic event is expected to intersect the repository footprint (the area within the repository outline) at an expected annual frequency of 1.5×10^{-8}. This frequency value has a 90-percent confidence interval of 5.4×10^{-10} to 4.9×10^{-8}. The major contributors to the uncertainty in the frequency of intersection are the statistical uncertainty in estimating the rate of volcanic events from small data sets and the uncertainty in modeling the spatial distribution of future events.

4.4.2.1 Direct Release Scenario

In the direct-release scenario, a volcanic eruption disperses contaminated ash on the ground. The components of this scenario are illustrated in Figure 4-41. The figure is constructed as a series of branch points; if an event or process occurs, the next element of the scenario is evaluated. If it does not occur, either the scenario is terminated with no adverse performance assessment consequences or another scenario is invoked.

The first branch asks whether igneous intrusion occurs in the Yucca Mountain (Figure 4-41a). This is the issue addressed by the *Probabilistic Volcanic Hazard Analysis* (CRWMS M&O 1996c), as discussed above. If igneous activity does occur, a branch on whether the igneous event causes an intrusion follows. If the intrusion is outside the repository footprint, the indirect-effects scenario is used (see Section 4.4.2.3). If the intrusion intersects the repository, the next branch asks if any waste packages are directly contacted. If the intrusion does not contact any waste packages, there is no adverse impact on performance assessment beyond that evaluated in the indirect-effects scenario.

If waste packages are directly contacted by ascending extrusive magma or by a pyroclastic flow, the next branch point is shown in Figure 4-41b. The branch determines whether the conditions allow the waste packages to be breached by the ascending hot material. The processes that can rupture a waste package include rapid corrosion by aggressive magmatic gases, deformation and rupture of the metal waste package, or blowout of the end plates from the high temperatures. The thick outer barrier of the waste package is made of materials that are very susceptible to attack by sulfur compounds normally identified in eruptions. Therefore, we assume that, during the period of eruption (typically between 5 and 40 days for igneous events in the Yucca Mountain region [Jarzemba 1997, Table II]), the outer barrier will be completely removed. The inner waste package wall is made of a superalloy composed of nickel, chromium, and molybdenum, that has been selected for its corrosion resistance. Although experiments have not directly confirmed it, the full 2-cm (3/4-in.) thickness of this superalloy is unlikely to be corroded through because the expected duration of typical Yucca Mountain eruptions appears to be too short. Only if the inner barrier has previously been degraded by normal corrosion processes will an igneous event breach the waste package. If the waste package is not breached, the scenario stops because the encapsulation of the waste packages in basalt is likely to have a beneficial effect on subsequent repository performance.

For those waste packages that are breached, the scenario investigates the mechanisms for removing waste from the opened packages. The moving

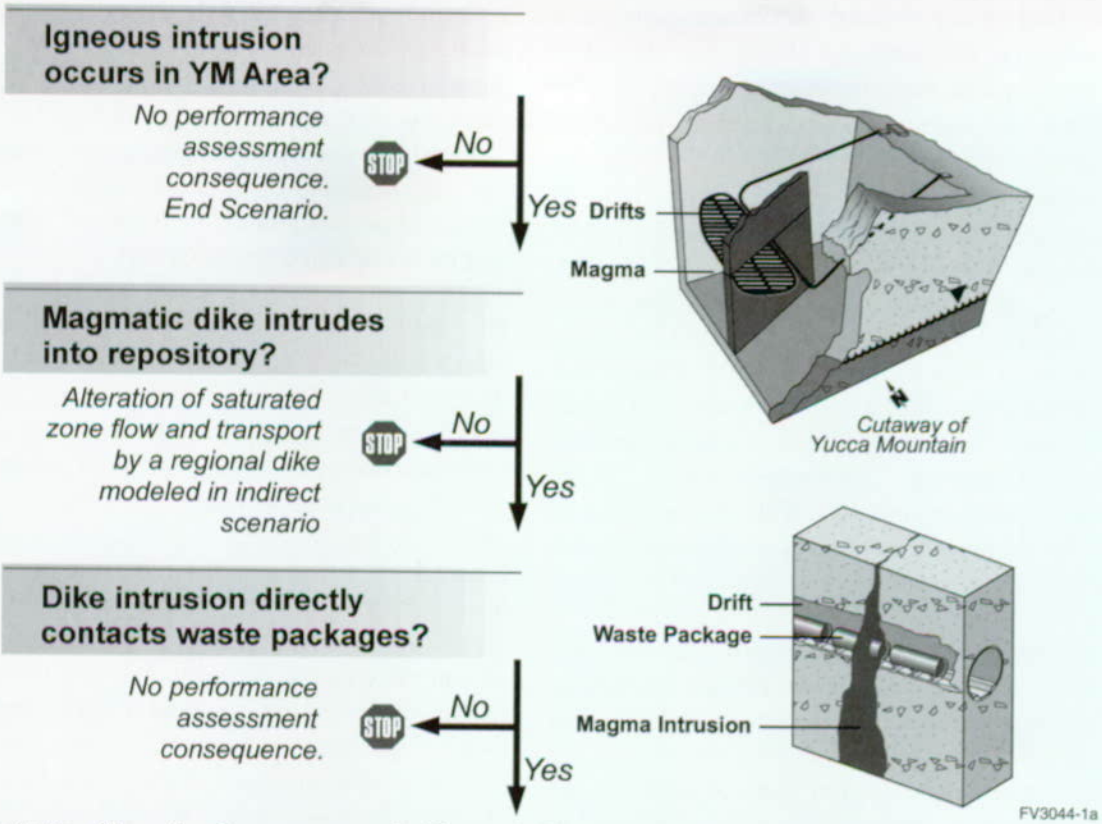

Figure 4-41a. Alternative Consequences of a Magmatic Dike Intruding the Repository
This figure illustrates some of the branch points for a dike interacting with the repository.

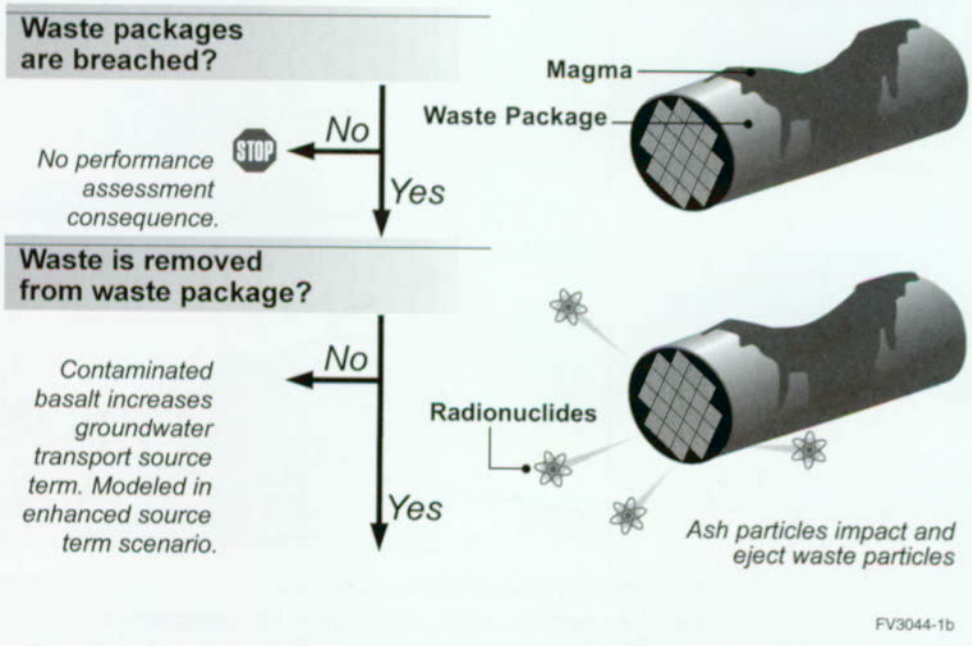

Figure 4-41b. Alternative Consequences of a Magmatic Dike Intruding the Repository-Part 2
If waste packages are directly contacted by magma or a pyroclastic flow what are the possible consequences? The chemically aggressive gases and high temperatures associated with a volcanic event could breach packages.

liquid magma or pyroclasts can cause waste to be ejected from the packages by hitting it. The density of waste material is considerably greater than that of magma (approximately 11 g/cm^3 [Glasstone and Sesonske 1991, Table 8.3] for waste and 0.8 to 2.5 g/cm^3 [Suzuki 1983, Figure 3] for magma). This density difference means that to cause waste to be ejected from the package, the magma material must be at least as large as the waste material that it hits. This relationship holds for the range of ascent velocities for magma that are typical of the Yucca Mountain area volcanoes. The process was simulated by comparing the sizes of magma fragments and waste materials. If the moving igneous material is unable to eject material from the waste package, then the enhanced-source-term scenario is examined (see Section 4.4.2.2).

The ascending magma or pyroclasts can transport the heavy waste material to the surface (see Figure 4-41c) if the upward magma velocity is faster than the downward settling velocity of the waste. An ascent velocity ranging from approximately 10 m/s (20 mph) to over 200 m/s (400 mph) is required to entrain the waste material. This component of the scenario completes the definition of the source term used by the ash-dispersal analysis. If the waste is not moved to the surface, it collects somewhere underground and could contribute to the enhanced-source-term scenario. This type of underground accumulation of waste material has not been evaluated for this TSPA.

The dose to humans from this scenario is calculated based on the dispersal of contaminants in volcanic ash. The ash-dispersal model (Jarzemba 1997, Section IV.B) uses information on eruption characteristics of volcanoes, wind direction and velocity, and ash and waste characteristics.

4.4.2.2 Enhanced Source Term Scenario

When liquid magma intersects the repository drifts, it can flow down the drifts and engulf the waste packages. In this environment of high temperatures and aggressive magmatic gases, even the corrosion-resistant parts of the waste packages are expected to fail. When this happens, the liquid

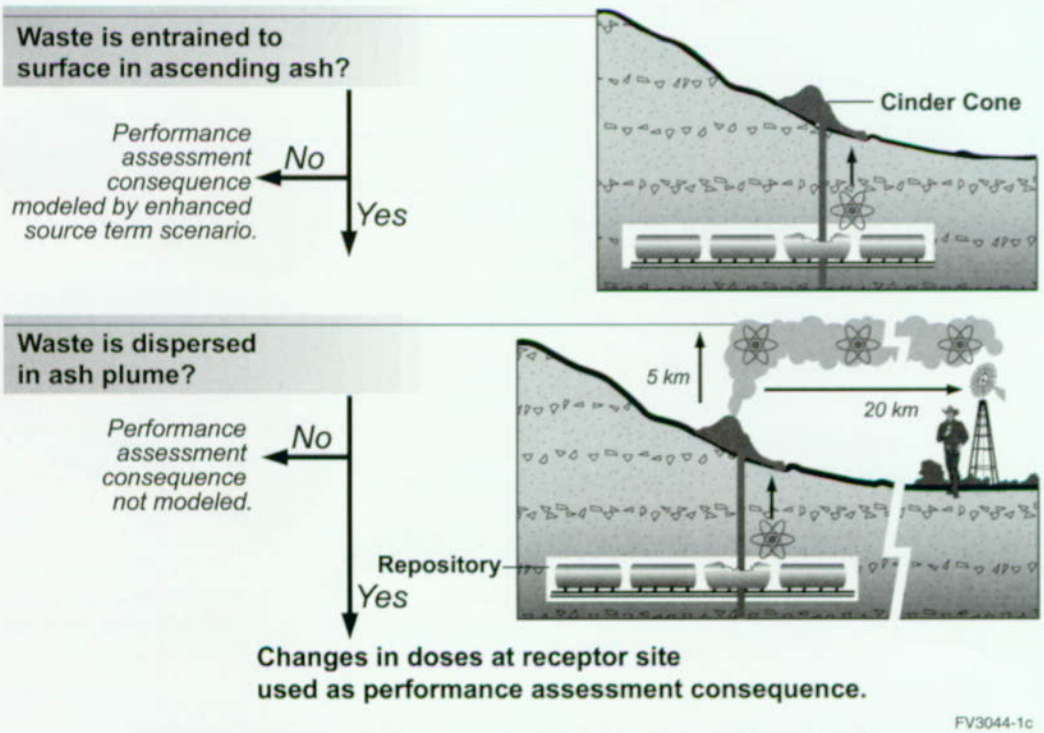

Figure 4-41c. Alternative Consequences of a Magmatic Dike Intruding the Repository-Part 3
If waste is incorporated in the eruption, what are the potential consequences? Contaminated ash may be transported to the surface and dispersed in an ash plume.

magma can dissolve some of the UO_2 in the spent nuclear fuel (Westrich 1982, Figure 3). When the basalt cools (in about 10 years for a 2-m [7 feet] wide intruded dike) groundwater returns to the drifts. As the basalt cools, it cracks, allowing the water to dissolve the UO_2 and other radionuclides in the contaminated basalt. The groundwater then carries the contaminants through the geologic media to the dose-exposure location (the location 20 km [12 miles] south of the potential repository where humans can be exposed to radionuclides). Figure 4-42 illustrates this scenario.

4.4.2.3 Indirect Igneous Effects Scenario

If an igneous event occurs near the Yucca Mountain repository, it could affect repository performance although magma does not contact the waste. This scenario is shown in Figure 4-43. As discussed in Section 3.7, groundwater flow and radionuclide transport through the saturated zone are controlled by the geologic features and their hydraulic properties. If an igneous event occurs in the saturated zone, it could potentially change flow and thus repository performance. The most likely places for dike intrusion are near sites of recent igneous or seismic activity (faults or existing dikes). The dike could change the flow pattern by

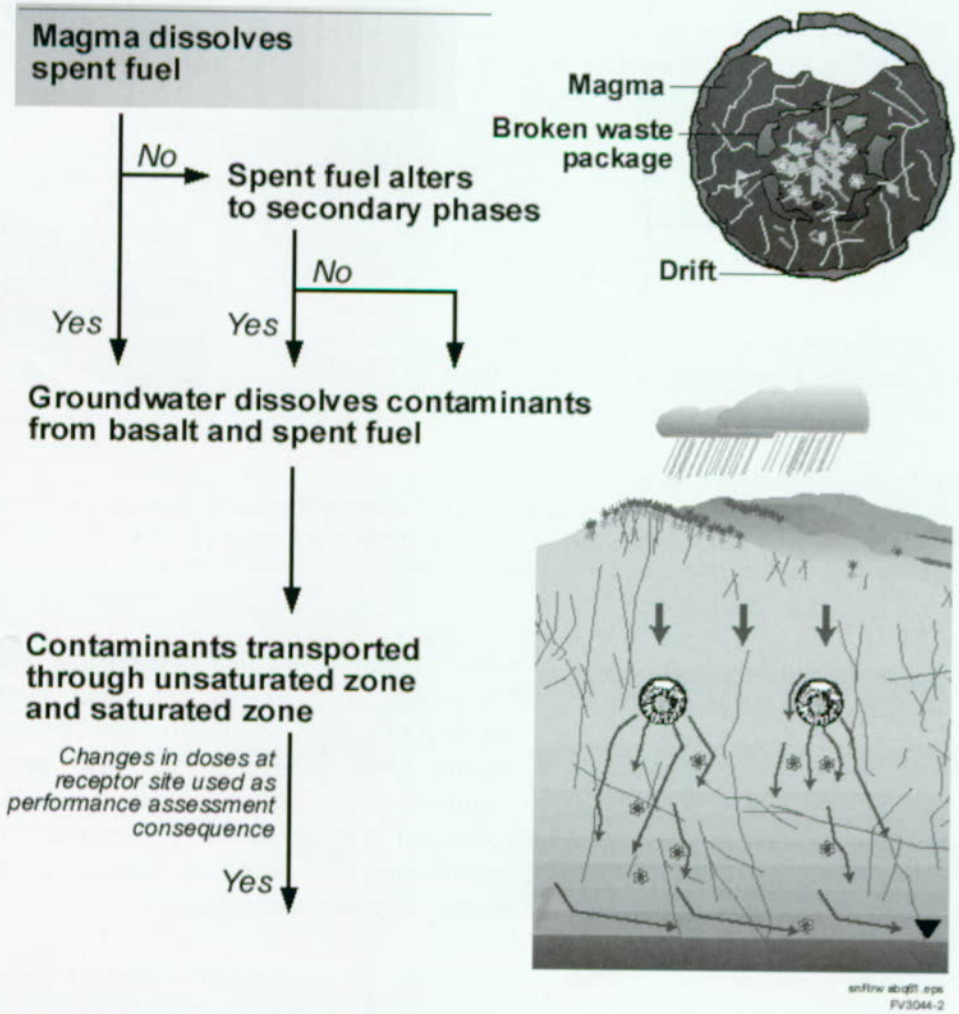

Figure 4-42. Source Term Enhanced by Igneous Activity
What are the possible outcomes if liquid magma intersects the repository, engulfing the waste packages and causing breaches? After the intrusive magma cools, and normal groundwater flow returns, radionuclides could be carried from the repository in groundwater.

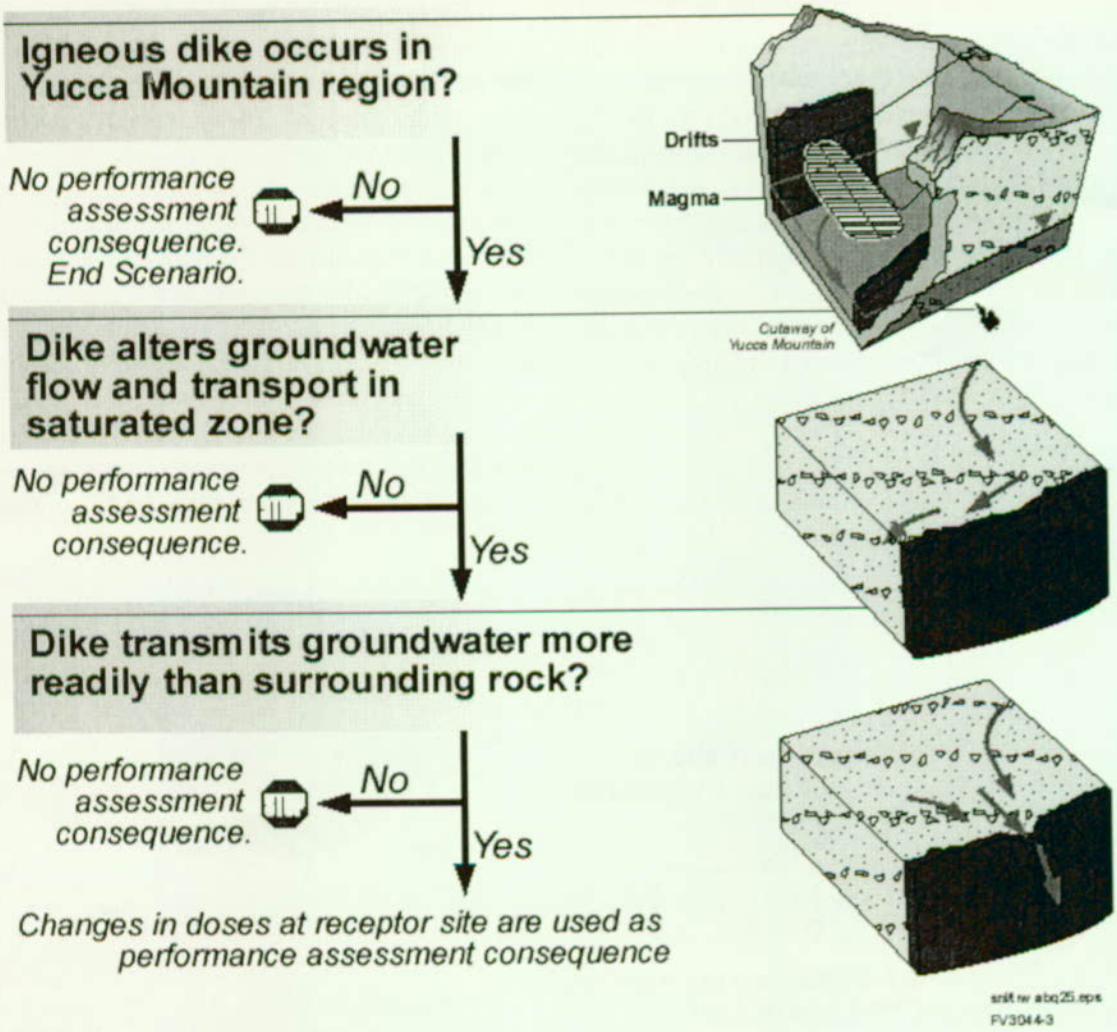

Figure 4-43. Indirect Igneous Effects Scenario
If magma intrudes near the repository, not directly contacting the waste, but possibly altering groundwater flow patterns in the area, could it affect the dose rate at the receptor site? If a magmatic dike alters the flow pattern, redirecting flow, there is the potential for an increase in radionuclide doses to humans.

redirecting flow. This change in flow could potentially increase the radionuclide doses to humans.

4.4.2.4 Results of Igneous Activity Analyses

Modeling of direct-release volcanism shows that there is very little impact from this scenario. When all the processes outlined in Section 4.4.1 are considered, less than 6 percent of all igneous events could cause releases of contaminants into an ash cloud. When combined with the probability that these events happen at all, the contribution to the base case repository performance is negligible. Figure 4-44a compares median dose rates. The median dose rates are also much smaller than the peak dose rates for the groundwater base case. Figure 4-44b compares the dose rates over 1 million years. The maximum dose rate from volcanism is approximately two million times less than the peak dose rates from the base case groundwater transport of radionuclides.

The model for the enhanced-source-term scenario examines the interaction underground of magma with waste packages. The magma is predicted to contact between 0 and 170 waste packages, with 40

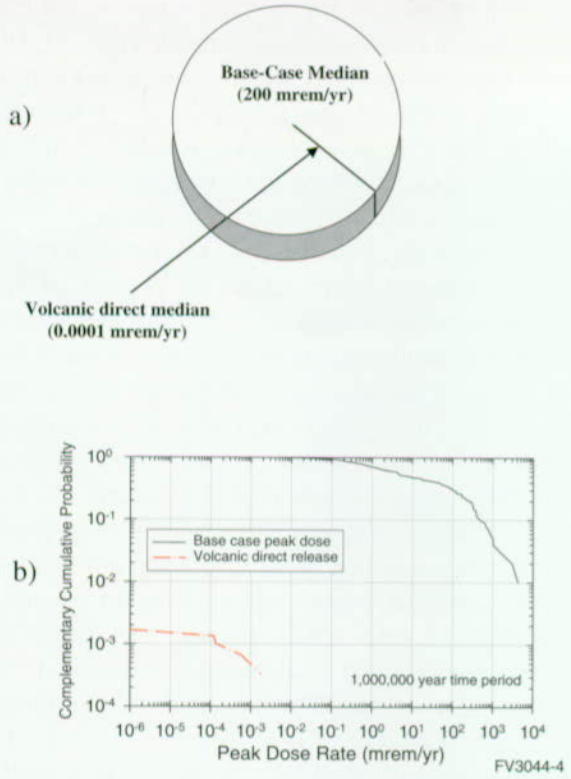

Figure 4-44. Volcanic Eruption Scenario Dose Rates (Top, a) Median dose rates from volcanic eruptions compared with median base-case dose rate. The median dose rates due to releases associated with volcanic eruption are significantly smaller than those modeled in the base case. (Bottom, b) CCDF showing combined peak dose rates and probabilities for the volcanic eruption scenario compared with the base case.

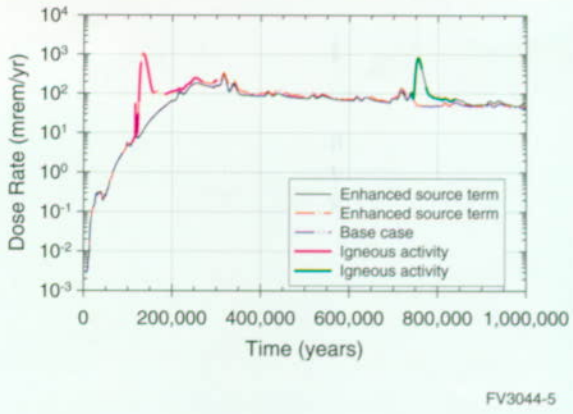

Figure 4-45. Dose-Rate Time Histories from Igneous Enhanced Source Term Scenario Compared with Base Case Dose Rate
Two examples of dike intrusion causing an enhanced source term release to groundwater are plotted, and result in an increased dose rate that occurs tens of thousands of years after the intrusion.

to 50 waste packages being the average. The sudden release of radionuclides in this scenario produces an increased source term for the base case groundwater flow and transport calculations. All other flow and transport modeling parameters are specified the same as for the base case. Two examples of dikes interacting with waste packages are shown in Figure 4-45. One event occurs at about 113,000 years and has a peak dose rate of 4 times the peak dose rate of the base case example shown in Figure 4-45 (that occurs at about 350,000 years).

The other event occurs at about 735,000 years and has a peak dose rate of 3 times the example base case. In both cases, the peak dose rate at the dose-exposure location is tens of thousands of years after the event because of the time needed for groundwater to transport the radionuclides. For all the modeled cases, the increase in dose rates range from less than 2 times to about 8 times the base case, although volcanic events that happen before about 100,000 years produce dose rates many times greater than the base case dose rate for the same time period. As Figure 4-45 shows, after the waste released by interaction with magma has been transported away, the dose histories again track the base case (this can take about 100,000 years). Figure 4-46 shows CCDFs for peak dose rates for 100,000 years (Figure 4-46a) and for 1 million years (Figure 4-46b). In both cases, the CCDFs are significantly less than the corresponding base case CCDFs. The peak dose rates are less than half those of the corresponding base case rates, and the probabilities are approximately one-tenth those of the base case dose rates.

Modeling of the indirect effects of igneous events has shown that recently formed geologic structures (faults or dikes) upstream from the repository have no effect on contaminant transport. In order to calibrate the flow model it was necessary to make the hydraulic conductivity of existing structures very low (Wilson et al. 1994, Table 11-1). Thus, making them even more of a barrier through

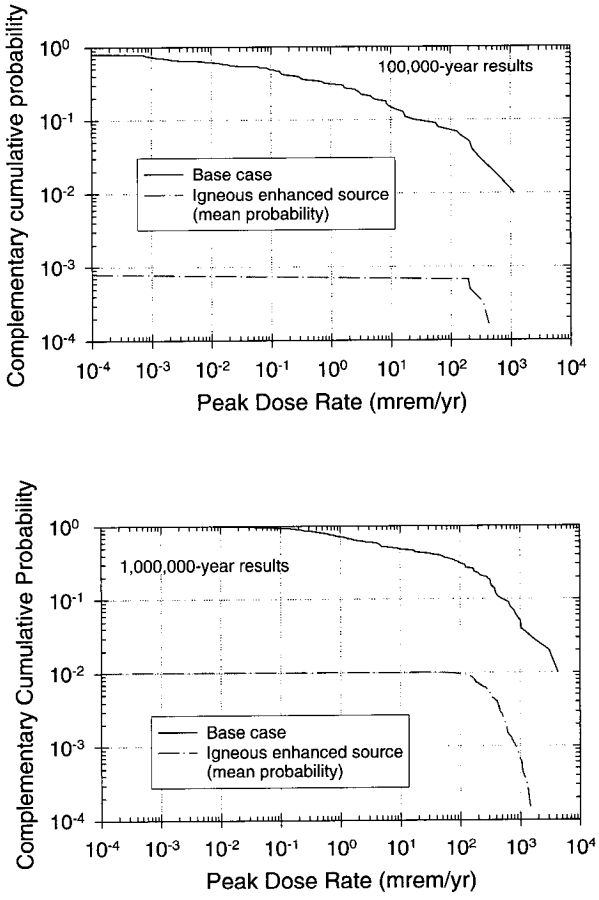

FV3044-6

Figure 4-46. Peak Dose Rate Complimentary Cumulative Distribution Function for 100,000 and 1 Million Years

Peak dose rate CCDFs for 100,000 years (Top, a) and 1 million years (Bottom, b). Probabilities and dose rates for both time periods are considerably less than the corresponding base case dose rates. (CCDF—complimentary cumulative distribution function)

igneous intrusion causes no noticeable change in the flow patterns. When the down-gradient dikes are modeled as being more transmissive, there is a small change in the flow pattern. Generally, the flow is directed more to the east and may be slower, which does not increase the dose rates significantly. Patterns of radionuclide concentration for the base case and for a more transmissive dike located along the Solitario Canyon fault are shown in Figure 4-47.

The probability that any of these igneous-activity scenarios will occur can be estimated. Over 10,000 years, there is less than one chance in 1,000 that there will be any igneous activity at all. If there is activity, there is a very low probability that a volcanic eruption will contain any high-level radioactive waste, because the waste packages still provide enough containment to withstand the forces of the eruption. About 60 percent of the time, an eruption would cause an enhanced source term for groundwater transport of radionuclides (regardless of the time of occurrence). Over one million years there is less than a 10 percent chance that there will be igneous activity. If an igneous event does occur, there is about a 5 percent chance that a volcanic eruption will contain high-level radioactive waste and a 60 to 70 percent chance that there will be more radionuclides in groundwater flow because of the eruption. The details of the igneous-activity analyses are contained in Section 10.4 of the *Total System Performance Assessment-Viability Assessment (TSPA-VA) Analyses Technical Basis Document* (CRWMS M&O 1998i). Table 4-3 summarizes the probabilities of volcanic effects.

4.4.3 Seismic Activity

Seismic activity has not previously been systematically included in TSPA analyses, although ancillary calculations have been made (Gauthier et al. 1996). Potential effects of seismic activity include the following:

- Vibratory ground motion and displacement from earthquakes (can cause rockfall on waste packages or other disruptions to the packages)
- Changes in site hydrologic properties (such as change in flow patterns of groundwater near the waste packages or a change in elevation of the water table)
- Indirect effects such as alteration of groundwater flow and transport paths from faulting near the repository site

Because these events have not been evaluated in a previous TSPA, their potential impact on a repos-

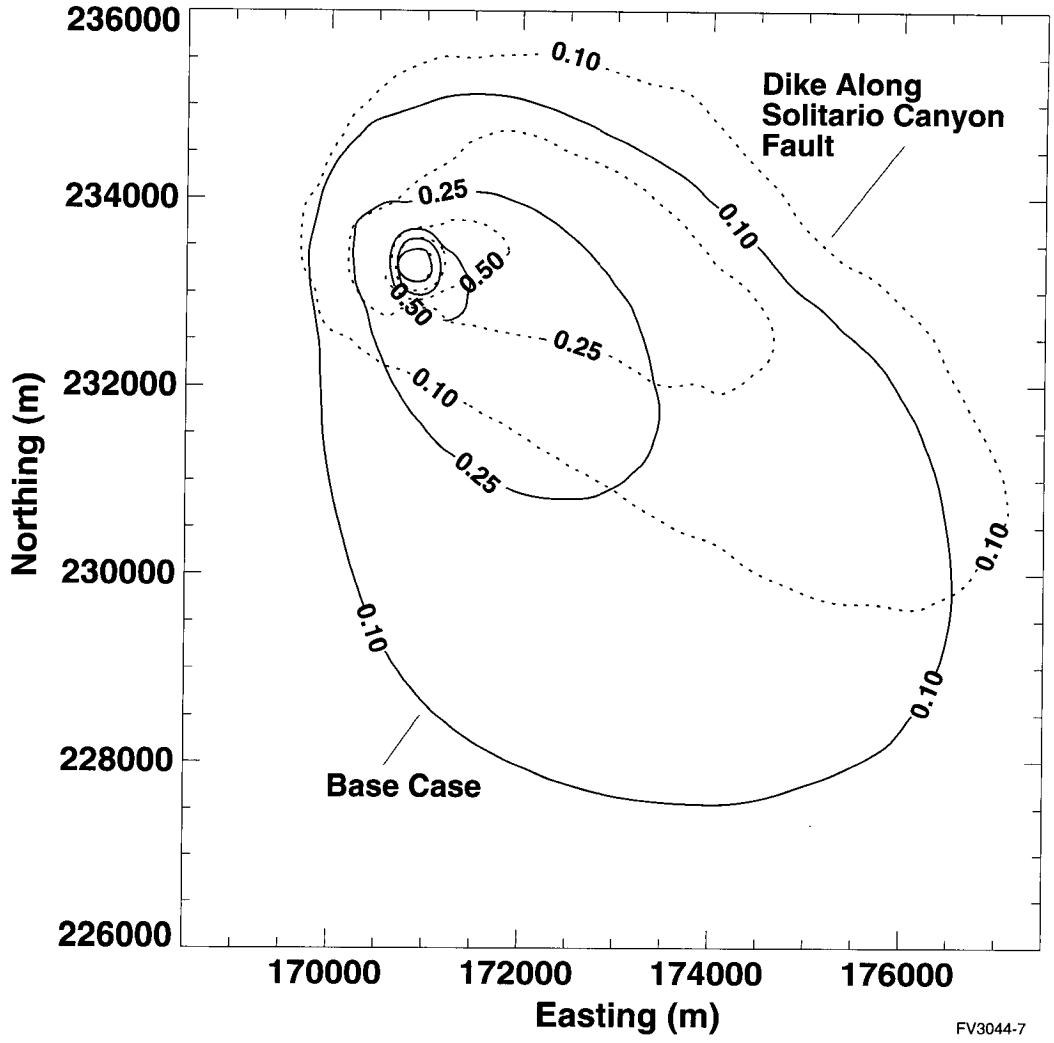

Figure 4-47. Contaminant Concentration Profiles Resulting from a Dike Intruding Along the Solitario Canyon Fault
A transmissive dike along the Solitario Canyon fault area could shift contaminant concentration flow patterns to the northwest (shown by the dotted contours).

itory has not been known until these analyses. The probability of earthquake occurrence is sufficiently high that these scenarios must be considered.

The *Probabilistic Seismic Hazard Analysis* (CRWMS M&O 1998h) led to the determination of fault displacement and vibratory ground motion hazards. The activities performed were as follows:

- Evaluation and characterization of seismic sources including the characterization of potential fault displacement
- Evaluation and characterization of vibratory ground motion, including earthquake source, wave propagation path, and the effects of the country rock
- Probabilistic seismic-hazard analyses for both fault displacement and vibratory ground motion

The hazards results are in the form of annual frequencies that various levels of fault displacement and vibratory ground motion are expected to exceed. The hazard analyses were based on evaluations of the seismic source charac-

Table 4-3. Probabilities of Igneous Impacts on Repository

	At 10,000 years	At 1,000,000 years
Probability of Occurrence	< 0.0001	< 0.1
Probability of Surface Releases	~0	~0.05
Probability of Increased Groundwater Doses	~0.6	0.6 – 0.7

teristics, earthquake ground motions, and fault displacement that reflect interpretations of different scientific hypotheses and models using available data.

The procedures used for evaluating seismic hazards allowed quantitative assessments based on interpretations provided by the experts. (Two expert groups were assembled: a panel of ground motion experts, and panel of seismic-source and fault-displacement experts. The latter panel was divided into teams covering the geology, tectonics, and geophysics of Yucca Mountain.) The quantification incorporates uncertainty in the hazard analyses because of uncertainty in the input interpretations as well as random variability in input parameters. The hazard results are presented as mean, median, and fractile hazard curves representing the total uncertainty in input interpretations.

4.4.3.1 Rockfall Scenario

Falling rock can affect repository performance if damage to the waste packages causes early leakage of radionuclides. Rockfall can either split the waste package, allowing immediate access of air and water, or cause dents in the package, providing locations for accelerated corrosion. Additionally, rockfall can knock waste packages from their supports, enhancing the chances of corrosion on the bottom. If the waste package is prematurely corroded, air and water can reach the waste earlier. Figure 4-48 illustrates this scenario.

Rocks from the drift walls can fall if the stresses on them change. Initially the drifts are lined with concrete, but the concrete is expected to decompose within a few hundred years (the base case assumption and the one used here is that the drifts are not backfilled). As the emplaced waste heats the repository area, the rock stresses change, primarily because of thermal expansion. In some cases, the effect on the rocks surrounding the drifts is a change from compression to tension, potentially causing rockfall.

Seismic activity can also cause rockfall. The magnitude of the sizes of rocks that fall has been correlated with vibratory ground motion. The *Probabilistic Seismic Hazard Analysis* (CRWMS M&O 1998h, Volume 1, Chapter 7) has provided the probabilities of occurrence of various levels of peak ground velocity. It should be noted that earthquake ground motion is greatly reduced underground. An earthquake that can collapse buildings on the surface has much less effect underground. Over any period (such as 10,000 years), there are expected to be numerous small earthquakes (with small ground velocity), but there is also a small probability that there can be large earthquakes. The *Probabilistic Seismic Hazard Analysis* (CRWMS M&O 1998h) provides estimates of these probabilities.

For waste packages to be damaged by falling rock, the following must occur:

- A sufficiently big rock is available
- The waste package wall is so thin that the rock can damage it
- The rock hits a package

The distribution of rocks available to fall has been estimated from a study of fracture spacing in the Exploratory Studies Facility. Most rocks are less than 1,000 kg (1 ton), with many weighing near 50 kg (100 lb). There are very few rocks greater than 3,500 kg (4 tons). The distance the rocks fall is approximately from the drift ceiling to the waste

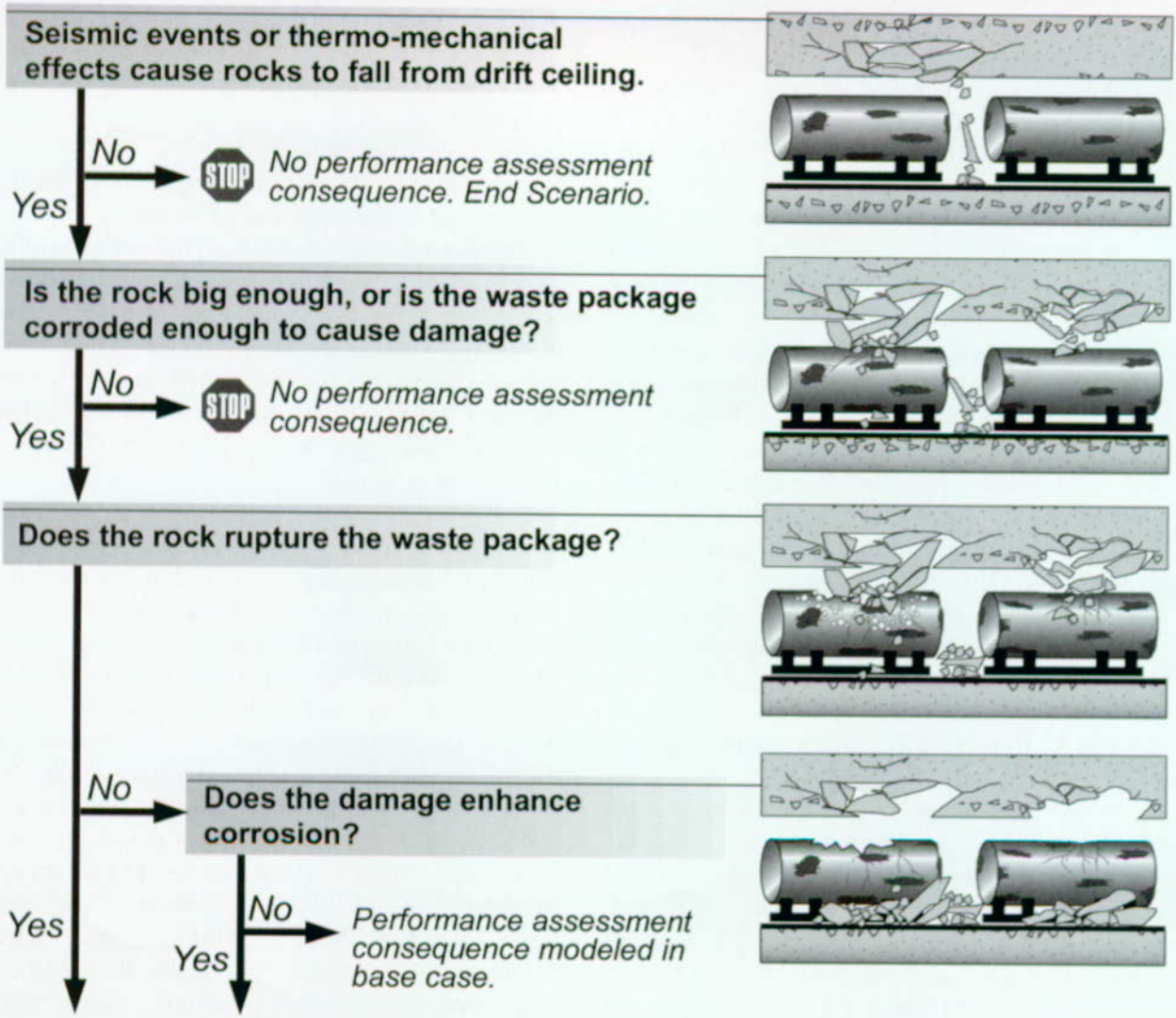

FV3044-8

Figure 4-48. Rockfall Scenario

Rockfall could damage packages causing acceleration of corrosion, and if packages are already damaged by corrosion, even faster exposure of waste could occur.

package—approximately 3.5 m (12 ft). When the waste package outer barrier is thick, the rock mass needed to damage it is very large (larger than 3,500 kg (4 tons)). As the waste package walls corrode, the rock mass that can damage it is correspondingly less (as small as 50 kg (100 lb) for severely corroded packages). Therefore, at later times (more than 100,000 years) rockfall damage is more likely because the waste packages have corroded and there is a much longer period of time in which a large earthquake can occur. Lastly, the waste packages occupy about 40 percent of the space along a drift. For the size rocks considered here, any that fall have an approximately 40 percent chance of hitting a waste package (or a 60 percent chance of falling to the drift floor without hitting a waste package).

4.4.3.2 Indirect Seismic Effects Scenario

Seismic activity near Yucca Mountain could affect repository performance even if a fault does not

intersect the repository. This scenario is shown in Figure 4-49. As discussed in Section 3.7, flow and transport through the saturated zone is controlled by the geologic structures and their hydraulic properties. If faulting occurs in the saturated zone, it could potentially change water flow patterns and, therefore, repository performance. The most likely places for faulting to occur are at locations of previous igneous or seismic activity. These locations include faults near the repository footprint (for example, Solitario Canyon and Drill Hole Wash) or faults in the Yucca Mountain region (for example, Stagecoach Road). A fault can change the flow pattern by either being a barrier to flow or a conduit for flow. Redirection of flow could increase the dose rate at the receptor location. However, recently observed seismic activity (the Little Skull Mountain earthquake) does not significantly affect flow. Over sufficiently long times, several earthquakes could cause substantial movement along existing faults.

4.4.3.3 Results of Seismic Activity Analyses

Based on modeling results, most waste package failure because of ground motion occurs when the waste package outer wall is completely corroded away. Figure 4-50 shows a distribution of waste package failure times because of rockfall. Analyses of the rock sizes that are required to break open a waste package show that, if the outer barrier is not corroded, a rock larger than any observed in the Exploratory Studies Facility is needed to damage it. When the outer barrier and about half the thickness of the inner barrier are gone, a rock similar to the average-sized rock in the Exploratory Studies Facility can damage a waste package. However, this type of failure requires more than 100,000 years under wet-corrosion conditions. The analysis combined failures from rockfall with those from normal corrosion. Waste package damage from corrosion and rockfall has been used in dose calculations similar to those for base case groundwater flow. The calculations show that there is almost no effect on repository performance over 1 million years. The model for waste form release after the waste package is breached assumes that just one hole is enough to permit substantial amounts of waste to be released (see Section 3.4). The rockfall analysis predicts that much larger (and more numerous) holes occur than for corrosion. However, this does not change the amount of waste released under the existing waste package model.

The results of the indirect-effects modeling are very similar to the modeling of the indirect effects of dikes (see Section 4.4.2.4). There is very little change in the flow pattern when a permeable fault is introduced to the region and no detrimental effect at all if the fault is a flow barrier. There is no difference between this concentration profile and the one for the base case. Modeling has shown that the concentration profiles change only if several faults occur.

Over 10,000 years, the probability of rockfall causing a waste package to split open is essentially zero because the waste package walls are thick enough to withstand hits from most falling rocks. There is less than a 1 percent probability that rockfall will accelerate corrosion during this time period. Over 1 million years, about 30 percent of the waste packages in the repository could be breached by rockfall. When these failures are added to the normal failures from corrosion, they do not significantly change the overall probability of failure because they mostly occur at very late times (more than 500,000 years after emplacement). Section 10.5 of the *Total System Performance Assessment-Viability Assessment (TSPA-VA) Analyses Technical Basis Document* (CRWMS M&O 1998i) contains a detailed description of the calculations.

4.4.4 Nuclear Criticality

Isolated nuclear criticality events could occur if the engineered control measures in the waste package fail and other conditions occur (such as the presence of water). Additionally fissile material in the waste can potentially form a critical configuration in the surrounding rock. Criticality has not previously been included in TSPA analyses, but the DOE waste package design team has extensively investigated the possibility (CRWMS M&O 1996b; CRWMS M&O 1997r; CRWMS M&O 1998f). Although criticality is very unlikely because multiple failures in designs and materials must occur, it cannot be ruled out during the period

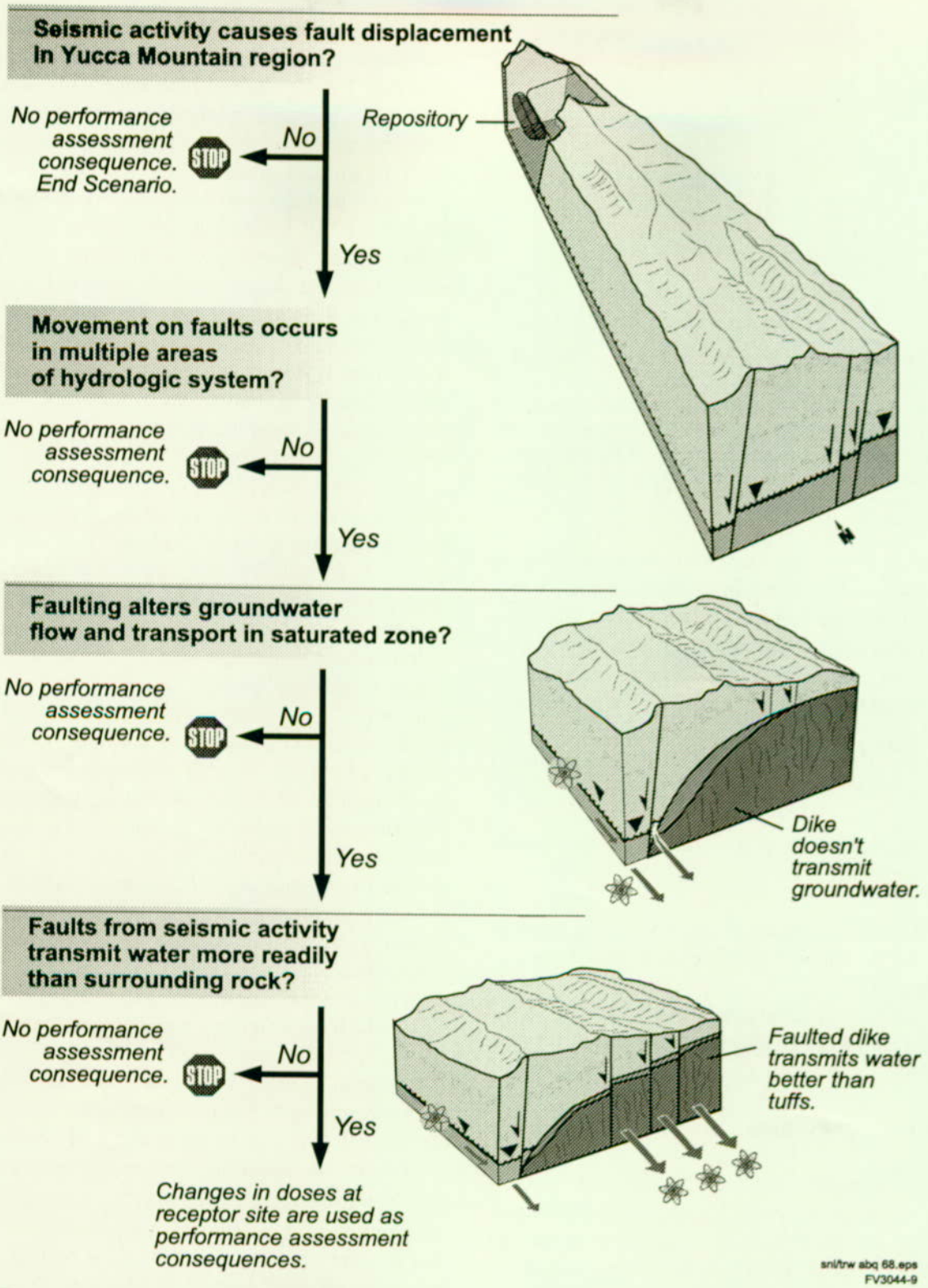

Figure 4-49. Indirect Seismic Effects Scenario
Could seismic activity in the repository area, not directly impacting the site, have an effect on groundwater flow? If groundwater flow patterns were affected in a manner that enhanced flow to the receptor site, there could be a change in dose rate.

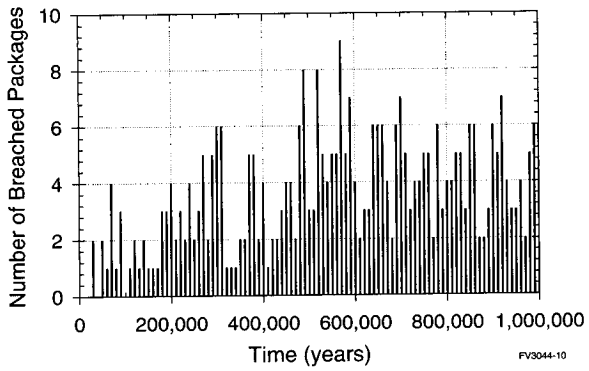

Figure 4-50. Number of Waste Package Failures from Rockfall as a Function of Time
Based on the size of rocks observed in the Exploratory Studies Facility, the packages would have to have lost the outer barrier and half of the inner barrier thickness in order to be significantly damaged by rockfall.

of repository performance. Criticality can occur in two locations in a repository system, inside a waste package or in the surrounding rock. The following three factors are required for nuclear criticality to occur in the Yucca Mountain repository environment (Kastenberg et al. 1996, Chapter 1):

- A sufficient quantity of fissile fuel (uranium or plutonium)
- A moderator (e.g., water) of the fission neutrons
- Insufficient neutron absorbers (e.g., boron) for the amount of fissile material present

In addition, the geometrical configuration of the fuel and moderator influences the likelihood of a criticality.

4.4.4.1 In-Package Criticality Scenarios

There is generally sufficient fissile fuel inside a waste package to form a critical configuration; however, the waste package is designed to provide sufficient neutron absorbers to prevent criticality. Furthermore, waste packages may be loaded in such a manner that in-package criticality, even in the worst degraded configuration, is an incredible event (CRWMS M&O 1997r, p. 75). If water can enter the waste package, a mechanism then exists to corrode the steel containing the neutron absorbers and remove any soluble neutron absorbers. If, in addition, the water fills most of the waste package, a moderator is present to support a criticality. Scenarios for in-package criticality investigate processes for introducing water to a waste package and dissolving out the neutron absorbers (CRWMS M&O 1997b). The processes differ slightly depending on the type of fissile material in the waste package, but the general scenario is the same. Figure 4-51 illustrates this general scenario. Criticality analyses for both commercial spent nuclear fuel (CRWMS M&O 1997r) and a bounding case for DOE-owned aluminum-clad spent nuclear fuel (CRWMS M&O 1997u) have been completed.

If a hole develops in the top of the waste package but not in the bottom, a "bathtub" that can hold water is formed in the waste package. For commercial spent nuclear fuel, the primary neutron absorber is boron carried in stainless steel plates. Certain of the assemblies will be so reactive as to require additional neutron absorber, less soluble than boron. For such a limited fraction of the waste packages, gadolinium, hafnium, or boron carbide could be suitable replacements for, or supplement to, the boron. As the steel rusts away, the boron can dissolve in the water and be flushed from the waste package or it can settle to the bottom of the package. Each spent nuclear fuel assembly is in the proper configuration to support criticality because it was in that configuration when it was in a nuclear reactor. As the waste form degrades, the fuel assemblies may shift. This shift may make the configuration more or less reactive.

The onset of a nuclear criticality is accompanied by an increased heat output. This heat will cause accelerated evaporation or boiling of the water moderator; the resulting loss of moderator will slow down, or stop the criticality[46]. A steady-state criticality can be maintained at a power level such that the rate of water evaporation, or boiling, will just equal the rate of water flowing into the waste package. Eventually, even the steady-state reactor will shut down because of reduction in the flow of

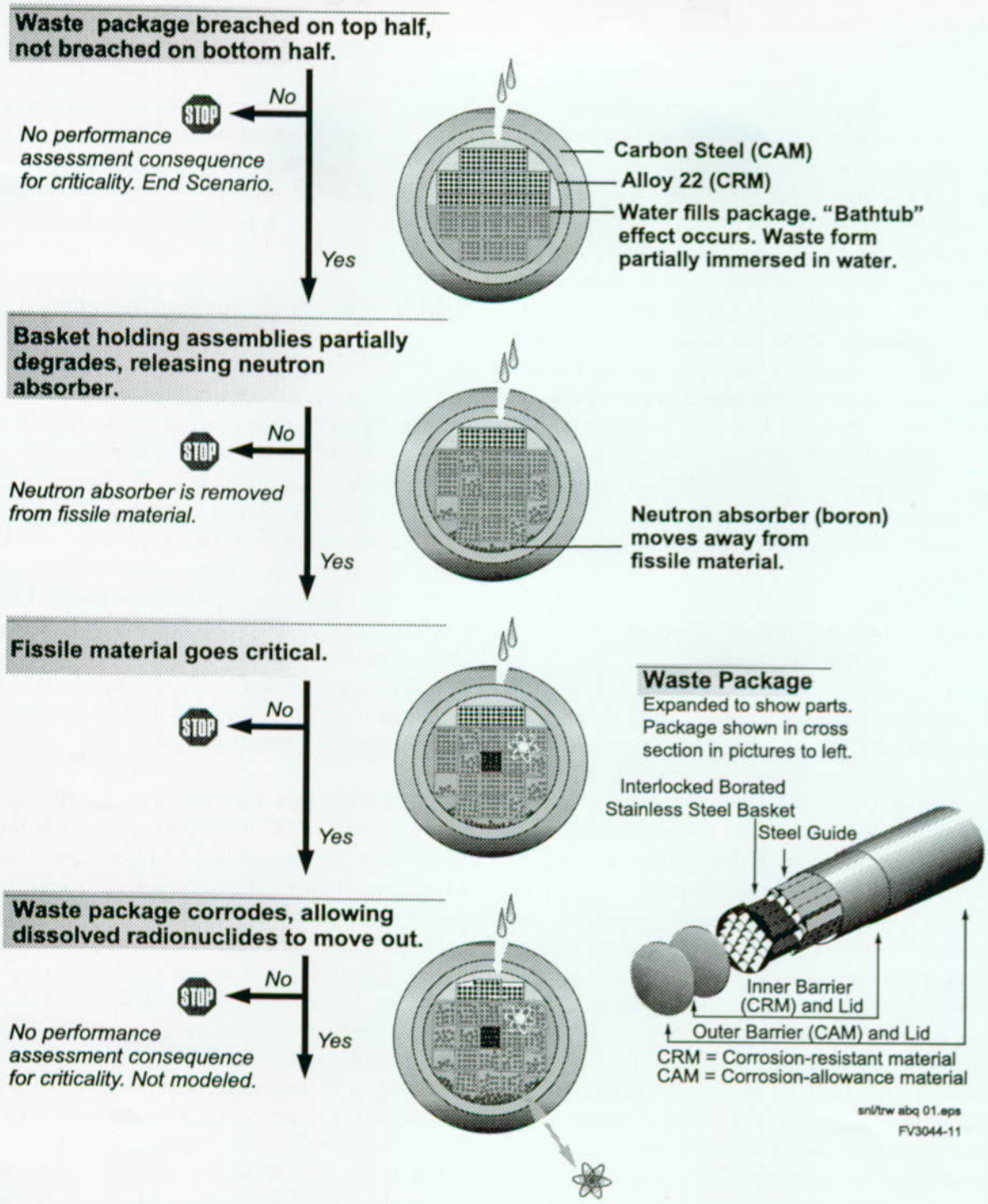

Figure 4-51. In-Package Criticality
Criticality is very unlikely, but a series of sequential steps that could lead to in-package criticality are shown. The result could be additional radionuclides available for transport; however, many would be short-lived and could decay away before reaching a receptor.

water into the waste package, or a loss of standing water due to failure of the package bottom.

Criticality increases the radionuclide inventory (in the waste package where the event occurred) that could be transported by groundwater to the dose-exposure location. The additional fission products initially have high activity but many are relatively short-lived. They can potentially cause increased doses at the dose-exposure location if both short-lived and long-lived radionuclides are transported there. The transport process for these radionuclides is expected to be the same as for the base case, thus the impact of any criticality on performance assessment can be judged by the change in source term. Because transport by groundwater ranges from several hundred to several thousand years (see Figure 3-73), the additional short-lived radionuclides that are produced by the criticality will mostly decay away before they reach the dose receptor point.

4.4.4.2 Out-of-Package Criticality Scenarios

As waste is transported from the waste package, it could accumulate in the surrounding rock. Transport as either solutes or colloids is possible. Mechanisms for accumulation include physical or topographic features (such as accumulation of contaminated water in geologic strata or ponding of water in low spots in the drifts). Flooding of drifts is considered quite unlikely because the calculated seepage rate is very low and the permeability of the rock is high. Other scenarios will be investigated for the LA, including those considering potential criticalities in the repository drifts. When the waste form dissolves, its chemical oxidation state usually increases. Accumulation mechanisms can occur if the contaminated water encounters reducing materials that cause the dissolved fissile materials to precipitate. Organic materials such as buried carboniferous logs are a possible source of reducing agents. The transport process separates the fissile materials and the neutron absorbers that may have left the waste package together. For example, transport of fissile-material colloids may separate them from the neutron-absorbing materials. If the fissile material forms a spherical shape in the rock, criticality is more likely to happen than if the material is in a flat plane. Fission products created by the criticality could be transported to the dose receptor point. Figure 4-52 illustrates some external criticality scenarios.

4.4.4.3 Results of Nuclear Criticality Analyses

The consequences of criticality have been evaluated by the waste package design team and found to be relatively small compared with the measures for nominal repository performance. An analysis of an in-package criticality scenario for commercial spent nuclear fuel has been completed, using conditions and waste characteristics that potentially maximize the effects of the criticality (CRWMS M&O 1997r, Section 6.2.2). Section 10.6 of the *Total System Performance Assessment-Viability Assessment (TSPA-VA) Analyses Technical Basis Document* (CRWMS M&O 1998i) contains details of these analyses.

The examples analyzed had criticality durations ranging from 1,000 to 10,000 years (the latter being the longest period that could be supported by a necessary, moist climate cycle). To be conservative, the example criticalities are assumed to start 15,000 years after emplacement, when commercial spent nuclear fuel is the most reactive (CRWMS M&O 1997r, Figures 6.2.2-1 and 6.2.2-2). For further conservatism, a criticality design-basis fuel is used (selected to be more reactive, with respect to criticality, than 98 percent of the commercial pressurized water reactor spent nuclear fuel). Figure 4-53 shows the time histories of the radioactivity for a waste package containing 21 pressurized water reactor design-basis fuel assemblies that undergo a criticality event of 1,000, 5,000 or 10,000 years. Also shown in the figure is

[46] The natural reactor occurring at Oklo, Gabon, depended on unique conditions in the surrounding rock that resulted from sufficient water to moderate the fission reaction. When the water was unavailable, the reactions stopped (Oversby 1996, pp. 37-38; Naudet 1975, pp. 589-601).

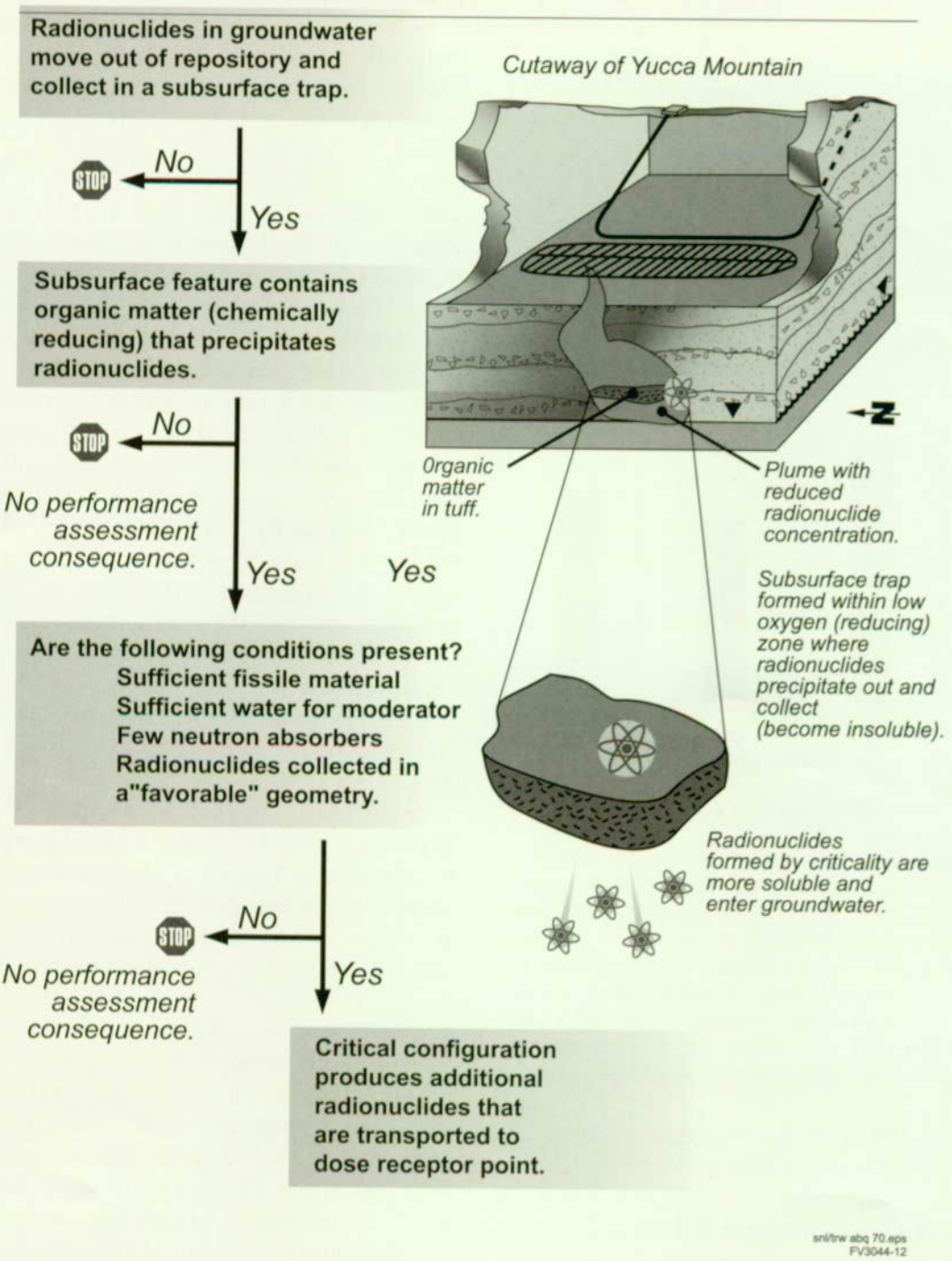

Figure 4-52. External Criticality Scenarios
Criticality in the rock away from the repository is very unlikely, but a series of processes that could lead to out-of package criticality are shown. The result could be additional radionuclides available for transport to a dose receptor.

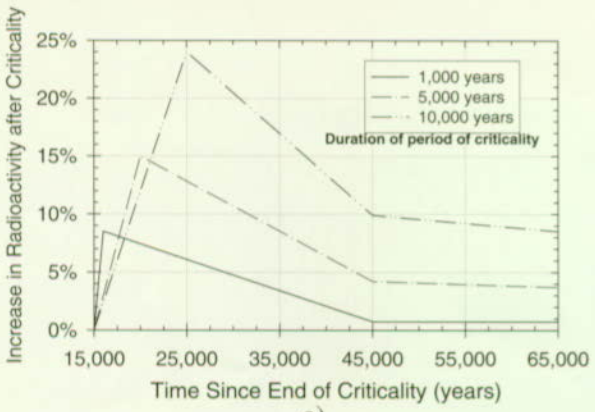

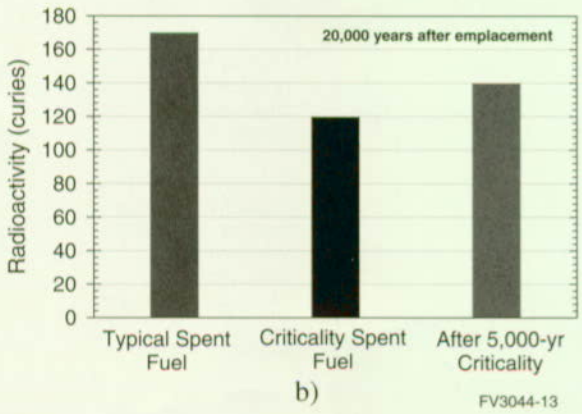

Figure 4-53. Radioactivity Levels for In-Package Criticality Model
(Top, a) Criticalities lasting for three different durations are shown: 1,000 years; 5,000 years; 10,000 years. All start at 15,000 years after emplacement. (Bottom, b) A comparison of total radioactivity developed for different fuel types from a 5,000-year criticality. ("Criticality spent fuel" is the waste that is modeled as going critical for 5,000 years.) The extra radioactivity from this criticality is less than the normal radioactivity from most waste.

the total radioactivity for the same package that does not undergo a criticality, and the radioactivity for a package containing average pressurized water reactor assemblies. It is seen that the design basis fuel has about 24 percent more radioactivity immediately after the criticality shuts down (at 25,000 years) than does the fuel not undergoing a criticality. It should, however, be noted that both these radioactivity curves are below that of the average pressurized water reactor spent-fuel package that does not undergo any criticality. The additional heat output from a steady-state criticality is only about 2 kW per package, which is inconsequential compared with the overall repository heat load. Because of the small increases in radioactivity and heat output, there is no chance that the waste package and engineered barrier system will be mechanically disrupted by a criticality.

Criticalities outside the waste package primarily require some mechanism to accumulate the fissile material in a localized area. To accumulate sufficient fissile material for a criticality, the mechanism must be fairly effective, since the concentration of dissolved uranium and plutonium in groundwater is very low (about 1 part in 100,000 or less, as is discussed in Section 3.3). An analysis of the potential for external criticality from plutonium has been completed (CRWMS M&O 1998f, Section 6). The waste packages contain sufficient neutron absorbers to prevent criticality inside the container. However, at high pH, uranium and plutonium are relatively soluble, while the neutron absorbers are not. These conditions provide the opportunity for the fissile materials to move away from the neutron absorbers and concentrate in the drift or the surrounding rock. Concentration mechanisms include reaction with the tuff or sorption on zeolites. Using the EQ6 reaction-path computer code (Wolery 1992a), precipitation and sorption of plutonium has been estimated. For both processes, the concentration of plutonium is less than 0.01 percent by volume, which is much too low to make criticality possible.

Another mechanism for external accumulation is the analog of the uranium ore deposits found in nature. The conditions for epigenetic (accumulating later than the surrounding host rock) formation of ore bodies are almost totally absent from the Yucca Mountain area (CRWMS M&O 1998f, Section 6.2). Uranium or plutonium precipitation occurs if the dissolved materials encounter a reducing environment. Potential reducing environments include hydrothermal fluids (can be associated with igneous activity, although these conditions have not been observed in the Yucca Mountain region), decayed organic material, or petroleum deposits. None of these features are located in the Yucca Mountain area, nor are they anticipated to occur.

In the extremely unlikely event that an external criticality occurs (with uranium or plutonium), the resulting radionuclide inventory increase is very small. For example, (CRWMS M&O 1998f, Section 9) a plutonium-fueled criticality operating at a power level of 590 watts was simulated for 4,000 years. Of the total radioactivity of 560 curies immediately after shutdown, 480 curies come from radioactive decay of the plutonium already present in the waste form and the balance (80 curies) from the result of the criticality (fission products and transuranic elements), so the criticality contributes only a minor amount to the radioactivity.

It has been suggested (Bowman and Venneri 1996) that a transient external criticality with a large mass of highly enriched fissile material could have sufficient positive reactivity feedback (due to overmoderation, a condition that can increase k_{eff} as water is removed from the system), and could be sufficiently confined by the rock, to produce a power pulse large enough to be classified as an explosion (Bowman and Venneri 1996, p. 280). The following are reasons why such a positive feedback transient event is far less likely than the already incredible external criticality:

- It will be nearly impossible to accumulate a large enough mass because the few waste packages containing highly enriched uranium (or plutonium) will be widely interspersed among the much greater number of packages containing low enriched material. As multiple waste packages fail near the highly enriched material, the effective enrichment would be reduced (Van Konynenburg 1996, p. 306).

- The slow accumulation of such a large mass of fissile material (over a million years) is entirely inconsistent with the rapid reactivity insertion necessary for a transient criticality. With slow accumulation, it would be nearly impossible to accumulate an overmoderated mass without going through a small criticality that would disrupt the mass and consequently preclude the possibility of reaching the overmoderated condition (Van Konynenburg 1996, pp. 316 ff.).

The following is a summary of the physical and chemical processes that act to make repository criticality an unlikely event (either inside or outside the waste package):

- Most of the waste packages cannot go critical because they do not have sufficient fissile material (or have sufficient enrichment) to form a critical mass.

- Of the waste packages that have sufficient fissile material for criticality, commercial spent nuclear fuel waste packages are a major fraction. The maximum fraction of commercial packages with sufficient fissile material for criticality never exceeds eight percent of the total. This amount drops by 30 percent for times beyond 40,000 years (CRWMS M&O 1997r, p. 46). This significantly decreases the criticality probability because only 10 percent of the waste packages are expected to even be breached by 40,000 years (see Figure 4-7).

- Of the waste packages that have sufficient fissile material for criticality once they are breached and degraded, most require some form of water retention to provide moderation. Models of the waste package corrosion process indicate that only 25 percent of the waste packages that are breached will hold a significant amount of water for the time required to flush the neutron absorbers that have been added for criticality prevention.

- External criticalities are extremely unlikely because of the low probability of accumulating significant amounts of fissile material by any credible geologic process. Specifically, there have been no identified deposits of carboniferous logs or other carbonaceous material near Yucca Mountain to cause accumulation to occur.

4.4.5 Human Intrusion

Human intrusion is generally interpreted to mean inadvertent penetration of the repository (such as by drilling operations) that either releases radionu-

clides at the surface or accelerates radionuclide transport to the dose-exposure location. Regulations specifically exclude consideration of deliberate intrusion of the repository. Human-intrusion drilling scenarios have been investigated in prior TSPA analyses and found to contribute less than 1 percent to the overall repository performance (Barnard et al. 1992, Chapter 6; Wilson et al. 1994, Chapter 16). Because of the uncertainties associated with evaluating future human technology and societies, the National Academy of Sciences has recommended that the probability of occurrence of human intrusion not be considered in any TSPA analysis (National Research Council 1995, Chapter 4). The consequences of human intrusion, in terms of potential increases in long-term doses to the exposed public, are used to measure the resilience of the repository to such disturbances. In the past, human intrusion requirements have been incorporated in NRC and EPA regulations.

4.4.5.1 Technical Bases for Human Intrusion Analyses

The stylized analysis of human intrusion assumes that, as a result of drilling into the repository, a waste package is penetrated by a drillhole. Waste then falls down the drillhole to the saturated zone beneath the repository. There, the flowing water dissolves the waste and carries it to the dose-exposure location. This analysis is meant to show whether a single drilling incident of this type can cause large doses.

The analysis does not consider the process that causes punctures to the waste package or how the waste gets down the drillhole to the water table. Instead, we make some assumptions about the amount of waste that can fall down the hole based on current drilling practices. The analysis assumes that the drilling is for water, an operation in which a 21-cm (8-in.) drill bit is typically used. The drilling operation is assumed to stop when the driller hits water at the water table. At this point, the hole is abandoned; it is neither cased (lined with pipe) nor plugged. Shortly thereafter it fills with rock debris. Consequently, most of the waste that reaches the saturated zone comes from the drilling incident; not from being washed down the hole later.

The waste that falls down the drillhole is assumed to be extensively pulverized. The water dissolves the waste according to the dissolution rate appropriate for saturated zone conditions and the surface area of the specific waste type. The dissolved waste is transported to the dose-exposure location, where it adds to the dose from the base case radionuclide transport. Figure 4-54 shows this scenario.

4.4.5.2 Results of Human Intrusion Analyses

Between 550 and 2,700 kg (1,200 and 6,000 lb) of waste are assumed to fall down the borehole (the amount depends on how much is removed by the drill). Because it is so finely pulverized, the waste can readily dissolve. Two dissolution rates for spent-fuel waste are used, representing the lower and upper ranges expected for saturated zone parameters that control dissolution. Some of the radionuclides included in the analysis are completely dissolved in about 20 years, while the low-solubility ones (like plutonium) continue to dissolve in groundwater for many thousands of years. The drilling incident is modeled as occurring at 10,000 years (the time at which the waste package is likely to be degraded enough that a drill can penetrate it). Figure 4-55 shows the dose-rate time histories for the extreme cases modeled (about 550 kg, or 1200 lb per low dissolution rate and 2700 kg or 6000 lb. per high dissolution rate). The inset graph in Figure 4-55 shows the dose rates from 10,000 to 20,000 years. The peak for the large-mass/high dissolution rate case in this period is approximately 145 times the base case dose rate at 12,000 years. The dose rate for the low mass/low dissolution rate case is approximately 3.7 times that of the base case at the same time. By about 15,000 years the dose rates again closely track the base case. At about 50,000 years the dose rates diverge again, as can be seen in Figure 4-55. After about 150,000 years the dose rates for all human-intrusion cases again track the base case time history.

In terms of the dose to a critical group over 100,000 years, the effects of human intrusion are

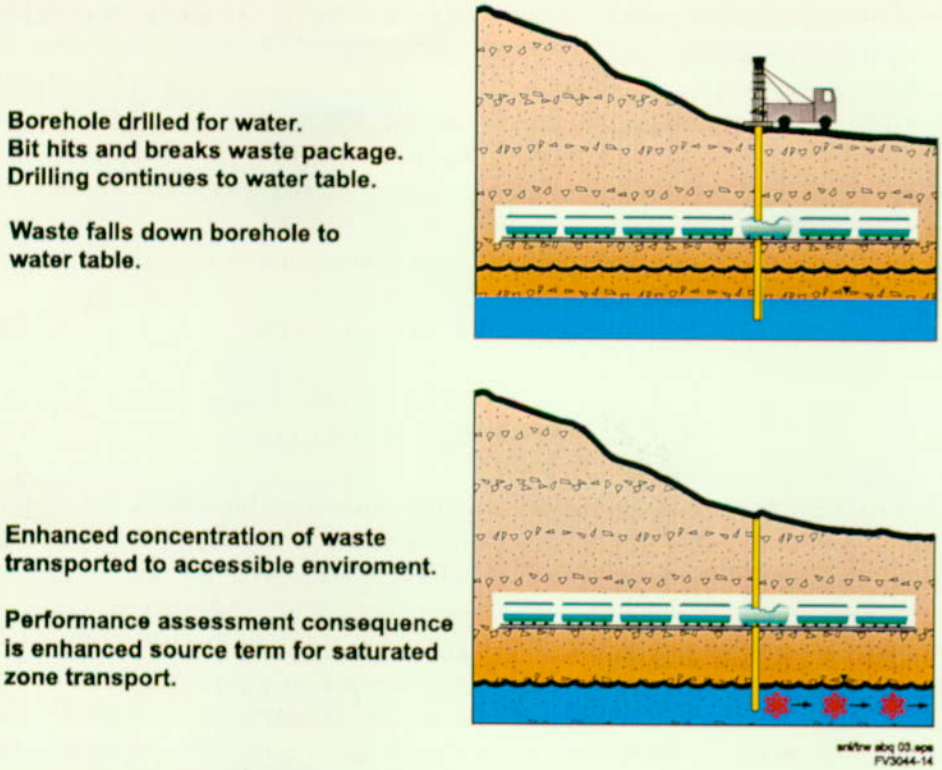

Figure 4-54. Human Intrusion Scenario
This figure is a stylized depiction of what might happen if a waste package were penetrated by a drill bit during drilling for water with drilling continuing to the water table. The assumption is that waste could be carried down the drillhole to the water table. This could add to the dose rate at the receptor.

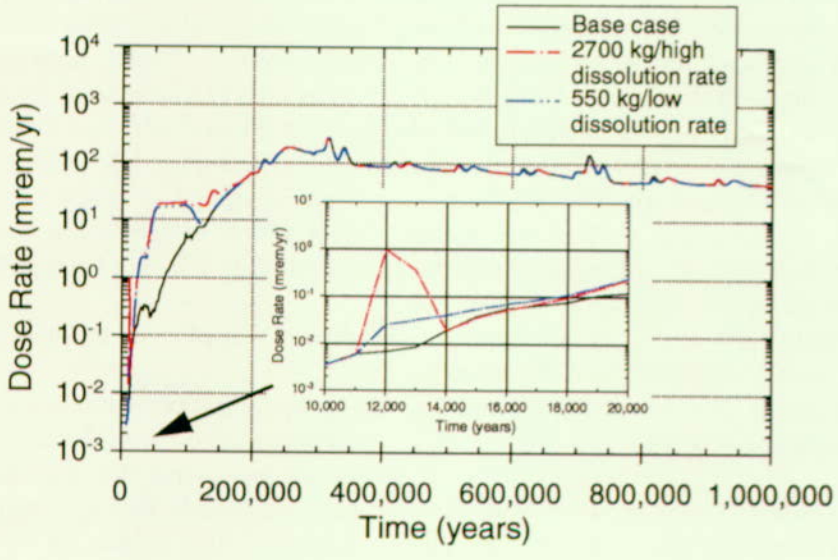

Figure 4-55. Comparison of Human-Intrusion Dose Rates with Base Case Dose Rates
This figure illustrates the case where the extremes of the amount of waste goes downhole and are dissolved in groundwater at the two different rates. The inset graph shows that the fastest moving radionuclides are transported to the accessible environment in about 2,000 years with the next radionuclides arriving in about 12,000 years.

small (an approximate four-times increase over the base case dose rate for about 50,000 years). Over 1 million years, this increase over the base case is unlikely to be significant. At times closer to the human-intrusion incident, the increased dose rates can be much larger than the corresponding base case rates. Section 10.7 of the *Total System Performance Assessment - Viability Assessment (TSPA-VA) Analyses Technical Basis Document* CRWMS M&O (1998i) contains details of the human-intrusion analyses.

4.4.6 Summary

The four scenarios modeled here have produced a wide range of performance impacts on the base case performance of the repository. Results from modeling direct volcanic effects show almost no impact on performance from either consequence or probability. The increased dose rates when a dike creates an enhanced source term can be larger than some base case analyses, but their probability of occurrence is less than 10 percent. The peak dose from volcanism occurs thousand years after the event because of the time required for transport by groundwater to the dose receptor point. Because the volcanic events can happen at any time, the peak dose rate can be much sooner than the peak dose rate for the base case. The models for rockfall do not predict a significant impact on performance. In-package nuclear criticalities have the potential to increase the radioactivity in a small number of emplaced waste packages by up to 25 percent, but the probability of this type of criticality is low, as is the probability of criticality outside the waste package after degradation. Human intrusion produces increased dose rates that are within the range of variability of base case results. In summary, the overall impact of these disturbances does not significantly change our assessment of base case performance.

One area of uncertainty that is apparent from these analyses is the behavior of waste package materials in magmatic environments. If DOE decides to analyze disruptive events in the future, a better understanding of the corrosion and deformation resistance of the waste package inner barrier material can help reduce these uncertainties.

4.5 EFFECTS OF DESIGN OPTIONS

Three enhancements to provide potential improved performance of the engineered barrier system have been identified as "design options" in Volume 2, Section 5.3. These enhancements are as follows:

- Emplaced drift backfill
- Drip shields
- Ceramic coating of the disposal container with backfill

These options are intended to reduce the amount of liquid water in contact with the waste package, which is the principle factor impacting waste package lifetimes. Backfill may cause a reduction in relative humidity for longer periods after waste emplacement, thus causing further delay in the initiation of corrosion. Backfill also may be considered to control the chemistry of the system, thus controlling waste package corrosion, waste from dissolution, engineered barrier system transport and to some extent geologic transport. However, the current analyses do not include such controls. Drip shields and ceramic coating may provide barriers to seepage into the waste package, which can reduce waste form degradation and mobilization. These three enhancements to the engineered barrier system are illustrated schematically in Figure 4-56 and are discussed in detail in Volume 2, Section 5.3. Additional "design alternatives" identified in Volume 2, Section 8.2, are not analyzed for the TSPA-VA, but will be considered as part of the EIS and LA analyses.

4.5.1 Emplacement Drift Backfill

The first enhancement is a design for covering the waste packages with backfill. This design was incorporated into the thermal-hydrologic model and the waste package degradation model to determine the effect on waste package and, ultimately, repository system performance. The backfill was assumed to have the thermal properties of crushed tuff, to be dry at emplacement, and to be introduced 100 years after waste emplacement. The initial moisture in the backfill may cause early corrosion, but this effect is

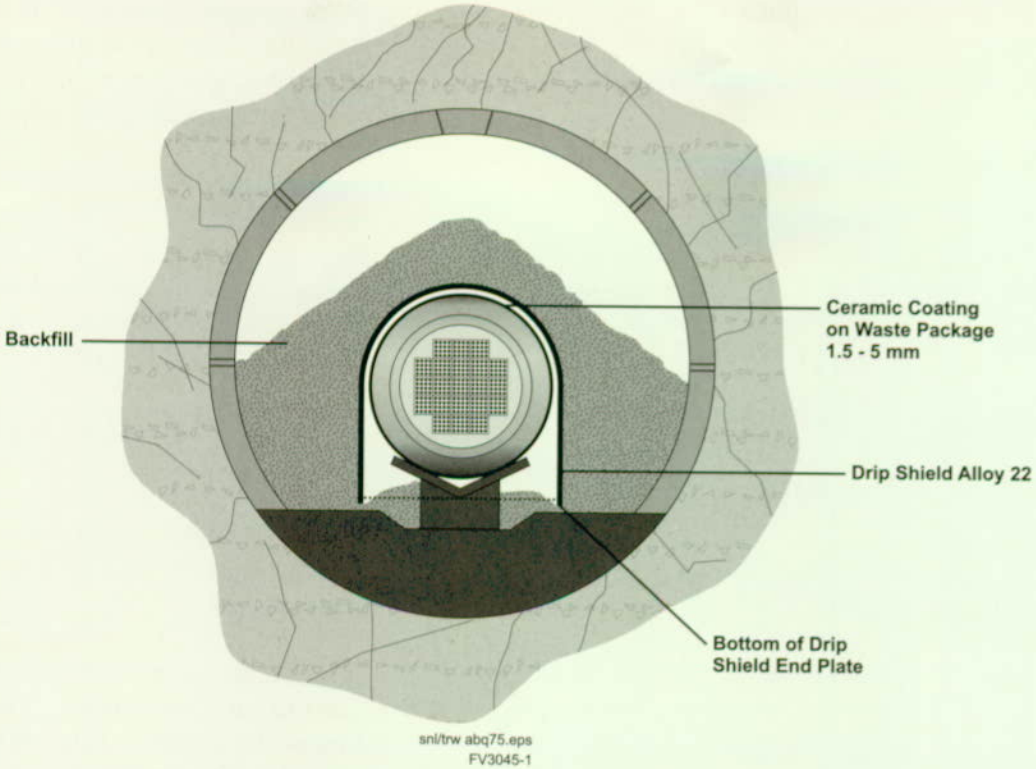

Figure 4-56. Engineered Barrier System with Design Enhancements (Backfill, Drip Shield, and Ceramic Coating)

expected to be small as temperatures in the repository quickly rise to drive off the moisture in the backfill. The primary effect on the system is an increase in temperature at the time of backfilling and a corresponding delay in the relative-humidity increase as the repository cools. While the effect of moisture control is an important potential benefit of backfill, no change in seepage contacting the waste package as a result of backfilling was included in the modeling. The full evaluation of the effects of backfill on system performance have not been completed because the effects of seepage have not been quantified and included in the analysis. For the model assumptions included herein, there is little difference in total system performance between backfill and no backfill cases.

The thermal-hydrologic results and waste package degradation analyses comparing the case with the reference design (no backfill in the emplacement drift) and a partially backfilled emplacement drift are illustrated in Figure 4-57. The large temperature increase at 100 years corresponds to the emplacement time of the backfill. For an emplacement drift without backfill, the dominant mode of heat transfer is radiation, which is an efficient mode of heat transfer between the waste package surface and the drift wall. For a backfilled drift, the resistance to heat transfer from the waste package surface to the drift wall is greatly increased; therefore, the waste package temperature increases. Accompanying the increase in surface temperature is a corresponding decrease in relative humidity around the waste package. These results are presented in Figure 4-57. The degradation of corrosion-allowance material (labeled CAM in the figure) for the backfill case is delayed over 1,000 years from the non-backfill case. The bend in the corrosion-allowance-material degradation curve, after about 80 percent of the waste packages are breached through the outer barrier, is caused by a few of the waste packages that have low relative humidity compared to the rest of the waste packages. This is a result of the thermal-hydrologic variability leading to some zones with low relative humidity. These packages have longer lifetimes for their corrosion-allowance material. The non-backfill case didn't have any such

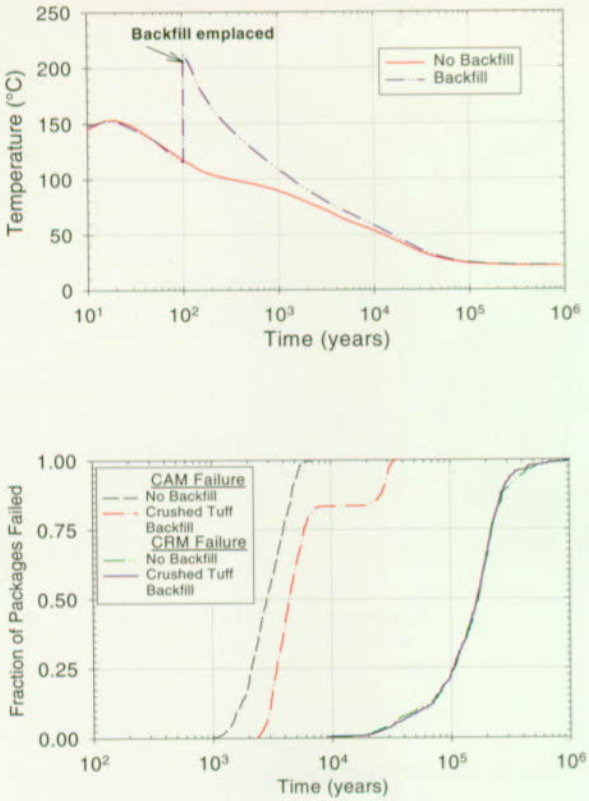

Figure 4-57. Effect of Backfill on Temperature and Fraction of Waste Packages Failed over Time
The top figure shows the average waste package temperature with and without backfill in the NE region (see Figure 3-20) for commercial spent nuclear fuel, long-term average climate, mean infiltration, and base case hydrologic properties. The bottom figure shows the corresponding waste package degradation history. (CAM—corrosion allowance material [outer layer of the waste package], CRM—corrosion resistant material [inner layer of the waste package])

packages. The degradation of corrosion-resistant material (labeled CRM in the figure) is essentially the same for the two cases because the primary factor for degradation of the corrosion-resistant material is whether dripping is occurring (the model assumes the same dripping conditions for both backfill and no backfill conditions). The TSPA results for the two cases are similar because the waste package degradation is similar, so those results are not presented here.

The effect of backfill on seepage is uncertain and additional testing is being conducted to better understand these effects. As noted, the backfill is assumed in these analyses not to alter the seepage onto the waste package. Some of the potential effects of backfill on seepage are as follows:

- Diversion of the seepage around the waste package.
- Reduction of seepage reaching waste package because of evaporation of incoming water that is at a low flow rate.
- Concentration of salts in the backfill from seepage water.
- Promotion of water condensation at the contacts between the backfill and the waste package surface.
- The backfill is not expected to restore the preconstruction unsaturated zone flow conditions. These effects have not been fully evaluated for their impact on overall system performance.

Also, if the drift is backfilled, the effect of rockfall on waste package failure is minimized.

4.5.2 Drip Shields

Performance assessment analyses have been conducted to evaluate the effect of a drip shield on waste package lifetime as well as on overall performance. Several configurations for a drip shield have been identified. However, only a single representative drip shield is evaluated here. The evaluated drip shield design was a 2-cm (0.8-in.) thick sheet made of Alloy 22, the same material as the inner barrier of the waste package. The drip shield was assumed to be placed over the waste package (waste package drip shield) and in the model measured half the surface area of the waste package (the failure of the sides of the drip shield is not important to performance of the waste package). The simulation assumed backfill emplacement at 100 years. The drip shield analyses do not include the potential effects of galvanic coupling of Alloy 22 over the carbon steel, although the design specifies a ceramic

coating on the carbon steel that could reduce the effect.

The degradation model for the drip shield assumed that the drip shield upper surface was 100 percent wet in dripping zones. The drip shield was assumed to fail only from general corrosion (no localized corrosion) because there is little potential for crevices on the wetted surface, and there are no significant oxidants (other than oxygen). Failure from rockfall was not considered in these analyses, but is not expected to contribute significantly to drip shield degradation because of backfill protection. Likewise, crevice corrosion between backfill and drip shield is not expected because temperature and oxidant availability would not be sufficient to initiate crevice corrosion of Alloy 22. The drip shield-corrosion rate was assumed to be the same as the benign conditions for Alloy 22 corrosion (moderately acidic pH 3 and moderately oxidizing, see Section 3.4). Although crevices could form between the drip shield and the corrosion-allowance material underneath the drip shield, they were assumed not to form because of the lack of chloride ions required for crevice corrosion (Fontana and Greene 1978, Chapter 3). Potential galvanic coupling between the drip shield and the corrosion-allowance material could reduce the general corrosion rate of the drip shield, but was not considered. The design specifies a ceramic coating on the carbon steel to reduce this potential effect. The waste package was assumed to undergo only humid-air corrosion during the time when the waste package drip shield was functioning. After failure of the waste package drip shield, water was assumed to drip on 10 percent of the waste package surface area because only a small area of the drip shield fails in the model, and only a fraction of the waste package surface area directly under the patch opening in the drip shield will get wet. Very few drip shield patches fail, so 10 percent wetting of waste package surface is conservative. This percentage is in contrast with the base case in that water is assumed to drip on 100 percent of the waste package surface area.

The degradation of the waste package and drip shield in dripping zones was evaluated. The results are presented in Figure 4-58 in a comparison with waste package failure for the base case.

The corrosion of the outer barrier of the waste package (corrosion-allowance material) proceeds at the same rate as the base case even though a drip shield was added. Humid-air corrosion of the outer barrier is unabated by elimination of water dripping onto the waste package. However, the drip shield does cause significant delay in inner-barrier corrosion. The drip shield is expected to be in a more benign environment than some portions of the waste package (because of lack of contact with the corrosion-allowance material), thus its failure is later than the corrosion-resistant material in the case with backfill. Deferring dripping until after drip shield failure significantly extends the lifetime of the waste package. The drip shield enhances the overall waste package lifetime by greater than 100,000 years. The effect on dose from the addition of the drip shield is illustrated in Figure 4-59. Doses are reduced from base case amounts by greater than an order of magnitude for the first 300,000 years of the simulation. However, once a significant number of the waste packages fail after the drip shield fails, the doses approach base case amounts; at about 500,000 years the doses become identical to those from the base case. This analysis indicates that the life span of the drip

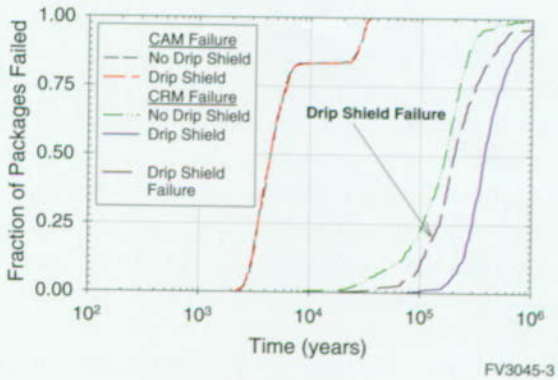

Figure 4-58. Effect of Dripshield on Waste Package Degradation
The drip shield fails after the no-drip shield waste package because of the less aggressive corrosion conditions on the drip shield in comparison with the waste package. This effect leads to significantly later failure of the waste package associated with the drip shield than in the base case.

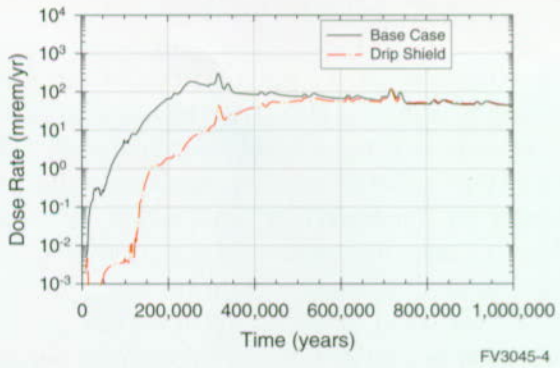

Figure 4-59. Effect of Dripshield on Dose Rate at 20 km (12 miles)
The drip shield substantially improves performance at early times up to 300,000 years because of later waste package failure than in the base case.

shield is the key determinant in providing improved performance. After the drip shield fails, the dose from the repository gradually returns to the dose simulated with non-drip shield conditions.

4.5.3 Ceramic Coating of the Disposal Container with Backfill

A third design enhancement specifies a coating of ceramic material on the waste packages, with the expectation that this coating will delay corrosion of the outer barrier for some period. The design includes backfill on top of the waste packages to prevent damage to the coating by rockfall, so thermal-hydrologic parameters from the backfill case are important in these analyses. The preliminary model for ceramic coating degradation was provided by the repository-design organization. This model was implemented in WAPDEG, a computer program for modeling various designs, waste package materials, and degradation mechanisms (see Section 3.4). The ceramic degradation model is based on a process by which the oxygen transport rate through water-filled pores in the ceramic coating on the carbon steel substrate is retarded. Because the corrosion rate for the carbon steel substrate is proportional to the rate at which oxygen is supplied to the substrate, ceramic coating performance as an oxygen transport barrier is expressed as the substrate-corrosion-rate reduction factor. The factor is expressed with a distribution to represent the uncertainty. The ceramic coating may have very low connected porosity, that may provide additional protection to the waste package (*Outer Barrier Corrosion Model with Ceramic Coating.* Interoffice Correspondence. V. Pasupathi to J. H. Lee, LV.WP.VP.05/98-102, May 24. Transmitted via QAP 3-12 on May 26 by D. Stahl).

Degradation of the ceramic coating was evaluated for two cases. In the first case, degradation of the ceramic coating was evaluated under humid-air conditions that were assumed to be effective for the first 1,000 years of the analysis. The first evaluation was only for 1,000 years and no failures occurred over this period. The relative humidity is low for the first 1,000 years, so the ceramic pores are assumed to not be filled with water. In the second case, degradation of the ceramic coating was evaluated for continual aqueous or dripping conditions. The failure of the ceramic coating for only the second condition is illustrated in Figure 4-60, since the first provides no failure over the period of interest. For humid-air conditions, the ceramic coating is not breached in the period of interest, the first 1,000 years of the simulation, after which aqueous conditions are assumed. For the aqueous conditions, the breach of the ceramic coating does not begin until after 300,000 years. After 1 million years, there is less than a 6 percent failure of the ceramic coating on the waste packages with dripping. For the preliminary ceramic coating model, there are few waste package failures under 1 million years. The ceramic model requires additional data and justification because it is in the early stages of development. The dose rate plot for the ceramic case is also presented in Figure 4-60 in comparison with the base case. The dose for the ceramic case starts much later and is reduced by over an order of magnitude from the base case.

The preliminary ceramic coating model that was used in the current analysis to evaluate the impact of the ceramic coating design option on the long-term waste package performance was developed based on the assumption that stress developed by the volume expansion of the corrosion products of the CAM substrate is the only mechanism leading to the coating failure. The analysis assumed two

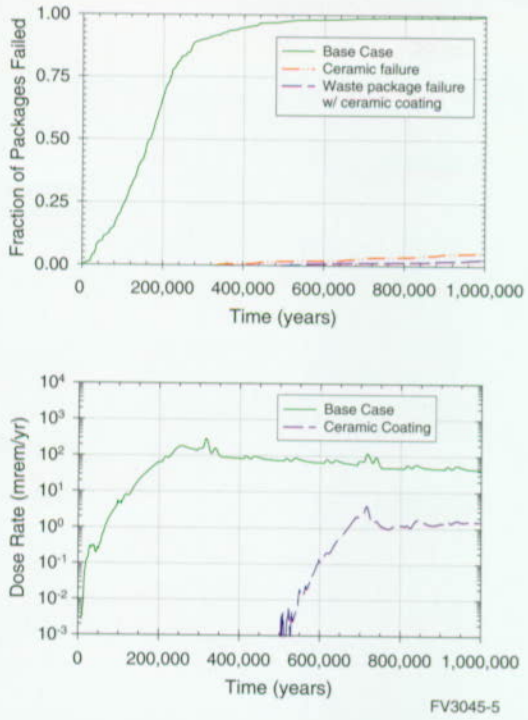

Figure 4-60. Effect of Waste Package Ceramic Coating on Waste Package Degradation
Use of ceramic corrosion factors for humid air and for aqueous conditions leads to a very small number of waste packages with ceramic coating failure. The humid-air corrosion factor was only applied for 1,000 years, so there were no waste packages failing in humid-air conditions. Waste packages affected by aqueous corrosion on the ceramic coating did not begin to fail until after 300,000 years, and only a few percent had failed ceramic coating by 1 million years.

percent interconnected porosity in the coating. As discussed previously, the sensitivity analysis results showed that the ceramic coating itself could last more than 300,000 years if the interconnected pores in the ceramic coating are filled with water, which provides a barrier to the oxygen transport to the corroding carbon steel substrate.

However, in the current analysis, the effect of other potential mechanisms that could cause damage to the proposed thin ceramic coating on the waste package have not been analyzed. Defects and flaws in the coating could be introduced from the fabrication process (application of the coating on the waste package). Differential thermal expansion between the ceramic-coating material and the waste package metal-barrier substrate could potentially cause cracks in the coating. Because of the extremely long time periods considered in the geologic repository, dissolution of the ceramic materials over such long-term periods (especially under locally perturbed acidic or alkaline conditions on the waste package) and its effect on the integrity of the coating need to be considered. In addition, damage to the coating could be caused by improper handling and transport of the ceramic-coated waste package), impact by a sufficiently large rockfall, and ground motion by earthquakes. A complete analysis of the effects of these processes should be conducted before potential benefits of the ceramic coating can be substantiated.

INTENTIONALLY LEFT BLANK

5. SENSITIVITY ANALYSES FOR COMPONENTS

The individual process model components of TSPA-VA are described in Section 3 of this volume. The construction of Section 5 of this volume parallels that of Section 3. In Section 5, the TSPA-VA is again discussed based on its component parts to assess the sensitivity of the results to changes in the various parameters used to construct the model of that component. An important task for the TSPA is performing the uncertainty and sensitivity analyses. They are one means of showing which parameters in the analysis have the most influence on repository system performance.

In general, the sensitivity analyses do not show, in an absolute sense, which parameters in the analysis are most important to performance. Instead, they show the parameters in which uncertainty most affects the results. Therefore, by holding a parameter constant in a comparative calculation, the relative reduction in uncertainty is obtained. In some cases, if future studies could reduce the range in uncertainty, the parameter might no longer appear as a parameter to which performance is highly sensitive. Conversely, if a parameter or component is assigned an inappropriately low uncertainty range, it might not show up as a particularly important parameter. Uncertainty analyses must be performed with care and implemented in many different configurations. This process allows analysts to gain the necessary understanding about which parameters are most important to actual repository performance. It can also provide DOE with an indication of which parameters might warrant additional study to achieve the confidence necessary for an adequate licensing argument.

5.1 UNSATURATED ZONE FLOW

5.1.1 Sensitivity to Climate

Three sensitivity studies were conducted to look at the effects of base case assumptions about climate. The sensitivity studies address timing and duration of climate conditions; assumptions about more extreme climate magnitudes or the sufficiency of using only three discrete climate states are not addressed. Climate magnitude is not considered, because the range of uncertainty in net infiltration (from one-third to three times the base value) is intended to cover the range of natural variability.

The first sensitivity study examines the duration of each climate state. In the base case, the long-term-average climate lasts about 90,000 years, the dry climate lasts about 10,000 years, and the superpluvial climate lasts about 10,000 years. There is some information in the paleoclimate record about how long the Great Basin pluvial lakes were present and how deep they were. This and other information indicates that both the dry and superpluvial climates lasted longer, perhaps as long as 50,000 years. Therefore, the expected-value base case is compared with a case having 50,000-year climate durations for all three climates but which is otherwise identical to the expected-value base case.

The comparison is shown in Figure 5-1. This figure shows that differences are relatively insignificant between the two cases, suggesting that climate duration, at least at the scale of thousands of years, is not important. There is a slight difference, generally less than a factor of two, in the magnitude of the peaks. The peaks mark the transition from one climate to another and primarily represent the effect of abrupt changes in water table elevation and saturated zone groundwater flux. The superpluvials do not occur at the same time in both cases, so the major peaks in dose rate do not occur at the same time.

The second sensitivity study examines the effect of the base case assumption of an instantaneous transition from one climate state to the next. In this sensitivity study, three calculations were performed, identical to the expected-value base case, except that climate was held constant in each. Therefore, one calculation used a dry climate for the entire 1 million years; one, a long-term-average climate; and one, a superpluvial climate. The results are shown in Figure 5-2. The figure shows that the base case and the case using only the long-term-average climate are virtually identical. The only difference is that the case using the long-term-average only does not show fluctuations in the

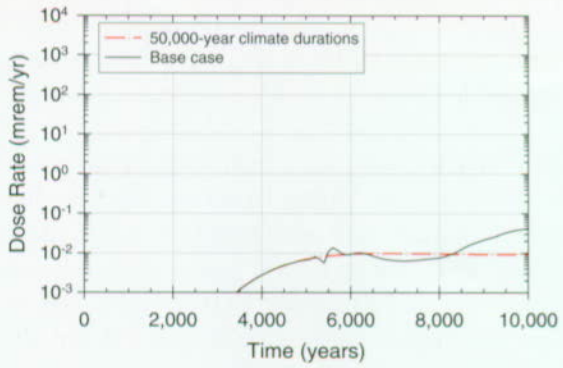

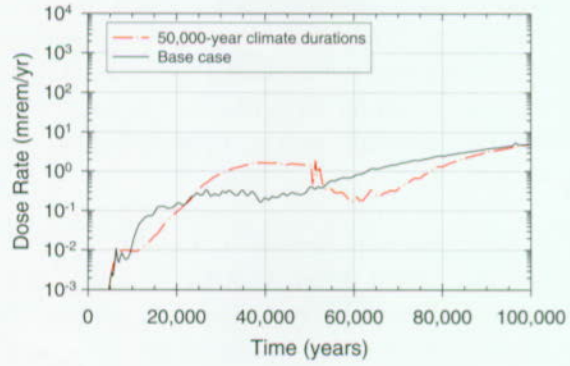

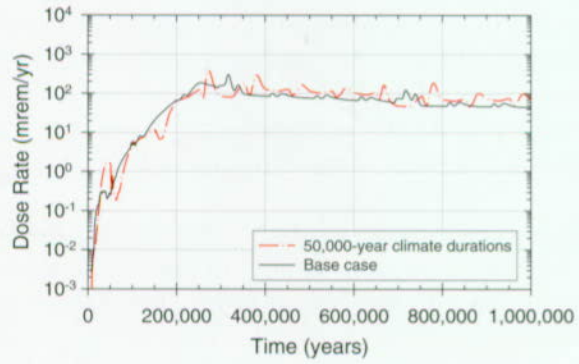

FV3051-1

Figure 5-1. Comparison of the Expected Value Base Case with a Sensitivity Case in Which all Climate Durations are 50,000 Years
The differences in total dose rate are relatively insignificant when climate durations are adjusted by thousands of years.

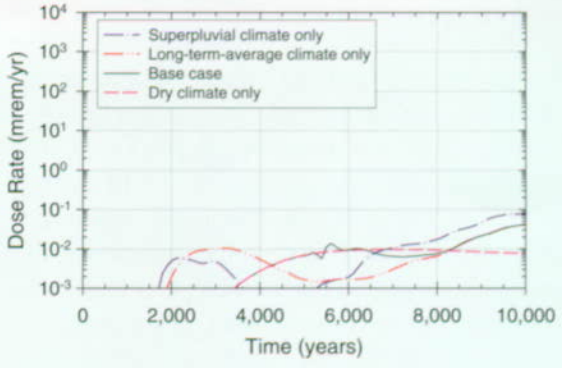

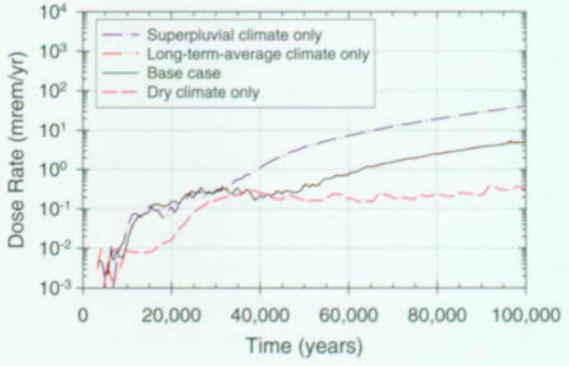

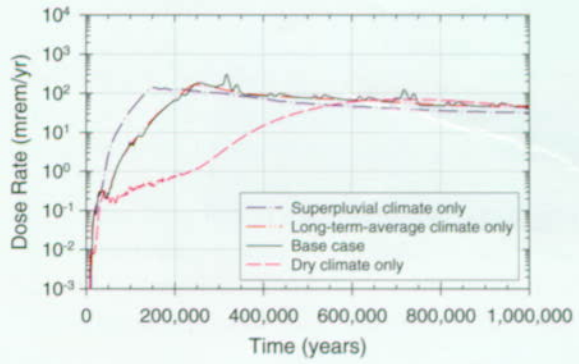

FV3051-2

Figure 5-2. Comparison of the Total Dose Rate for Expected-Value Base Case with Three Sensitivity Cases in Which There are no Climate Changes
The indicated climate state is in effect for the full time period.

magnitude of the dose rate associated with the times of climate changes in the base case.

Figure 5-2 also shows something unexpected. For a 1-million-year period, peak dose rate varies little because of the climate type. The time of the peak dose rate changes in response to the wetter repository conditions associated with wetter climates. However, the additional water that comes with wetter climates tends to compensate for the additional releases of radionuclides by creating additional dilution. The time of the peak dose rate for the dry climate is about 700,000 years; for the long-term average, it is 250,000 years; for the superpluvial, it is 150,000 years. Therefore, the time of peak dose rate is affected by climate, but the magnitude of the peak dose rate is not particularly sensitive to the magnitude of the climate. Indeed, radionuclide decay might be responsible, at least in part, for making the dry-climate peak lower than the other two.

The third sensitivity study investigates the assumption in the base case that climate magnitudes are correlated over time. In the base case, when a high infiltration (i.e., base infiltration times three) is selected for a given realization, all the future climates have infiltrations that are times three, including commensurately high seepage rates. For the third sensitivity study, climate magnitudes were uncorrelated and 100 realizations were simulated. The results are presented as a distribution of peak dose rate in Figure 5-3. Variable climate magnitudes produce higher peak dose rates than more uniform magnitudes. It might seem reasonable that, with variable climate magnitudes, there is a greater chance of getting more extreme climates in any given realization. However, the sensitivity studies show that climate magnitude is relatively unimportant, and the transitions between climates are important for peak dose rate. Variable climate magnitudes create instances when the change from one climate to the next is even greater than in the base case, and the contrast creates the greater dose rate.

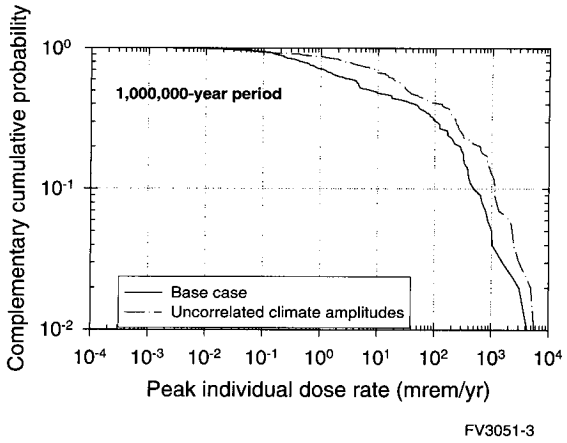

Figure 5-3. Comparison of the Base Case Peak-Dose-Rate Distribution with a Sensitivity Case in Which Infiltration and Climate are Uncorrelated
For example, an "infiltration divided by 3" dry climate could be followed by an "infiltration multiplied by 3" long-term average climate.

5.1.2 Sensitivity to Infiltration

One sensitivity analysis was performed to examine further the effect of the uncertainty in infiltration. In the unsaturated zone flow model expert elicitation (CRWMS M&O 1997n), some experts favored relatively high net infiltration values for Yucca Mountain, so the effect of higher infiltration is particularly of interest.

Performing additional simulations with the infiltration model and the mountain-scale unsaturated zone flow model is very difficult, but changing the probabilities associated with the existing simulations (within a probabilistic TSPA simulation) is relatively easy. Therefore, the effect of infiltration uncertainty was investigated further by changing the probabilities of the three infiltration cases ("base infiltration," "base infiltration divided by 3," and "base infiltration multiplied by 3"). In the base case, the probabilities are skewed to lower infiltrations, so that "infiltration divided by 3" has a 30 percent probability while "infiltration multiplied by 3" has a 10 percent probability. For this sensitivity analysis, the probabilities are reversed so that they are skewed to higher infiltrations: "infiltration divided by 3" is given a 10 percent probability and "infiltration multiplied by 3" is given a 30 percent probability. This change

increases the mean infiltration by approximately 50 percent. In the base case, the mean net infiltration averaged over the repository area is a little under 8 mm/year; in this sensitivity analysis the mean net infiltration is about 11 mm/year.

The distribution of peak dose rates over a 100,000-year period for this sensitivity case is compared with the base case distribution in Figure 5-4. There is surprisingly little difference in the two curves, with the base case being higher part of the time and the higher-infiltration case being higher part of the time. The means of the two distributions are nearly the same, both of them about 30 mrem/year. Other factors, such as seepage and waste package corrosion uncertainties, dominate both of these distributions.

5.1.3 Sensitivity to Mountain-Scale Unsaturated Zone Flow

As discussed in Section 3.1.2.3, the base case includes five calibrated, mountain-scale flow fields to account for uncertainty in net infiltration and hydrologic properties, plus the same cases calculated for projected future climates. Figure 5-5 shows a comparison of dose rates calculated for the five base case flow fields, with all other parameters

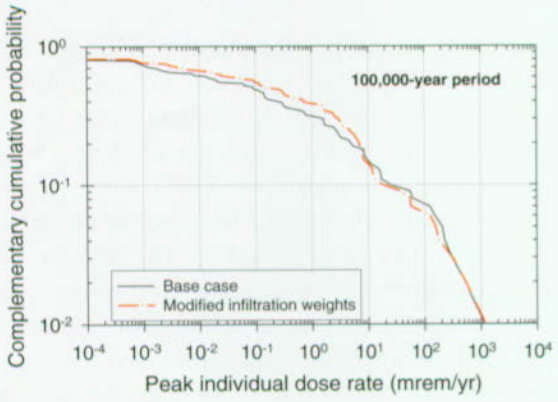

Figure 5-4. Comparison of the Base Case Dose Rate Results with a Sensitivity Case Involving Infiltration
Comparison of the base case peak-dose rate distribution with a sensitivity case in which infiltration probabilities are changed so that the mean infiltration is 50 percent higher.

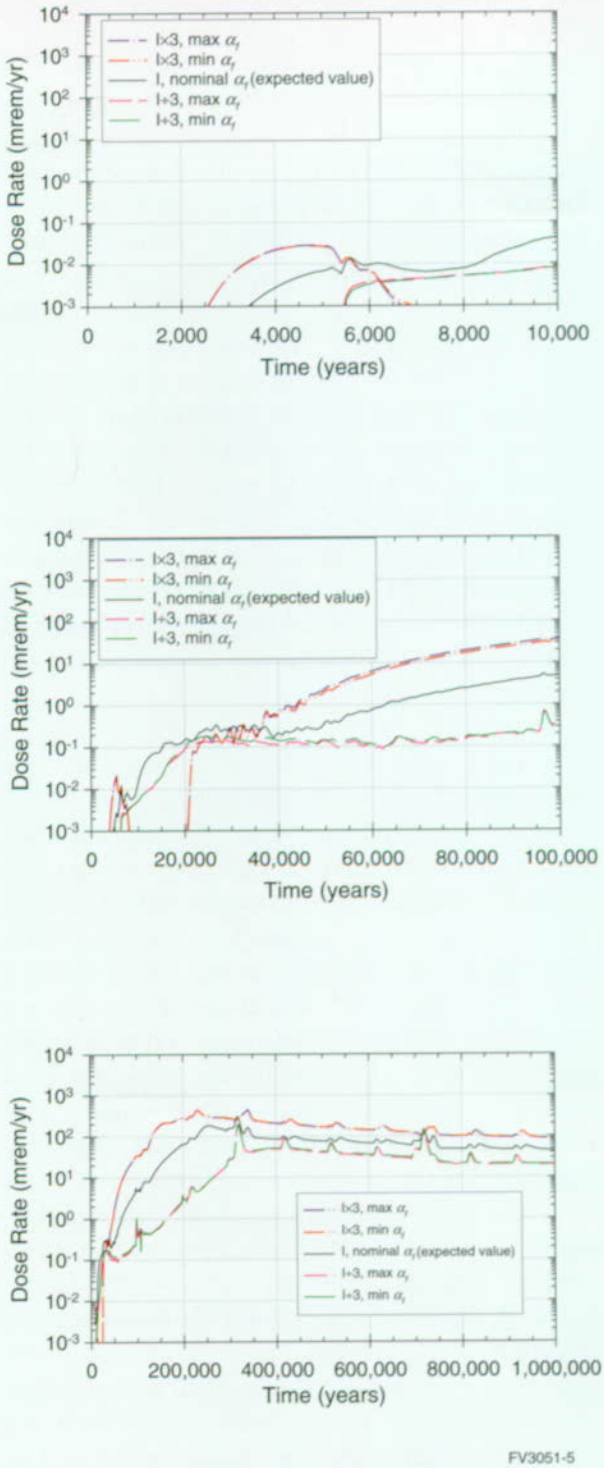

Figure 5-5. Total Dose Rate History Curves for the Five Base Case Flow Fields, with all Other Parameters Set to Their Expected Values
The middle curve is the expected value base case.

kept the same at their expected values. The infiltration varies from one-third of the base infiltration ("I ÷ 3") to three times the base infiltration ("I × 3"). The fracture air-entry parameter α_f (proportional to fracture aperture) varies over a range that is different for each hydrogeologic unit, but typically the range from minimum to maximum is one to one and one-half orders of magnitude. See CRWMS M&O (1998i, Sec. 2.4.3.2.2) for more detail. The curve marked "I, nominal α_f" is the expected-value base case.

Figure 5-5 shows a fairly large effect on dose rate from the variation in infiltration but very little effect from the variation in fracture air-entry parameter. These observations are consistent with those made for the effects on unsaturated zone groundwater travel time (Figure 3-11). However, most of the effect on dose rate from varying the infiltration is because of the corresponding change in the amount of seepage and not because of changes in transport times. One surprising aspect of the high-infiltration dose-rate histories is that, after an initial peak, the dose rate drops to a very low rate from approximately 7,000 to 20,000 years and is below the base-infiltration dose rate until about 35,000 years. This sharp drop occurs because temperatures are lower for higher net infiltrations (see Section 3.2.3), leading to lower corrosion rates and later onset of waste package failures because of corrosion (see Section 3.4). The initial peak in the high-infiltration dose rate at about 5,000 years is caused by releases from a juvenile-failure waste package; corrosion failures do not start contributing until after 20,000 years. The mean and low infiltration cases also have early releases from a juvenile-failure waste package, but releases from corrosion-failed waste packages follow soon thereafter (see Section 3.4).

Figure 5-6 shows a comparison of dose-rate histories for the expected-value base case and for a sensitivity case; the calculations are the same except that the base-infiltration flow field from the dual-permeability/Weeps model was used. Note that, for this set of calculations, the base case thermal-hydrology and waste package degradation results were used for the dual-permeability/Weeps runs in order to show the effect of the difference in

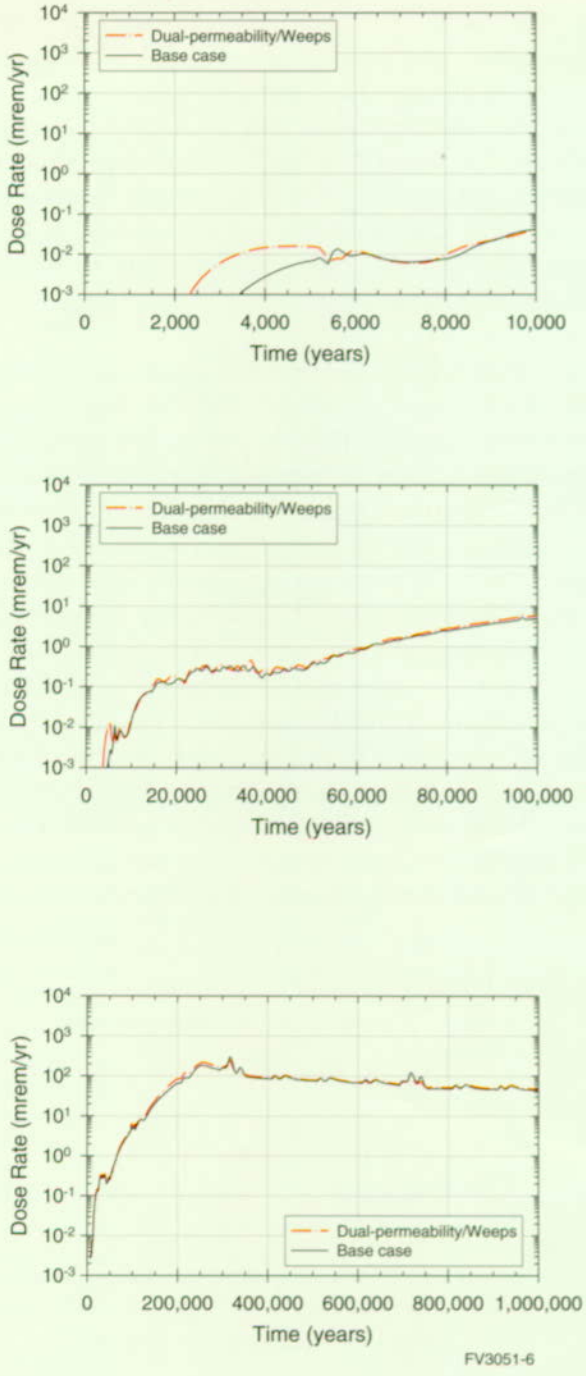

Figure 5-6. Comparison of the Total Dose Rate for Expected-Value Base Case with a Sensitivity Case that Used the Dual-Permeability/Weeps Flow Model Rather than the Base Case Flow Model
The two are nearly identical except that the dual-permeability/Weeps results show an earlier initial breakthrough.

mountain-scale flow only. Dual-permeability/Weeps results including more consistent thermal-hydrology and waste package degradation are given in Section 5.2. The dose-rate histories for the two cases in Figure 5-6 are nearly the same except for an earlier breakthrough and slightly higher early peak for the dual-permeability/Weeps case, both caused by the greater amount of fast fracture flow in the dual-permeability/Weeps model (see Figure 3-12).

A probabilistic comparison was also made between the base case flow model and the dual-permeability/Weeps flow model. Figure 5-7 shows the distributions of peak dose rate over 100,000 years. The two distributions are very similar except in the low-probability tail. About 3 to 4 percent of the time, the peak dose rates from the dual-permeability/Weeps model are significantly higher than the base case (about a factor of three higher). This increase in the lower part of the curve can be traced to transport of colloidal plutonium. Because of the greater prevalence of fast fracture flow in the dual-permeability/Weeps model, more of the colloids are able to travel through the system quickly to the biosphere for those realizations that have very mobile plutonium colloids. This happens a small

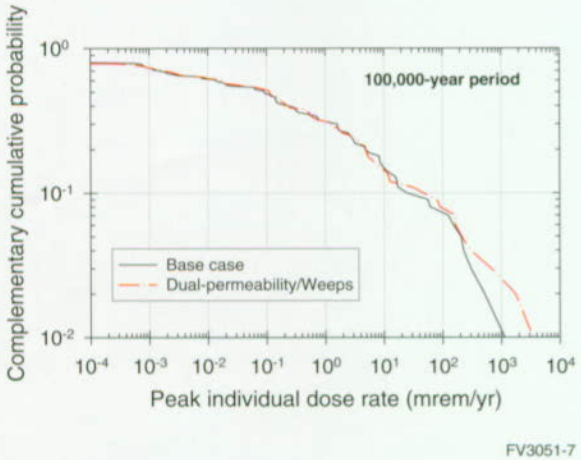

Figure 5-7. Comparison of the Base Case Peak-Dose-Rate Distribution with a Sensitivity Case in Which Dual-Permeability/Weeps Flow Fields are Used Instead of Base Case Flow Fields
About 3 to 4 percent of the time, the peak dose rates from the dual-permeability/weeps model are significantly higher than the base case because of faster transport of colloidal plutonium.

percentage of the time with the base case assumptions (see Section 4.3.1.1).

5.1.4 Sensitivity to Seepage into Drifts

The sensitivity of individual dose rate at 20 km (12 miles) from the repository to seepage into drifts is illustrated in Figure 5-8, which shows dose-rate time histories for three discrete cases: the expected-value base case plus runs in which seepage fraction (fraction of waste packages contacted by seeps) and seep flow rate are assigned values at the fifth and ninety-fifth percentiles of their probability distributions (see Figure 3-13), with all other parameters being held fixed at their expected values. The effect is strongest on the low end, with the fifth-percentile case having no waste package failures except for a single juvenile failure until after 700,000 years. The lack of waste package failures is a direct result of the very low seepage fraction—so low that no waste packages are wetted by seepage in the fifth-percentile case. Because the juvenile failure dominates radionuclide releases for the first 10,000 years, and juvenile-failure waste packages are always assumed to be contacted by seeps, the dose results are fairly similar for all three cases for the 10,000-year period (Figure 5-8, top), but for the 100,000-year and 1-million-year periods the dose results are quite different for the fifth-percentile case because of the lack of corrosion failures.

Because of the importance of seepage to the final results and the large uncertainty in the seepage model, several probabilistic sensitivity analyses were performed for seepage. Similar to the situation with infiltration and mountain-scale unsaturated zone flow, the process-model computations on which the TSPA-VA seepage model is based are very time consuming. However, the probabilities assigned to the various process-model cases can easily be modified to explore the impact on the final dose results.

The results of two kinds of modifications to the seepage-model inputs are presented here. One is to narrow the fracture-property distributions (i.e., assume that the fracture properties have less uncertainty than in the base case) and the other is to

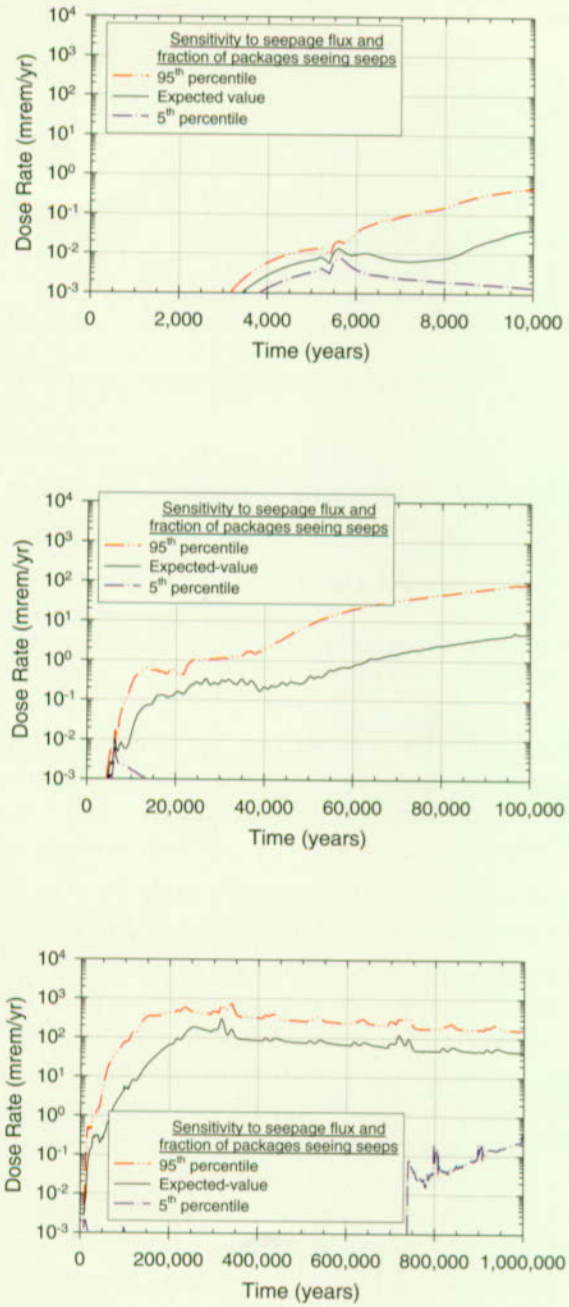

Figure 5-8. Total Dose Rate History Curves with Seepage Influence
Dose-rate history curves for the expected-value base case and cases that have seepage fraction and seep flow rate at the 5th and 95th percentiles of their base case distributions.

skew the distributions toward higher or lower fracture apertures.

As discussed in Section 3.1.2.4, three values of mean fracture permeability (k_f) and three values of fracture air-entry parameter (α_f) were used in the drift-scale flow simulations that were performed to calculate the amount of seepage into emplacement drifts. The base case probabilities for both parameters were assigned as (0.25, 0.5, 0.25); that is, the lowest value was weighted 25 percent, the middle value 50 percent, and the highest value 25 percent. The middle value is the preferred value, based on the available data, and the low and high values were chosen to span a reasonable range based on the variability in the data. For the first sensitivity analysis, the probabilities of the outlying values were cut in half, giving probabilities of (0.125, 0.75, 0.125). These probabilities emphasize the best-estimate parameter values considerably more. They are also reasonable, given what is known about fracture properties. Taking fracture permeability as an example, the base case probabilities imply a log standard deviation (i.e., the standard deviation of the logarithm of permeability) of 0.7, while the narrower distribution implies a log standard deviation of 0.5. These standard deviations are near the low and high ends of the observed range for air permeability measurements in the repository host rock (see Table 7.11 of Bodvarsson et al. 1997).

This modified set of probabilities was applied to the process-model results to generate new seepage distributions, and then calculations were rerun with the modified seepage distributions. The results are shown in terms of dose-rate history for the mean parameter values in Figure 5-9 and in terms of distribution of peak dose rates in Figure 5-10. This first sensitivity case is shown as the curves labeled "Narrower variance on fractures" in the figures. The results are not very different from the base case results, although the peak dose rates tend to be slightly smaller.

The other two curves shown in Figures 5-9 and 5-10 are for sensitivity cases with modified probabilities that represent systematically smaller or larger fractures. These cases could approximate

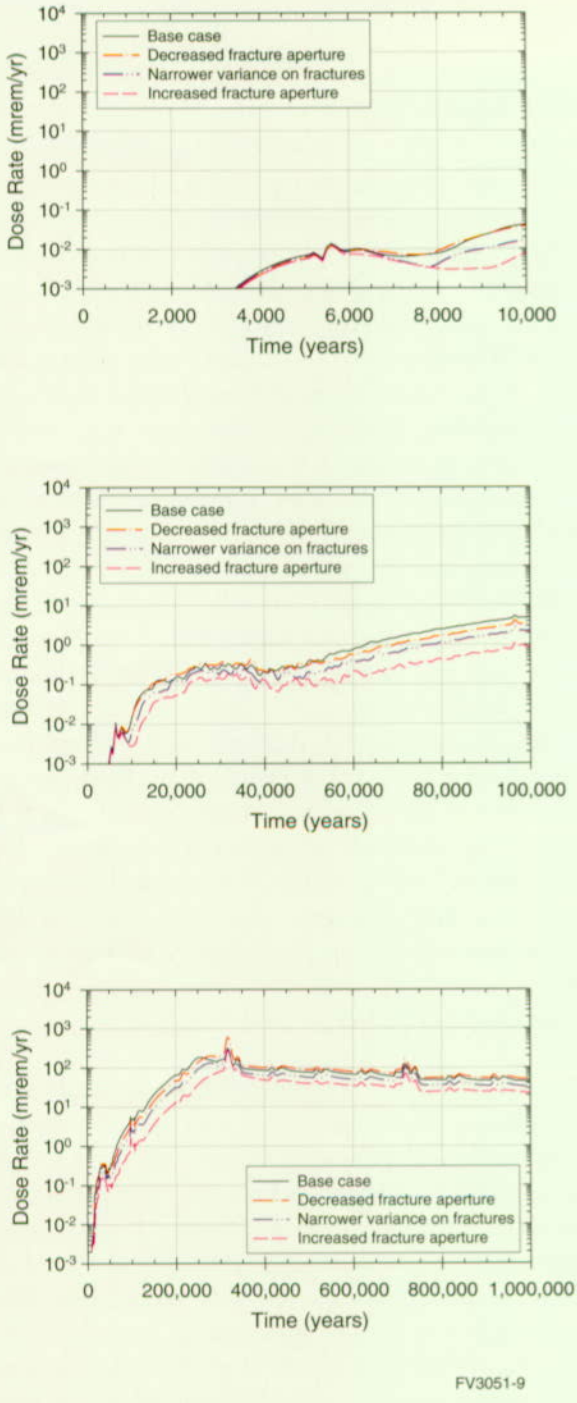

Figure 5-9. Dose Rate History Curves for Three Sensitivity Cases

Total dose-rate history curves for the expected-value base case and for three sensitivity cases in which the probabilities of the fracture-property inputs to the seepage model are modified.

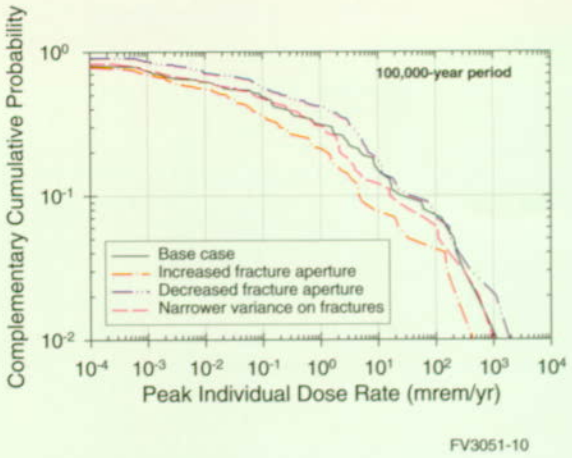

Figure 5-10. Comparison of Base Case Peak Dose Rate with Sensitivity Cases Involving Fracture Aperture

Comparison of the base case peak-dose-rate distribution with three sensitivity cases in which the probabilities of the fracture property inputs to the seepage model are modified.

the possibility of smaller or larger fracture apertures caused by thermal-hydrologic-chemical or thermal-hydrologic-mechanical processes. Smaller fracture apertures imply both lower k_f and lower α_f, because α_f is proportional to the effective fracture aperture and k_f is proportional to the cube of fracture aperture. Therefore, to simulate smaller fracture apertures, the probabilities for the parameter values were shifted to smaller values, giving (0.67, 0.33, 0) as the low, middle, and high parameter values. Similarly, to simulate larger fracture apertures the probabilities were changed to (0, 0.33, and 0.67). Time-history curves for the mean parameter values are shown in Figure 5-9 and the distributions of peak dose rate are shown in Figure 5-10. For smaller fracture apertures, the peak dose rates are somewhat higher, and for larger fracture apertures, the peak dose rates are somewhat lower. Basically, the probability shift to smaller apertures causes more seepage, and the shift to larger apertures causes less seepage. The differences in seepage are then reflected in the final dose results. None of these seepage sensitivity cases causes greatly different dose rates; the one that has the most effect is the increased-fracture-aperture case, which has peak dose rates lower than the base case by a factor of about 3 to 10 for the

100,000-year period, and somewhat less for the other two time periods.

5.2 THERMAL HYDROLOGY

The most important thermal hydrology issues are related to hydrologic parameters and fracture-matrix interaction and to repository design, including backfill, thermal load, and waste package spacing. Some variations in repository design were considered in this TSPA, including emplacement of backfill 100 years after emplacement of waste. Analyses of alternative designs are discussed in Section 4.5. Issues related to hydrologic parameters and fracture-matrix interaction are discussed in Section 5.1 on unsaturated zone flow. In most cases, the thermal-hydrologic implications of hydrologic issues such as climate change, infiltration uncertainty, hydrologic-property uncertainty, and alternative flow models were included. These issues are incorporated in the sensitivity analyses in Section 5.1, particularly in Section 5.1.3, where lower temperatures related to high infiltration rates are shown to have a strong effect on doses for approximately the first 20,000 years. One exception is the sensitivity to alternative conceptual models of mountain-scale unsaturated zone flow, exemplified by the dual-permeability/Weeps model. The results shown in Figures 5-6 and 5-7 were obtained using base case thermal hydrology rather than incorporating thermal-hydrology results calculated using the dual-permeability/Weeps model. Figure 5-11 shows results of a more consistent set of calculations, in which the dual-permeability/Weeps model was used for the thermal-hydrology calculations as well as for the mountain-scale flow calculations. In addition to the earlier breakthrough noted in Figure 5-6, the dual-permeability/Weeps dose rate in Figure 5-11 remains a little bit higher than the base case dose rate for approximately the first 250,000 years. The higher dose rate results from a slightly higher rate of waste package failures at early times, caused by small differences in temperatures and relative humidities.

Figure 5-11 also shows two sets of curves for the "thermal-hydrologic" property set that was mentioned in Section 3.2.3. The curves labeled

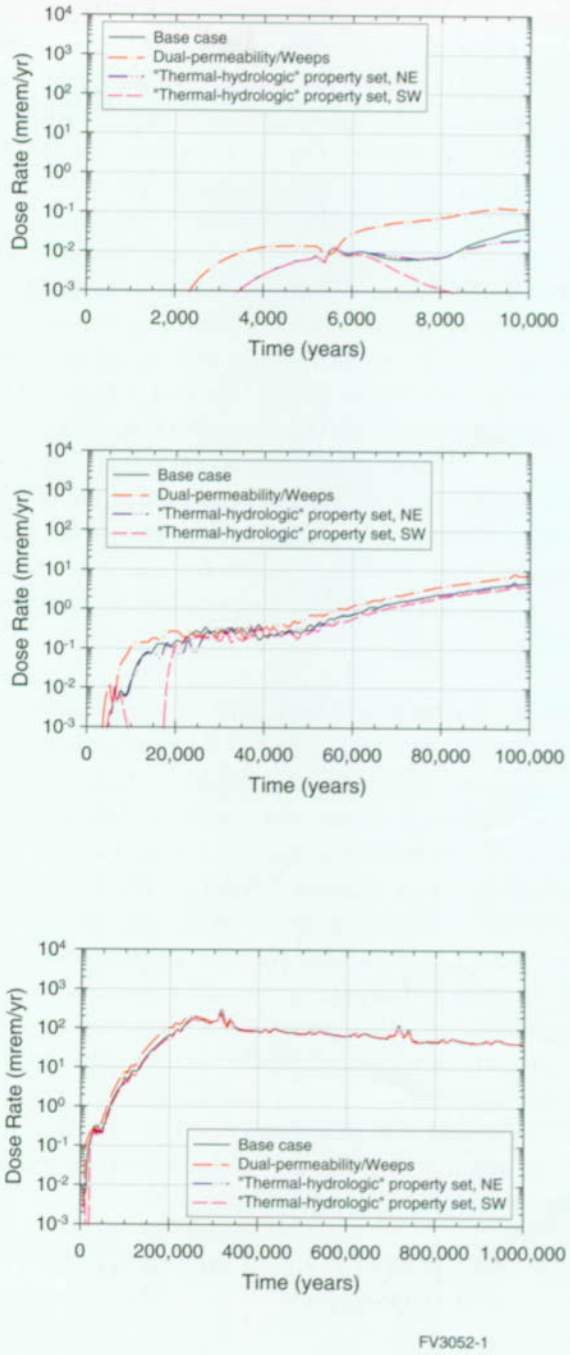

Figure 5-11. Total Dose Rate History Curves for the Expected-Value Base Case and for Three Sensitivity Cases in Which Different Hydrologic Properties Were Used
The greatest difference is for the case in which the "thermal-hydrologic" property set was used and temperature and relative humidity for Region SW (see Figure 3-20) were applied to the entire repository.

"NE" use the thermal-hydrologic results for Region NE for the entire repository, which was the approximation used for the base case (see Section 4.1.4), while the curves labeled "SW" use the thermal-hydrologic results for Region SW for the entire repository. For the base case, the results for Regions NE and SW are nearly the same, but for the thermal-hydrologic property set results for Region SW are significantly different for about the first 20,000 years. The difference is a result of significantly different matrix hydrologic properties for Region SW in the thermal-hydrologic property set (CRWMS M&O 1998i, Section 3.6.2). It is important to note that the large difference shown in Figure 5-11 exaggerates the actual effect, because of using the Region SW results for the entire repository. Region SW is actually rather small (see Figure 3-20), and the results for the rest of the repository are more like Region NE than Region SW.

Other potentially important issues—thermal-hydrologic-chemical and thermal-hydrologic-mechanical processes and effects—have largely been neglected. Some subsystem-level analyses of these effects are discussed in Section 3.2.1 of this volume, and in Section 3.6.8 of CRWMS M&O (1998i). At the system level, the effects of decreasing or increasing fracture apertures because of thermal-hydrologic-chemical or thermal-hydrologic-mechanical processes were evaluated approximately by modifying the seepage-model input parameters (see Section 5.1.4). The change in calculated peak doses was relatively modest, but these aperture changes do not necessarily represent the full range of possibilities.

5.3 NEAR-FIELD GEOCHEMICAL ENVIRONMENT

The models and results for the near-field geochemical environment component are discussed in Section 3.3. Analyses for the TSPA-VA base case used a water composition that represents the incoming, thermally perturbed fluid that reacted with corrosion products (iron oxides). Changes to the composition of this water as it reacts with freshly exposed spent nuclear fuel and subsequent alteration products were also evaluated in Section 3.3 and those analyses were used as part of the conceptual representation of secondary-phase evolution for the waste form (see Sections 3.5 and 5.5). Because concrete is a major component of the repository design, near-field geochemical analyses were also performed to simulate the reaction of concrete and water. These analyses and results (Section 3.3), although not part of the base case, are used for some of the sensitivity studies in this section. These sensitivity studies evaluate the effect of concrete on both the total system performance and the engineered barrier system performance. Near-field geochemical analyses were also used to develop the conceptual scenarios for sensitivity studies of other component models. The conceptual linkage between the near-field geochemical environment and the sensitivity studies for other TSPA components are discussed below, but the results of those analyses are provided in other sections as indicated below.

5.3.1 Sensitivity of Water Composition to Spent Fuel Alteration

For periods in which water composition is dominated by spent nuclear fuel reactions, different source-term constraints may be necessary than for periods of unaltered water composition. Spent fuel dissolution rates, radionuclide solubility limits, and radionuclide transport (colloidal and aqueous) should particularly reflect the altered solution composition. The impacts on performance from reaction with spent nuclear fuel depend on the magnitude of the water composition changes and the period over which the changes exist.

The near-field geochemical analyses showing the effects of spent-fuel reaction on water composition are presented in Section 3.3.3. Those results indicate that the water composition will change the most where most of the fuel is available for reaction, with lesser effects if only a portion of the fuel is exposed to the water. In addition, maintaining such water composition changes depends on active alteration of primary spent nuclear fuel to secondary uranium phases. Once the fuel is completely altered, the secondary-phase evolution causes only minor changes to water composition. The modeled period for completely

altering the spent nuclear fuel once it is exposed is about 1,000 years for the analyses discussed in Section 3.3.3, but the calculated evolution of secondary phases continues over hundreds of thousands of years. These time differences indicate that reaction of spent nuclear fuel with water will produce either major changes to the fluid composition for relatively short times or minor effects over longer times. For the latter case, the current representations should be sufficient to bound the behavior of radionuclide release from the waste form. For the former case, the analyses could be improved by considering a short time period when water composition is dominated by releases from spent nuclear fuel followed by evolution of secondary uranium phases over geologic time.

Although changes to both solubility limits and colloid stabilities have not yet been evaluated for the geochemical conditions during the period of active alteration, changing spent nuclear fuel dissolution rates are explicitly coupled to changing water chemistry in the completed near-field geochemical analyses. Because of the potential for incorporating other actinides (for example, neptunium) into the secondary uranium phases, the primary focus of these sensitivity studies was the long period of secondary-phase evolution. Also, these secondary phases dissolve or alter at a much lower rate than the primary spent nuclear fuel (Section 3.5.3). The model incorporating neptunium into secondary uranium minerals and the resulting rates of release of uranium and neptunium is presented in Section 3.5. The results of sensitivity studies using secondary-phase constraints on releases of both uranium and neptunium over long time frames are shown in Section 5.5.

5.3.2 Sensitivity to Concrete-Modified (Alkaline) Water Compositions

This section provides a discussion of the effect of concrete modified water on performance. The components affected by the concrete-modified water are described followed by performance results for such a system.

5.3.2.1 Components Affected by Concrete-Modified Water

The near-field geochemical analyses for the composition of water reacting with concrete support components in the emplacement drifts indicate that water will have a pH near 11 for at least 10,000 years but for much less than 100,000 years. This pH change represents a substantial change to ambient water composition and may affect the ability of the engineered barrier system to contain radionuclides within the drift. This would in turn change the source term for total system performance analyses. In addition, higher pH fluids migrating into the geosphere can react with the host rock, potentially altering minerals along flow paths and providing an aqueous medium that enhances actinide transport in the unsaturated zone. Both of these aspects of the analysis were assessed with sensitivity studies. As described in the following paragraphs, impacts on the source term and the engineered barrier system were explicitly addressed based on the changed fluid composition. The impacts on transport through the geosphere were evaluated through simulations using conservative assumptions.

Source Term and Engineered Barrier System. The effects of concrete-modified water on a number of the components related to the source term have been explicitly evaluated. The waste package corrosion models (Section 3.4) include a submodel for aqueous corrosion of the outer barrier, specifically designed to address pH conditions above 10. This submodel was used to generate a set of waste package degradation histories for concrete-modified water. These waste package models and results are presented in Sections 3.4 and 5.4. The waste form dissolution models directly incorporate rates that depend on pH and total dissolved carbonate (Section 3.5). Changes to the ionic strength for concrete-modified water were reflected in changes to colloid amounts (Sections 3.3 and 3.5). These results are provided directly to the TSPA integration model, and impacts on performance were analyzed in a sensitivity analysis based on the expected value compositions for concrete-modified water. The effects on the source term are presented in the following paragraphs of this section. Additional

discussion of these results that are related to changes in waste package degradation is included in Section 5.4.

Transport Through the Geosphere. The migration of alkaline fluids into the unsaturated zone may have a number of effects, depending on the flow pathway and diffusion rates. Such fluids can alter the siliceous host rock, both along fracture pathways and in the matrix. The mineralogical changes, the distance over which they may occur, and the distribution of such alterations are still very uncertain but could produce changes in the amount of fracture-matrix interaction and the sorption of radionuclides within the unsaturated zone host rock (CRWMS M&O 1998i, Chapters 4 and 7). Because of the complex and uncertain nature of this alteration, current process models do not include any explicit representation of these potential changes to minerals along radionuclide migration pathways. In addition, the migration of a high-pH (alkaline) plume through the unsaturated zone would create aqueous pathways with little or no actinide sorption capability (CRWMS M&O 1998i, Chapters 4 and 7). Also, this potential effect has not been incorporated explicitly into process models. Because of the likelihood that alkaline fluids will be generated by water in contact with concrete in the repository (Section 3.3.3), this effect was included in sensitivity analyses. To bound the consequences of this effect, the unsaturated zone sorption coefficients for actinides (uranium, neptunium, plutonium, and protactinium) were set to zero (Section 5.6). The changes to dose rates specifically caused by impacts to transport in the unsaturated zone, as well as the changes caused by combining the impacts to the source term with the transport impacts, are presented in Section 5.6.

5.3.2.2 Effect on Dose Rate and Engineered Barrier Release Rate

In this section, sensitivity analyses are presented based on changes to the source term only (waste package degradation and waste form degradation) caused by concrete-modified water.

Release Rate from the Engineered Barrier System. The expected value release rates from the engineered barrier system for the total activity of nine main radionuclides (carbon-14, selenium-79, technetium-99, iodine-129, protactinium-231, uranium-234, neptunium-237, plutonium-239, and plutonium-242) through 10,000 years are shown in Figure 5-12. The rates for both the concrete-modified water case and the base case are shown. In Figure 5-12, the total activity release rate for the concrete-modified water case is higher than that for the base case for all times to 10,000 years. Early in this period, the difference is about two to three orders of magnitude but is only about 1.5 orders of magnitude at 10,000 years. For the concrete-modified water case, the peak total release rate from the engineered barrier system is increased by slightly more than three orders of magnitude over that for the base case. These two peaks both occur at about 5,200 years, reflecting the climate change that is imposed at 5,000 years. These higher total release rates from the engineered barrier system primarily reflect a larger amount of exposed inventory at earlier times caused by higher rates of waste package degradation (see Section 5.4).

The differences between these two cases become less extreme between 10,000 years and 100,000 years, as shown in Figure 5-12. The release rate in the engineered barrier system for the concrete-modified water case is a factor of two to six times higher than for the base case after about 15,000 years. The individual radionuclide contributions to the total activity release rate for the concrete-modified water case over the three time frames are shown in Figure 5-13. Technetium-99 is the major component of this total activity release rate for the entire time. At times less than about 15,000 years, carbon-14 and iodine-129 were the next highest contributors. At times greater than 30,000 years, plutonium-239 and neptunium-237 were the second and third largest contributors, respectively, to the total activity release rate. The activity release rates for these radionuclides increase in a relatively uniform manner over the base case results because of an increase in the inventory available for release compared to the base case.

Dose Rate at the 20-km (12-mile) Boundary (Accessible Environment). The increases in the source term directly impact expected-value dose

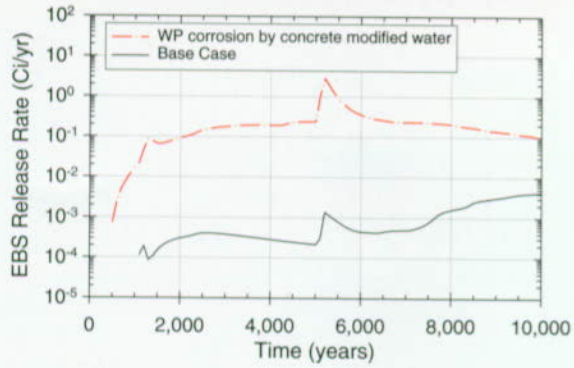

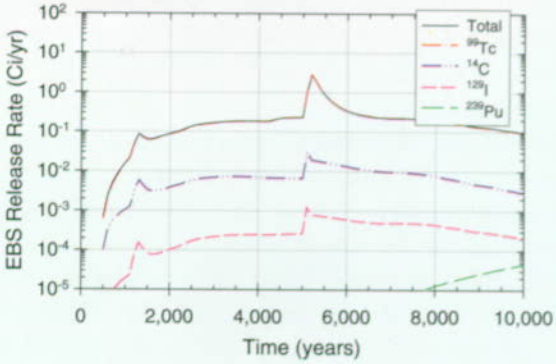

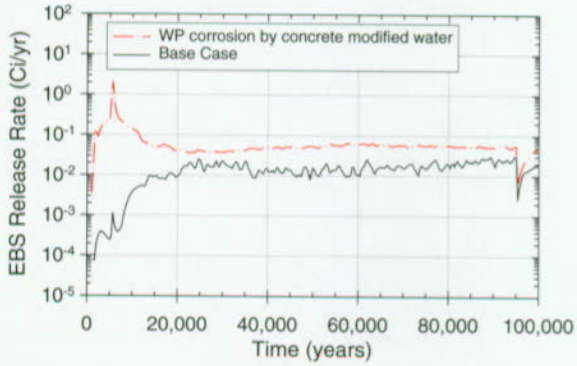

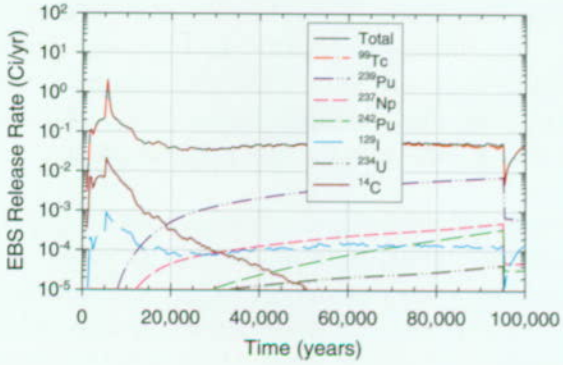

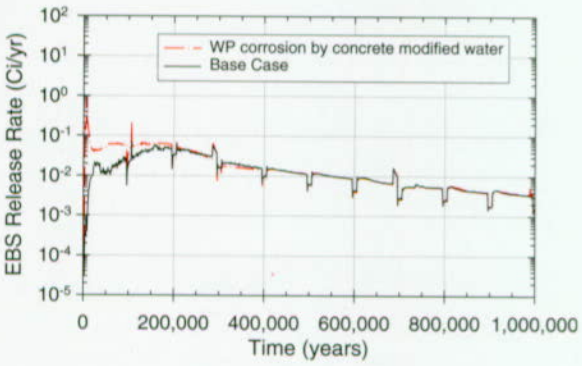

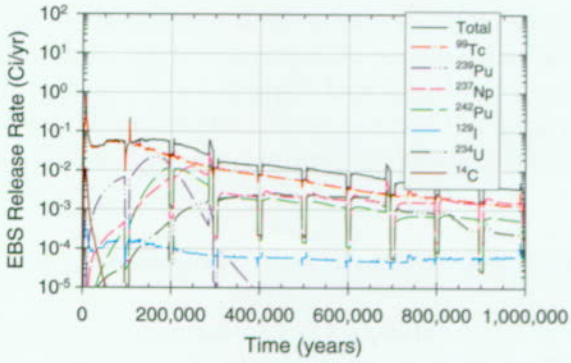

FV3053-1

FV3053-2

Figure 5-12. Comparison of Expected-Value Total Release-Rate Histories from the Engineered Barrier System for Concrete-Modified Water and the Base Case
The release rates include the total activity of nine radionuclides.

Figure 5-13. Expected-Value Time Histories for Individual and Total Radionuclide Release Rates from the Engineered Barrier System for the Concrete-Modified Water Case

rates at the 20-km (12-mile) boundary, which are shown in Figure 5-14 for both the concrete-modified water case and the base case over 10,000 years, 100,000 years, and 1 million years. The orders-of-magnitude increases in activity release rate for the engineered barrier system are reproduced in the orders-of-magnitude increases in expected values of dose rate over 10,000 years. Note that for the concrete-modified water case, the peak value at about 6,100 years is slightly more than three orders of magnitude higher than the values for the base case at that time. One qualitative change that can be seen for the concrete-modified water case in Figure 5-14 is that the peak dose rate at about 6,100 years is the peak dose rate over the first 100,000 years after repository closure; this is not true for the base case results. Figure 5-14 also shows that the expected value dose rate histories for these two cases later converge, similar to the source term behavior.

In the concrete-modified water case for the 10,000-year time frame, technetium-99 is the major dose contributor as well as the major contributor to activity release rate from the engineered barrier system. At times approaching 100,000 years, plutonium-239 and neptunium-237 are the biggest contributors to dose rate, even though technetium-99 was still the largest contributor to the activity release rate for the engineered barrier system. Further discussion of the impacts on the engineered barrier system and system performance as evaluated in the sensitivity analyses for concrete-modified water is given in Sections 5.4, 5.5, and 5.6.

5.4 WASTE PACKAGE DEGRADATION

The key uncertainties in the waste package degradation analyses were identified in Sections 3.4 and 4. The results in Section 4 indicate that the general corrosion rates for Alloy 22 under dripping conditions are a key determinant of overall performance. These corrosion rates are highly uncertain. The corrosion rates provided by the experts have a range of more than five orders of magnitude. This is mostly caused by a lack of information on local chemical and electrochemical conditions on Alloy 22 and limited experience with the alloy.

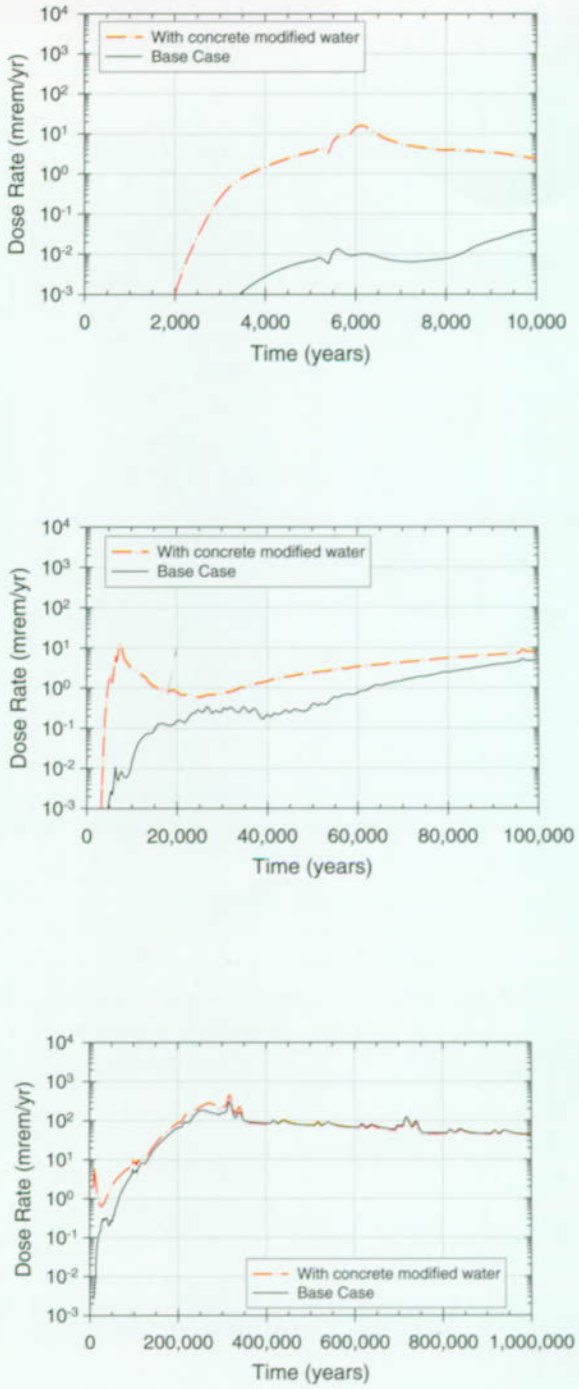

Figure 5-14. Comparison of Expected-Value Total Dose-Rate Histories for the Concrete-Modified Water Case and the Base Case

Also, the effect of the emplacement environment on waste package degradation has been identified as very important, especially in terms of overall performance of the potential repository. The number of waste packages that will be exposed to dripping water, the percentage of the waste package surface that gets wet in the dripping zones, and the chemistry of the drift seepage are also uncertain factors in the analyses. The effects of these uncertainties on repository performance are evaluated in the following sensitivity cases. In addition, the importance of juvenile failures on system performance is evaluated. A final sensitivity analysis is presented concerning the effect on total dose of the corrosion patch size, which is the area over which the corrosion model parameters are relatively constant.

5.4.1 Sensitivity to Uncertainty/Variability Assumptions in Alloy 22 General Corrosion Rates

There are limited data for the general corrosion rate for Alloy 22. However, the corrosion rate over long periods is highly uncertain due to limited experience with the material and lack of information on local exposure conditions on the inner barrier. Panelists for the waste package degradation expert elicitation (CRWMS M&O 1998b) estimated the Alloy 22 general corrosion rate and the allocation of the total variance to its variability and uncertainty. The effect on dose of the corrosion rate variability among waste packages and patches and the corrosion rate uncertainty on waste package failure was evaluated by splitting the total variance into three different variability and uncertainty combinations: 75 percent variability and 25 percent uncertainty, 50 percent variability and 50 percent uncertainty, and 25 percent variability and 75 percent uncertainty. For each variability and uncertainty split, the median general corrosion rate was sampled from the 5th, 50th, and 95th percentile of the uncertainty variance respectively. This sampling scheme creates a matrix of nine pairs of values for the median general corrosion rate and the degree of variability in the corrosion rates when spread over corrosion patches on a given package and from package to package.

The expected-value base case described in Section 4.2 allocates a split of 50 percent variability and 50 percent uncertainty of the total variance, with the median general corrosion rate at the 50th percentile of the uncertainty variance. The results for the cases with different variability-uncertainty splits and the median general corrosion rate at the 50th percentile of the uncertainty variance show a difference in the performance of the waste package, with a large spread in the failure times and rates (CRWMS M&O 1998i). The results for the base case variability-uncertainty split (50/50) with the median corrosion rate sampled at the 5th, 50th, and 95th percentile from the uncertainty variance show a considerable difference in waste package failure rate, as indicated in Figure 5-15. The failure curves in this figure are shown only for the waste packages that are dripped on. The impact of this range of Alloy 22 general corrosion rate on the uncertainty range of dose rate is demonstrated in Figure 5-16 for the TSPA-VA base case. These dose rate histories further confirm the results shown in Figure 4-34 that the Alloy 22 corrosion rate has more impact on dose than most other TSPA-VA model parameters, especially over the 10,000-year and 100,000-year periods.

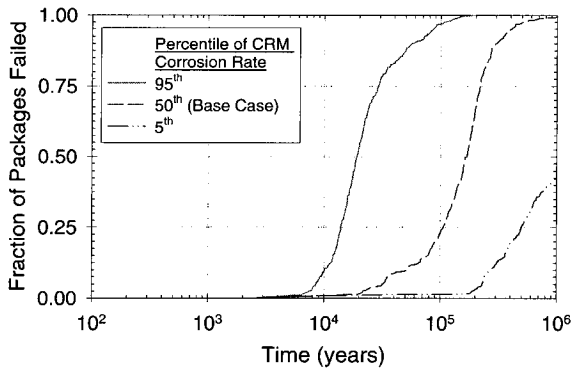

Figure 5-15. Effect of Uncertainty in Alloy 22 Corrosion Rate on Package Failure Time
The effect on waste package degradation is shown for the 5th, 50th and 95th percentile corrosion rates for Alloy 22.

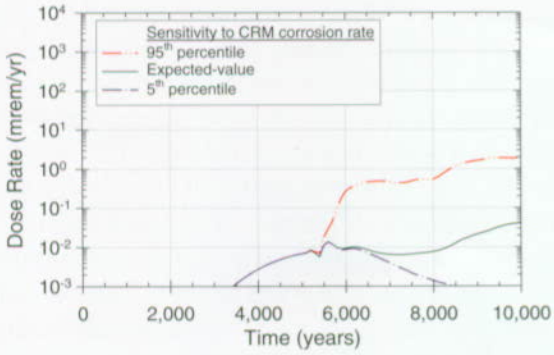

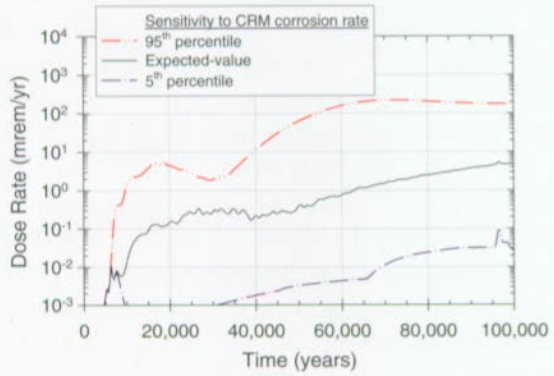

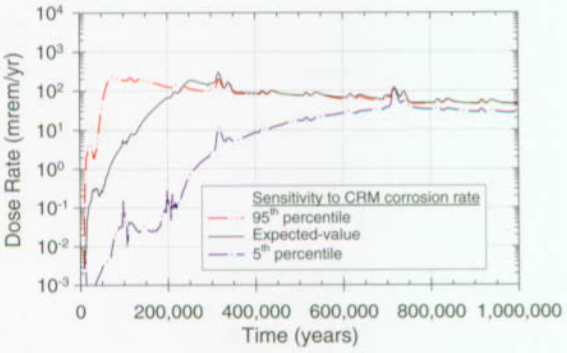

FV3054-2

Figure 5-16. Effect of Uncertainty in Alloy 22 Corrosion Rate on Total Dose Rate
Results are shown for the 5th, 50th, and 95th percentile corrosion rates for Alloy 22 for the base case uncertainty distribution.

5.4.2 Sensitivity to Environment (Drip Versus No Drip Conditions)

Waste package degradation is sensitive to the impacts of water dripping onto the waste package, as noted in Section 3.4. The general corrosion rate of Alloy 22 is extremely low under moist conditions (a thin water film on the surface, but no flowing water), but the material may undergo a more rapid, although still relatively slow, general corrosion under dripping conditions. Figure 5-17 shows the difference in waste package degradation for the two conditions in the base case. The first penetration of the waste packages in the dripping zone occurs several hundred thousand years before penetration of the waste packages that are not dripped on. Only a small fraction of the waste packages in the nondripping portion of the repository are penetrated over 1 million years, while the simulation indicates nearly 100 percent of the waste packages in the dripping zone develop at least one penetration.

5.4.3 Sensitivity to Percent of Waste Package Surface Wetted Under Dripping Conditions

Uncertainty about seepage into the drift, and subsequently onto waste package surfaces, is present at a variety of different spatial-temporal scales. A

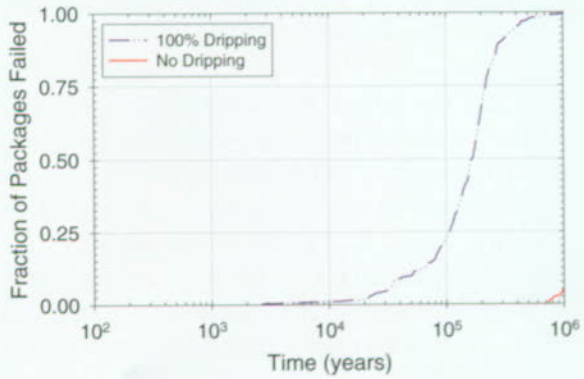

Figure 5-17. Effect of Dripping Conditions on Waste Package Failure for the Base Case
Waste packages in dripping conditions fail more rapidly than those in nondripping zones.

variety of different alternative models might be imagined for the percentage of waste package surface area that is wet as a function of time and location. To determine the sensitivity of performance to the wetted surface area, three different models have been examined. These three cases represent a combination of two main factors: percent of waste package area corroded and percent of drift seepage that enters the package through the corroded area and subsequently interacts with all the exposed (i.e., non-clad) fuel:

1. *TSPA-VA base case.* In this case 100 percent of the surface area of a dripped-on package is assumed to be dripped upon and to corrode under dripping conditions for all time. The flux of dripping water that is allowed to flow through the waste package is set equal to the flux of water seeping into a drift multiplied by the combined patch-pit area divided by the total waste package surface area. This seeping water flowing through the package is assumed to interact with all the exposed waste in the package (i.e., all waste that is either unclad or whose cladding has failed). The conceptual scenario most suited for this model is one where a spatially focused seep moves back and forth across the package on a rather short time scale such that it contacts the entire package area (at least the top half of the package) within this short time span, say, within 100 years, which is the numerical timestep size for the total system model. As the seep moves, sometimes it will encounter a fully corroded patch or pit and is able to flow through the package and sometimes it will encounter a still-intact area of the package surface and be unable to enter. (This model is mathematically equivalent to assuming that the seep is spread uniformly across the entire package area at all times, such that the flux of water able to enter the package is proportional to the fully corroded area.)

2. *Ten-percent-wet model.* In this case it is assumed that only 10 percent of the waste package surface area ever corrodes under dripping conditions throughout time. Further, the fraction of drift-seepage water that can enter the package and interact with all the non-clad waste is equal to the combined patch-pit area divided by one-tenth of the total package surface area. The conceptual model corresponding to this case is that a seep does not move with time and has a high enough flux that it splashes over 10 percent of the package area. Then the fraction of drift seepage able to enter the package is limited by the corroded area. Equivalently, it could be a narrow focussed seep that only moves back and forth across 10 percent of the surface area, sometimes encountering a fully corroded patch and sometimes not. (The scenario where the flux entering the package is not scaled by the corroded area but is equal to the entire drift seepage is discussed in Section 5.5.)

3. *One-percent-wet-model.* In this case it is assumed that only 1 percent of the waste package surface area ever corrodes under dripping conditions throughout time. This would be the conceptual scenario of an even more spatially concentrated seep that does not move with time. Furthermore, although the fraction of drift seepage water entering the package is again scaled by the combined patch-pit area (specifically, equal to this patch-pit area divided by one-hundredth of the total waste package surface area), the scaling for this scenario results in almost all the drift seepage entering the package. Specifically, one patch has an area approximately equal to 1/1,000 of the total package area. Dividing this by the 1/100 of the package area exposed to dripping yields a factor of 0.1, which would mean that one-tenth of the drift seepage enters the package and reacts with all the non-clad fuel. However, for the expected-value base case realization, the seepage collection factor mentioned in Section 4.3.2.2 is equal to 5.5, which when multiplied by the 0.1 yields 0.55. This means that about one-half of the drift seepage flows through the waste package

in this case. (Note that the collection factor is applied in all three of the above cases.)

Figure 5-18 shows the waste package failure curves for the above three scenarios. Generally, fewer waste packages fail, and waste packages fail later when a smaller percentage of the waste package surface is assumed to get wet. Figure 5-19 shows the effect on dose rate for these three dripping scenarios. The effect is generally small at all three time scales and seems to be an unimportant uncertainty as far as total system performance is concerned.

5.4.4 Sensitivity to High-pH (Concrete-Modified) Seepage Water

The base case does not include the effect of seepage water interacting with the concrete drift lining, because the assumption in the base case is that the drift lining collapses very early in the simulation. The simulations of geochemical conditions reported in Section 3.3 indicate that seepage water may have a high pH (>10) for some time, because the seepage water interacts with the concrete drift lining. The sensitivity of waste

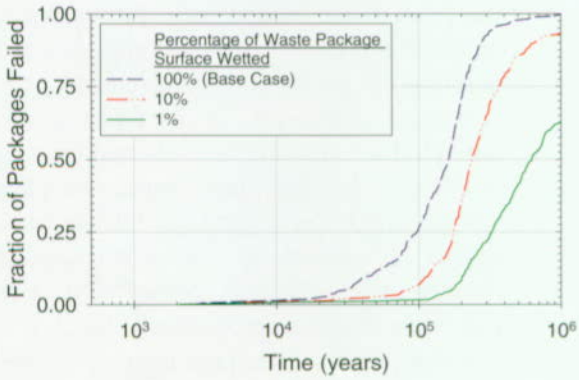

Figure 5-18. Waste Package Degradation Curves for Different Percentages (Alternative Models) of Wetted Surface Area
a) 100 percent of surface area corrodes under dripping conditions (base case), b) 10 percent of surface area corrodes under dripping conditions, and (c) 1 percent of surface area corrodes under dripping conditions. (WP—waste package)

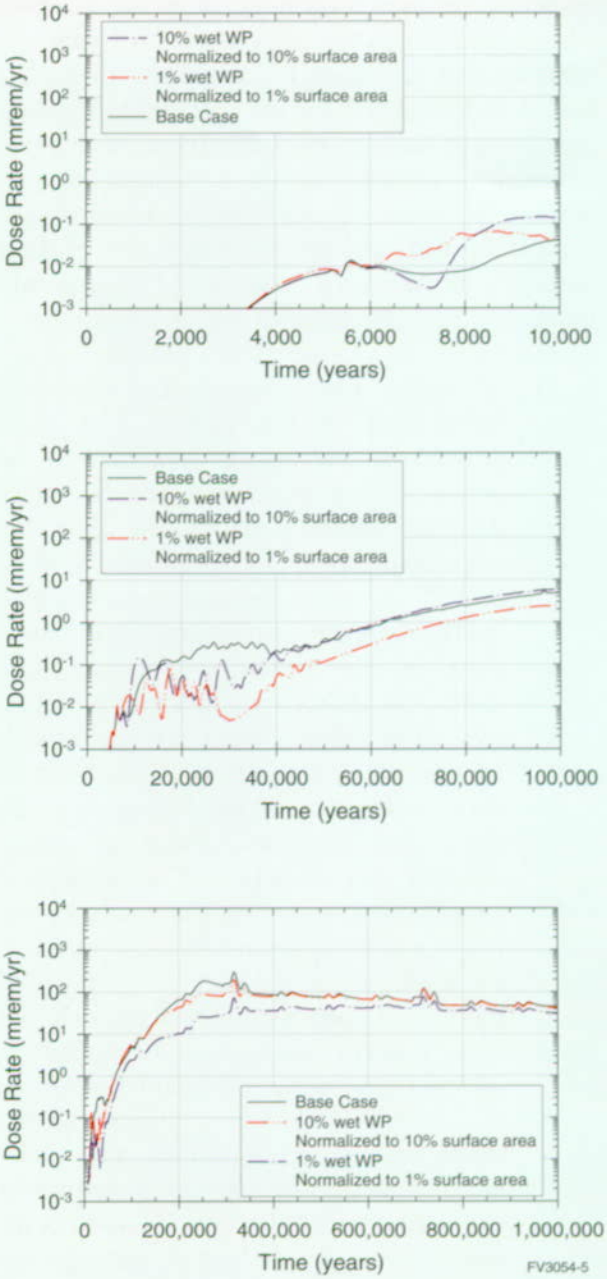

Figure 5-19. Total Dose Rate Histories for Different Percentages (Alternative Models) of Wetted Waste Package Surface Area
a) 100 percent of surface area corrodes under dripping conditions (base case), (b) 10 percent of surface area corrodes under dripping conditions, and (c) 1 percent of surface area corrodes under dripping conditions. For all of these models the fraction of drift seepage entering the package is proportional to the fully corroded surface area divided by the fraction of the area that is wetted (i.e., either 1.0, 0.1, or 0.01) times the seepage collection factor.

package degradation to elevated pH of incoming water is shown in Figure 5-20. As discussed in Section 3.4, while the seepage water pH > 10, the carbon-steel outer barrier undergoes high-aspect ratio pitting corrosion, which fails the outer barrier shortly after corrosion starts. The early failure of the outer barrier leads to early, rapid failure of the waste package because of higher probability of localized corrosion of the inner barrier and associated early release of radionuclides. At later times, the dose from the two cases is not significantly different, because advective release rates through patch openings from general corrosion would be about the same. The one-year data for carbon steel in a concentrated J-13 water condition underway at Lawrence Livermore National Laboratory in Livermore, California, do not show such high-aspect ratio pitting corrosion (McCright 1998). The testing solution is maintained at pH 9.7. Mixed anions in the concentrated testing solution may prohibit pitting corrosion of carbon steel even in such elevated pH conditions. Thus, the current pitting model from the expert elicitation may be unrealistically conservative.

The effect of the high-pH alternative model on dose rate at 20 km (12 miles) has already been demonstrated in Figure 5-14 where it was found to have a very large effect within the first 10,000 years. But, again this is based on corrosion model for carbon steel that is probably overly conservative.

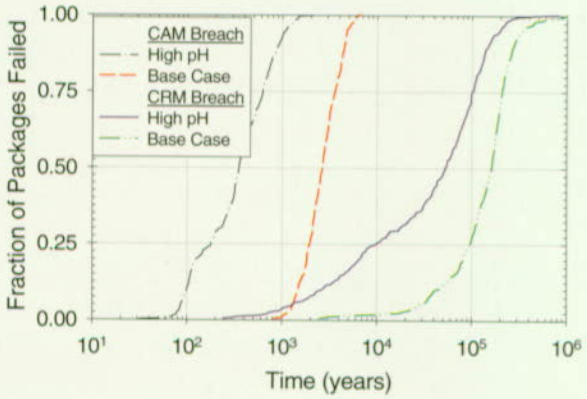

FV3054-6

Figure 5-20. Effect of High-pH (Concrete-Modified) Seepage Water on Waste Package Degradation
The high-pH alternative model has a major effect on waste package degradation at early times.

5.4.5 Sensitivity to Microbiologically Influenced Corrosion

Microbiologically influenced corrosion was not included in the base case in part because the potential for this corrosion of the waste packages was discounted in the recent expert elicitation (CRWMS M&O 1998b). However, the process has uncertainty and could affect long term performance. In order to assess this uncertainty on repository performance an alternative model for microbiologically influenced corrosion effects on corrosion allowance material corrosion was implemented.

In this sensitivity analysis, sustained and sufficient microbe activities are assumed to exist all the time in the postclosure repository at a level high enough to affect waste package corrosion. The Waste Package Degradation Expert Elicitation Expert Panel generally agreed that Alloy 22 would not be affected by the microbiologically influenced corrosion, thus it was assumed only the corrosion allowance material is affected by the microbiologically influenced corrosion. In addition, since drips are required for microbe growth (as indicated by the expert panel), microbiologically influenced corrosion is assumed to be operative only for the dripping case.

The sensitivity analysis was conducted using a simple microbiologically influenced corrosion-enhancement factor (or multiplication factor) to the corrosion allowance material general corrosion rate. The enhancement factor was derived from the corrosion current differences between inoculated and "sterile" samples that were measured at ambient temperature (Horn et al. 1998). This study reported an increase of the corrosion current of five- to six-fold for the inoculated samples over the sterile samples. For this analysis the enhancement factor to the corrosion allowance material general corrosion rate was assumed to have uniform distribution between 1 and 5. In the simulation, the factor was sampled randomly from the distribution

and applied as a multiplier to the corrosion allowance material aqueous general corrosion rate. The simulations were conducted with the base case parameter values: NE region, spent nuclear fuel waste packages, always dripping, and 100 percent of the surface wetted by drips.

The effect of microbiologically influenced corrosion on waste package failure time is shown in Figure 5-21 and shows that early failures are significantly increased but the average failure time is not changed that much. The early exposure of the corrosion resistant material from the early corrosion allowance material breaches results in an earlier waste package breach initiation and a substantially greater number of breached waste packages. Compared to the base case results, much more extensive pit perforation is predicted for the microbiologically influenced corrosion case; however, there is not much difference in the patch perforations by corrosion resistant material general corrosion. The effect of microbiologically influenced corrosion on peak dose rate is very similar to the effect of concrete-modified water (Figure 5-14) and is shown in Figure 5-22 for the three periods. The main effect on peak dose rate is the large (over two orders of magnitude) increase in the first 10,000 years due to more aggressive degradation of the carbons steel outer barrier.

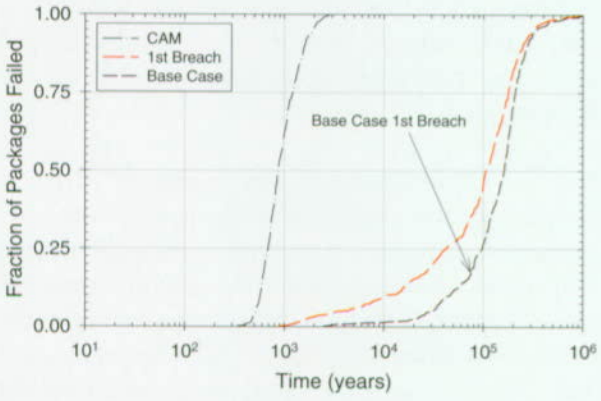

Figure 5-21. Effect of Microbiologically Influenced Corrosion on Waste Package Degradation
The microbiologically influenced corrosion alternative model has a major effect on waste package degradation at early times. (CAM—corrosion allowance material)

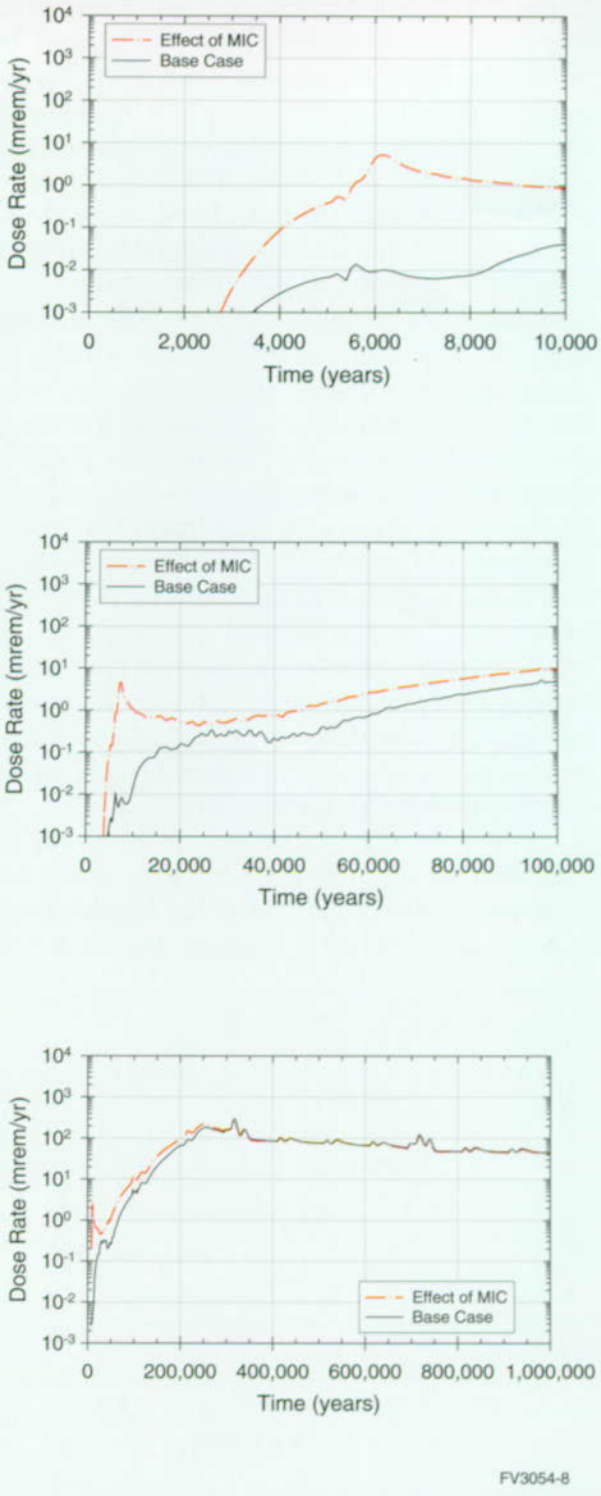

Figure 5-22. Total Dose Rate Histories for Microbiologically Influenced Corrosion Waste Package Degradation Versus the Base Case
The effect is similar to the high-pH alternative model. (MIC—microbiologically influenced corrosion)

5.4.6 Sensitivity to Juvenile Failures

Another uncertainty in the waste package degradation model is the number of early, or juvenile, failures that may occur in the repository. The effect of such failures is also uncertain. Failure could be a merely a slight crack in the waste package that provides a little opening for radionuclide transport out of the waste package or a more general failure such as that caused by corrosion patch failure. The expected-value base case assumes that a single waste package fails at 1,000 years in a dripping zone. The failure is assumed to be one general corrosion patch (about 300 cm^2) that allows advective release to begin at the failure time. This juvenile-failure model implemented in the base case has an effect on the early-time dose, as expected but does not affect the long-term peak dose. This is demonstrated in Figure 5-23 which compares the base case model to a case (alternative model) where there are no juvenile failures. The effect of juvenile failures is to cause earlier appearance of radionuclides at the 20-km (12-mile) boundary, by about two to three thousand years. The 95th percentile, juvenile-failure scenario in the TSPA-VA base case, which assumes that eight waste packages fail at 1,000 years, is also shown in Figure 5-23. It indicates that the early-time peak dose rate increases by about eight times but there is no affect on the long-term dose.

5.4.7 Sensitivity to Corrosion Patch Size

In the waste package degradation model, the size of the corrosion patches used in the stochastic waste package degradation to model general corrosion of Alloy 22 is also uncertain. The individual patches are intended to represent a minimum area on the waste package, that has a uniform, local exposure condition and thereby uniform general corrosion rate within a patch. The base case corrosion patch size is assumed to be 310 cm^2 (48 $in.^2$), close to the surface area of the standard atmospheric corrosion test coupon, or sample. The total number of corrosion patches on a single waste package for the base case is assumed to be 964.

If the patch size is increased by a factor of 10, there are early failures because there are more pits per patch, which leads to early pit failure. But the average waste package failure time for dripping conditions is later than the base case, and the number of waste packages failing in 1 million years is reduced by about 10 percent (Figure 5-24). If the corrosion patch size is decreased by a factor of 10, giving 9,641 corrosion patches per waste package, average waste package failure occurs earlier for dripping conditions than it does in the base case.

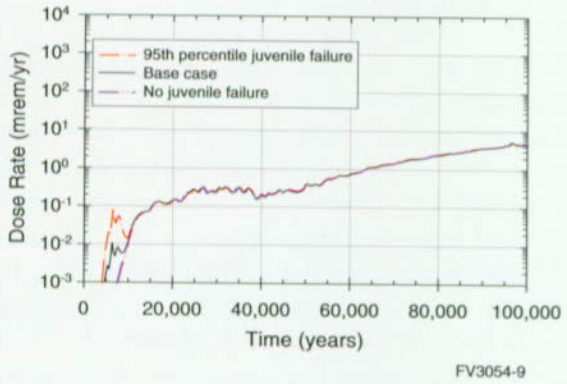

Figure 5-23. Sensitivity of Dose to Juvenile Failure of Waste Packages
Early-time dose is linearly increased by additional juvenile waste package failures.

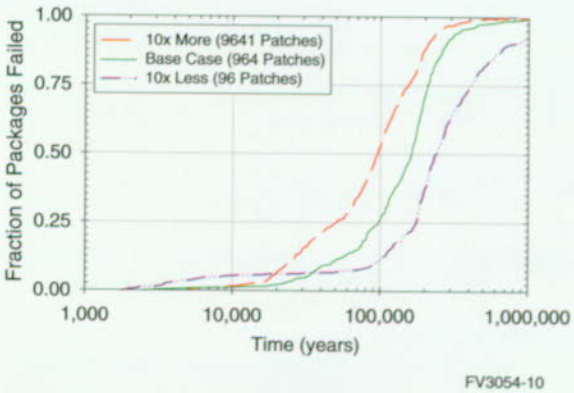

Figure 5-24. Sensitivity of Waste Package Degradation to Corrosion Patch Size

When the alternative-model corrosion-patch-size curves are implemented into the total system analysis, the dose rate results differ in the first part of the time period but not at late time (see Figure 5-25). Some of the larger patches fail earlier, and they have larger area for seepage into and release from the waste package. The smaller patch case fails earlier in general than the other two cases, but there is less seepage into the waste package and smaller openings for radionuclide release from the waste package, so the dose rates are similar to the base case.

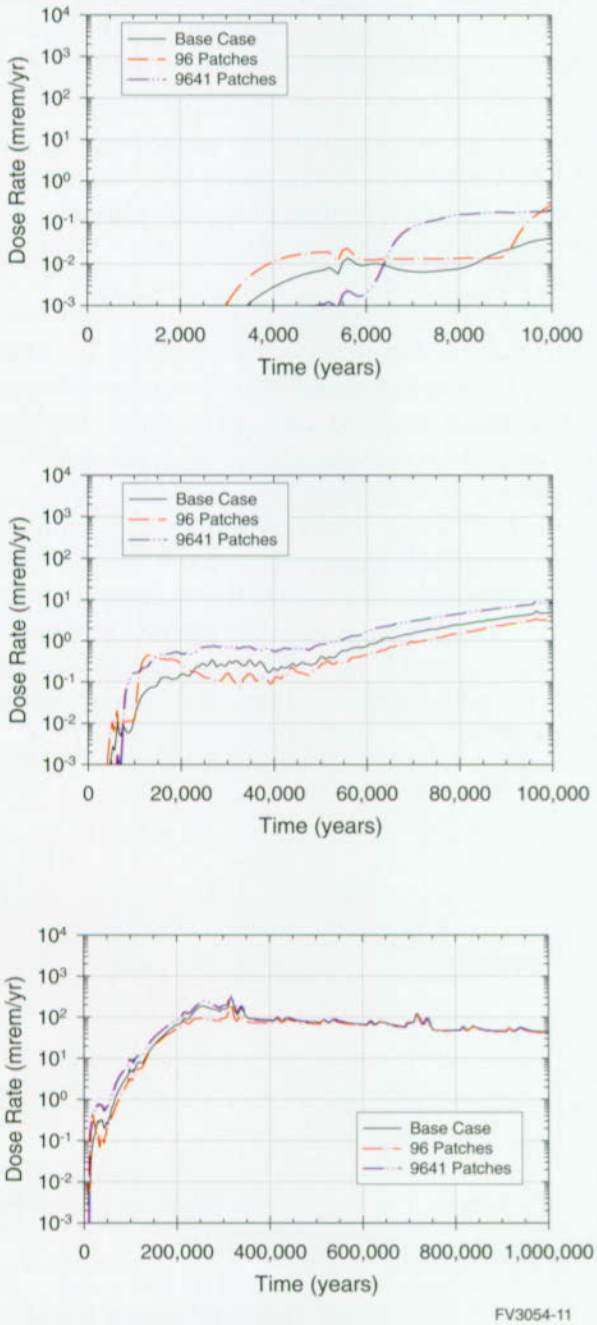

Figure 5-25. Total Dose Rate Histories for Different Sizes of Corrosion Patch Failure
There is little effect on dose rate for these alternative models.

5.5 WASTE FORM ALTERATION, RADIONUCLIDE MOBILIZATION, AND TRANSPORT THROUGH THE ENGINEERED BARRIER SYSTEM

The key uncertainties in waste form degradation and mobilization and transport of radionuclides through the engineered barrier system are discussed in this section. These uncertainties were identified in Section 3.5 and Section 4.3. Evaluations of the importance of seepage through the waste package, integrity of the spent nuclear fuel cladding, secondary phase retention of neptunium, neptunium solubility, the formation and transport of radionuclide-bearing colloids, and radionuclide retardation in the invert are included in this section.

Additional sensitivity analyses comparing the defense spent nuclear fuel with an equivalent amount of commercial spent nuclear fuel, and the plutonium waste forms with an equivalent amount of commercial spent nuclear fuel and high-level radioactive waste are also presented in this section.

5.5.1 Sensitivity to Seepage into the Waste Package

The flux into the waste package is an important parameter affecting release from the waste package, and little is known experimentally about how much of the seeping water will flow into the waste package. Some of the water seeping into a drift and dripping onto a package is expected to flow around the package without entering it. The releases from the waste package are directly proportional to the amount of seepage that flows through the waste package. As discussed in Section 5.4.3, a base case assumption is that the seepage into the waste package is directly proportional to the size of the corroded openings in the waste package (divided by the total package surface area) and multiplied by a "seepage collection factor" that varies uniformly between

1 and 10, with a mean of 5.5. A sensitivity evaluation of the importance of this parameter was conducted using the 5th and 95th percentile values for the seepage collection factor. The results are shown in Figure 5-26. The effect is small at all times but is most noticeable between 50,000 and 250,000 years when the dose is dominated by solubility-limited releases of neptunium-237. During this time a change in seepage produces a change in the dose that is linear with the increase or decrease in the seepage fraction into the waste package. However, at later times the effect is masked by the cladding model, which is not exposing enough additional waste to reach the solubility limit of the highest dose contributor, neptunium.

As a further investigation into the effect of seepage through the package on total dose rate, an alternative model was examined which is similar to Case 2 in Section 5.4.3. In this case, 10 percent of the package area is corroded under dripping conditions for all time. However, in contrast to the aforementioned case (which has seepage into the package scaled by the corroded patch-pit area), in the alternative model all of the drift seepage is assumed to flow through the package. These two seepage models are compared to the base case seepage model in Figure 5-27. As with the seepage collection factor, the effect is relatively minor over all periods.[1]

5.5.2 Sensitivity to Cladding Degradation

Commercial spent fuel cladding degradation through time is another uncertain process. The comparison of the total dose rate arising from the expected-value cladding degradation is compared to the total dose rate for the 5th and 95th percentiles of the cladding-failure distribution in Figure 5-28 for the TSPA-VA base case. The base case cladding degradation distribution is defined with an expected value of 31 percent, a maximum of 47 percent, and a minimum of 1 percent for the amount of exposed surface area of the commercial spent nuclear fuel at 1 million years. The base case

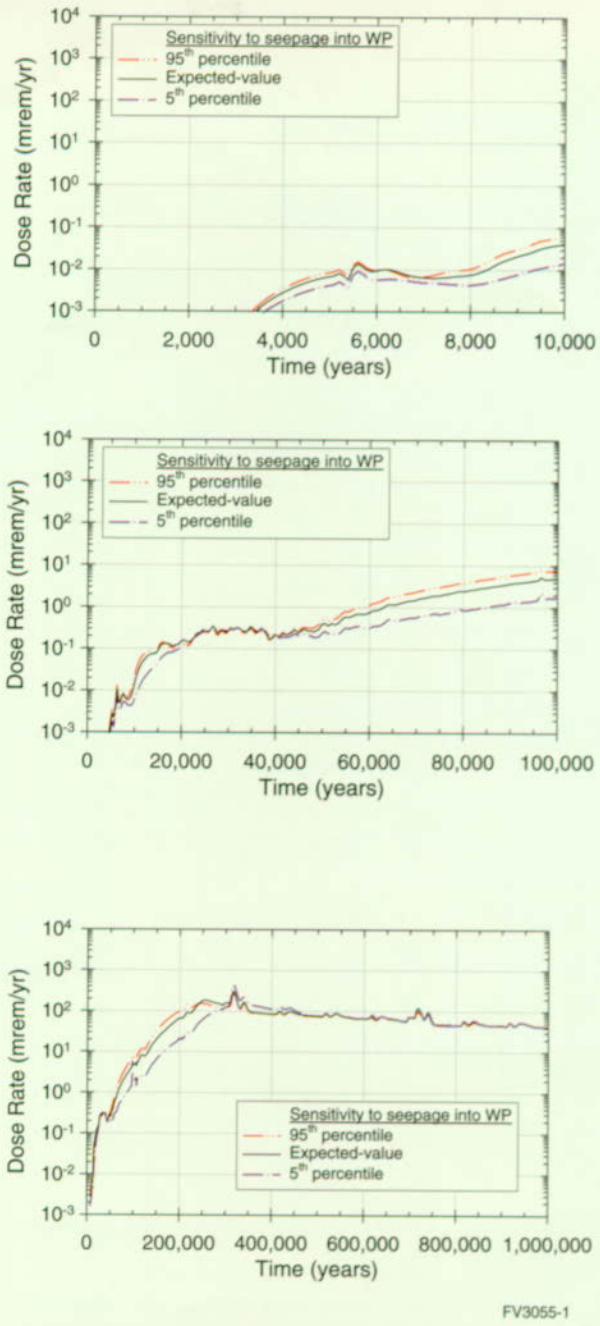

Figure 5-26. Effect of Seepage Collection Factor on Total Dose Rate

Comparison of base case expected-value seepage collection factor with the base case 5th and 95th percentile values. This factor partially determines the amount of liquid flowing through the corroded areas of the waste packages. (WP—waste package)

[1] For all three of these cases the water flowing through the package is assumed to react with all of the exposed fuel (that is, all fuel for which the cladding has degrading or which had no cladding at emplacement).

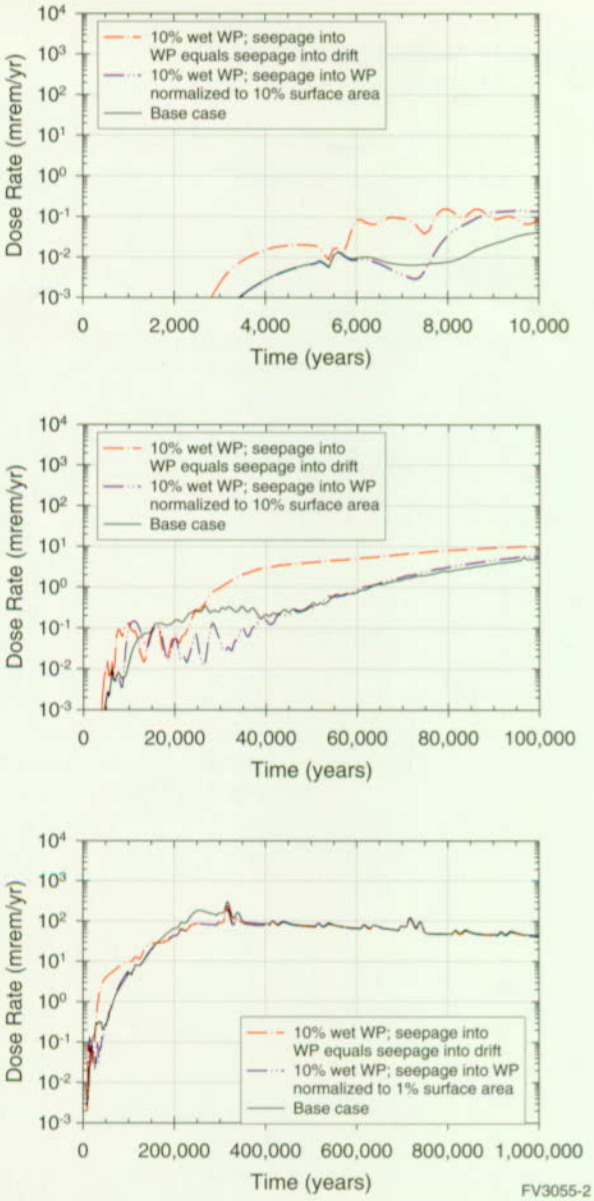

Figure 5-27. Effect of Alternative Seepage Model on Total Dose Rate

a) Base case model assumes that the entire waste package surface area corrodes under dripping conditions but the seepage flux through the waste package is proportional to the corroded area divided by the total surface area; b) "10 percent wet waste package model combined with seepage into package normalized by 10 percent of surface area" means that 10 percent of the waste package surface corrodes under dripping conditions and that the seepage flux through the waste package is proportional to the corroded area divided by one-tenth of the total surface area; (c) "10 percent wet waste package model combined with drift seepage equals seepage into package" means that 10 percent of the waste package surface corrodes under dripping conditions and that the seepage flux through the waste package is equal to the drift seepage flux.

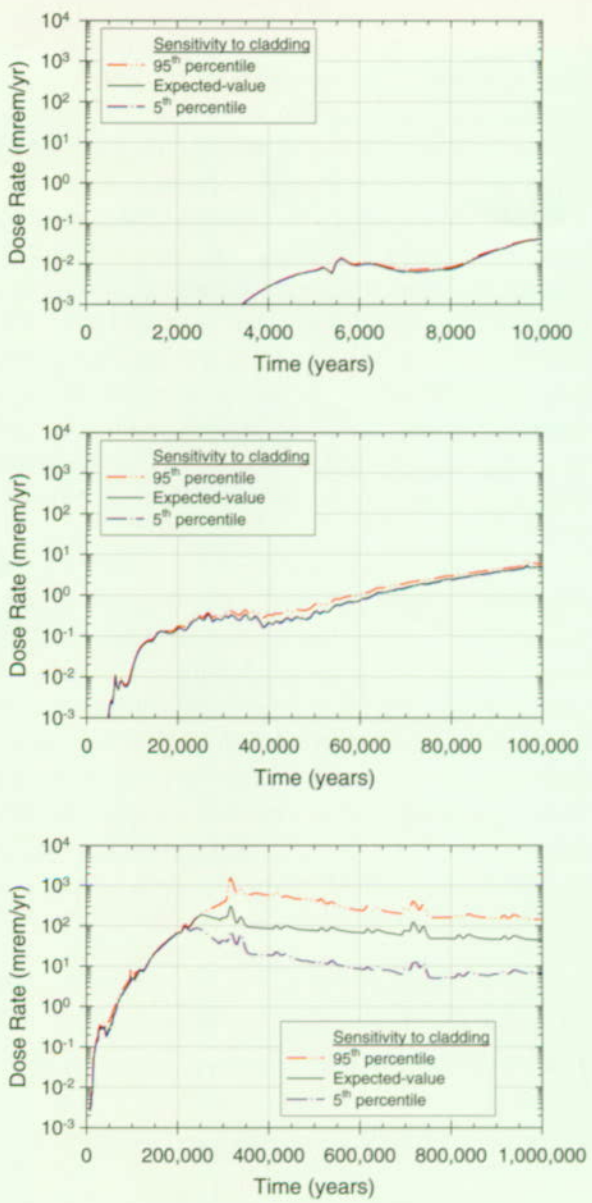

Figure 5-28. Effect of Cladding Failure Fraction on Total Dose Rate

Comparison of base-case expected-value cladding failure fraction with the base-case 5th and 95th percentile values.

model does not have a significant range for the surface area until 100,000 years after waste package failure, when mechanical and corrosion degradation processes begin to increase. The delay in initiation of these processes is one reason why the spread, or variance, in the dose is not observed until after 250,000 years. The other reason is that releases become cladding-degradation-rate-limited after 250,000 years, as explained in Section 4.2. Prior to that time, between 50,000 years and 250,000 years, the dose rate is dominated by solubility-limited neptunium releases, implying that within the range of the base case cladding model, the variations in cladding degradation would not have an effect on dose rate prior to 250,000 years.

The base case cladding model does not have a very wide uncertainty range, so the parameter does not show up in section 4.3 as a top rank-regression parameter. For example, the extreme of no cladding credit is not part of the base case model uncertainty range. Thus, additional analyses are conducted to evaluate alternative conceptual models of cladding failure. The alternative models range from immediate cladding failure to total failure of the cladding at either 100,000 years or 1 million years. These are compared to the base case model in Figure 5-29. The most significant difference in the models up through 100,000 years is that the no-cladding model has significantly higher releases. This is primarily due to the increased release of technetium-99 at early times from the fully exposed spent fuel rods. After the technetium is exhausted, the releases are dominated by solubility-limited neptunium releases up till about 250,000 years, which is the reason that all models yield approximately the same dose rates. Beyond 250,000 years, the no-cladding model and 100,000-year-failure model yield similar results, as might be expected, with their predicted dose rates being higher than the other two models (the base case and 1-million-year models). At close to 1 million years the fuel inventory from these two models is starting to be exhausted, so their predicted dose rates fall below the 1-million-year-failure model. The other two models, the base case and 1-million-year-total-failure have similarly shaped dose rate curves, but

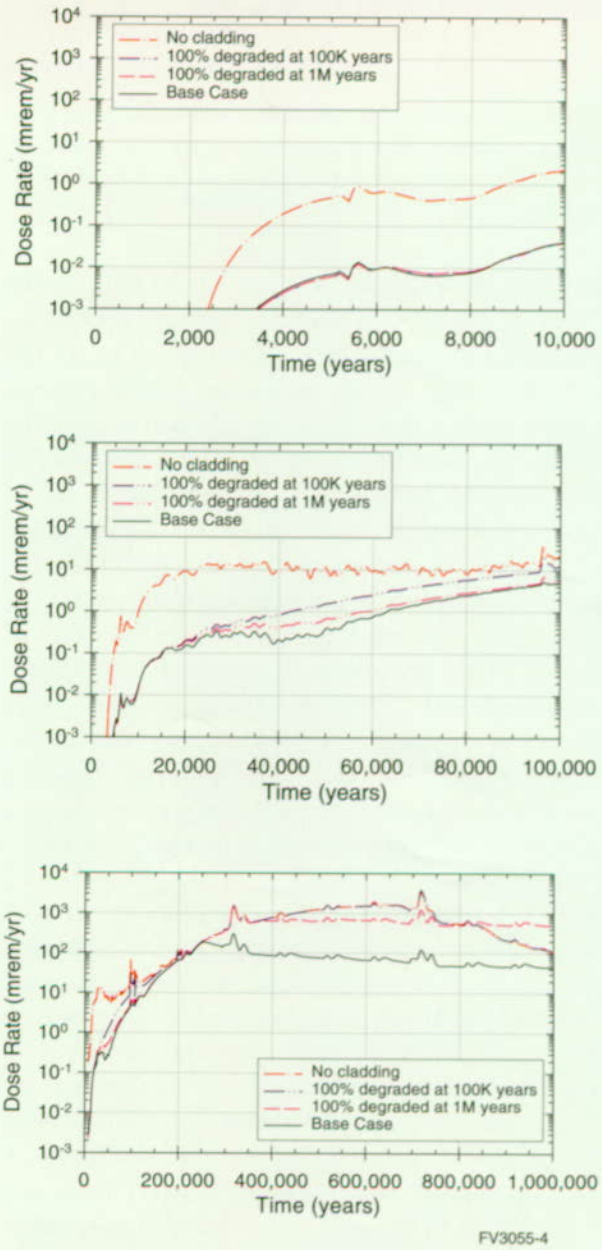

Figure 5-29. Effect of Alternative Models for Cladding Failure on Total Dose Rate
One model assumes no cladding credit at any time. The "100 percent degraded at 100,000 years" model assumes a linear relationship between log (clad failure fraction) and log (time) with 1 percent failure at 10,000 years and 100 percent failure at 100,000 years. The "100 percent degraded at 1 million years" model assumes a linear relationship between log (clad failure fraction) and log (time) with 1 percent failure at 10,000 years and 100 percent failure at 1 million years. These three models are compared to the base case model, which has several different failure modes as shown in Figure 3-54.

separated by a constant factor. This behavior is not unexpected, since the cladding failure curves for the two models are about the same, only differing with respect to the endpoint value at 1 million years, which is 31 percent failure for the base case and 100 percent failure for the 1-million-year-total-failure model.

Because there might be more uncertainty in the cladding degradation than that included in the base case and because the base case cladding model did not show up as an important rank-regression parameter in Figure 4-34, an alternative cladding model was investigated besides those discussed in the previous paragraph. The alternative model assumes a much wider range on the cladding uncertainty by assuming that the percentage of failed cladding in a waste package is log-uniformly distributed between 0.01 and 1.0, with a mean of 0.215. This percentage is assumed to be failed instantaneously when the waste package inner barrier is breached. To evaluate the differences between the base case and modified cladding models, probabilistic simulations were conducted for each of the three simulation periods. The distributions of peak dose rates to an individual located at 20 km (12 miles) from the repository for the base case and the modified cladding case are compared in Figure 5-30. The case with the modified cladding model gives higher peak dose rates than the base case in all three time. This increase in peak dose rates is primarily due to the fact that the fraction of fuel exposed because of cladding failure is available immediately for dissolution after waste package failure rather than gradually increasing with time as in the base case. Note that differences in dose rates tend to be more pronounced on the low probability regions of the curves, except in the 10,000-year period where differences tend to be significant for the entire range of doses. Figure 5-31 is a comparison of the most important model parameters for total system performance, similar to Figure 4-34, for the modified cladding case. Based on the R^2-loss, the modified cladding case indicates that cladding degradation is a key parameter in the 10,000-year and 1-million-year periods. However, it is not a key parameter in the 100,000-year period because of the dominance of solubility-limited neptunium releases, which

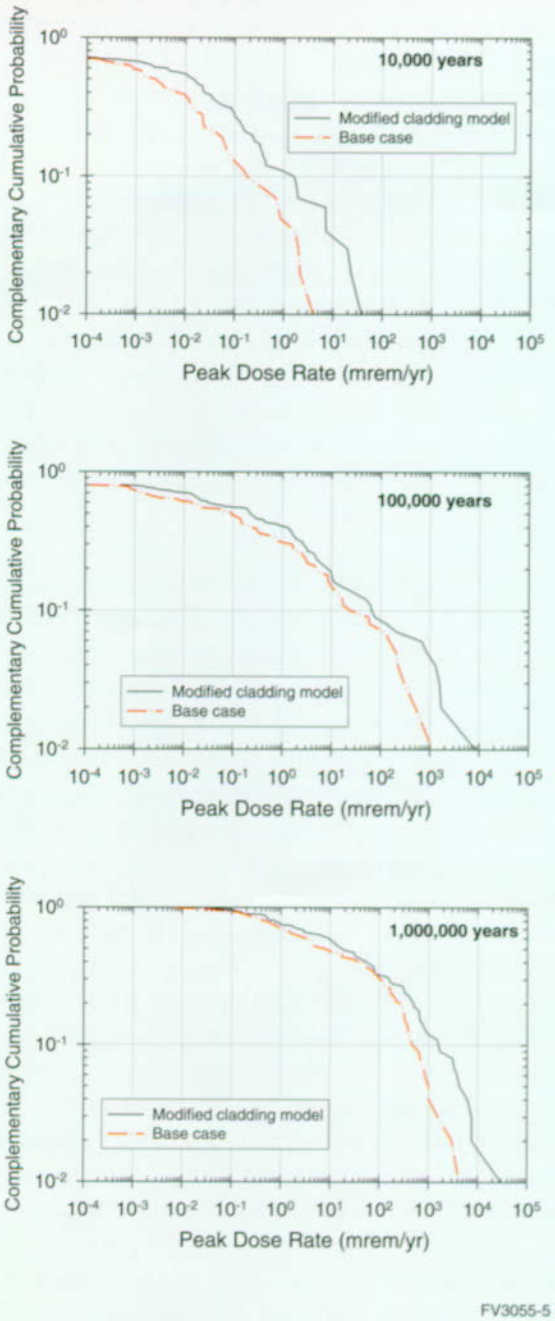

Figure 5-30. Effect of an Alternative Cladding Model on 10,000-Year, 100,000-Year, and 1 Million Year Peak Dose Rate over Multiple Realizations
The alternative model assumes a wider uncertainty band for cladding failure fraction than used in the base case (see Figure 3-54). The fraction is assumed to be log-uniform from 0.01 to 1.0 and it is assumed that the cladding is failed instantaneously when the waste package fails.

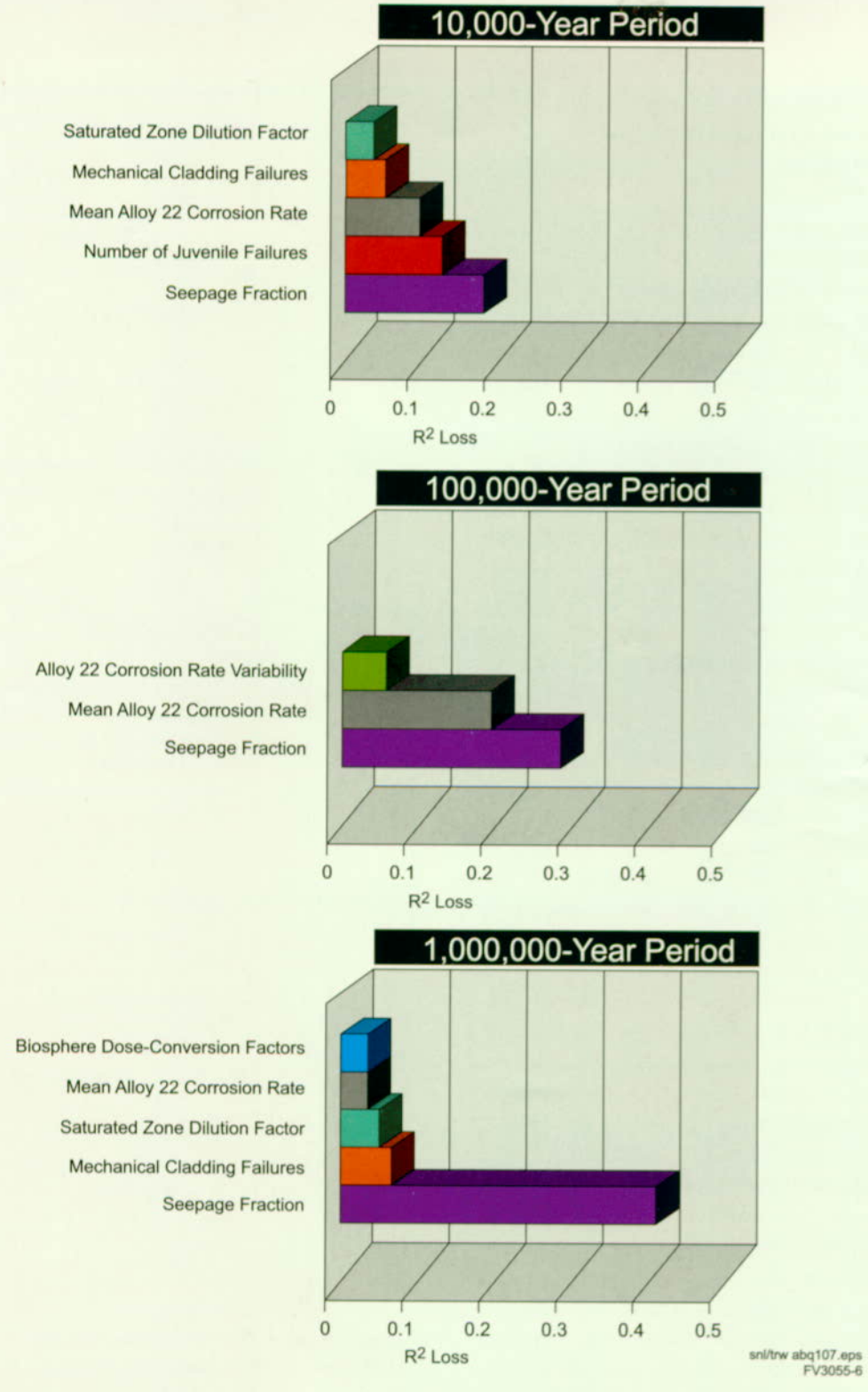

Figure 5-31. Most Important Parameters for the Modified Cladding Model Case
Results are from stepwise regression analysis for three time periods. These charts show the relative importance of various parameters to the calculated uncertainty in dose rate for the three time periods. Importance of an individual parameter is shown by R^2-loss, the reduction of goodness of the regression fit.

prevents the cladding from having much of an effect.

5.5.3 Sensitivity to Dissolution Rate and Secondary-Phase Retention of Neptunium

The dissolution rates of commercial spent nuclear fuel and high-level glass waste are potentially important parameters for repository performance, although they did not appear in the R^2-loss ranking in Figure 4-34. To examine their possible effect on dose rate, the single realizations of their 5th and 95th percentile values are compared to the expected-value base case in Figure 5-32. The uncertainty ranges in these parameters are derived from experimental studies described in Chapter 6 of the *Total System Performance Assessment-Viability Assessment (TSPA-VA) Analyses Technical Basis Document* (CRWMS M&O 1998i). Clearly for the uncertainty ranges considered, there is almost no effect on dose rate.

The uncertainty in dissolution rate in the base case did not consider a potentially important phenomenon: the retention (re-precipitation) of neptunium in secondary phases after initial dissolution. This effect is observed in laboratory experiments (Finn et al. 1997) The effect of such retention is analyzed as an alternative model described in Section 3.5 and in Chapter 6 of the *Total System Performance Assessment-Viability Assessment (TSPA-VA) Analyses Technical Basis Document* (CRWMS M&O 1998i). The retention effect is gained by reducing the solubility of neptunium by a factor of 45 to approximate the results of reactive transport modeling discussed in Section 3.5.2.5. The dose rate resulting from this alternative model is shown for all three time frames in Figure 5-33. At early times, prior to about 50,000 years, the alternative model has no effect because doses are dominated by technetium. The greatest effect is noticed at about 200,000 years when neptunium comprises more than 99 percent of the total dose in the base case (see Figure 4-12). At this time, the total dose from the alternative neptunium solubility model is about a factor of 25 lower than the base case total dose rate. If the total dose rate at this time in the alternative model were

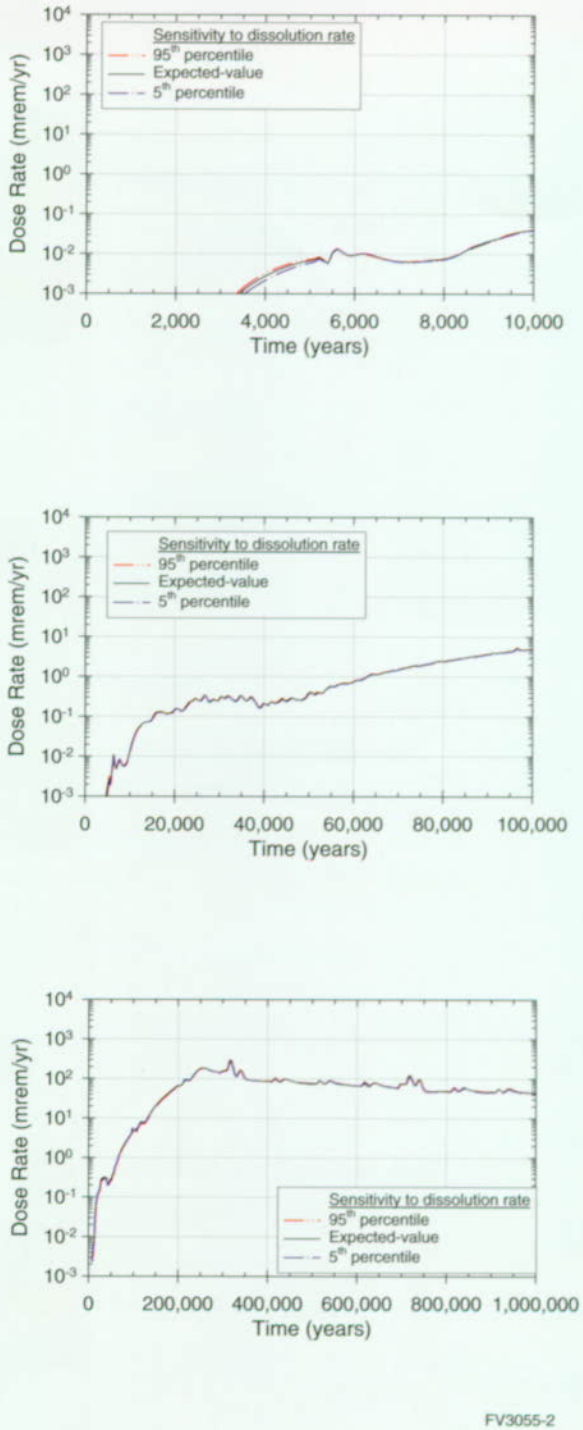

Figure 5-32. Effect of Commercial-Spent-Fuel and High-Level-Glass Dissolution Rates on Total Dose Rate

Comparison of base case expected-value dissolution rates with the base case 5th and 95th percentile values.

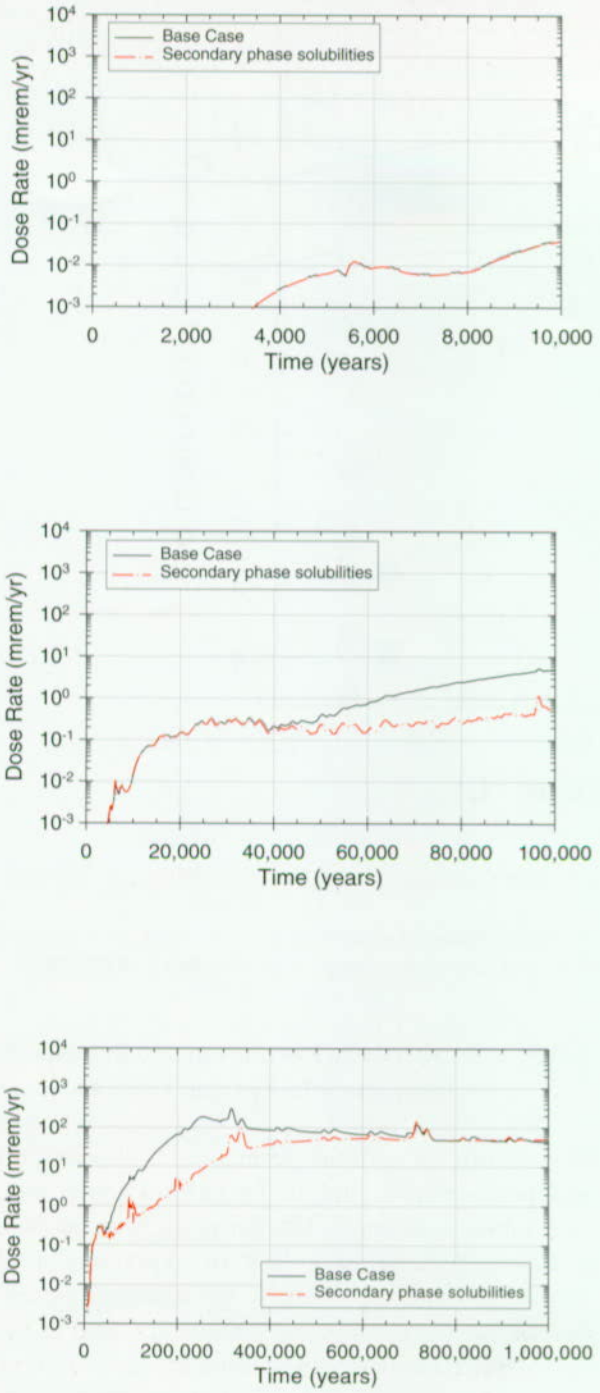

Figure 5-33. Sensitivity of Total Dose Rate to Reprecipitation of Neptunium in Secondary Mineral Phases
These phases have lower solubility than the primary mineral phases. This effect is implemented by dividing the base case neptunium solubility by 45.

composed almost solely of neptunium, as it is in the base case, then the difference between the two models would be exactly a factor of 45 because of the difference in neptunium solubility. However, in the alternative model the neptunium dose is low enough at this time that some of the other radionuclides, such as plutonium-242, uranium-234, and technetium-99 (see Figure 4-12) have a non-negligible contribution to dose. At a later times (> 250,000 years), the effect of the alternative neptunium model is not as significant because neptunium is no longer solubility limited (all waste packages have failed) and the cladding degradation rate limits the surface area available for dissolution and release.

The retention of neptunium as a secondary phase, while a potentially important effect in repository performance, is still being evaluated in laboratory testing and corresponding reactive transport modeling. Further analyses are necessary before including such effects in the base case TSPA.

5.5.4 Sensitivity of Dose to Neptunium Solubility

The solubility of neptunium is uncertain to within at least a three-order of magnitude range as shown by the shaded region in Figure 5-34. This shaded region was the range of neptunium solubility used in the TSPA-VA base case. It does not encompass all experimental measurements, as shown in the figure, but the measurements outside of this range are thought to be unrepresentative of any potential repository conditions, as described briefly in Section 3.5.1.8 and in much more detail in Chapter 6 of the *Total System Performance Assessment-Viability Assessment (TSPA-VA) Analyses Technical Basis Document* (CRWMS M&O 1998i). Neptunium solubility did not appear as one of the most important rank-regression parameters in Figure 4-34, however, it did appear as an important parameter in Figure 4-40 for the 100,000-year time span, when the seepage and corrosion-rate parameters were held at their mean values. In other words it was in the second-tier of key R^2-loss parameters. However, it only appears in the second tier during the 100,000-year time frame because this is the time frame when

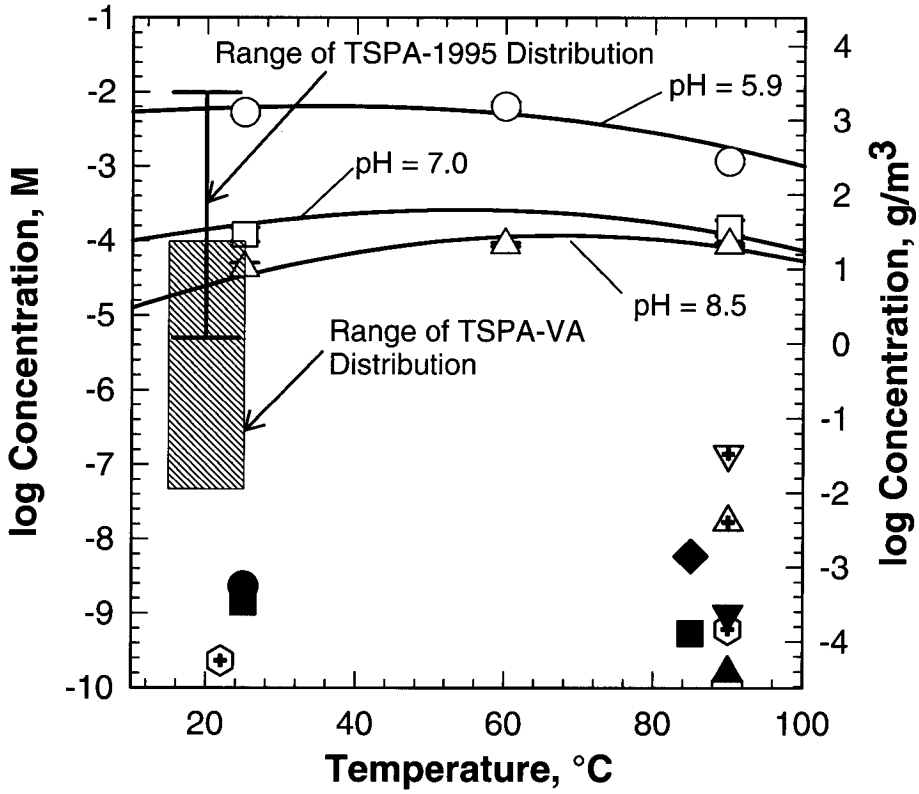

Figure 5-34. TSPA-VA Base Case Neptunium Solubility Distribution Compared to TSPA-1995 Distribution and to Eleven Different Precipitation/Dissolution Experiments
The open symbols at the top of the diagram are precipitation (oversaturation) experiments. The filled symbols at the bottom are dissolution studies, including batch, flow-through, and drip experiments. See Chapter 6 of CRWMS M&O 1998i for more detail.

solubility-limited neptunium tends to dominate doses. This is born out in the total-dose time-history comparison shown in Figure 5-35, comparing the expected-value neptunium solubility case to the dose rate arising from the 5th and 95th percentile values from the base case neptunium solubility range.[2] As with the secondary-phase model described by Figure 5-33, the greatest effect on dose for the base case model is in the time frame of 50,000 to 250,000 years when the total dose is dominated by solubility-limited neptunium releases. At later times the cladding degradation rate controls total dose rate.

5.5.5 Sensitivity to Formation and Transport of Radionuclide-Bearing Colloids

Uncertainty in colloid formation and transport parameters is quite high in the TSPA-VA base case (see Tables 3-16 and 3-18), particularly in far-field transport, because of a lack of experimental or field-scale evidence to verify the models. Nevertheless, for the models and parameters used in the base case, colloid model parameters do not show up in the key rank-regression parameters in Figures 4-34 or 4-40, even though Figure 4-29 indicates that plutonium dose rate is the most significant contributor to total dose rate for 2 percent of the 100,000-year multiple realizations

[2] Neptunium solubility was modeled as a log-beta distribution and the 5th, 95th, and expected values were chosen for the log of solubility, not for the solubility itself.

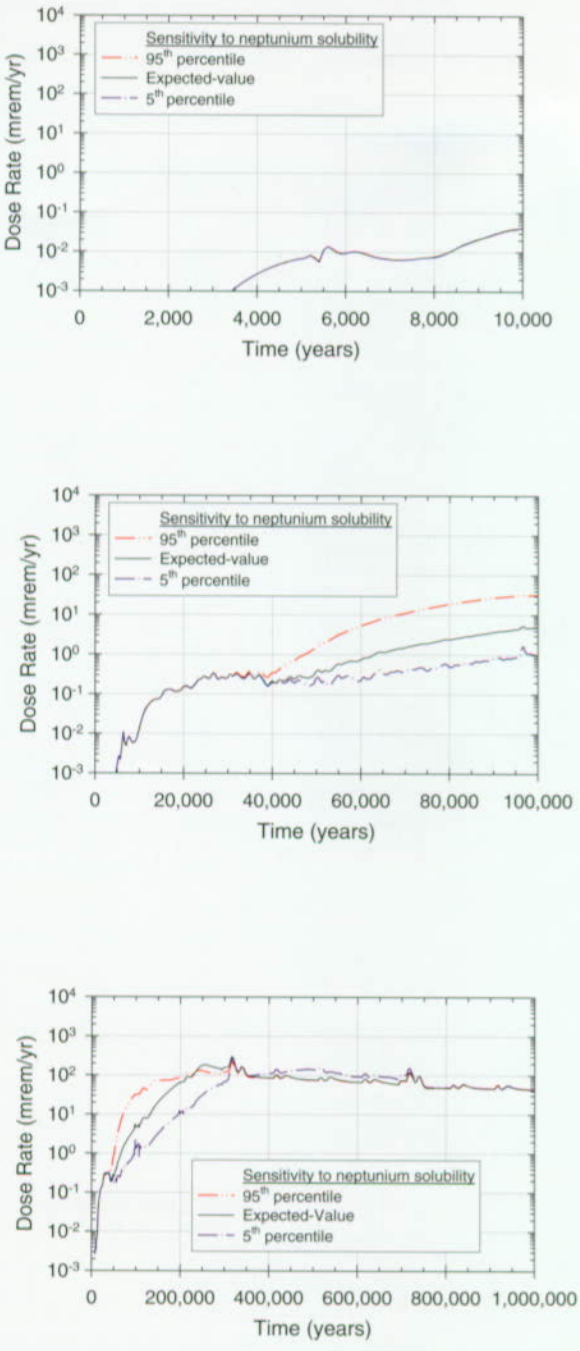

Figure 5-35. Effect of Neptunium Solubility on Total Dose Rate
Comparison of base case expected-value solubility with the base case 5th and 95th percentile values.

and 8 percent of the 1-million-year multiple realizations. However, in examining the sensitivity to the 95th percentile value of the K_c range ($K_c = 5.0$) in the base case, it is evident that there is an effect on dose rate during the 50,000-year to 250,000-year time period, as indicated in Figure 5-36. The K_c parameter is high enough at this percentile to allow a significant fraction of plutonium to be transported as reversibly sorbing on colloids. There is no difference in this figure between the 5th percentile value for K_c and the expected-value because the expected value is already too low to allow a significant fraction of aqueous plutonium to be transported in colloidal form.

5.5.6 Sensitivity to Transport in the Engineered Barrier System

The TSPA-VA base case evaluation includes radionuclide retardation in the concrete invert (i.e., the structure that supports the waste package) for neptunium, plutonium, uranium, and protactinium. There is uncertainty in the appropriate values for these retardation factors (as indicated by the ranges given in Section 4.1.10) and about what will happen to the retardation capability of the invert over a long time as the system degrades. To evaluate the effect on dose rate of the retardation capability of the invert, a sensitivity case was conducted (Figure 5-37) using the 5th and 95th percentiles of these K_d ranges. The results indicate that for early times (< 35,000 years) when the dose is dominated by technetium release (no retardation), there is no change. At later times when the dose is primarily a result of neptunium release, the difference in total dose rate mimics the change in neptunium dose rate, but the increase is less than a factor of two. At much later times (> 250,000 years) cladding degradation rate eliminates any difference between the cases.

An additional sensitivity analysis was carried out to examine retardation in the invert. This is an alternative model wherein all the distribution coefficients (K_ds) in the invert are set to zero (i.e., no retardation in the invert). Figure 5-38 presents the results of these analyses, which are about the same as the 5th percentile case in Figure 5-37. In

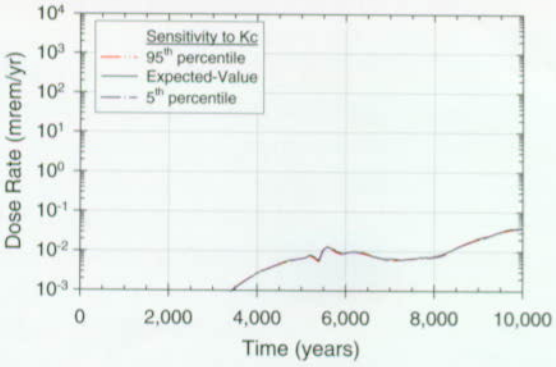

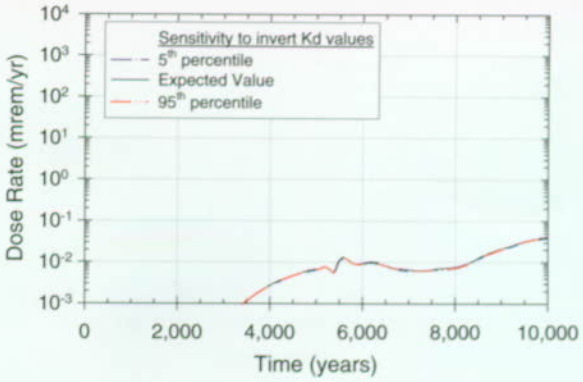

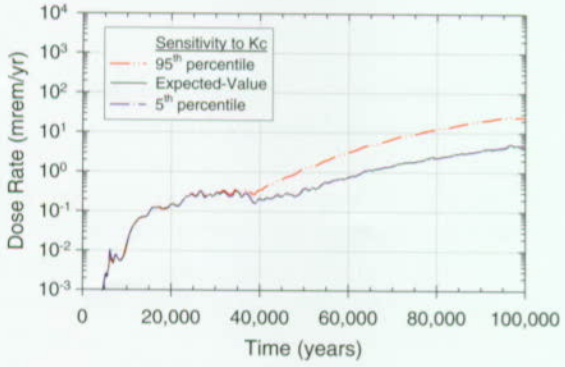

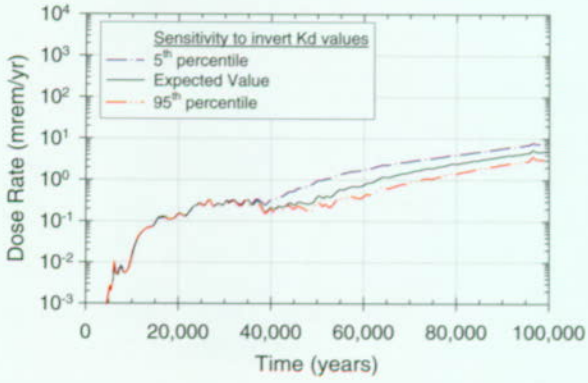

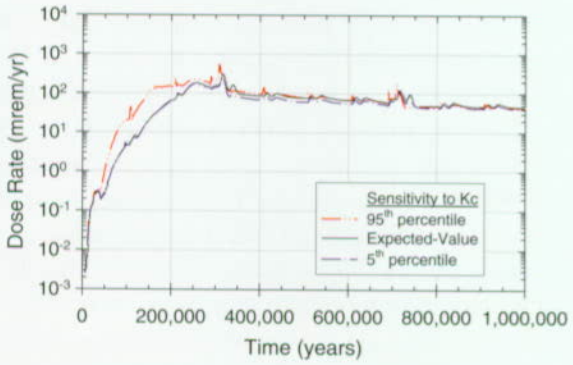

FV3055-11

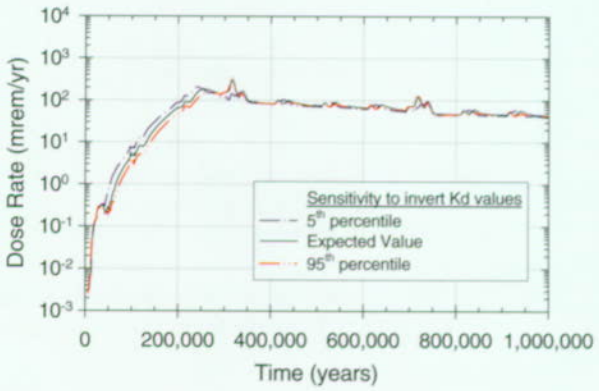

FV3055-12

Figure 5-36. Effect of Colloid Distribution Coefficient on Total Dose Rate
Comparison of base case expected-value K_c with the base case 5th and 95th percentile values.

Figure 5-37. Effect of Radionuclide Distribution Coefficients in the Concrete Invert on Total Dose Rate at 20 km (12 miles)
Comparison of base case expected-value K_ds with the base case 5th and 95th percentile values. The primary effect is from the neptunium K_d.

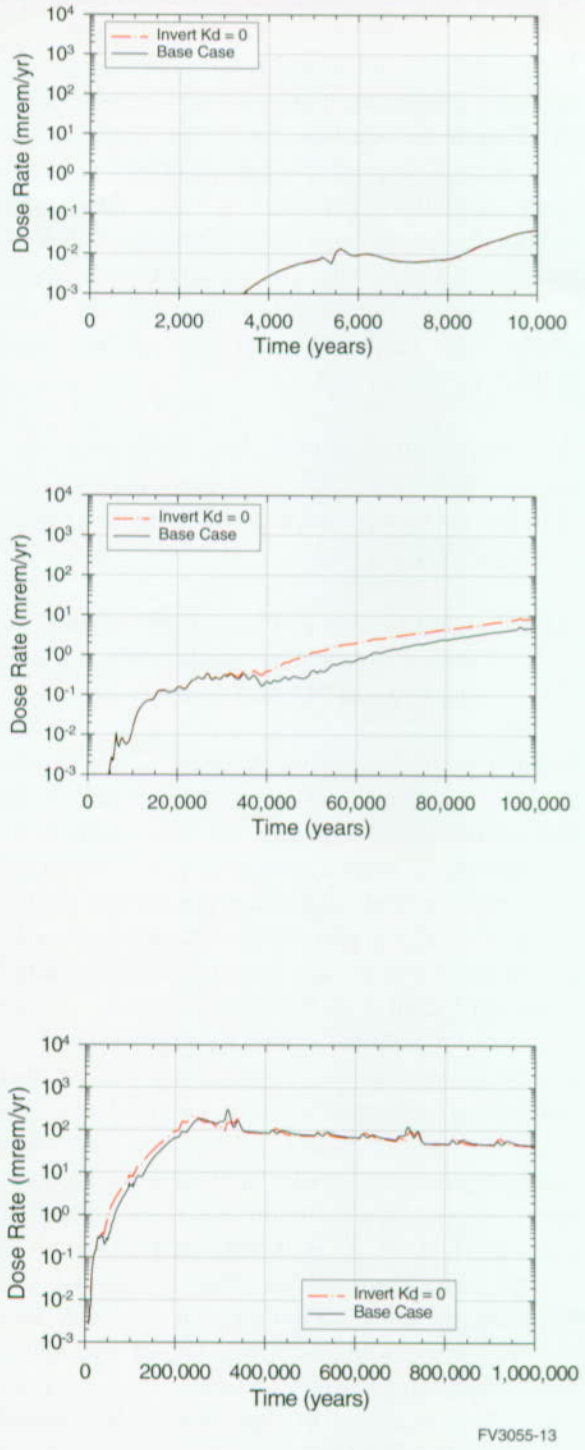

Figure 5-38. Sensitivity of Total Dose Rate to an Alternative Engineered Barrier System Transport Model that Assumes the Radionuclide K_ds in the Invert are Equal to Zero
In the top figure, the two curves overlay.

summary, the retardation in the invert appears to have little significance to total dose, and this is in spite of the fact that the expected-value K_d in the base case is quite high.

5.5.7 Comparison of the Surrogate U.S. Department of Energy Spent Nuclear Fuel to DOE Spent Nuclear Fuel Total

The base case analyses reported in Sections 3.5, 4.2, and 4.3 used a surrogate inventory for DOE spent nuclear fuel rather than explicitly modeling each of more than 250 types of the fuel. The surrogate was based on the key dose contributors from the 15 categories of DOE spent nuclear fuel that were determined in the original inventory. To determine the key dose contributors, each individual DOE spent nuclear fuel category was analyzed by placing it in the environment of the base case, one category at a time, and calculating the expected dose to humans located 20 km (12 miles) downgradient from the repository. The 2,333 metric tons of heavy metal (MTHM) of surrogate have a radionuclide inventory that is a weighted average (on an MTHM basis) of the radionuclide inventories of Categories 1, 4, 5, 6, 8, and 11. These six categories were found to contribute significantly to the dose from all DOE spent nuclear fuel (Duguid et al. 1997, pp. 4-1 to 4-10, 6-2 to 6-3). Because the majority of the DOE spent nuclear fuel is metallic, the metallic dissolution model was assumed for the surrogate. In addition to these six categories, Categories 7 and 16 were also found, in the current analyses, to contribute significantly to the dose from all DOE spent nuclear fuel (CRWMS M&O 1998i). In the base case, these categories are represented by the surrogate spent nuclear fuel, which would yield conservative results. (For more detail on this analysis, see Chapter 6 of *Total System Performance Assessment-Viability Assessment (TSPA-VA) Analyses Technical Basis Document* [CRWMS M&O 1998i].)

The dose rate from each DOE spent nuclear fuel category is presented in Figure 5-39 over the first 100,000 years after repository closure. Figure 5-39 also compares the total dose from the surrogate DOE spent nuclear fuel to the total DOE spent

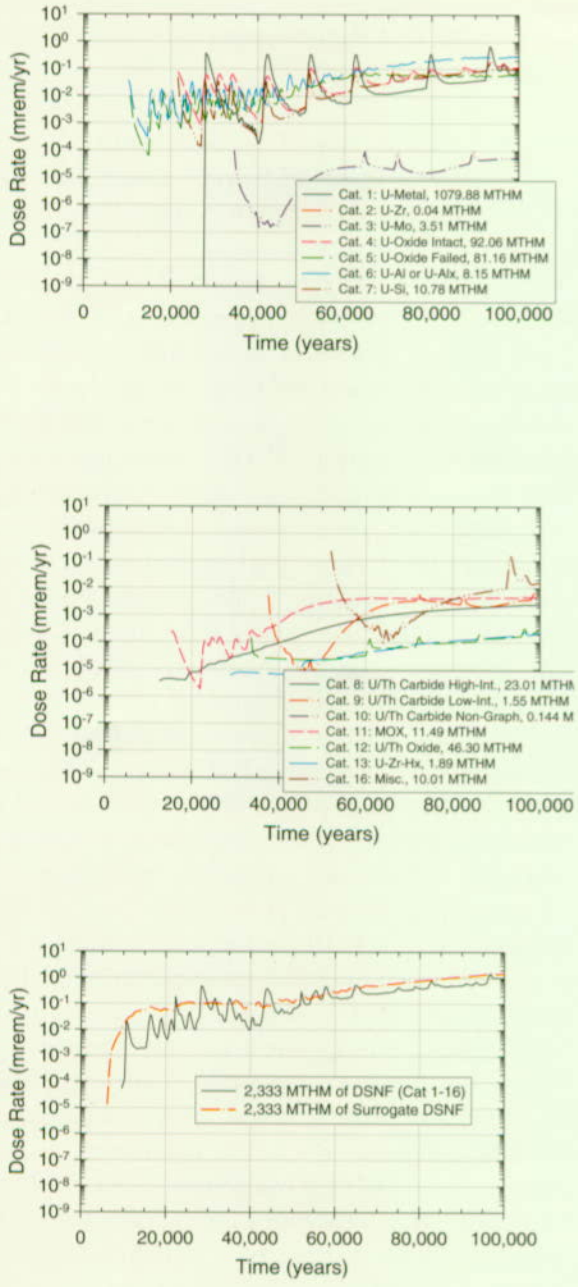

Figure 5-39. Expected-Value Total Dose-Rate History at 20 km (12 miles) over 100,000 Years for Sixteen Categories of U.S. Department of Energy Spent Nuclear Fuel
Total dose rate for all DOE spent nuclear fuel, found by summing the individual categories, compared to the surrogate DOE spent nuclear fuel (bottom figure). Fuel is assumed to be exposed upon waste package failure (no credit for cladding).
(DSNF—DOE Spent Nuclear Fuel)

nuclear fuel, where the latter is defined as the sum of the dose rates from the various categories 1-16. The spikes on the total DOE spent nuclear fuel curve are caused by individual package failures of DOE spent nuclear fuel, with the highest spikes being from Category 1. They occur because of the small number of packages in some DOE spent nuclear fuel categories (e.g., Category 1 has 107 packages). In contrast, the surrogate spent nuclear fuel curve is smoother because of the larger number of disposed packages (2,546 waste packages).

The contributions to total dose from naval spent nuclear fuel (Category 15) that had not been analyzed previously were found to be insignificant (CRWMS M&O 1998i).

5.5.8 Comparison of Plutonium Waste Form with Commercial Spent Nuclear Fuel Equivalent Waste Form

Another waste form currently planned for disposal in the repository is plutonium waste. The plutonium waste consists of two subtypes: a Zircaloy-clad, mixed uranium-plutonium oxide spent nuclear fuel, and a can-in-canister, ceramic waste, which is a plutonium ceramic in cans that are encapsulated in high-level radioactive waste in a standard high-level radioactive waste canister. The cans of ceramic comprise approximately 12 percent of the canister volume, and four of these canisters are assumed to be disposed of in a high-level radioactive waste package. The mixed uranium-plutonium oxide fuel contains approximately 5 percent plutonium and is assumed to be used as fuel in a standard, pressurized water reactor. The spent nuclear fuel is assumed to be disposed of in 21 assembly, pressurized water reactor waste packages. There are 75 packages of mixed uranium-plutonium oxide spent nuclear fuel and 159 packages of can-in-canister ceramic (CRWMS M&O 1998i).

The effects of disposal of the 50 tons of surplus plutonium was analyzed by simulating the emplacement of the plutonium waste forms, one at a time, in the base case environment and analyzing the expected value dose history 20 km (12 miles) from the repository (CRWMS M&O 1998i).

Figure 5-40 compares the doses from 33 tons of plutonium as mixed uranium-plutonium oxide spent nuclear fuel and 17 tons of plutonium as can-in-canister ceramic with equivalent commercial spent nuclear fuel and high-level radioactive waste.

A comparison of the mixed uranium-plutonium oxide spent nuclear fuel with an equivalent amount of commercial spent nuclear fuel shows that the dose from both is nearly identical, with the mixed uranium-plutonium oxide being negligibly higher. A comparison of the can-in-canister ceramic with an equal number of packages of high-level radioactive waste indicates that the dose from the high-level radioactive waste is negligibly higher than from the can-in-canister ceramic. These results show that the dose attributed to mixed uranium-plutonium oxide fuel and can-in-canister ceramic is essentially the same as that from commercial spent nuclear fuel and high-level radioactive waste, respectively. These results can be interpreted to mean that the effects on dose from disposal of plutonium are not significant, because the spent nuclear fuel equivalent and equivalent number of high-level radioactive waste packages would have been disposed of anyway.

5.6 UNSATURATED ZONE TRANSPORT

This section examines the sensitivities of the total system performance to variations in matrix diffusion, sorption, and a coupled sorption and source term scenario. These sensitivity analyses are intended to complement the unsaturated zone subsystem calculations presented in Section 3.6 and provide information on how changes in the subsystem affect performance of the total system.

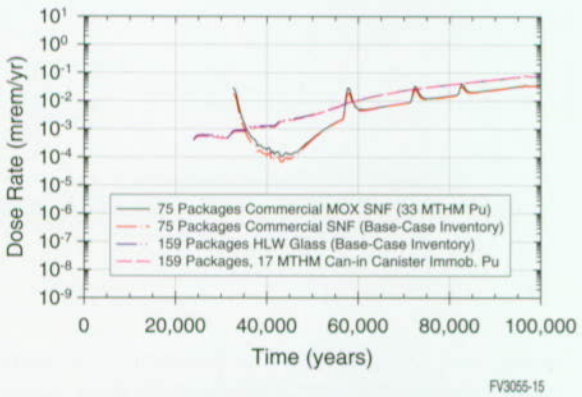

Figure 5-40. Comparison of Total Dose Rate for Plutonium Waste Forms (Mixed Oxide Fuel and "Can-in-Canister")

(CSNF—commercial spent nuclear fuel; HLW—high-level radioactive waste; MOX—mixed oxide fuel)

5.6.1 Sensitivity to Matrix Diffusion

Analyses of matrix diffusion sensitivity for unsaturated zone flow were carried out for different infiltration rates and conceptual models. The relationship between matrix diffusion and flow is important because the relative rates of these processes influence how matrix diffusion affects unsaturated zone transport. In particular, the relative rates of advective transport in the fractures to diffusion in the matrix (coupled with matrix sorption) determine how strongly matrix diffusion influences transport in the unsaturated zone.

The base case, expected-value dose-rate history is shown in Figure 4-12. This figure shows that early dose (up to about 50,000 years) is dominated by technetium; after that time, the dose is dominated by neptunium. The dominant radionuclide for dose affects the sensitivity analyses discussed below because of the differences in matrix diffusion and sorption between these radionuclides (see Section 3.6). Sorption enhances the effects of matrix diffusion because it sharpens concentration gradients, the driving force for diffusion, between the fractures and matrix. Technetium is nonsorbing and in the aqueous phase is expected to be in the form of the negatively charged pertechnetate anion, TcO_4^- (Triay et al. 1997, p 177). Mineral surfaces also are commonly negative in charge, so pertechnatate tends to be repelled slightly by the rock matrix surfaces (ibid, p.182). Both these characteristics of technetium lead to less matrix diffusion. Neptunium is weakly sorbing on the different rock matrix types in the unsaturated zone. For oxidizing conditions at values of pH less than about 7, the aqueous form of neptunium is expected to be predominantly the positively charged neptunyl cation, NpO_2^+ (ibid, p. 124, Table 47). Therefore, neptunium transport is expected to be more strongly influenced by matrix diffusion. Although values of pH are likely to be larger than 7 (see

Section 3.3), we have used the matrix diffusion coefficient for a positively charged species as a conservative measure.

Figure 5-41 shows the change in dose at the 20-km (12-mile) boundary for the expected value base case with and without matrix diffusion. In general, matrix diffusion is found to have little influence on dose; some slight variations at very early times (< 5,000 years) and then at longer times (about 70,000 to 250,000 years) are seen in the figure. Matrix diffusion is expected to have greater influence at the leading edge of the releases because the concentration gradients at the front are larger. The slight variation in responses at longer times is believed to be caused by the dominance of neptunium for total dose after about 50,000 years. Before this time, dose is dominated by technetium. The greater sensitivity of neptunium to matrix diffusion (after the leading edge of the concentration front passes through the system) is expected because of the differences discussed above the respect to matrix diffusion and sorption. The fact that matrix diffusion has much less effect on dose at the 20-km (12-mile) boundary than on the unsaturated zone radionuclide transport results (see Section 3.6) suggests that other aspects of the total system, such as engineered barrier system releases and saturated zone transport, tend to dominate the total system response.

The effect of matrix diffusion on other flow models besides the expected-value base case model was also analyzed, but not shown here because of the negligible effect. The other four flow fields in the base case (see Section 5.1) showed similar behavior to the expected-value flow field (the "base infiltration with mean fracture alpha" case), with relatively little effect on total dose rate from matrix diffusion in the unsaturated zone. The DKM/Weeps model also showed similar behavior to the expected-value base case flow field.

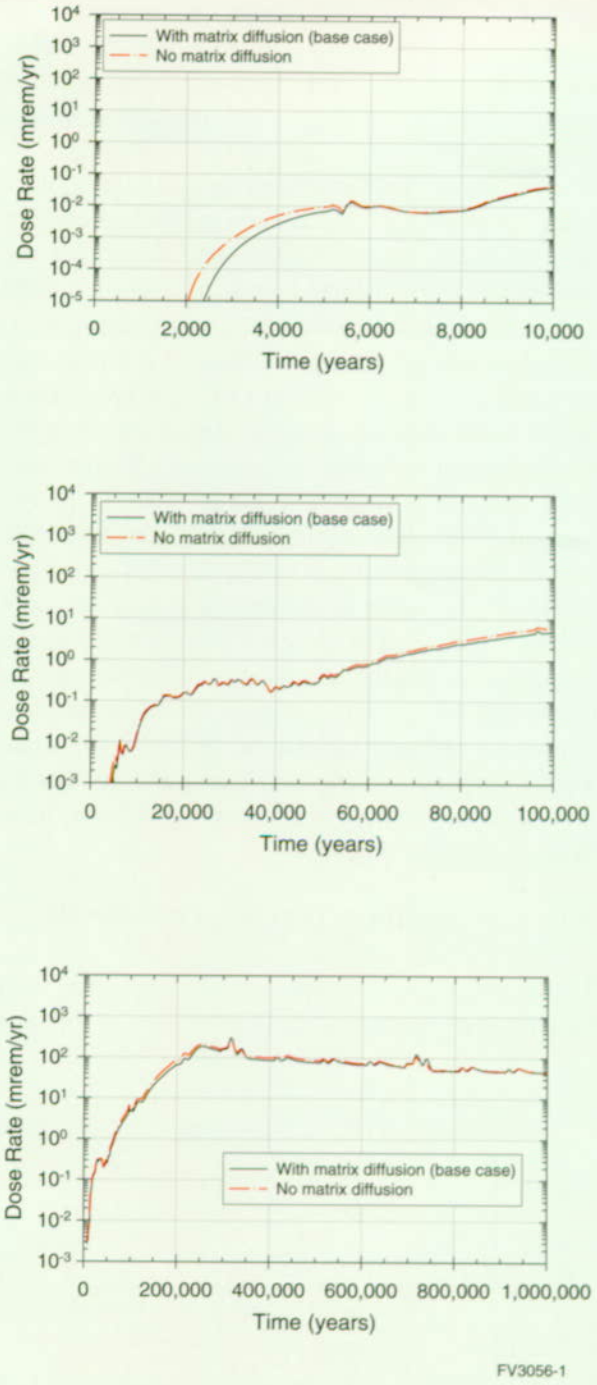

Figure 5-41. Comparison of Zero-Matrix-Diffusion (in the Unsaturated Zone) Model with Base Case Model
Effect on total dose rate at 20 km (12 miles) for three different periods.

5.6.2 Sensitivity to Sorption

This section considers the sensitivity of performance to sorption in the unsaturated zone and does not consider changes to sorption in the saturated zone.

The first sensitivity examined is to the uncertainty ranges for the distribution or sorption coefficients (K_ds) in the base case, specifically for neptunium, plutonium, uranium, selenium, and protactinium. Figure 5-42 shows the total dose rate histories resulting from using the 5th and 95th percentile values for these K_ds. The effect is negligible.

To account for other effects on sorption besides those encompassed by the base case ranges of the K_ds, an extreme alternative sorption model was examined. In particular, a model of zero sorption for the actinides (neptunium, uranium, protactinium, and plutonium) in the unsaturated zone is examined. One of the reasons that actinide sorption could disappear is that the repository may create thermal-chemical effects that could reduce sorption. One interaction that may lead to reduced actinide sorption in the unsaturated zone is an increase in pH. Higher values of pH may occur because of the interaction of water with concrete in the repository (see Section 3.3). The higher pH is believed to reduce sorption through geochemical effects on speciation of the actinides. For example, at lower values of pH (below 7), neptunium is expected to be primarily NpO_2^+, while at higher values of pH the dominant species is $NpO_2(CO_3)$ (Triay et al. 1997, p. 124, Table 47). The positively charged species of neptunium has a weak tendency to sorb onto matrix rock, but the negatively charged species is essentially nonsorbing.

Figure 5-43 compares total dose rates over the three time frames for the base case and the zero sorption case. It indicates that the early doses are not affected by sorption (primarily because of technetium), but that sorption helps to reduce the total dose rate between 50,000 and 250,000 years (primarily because of neptunium and plutonium) by about a factor of three.

The effects of neptunium sorption for this alternative model are given in Figure 5-44 over the first 100,000 years. When compared to the base case, the effect of K_d=0 of neptunium is found to be relatively small because neptunium is only weakly sorbing in the base case. Similar results are found

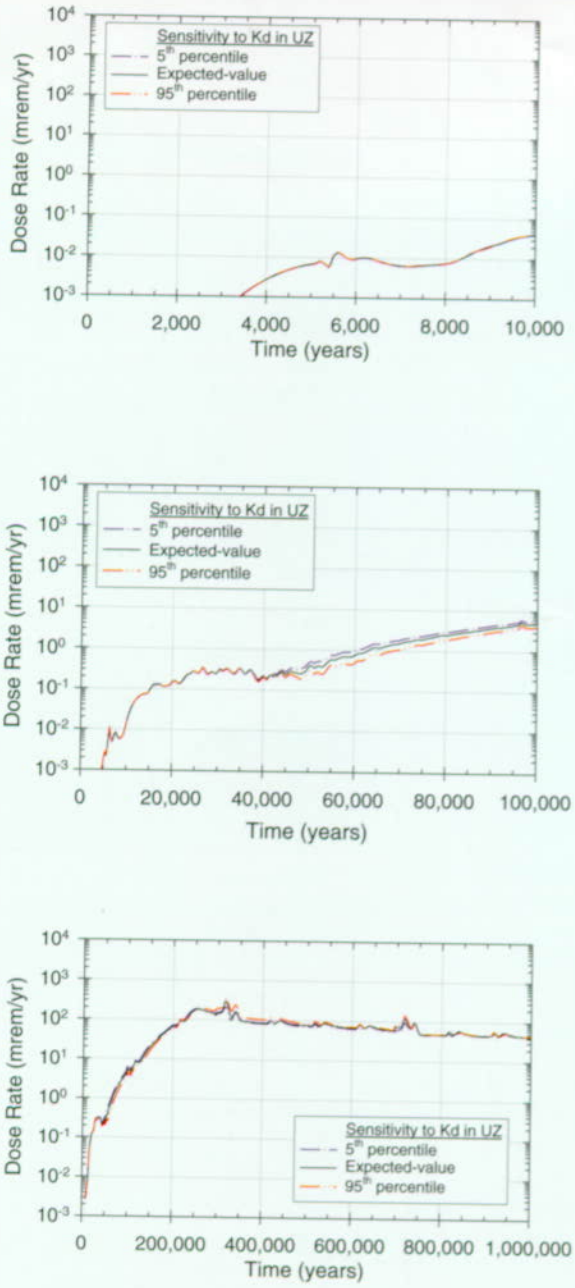

Figure 5-42. Effect of Radionuclide Distribution Coefficients in the Unsaturated Zone Matrix on Total Dose Rate at 20 km (12 miles)
Comparison of base case expected-value K_ds with the base case 5th and 95th percentile values. The primary effect is from the neptunium K_d.

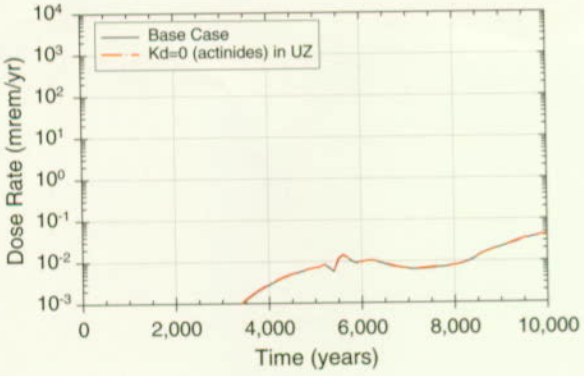

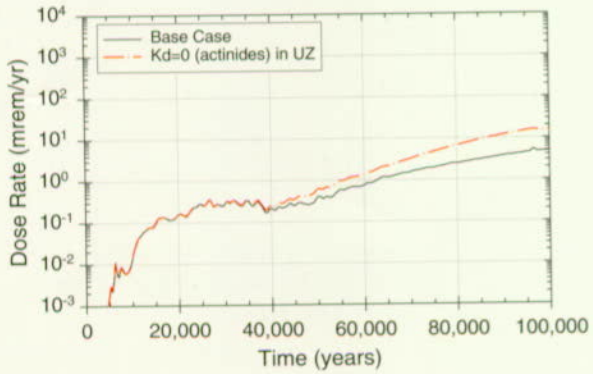

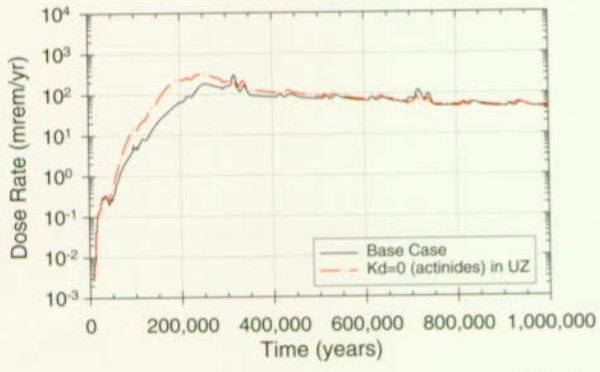

Figure 5-43. Sensitivity of Total Dose Rate to an Alternative Unsaturated Zone Transport Model that Assumes the Actinide K_ds in the Unsaturated Zone Rock Matrix are Equal to Zero
The primary effect is from the plutonium K_d.

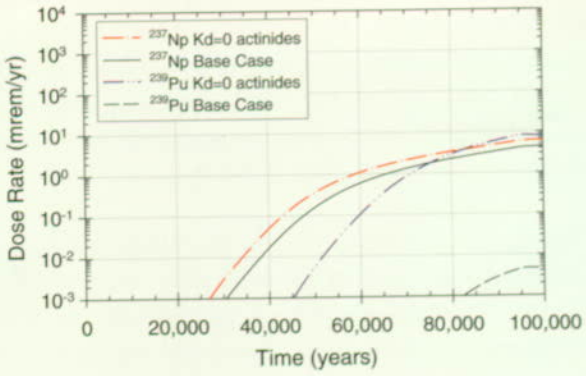

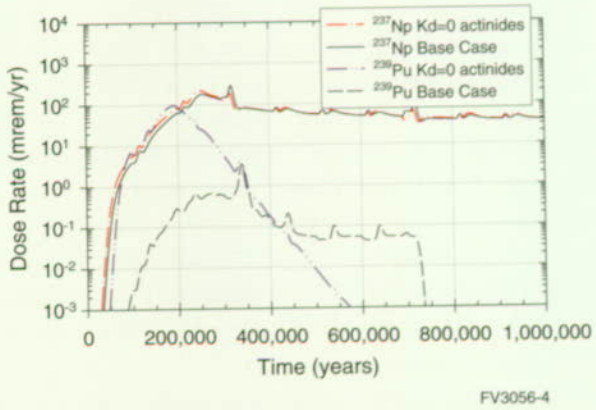

Figure 5-44. Sensitivity of Neptunium-237 and Plutonium-239 Dose Rate to an Alternative Unsaturated Zone Transport Model that Assumes the Actinide K_ds in the Unsaturated Zone Rock Matrix are Equal to Zero

for uranium, which is also a weakly sorbing element.

The effects of sorption on plutonium transport are more complex. Plutonium is a strongly sorbing radionuclide, but is also subject to colloidal transport. A portion of the colloid interaction is believed to be caused by sorptive mechanisms. Sorption on the rock matrix retards plutonium transport, while sorption on colloids facilitates plutonium transport. Therefore, the sensitivity of plutonium transport to sorption is a result of two competing effects. The overall effect of eliminating sorption on plutonium transport is shown in Figures 5-44 and 5-45 for plutonium-239 and plutonium-242, respectively. For both plutonium

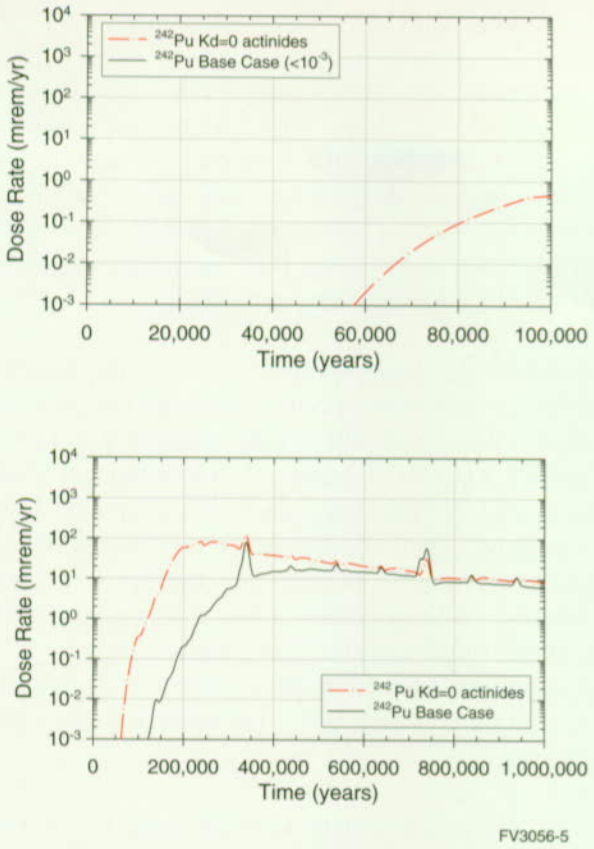

Figure 5-45. Sensitivity of Plutonium-242 Dose Rate to an Alternative Unsaturated Zone Transport Model that Assumes the Actinide K_ds in the Unsaturated Zone Rock Matrix are Equal to Zero

isotopes, the elimination of sorption causes higher dose rates. In fact, plutonium-239 dose rates slightly exceed those of neptunium-237 for the zero-sorption model between 100,000 and 200,000 years. These sensitivity results indicate that the sorption of aqueous plutonium on the rock matrix is dominant over the sorption of plutonium on colloids. Also, it is evident that the factor-of-3 increase in total dose indicated on Figure 5-43 between 100,000 and 200,000 years is caused by the plutonium isotopes becoming as important as neptunium-237.

5.6.3 Sensitivity to Combined Effects of Source Term and Unsaturated Zone Sorption

In addition to reducing sorption, increased pH from concrete dissolution may also promote waste package corrosion and waste form dissolution, as discussed in Sections 5.3 and 5.4, accelerating releases from the engineered barrier system. The dose effects at 20 km (12 miles) caused by the combined effects of zero sorption in the unsaturated zone and concrete-modified waste package and waste form degradations are shown in Figure 5-46. Dose is much higher before 10,000 years.

This early peak in dose is caused by greater releases of technetium from the engineered barrier system (see Section 5.3). Similarly to Figures 5-44 and 5-45, neptunium and plutonium are the primary causes of the later increase in doses. These increases in dose for neptunium and plutonium may be attributed to a combination of greater transport rates (see Section 5.6.1) and greater releases from the engineered barrier system (see Section 5.3). Changes in releases from the engineered barrier system indicate that plutonium-242 would always provide a greater portion of the dose than neptunium. However, sorption in the saturated zone is found to retard plutonium release to the accessible environment sufficiently so that the neptunium, which is less strongly sorbing, provides a greater portion of the dose following the technetium peak but before the arrival of plutonium.

By comparing Figures 5-14 and 5-43, it is apparent that most of the change in total dose rate for this alternative model is due to the effect on engineered barrier system releases up until 50,000 years and due to the effect on sorption in the unsaturated zone after 100,000 years. Between those two times, it is a combination of the two effects.

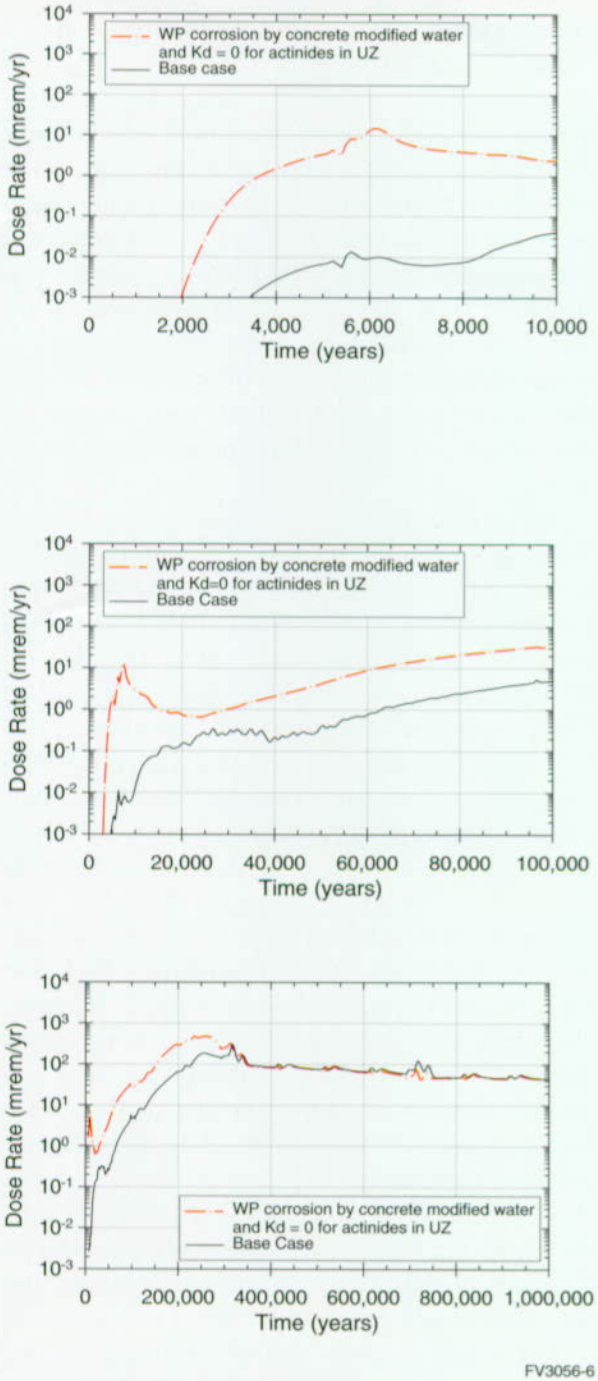

Figure 5-46. Sensitivity of Total Dose Rate to the "Alkaline Plume" Model
This model is a result of concrete degradation in the drift which raises the pH in the engineered barrier system and in the unsaturated zone. This causes an increased rate of waste package and waste form degradation and decreased (zero) sorption in the unsaturated-zone. Compare Figures 5-14 and 5-42. (UZ—unsaturated zone)

5.7 SATURATED ZONE FLOW AND TRANSPORT

Three sensitivity studies were conducted to look at the effects of base case assumptions about saturated zone flow and transport. The sensitivity studies addressed the importance of the dilution factor, the fraction of the saturated-zone flow path in alluvium, and how six flow tubes are combined to calculate the final concentration.

Assumptions about the flow model and parameters were not addressed because estimated variation in these areas would affect only radionuclide travel times and not significantly affect dilution and peak dose rate. Therefore, they are relatively less important. Also, changes in the effective-porosity parameter cause changes in the groundwater velocity. The effective porosity was considered probabilistically in the base case (Section 3.7). Assumptions about transport variables (other than the dilution factor) were not addressed for two reasons:

- These parameters also primarily influence radionuclide travel time, not dose rate
- They are defined with probability distributions and covered in the probabilistic analyses (Section 4.3)

One issue that cannot be addressed yet is the amount of dilution at the interface between the unsaturated and saturated zones. No additional dilution is allowed when contaminated water from the unsaturated zone enters the saturated zone. However, the contamination is assumed to uniformly spread through the water in each of the six areas at the base of the unsaturated zone so that dilution is implicitly considered. This assumption might overestimate dilution when a small number of containers release waste. As the number of releasing containers increases, the assumption becomes more appropriate.

5.7.1 Sensitivity to Dilution

The first sensitivity study addresses how the variation in the dilution-factor distribution affects

dose rate. Figure 5-47 shows the results of the expected-value base case. Also shown are two calculations that are the same as the expected-value base case, except that one calculation uses the 5th-percentile value of the base case dilution-factor distribution and the other calculation uses the 95th-percentile value. In the dilution-factor distribution, the median value is 10; the 95th-percentile value is a dilution factor of 49, or approximately a factor of 5 above the median. The 5th-percentile value is a dilution factor of 1.7, approximately a factor of 6 below the median. The dose is proportional to the radionuclide concentrations in the groundwater, and the concentration is inversely proportional to the dilution. The 95th-percentile dilution factor does decrease the expected-value-case dose rate by about a factor of 5. The 5th-percentile dilution factor does not increase the dose by a factor of 6. The 5th-percentile dilution is small enough so that the usual method of calculating the final concentration—adding the six stream tubes—exceeded the maximum undiluted concentration in the stream tubes (Sections 3.7.2.3 and 5.7.3). Hence, the dose-rate curve for the 5th-percentile dilution factor is calculated using the maximum undiluted concentration. It is significant that the dose rate does not increase in proportion to the dilution factor at very small dilution factors. The final difference between the 5th-percentile and 95th-percentile curves ranges between approximately a factor of 10 at early times and during superpluvials, and approximately a factor of 7 at other times. This difference is enough to cause the dilution factor to be one of the most important parameters (Section 4.3).

5.7.2 Sensitivity to Alluvium Fraction

The second sensitivity study addresses how the fraction of the saturated zone flow path in alluvium affects dose rate. Alluvium has higher effective porosity and higher radionuclide retardation as compared to the fractured tuff, so transport tends to be significantly slower through the alluvium. Figure 5-48 shows dose-rate history curves for the expected-value base case plus two additional cases defined by setting the alluvium fraction to the 5th percentile and the 95th percentile of its base case probability distribution while keeping all other

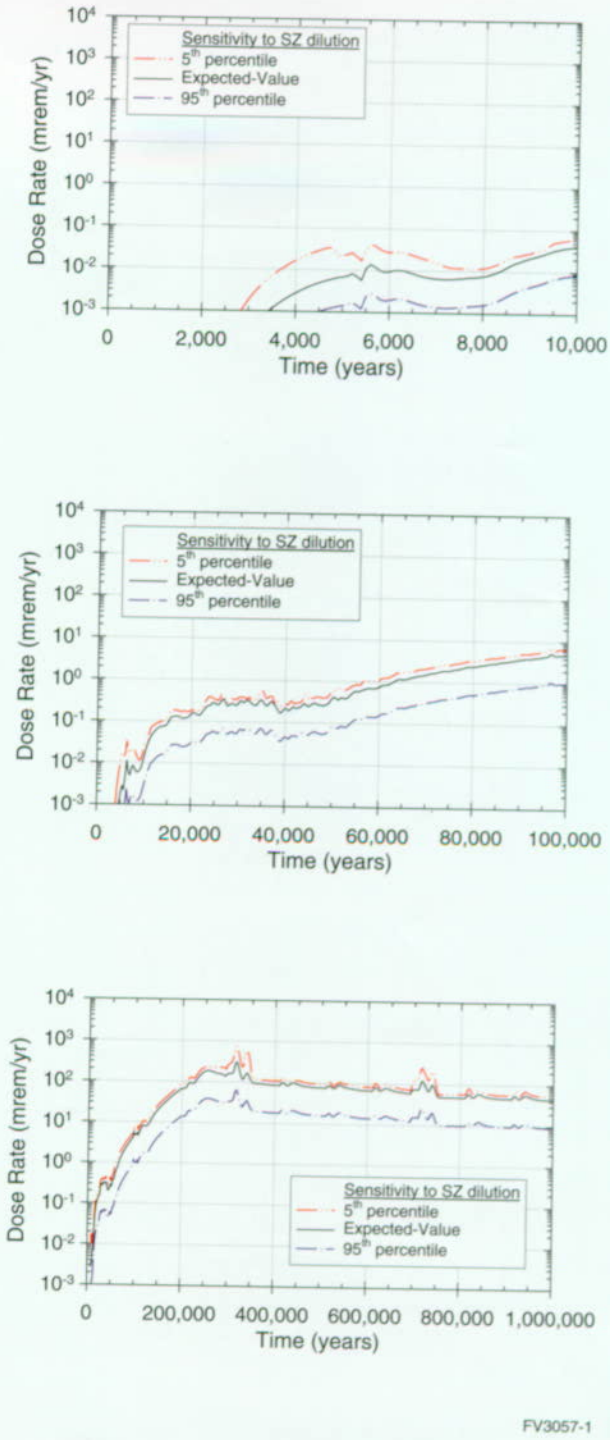

Figure 5-47. Total Dose-Rate History Curves for the Expected-Value Base Case and Cases that Have Saturated Zone Dilution Factor at the 5th and 95th Percentiles of its Base Case Distribution (SZ—saturated zone)

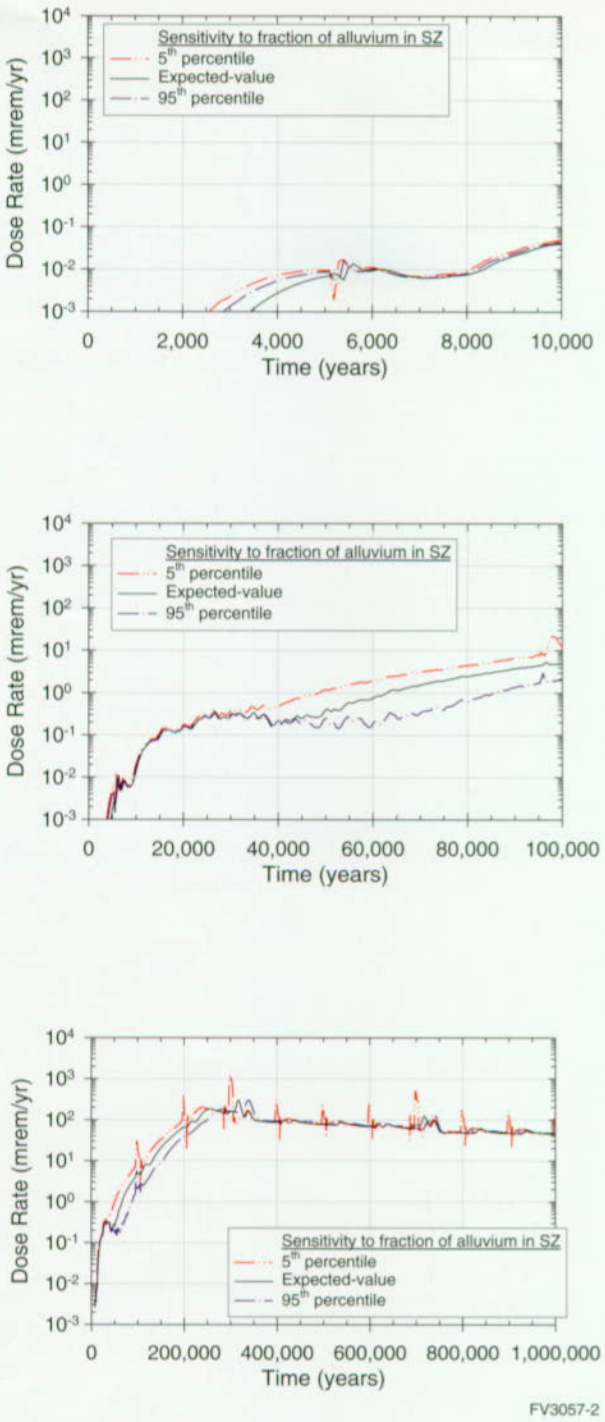

Figure 5-48. Total Dose-Rate History Curves for the Expected-Value Base Case and Cases that Have the Fraction of the Saturated Zone Flow Path in Alluvium at the 5th and 95th Percentiles of its Base Case Distribution
(SZ—saturated zone)

parameters fixed at their expected values. Figure 5-48 shows that alluvium fraction affects the dose rate by a moderate amount. The most interesting behavior is shown in the 1-million-year plot (Figure 5-48, bottom). The spikes caused by climate changes are much more pronounced in the fifth-percentile case. This behavior results because the alluvium in the flow path has a damping effect on the climate-change spikes, so when there is less alluvium the spikes are larger.

5.7.3 Sensitivity to Method of Flow-Tube Combination

The third sensitivity study examines the effect on the dose-rate results of how the six one-dimensional flow tubes are combined, for the saturated zone, to estimate the final, diluted concentration at the biosphere/geosphere interface. Radionuclide concentrations at a distance of 20 km (12 miles) were calculated separately for each of the six flow tubes (Section 3.7). The goal is to preserve the spatial variability but allow diffusion and dispersion out of the individual flow tubes and potentially into neighboring flow tubes. Three methods are considered for calculating the concentration used for determining dose:

- The final concentrations in the six flow tubes are summed. If the sum is larger than the greatest initial concentration in one of the flow tubes, then that initial concentration is substituted for the result. It is not physically realistic for concentrations to increase above the initial maximum concentration. This method overestimates the concentration; it is the method used in the base case.

- The final concentration in the flow tube that is the greatest of all the flow tubes is selected as the maximum concentration. This method underestimates the final concentration because radionuclides from other flow tubes might diffuse or disperse into the selected flow tube. (By the principle of linear superposition of solutions, two spreading plumes that overlap must have at least as high a maximum concentration as if they did not overlap.)

- One flow tube is used in place of the six flow tubes to calculate the final concentration. This method also underestimates the final concentration, because initially all radionuclides are distributed in all the water from the unsaturated zone, thereby ignoring spatial variability and omitting any potential high-concentration regions.

The results of the concentration-combination study are presented in Figure 5-49. The first method is incorporated in the expected-value base case. The other methods are modifications of the expected-value base case. As anticipated, the first method—summing the concentrations—causes the greatest doses. The second method—using the highest concentration flow tube—causes doses that are approximately a factor of four below the first method. The third method—using one flow tube—causes doses that are approximately a factor of six below the first method. The relationship depends on the distribution of radionuclides in the flow tubes at the boundary between the unsaturated and the saturated zones. The calculated dose depends on the method of determining the final concentration. However, the differences in dose are less than the differences caused by parameters such as the dilution factor that are significant to the final results (compare Figures 5-47 and 5-49).

5.8 BIOSPHERE

Three sensitivity studies were conducted to look at the effects of assumptions about the biosphere on the TSPA calculations. Other assumptions internal to the biosphere modeling that affected calculation of biosphere dose conversion factors also were considered (see Section 3.8.3).

The sensitivity studies address how the variability in biosphere dose conversion factors influences the final calculated dose rates, how assumptions related to dilution at the well and in the biosphere affect the calculated dose rates, and how assumptions about the critical group affect calculated dose rates.

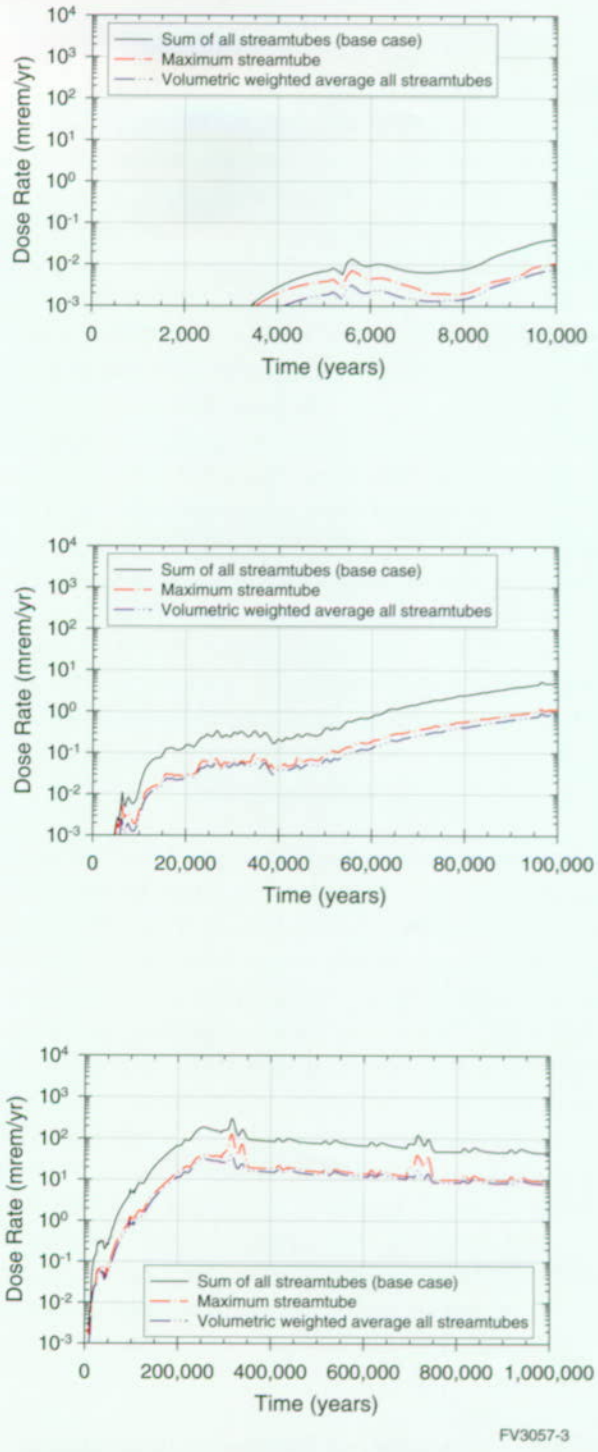

Figure 5-49. Total Dose-Rate History Curves for the Expected-Value Base Case and for Two Sensitivity Cases that Use Different Methods for Combining the Six Flow Tubes Used to Model the Saturated Zone

5.8.1 Sensitivity to Biosphere Dose Conversion Factor

The first sensitivity study addresses how the final dose calculation is affected by the spread in the distributions used to define the biosphere dose conversion factors. Figure 5-50 shows the results of the expected-value base case. Also shown are two calculations that are the same as the expected-value base case, except that in one the 5th-percentile values of each biosphere dose conversion factor distribution for each radionuclide is used and, in the other calculation, the 95th-percentile values are used. In the figure, using the 5th-percentile, biosphere dose conversion factors decreases expected-value-case dose rates by about a factor of 3; using the 95th-percentile biosphere dose conversion factors increases the dose rates by about the same amount. The spread in most of the biosphere-dose-conversion-factor distributions is about an order of magnitude (a factor of 10), and thus the difference in doses calculated by the 5th-percentile and 95th-percentile values also is about an order of magnitude.

The three curves shown in Figure 5-50 have an identical shape. The dose is proportional to the concentration of radionuclides in the groundwater, and the biosphere dose conversion factors for the radionuclides are the constants of proportionality. Although this is a linear relationship, when combined with the relatively large uncertainty in biosphere dose conversion factors as shown by the order-of-magnitude spreads in the distributions, it is enough to cause the biosphere dose conversion factor to be an important parameter in TSPA-VA. (That is, out of 177 parameters defined with probability distributions in the base case, the biosphere dose conversion factors are number three in importance over the one-million-year time frame, as shown in Figure 4-34.)

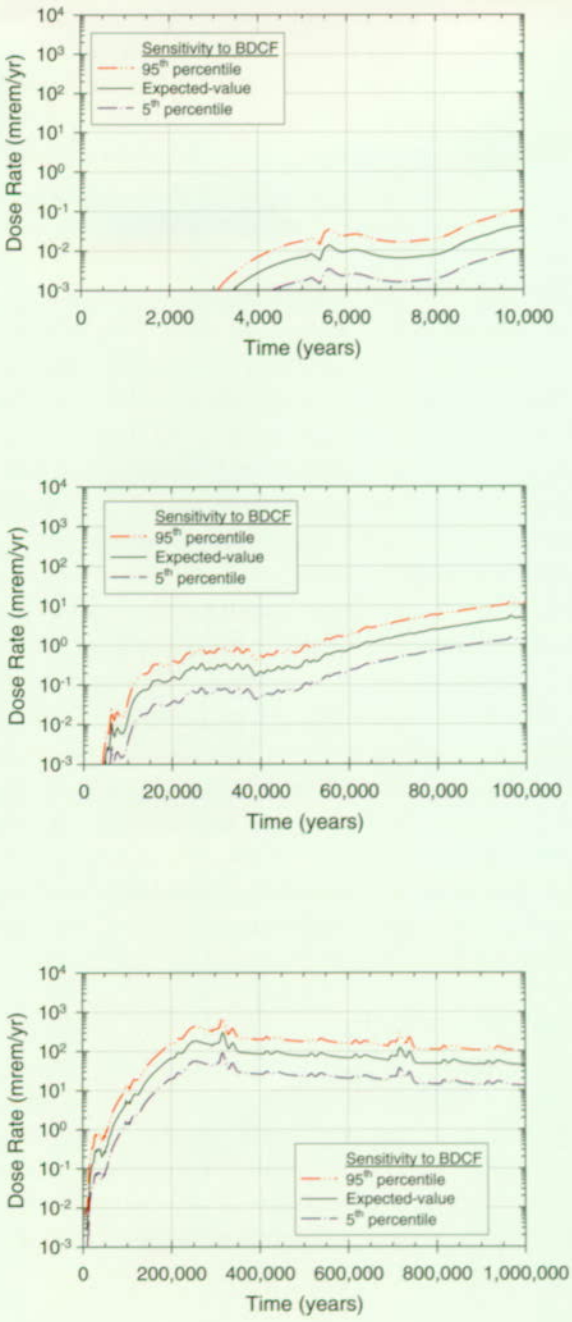

Figure 5-50. Total Dose-Rate History Curves for the Expected-Value Base Case and Cases that Have Biosphere Dose Conversion Factors at the 5th and 95th Percentiles of Their Base Case Distributions (BDCF—biosphere dose conversion factors)

5.8.2 Sensitivity to Dilution at the Well and in the Biosphere

The second sensitivity study examines assumptions made in the base case analyses concerning well-water withdrawal, well location, and food-source

location; these assumptions are related to the choice of an individual-dose performance measure. Some of these assumptions are as follows:

- The individual's water source is always at the point of maximum contamination in the aquifer.
- There is no dilution during withdrawal of water from the aquifer; that is, there is no mixing of contaminated water with uncontaminated water when the water is pumped from the ground or when the water is stored in a tank.
- The locally produced foodstuffs that this individual consumes, as determined by a survey of existing inhabitants of the Amargosa Valley region (Section 3.8.1), were all grown with this maximally contaminated groundwater. In other words, consumables, possibly grown away from contaminated groundwater, but still in the Amargosa Valley region, were considered to be contaminated.

If the plume of contaminated groundwater is large and dispersed, these assumptions are reasonable. In the saturated zone modeling, the contaminated groundwater travels in flow tubes and is typically diluted by a factor of 10. The original plume has cross-sectional dimensions of about 3,000 m (10,000 ft) horizontally and 10 m (30 ft) vertically. The plume at 20 km (12 miles) downgradient has an undefined cross section, but with a dilution factor of 10, it might have dimensions of about 10,000 m (30,000 ft) horizontally and 30 m (100 ft) vertically. At the estimate groundwater flux of 0.6 m/year (2 ft/year), such a plume would constitute approximately 180,000 m^3/year (50 million gal/year) of water. (This approximation is somewhat less than the volume actually used in the expected-value base case.)

To examine the assumptions that all drinking water and all local consumables are produced using well water containing the highest concentration of radionuclides, the average dose rate per person is introduced. To calculate an average dose rate per person, all contamination is assumed to be spread equally in all water available to a group of people. Also, each member of the group is assumed to use the same amount of water—the average water usage per person. For a given volume of contaminated water, the size of group of people can be estimated. For a given mass of radionuclides, the radionuclide concentration—and thus the average dose rate per person—can be estimated.

The mass of each radionuclide reaching the 20-km (12-mile) distance from Yucca Mountain at a given time can be taken from the TSPA-VA expected-value base case results. This mass is dissolved in a certain amount of water, for example, if the approximate base case volume is assumed, then this mass is dissolved in 180,000 m^3/year of water directly linked to the repository. If, however, it is assumed that this mass is dissolved in all of the groundwater that is currently being pumped from the Amargosa Valley, which includes water sources not linked to the repository, then this mass is dissolved in an estimated 12 million m^3/year (3 billion gal/year), resulting in a lower concentration of radionuclides in water. Note that based on this estimate of present-day water production, the average water usage for a member of the Amargosa Valley population (approximately 1,300 people) is about 9,300 m^3/year or 2.5 million gal/year.

The peak radionuclide release over a one-million-year period is estimated to occur 317,000 years in the future and the major contributor to the dose rate is neptunium-237, which reaches 20 km (12 miles) at the peak rate of 12 g/year. If this mass of radionuclide is dissolved in the amount of water corresponding to the current estimated volume of water produced in Amargosa Valley instead of the base case volume, then the resulting radionuclide concentration is 1.0×10^{-6} g/m^3. The dose rate resulting from using this contaminated water is found by multiplying the radionuclide concentration by the biosphere dose conversion factor, which for neptunium-237 is 4.6×10^{6} mrem/year per g/m^3. The result is an average peak dose rate of 4.6 mrem/year. If, however, the approximate base case volume is assumed, the resulting neptunium-237 concentration is 6.7×10^{-5} g/m^3, and a corresponding average peak dose rate is 308 mrem/year.

(This dose rate does not correspond exactly to the value calculated for the expected-value base case described in Section 4.2. The peak dose rate in the expected-value base case occurred during the long-term-average climate and was calculated for a larger groundwater flux. However, the concentrations for the various flow tubes used were combined in the expected-value base case, yielding a similar concentration and dose rate to the values presented here.) This sensitivity analysis shows that dose rate is 67 times higher for the base case than if the entire water-production dilution is assumed. Based on the current Amargosa Valley water usage per resident (9,300 m^3/year), the approximate base case volume of groundwater (180,000 m^3/year) could only support about 20 people. Figure 5-51 presents the relationship between the average dose rate per person and the size of the group using contaminated water, calculated using the peak radionuclide release from the expected-value base case results for the one-million-year period.

This analysis indicates that assumptions related to how radionuclides are distributed in the biosphere

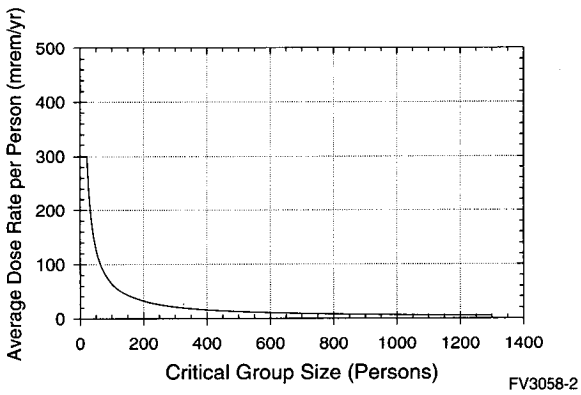

Figure 5-51. Average Dose Rate as Function of Critical Group Size for the Amargosa Valley, Estimated for the Expected-Value Base Case
The line indicates the average dose rate per person; the plateau value corresponds to the 300 mrem/year maximum dose rate calculated in the base case for the reference person. Approximately 20 people could incur this dose rate based on the calculated amount of radionuclides released to the biosphere and the average water usage per person in the Amargosa Valley. The distribution of these radionuclides among the entire population would reduce the dose rate to an average of approximately 5 mrem/year.

(i.e., the volume of water the radionuclides are dissolved into) could affect calculations of dose rates by possibly a factor of 70. It also sets approximate limits on how many people (20) can incur the maximum dose rate calculated for the base case for the assumed usage.

5.8.3 Sensitivity to Critical-Group Definition

The third sensitivity study examines the effect on calculated doses of the assumptions made for the base case regarding what constitutes the critical group. In the base case, radiation doses were calculated for a reference person based on an average resident of Amargosa Valley, using distributions for consumption of water and locally grown food taken from a survey of residents (Section 3.8.1). In this section the base case is compared with two other possible dose receptors. One alternative is a "subsistence farmer," who lives entirely on water taken from the maximally contaminated part of the contaminant plume, including all drinking water and all water used to grow produce and livestock. The other alternative is a "resident farmer," who is assumed to consume 50 percent locally grown food that is contaminated by water from the maximally contaminated part of the contaminant plume.

Figure 5-52 compares the two alternative dose calculations with the base case. The spread between the highest method (the subsistence farmer) and the lowest method (the base case) is a factor of 4 to 5. These results are consistent with the differences in these receptors types presented in Figure 3-80.

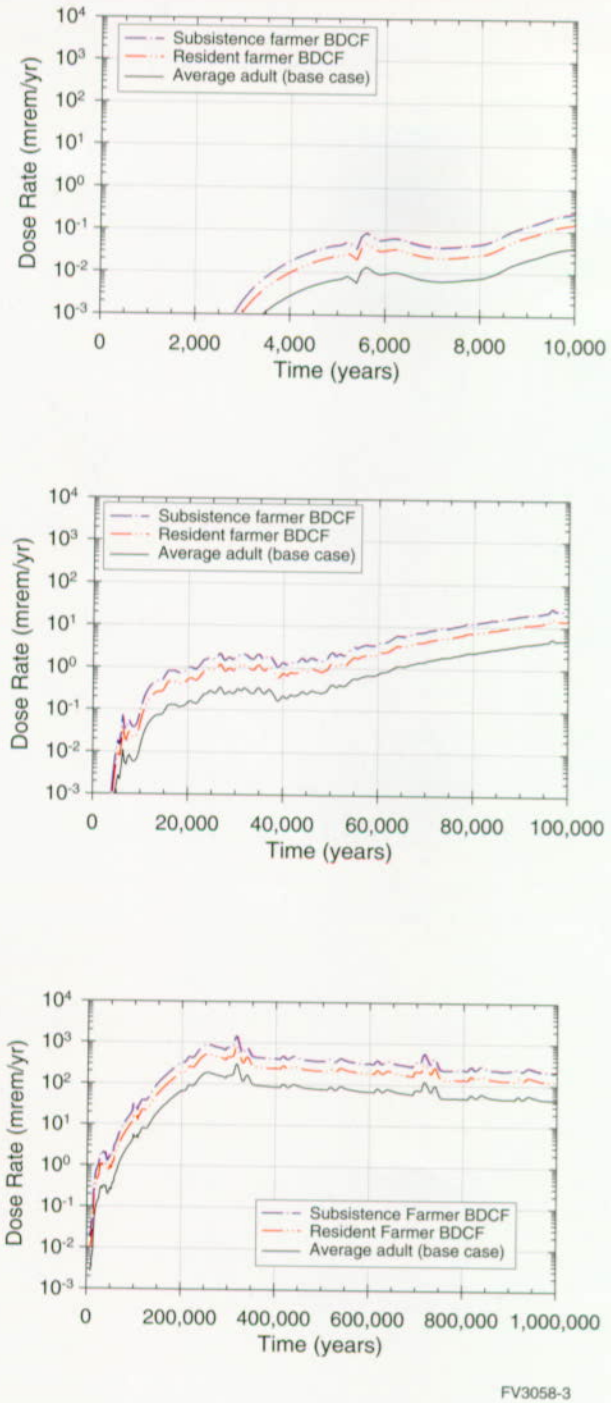

Figure 5-52. Total Dose-Rate History Curves for the Expected Value Base Case and for Two Sensitivity Cases in Which Different Critical Groups are Assumed

INTENTIONALLY LEFT BLANK

6. SUMMARY AND CONCLUSIONS

The objective of the TSPA-VA was to conduct and document "a total system performance assessment based upon the design concept and the scientific data and analysis available by March 1998, describing the probable behavior of the repository in the Yucca Mountain geological setting relative to the overall system performance standards" (Public Law 104-206). This volume of the VA contains the information, analyses, and interpretations used to describe "probable" behavior of the proposed Yucca Mountain repository system.

The projected behavior of the Yucca Mountain repository system is based on the site-specific scientific data and analyses summarized in Volume 1, and in Section 3 of this volume. The Yucca Mountain repository and waste package design concepts used in this TSPA are described in detail in Volume 2, and the relevant scientific data and analyses used to evaluate the behavior of these designs are summarized in Section 3 of this volume. This information has been used to develop an estimate of the probable behavior of the repository disposal system, comprised of both engineered and natural components. The results of these analyses have been presented in Section 4 of this volume.

In examining and summarizing results describing the "probable" behavior of the Yucca Mountain repository system, it is important to understand that the evaluations are indicators of the postclosure performance impacts of the proposed repository. The analyses should not be construed as predictions in the normal sense of the word. Although an attempt has been made to incorporate the most current understanding of key processes affecting the long-term behavior of Yucca Mountain, such projections are uncertain. Although many of these uncertainties will still remain at the time of the License Application (LA), DOE will reduce the significant uncertainties sufficiently and modify the design as appropriate to provide NRC with reasonable assurance that post closure performance objectives can be met. The uncertainty is a result of several factors:

- The periods are long. The period for the quantitative analyses extends to 10,000 years and beyond. Over these long periods, there is uncertainty in the definition of likely future environments. This period is also long compared to available information about a number of principal factors affecting repository performance such as the degradation rates of corrosion-resistant metals.

- The site is heterogeneous. Water movement in the unsaturated and saturated zones at Yucca Mountain is expected to vary with location and with time because of the heterogeneous nature of the fractured rocks. Precisely defining the flow paths and volume and geochemical interactions along the flow paths is not possible.

- The system is coupled. Coupled interactions are expected to occur near the emplaced wastes. These interactions include thermal, chemical, hydrologic, and mechanical processes that can influence one another. For example, the chemical alteration of the rock caused by a temperature increase may cause the hydrologic properties of the rock to change. It is difficult to predict the magnitude and extent of these changes with any precision.

- Future populations are unknown. It is not possible to reasonably forecast changes in human activities. Therefore, the doses calculated are based on the activities of the present-day population in the region around Yucca Mountain. This assumption, which is consistent with internationally accepted recommendations (see Section 3.8), implies that the doses represent the range of likely performance of a repository for a hypothetical population.

Although these uncertainties are recognized in the analyses and interpretation of results, they do not detract from the goal of objectively evaluating how the system is likely to perform. To precisely identify the exact magnitude of the effects and consequences for disposing 70,000 metric tons of nuclear waste at Yucca Mountain is not expected

by the regulators. For example, NRC has noted in 10 CFR Part 60.101 (a)(2):

> While these performance objectives and criteria are generally stated in unqualified terms, it is not expected that complete assurance that they will be met can be presented. A reasonable assurance, on the basis of the record before the Commission, that the objectives and criteria will be met is the general standard that is required. For 60.112, and other portions of this subpart that impose objectives and criteria for repository performance over long time periods into the future, there will inevitably be greater uncertainties. Proof of the future performance of engineered barrier systems and the geologic setting over time periods of many hundreds or many thousands of years is not to be had in the ordinary sense of the word. For such long-term objectives and criteria, what is required is reasonable assurance, making allowance for the time period, hazards, and uncertainties involved, that the outcome will be conformance with those objectives and criteria.

In addition, EPA has noted the following with respect to the degree of confidence that is expected (40 CFR 191):

> Performance assessments need not provide complete assurance that the requirements of 191.13(a) will be met. Because of the long period involved and the nature of the events and processes of interest, there will inevitably be substantial uncertainties in projecting disposal system performance. Proof of the future performance of a disposal system is not to be had in the ordinary sense of the word in situations that deal with much shorter time frames.

The assessment provided here is not final. It does not include the type of evaluation of a number of design options that will be conducted for the LA. Also, analyses to address design margin and defense in depth have not yet been completed. However, this assessment does include sufficient sensitivity and uncertainty analyses to illustrate the range of possible behaviors that might be anticipated. These analyses have assisted DOE in focusing the data-collection, model-validation, and design-development activities between now and the LA. While the projections of future behavior presented appear reasonable, additional information may be needed to demonstrate regulatory compliance in a licensing proceeding.

Although uncertainties exist regarding many factors affecting repository performance, these uncertainties have been reasonably bounded and analysis have been satisfactorily completed using these bounded values. Therefore some uncertainties and areas of limited data will remain as they are while other uncertainties may require further study in order to provide a sufficiently robust analysis of repository performance for the LA.

As noted above, it would be ideal to be able to make all decisions based on complete information. However, the behavior of the repository system over tens of millennia will never be known with certainty. The regulatory agencies agree that reasonable conclusions about whether a repository system can be expected to provide the public with adequate protection from nuclear waste need not include this degree of absolute certainty.

6.1 SCIENTIFIC DATA AND ANALYSES IN THE TOTAL SYSTEM PERFORMANCE ASSESSMENT FOR THE VIABILITY ASSESSMENT MODELS

One of the principal objectives of the analyses for this TSPA was to use all the available scientific data and analysis in the performance evaluation of the Yucca Mountain repository system. The data consist of a suite of laboratory, surface based, and in situ tests and observations conducted as part of the YMP. These tests and observations provided data that have been used in analytical tools consisting of conceptual, process, abstracted, and numerical models. These models, in conjunction

with the test data for defining a range of parameter values, have been used as the basis for this TSPA.

An evaluation of total system performance is a projection or estimate of the expected future behavior of the repository system. With the possible exception of some naturally occurring uranium ore bodies and other natural analogs, there are no directly observable phenomena that are comparable to the potential repository system at Yucca Mountain. Because of this, it is necessary to extrapolate the projections of future behavior based on present-day observations of the same phenomena. The extrapolation of the relevant phenomena into the future is accomplished using models based on laboratory, surface based and in situ test data and observations. These models describe the behavior of the relevant processes.

Laboratory test data are valuable in improving confidence in models used for future projections of behavior because they can be conducted under well-controlled conditions and can be designed to address specific data needs.

Examples of laboratory testing that has been used in the development of models for this TSPA include:

- Corrosion testing of candidate waste package metals, including the outer corrosion allowance and the inner corrosion resistant barrier (Alloy 22)
- Intrinsic dissolution testing of the spent nuclear fuel and glass waste forms
- Alteration tests and secondary phase formation of spent nuclear fuel and glass
- Radionuclide mobility tests including solubility and colloid formation
- Radionuclide sorption tests
- Coupled thermal, mechanical, chemical, and hydrologic tests of rock alteration
- Rock matrix property tests to determine hydrologic properties

Surface based tests and observations are valuable in determining site-specific properties necessary to define how water moves through the unsaturated and saturated zones of the Yucca Mountain repository system. Surface based tests are conducted from a range of shallow (about 10 m, or 33 ft, deep) and deep (over 1,000 m, or 3,300 ft, deep) boreholes. The types of surface based tests and observations include:

- Mapping geologic features and hydrostratigraphy
- Mapping fracture characteristics and lithology
- Testing hydrologic properties
- Observing ambient water content and matrix potential in the unsaturated zone
- Measuring precipitation, temperature, and other meteorological variables
- Measuring moisture transients in the near surface (net infiltration)
- Measuring seismological disturbances
- Mapping and analyzing volcanic features
- Observing water potential in the saturated zone
- Observing ambient temperature and aqueous geochemistry
- Cross-hole testing of transport characteristics

In situ tests and observations are valuable in determining the site-specific properties necessary to define environmental conditions that control performance of the engineered barriers of the Yucca Mountain repository system. In situ tests and observations at Yucca Mountain have been made from a number of niches constructed in the Exploratory Studies Facility and other test facilities near Yucca Mountain, such as at Busted Butte. Although in situ tests are expensive because of the

construction and operational costs of the underground facilities, they are the principal means of testing the host rock under conditions similar to what might be expected in the presence of a repository. Examples of in situ tests and observations include:

- Single and drift scale heater tests to evaluate the thermal, hydrologic, chemical, and mechanical response of the rock when heated
- Observations of in situ water content, chemistry, isotopes, and mechanical stress of the rock mass around the underground tunnels
- Tests of in situ hydrologic, geochemical, and transport properties of the rock mass

These observations and tests form the basis for a suite of process and numerical models that have been used to develop this TSPA analyses. Each of these models and their abstraction into the TSPA model are described in Section 3. The term "abstraction" is used to indicate the extracting of essential information. The TSPA models are usually referred to as abstracted models. Details of this abstraction are presented in the *Total System Performance Assessment-Viability Assessment (TSPA-VA) Analyses Technical Basis Document* (CRWMS M&O 1998i).

While these tests and observations form the scientific basis for the models used, it is important to acknowledge the uncertainty in these models. Part of this uncertainty is caused by the complexity of the individual processes and their interactions. Another component of the uncertainty is caused by the variability of the natural system and the inability to completely characterize this variability. To address the uncertainty in each of these process models, DOE has conducted a number of different expert elicitations. The results of these elicitations have provided this TSPA analyses with a reasonable range of expected parameters and models that extend the range beyond what might be determined solely by the test information.

6.2 PROBABLE BEHAVIOR OF THE REFERENCE DESIGN

The performance assessments provide a picture of the repository system evolution and probable behavior, where probable behavior is defined as the behavior specified by the base case. The assessment considers the potential for radionuclide release from the repository system and transport 20 km (12 miles) from the repository, where the radionuclides could be drawn in water from a hypothetical well. The assessment is made for the repository design concept under consideration as described in Volume 2. The behavior of other design concepts could be somewhat different. These analyses, including the sensitivity studies, provide a broad indication of the kind of behavior expected for the system, the probable behavior. This section briefly describes the design concept and discusses the probable behavior of the system.

The design concept for the Yucca Mountain repository system is to place the various waste forms, whether commercial spent nuclear fuel, defense high-level nuclear waste glass, or DOE-owned spent nuclear fuel, into large waste packages. These waste packages are made of an inner highly corrosion resistant nickel alloy (Alloy 22) and an outer layer of carbon steel. The waste packages are placed on supports within mined drifts located about 300 m (1000 ft) beneath the surface. Following emplacement of individual waste packages, the drifts are sealed to prevent access, but otherwise the facility will be designed to remain open for 100 years (and perhaps several hundred years) after the start of waste loading to allow maintenance and observation until a decision is made to permanently close the facility. This design forms the basis of this TSPA. The details of this design concept are presented in Volume 2.

The presentations in Sections 3 and 4 showed the probable behavior of the system from the viewpoint of a series of model results that, when integrated, yielded a description of the overall system behavior. This description was summarized in Section 2.4 as a series of time slices that synthesize the system response to the proposed design concept. These time slices were:

- Time of waste emplacement to time of repository closure
- Time of repository closure to several hundred years after closure
- Several hundred years to several thousand years after closure
- Several thousand years to ten thousand years after closure
- Ten thousand years to several tens of thousands of years after closure
- Several tens of thousands of years to one hundred thousand years after closure
- Several hundred thousand years to as long as a million years after closure

The assessment described in Section 4 indicates that the vast majority of radionuclides in the waste is immobile and never leaves the repository even if in contact with water. A small number of radionuclides, notably technetium-99, iodine-129, neptunium-237, and those radionuclides transported by colloids, are sufficiently mobile under some conditions that they could reach the biosphere downgradient from the repository. Therefore, these analyses indicate that the most important factors for system performance over time are the amount of water likely to contact the waste packages and the amount of waste exposed to that water. Consequently, long lived waste packages and engineered barriers or other factors that are effective in further limiting the contact of water with the waste will also be highly important to performance.

Under the base case scenario the quantities calculated to reach the biosphere are small: a negligible amount in 10,000 years and a dose rate for hundreds of thousands of years that is comparable to natural background activity. Although the assessment is conservative by virtue of overestimating the effects leading to release and transport, there are still some uncertainties in the estimates that will require further analysis. The sensitivity of the results to these uncertainties is discussed in Section 6.3.

6.3 SENSITIVITY ANALYSES OF THE REFERENCE DESIGN

One of the principal objectives of any total system performance assessment is to evaluate the significance of the assumptions made in defining the "probable" system behavior. One of the primary goals of this TSPA is to assist DOE in identifying, based on the reference repository design, the principal factors that affect the postclosure performance. A part of this objective is met by examining a range of possible outcomes predicated on a range of conceptual and parameter values. These results are presented in Sections 4.3 and 5. In addition, the possibility of some low-probability, potentially high-consequence disruptive scenarios has also been evaluated (Section 4.4). Finally, the effects of using different design options to compensate for some of the uncertainty in the various components of the natural and engineered system, and thus provide greater assurance of repository performance has been investigated (Section 4.5).

The sensitivity analyses conducted as part of this TSPA are summarized in this section. The summary includes a discussion of general insights gained during the course of the analyses. These insights include not only the direct quantitative sensitivity analyses, but also the understanding gained from a range of comparative analyses. Just as the individual results associated with a deterministic evaluation need to be tempered with realization of the uncertainty in the results, so too should the interpretation of a range of uncertainty analyses. For example, the importance of one component of the system can sometimes be masked by other, seemingly more significant components. It is also possible that the complete range of uncertainty for a particular component in the evaluation has not been fully evaluated. To address this issue, in some instances additional sensitivity analyses were conducted with wider uncertainty bounds. However, some judgment regarding the unquantified uncertainty must be used in assessing the overall significance of the principal factors in the repository safety strategy.

Finally, the significance of individual components at different locations and times must be examined because their importance can change depending on the performance measure used.

Evaluations of repository system performance are sensitive to different factors over different time frames. The analyses indicate no releases for the first several thousand years and the sensitivity studies indicate that this observation holds over a wide variety of variations of the components that could affect performance. The following summary addresses the sensitivities in the longer term. The summary has been broken into three time scales; up to 10,000 years, from 10,000 years to 100,000 years, and after 100,000 years.

6.3.1 Sensitivity Analyses over the First 10,000 Years

Over the first 10,000 years after waste emplacement, the overall performance is controlled principally by waste package failure. During this period, with few exceptions, the waste packages completely prevent water from contacting the wastes. A small fraction (on the order of 1/10 of 1 percent), of the waste packages may develop one or more small openings through the corrosion-resistant metal during the first 10,000 years. These packages would generally be located in areas of the repository either with a higher probability of more aggressive geochemical conditions or containing waste packages with a higher Alloy 22 corrosion rate. Because the reference design contains approximately 10,500 waste packages, some waste packages are anticipated to undergo more rapid degradation than others, simply because of the range in possible corrosion rates.

In addition to these "expected" failures, some low probability of failures may occur as a result of unanticipated events. These include:

- Waste packages that might fail prematurely by improper quality control of the welds or fabrication
- Impurities in the metals, leading to higher corrosion rates
- An unforeseen degradation mechanism acting on the waste package materials

Although procedures will be developed and implemented to minimize or eliminate these early failures, they have been included in this analyses in order to evaluate the sensitivity of the results to them.

Once the waste package has been breached, the next significant component is the amount of the waste form surface that is exposed and in contact with water. The amount of water entering the waste package is assumed to be proportional to the perforation area. For the commercial spent nuclear fuel and naval spent nuclear fuel, the negligible corrosion rate of the Zircaloy cladding minimizes the amount of exposed waste form surface. For the other waste forms, once the package is breached the entire surface area of the waste form is assumed to be exposed. In all of the TSPA-VA analyses, water is assumed to contact all of the exposed waste. This is a conservative assumption, but to do otherwise in a quantitative fashion would require a degree of sophistication that would be difficult to substantiate. For the highly soluble radionuclides that dominate the 10,000-year dose rates, the rate at which fuel is exposed and contacted by water dominates the release rate from the engineered barriers.

The calculated dose rate from radionuclides released from the waste package in this period is influenced by their travel time and by the degree of dilution that occurs as the radionuclides migrate to the biosphere. The travel time depends on the flow velocities in the unsaturated and saturated zones. The climate at Yucca Mountain is expected to change from the present-day dry conditions to a presumed wetter environment associated with what is believed to be the long-term average climate. The timing of this climate change and the net infiltration have a significant effect on the travel time of any dissolved radionuclides released from the engineered barriers in the first 10,000 years. Under present-day conditions, the time for 50 percent of the mass of highly soluble, unretarded species to travel from the repository to the water table is a few thousand years. It takes an additional few thousand years for 50 percent of the mass to travel

in the saturated zone from the repository footprint to the assumed compliance point 20 km (12 miles) downgradient. Retarded species take significantly longer than these times. Therefore, if no releases occurred from the engineered barriers for thousands of years, then the present-day climate regime indicates that only a small fraction of the released inventory would be transported 20 km (12 miles) in the first 10,000 years. Invoking a climate change within the first 10,000 years significantly reduces these travel times. As the amount of water moving through the rocks increases, the velocity of the groundwater increases, causing a greater percentage of the groundwater to flow more rapidly through fractures in the nonwelded tuff units.

The effective amount of dilution as radionuclides move through the unsaturated and saturated rocks to the biosphere depends on several things. The dilution is influenced by the degree to which water contacting the waste is mixed with uncontaminated water in the emplacement drifts. It is also altered as the water bearing the radionuclides mixes with the water that has never entered the drift in the rock in and around the drifts, in the path to the water table, and in the paths through the saturated zone. Finally, the degree of dilution is affected by pumping at a well.

As noted in Section 4.1, the flux through the unsaturated zone within each of six different repository regions is assumed to mix the different sources of radionuclides created when each individual package is breached and begins to release radionuclides. In areas of the repository underlain by perched water bodies and/or significant lateral flow this is a reasonable assumption. At times when a significant number of waste packages have been breached and are releasing radionuclides this is also a reasonable assumption given the relatively close spacing of the waste packages. However, there is more uncertainty implicit in this assumption at early times (less than 10,000 years), when only a very few waste packages have been breached. If those breached packages are located in the southern half of the repository (where the flow is predominantly vertical), the degree of transverse mixing that might be anticipated between the breached waste package in the repository and the water table may not have been adequately captured in the model. Quantifying the effect of this uncertainty is not currently possible, given the degree of spatial averaging and numerical discretization used in the unsaturated zone radionuclide transport model. Although the significance of this uncertainty may be minimized by possible mixing in the saturated zone or at the well, it is anticipated that additional analyses will be required before licensing to define the significance of this issue.

In summary, the most significant components in the determination of the dose rates at 20 km (12 miles) from the Yucca Mountain repository over the first 10,000 years are the following:

- Seepage contacting the waste packages and waste forms
- Waste package containment, including effects both of premature waste package failures and of waste package degradation rates
- Rate of cladding failure
- Chemistry of water contacting waste package surfaces
- Travel time, including the effect of timing and the magnitude of climate change
- Degree of mixing in the unsaturated and saturated zones
- Biosphere dose conversion factor

The peak dose rates during this period are forecast to be small. The median (50th percentile) dose is 0.002 mrem/year with the 5th and 95th percentiles of 0 and 0.8 mrem/year, respectively. The mean peak dose rate is forecast to be 0.1 mrem/year. The variations in the forecasted dose results primarily in variations in the first two components. Finally, it should be noted that, in the event of immediate cladding failure, Figure 5-29 indicates that the median dose could be about 1 mrem/year in the 10,000 year time frame.

6.3.2 Sensitivity Analyses from 10,000 to 100,000 Years

It is expected that the potential future regulatory requirements for Yucca Mountain will focus on dose assessments to 10,000 years. However, analyses beyond 10,000 years will be conducted to gain additional insights into repository system behavior. It is likely that the goal of the analyses beyond 10,000 years will be determining the average behavior and its confidence interval. This is different than examining the full range of potential performance (as has been done in Sections 4.3 and 5) that has been used as the basis for defining the significance of the principal factors of the repository safety strategy. Therefore, although useful insights into factors affecting dose rates beyond 10,000 years are discussed below, the degree to which these uncertainties need to be addressed before licensing requires consideration of how these long-term projections will be used in the LA.

From 10,000 to 100,000 years after the repository is closed, the important factors controlling the dose rate at 20 km (12 miles) change from those that were important in the first 10,000 years. The principal reason is the change in the radionuclides that dominate the dose rate. As the period is extended, the controlling radionuclides generally (but not always) change from being the highly soluble, unretarded radionuclides such as technetium-99 and iodine-129 to low solubility, slightly retarded species dominated by neptunium-237. Even at extended times the high solubility radionuclides may dominate the predicted dose rate if any of the following conditions are present:

- The rate of waste package failures is low.
- The amount of seepage into the drifts or into the waste packages is low.
- The solubility of the solubility-limited radionuclides is low.

An additional explanation for the change in key components as the period of interest is extended beyond 10,000 years is the difference caused by the groundwater flow regime. While the advective travel time can make a difference when considering the present-day climate over 10,000 years, over a longer period the nonsorbed or poorly sorbed radionuclides that are released from the engineered barriers will reach the hypothetical well located 20 km (12 miles) downgradient. However, once the climate state switches to being the long-term average precipitation, the net infiltration, percolation flux, and advective velocity all increase significantly. This decreases the travel time for any radionuclides that may be traveling through the unsaturated or saturated zones. Even over this period, the more highly sorbed radionuclides are effectively immobile in the Yucca Mountain environment.

The dominance of specific radionuclides in the dose rate changes over the 100,000-year period. For example in the expected value base case realization presented in Section 4.2, the time at which neptunium-237 begins to dominate the dose occurs about 40,000 years after repository closure. Because of this change, the significant components driving the performance are some combination of those that affect the concentration and dose rate of technetium-99 and those that affect the concentration and dose rate of neptunium-237. The controlling factors are examined separately in the following paragraphs.

High solubility, low retardation radionuclides such as technetium-99 are generally called "release-rate-limited" radionuclides. The release rate from the engineered barriers is controlled by the rates of waste package failure, the surface of the waste form exposed through clad failures and contact with water. The rate of waste package failure is a function of the presence or absence of seeps and the degradation rate of the Alloy 22 metal in the waste package. If the clad is failed and water contacts the waste, the advective or diffusive travel times through the engineered barriers are generally short in comparison to the 100,000-year period of the analyses. This short travel time is, in part, a result of the conservative assumption that the water pathways inside the waste package and the water film along the waste form surface are continuous. Therefore, the advective and diffusive travel times are short for the highly soluble radionuclides

released from the engineered system after the waste packages have been breached.

After the low-retardation radionuclides are released from the engineered barriers, their travel times to the 20-kilometer (12-mile) hypothetical well are on the order of several thousand years for the present-day climate. This delay time is reduced if there is a change to a wetter climate. In addition to the delay, the radionuclides released from the engineered barriers are diluted as the water containing the dissolved radionuclides mixes and disperses through both the unsaturated and saturated zones. Because not all the water that enters the drift has entered waste packages, some has diverted around the waste package, this mixing starts as soon as the water containing the dissolved radionuclides leaves the waste package and enters the drift. Because not all the water that intersects the drift has entered the drift, some has diverted around the drift, the mixing continues as the water containing dissolved radionuclides leaves the drift and enters the rock. This mixing effectively reduces the concentrations of the dissolved radionuclides.

The release rate of the less mobile radionuclides such as neptunium-237 is controlled by their solubility in the water. For these radionuclides, the solubility of the radionuclide in the water film on the waste form surface and the advective flux of water over the waste form surface control the release rate from the engineered barriers. For any repository region, the mass release rate for the solubility-limited radionuclides is a function of the cumulative number of waste packages that have been breached and the amount of water that seeps into each waste package. These aspects of the system are, in turn, controlled by the fraction of the waste packages in contact with seepage water, the amount of water that seeps, and the Alloy 22 degradation rate. This fact has been reinforced by the identification of the key parameters in the multiple-realization analyses presented in Section 4.3.

The solubility of some radionuclides, including neptunium, in the water on the waste form surface can be significantly affected by geochemical reactions of that water with the waste form as it alters. Spent fuel may progress through a complex series of alteration states. The different altered forms of the spent nuclear fuel can have neptunium retained in the solid state rather than being released to the aqueous phase. If neptunium is contained within these alteration products, then it will be immobile until the secondary and tertiary alteration phases have dissolved. The effect of these alteration phases on limiting the neptunium-237 dose has been investigated in Section 5.5.

Because the solubility limit is applied separately to each waste package, the total inventory exposed and in contact with water does not make an appreciable difference in the release rate of neptunium-237 from the repository. In part this is caused by the model not explicitly linking the solubility constraints to the clad failure model. Neptunium release remains almost unaffected by cladding degradation until the inventory in the initially breached waste packages has been depleted. With a 2 million year half-life, neptunium-237 does not significantly decay during the period of the analyses. The depletion time is a function of the amount of water that enters each waste package and the percent of the cladding that has been degraded (for commercial spent nuclear fuel). The analyses presented in Section 4.2 and 5.5 show that this time is several hundred thousand years.

Once the solubility-limited radionuclides are released from the waste package and transported through the invert, their transport through the unsaturated tuffs is controlled by the retardation characteristics of the rock. Many solubility-limited radionuclides are very highly sorbed on tuffs (they are essentially immobile in the Yucca Mountain setting). Neptunium-237 is slightly retarded on the tuffaceous rocks within the unsaturated zone. Therefore, in the time periods of interest, neptunium-237 released from the repository will travel through an average of 300 m (1,000 ft) of unsaturated tuffs to the water table. During the long-term climate state, this distance would be reduced to 220 m (720 ft) due to an assumed 80-meter (260-ft) rise of the water table. Eventually, these radionuclides will be transported through the saturated zone to the hypothetical well

located 20 km (12 miles) downgradient from the repository.

Another factor that could have an impact on overall performance is the colloidal transport of plutonium. There is significant uncertainty about the nature, stability, filtration, and adsorption and desorption characteristics of naturally occurring and waste form generated colloids. For the anticipated range in colloid properties considered, the dose rate attributed to colloidal plutonium-242 and plutonium-239 is less than the dose rate caused by neptunium-237. However, either expanding the possible range in colloid properties or reducing the neptunium solubility may cause colloidally transported plutonium-242 to be the dominant dose contributor at times in excess of 100,000 years.

In summary, the most significant components in determining the dose rates at 20 km (12 miles) from the Yucca Mountain repository over the first 100,000 years are the following:

- Fraction of waste packages with seepage
- Waste package degradation rate
- Cladding degradation rate
- Dilution and mixing in the unsaturated and saturated zones
- Timing and magnitude of climate changes
- Formation and transport of radionuclide-bearing colloids
- Formation of secondary neptunium mineral phases (related to waste form degradation rate)
- Neptunium solubility (related to the alteration rate of spent nuclear fuel)
- Biosphere dose conversion factor

The median (50th percentile) peak dose rate during this period is forecast to be 0.09 mrem/year, with the 5th and 95th percentiles at 0.0 and 200 mrem/year, respectively. The mean peak dose rate is forecast to be 30 mrem/year.

6.3.3 Sensitivity Analyses for Times Greater than 100,000 Years

At times longer than 100,000 years, neptunium-237 is again the dominant radionuclide. As time proceeds, several events occur:

- The number of degraded waste packages (with at least one opening through Alloy 22 inner barrier) continues to increase
- The amount of degradation (the extent of the openings) through each waste package continues to increase
- The amount of seepage that enters each degraded waste package continues to increase
- The fraction of the waste form surface area exposed (because of cladding degradation) and in contact with water continues to increase

All of these factors tend to cause the release of neptunium-237 from the waste packages to continue to increase with time. This continued increase is illustrated in the base case deterministic results described in Section 4.2. As the releases from the engineered barriers increase with time, the concentrations and dose rates downgradient from the repository increase accordingly.

Eventually the neptunium-237 inventory will be depleted from the degraded waste packages. The length of time for depletion to occur is a function of the neptunium-237 inventory as well as the factors listed in the previous paragraph. For the base case deterministic analyses, this period is several hundred thousand years. After this time, the release rate from the engineered barriers for neptunium-237 decreases, as do the corresponding concentrations and, ultimately, dose rates.

Because the release rate depends on the seepage amount and fraction of waste packages contacting seepage water, climate affects release from the

engineered barriers. In particular, during the superpluvial climate, the presumed increase in net infiltration causes an increase in percolation and, therefore, seepage. As a result, at the time of the superpluvial climate, which is assumed to be several hundred thousand years from the present, the dose rate could increase. Although this increase is in part an artifact of the presumed instantaneous change in the climatic regime from the long-term average to the superpluvial climate, some increase would be expected when the seepage increases.

As noted in the discussion of the 100,000-year sensitivity analyses, the travel time of the nonsorbed and partially sorbed radionuclides from the repository to the water table and then to the 20 km (12 mile) hypothetical well is short compared to the overall period of the analyses. However, some dilution occurs when the water containing dissolved radionuclides is released from the engineered barriers and mixes with the moving groundwater in the rock. Although not considered in the base case analyses, additional dilution could occur if the hypothetical well pumps more water than contained within the maximally contaminated zones of the aquifer.

In summary, the most significant components in determining the dose rates at 20 km (12 miles) from the Yucca Mountain repository over the first million years are the following:

- Fraction of waste packages contacting seepage water
- Waste package degradation rates
- Cumulative amount of degraded cladding
- Dilution in the unsaturated and saturated zones
- Biosphere dose conversion factors

The median peak dose rate calculated in this period is 8 mrem/year. The 5th and 95th percentiles are 0.07 and 1000 mrem/year, respectively. The mean peak dose rate is forecast to be 200 mrem/year.

6.4 PRINCIPAL FACTORS AFFECTING POSTCLOSURE PERFORMANCE

The principal factors affecting the repository system are those factors that bear directly or indirectly on one or more of the components identified in the sensitivity studies as being potentially important to performance. These factors are summarized in Table 6-1. They are grouped according to the system attributes of the *Repository Safety Strategy* (DOE 1998).

The major insights gained from the sensitivity analyses for the reference design are summarized in Section 6.3. These results have been interpreted to guide the definition of the information required to enhance confidence in the performance-assessment analyses for the LA. Each of the principal factors affecting postclosure performance was examined to determine whether that factor has a high, medium, or low contribution to the overall system performance.

The significance of the uncertainty in the principal factors on the assessment of the postclosure system performance may be identified in several different ways. One method is to examine the multiple realization performance analyses and their corresponding regression analyses presented in Section 4.3 to identify which parameters within the TSPA-VA base case simulations are most significant. This is an appropriate technique and provides very useful insights into what is driving the system behavior, but is predicated on the degree of uncertainty included in the base case models and parameters. However, it is possible that a few very uncertain parameters will mask the potential contribution to the uncertainty of other parameters. Therefore, this method can not be used in isolation or without examining the contribution of the other parameters to the system performance.

In order to examine the significance of alternative models and to examine more explicitly the role that some parameters may have in the system performance, a range of comparative analyses have been presented for each of the TSPA-VA model components in Chapter 5. These comparative analyses include sampling the uncertain parameter at

Table 6-1. Significance of Uncertainty in Principal Factors on Post Closure System Performance - Summary of Sensitivity Analysis for Viability Assessment Reference Design

Key Attribute of the Repository Safety Strategy	TSPA Model Components	Principal Factor for the Repository Safety Strategy	Significance of Uncertainty in TSPA[1] Performance Period (years)			Reference Figure Location	
			10k	100k	1M	Base Case	Alternative Models
Limited water contacting waste packages	Unsaturated Zone Flow	Precipitation and infiltration into the mountain	L	M	L	5-5	5-1, 5-2, 5-3
		Percolation to depth	L	L	L	5-5	5-6, 5-7
		Seepage into drifts	H	H	H	4-34, 5-8	NA
	Thermal Hydrology	Effects of heat and excavation on flow (mountain-scale)	NA	NA	NA	NA	NA
		Effects of heat and excavation on flow (drift-scale)	L	M	L	NA	5-9, 5-10
		Dripping onto waste package	L	L	L	NA	5-18
		Humidity and temperature at the waste packages	L	L	L	NA	5-11
Long waste package lifetime	Near-Field Geochemical Environment Waste Package Degradation	Chemistry of water on waste package	H	L	L	NA	5-14, 5-22
		Integrity of the outer carbon steel waste package barrier	NA	NA	NA	NA	NA
		Integrity of the inner corrosion-resistant waste package barrier	H	H	M	4-34, 5-16	NA
Low rate of release of radio-nuclides from breached waste packages	Waste Form Alteration and Mobilization	Seepage into waste packages	L	L	L	5-26	5-27
		Integrity of spent nuclear fuel cladding	H	M	M	5-28	5-29, 5-30, 5-31
		Neptunium solubility	L	M	L	5-32	5-33
		Dissolution of uranium oxide and glass waste forms	L	M	L	4-40, 5-35	NA
		Formation and transport of radionuclide-bearing colloids	L	M	L	5-36	NA
		Transport through and out of the engineered barrier system (including waste packages)	L	L	L	5-37	5-38
Radionuclide concentration transport from the waste packages	Unsaturated Zone Transport	Transport through the unsat-urated zone	L	L	L	5-42	5-41, 5-43, 5-44, 5-45
	Saturated Zone Flow and Transport	Flow and transport in the saturated zone	M	M	M	4-34, 4-40	5-47, 5-48, 5-49
		Dilution from pumping	H	H	H	NA	5-51
	Biosphere Transport	Biosphere transport and uptake	M	M	M	4-34, 5-50	5-52

[1]H —High Significance (Uncertainty in principal factor, or its absence, results in a factor over 50 increase or decrease in peak dose rate from the "expected" value)
M—Medium Significance (Uncertainty in principal factor, or its absence, results in a factor of 5 to 50 increase or decrease in peak dose rate from the "expected" value)
L—Low Significance (Uncertainty in principal factor, or its absence, results in a factor less than 5 increase or decrease in peak dose rate from the "expected" value)

discrete probabilities (principally the 5th and 95th percentiles of the distribution as well as the mean of the distribution for comparison to the expected-value realization described in Section 4.2). The results of these analyses confirmed the significance of the parameters identified in the regression analyses described in Section 4.3 and also provided a method to rank the relative contribution of each of the principal factors.

The ranking of the significance of the principal factors presented in Table 6-1 has therefore been

based on both the multiple realization regression analyses and the one-off comparative analyses. Where both methods indicated the same high significance, the decision to label that factor as having a high significance was straightforward. Where the two methods gave differing results or, more commonly, where the significance based on multiple realizations was masked by more significant factors, the factor was assigned the significance based on the comparative analyses. In some cases the comparative analyses included alternative conceptual models which, if true, could lead to substantially improved or degraded performance. The results of calculations using these alternative representations (presented in Chapter 5) were also used to adjust the rankings, as appropriate. This was done to ensure that the assessment of the significance of the each principal factor is reasonably complete, is defensible and that it accommodates the full breadth of current understanding as well as the factor's potential effect on postclosure performance.

The analyses of significance have been conducted over different time scales to reflect that the behavior of the system changes with time as does the significance of the principal factors of the repository safety strategy.

Table 6-1 focuses on the principal factors affecting the expected or probable repository postclosure performance. Other factors relating to potentially disruptive processes and events have been described in Section 4.4. These consequence analyses, when combined with the understanding of the probabilities of these disruptive scenarios occurring, implies that the long-term risks to public health and safety associated with these scenarios are minimal. Therefore, the uncertainties in these processes and events (seismicity, volcanism, nuclear criticality, and human intrusion) are deemed to have a low significance on overall performance.

An evaluation of significance requires combining both objective and subjective assessments of appropriate information. To provide objective evidence of significance, a range of sensitivity analyses have been performed. These sensitivity analyses have been used to define significance with respect to the magnitude of the effect of the uncertain parameter or model on the dose rate at a hypothetical well located 20 km (12 miles) downgradient from the repository. This section reports the results of those analyses in terms of "high," "medium," or "low" sensitivity to uncertainty. For the assessment of uncertainty given in this section and in Table 6-1, the following definitions were used to assign a ranking of high, medium or low. To rate a particular factor as having high significance on dose rate, varying the range between the mean and the 95th percentile of that parameter causes a change of over 50 times in the dose rate. In addition, if the absence of such a factor could result in a change in the projected dose of a factor of over 50, it also would be deemed to have a high significance. A medium significance corresponds to a change of 5 to 50 times the dose rate and a low significance indicates a change of less than 5 times the dose rate. These criteria were applied over the range of time periods of concern: 10,000 years, 10,000 to 100,000 years, and 100,000 to 1 million years.

Objective measures of significance are useful, but they presuppose that the uncertainty in the parameter or model is well characterized. One source of uncertainty may arise from the fact that not all possible alternative conceptual models have been considered. Also, the models themselves may have inaccuracies that are not captured in the analyses. For example, a parameter may impact the results significantly over a certain range of values, but outside that range the results are insensitive to the value of that parameter. If the parameter range does not extend into the significance range, then the analyst may falsely conclude that the parameter is not important. Therefore, judgment must be used to assign significance to a particular parameter or model because a range and synergistic effects that may not have been fully evaluated in the sensitivity analyses can be an exercise in judgment. The determinations of significance in the following paragraphs have been based on objective criteria. However, the influence of judgment in modifying the significance ratings for each of principle factors is given in Section 2.2-1 of Volume 4. The changes in the values that have resulted from the incorporation of judgment are shown in Volume 4, Table 2-2.

6.4.1 Precipitation and Infiltration of Water into the Mountain

The amount of water that enters the unsaturated zone at the surface controls the amount of water that percolates to depth and, ultimately, the amount and location of seeps into the repository drifts. Generally, the lower the infiltration, the less seepage into the drifts and the less water that can contact the waste package and the waste form. Therefore, the time and location variability in precipitation and infiltration are significant factors in overall system performance. The significance of this principal factor is estimated to be higher in the period from 10,000 to 100,000 years because the solubility-limited radionuclides control the dose rate in this period. The release of these radionuclides from the engineered barriers is, in large part, a function of the volumetric flow rate into the drifts and into the waste packages. The net infiltration has a moderate significance on the projected dose rate based on variation in the range of plausible infiltration rates (Section 5.1).

6.4.2 Percolation to Depth

Percolation flux is closely correlated with net infiltration. The uncertainty in percolation flux is directly related to the uncertainty in net infiltration. Percolation flux controls the fraction of the repository with seeps and the seepage amount. Therefore, percolation is likely to have an effect similar to infiltration on the dose rate. However, the base case analyses only showed a low significance of this factor, based on the fracture flow properties, which was the only parameter related to percolation varied in this set of analyses (Section 5.1).

6.4.3 Seepage into Drifts

Seepage into the drifts is a significant factor for many reasons. Seepage controls waste package degradation because Alloy 22 only corrodes in the presence of liquid water. Following the creation of openings through the Alloy 22, the seepage volume controls the amount of water that can enter the waste package and dissolve the waste form. The flux of water into and through the waste package in turn controls the release rate of the solubility-limited radionuclides from the waste package. The high significance of seepage at all time periods can be ascertained from the Monte Carlo analyses presented in Section 4.3 (where seepage fraction or seepage amount were consistently in the top four of the most significant variables) and in Section 5.1.

6.4.4 Effects of Heat and Excavation on Flow (Drift Scale)

Heat can drive water away from the emplacement drifts and enhance flow because of condensation and refluxing in the earliest time period. Therefore the heat can modify waste package corrosion rates and other aspects important to performance. However, the effects of heat are shown to only have a low impact on repository performance in the period up to 10,000 years. In the later period, the heat will have diminished and its direct impact on the redistribution of flow will also be minor. However, heat can cause permanent effects on the flow system. For example, the heat can modify flow properties by altering minerals in fractures and creating mineral caps above the heated area, similar to those observed at geothermal sites. Likewise, excavation can alter the flow properties, increasing bulk permeabilities near the drifts. These alterations have been approximated by changing the fracture properties contained in the seepage sensitivity analyses described in Section 5.1. This aspect of altering properties of the host rock leads to an assessment of moderate importance to performance in the middle time period, as illustrated in the sensitivity analyses described in Section 5.1.

6.4.5 Dripping onto Waste Packages

In the current analyses, any seep located half way up the drift wall is conservatively assumed to directly hit the waste package. However, many seeps may simply form a film around the drift wall or fall on rubble around the waste package and not directly intercept the waste package. This diversion of water may be significant, but is believed to be less significant than the presence of the seep itself. Variations in the surface area of the waste package that becomes wetted show this factor to be of low significance to performance.

6.4.6 Humidity and Temperature Effects on Waste Packages

Corrosion of the carbon steel layer on the outside of the waste package can be initiated and sustained at values for relative humidity greater than about 70 percent and temperatures less than about 100°C (212°F). Although most of the waste package performance is caused by the very slow corrosion rates of the Alloy 22 inner barrier of the waste package, during earlier periods (less than 10,000 years) the outer barrier does provide some protection. However, the overall significance of this factor is shown to be low during all time periods (Section 5.2).

6.4.7 Chemistry Effects on Waste Packages

The chemistry of the water on the waste package surface can significantly affect the degradation rate of both the carbon steel material of the outer waste package and the inner corrosion-resistant layer. As noted in Section 3.4, the degradation rate of Alloy 22 under benign water compositions is less than the degradation rate under more aggressive chemical conditions. The presence of microbes also changes the chemistry, and thus the corrosion rates. In addition, the chemistry of the water can affect both the degradation rate of the waste form and the solubility of neptunium-237. This factor, therefore, has a high impact on performance during the first 10,000 years when water is modified as it travels through the concrete liner, but drops to low significance at later times (Sections 5.3 and 5.4).

6.4.8 Integrity of Inner Waste Package Barrier

In the reference design, the corrosion degradation rate of the Alloy 22 corrosion-resistant alloy is seen as one of the dominant factors affecting the postclosure performance. The effect is illustrated in the regression analyses presented in Section 4.3 and the comparative analyses presented in Section 5.4. Not only does the degradation control the time at which the initial opening is formed through each waste package, but it also affects the number of openings generated through each waste package. The number of openings significantly affects the amount of seepage that can enter each waste package, which in turn controls the advective release of solubility-limited radionuclides, notably neptunium-237, from the waste package. This factor has a high significance over all but the longest time frames in the analyses of reference design postclosure performance, as documented in Section 5.4.

6.4.9 Seepage into Waste Packages

After the waste package has failed because of at least one opening through the corrosion-resistant inner container, the amount of water that enters the waste package controls the advective release of solubility-limited radionuclides. However, changing the percentage of waste packages wetted and changing the resulting flux through the waste package only showed a small change in dose rates, resulting in an assignment of low for significance (Section 4.2).

6.4.10 Integrity of Spent Fuel Cladding

The degree of degradation of the cladding significantly affects the amount of the inventory potentially exposed to liquid water. The dose rates of the high-solubility radionuclides, such as technetium-99, depend on the fraction of exposed inventory. Because the dose rates during earlier periods are controlled by the high-solubility radionuclides, the significance of cladding is greater at early times. The significance of cladding is high for the first 10,000 years and relatively less significant, but still of moderate importance at late times.

6.4.11 Dissolution of UO_2 and Glass Waste Form (Waste Form Integrity)

The alteration rate of the different waste forms is relatively rapid (thousands of years) compared to the period of interest (tens to hundreds of thousands of years). Therefore, the dissolution rate is not a significant factor in the overall dose evaluation at early times. Before 50,000 years technetium is the most important contributor to dose, after that time neptunium becomes the dominant contributor. However, the possibility that secondary phases are created at the spent nuclear fuel can effectively reduce the mobile

concentration of neptunium-237. Therefore, this factor has the potential to be moderately important in the period between 10,000 and 100,000 years. After the secondary phases have been dissolved, the effect is mitigated, resulting in a reduction of the significance at times greater than 100,000 years.

6.4.12 Solubility of Neptunium-237

Neptunium solubility is a moderately significant contributor to the long-term dose assessment. The contribution of neptunium-237 is less significant at earlier times when the doses are primarily attributed to more mobile radionuclides such as technetium. However, at times greater than several tens of thousands of years, or in cases where the seepage flux is high, neptunium solubility can be a significant factor in postclosure performance projections. The solubility of the secondary phases of the fuel/glass is also important, because it may lead to a delay or reduction in the overall release of neptunium at times less than 100,000 years.

6.4.13 Formation of Radionuclide-Bearing Colloids

Plutonium colloids are responsible for the peak dose in a significant number of the TSPA-VA realizations during later times. It is one of the more significant findings in TSPA-VA that, under certain conditions, colloid-facilitated transport is moderately important to performance in the time period from 10,000 to 100,000 years.

6.4.14 Transport Within and out of the Engineered Barrier System

In the current TSPA analyses, if water gets into the waste package it was conservatively assumed to contact the entire exposed waste form surface. No credit is taken for the fact that a drip entering the waste package at one opening has a low likelihood of encountering the waste form at the other end of the waste package. In addition, the time it may take radionuclides to diffuse along a thin water film layer within the waste package was not considered. Quantifying the effects of these conservative assumptions is difficult. Therefore, the transport of radionuclides through the engineered system elements beneath the waste package (sorption in the invert) for any time period was shown to be of only low significance to performance.

6.4.15 Transport Through the Unsaturated Zone

Based on the current unsaturated zone flow model, the advective travel time through the unsaturated zone depends on the percolation flux distribution that is in turn controlled by the climatic conditions. Under the current dry climate, the unsaturated zone may provide a significant barrier to the migration of highly and slightly sorbed radionuclides. Under climate states with higher percolation flux, only the highly sorbed radionuclides are still retained in the unsaturated zone. Therefore, the significance of this barrier to release to the saturated zone may change with time as the climate state varies. In addition to the transport time, the unsaturated zone dilutes the concentration of the radionuclides released from the engineered barriers. The effects of unsaturated zone transport were investigated by changing sorption coefficients, assigning a value of zero for matrix diffusion, and assigning zero for sorption coefficient of the actinides (Section 5.6). However, the range investigated for these parameters only showed this factor to be of low significance at all periods.

6.4.16 Transport in the Saturated Zone

The time it takes for radionuclides to advectively travel through the saturated zone to a distance of 20 km (12 miles) is a significant fraction of the period of interest for 10,000 years. This is especially true for those radionuclides sorbed on the alluvial sediments. For longer periods and during climate regimes characterized by the long-term average climate, travel times in the saturated zone may not provide as much of a barrier to radionuclide migration. The saturated zone also provides some dilution of those radionuclides released from the unsaturated zone. The TSPA-VA sensitivity analyses of the saturated zone flow and transport has a moderate significance relative to other factors (as noted in Sections 4.3 and 5.7) for the three time periods.

6.4.17 Dilution from Pumping

If the volume of water extracted in the hypothetical well is significantly greater than the volume of water within an individual stream tube in the saturated zone, then significant dilution can occur at the well head. The effect of this dilution would diminish as the natural dilution in the saturated zone is increased. No credit is taken for the pumping dilution in the base case analyses of the reference design. The significance of this dilution depends on the size of the pumping well and the magnitude of the natural dilution in the saturated zone. Depending upon the assumptions concerning the amount of water pumped, the dilution factors investigated showed, at all times, a high significance in changing the dose to the average members of the critical population (Section 5.8).

6.4.18 Biosphere Uptake

After water containing dissolved radionuclides is extracted from the hypothetical well, the projected dose rate is a function of the range of possible water uses and food consumption habits of the exposed population. Although there is a linear relationship between the dose conversion factor and the dose rate (for a given radionuclide concentration at the well head), the changes in the dose rates show this factor to be of moderate importance in all time periods. (Sections 4.3 and 5.8).

6.5 IMPROVING CONFIDENCE IN THE TOTAL SYSTEM PERFORMANCE ASSESSMENT FOR THE LICENSE APPLICATION

The data and analyses summarized in Section 6.1-6.4 of this volume comprise a portion of the information needed to construct a complete postclosure repository safety case. In order to provide reasonable assurance that a repository at the Yucca Mountain site will not result in a significant long-term risk to public health or safety, the postclosure safety case must include:

- Explicit evaluation of expected repository performance
- Analyses of the degree of design margin and defense in depth that could improve performance and mitigate uncertainties in performance
- Explicit consideration of processes and events that, if present, have the potential to disrupt the repository system
- Supporting information regarding long-term behavior from natural and man-made analogs
- Plans for long-term testing and monitoring of the repository system

The purpose of the TSPA-VA described in this volume has been to examine the current understanding related to the first and third elements of the safety case, that is, the expected repository performance and the process and events that, if present, have the potential to disrupt the expected repository performance. The probable performance has been described in the context of how the four elements of the repository safety strategy work in concert to first minimize the contact of water with the waste and then reduce the concentration of any radionuclides that are released from the engineered barriers.

Based on the results of the TSPA analyses presented and discussed in this volume, areas of potential improvements in the analyses can be identified. Possible model enhancements and analyses that have the potential for improving the confidence in the TSPA for the site recommendation and LA are provided in Section 6.5.1. In addition, many important observations and insights have also been provided by independent groups, most notably by the TSPA Peer Review Panel and NRC. These comments are discussed in Sections 6.5.2 and 6.5.3, respectively. Section 6.5.4 provides some concluding remarks.

6.5.1 Assessment of Potential Activities to Increase the Confidence in the Total System Performance Assessment Based on the Results of the Total System Performance Assessment for the Viability Assessment

For each of the principal factors associated with the TSPA model components, the potential significance of some of aspects of model uncertainty has not been investigated in the TSPA-VA. This is in part a function of the objective of focussing the analyses on the probable behavior of the repository system which implies evaluating the expected performance as opposed to the performance associated with all the possible alternative hypotheses and models. The sensitivity analyses presented in Section 4.3 and Chapter 5 provide an indication of the possible range of performance, but can not be construed as being exhaustive. It is expected that the TSPA analyses developed for the site recommendation and LA will address these remaining uncertainties. The following paragraphs present possible model enhancements and analyses that have the potential for improving the confidence in the future assessments of repository performance.

6.5.1.1 Precipitation and Infiltration into the Mountain: Unsaturated Zone Flow

- *Abruptness of transition of climate changes.* The relation between the magnitude of the dose-rate "spikes" and the time of transition from one climate to another is not known. It is possible that noninstantaneous transitions would lead to lower peak dose rates.

- *Climate analogs.* The current approach is to base infiltration modeling on appropriate climate analogs (i.e., places that currently have climate conditions like those expected at Yucca Mountain for the future climate). The approach could be improved by taking temperature and other factors into account in addition to precipitation when defining the analogs.

- *Timing and duration of climate states.* The current model, using three distinct climate states, is simplistic and without a strong basis. Developing a more defensible basis for the number, timing, and duration of climate states could enhance confidence in the model.

- *Infiltration uncertainty.* A more quantitative basis for the uncertainty distribution for net infiltration (i.e., the probabilities in Table 3-5) could be obtained by running the infiltration model in a probabilistic mode (e.g., using Monte Carlo simulation, which is described in Section 4.3) to derive the infiltration uncertainty from the uncertainties in the model input parameters.

- *Infiltration for future climates.* Estimates of infiltration for future climates could be improved by explicit inclusion of processes that should be different for future climates, including effects of temperature, cloudiness, vegetation type, surface water runoff/run-on, and snow cover. Even for current conditions, some experts in the unsaturated zone flow model expert elicitation (CRWMS M&O 1997o) suggested that runoff and run-on might be more important than is assumed in the current infiltration model.

- *Model testing.* Confidence in the infiltration model could be enhanced by testing it using analogs with better-known infiltration, such as Rainier Mesa and Apache Leap.

6.5.1.2 Percolation to Depth: Mountain-Scale Unsaturated Zone Flow

- *Localized flow channeling.* An important uncertainty in the mountain-scale unsaturated zone flow modeling is the effect of localized channeling of flow, and in particular, the effect of flow in discrete fractures. Current modeling uses continuum models with very coarse spatial discretization, and the adequacy of this approach is not fully established. There are indications from geochemical and isotopic tracers (chloride concentration, chlorine-36 to

chlorine ratio and carbon-14 to carbon ratio) that channeling of flow might be important. Better integration of geochemical, isotopic, and temperature data could improve the calibration procedure because they provide important information about flow through fractures.

- *Perched water.* The role of perched water in unsaturated zone flow is uncertain. The current model assumes that the water is perched on a very-low-permeability underlying layer and flow is forced to go around it. Other interpretations are possible, such as mixing within the perched water and matrix flow out the bottom.

6.5.1.3 Seepage into Drifts

- *Model testing.* Confidence in the seepage model could be enhanced by more comparisons between field data and model predictions. The Exploratory Studies Facility niche test is an important first step, but it is primarily a test of the overall conceptual model of the drift opening acting as a capillary barrier. The test offers little validation of the calculated values of seepage fraction, which the TSPA results show to be the most important aspect of seepage, indeed, the most important aspect of repository performance. Seepage fraction, or the fraction of waste packages contacted by seepage water, is related to the average spacing of seeps along the drift, which is presumably related to quantities such as fracture and fault spacing, permeability distribution, and permeability correlation length. Field data relating these quantities to seep spacing, possibly from analog sites such as Rainier Mesa or Apache Leap, would lend confidence to the model.

- *Localized flow channeling.* Even more so than for mountain-scale flow, seepage into drifts is potentially strongly affected by channeling of flow and discrete-fracture effects. The adequacy of the current fracture-continuum model to represent these effects is uncertain.

- *Stability of seep locations.* A potentially important issue that was not addressed in the TSPA-VA is the stability of seep locations over time. In the present models, seeps are assumed to occur at the same locations indefinitely, so that a fraction of the waste packages (the seepage fraction) is always wet and the rest are always dry. If seep locations changed with time, more waste packages would be contacted by seeps, but only for a fraction of the time. This effect could result in more waste packages failing, but over a longer period of time, which could be important for performance.

- *Drift collapse and thermal alterations of hydrologic properties.* The effect of drift collapse on seepage has not yet been investigated. Also, thermal-hydrologic-chemical or thermal-hydrologic-mechanical alteration of hydrologic properties around the drifts could have an important effect on seepage.

- *Episodic percolation.* The potential for episodic percolation pulses at the repository is uncertain. Also, drainage of thermally mobilized water could potentially cause an increase in seepage for a period of time.

6.5.1.4 Effects of Heat and Excavation on Flow: Mountain- and Drift-Scale Thermal Hydrology

- *Conceptual model of flow.* Differences have been found between results using the dual-permeability flow model and the equivalent-continuum flow model. The dual-permeability model allows for greater mobility of water in fractures, which has a great effect on modeled condensate buildup and drainage. A related flow issue, which could be important to thermal hydrology, is channelized flow, especially in discrete fractures. Such flow could greatly increase the spatial variability in the results by increasing the range of water-flow rates seen by individual waste packages.

- *Coupled processes.* A potentially important shortcoming of the thermal-hydrologic

calculations is the lack of coupling to thermal-mechanical and thermal-chemical processes. These issues have been addressed to a limited extent (see Section 3.2.1), but the full range of possible (or even likely) behaviors has not been analyzed. The Near Field Environment Expert Elicitation (CRWMS M&O 1998d) will aid in considering these issues, but it was not completed until after the TSPA-VA analyses were finished. Therefore, implementing the recommendations from the expert elicitation remains to be done.

- *Thermal alterations of hydrologic properties.* Thermal alterations of flow and thermal-hydrologic-chemical or thermal-hydrologic-mechanical alterations of hydrologic properties are potentially important. In the current TSPA structure, these effects fall under the thermal-hydrology component, but thermal-hydrologic effects could be more closely coupled with mountain-scale unsaturated zone flow and transport if necessary.

- *Infiltration rate.* As shown in Section 3.2.3, infiltration rate influences computed repository temperatures. Within the range of infiltration uncertainty incorporated in the base case, the changes in temperature are not large. However, as shown in Section 5.1.3, temperature changes can still have a significant effect on computed dose rates during approximately the first 20,000 years.

- *Matrix hydrologic properties.* Almost all of the available data on matrix hydrologic properties have been obtained from drying experiments. For modeling the thermal-hydrologic behavior during rewetting and condensate drainage, data obtained from wetting experiments would be more appropriate. Wetting and drying properties can be very different because of hysteresis. The thermal-hydrologic property set mentioned in Section 3.2.3 was intended as a better representation of wetting hydrologic properties. It was found to make a significant difference to waste package failure and calculated doses for approximately the first 20,000 years, especially in the part of the repository that lies in the Topopah Spring lower nonlithophysal hydrogeologic unit (primarily Region SW of Figure 3-20).

- *Thermal response of different hydrogeologic units.* The single heater test and the heated-drift test are both located in the Topopah Spring middle nonlithophysal hydrogeologic unit. However, in the current repository design most of the emplacement drifts are in the Topopah Spring lower lithophysal unit, with some drifts in the middle nonlithophysal unit and others in the lower nonlithophysal unit. Confidence in the models would be enhanced by obtaining thermal-response data in the other two units.

- *Continued in-situ testing of thermal hydrologic models–single heater test.* The small-scale, single heater test at the Exploratory Studies Facility has provided valuable thermal-hydrologic information, including that the dual-permeability flow model and hydrologic properties used in the base case fit the measurements reasonably well, at least for the Topopah Spring middle nonlithophysal hydrogeologic unit. The single heater test results helped to guide the selection of hydrologic-property sets thermal-hydrologic models using the base case hydrologic properties match the test results better than an earlier, preliminary-base case property set (CRWMS M&O 1998i, Sec. 3.4.5).

- *Continued in-situ testing of thermal hydrologic models–drift scale test.* An important source of new information for improving thermal-hydrologic models will be the heated-drift test at the Exploratory Studies Facility. This test will provide information on drift-scale movement of heat through rock at Yucca Mountain and its impact on the flow system above and below an emplacement-sized drift. The test will include a detailed investigation of the heating period and movement of heat-driven water as well as the cooling period and subsequent rewetting analogous to the

processes that would occur in the repository. Indirect measurements to detect water flow into the drift during heating will provide crucial information related to thermal refluxing processes driven by larger-scale heat-transfer processes. The data obtained from the heated-drift test will:

- Allow important verification of the conceptual flow models currently being used (or show the degree to which the current models are not adequate).

- Provide information on the effective hydrologic properties during the various stages of heating and cooling.

- Provide information on the spatial and temporal extent of mechanical and chemical changes to the fracture-flow system surrounding the heated drift. It is important to note, however, that only the results of the early heating period of the heated-drift test will be available in time for the TSPA for the LA; information on the cooling period will not yet be available.

6.5.1.5 Chemistry of Water on Waste Package: Near-Field Geochemical Environment

- *Effects of concrete-modified water.* The potential impacts from concrete-modified water compositions assessed in the sensitivity results discussed above and in Sections 5.4 and 5.6 appear to be greatest for the 10,000-year time period. The greater effects during the first 10,000 years are mainly caused by impacts to waste package performance because earlier and more frequent failures allow greater exposure of the waste form inventories at earlier times. These results suggest that further consideration be given to substituting other ground support materials for the concrete in the VA design. However, there are uncertainties within the models currently employed to evaluate the near-field geochemical environment. To better constrain changes from materials evolution in the drift, further improvements could be made in the following areas:

  - Thermal-chemical data (both equilibrium and kinetic) for phases in the cement system, in particular at the higher temperatures expected for this system

  - Gas composition changes in the unsaturated, thermally perturbed system

  - Development and implementation of a two-phase, reactive transport model of concrete alteration

- *Precipitate and/or salt build up in the waste package.* Alternate conceptual models for water in the drifts and on the waste package may need to be considered. Similarly, preliminary bounds on biomass production suggest that microbial growth may be nutrient limited within the potential drifts for long periods.

- *Thermomechanical-hydrochemical coupling.* Coupled models would benefit from incorporation of more details of drift materials, both their physical-mechanical evolution and chemically-induced changes to the hydrologic properties of the engineered materials. These aspects would improve the description of water flow and radionuclide transport pathways and allow for development of more specific near-field geochemical environment scenarios.

- *Conceptual model of the near-field geochemical environment.* The updated near-field geochemical model could consider such topics as:

  - Heterogeneity of water composition flowing through the fracture system and interacting with the drift environment

  - Explicit CO_2 evolution from water and minerals coupled to the gas flow in the thermohydrologic system

– Explicit coupling of flow and geochemical reactions

– Thermal aging of all emplaced materials in dividing concrete

– Biomass production and specific microbial activity for local waste package corrosion effects

6.5.1.6 Waste Package Degradation

- *Chemical and electrochemical conditions.* The uncertainty in the current Alloy 22 corrosion model is mostly caused by the uncertainty in the local chemical and electrochemical conditions on the inner barrier and limited data on the long-term behavior of this material in the expected environment of the repository.

- *Corrosion rate of Alloy 22.* The Alloy 22 corrosion uncertainties include the general corrosion rate, localized (pitting and crevice) corrosion rate, localized corrosion initiation threshold, and understanding of the pitting and crevice corrosion stifling process.

- *Potential salt build up.* For waste packages under dripping conditions, the potential exists for salt deposit buildup on the package surface, which could produce concentrated salt solutions near the deposit. This condition could enhance corrosion of the carbon-steel outer barrier, thereby exposing the inner barrier to corrosive conditions earlier than the case without salt deposits. Long-term corrosion of carbon steel under dripping and in the presence of salt deposits is uncertain.

- *Potential galvanic coupling.* The effect of potential galvanic coupling between the Alloy 22 inner barrier and the carbon-steel outer barrier is also uncertain. The most important issue with this process is hydrogen embrittlement of Alloy 22, which could result from hydrogen pick-up by Alloy 22 over a long period and subsequent hydride precipitation inside the alloy, thus potentially shortening its lifetime. Potentially enhanced corrosion of the outer barrier from a galvanic coupling with the inner barrier is another area of uncertainty.

- *Incomplete annealing of welds.* Strengthening of the closure weld could lead to incomplete annealing of the weld. In this case, the closure weld could be subject to stress corrosion cracking.

- *Microbiologically influenced corrosion.* Microbiologically influenced corrosion was not included in the base case in part because the potential for this corrosion of the waste packages was discounted in the recent expert elicitation (CRWMS M&O 1998b). However, the process has uncertainty and could affect long term performance.

- *Long-term structural integrity.* The long-term structural integrity of the waste package is uncertain as to timing and effect. After substantial progress of degradation and under static loads from rockfall, the waste package is expected to lose its structural integrity and collapse, no longer providing a physical barrier to water ingress and radionuclide release. The threshold for waste package structural failure is currently unknown and has a potential impact on long-term repository performance.

6.5.1.7 Waste Form Alteration and Mobilization Models

- *Degradation of invert.* The invert is assumed not to degrade with time but to retain the same transport characteristics for the duration of the analyses. However, the chemistry of the invert will probably change as the system is heated during the thermal period. Heating may alter the transport characteristics of the invert. Likewise, the invert sorption characteristics are not well known and are under study. The impact of more complex invert analysis on overall system performances is not expected to be significant because of the small transport

length involved relative to the total transport length.

- *Degradation of drifts.* The base case does not directly account for rock falling into the drift at later times, which is an expected condition. Although the cladding model evaluates the effects of rockfall on the cladding, the rest of the analyses do not incorporate rockfall at later times. A sensitivity to rockfall alteration of the thermal-hydrologic characteristics has been presented in Chapter 3 of the *Total System Performance Assessment-Viability Assessment (TSPA-VA) Analyses Technical Basis Document* (CRWMS M&O 1998i).

- *Secondary phases.* The effect of the secondary phases on subsequent radionuclide transport has been initially analyzed in Section 5.5 of the TSPA-VA. Neither the dissolution rate of the secondary phase nor the identity of radionuclides that will become fixed in the secondary phases has been well characterized. This process could have the effect of delaying radionuclide releases.

- *Seepage into the waste package.* The amount of seepage into the waste package and onto the waste form is a significant factor in releases from the engineered barrier system. How much water actually enters the waste package once it is breached is uncertain.

- *Transport resistance of failed Zircaloy cladding.* Diffusive transport out of a locally failed fuel rod is not explicitly considered and could significantly reduce release rates.

- *Chemistry-dependent solubility limits.* Additional modifications to the waste form model to improve confidence in the model include solubility-limited radionuclide distributions that are explicitly dependent on the pH and the total water composition as indicated by changing phase relations in the chemical system.

- *Chemistry-dependent sorption in the engineered barrier system.* Identifying sorption mechanisms and evaluating the dependence of sorption on the composition and mineralogy of the specific material would help to better incorporate sorption processes into the model.

- *Cladding degradation.* The current version of the cladding model provides benefit to performance but is based on assumptions about cladding degradation modes and rates. Potential cladding-failure mechanisms, such as localized corrosion and their rates, are important remaining uncertainties in the cladding analyses.

- *Water contact of waste form.* In the TSPA-VA analyses, the entire waste form surface is assumed to be exposed to aqueous conditions after the cladding fails. Detailed analyses of possible alternative models of water flow in the degraded waste package, including alternative conceptual models such as "bathtub" model would aid in evaluating the significance of the water contact mode.

- *Use of natural analogs.* The analysis of numerous uncertainties in the models, data sets, and assumptions for predicting repository performance would benefit from the use of natural analogs. Waste form degradation and mobilization and transport of radionuclides are very long-term phenomena that are difficult to evaluate with a high degree of certainty, especially if limited to information gained through short-term laboratory and field studies. Natural formations and deposits that have existed for very long periods of time show how these processes have taken place and the factors that most affect the processes. The natural "reactors" at Oklo in Gabon, Africa, have been studied extensively to evaluate the mobilization and transport of radionuclides, including plutonium, in both reducing and oxidizing environments (see, for example, Jakubick and Church 1986 p. 1; Curtis et al. 1989 p. 49; Brookins 1990 pp. 285-287; Cramer and Smellie 1994). Pena Blanca in

Chihuahua, Mexico, is a natural, high-grade uranium deposit located in unsaturated tuff that is believed to be a good analog to the Yucca Mountain repository. Further analog-oriented studies of this 8 million-year-old-deposit may provide important transport information (Murphy 1995 p. 44; Murphy et al. 1997 pp. 105-111). In addition, DOE participated in a three-year analog study at Pocos de Caldas, Brazil, which focused on radionuclide transport issues (Chapman et al. 1991 p. v).

6.5.1.8 Unsaturated Zone Transport

- *Effects of thermal-hydrologic-chemical alteration.* The current model does not account for alteration of the unsaturated zone because of thermal alteration of minerals, chemical interactions of repository materials, mineral dissolution, and precipitation. These effects are potentially important to transport behavior in the unsaturated zone. Thermal-chemical alteration could cause reduced matrix sorption and fracture/matrix interaction. The potential effects associated with alteration of the host rock and radionuclide transport pathways caused by alkaline plumes derived from the concrete masses and extending into the geosphere is not well constrained. The development of a coupled, reactive transport representation would aid the assessment of these potential effects. These effects could cause increased release rates from the unsaturated zone for base case transport results; however, the sensitivity studies (illustrated in Section 5.6) are expected to bound most of these potentially nonconservative interactions.

- *Colloid Filtration.* The ability of colloids to facilitate radionuclide transport is a function of their ability to migrate over large distances without being filtered by the host rock. This filtration effect was not included in the TSPA because of inadequate information to bound the mechanism. The filtration effect is particularly important for the fraction of radionuclides that are irreversibly bound to colloids. The assumption that there is no colloid filtration is conservative for transport in the unsaturated zone.

- *Fracture Sorption.* The effects of higher infiltration evaluated in this TSPA imply that transport will be fracture-dominated in many of the unsaturated zone units. Minerals that line fractures are known to sorb radionuclides, but more information is needed to define the distribution and character of the fracture materials so that sorption on fracture surfaces may be included. However, the assumption that radionuclides do not sorb onto fracture surfaces is conservative for transport in the unsaturated zone.

- *Matrix Diffusion.* Radionuclide transport in the unsaturated zone can be sensitive to changes in matrix diffusion depending on the nature of the release from the engineered barriers. The way in which the fracture/matrix contact area is used for calibrating the flow model suggests that some type of coupling strength may be appropriate for matrix diffusion. Sensitivity studies presented in Section 5.6 suggest that the influence of matrix diffusion on total system performance is small.

6.5.1.9 Saturated Zone Flow and Transport

- *Additional potentiometric and transport data.* Data are lacking in the saturated zone from approximately 10 km (6 miles) downgradient of the repository to the 20-km (12-mile) boundary used in the analyses. Available data in water levels, hydrochemistry and the characteristics of the alluvium are lacking in this area. Water-level measurements would improve understanding of the groundwater flow directions in this area and provide additional data for flow modeling calibration. There is uncertainty about where flow in the shallow saturated zone enters the alluvium along the flow path from the repository or even if flow occurs in the alluvium within 20 km (12 miles) of the repository. This uncertainty is particularly important given the potentially higher

sorption coefficients of some radionuclides such as neptunium in the alluvium. Hydrochemical data could provide information to constrain flow paths in the model for the saturated zone in this area. Additionally, there are little site-specific data on the hydraulic, mineralogic, or geochemical characteristics of the alluvium in the saturated zone from this area.

- *Geochemical and isotopic data.* Additional geochemical and isotopic data from the saturated zone could provide important constraints on conceptual models of groundwater flow and on some key parameters for performance assessment. Enhanced vertical resolution of hydrochemical sampling could provide information on the degree of mixing in the flow system, with implications for the amount of transverse dispersion that would occur in contaminant transport from the repository. The data could also provide a better understanding of the flow paths in the saturated zone downgradient from the repository and of the magnitude of recharge to the system from Fortymile Wash. Reliable age dating of groundwater along the flow path from beneath the repository would constrain the travel times through the system and the appropriate range of values of effective porosity in the fractured volcanic tuff units. By inference, these data would provide information on the process of matrix diffusion in the fractured units. Additional electro-chemical-potential data to determine oxidation/reduction states in the saturated zone could improve sorption and solubility parameters for calculating radionuclide transport, as well as aid in the understanding of the connection between the shallow and deep aquifers at the site.

- *Three-dimensional flow and transport model.* A three-dimensional flow model for the saturated zone could provide the basis for radionuclide transport simulations that explicitly model relevant processes. An improved, site-scale flow model should be consistent with all the available data from the site. In addition, development of the flow model should be focused on simulation capabilities that are important for accurate transport modeling. These capabilities include incorporating variability and uncertainty in aquifer properties and numerical methods for simulating solute transport with minimal numerical dispersion.

- *Dispersivity and dilution.* The dilution factor for the saturated zone has been shown to be a sensitive parameter in TSPA-VA. The appropriate range for dilution and vertical transverse dispersivity is also uncertain. Reduction in the uncertainty in this parameter can benefit from inferences from analog sites or possibly from analyzing natural solute tracers in the saturated zone at the site. Additional effort could be devoted to evaluating potential analog systems of saturated flow in fractured media or in highly heterogeneous porous media.

- *Effects of climate change.* Climate change has an effect on the saturated zone that was simplified in the TSPA. For example, changes in flow paths were not considered. Changes in groundwater flux were based on regional-scale modeling but without an estimate of uncertainty. The effects of additional discharge locations and the presence of surface water were not considered. The effects of additional recharge at Yucca Mountain, Fortymile Wash, and the regions that are up gradient were also not considered. The saturated zone modeling should attempt to better reflect the wetter climates that might be normal for the Yucca Mountain region.

- *Colloid transport.* More realistic models of colloid-facilitated transport should be implemented in the saturated zone models. These models should be tied to site-scale observations of colloidal transport.

6.5.1.10 Dilution from Pumping

- *Geosphere/biosphere interface.* The geosphere/biosphere interface was defined as a well located at the point of highest

concentration of contaminants in the groundwater. Natural discharge points were not considered. Dilution from mixing contaminated water with uncontaminated water during well pumping was not considered. An improved definition and modeling of this interface would lend further credibility to the calculations.

- *Pumping from Wells.* Pumping from a well could mix contaminated and uncontaminated waters—as might storing water from multiple sources in tanks—diluting any contamination. These effects have not been included in TSPA-VA (although they have been estimated in a sensitivity study presented above in Section 5.8.1). If it is determined that dilution of radionuclides by the natural environment during transport is less than the values used in TSPA-VA, it would be reasonable to examine the dilution produced during well withdrawal and storage.

6.5.1.11 Biosphere Transport and Uptake

- *Site-specific data.* The biosphere modeling indicated that the pathways that contribute the most to the calculated radiation dose rate are drinking-water ingestion, leafy-vegetable ingestion, and meat ingestion. The parameters that create the most uncertainty in these pathways are the related consumption rates, crop-interception fraction, crop-resuspension factor, grain irrigation rate, animal-uptake scale factor, and egg yield. Some of these pathways and parameters were defined based on the regional-survey data; however, additional site-specific data could improve the dose-rate calculations. The crop-interception fraction could be measured. The scaling factors for animal uptake and soil-to-plant transfer could be refined to appropriately reflect the bioavailability of radionuclides in the Amargosa Valley region and the vicinity of Yucca Mountain in general.

- *Definition of critical group and individual receptor.* For TSPA-VA, the receptor for radionuclides released from a repository at Yucca Mountain is an average member of the critical group (the reference person), to be consistent with guidance from the National Research Council (1995; p. 52). Several simplifying assumptions are made concerning the critical group: it comprises only adults; the members have habits similar to those people residing in the Amargosa Valley region today; all water for drinking and production of (locally produced) foodstuffs is the most contaminated water at 20-km (12-miles) downgradient from Yucca Mountain. It is recognized that some persons in the Amargosa Valley might be more susceptible to radionuclide contamination than the average person. Consideration of a child receptor in particular would improve the estimation of radiological effects on the critical group. It is also recognized that a better understanding of water usage and food-distribution patterns would improve the estimation of radiological effects.

- *Biosphere changes with climate.* Attempting to quantify the effect of the technological and societal advances or declines over many thousands of years is speculative. To address the influence of climate on the critical group, a comparatively small survey was conducted in Lincoln County, Nevada. This area was selected as an analog because the climatic conditions in Lincoln County are similar to those predicted for a future Amargosa Valley region. Lincoln County is approximately 200 km (120 miles) northeast of the repository site. This county is generally higher in elevation and is characterized by cooler temperatures and higher precipitation (mean annual rainfall is 2-3 times greater, depending upon elevation) than the Yucca Mountain area. However, the results from this survey were being analyzed and are not included in this report. The data gathered in the Lincoln County survey should be available to support a future TSPA.

- *Long-term build-up of radionuclides at natural discharge locations.* Modeling did

not include assessments of surface soil contamination and subsequent buildup from natural discharge locations (e.g., from Franklin Lake Playa). Long-term buildup of radionuclides in natural discharge areas could alter dose calculation, especially if natural discharge affects sites of future habitation. Of interest is the amount that radionuclides might be concentrated at a natural discharge site; how these sites might be used by future inhabitants; and how much these radionuclides might subsequently be dispersed via wind or other erosional processes.

- *Well-location assumption.* All of the locally produced food consumed by the reference person was assumed to be grown with water having the same maximum levels of contamination. This assumption might be appropriate if the contaminant plume is large and well-dispersed; however, in the TSPA-VA modeling, the contamination plumes generated by a repository at Yucca Mountain would not cover the entire Amargosa Valley. This assumption might also be appropriate for a subsistence farmer; however, no one currently in the Amargosa Valley region fits this profile. Therefore, to be consistent with the current demographics and population locations, food sources could be more carefully investigated to estimate the amount of possible contamination.

- *Soil build-up.* Using contaminated water for crop irrigation can cause the buildup of radionuclide in the soils. These radionuclides can then produce an external dose and may cause additional internal doses if resuspended and contaminated soil particles are inhaled or ingested. The process of retention and buildup of radionuclides through continued irrigation with contaminated groundwater and the subsequent impacts on the various pathways defined for the biosphere could be further investigated.

6.5.2 Insights from the Total System Performance Assessment Peer Review Panel

An independent peer review of the TSPA-VA is being conducted. This peer review has the objective of providing a formal, independent evaluation and critique of the TSPA-VA in order that technical issues associated with the approach, methodology, and assumptions can be addressed prior to initiating the TSPA for the site recommendation and license application. The peer review has consisted of three interim reports to date (Whipple et al. 1997a, 1997b, and 1998) and will culminate in a final report due to be completed by the end of 1998. The Peer Review Panel consists of 6 individuals who have technical backgrounds that span the major disciplines of significance to postclosure performance, namely geohydrology, geoengineering, geochemistry, materials science, materials engineering, health physics, and risk assessment.

The Peer Review Panel has reviewed preliminary draft materials describing the approach, methodology, and assumptions to be used in the TSPA-VA as well as presentations made by the TSPA analysts to external review organizations such as NRC and the NWTRB. These materials have been supplemented by interactions of the panel members with TSPA-VA and other Yucca Mountain project staff. Although the review of the panel has been limited to date, the panel was impressed with the initial draft of Volume 3 of the Viability Assessment (Whipple et al. 1998, p. 45). However, the panel did not comment on the draft documentation of the TSPA-VA at the time of their third interim report. Ultimately the TSPA-VA Peer Review Panel will review this Volume 3 of the VA and the associated *Total System Performance Assessment-Viability Assessment (TSPA-VA) Analyses Technical Basis Document* (CRWMS M&O 1998i) which is being prepared concurrently. This review will be completed in fiscal year 1999, with the results being used to assist DOE in prioritizing the development of the approach and methods to be used for the TSPA for the site recommendation and LA.

Based on the Peer Review Panel's reviews of the preliminary materials available to them, they have provided a range of observations, conclusions, and

recommendations that must be considered in the development of the approach and methodology for the next iteration of the TSPA for the site recommendation and LA. The conclusions of the panel have been grouped into the following categories:

- Physical events and processes considered
- Use of appropriate and relevant data
- Assumptions made
- Abstraction of process models
- Application of accepted analytical methods
- Treatment of uncertainties
- Other issues

In the following paragraphs, these issues are discussed with the goal of identifying the additional models and analyses that will ultimately be required in the development of the TSPA for the site recommendation and LA. These issues may be treated as critiques of some of the assumptions made in TSPA-VA and as such some discussion is included to note the potential significance of the criticism to the conclusions reached in the TSPA-VA.

6.5.2.1 Physical Events and Processes Considered

The panel notes in their review of preliminary draft materials that the TSPA-VA has not fully addressed the potential effects associated with a number of processes. The examples they cite include coupled phenomena such as the chemical and mechanical interactions in the thermohydrologic analyses, degradation of the drift with time and the effects this may have on waste package performance, and dispersion and dilution of radionuclides in the groundwater especially at early times when small source areas may be more likely. In addition, the panel believes that too much attention may have been devoted to the potential consequences associated with low-probability disruptive events such as volcanic events.

It is acknowledged that the TSPA-VA has not addressed all processes that must eventually be evaluated as DOE proceeds from the VA to the site recommendation and licensing. Nevertheless, bounding sensitivity analyses have been performed of the potential effects associated with coupled processes by varying the fracture characteristics of the rock mass around the drift opening. These changes in fracture properties would be the principal effect of the coupled phenomena identified by the panel. The analyses presented in Section 5.1 illustrate that, within the range of parameters examined, these effects are minimal on the dose rate.

Although additional analyses are also required of the effects of drift degradation to support the site recommendation, assuming the VA reference design of no long-term support or backfill placed in the drift, some sensitivity analyses of these effects have been examined in the VA. For example, the chemical degradation of the drift liner has been examined in Section 5.3. The mechanical effects associated with drift degradation are examined in the rock fall disruptive event scenario described in Section 4.4.3. The hydrologic effects associated with drift degradation were addressed in the same sensitivity analyses related to coupled processes described above. Finally, the potential thermal effects associated with the degradation of the drift have been examined in Chapter 3 of the *Total System Performance Assessment-Viability Assessment (TSPA-VA) Analyses Technical Basis Document* (CRWMS M&O 1998i) and found to be inconsequential.

DOE agrees with the panel's observation that the degree of dispersion and dilution in the transport modeling should be related to the fraction of the area of the repository represented by degraded waste packages. This issue will be addressed in the analyses planned for the site recommendation and the LA. It is also important to note that the dispersion/dilution models used in the unsaturated and saturated zones as well as the assumptions made regarding the probability of the single well intersecting any dispersed plume in the alluvial aquifer must be internally consistent. In the case of TSPA-VA, it was conservatively assumed that the well intersected the highest concentration area of the plume and that there was minimal dilution in the saturated zone. This latter assumption was predicated on an expert elicitation of the saturated zone flow and transport model, in which the experts assumed that the source region was relatively large (on the order of several hundred

meters) and therefore the additional dispersion effects expected in the saturated zone were minimal. If, as pointed out by the Peer Review Panel, the source region in the unsaturated zone is small, then the consistent saturated zone model should include the expected dispersive effects which are much larger (Whipple et al. 1998, p. 38). This alternative representation has been acknowledged in the assessment of the significance of unsaturated zone transport in Section 6.4. It is acknowledged that refined unsaturated and saturated zone transport models need to be investigated as part of the site recommendation and LA.

Some disruptive events are of very low probability. The probabilities of some disruptive events of interest to the long-term performance of the Yucca Mountain repository system are described in Section 4.4. Although DOE agrees that these low probability events pose very low risk to the public (as documented in Section 4.4), they are of interest to both the public and regulatory agencies such as NRC. Given this interest, DOE believes this effort has been given about the right level of attention in the TSPA-VA.

6.5.2.2 Use of Appropriate and Relevant Data

The panel notes in their review of preliminary draft materials that the TSPA-VA lacks site-specific data citing as examples the saturated zone from Forty Mile Wash to the Amargosa Valley, soil properties for determination of sorption characteristics, data on colloid transport, and radionuclide plant uptake factors. They also note that experimental data are needed to confirm the processes that control neptunium solubility and their belief that there are insufficient data to support the selection of the materials for use in the final waste package design. Finally, the panel believes that there is an over-reliance on the use of data generated by YMP scientists and only limited use of the published literature.

As DOE moves forward from the VA to the site recommendation and LA, all relevant site-specific data must be used to improve the basis for the process models. A wealth of site-specific, laboratory-derived and published literature information has been used in the course of developing the TSPA-VA. The unsaturated zone flow model has been based on extensive surface-based geologic and hydrogeologic testing, in situ observations of thermo-hydro-chemical conditions that are indicators of water movement, and laboratory studies of fundamental processes affecting water movement in fractured unsaturated media. The thermal hydrologic models have been based on in situ tests such as the single heater test and laboratory tests. These models have been compared to a wide range of similar models available in the published literature to add confidence in their relevance to the performance of the Yucca Mountain repository system. Similarly, a significant amount of laboratory testing has been conducted to evaluate the degradation characteristics and rates of the materials that are proposed to contain the wastes, in particular the candidate metals for the waste package. These tests have been complemented by information available in the published literature.

DOE will carefully consider the panel's input with regard to data availability. However, it is appropriate to acknowledge that uncertainty exists in many of the models that are used to evaluate the behavior of the Yucca Mountain repository system. This uncertainty is documented throughout this volume and in the companion *Total System Performance Assessment-Viability Assessment (TSPA-VA) Analyses Technical Basis Document* (CRWMS M&O 1998i). Some of these uncertainties can and indeed will be reduced in the next years with an appropriate combination of site-specific field testing, laboratory testing and literature data. These additional data will be used to enhance the current understanding in those factors most significant to long term performance for use in the site recommendation and LA. The activities identified as being most important for continued testing are discussed in Volume 4, which was not available for the Peer Review Panel to review.

Despite the desire to reduce the uncertainty in many of the key components of the TSPA, it must nevertheless be acknowledged that some uncertainty will remain. As noted in the introduction to Chapter 6, this uncertainty is the result of the time and space scales of interest. The goal of the TSPA

analyses is to reasonably bound this remaining uncertainty. DOE believes that the uncertainty has been reasonably bounded in the TSPA-VA. Even as efforts are made to reduce the uncertainty in the coming years, DOE will continue to assure that the remaining uncertainty, and its potential effects on postclosure performance, are appropriately addressed in the TSPA for the site recommendation and LA.

6.5.2.3 Assumptions Made

The panel notes in their review of preliminary draft materials that the TSPA-VA made some assumptions that need to be appropriately justified. They cite an example of the fully coupled thermal-hydraulic-mechanical-chemical interactions being of second order importance. In addition, they believe that incorporating other assumptions could provide useful insights into repository performance. They cite an example of prolonged ventilation of the repository.

DOE agrees that all assumptions need to be appropriately justified and their significance to long term performance evaluated. The purpose of the *Total System Performance Assessment-Viability Assessment (TSPA-VA) Analyses Technical Basis Document* (CRWMS M&O 1998i) is to provide the appropriate rationale with the supporting data, analyses and references to relevant project information, including the process model for each TSPA component. In the particular example cited by the panel, the significance of the complex process interactions mentioned has been evaluated with a range of individual sensitivity studies. For example, the seepage model has been modified to account for either an increase or decrease in fracture permeability and capillarity that might be the result of these coupled processes. These results indicate that the overall performance is not significantly sensitive to such changes, which is the basis of the assumption. DOE acknowledges that it will be very difficult to predict with any degree of robustness the exact thermal-hydraulic-mechanical-chemical interactions that might occur in each drift in the vicinity of each waste package. However, such fidelity in the analysis is not required. What is required is to reasonably bound the potential effects so that informed decisions can be made about the potential safety of the repository system.

DOE agrees that a range of alternative assumptions needs to be evaluated to gain sufficient understanding of how the system is likely to perform. Many of these alternative assumptions have been explored in Chapters 4 and 5 of this volume. Most of these have relied on the VA reference design, which does not include long term ventilation. Many others, including a range of alternative designs such as the long-term ventilation design mentioned by the panel, are worthy of investigation. These alternative designs and design features will be a major emphasis of the Project in fiscal year 1999 as DOE moves forward to selecting the appropriate site recommendation and LA design.

6.5.2.4 Abstraction of Process Models

The panel notes in their review of preliminary draft materials that the abstraction process used in the TSPA-VA needs to be reviewed. In particular they note that an abstracted model should only be used if the process-level model upon which the abstraction is based confirms its use is justified. They also note that there needs to be appropriate integration of the abstracted models among the different groups developing the TSPA. They cite an example related to the consistency between unsaturated zone and saturated zone transport model assumptions.

The abstracted models used in TSPA-VA have been based either on an underlying process model or the basic data that describe the relevant process. All models, whether process-based or abstracted, are abstractions of reality. All models, whether process-based or abstractions, need to be compared to appropriate in-situ or laboratory observations. Unfortunately, there are minimal opportunities to compare the results of the models over the spatial and temporal scales of interest to direct observations, with the exception of some natural analogs.

The *Total System Performance Assessment-Viability Assessment (TSPA-VA) Analyses Technical Basis Document* (CRWMS M&O 1998i) describes the details of the abstraction for each of

the components of the TSPA-VA. In the case of the abstracted models of unsaturated zone flow, seepage into drifts, thermal hydrology, waste package degradation, cladding degradation, unsaturated zone transport, and biosphere transport the abstracted models are based directly on the underlying process model. In some cases the model was directly used in the TSPA analyses while in other cases a response surface capturing the relevant results of the process model was used. In the case of abstracted models of climate change, waste form degradation, radionuclide solubility, colloid stability and mobility, and saturated zone transport the abstracted models are based directly on available externally published or project-generated global, regional, site and laboratory data. Therefore, DOE believes there is a good, even if preliminary, technical basis for all the models used in the TSPA-VA.

Nevertheless, DOE understands the Peer Review caution that all models and assumptions need to be appropriately justified when used in the development of a license application. Therefore, a range of activities that are summarized in Volume 4 will be undertaken over the next few years with their aim being to enhance the confidence in all models used to make projections of repository performance.

DOE agrees that the assumptions made between different abstracted models need to be self consistent. Every effort was made in the TSPA-VA to assure this. For example, if different assumptions were made about infiltration rates, these were consistently applied through the system to evaluate changes in percolation flux, seepage fraction and flux, thermal hydrologic response, unsaturated zone groundwater velocity, and the water table elevation. An additional example is the propagation of transient changes through the system. If the climate was assumed to change at a particular time, then this change was propagated through changes in the unsaturated zone flow and transport, seepage, water table elevation and saturated zone flow and transport. DOE will continue to strive to assure that assumptions made between different components of the TSPA remain consistent.

An additional consistency issue noted by the panel centers around the depiction of contaminant plume dispersion in both the unsaturated and saturated zones. DOE agrees these need to be consistent. As noted above in the discussion in Section 6.5.2.1, the TSPA-VA assumed that the pumping well directly intersected the maximum concentration of the plume, that there was no mixing in the pumping well and that there was minimal dispersion in the saturated zone. This was the result of basing the dispersion effects on an expert elicitation which assumed the plume size entering the saturated zone was on the order of several hundred meters in width, that is the plume had already been dispersed in the unsaturated zone. As the panel points out, this assumption, may be appropriate at late times (several hundred thousand years) when waste packages located over a significant fraction of the area of the repository may be expected to be contributing to releases. However, this assumption is probably inappropriate at early times (less than 10,000 years) when only a very few breached waste packages are contributing to the dose rate. To be consistent, if a model of transport from discrete waste packages is invoked in the unsaturated zone, then the likely dispersion in the saturated zone and well intersection probability should be included in the analyses. These will be investigated in the TSPA for the site recommendation and LA.

6.5.2.5 Application of Accepted Analytical Methods

The panel notes in their review of preliminary draft materials that the TSPA-VA may contain models that contain uncertainties. In some cases they note that these models may have been applied without recognition of their potential limitations. They comment that these limitations could call into question the usefulness of the sensitivity and uncertainty analyses that have been conducted. They cite several models that exemplify their concern:

1. The saturated zone flow model

2. The thermal hydrology model including the coupled effects of thermochemical and thermo-mechanical interactions

3. The unsaturated zone flow model including the seepage model

4. The unsaturated zone transport model including the mechanisms of colloid migration

5. The waste package degradation model including the effects of crevice corrosion, chemical conditions on the waste package surface, stress corrosion cracking, and the generation of corrosion products in crevices between the outer and inner waste package materials

6. The cladding degradation model including its uncertainty

7. The saturated zone flow and transport model including greater resolution of the numerical representation

In addition to these individual models, they note that the relevant hypotheses, models and abstractions need to be verified by comparison to appropriate site-specific, laboratory or literature data.

DOE agrees that uncertainties exist in all the cited models. These uncertainties have been the focus of a number of workshops that DOE has held on the key components of the TSPA (see Table 2-2 for a complete listing of these workshops and expert elicitations). These uncertainties have also been documented in the *Total System Performance Assessment-Viability Assessment (TSPA-VA) Analyses Technical Basis Document* (CRWMS M&O 1998i).

One of the goals of the TSPA-VA is to examine the significance of these uncertainties on postclosure performance to assist in identifying the key factors requiring additional information prior to the submittal of the site recommendation and LA. As noted in Section 4.3 and Chapter 5, the significance of these uncertainties was investigated using both a range of parameters and models to describe the base case performance, as well as a suite of alternative models that were tested to determine whether differing assumptions would significantly change the results.

In all of the examples cited by the Peer Review Panel, at least one and in many cases several sensitivity analyses have been conducted to investigate the potential significance of the noted uncertainty. For example, a range of different seepage models has been studied to accommodate the most significant aspect of coupled processes (Section 5.1). A range of different assumptions regarding the waste package degradation model (including the fraction of the waste package with seepage, the size of the patches, and the distribution of the local chemistry on the waste package surface) has also been investigated (Section 5.4). Analyses have been performed using a range of distributions for the Zircaloy cladding degradation (Section 5.5). These included one case in which it was assumed there was no performance credit for the cladding.

DOE believes that the above sensitivity analyses and others described in Chapter 4 and 5 capture the range of likely performance of the repository system. Although it is possible to combine low probability models and parameters to further investigate the full range of performance, the results of these scenarios would have to be appropriately weighted by their low probability. Such analyses may be required in the licensing of the Yucca Mountain repository, but they were not the focus of the Viability Assessment, which was designed to investigate the probable behavior of the repository system.

DOE agrees that uncertainties other than those quantified in the TSPA-VA do exist. The panel correctly points out some of these. These uncertainties, as well as their potential significance need to be investigated prior to the site recommendation and LA.

In several instances, the Peer Review Panel notes the need to reduce the uncertainty that has been identified (whether that identification was by DOE, by the Peer Review Panel, by the NWTRB or by NRC). Although in many areas, there will be significant work performed over the next several years to minimize the uncertainty in models and abstractions for use in the TSPA for the site recommendation and LA, DOE acknowledges that even after this effort, uncertainties will still remain. The goal of the next TSPA analyses will be to address

the significance of the remaining uncertainties and assure that the site and associated engineered barriers meets with a sufficient safety margin all applicable environmental and safety standards.

6.5.2.6 Treatment of Uncertainties

The panel notes in their review of preliminary draft materials that the TSPA-VA has "lumped" many types of uncertainties and that the results may be inappropriately insensitive to some aspects of the actual behavior of the repository system. In addition, the panel observes that the TSPA-VA has not provided adequate consideration of the multitude of factors that are necessary for estimating dose rates to the public.

DOE agrees that many types of uncertainty have been evaluated as part of the TSPA-VA. Assuming that all the relevant uncertainties were adequately characterized, quantified and incorporated in the models used for projecting system behavior, the system model should be able to determine the relative sensitivity of the system behavior to each of the model components. However, it must be acknowledged that not all uncertainties of all types have been included in the single system model used in TSPA-VA. To better investigate the complex interrelationships between the different system components, a number of alternative model sensitivity analyses were developed and documented in Chapter 5. These analyses were conducted in part to examine whether the initial results were indeed "inappropriately insensitive". DOE believes that the combined suite of sensitivity analyses have captured the range in probable behavior of the Yucca Mountain repository system.

DOE is aware of the many factors that contribute to the estimate of dose from a given radionuclide concentration in the groundwater. All of these factors are included in the model used to estimate biosphere dose conversion factors. Reasonable ranges for the key factors have been used in the development of the distribution of biosphere dose conversion factors. These distributions will be examined, including the sources and magnitudes of their uncertainty, prior to the development of the TSPA for the site recommendation and LA.

6.5.2.7 Other Issues

Based on the preliminary information available to the panel, they questioned the apparent focus of the TSPA-VA almost exclusively on the time period from 10,000 to 1 million years. They also note the need for additional supporting research in a number of areas, including water compositions in contact with the waste package, critical crevice corrosion temperatures, neptunium solubility and technetium sorption on degraded waste package materials.

DOE does not believe it focussed on any particular time frame in the analyses presented in Chapters 4 and 5. Generally, the results are displayed and discussed in three different time periods, the time from closure to 10,000 years, the time from 10,000 to 100,000 years and finally the time period from 100,000 to 1 million years. This has been done for several different reasons. First, the significance of the overall system response is difficult to examine in a single time period. Second, different insights are gained by examining the results over different time periods. Third, DOE does not know over what time period the environmental and regulatory performance objectives will be applied although preliminary indications are that the 10,000 year period will likely be addressed with quantitative performance requirements in the new regulations being prepared for Yucca Mountain. Finally, it is believed that conducting analyses to the time of the peak dose, whenever that occurs, allows some confidence in a more comprehensive, even if more qualitative, evaluation of the performance of the entire system.

As noted by the panel, the time period of interest is an important aspect of the defense in depth strategy that will evolve during development of the license application, and will undoubtedly be the subject of extensive discussion between NRC and DOE during licensing proceedings. The performance allocation approach presented in Volume 4 is consistent with the general approach taken to date, which assumes that both 10,000 year performance and peak dose are important performance measures.

DOE acknowledges the need for additional investigations in a number of areas, including those mentioned in the panel's report. The investigations that are planned over the next few years are those that would significantly improve upon the current understanding and which are significant to the system performance. The planned activities are described in Volume 4.

In summary, interactions with the Peer Review Panel continue to provide useful feedback as DOE moves forward to develop the basis for the next iteration of TSPA. Their Third Interim Report points to a number of areas where attention will need to be placed as the basis for the site recommendation and license application is prepared.

6.5.3 Comments from the Nuclear Regulatory Commission

NRC has recently provided DOE with initial comments on the TSPA-VA (Letter from Michael J. Bell, NRC to Stephan J. Brocoum, DOE, dated July 6, 1998). These comments were based on a series of three Technical Exchanges held between DOE and NRC staffs and their contractors, the most recent being in March, 1998. As noted in the letter, NRC comments are intended to facilitate DOE's effort to identify the future work that may be needed to develop a complete and acceptable license application.

DOE appreciates the opportunity to interact with NRC staff on the significant issues associated with assessing the long-term performance of the Yucca Mountain repository system. The comments provided by NRC during the Technical Exchanges and the above letter, in conjunction with the recently published Issue Resolution Status Report for Total System Performance Assessment and Integration (NRC 1998a) assist DOE in identifying the most relevant issues to NRC which can then be a basis for continued discussion and ultimately closure.

In the following paragraphs, each of the NRC comments is presented and briefly discussed. Where appropriate, the reader is referred to Volume 4, which contains descriptions of the activities DOE intends to conduct between now and the completion of the Site Recommendation Report and the submittal of the LA.

6.5.3.1 Radionuclides Tracked in the Performance Assessment

DOE concurs that the approach used for screening out unimportant radionuclides from the TSPA analyses needs to be well documented and the potential impacts of not considering the full suite of possible radionuclides present needs to be demonstrated. The radionuclide screening process is summarized in Section 3.5 of the TSPA-VA. The details of the implementation of this process and the small differences arising from not considering a full suite of radionuclides are discussed in Chapter 6 of the *Total System Performance Assessment-Viability Assessment (TSPA-VA) Analyses Technical Basis Document* (CRWMS M&O 1998i). Given that the suite of potentially important radionuclides may vary with the specific design, modeling assumptions, and scenarios analyzed, it is agreed that each TSPA analysis should address this issue and justify the inclusion or exclusion of certain radionuclides. DOE will continue to carefully review the assumptions of the radionuclides included in the TSPA analyses for the site recommendation and LA.

6.5.3.2 Consideration of all Significant Features and Processes in the Performance Assessment

DOE agrees that the rationale for including or excluding any potentially significant feature, event or process needs to be technically justified and clearly articulated. The rationale used in the TSPA-VA has been presented in the detailed descriptions of each component model documented in the *Total System Performance Assessment-Viability Assessment (TSPA-VA) Analyses Technical Basis Document* (CRWMS M&O1998i). Acknowledging that there is uncertainty in exactly what features, events and processes are most significant to long-term performance, a range of total system sensitivity analyses have been conducted in the TSPA-VA (Chapter 5). These analyses, together with subsystem and component model sensitivity analyses that are presented in the *Total System Performance Assessment-Viability*

Assessment (TSPA-VA) Analyses Technical Basis Document (CRWMS M&O 1998i) form the basis for the determination of importance. As DOE proceeds from the VA to the site recommendation and LA, these analyses will be expanded to include other potentially important features, events and processes, along with appropriate auxiliary analyses to support the resolution of relevant sub-issues in some of the NRC KTIs. All of these analyses will be documented in the LA.

6.5.3.3 Model Abstraction

DOE agrees that modeling assumptions should be consistent across different process models, unless there is a defensible technical rationale. An example of a case where different assumptions may be appropriate is the spatial and temporal averaging of hydraulic properties. Flow properties applicable at the scale of tens of meters (e.g., analyses in the vicinity of the drift) would be different than hydraulic properties hundred of meters (e.g., analysis of flow from the repository to the water table). Although the two parameter sets should be consistent, they may be different.

Every effort is being made through the document review process to ensure consistency of key parameters across both process models and abstracted models used in the TSPA-VA. For example, the climate change is propagated through the system by affecting the infiltration rate, percolation rate, seepage rate, groundwater velocity, water table rise and saturated zone flux. DOE will continue to rely on its internal and external review processes to ensure that the individual models and their coupling are appropriately consistent. In addition, DOE will use pre-licensing interactions and technical exchanges with NRC to check its effectiveness, as it proceeds with preparing the TSPA for the LA.

6.5.3.4 Documentation of Assumptions

DOE agrees that detailed documentation of the assumptions used in performance assessments is of fundamental importance to the transparency (and credibility) of the TSPA. This was the objective of producing a companion document, the *Total System Performance Assessment-Viability Assessment (TSPA-VA) Analyses Technical Basis Document* (CRWMS M&O 1998i), which augments the TSPA-VA documentation contained in Volume 3 of the VA. This documentation has undergone several internal reviews, with part of the review criteria being based on the NRC criteria noted in their Issue Resolution Status Report on Total System Performance Assessment (NRC 1998a). The documentation of the TSPA-VA model assumptions will ultimately be reviewed by the TSPA-VA Peer Review Panel, NRC and their contractors, the NWTRB, the State of Nevada, and by other interested parties. All comments received will help DOE ensure that the documentation for the TSPA for the site recommendation and LA is sufficient to facilitate regulatory review.

6.5.3.5 Transparency and Traceability of Analysis

DOE concurs with NRC comment that the performance assessment results should allow the importance of alternative models to be evaluated. This was the goal of the sensitivity analyses presented in Section 5. Based on previous NRC comments on this subject, as those from the NWTRB on this same subject, DOE is making a concerted effort to improve the graphical presentation and documentation of these diverse and multifaceted analyses. DOE expects to discuss this issue at future Technical Exchanges with NRC on their TSPA Methodology Issue Resolution Status Report, and through DOE's internal review process for technical reports.

6.5.3.6 Container Life

DOE agrees that the technical basis for the degradation characteristics and rates of the candidate waste package materials needs to be adequately justified. The basis for the model used in the TSPA-VA is described briefly in Section 3.4 of Volume 3 of the VA and in Chapter 5 of the *Total System Performance Assessment-Viability Assessment (TSPA-VA) Analyses Technical Basis Document* (CRWMS M&O 1998i) along with the supporting documentation that is cited in these documents. DOE agrees that the basis must be enhanced further in the next few years leading to the LA design and performance assessment. The

work to provide this additional confidence is described in Volume 4.

6.5.3.7 Role of Rockfall in Assessing Waste Package Lifetime

DOE agrees that rockfall effects need to be considered in the design and performance of the Yucca Mountain repository system. In the TSPA-VA this has been addressed with some explicit analyses of seismically-induced rockfall damage in Section 4.4.3 and an implicit incorporation of early waste package failures caused by unanticipated processes. These early juvenile failures were incorporated in the base case analyses after the NRC-DOE Technical Exchange in March, 1998. Continued definition of the potential consequences of early waste package failures will occur as part of the multiple barrier analyses expected to be performed for the TSPA for the site recommendation and LA. In addition, DOE plans to pursue dialog on this topic through its interactions with NRC in future Technical Exchanges.

6.5.3.8 Effectiveness of Engineered Barriers in the Event of Volcanic Activity

In the TSPA-VA, DOE has analyzed the potential consequences associated with low probability volcanic activity at Yucca Mountain. In these analyses, reasonably conservative assumptions were made regarding the potential waste package failure modes (presuming that such an event occurred.) Although alternative failure modes could be postulated, DOE believes that the analyses presented in the VA are sufficient to bound the potential risk (equal to the probability of the event times the consequences of the event) of the direct volcanic intrusion scenario. Alternative failure modes may be addressed in the TSPA for the site recommendation and LA and DOE plans to pursue dialog on this and other disruptive events and processes with NRC staff and their contractors as part of the ongoing DOE/NRC Technical Exchanges on TSPA and future interactions on the NRC TSPA Methodology Issue Resolution Status Report (i.e., as part of resolution activities on the scenario analysis subissue).

6.5.3.9 Neptunium Solubilities

DOE concurs that the basis for the selection of the neptunium solubility used in the TSPA analyses needs to be supported by applicable measurements under suitable conditions. The rationale for the statistical distribution used in TSPA-VA has been based on available laboratory measurements combined with information on the stability of various neptunium phases in different geochemical environments. This rationale is presented in Section 3.5. Because of the importance of neptunium to long-term dose assessments (see Section 5.5), DOE will continue to refine the estimates of the range of neptunium solubility values for use in the TSPA for the site recommendation and LA.

6.5.3.10 Matrix Diffusion

DOE agrees that the technical basis for differing assumptions about matrix diffusion need to be documented. These have been included in Section 3.6 and in Chapter 7 of the *Total System Performance Assessment-Viability Assessment (TSPA-VA) Analyses Technical Basis Document* (CRWMS M&O 1998i). In addition, a range of sensitivity analyses have been conducted with differing assumptions about matrix diffusion. These results are presented in Sections 5.6 and 5.7. DOE will continue to review this issue with NRC in future Technical Exchanges and Appendix 7 meetings to ensure that a defensible and reasonably conservative representation of this transport process is included in subsequent TSPAs for the repository.

6.5.3.11 Saturated Zone Transport

NRC notes that there are limited data to define the saturated zone transport along the groundwater pathway south of the repository to the postulated receptor location at 20 km (12 miles). DOE also recognizes the current dearth of hydrogeologic data in this region of the flow system. DOE also agrees that both the incorporation of additional field data, such as the data to be collected from the Nye County well network, and models which incorporate the uncertainty in the flow and transport characteristics are essential to the preparation of a

complete and defensible TSPA for the proposed repository system.

6.5.3.12 Radionuclide Retardation

DOE agrees that the technical basis for sorption coefficients used in the TSPA analyses needs to be improved and more substantive. For the TSPA-VA, this basis is presented in Chapter 7 of the *Total System Performance Assessment-Viability Assessment (TSPA-VA) Analyses Technical Basis Document* (CRWMS M&O 1998i). The basis for application of any laboratory-derived sorption coefficients, and the analogs that are used to define correlations, needs to reasonably represent the uncertainty in this parameter. DOE will continue its effort to enhance the documentation of the basis for all assumptions as it moves forward from the VA to the site recommendation and LA.

6.5.3.13 Treatment of Colloids

DOE agrees that the mechanistic basis for the partitioning coefficient for plutonium sorption onto colloids, as well as the stability and filtration characteristics of these colloids, needs to be better defined between the VA and the site recommendation and LA. Efforts to better characterize the colloid distribution and reversibility are planned. These efforts are summarized in Volume 4.

6.5.3.14 Basis for Assigning Probabilities to Corrosion Potential Values

NRC notes that specific probabilities of different corrosion potentials, that have been derived from expert elicitation, have been used in the waste package degradation model of the TSPA-VA. The basis for these distributions is presented in Chapter 5 of the *Total System Performance Assessment-Viability Assessment (TSPA-VA) Analyses Technical Basis Document* (CRWMS M&O 1998i) as well as the expert elicitation report on waste package degradation (CRWMS M&O 1998b). As described in Volume 4, continued testing is underway to verify the corrosion potential distributions that should be used in future TSPAs.

6.5.3.15 Uncertainty in the Results of Expert Elicitation

NRC comments that the significance of the uncertainty representations in the expert elicitation results should be propagated through the total-system calculation. They cite an example of the point-value probabilities used to define the corrosion potential of Alloy 22. DOE concurs with this assessment. In fact, the sensitivity to this parameter was evaluated and documented in Chapter 5 of the *Total System Performance Assessment-Viability Assessment (TSPA-VA) Analyses Technical Basis Document* (CRWMS M&O 1998i). As DOE continues toward the development of the site recommendation and LA, the uncertainty in all significant factors affecting postclosure performance will be investigated.

6.5.3.16 Development of Expert Elicitation Results for Use in Performance Assessment

NRC comments that in some cases, the cited example being the Probabilistic Seismic Hazard Analysis, the panel of experts did not have a clear understanding of how their results would be used in the performance assessment. In all of the elicitations conducted specifically for TSPA-VA, however, the CRWMS M&O presented the goals and objectives of the elicitation as well as exactly how the results were to be used. The goal of the cited seismic hazard analysis was focussed on inputs to the preclosure design and safety aspects of the surface and subsurface facilities as opposed to the postclosure performance assessments. DOE agrees that experts used in formal elicitations should be informed at the outset how the results of the elicited judgments will be used.

In summary, DOE finds the comments that NRC (and their contractors at the Center for Nuclear Waste Regulatory Analyses at the Southwest Research Institute) have made during and after the Technical Exchanges held over the last year to be very constructive and helpful. DOE anticipates that NRC will comment on the Viability Assessment when it is formally released. DOE believes that these comments in conjunction with meetings on each of the individual Issue

Resolution Status Reports will assist DOE in working towards a defensible LA.

6.5.4 Concluding Remarks

Current data and analyses indicate that the Yucca Mountain site provides favorable features for limiting the contact of water with the waste. The location of the site in a semiarid region and the nature of the site itself limit the amount of water that can reach the repository. The site provides a thick unsaturated zone where the waste can be placed deep below the surface and well above the water table; the waste packages would therefore be protected from changes in conditions at the surface while still being kept well away from the saturated zone. The site would therefore provide predictable and stable environments for design of engineered barriers that could further limit the exposure of waste to water.

Performance assessment and design studies indicate that there are a number of options for the design to keep water away from the waste. They indicate, for example, that the highly corrosion-resistant inner container and the thick steel outer container of the reference design of this VA each provide effective barriers against water. Although as noted above there are some issues that must still be addressed, the estimates indicate that robust waste packages could be designed to remain intact for thousands of years in the repository environments. The studies also indicate that the spent nuclear fuel cladding would likely provide an additional barrier to water contacting the waste, once the outer and inner waste package barriers are breached.

In addition to expected repository performance, the postclosure safety case also explicitly considers processes and events that could disrupt a repository at the Yucca Mountain site. These include disruptive natural processes (seismicity and volcanism), potential human intrusion associated with exploration for natural resources, and nuclear criticality. Each of these potentially disruptive processes and events has been examined in this volume. The analyses presented in Section 4.4 indicate these disruptive scenarios introduce no substantial increase in the risk to long-term public health or safety.

As noted in the Introduction (Volume 1), a number of investigations are required to assist DOE in developing the safety case for the Yucca Mountain repository system. The safety case is comprised not only of evaluations of total system performance similar to those documented in this volume, but also of evaluations of multiple barriers, treatment of the safety margin, and use of natural analogs as qualitative indicators of expected behavior. In addition, the total safety case must consider the operational and preclosure safety of the workers and the public, rather than solely the long-term postclosure aspects evaluated in TSPA.

The goal of each successive total system performance assessment iteration is to refine the analyses based on improved site understanding and the maturation of the design concepts for the engineered system. Using the results of the performance assessments documented in this volume and summarized in the previous portions of this section, the key attributes and principal factors likely to affect the LA performance assessment have been identified and prioritized.

The effects of uncertainty included in the analyses of the principal factors affecting postclosure performance projections for the reference design were identified and ranked in Section 6.4. These rankings provide a partial basis for prioritizing investigations to reduce the uncertainty in these factors. However, there is also additional information in the form of judgment that must also be incorporated in the rankings. Finally, although uncertainty in a specific factor may have a large effect on the final result of a TSPA analysis, reduction of that uncertainty may not be possible. This may be true because of prohibitive cost of a study, lack of technology to address a specific question, or lack of adequate time to complete a study before the LA submission deadline.

Therefore, prioritization of the principle factors, and the work needed to characterize each of them in the TSPA, is conditional based on the reference design and the TSPA modeling and assumptions. Reduction in uncertainty may not be practical, or

even possible, for some of the factors that are most important to performance. Some of the factors that are most important to performance may already be sufficiently well characterized. The importance of some factors may be obviated by a change in the repository design. Only where data are deemed inadequate and can be improved from a practical perspective, and should be improved from a licensing perspective, will additional work be performed.

The TSPA-VA indicates that for the first 10,000 years the expected dose rate derived from the repository at Yucca Mountain is essentially zero. Even within the first 100,000 years, the anticipated dose rate from a repository at Yucca Mountain is less than the national average for radiation from non-medical sources (approximately 300 mrem/year). Only at time scales of greater than 100,000 years does the additional dose rate from a repository approach the average background dose rate. The TSPA-VA also finds that the engineered system in the reference design has considerable impact on repository performance for a long period, on the order of several hundred thousand years. For even longer periods of time, however, the natural system dominates performance. The TSPA-VA shows that some factors and how they are modeled can have especially important influences on performance: for example, the corrosion characteristics of Alloy 22, the dilution of radionuclides in the transport pathways, and the transport of radionuclides as colloids. The TSPA-VA reinforces some ideas about performance; for example, that it is important to isolate waste from advective flow and that, for a dose-based standard, the rate of releases of radionuclides from a repository and the dilution in the environment are important. And finally, the TSPA-VA points out areas where improvements could be made to the TSPA models and data, including the most important uncertainties that could be reduced and the most important assumptions that could be addressed in the future.

The prioritization of the information needed to address the principal factors affecting expected postclosure performance allows focusing the testing and analysis programs on the key remaining questions related to repository performance. This prioritization and the rationale behind the allocation for each principle factor is given in Volume 4. The schedule for addressing these issues is also found in Volume 4.

The analyses of the TSPA-VA will provide a large part of the basis for the work required for construction of the TSPA for the site recommendation and the LA. However, as discussed above, the specific analysis results do not tell the entire story. In some cases, there was little applicable data available at the time for developing a model of a given factor. In other areas, because site characterization and design activities are still ongoing, new information has indicated that the ranges of values used may have been incomplete or too large. In each such case, it was necessary for the analysts to use judgment, based on their experience, to interpret the validity of their results. Where judgment has been used to modify the relative influence of uncertainty of a factor to be different than that shown by analysis (as documented in Volume 4), there is clearly a need to improve the confidence in the model for that factor. In addition, independent groups, such as the TSPA Peer Review Panel and the Nuclear Regulatory Commission, have provided suggestions of areas where more work is necessary to develop adequate TSPA models.

The next step for the Yucca Mountain TSPA team is to develop a comprehensive plan for addressing the important issues. While the general outline of this plan is contained in Volume 4, many details of the specific modeling activities must still be developed. A series of abstraction and testing activities, involving investigators from site characterization, design, and the performance assessment organizations will be convened to determine how to best incorporate the available information into appropriate representations of the total system. Because it will not be possible to develop these models to the same degree of complexity, the relative sensitivity of the factor will determine how much effort will be expended to improve any specific model or parameter. The outcome of these activities is anticipated to result in an improved set of total-system performance assessment models. These models will provide DOE with the reasonable assurance required to

understand how the system will behave and the degree of safety the system will provide to the public.

7. REFERENCES

The numbers at the end of each reference are Office of Civilian Radioactive Waste Management document accession numbers. See the inside front cover of this document for whom to contact regarding more information.

7.1 DOCUMENTS CITED

Andersen, R.; Kasper, J.; and Frankel, M., eds. 1979. *A Model of Survey Error,* 1–14. San Francisco, California: Jossey-Bass. 236464.

Andrews, R.W.; Dale, T.F.; and McNeish, J.A. 1994. *Total System Performance Assessment - 1993: An Evaluation of the Potential Yucca Mountain Repository.* B00000000-01717-2200-00099 Rev. 01. Las Vegas, Nevada: CRWMS M&O. NNA.19940406.0158.

Baca, R.G. and Brient, R.D. eds., 1996. *Total System Performance Assessment 1995 Audit Review.* San Antonio, Texas: U.S. Nuclear Regulatory Commission, Center for Nuclear Waste Regulatory Analyses. MOL.19970404.0012.

Barnard, R.W. and Dockery, H.A., eds. 1991. *Technical Summary of the Performance Assessment Calculational Exercises for 1990 (PACE-90), Volume 1: "Nominal Configuration" Hydrogeologic Parameters and Calculational Results.* SAND90-2726. Albuquerque, New Mexico: Sandia National Laboratories. NNA.19910523.0001.

Barnard, R.W.; Wilson, M.L.; Dockery, H.A.; Gauthier, J.H.; Kaplan, P.G.; Eaton, R.R.; Bingham, F.W.; and Robey, T.H. 1992. *TSPA 1991: An Initial Total-System Performance Assessment for Yucca Mountain.* SAND91-2795. Albuquerque, New Mexico: Sandia National Laboratories. NNA.19920630.0033.

Barr, G.E.; Borns, D.J.; and Fridrich, C. 1996. *Scenarios Constructed for the Effects of the Tectonic Processes on the Potential Nuclear Waste Repository at Yucca Mountain.* SAND96-1132. Albuquerque, New Mexico: Sandia National Laboratories. MOL.19970610.0644.

Barr, G.E.; Dunn, E.; Dockery, H.; Barnard, R.; Valentine, G.; and Crowe, B. 1993. *Scenarios Constructed for Basaltic Igneous Activity at Yucca Mountain and Vicinity.* SAND91-1653. Albuquerque, New Mexico: Sandia National Laboratories. NNA.19930811.0013.

Beckett, T.H. 1998. *Naval Spent Nuclear Fuel Package Source Term Release Data.* Arlington, Virginia: U.S. Department of the Navy. MOL.19980617.0476.

BIOMOVS II (Biosphere Model Validations Study II Steering Committee) 1994. *An Interim Report on Reference Biospheres for Radioactive Waste Disposal Developed by a Working Group of the BIOMOVS II Study.* Technical Report No. 2. Stockholm, Sweden: Swedish Radiation Protection Institute. 238733.

BIOMOVS II 1996. *Development of a Reference Biospheres Methodology for Radioactive Waste Disposal.* Technical Report No. 6. Stockholm, Sweden: Swedish Radiation Protection Institute. 238329.

Boak, J.M. and Dockery, H.A. 1998. "Providing Valid Long-Term Projections of Geologic Systems for Policy Decisions: Can We Succeed? Should We Try?" *A Paradox of Power Voices of Warning and Reason in the Geosciences 12, Reviews in Engineering in Geology.* 177–184. Welby, C.W. and Gowan, M.E., eds. Boulder, Colorado: Geologic Society of America. 238137.

Boden, P.J. 1994. "Effect of Concentration, Velocity and Temperature." *Corrosion, 3rd ed., Vol. 1,* 2:3–2:30. Shreir, R.A.; Jarmen, A; and Burstein, G.T. eds. Houston, Texas: National Association of Corrosion Engineers, Butterworth-Heinemann. 236653.

Bodvarsson, G.S.; Bandurraga, T.M.; and Wu, Y.S., eds. 1997. *The Site-Scale Unsaturated Zone Model of Yucca Mountain, Nevada, for the Viability Assessment.* LBNL-40376. Berkeley, California: Lawrence Berkeley National Laboratory. MOL.19971014.0232.

Bourcier, W.L.; Carroll, S.A.; and Phillips, B.L. 1994. "Constraints on the Affinity Term for Modeling Long-Term Glass Dissolution Rates." *Materials Research Society Symposium Proceedings 33,* 507–512. Barkatt, A. and Van Konynenburg, R.A, eds. Pittsburgh, Pennsylvania: Materials Research Society. 237858.

Bowman, C.D. and Venneri, F. 1996. "Comments On the Draft Paper 'Underground Supercriticality from Plutonium and Other Fissile Material.'" *Science and Global Security.* Amsterdam, Holland: Gordon and Breach Science Publishers. 238269.

Brady, Nyle C. 1984. *The Nature and Properties of Soils*, Ninth Edition. 371. New York, New York: MacMillan Publishing Company. 238332.

Brookins, D.G. 1990. "Radionuclide Behavior at the Oklo Nuclear Reactor, Gabon." *Waste Management 10,* 285–296. Amsterdam, Holland: Pergamon Press. 237759.

Buck, E.C.; Finch, R.J.; Finn, P.A.; and Bates, J.K. 1998. "Retention of Neptunium in Uranyl Alteration Phases Formed During Spent Fuel Corrosion. Scientific Basis for Nuclear Waste Management XXI." *Materials Research Society Symposium Proceedings, Davos, Switzerland, September 28-October 3, 1997, 506,* 87–94. McKinley, I.G. and McCombie, C., eds. Warrendale, Pennsylvania: Materials Research Society. 234676.

Burns, P.C.; Ewing, R.C.; and Miller, M.L. 1997. "Incorporation Mechanisms of Actinide Elements Into the Structures of U6+ Phases Formed During the Oxidation of Spent Nuclear Fuel." *Journal of Nuclear Materials 245 (1),* 1–9. Amsterdam, Holland: North Holland Publishing Company. 235501.

Chapman, N.A.; McKinley, I.G.; Shea, M.E.; and Smellie, J.A.T. 1991. *The Pocos de Caldas Project: Summary and Implications for Radioactive Waste Management.* SKB Technical Report TR 90-24. NAGRA Technical Report NTB 90-33. Stockholm, Sweden: Swedish Nuclear Fuel and Management Company. 205593.

Chen, Y.; Engel, D.W.; McGrail, B.P.; and Lessor, K.S. 1995. *AREST-CT V1.0 Software Verification.* PNL-10692/UC-510. Richland, Washington: Pacific Northwest National Laboratory. MOL.19960415.0236.

Chen, Y.; McGrail, B.P.; and Engel, D. 1996. "A Reaction-Transport Model and Its Application to Performance Assessment of Nuclear Waste Disposal." *Proceedings of the 1996 International Conference on Deep Geological Disposal of Radioactive Waste, Winnipeg, Manitoba, Canada, September 16-19, 1996,* 8–21 through 8–30. Toronto, Canada: Canadian Nuclear Society. 235084.

Chen, Y.; Chen, W.; Mu, J.; Park, A.; and Ortoleva, P. 1997a. *A General, Coupled Model for Solute Transport and Reactions and Porous Medium Alteration.* Las Vegas, Nevada: Duke Engineering & Services. 238119.

Chen, Y.; McGrail, B.P.; and Engel, D.W. 1997b. "Source-Term Analysis for Hanford Low-Activity Tank Waste Using the Reaction-Transport Code AREST-CT." *Scientific Basis for Nuclear Waste Management XX, Materials Research Society Symposium Proceedings Boston, Massachusetts, December 2-6, 1996, 465,* 1051-1058. Gray, W.J. and Triay, I.R., eds. Pittsburgh, Pennsylvania: Materials Research Society. 236519.

Chen, Y. 1998. *AREST-CT V1.2 Software Routine Report.* Las Vegas, Nevada: CRWMS M&O. 237968.

Conca, J. 1990. "Diffusion Barrier Transport Properties of Unsaturated Paintbrush Tuff Rubble Backfill." *High Level Radioactive Waste Management Conference,* 394-401. Las Vegas, Nevada: CRWMS M&O. 239067.

Conca, J.L. and Wright, J., 1992. "Diffusion and Flow in Gravel, Soil, and Whole Rock." *Applied Hydrology, 1,* 5-24. Hannover, Germany: Verlag Heinz-Heise. 224081.

Cramer, J.J. and Smellie, J.A.T. 1994. *Final Report of the AECL/SKB Cigar Lake Analog Study.* AECL-10851, COG-93-147, SKB TR 94-04.

Pinawa, Manitoba, Canada: Whiteshell Laboratories. 212783.

CRWMS (Civilian Radioactive Waste Management System) M&O (Management and Operating Contractor) 1995. *Total System Performance Assessment-1995: An Evaluation of the Potential Yucca Mountain Repository.* B00000000-01717-2200-00136 REV 01. Las Vegas, Nevada: CRWMS M&O. MOL.19960724.0188.

CRWMS M&O 1996a. *Emplaced Waste Package Structural Capability Through Time Report.* BBAA00000-01717-5705-00001 REV 00. Las Vegas, Nevada: CRWMS M&O. MOL.19961108.0075.

CRWMS M&O 1996b. *Probabilistic Criticality Consequence Evaluation.* BBA000000-0717-0200-00021 REV 00. Las Vegas, Nevada: CRWMS M&O. MOL.19970211.0203.

CRWMS M&O 1996c. *Probabilistic Volcanic Hazard Analysis for Yucca Mountain.* Nevada. BA0000000-1717-2200-00082 REV 00. Las Vegas, Nevada: CRWMS M&O. MOL.19961119.0034.

CRWMS M&O 1996d. *Scientific Investigation Implementation Package For Developing Biosphere Dose Conversion Factors.* B00000000-01717-4600-00073 REV 00. Las Vegas, Nevada: CRWMS M&O. MOL.19970616.0412.

CRWMS M&O 1996e. *Thermohydrologic Modeling and Testing Program Peer Review Record Memorandum.* Part I. Las Vegas, Nevada: CRWMS M&O. MOL.19960618.0060.

CRWMS M&O 1996f. *Total System Performance Assessment-Viability Assessment (TSPA-VA) Plan.* B00000000-01717-2200-00179. Las Vegas, Nevada: CRWMS M&O. MOL.19970320.0078.

CRWMS M&O 1997a. *Biosphere Abstraction/ Testing Workshop Results.* B00000000-01717-2200-00192. Las Vegas, Nevada: CRWMS M&O. MOL.19980618.0032.

CRWMS M&O 1997b. *Construction of Scenarios for Nuclear Criticality at the Potential Repository at Yucca Mountain, Nevada.* B00000000-01717-2200-00194. Las Vegas, Nevada: CRWMS M&O. MOL.19980204.0281.

CRWMS M&O 1997c. *Controlled Design Assumptions Document.* B00000000-01717-4600-00032 REV 04, ICN 2. Las Vegas, Nevada: CRWMS M&O. MOL.19970130.0039; MOL.19971028.0583; MOL.19980130.0128.

CRWMS M&O 1997d. *Near-Field Geochemical Environment Abstraction/Testing Workshop Results.* B00000000-01717-2200-00188. Las Vegas, Nevada: CRWMS M&O. MOL.19980612.0027.

CRWMS M&O 1997e. *Preliminary Design Basis for WP Thermal Analysis.* BBAA00000-01717-0200-00019 REV 00. Las Vegas, Nevada: CRWMS M&O. MOL.19980203.0529.

CRWMS M&O 1997f. *Report of Results of Hydraulic and Tracer Tests at the C-Holes Complex.* SP23APM3. Las Vegas, Nevada: CRWMS M&O. MOL.19971024.0074.

CRWMS M&O 1997g. *Repository Thermal Loading Management Analysis.* B00000000-01717-0200-00135 REV 00. Las Vegas, Nevada: CRWMS M&O. MOL.19971201.0601.

CRWMS M&O 1997h. *Waste Package Degradation Abstraction/Testing Workshop Results.* B00000000-0717-2200-00182 REV 00. Las Vegas, Nevada: CRWMS M&O. MOL.19980505.0604.

CRWMS M&O 1997i. *Suitability of Amargosa Valley Soils for Farming.* B00000000-01717-5705-00084 REV 00. Las Vegas, Nevada: CRWMS M&O. MOL.19980105.0149.

CRWMS M&O 1997k. *The 1997 "Biosphere" Food Consumption Survey - Summary Findings and Technical Documentation.* Las Vegas, Nevada: CRWMS M&O. MOL.19980202.0239.

CRWMS M&O 1997l. *Thermohydrology Abstraction/Testing Workshop Results.* B00000000-01717-2200-00184 REV 00. Las Vegas, Nevada: CRWMS M&O. MOL.19980528.0037.

CRWMS M&O 1997m. *Total System Performance Assessment-Viability Assessment (TSPA-VA) Methods and Assumptions.* B00000000-01717-2200-00193, REV 01. Las Vegas, Nevada: CRWMS M&O. MOL.19980213.0418.

CRWMS M&O 1997n. *Unsaturated Zone Flow Model Expert Elicitation Project.* Las Vegas, Nevada: CRWMS M&O. MOL.19971009.0582.

CRWMS M&O 1997o. *Waste Form Degradation and Radionuclide Mobilization Abstraction/Testing Workshop Results.* B00000000-01717-2200-000189. Las Vegas, Nevada: CRWMS M&O. MOL.19980602.0479.

CRWMS M&O 1997p. *Unsaturated Zone Radionuclide Transport Abstraction/Testing Workshop Results.* B00000000-01717-2200-00185 REV 00. Las Vegas, Nevada: CRWMS M&O. MOL.19980528.0035.

CRWMS M&O 1997q. *Waste Package Design Basis Events.* BBA000000-01717-0200-00037 REV 00. Las Vegas, Nevada: CRWMS M&O. MOL.19971006.0075.

CRWMS M&O 1997r. *Waste Package Probabilistic Criticality Analysis: Summary Report of Evaluations in 1997.* BBA000000-0717-5705-00015 REV 00. Las Vegas, Nevada: CRWMS M&O. MOL.19980204.0095.

CRWMS M&O 1997s. *Saturated Zone Flow and Transport Abstraction/Testing Workshop Results.* B00000000-01717-2200-00190. Las Vegas, Nevada: CRWMS M&O. MOL.19980528.0038.

CRWMS M&O 1997t. *Unsaturated Zone Flow Abstraction/Testing Workshop Results.* B00000000-01717-2200-00183. Las Vegas, Nevada: CRWMS M&O. MOL.19980528.0039.

CRWMS M&O 1997u. *Evaluation of Codisposal Viability for Aluminum-Clad DOE-Owned Spent Fuel: Phase II Degraded Codisposal Canister Internal Criticality.* BBA000000-01717-5705-00017 REV 00. Las Vegas, Nevada: CRWMS M&O. MOL.19980216.0440.

CRWMS M&O 1997v. *Constraints on Solubility-Limited Neptunium Concentrations for Use in Performance Assessment Analyses.* B00000000-01717-2200-00191 REV 00. Las Vegas, Nevada: CRWMS M&O. MOL.19980213.0484.

CRWMS M&O 1998a. *Design Basis Cladding Analysis.* BBAA000000-01717-0200-00054 REV 01. Las Vegas, Nevada: CRWMS M&O. MOL.19980325.0102.

CRWMS M&O 1998b. *Waste Package Degradation Expert Elicitation Project.* Revision 1. Las Vegas, Nevada: CRWMS M&O. MOL.19980727.0002.

CRWMS M&O 1998c. *Near-Field/Altered-Zone Models Report.* Milestone SP3100M4, UCRL-ID-129179 DR. Las Vegas, Nevada: CRWMS M&O. MOL.19980504.0577.

CRWMS M&O 1998d. *Near-Field/Altered Zone Coupled Effects Expert Elicitation Project.* Las Vegas, Nevada: CRWMS M&O. MOL.19980729.0638.

CRWMS M&O 1998f. *Report on External Criticality of Plutonium Waste Forms in a Geologic Repository.* BBA000000-01717-5705-00018 REV 01. Las Vegas, Nevada: CRWMS M&O. MOL.19980318.0412.

CRWMS M&O 1998g. *Saturated Zone Flow and Transport Expert Elicitation Project.* Deliverable No. SL5X4AM3. Las Vegas, Nevada: CRWMS M&O. MOL.19980825.0008.

CRWMS M&O 1998h. *Probabilistic Seismic Hazard Analyses for Fault Displacement and Vibratory Ground Motion at Yucca Mountain, Nevada.* Volume 1. Las Vegas, Nevada: CRWMS M&O. MOL.19980619.0640.

CRWMS M&O 1998i. *Total System Performance Assessment-Viability Assessment (TSPA-VA) Analyses Technical Basis Document.* Las Vegas, Nevada: CRWMS M&O.

Chapter 1, "Introduction." B00000000-01717-4301-00001 REV 01. MOL.19981008.0001.

Chapter 2, "Unsaturated Zone Hydrology Model." B00000000-01717-4301-00002 REV 01. MOL.19981008.0002.

Chapter 3, "Thermal Hydrology." B00000000-01717-4301-00003 REV 01. MOL.19981008.0003.

Chapter 4, "Near-Field Geochemical Environment." B00000000-01717-4301-00004 REV 01. MOL.19981008.0004.

Chapter 5, "Waste Package Degradation Modeling and Abstraction." B00000000-01717-4301-00005 REV 01. MOL.19981008.0005.

Chapter 6, "Waste Form Degradation, Radionuclide Mobilization, and Transport Through the Engineered Barrier System." B00000000-01717-4301-00006 REV 01. MOL.19981008.0006.

Chapter 7, "Unsaturated Zone Radionuclide Transport." B00000000-01717-4301-00007 REV 01. MOL.19981008.0007.

Chapter 8, "Saturated Zone Flow and Transport." B00000000-01717-4301-00008 REV 01. MOL.19981008.0008.

Chapter 9, "Biosphere." B00000000-01717-4301-00009 REV 01. MOL.19981008.0009.

Chapter 10, "Disruptive Events." B00000000-01717-4301-00010 REV 01. MOL.19981008.0010.

Chapter 11, "Summary and Conclusions." B00000000-01717-4301-00011 REV 01. MOL.19981008.0011.

CRWMS M&O 1998j. *Software Routine Report for WAPDEG.* 30020-2999 REV 01. Las Vegas, Nevada: CRWMS M&O. MOL.19980604.0119.

CRWMS M&O 1998k. *Waste Form Degradation and Radionuclide Mobilization Expert Elicitation Project.* Las Vegas, Nevada: CRWMS M&O. MOL.19980804.0099.

CRWMS M&O 1998l. *Waste Package Materials Selection Analysis.* BBA000000-01717-0200-00020 REV 01. Las Vegas, Nevada: CRWMS M&O. MOL.19980324.0242.

CRWMS M&O 1998m. *Yucca Mountain Site Description.* B00000000-01717-5700-00019, REV 00. Las Vegas, Nevada: CRWMS M&O.

Section 1, "Geography and Demography." MOL.19980729.0047.

Section 2, "Nearby Industrial, Transportation, and Military Facilities." MOL.19980729.0048.

Section 3, "Geology." MOL.19980729.0049.

Section 4, "Climatology and Meteorology." MOL.19980729.0050.

Section 5, "Hydrologic System." MOL.19980729.0051.

Section 6, "Geochemistry." MOL.19980729.0052.

Section 7, "Integrated Natural System Response to Thermal Loading." MOL.19980729.0053.

Curtis, D.B.; Benjamin, T.M.; Gancarz, A.J.; Loss, R.J.; Rosman, K.R.; DeLaeter, J.R.; Delmore, J.E.; and Maeck, W.J. 1989. "Fission Product Retention in the Oklo Natural Fission Reactors." *Journal of*

Applied Geochemistry, 4, 49–62. New York, New York: Pergamon Press. 237970.

Czarnecki, J.B. 1990. *Geohydrology and Evapotranspiration at Franklin Lake Playa, Inyo County, California.* Open-File Report 90-356. Denver, Colorado: USGS. NNA.19901015.0195.

Czarnecki, J.B.; Faunt, C.C.; Gable, C.W.; and Zyvoloski, G.A. 1997. *Hydrogeology and Preliminary Calibration of a Preliminary Three-Dimensional Finite-Element Ground-Water Flow Model of the Site Saturated Zone, Yucca Mountain, Nevada.* Denver, Colorado: USGS. MOL.19980204.0519.

D'Agnese, F.A.; Faunt, C.C.; Turner, A.K.; and Hill, M.C. 1997a. *Hydrogeologic Evaluation and Numerical Simulation of the Death Valley Regional Ground Water Flow System, Nevada and California.* Water-Resources Investigations Report 96-4300. Denver, Colorado: USGS. MOL.19980306.0253.

D'Agnese, F.A.; O'Brien, G.M.; Faunt, C.C.; and San Juan, C.A. 1997b. *Simulated Effects of Climate Change on the Death Valley Regional Ground-Water Flow System, Nevada and California.* Regional Saturated-Zone Syntheses Report. Milestone Report SP23OM3. Denver, Colorado: USGS. MOL.19980130.0211.

De Marsily, G. 1986. *Quantitative Hydrogeology.* Orlando, Florida: Academic Press. 208450.

Dillman, D. 1978. *Mail and Telephone Surveys: The Total Design Method.* New York, New York: Wiley-Interscience. 236961.

DOE (U.S. Department of Energy) 1988. Nuclear Waste Policy Act (Section 113). *Site Characterization Plan, Yucca Mountain Site.* DOE/RW-0199, Volume VII, Part B. Washington, D.C.: OCRWM. HQO.19881201.0002.

DOE 1995. *Principles and Guidelines for Formal Use of Expert Judgment by the Yucca Mountain Site Characterization Project.* Rev. 00. Las Vegas, Nevada: YMSCO. MOL.19960710.0060.

DOE 1998. *Repository Safety Strategy.* YMP/96-01, REV 02. Washington, D.C.: OCRWM MOL.19980727.0001.

Doubt, G. 1984. *Assessing Reliability and Useful Life of Containers for Disposal of Irradiated Fuel Waste.* AECL-8328. Chalk River, Ontario, Canada: Atomic Energy of Canada Ltd., Chalk River Nuclear Laboratories. 227332.

Duguid, J.O.; McNeish, J.A.; Vallikat, V.; Cresap, D.; and Erb, N.J. 1997. *Total System Performance Assessment Sensitivity Studies of U.S. Department of Energy Spent Nuclear Fuel.* A00000000-01717-5705-00017 REV 01. Las Vegas: CRWMS M&O. MOL.19980618.0474.

Ehrhorn, T.F. and Jolley, D.M. 1998. *Software Routine Report: MING, Microbial Impacts to the Near-Field Environment Geochemistry.* 30018-2004 Rev. 0. Las Vegas, Nevada: CRWMS M&O. MOL.19980803.0618.

Einziger, R.E. 1994. "Preliminary Spent LWR Fuel Oxidation Source Term Model." *High Level Radioactive Waste Management International Conference, May 1994,* 554. LaGrange Park, Illinois: American Nuclear Society. 233158.

EPRI (Electric Power Research Institute) 1992. "Source Term in the EPRI Performance Assessment." Presented by R. Shaw to the Nuclear Waste Technical Review Board, Las Vegas, Nevada, October 15, 1992. Palo Alto, California: EPRI. 238962

EPRI 1997. *The Technical Basis for the Classification of Failed Fuel in the Back-End of the Fuel Cycle.* EPRI-TR-108237. Palo Alto, California: EPRI. 236839.

Eslinger, P.W.; Doremus, L.A.; Engel, D.W.; Miley, T.B.; Murphy, M.T.; Nichols, W.E.; White, M.D.; Langford, D.W.; and Ouderkirk, S.J. 1993. *Preliminary Total-System Analysis of a Potential High-Level Nuclear Waste Repository at Yucca Mountain.* PNL-8444. Richland, Washington: Pacific Northwest Laboratory. HQO.19930219.0001.

Farmer, J.C. and McCright, R.D. 1998. *Crevice Corrosion and Pitting of High-Level Waste Containers: Integration of Deterministic and Probabilistic Models.* UCRL-JC-127980. Livermore, California: Lawrence Livermore National Laboratory. MOL.19980812.0118.

Finn, P.A.; Hoh, J.C.; Wolf, S.F.; Slater, S.A.; and Bates, J. K. 1995. "The Release of Uranium, Plutonium, Cesium, Strontium, Technetium, and Iodine from Spent Fuel Under Unsaturated Conditions, Migration '95." *Fifth International Conference on the Chemistry and Migration Behavior of Actinides and Fission Products in the Geosphere, Saint-Malo, France, Sept 10–15, 1995.* 65–71. Amsterdam, Holland: Elsevier Publishing. 238155.

Finn, P.A.; Wronkiewicz, D.J.; Finch, R.J.; Hoh, J.C.; Emery, J.W.; Buck, E.C.; Fortner, J.A.; Wolf, S.F.; Neimark, L.A.; and Bates, J.K. 1997. *Yucca Mountain Project—Argonne National Laboratory, Annual Progress Report, FY 1997 for Activity WP1221 Unsaturated Drip Condition Testing of Spent Fuel and Unsaturated Dissolution Tests of Glass.* ANL-98/12. Argonne, Illinois: Argonne National Laboratory. MOL.19980818.0230.

Finsterle, S., Pruess, K., and Fraser, P. 1996. *ITOUGH2 Software Qualification.* LBNL-39489. UC-800. Berkeley, California: Lawrence Berkeley National Laboratory. MOL.19970619.0040.

Flint, L.E. and Flint, A.L. 1995. *Shallow Infiltration Processes at Yucca Mountain, Nevada -- Neutron Logging Data 1984-93.* Water-Resources Investigations Report 95-4035. Denver, Colorado: USGS. MOL.19960924.0577.

Flint, A.L.; Hevesi, J.A.; and Flint, L.E. 1996. *Conceptual and Numerical Model of Infiltration for the Yucca Mountain Area, Nevada.* Denver, Colorado: USGS. MOL.19970409.0087.

Fontana, M.G. and Greene, N.D. 1978. *Corrosion Engineering.* 2nd edition. New York, New York: McGraw-Hill, Inc. 218346.

Gauthier, J.H.; Wilson, M.L.; Borns, D.J.; Arnold, B.W. 1996. "Impacts Of Seismic Activity on Long-Term Repository Performance At Yucca Mountain." *Methods of Seismic Hazards Evaluation-Focus-95.* 159-168. La Grange Park, Illinois: American Nuclear Society. 231913.

Geldon, A.L. 1996. *Results and Interpretation of Preliminary Aquifer Tests in Boreholes UE-25c #1, UE-25c #2, and UE-25c #3, Yucca Mountain, Nye County, Nevada.* Water-Resources Investigations Report 94-4177. Denver, Colorado: USGS. MOL.19980724.0389.

Geldon, A.L.; Umari, A.M.A.; Fahy, M.F.; Earle, J.D.; Gemmell, J.M.; and Darnell, J. 1997. *Results of Hydraulic and Conservative Tracer Tests in Miocene Tuffaceous Rocks at the C-Hole Complex, 1995 to 1997, Yucca Mountain, Nye County, Nevada.* Milestone Report SP23PM3. Denver, Colorado: USGS. MOL.19980122.0412.

Glasstone, S. and Sesonske, A. 1991. *Reactor Engineering.* Malabar, Florida: Krieger Publishing Company. 239377.

Golder Associates, Inc. 1993. *Application of the RIP (Repository Integration Program) to the Proposed Repository at Yucca Mountain: Conceptual Model and Input Data Set.* Redmond, Washington: Golder Associates. 235334.

Golder Associates, Inc. 1998. *RIP Theory Manual and User's Guide.* Redmond, Washington: Golder Associates Inc. 238560.

Goode, D. J. and Shapiro, A. M. 1991. "Comment on 'Macrodispersion in Sand-Shale Sequences' by A. J. Desbarats." *Water-Resources Research, 27(1),* 135–139. Washington D.C.: The American Geophysical Union. 238386.

Grambow, B. 1987. *Nuclear Waste Glass Dissolution: Mechanism, Model and Application.* JSS-TR-87-02. Stockholm, Sweden: Swedish Nuclear Fuel and Waste Management Co. 239007.

Guenzel, P.J.; Berckmans, T.R.; and Cannell, C.F. 1983. *General Interviewing Techniques: A Self-Instructional Workbook for Telephone and Personal Interviewer Training*. Ann Arbor: University of Michigan, Survey Research Center, Institute for Social Research. 239394.

Helton, J.C. 1993. "Uncertainty and Sensitivity Analysis Techniques for Use in Performance Assessment for Radioactive Waste Disposal." *Reliability Engineering & System Safety, 42 (2-3),* 327–367. Barking, Essex, England (New York, New York): Elsevier Applied Science Publishers. 237878.

Henshall, G.A. 1992. "Modeling Pitting Corrosion Damage of High-Level Radioactive-Waste Containers Using a Stochastic Approach." *Journal of Nuclear Materials, 195 (1-2),* 109–125. Amsterdam, The Netherlands: North Holland Publishing Company. 237758.

Henshall, G.A.; Halsey, W.G.; Clarke, W.L.; and McCright, R.D. 1993. *Modeling Pitting Corrosion Damage of High-Level Radioactive-Waste Containers, With Emphasis on the Stochastic Approach*. UCRL-ID-111624. Livermore, California: Lawrence Livermore National Laboratory. NNA.19921222.0001.

Henshall, G.A. 1997. "Numerical Predictions of Dry Oxidation of Iron and Low-Carbon Steel at Moderately Elevated Temperatures." *Scientific Basis for Nuclear Waste Management XX, Materials Research Society Symposium Proceedings, 465,* 667–673. Pittsburgh, Pennsylvania: Materials Research Society. 238717.

Hillner, E.; Franklin, D.G.; and Smee, J.D. 1998. "The Corrosion of Zircaloy-Clad Fuel Assemblies in a Geologic Repository Environment." WAPD-T-3193. West Mifflin, Pennsylvania: Bettis Atomic Power Laboratory. 237127.

Ho, C.K. and Francis, N.D. 1998. "Coupled Thermo-Hydro-Mechanical Simulations of the Potential Repository at Yucca Mountain." *High-Level Radioactive Waste Management, Proceedings of the Eighth International Conference, Las Vegas, Nevada, May 11-14, 1998.* SAND97-2711C. 113-115. La Grange Park, Illinois: American Nuclear Society. 239064.

Horn, J.M.; Rivera, A.; Lian, T.; Jones, D. 1998. "MIC Evaluation and Testing for the Yucca Mountain Repository." *Proceedings of Corrosion/98, Paper No. 152, National Association of Corrosion Engineers, 22-27 March.* 152/2-152/14. Houston, Texas: National Association Corrosion Engineers. 237146.

International Atomic Energy Agency 1994. *Handbook of Parameter Values for the Prediction of Radionuclide Transfer in Temperate Environments*. Technical Report Series No. 364. Vienna, Austria: International Atomic Energy Agency. 232035.

Jakubick, A.T. and Church, W. 1986. *Oklo Natural Reactors: Geological and Geochemical Conditions-A Review*. INFO-0179. Ottawa, Canada: Atomic Energy Board of Canada. 238711.

Jarzemba, M.S. 1997. "Stochastic Radionuclide Distributions After a Basaltic Eruption for Performance Assessments At Yucca Mountain." *Nuclear Technology, 118,* 132–141. LaGrange Park, Illinois: American Nuclear Society. 237944.

Kastenberg, W.E.; Peterson, P.F.; Ahn, J.; Burch, J.; Casher, G.; Chambre, P.; Greenspan, E.; Olander, D.R.; and Vujic, J.; 1996. *Mechanisms for Autocatalytic Criticality of Fissile Materials in Geologic Repositories*. UCB-NE-4214. Berkeley, California: University of California. 238975.

Kessler, J. and McGuire, R. 1996. *Yucca Mountain Total System Performance Assessment: EPRI "Phase 3" Report*. EPRI TR-107191. Palo Alto, California: Electric Power Research Institute. MOL.19980211.0367.

Kotra, J.P.; Lee, M.P.; Eisenberg, N.A.; and DeWispelare, A.R. 1996. *Branch Technical Position on the Use of Expert Elicitation in the High-Level Radioactive Waste Program*. NUREG-1563. Washington, D.C.: NRC, Division of Waste Management. MOL.19961216.0119.

Kreyns, P.H.; Bourgeous, W.F.; White, C.J.; Charpentier, P.L.; Kammenzind, B.F.; Franklin, D.G. 1997. "Embrittlement of Reactor Core Materials." *Zirconium in the Nuclear Industry: Eleventh Symposium.* ASTM STP 1295, 758–782. Bradley, E.R. and Sabol, G.P. eds. West Conshohacken, Pennsylvania: American Society for Testing and Materials. 237256.

LaPlante, P.A. and Poor, K. 1997. *Information and Analyses to Support Selection of Critical Groups and Reference Biospheres for Yucca Mountain Exposure Scenarios.* CNWRA-97-009. San Antonio, Texas: The Center for Nuclear Waste Regulatory Analyses. 236454.

Lee, J.H.; Atkins, J.E.; and Dunlap, B. 1997. "Incorporation of 'Corrosion-Time' and Effects of Corrosion-Product Spalling in Waste Package Degradation Simulation in the Potential Repository at Yucca Mountain." *Scientific Basis for Nuclear Waste Management XX. Materials Research Society Symposium Proceedings, Boston, Massachusetts, December 2-6, 1996, 465,* 1075–1082. Gray, W. and Triay, I.R., eds. Pittsburgh, Pennsylvania: Materials Research Society. 235596.

Leigh, C.D.; Thompson, B.M.; Campbell, J.E.; Longsine, D.E.; Kennedy, R.A.; and Napier, B.A. 1993. *User's Guide for GENII-S: A Code For Statistical and Deterministic Simulations of Radiation Doses to Humans From Radionuclides in the Environment.* SAND91-0561A. Albuquerque, New Mexico: Sandia National Laboratories. 231133.

Los Alamos National Laboratory 1997. *Summary Report, Geochemistry/Transport Laboratory Tests.* Milestone SP23QM3. Los Alamos, New Mexico: Los Alamos National Laboratory. MOL.19980122.0053.

Luckey, R.R.; Tucci, P.; Faunt, C.C.; Ervin, E.M.; Steinkampf, W.C.; D'Agnese, F.A.; and Patterson, G.L. 1996. *Status of Understanding of the Saturated-Zone Ground-Water Flow System at Yucca Mountain, Nevada as of 1995.* Water-Resources Investigations Report 96-4077. Denver, Colorado: USGS. 227084.

Marsh, G.P.; Bland, I.D.; and Taylor, K.J. 1988. "Statistical Study of Pit Propagation in Carbon Steel Under Nuclear Waste Disposal Conditions." *British Corrosion Journal, 3 (3),* 157–164. London, England: The Metals Society. 236435.

McCartin, T. and Baca, R. 1998. "TPA 3.1.3 Approach and Reference Case," presented March 17-19, 1998, at *DOE/NRC Technical Exchange on Total System Performance Assessment for Yucca Mountain.* Washington, D.C.: Nuclear Regulatory Commission. MOL.19980701.0043.

McCright, R.D. 1998. *Engineered Materials Characteristics Report for the Yucca Mountain Site Characterization Project, Volume 3 Rev 1.1: Corrosion Data and Modeling.* UCRL-ID-119564. Livermore, California: Lawrence Livermore National Laboratory. MOL. 19980806.0177.

Meijer, A. 1992. "A Strategy for the Derivation and Use of Sorption Coefficients in Performance Assessment Calculations for the Yucca Mountain Site." *Proceedings of the DOE/Yucca Mountain Site Characterization Project Radionuclide Adsorption Workshop at Los Alamos National Laboratory, September 11-12, 1990.* Compiled by J. A. Canepa, LA-12325-C. Los Alamos, New Mexico: Los Alamos National Laboratory. 224112.

Merriam-Webster, Inc., 1993. *Merriam-Webster's Collegiate Dictionary (Tenth Edition).* Springfield, Massachusetts: Merriam-Webster Inc. 8883.

Murphy, W.M. 1995. "Natural Analogs for Yucca Mountain." *RADWASTE Magazine, 2(6),* 44-50. La Grange Park, Illinois: American Nuclear Society. 237929.

Murphy, W.M.; Pearcy, E.C.; and Pickett, D.A. 1997. *Natural Analog Studies at Pena Blanca and Santorini.* Seventh EC Natural Analogue Working Group Meeting. Von Maravic, H. and Smellie, J. eds. 105–112. EUR 17851 EN. Luxembourg, Belgium: CEC. 239077.

National Research Council 1995. *Technical Bases for Yucca Mountain Standards.* Washington, DC: National Academy Press. 104273.

National Research Council 1990. *Health Effects of Exposure to Low Levels of Ionizing Radiation, BEIR V.* Committee on the Biological Effects of Ionizing Radiations Board on Radiation Effects Research, Commission on Life Sciences, National Research Council. Washington, D.C.: National Academy Press. 203650.

Naudet, R. 1975. "Mechanisms de Regulation des Reactions Nucleaires." *Le Phenomene d'Oklo*, 589–601. Vienna, Austria: International Atomic Energy Agency. 238831.

NCRP 1987. *Exposure of the Population in the United States and Canada From Natural Background Radiation.* NCRP Report No. 94. Bethesda, Maryland: National Council on Radiation Protection and Measurements. 101308.

NEA (Nuclear Energy Agency) 1991a. *Disposal of Radioactive Wastes: Can Long-Term Safety Be Evaluated? An International Collective Opinion.* Paris, France: Nuclear Energy Agency, Organization for Economic Cooperation and Development. 226870.

NEA 1991b. *Disposal of Radioactive Waste: Review of Safety Assessment Methods.* Report of the Performance Assessment Advisory Group. Paris, France: Nuclear Energy Agency, Organization for Economic Cooperation and Development. 226871.

NEA 1991c. *Systematic Approaches to Scenario Development: A Report of the NEA Working Group on Identification and Selection of Scenarios for Performance Assessment of Nuclear Waste Disposal.* Paris, France: Nuclear Energy Agency, Organization for Economic Cooperation and Development. 8083.

NEA 1995. "The Role of Conceptual Models in Demonstrating Repository Post-Closure Safety." *Proceedings of an NEA Workshop, November 16-18, 1993.* Paris, France: Nuclear Energy Agency, Organization for Economic Cooperation and Development. 238177.

Neuman, S.P. 1990. "Universal Scaling of Hydraulic Conductivities and Dispersivities in Geologic Media." *Water Resource.* 26 (8), 1749–1758. Washington, D.C.: American Geophysical Union. 237977.

Nitao, J.J. 1998. *Reference Manual for the NUFT Flow and Transport Code, Version 2.0.* UCRL-MA-130651. Livermore, California: Lawrence Livermore National Laboratory. 238072.

NRC 1995. *NRC Iterative Performance Assessment Phase 2.* NUREG-1464. Washington, D.C.: NRC. 221527.

NRC 1997a. *Issue Resolution Status Report Key Technical Issue: Repository Design and Thermal-Mechanical Effects.* Rev. 00. Washington, D.C.: NRC. MOL.19980219.0570.

NRC 1997b. *Issue Resolution Status Report Key Technical Issue: Thermal Effects on Flow.* Rev. 00. Washington, D.C.: NRC. MOL.19980219.0091.

NRC 1997c. *Issue Resolution Status Report Key Technical Issue: Evolution of the Near-Field Environment.* Rev. 00. Washington, D.C.: NRC. 237920.

NRC 1997d. *Issue Resolution Status Report Key Technical Issue: Structural Deformation and Seismicity.* Rev. 00. Washington, D.C.: NRC. MOL.19980219.0882.

NRC 1997e. *Issue Resolution Status Report Key Technical Issue: Unsaturated and Saturated Flow Under Isothermal Conditions.* Rev. 00. Washington, D.C.: NRC. MOL.19980219.0572.

NRC 1997f. *Issue Resolution Status Report on Methods to Evaluate Climate Change and Associated Effects at Yucca Mountain Key Technical Issue: Unsaturated and Saturated Flow Under Isothermal Conditions.* Washington, D.C.: NRC. MOL.19980219.0880.

NRC 1998a. *Issue Resolution Status Report Key Technical Issue: Total System Performance Assessment and Integration,* Rev. 00. Washington, D.C.: NRC. MOL. 19980729.0483.

NRC 1998b. *Issue Resolution Status Report Key Technical Issue: Container Life and Source Term.* Rev. 00. Washington, D.C.: NRC. MOL.19980416.0784.

NRC 1998d. *Issue Resolution Status Report Key Technical Issue: Igneous Activity.* Rev. 00. Washington, D.C.: NRC. MOL.19980514.0576.

NWTRB (Nuclear Waste Technical Review Board) 1997. *Report to the U.S. Congress and the Secretary of Energy - 1996 Findings and Recommendations.* Arlington, Virginia: Nuclear Waste Technical Review Board. 232686.

NWTRB 1998. *Report to the U.S. Congress and the Secretary of Energy - 1997 Findings and Recommendations.* Arlington, Virginia: Nuclear Waste Technical Review Board. 236563.

O'Connell, W.J.; Bourcier, W.L.; Gansemer, J.; and Ueng, T.S. 1997. *Performance Assessment Modeling for Savannah River Glass HLW Disposal in a Potential Repository at Yucca Mountain.* UCRL-JC-127352. Livermore, California: Lawrence Livermore National Laboratory. MOL.19980211.0541.

Office of Management and Budget 1983a. "Approaches To Developing Questionnaires." *Statistical Policy Working Paper No. 10* [Online]. Washington, D.C.: Office of Management and Budget, Federal Committee on Statistical Methodology. Available: http://www.bts.gov/smart/cat/wp10.html [December 1, 1998]. 237085.

Office of Management and Budget 1983b. "Contracting For Surveys." *Statistical Policy Working Paper No. 9.* Washington, D.C.: Office of Management and Budget, Regulatory and Statistical Analysis Division, Office of Information and Regulatory Affairs. 237086.

Oversby, V.M. 1996. *Criticality in a High-Level Waste Repository.* SKB Technical Report 96-07. Stockholm, Sweden: Swedish Nuclear Fuel and Waste Management Company. 238574.

Pearcy, E.C.; Prikryl, J.D.; Murphy, W.M.; and Leslie, B.W. 1994. "Alteration of Uraninite From the Nopal I Deposit, Pena Blanca District, Chihuahua, Mexico, Compared to Degradation of Spent Nuclear Fuel in the Proposed U.S. High-Level Nuclear Waste Repository at Yucca Mountain, Nevada." *Applied Geochemistry 9(6),* 713–732. New York, New York: Elsevier Science. 236934.

Pruess, K. 1991. *TOUGH2: A General-Purpose Numerical Simulator for Multiphase Fluid and Heat Flow.* LBL-29400. Berkeley, California: Lawrence Berkeley National Laboratory. NNA.19940202.0088.

RamaRao, B.S.; Mishra, S.; Sevougian, S.D.; and Andrews, R.W. 1998. "Uncertainty Importance of Correlated Variables in the Probabilistic Performance Assessment of a Nuclear Waste Repository." *SAMO 98: Second International Symposium on Sensitivity Analysis of Model Output, Venice, Italy, April 19-22, 1998.* Luxembourg, Belgium: Office for Official Publications of the European Communities. 237987.

Robinson, B.A.; Wolfsberg, A.V.; Zyvoloski, G.A.; and Gable, C.W. 1995. *An Unsaturated Zone Flow and Transport Model of Yucca Mountain.* Milestone 3468. Draft. Los Alamos, New Mexico: Los Alamos National Laboratory. MOL.19960415.0218.

Robinson, B.A.; Wolfsberg, A.V.; Viswanathan, H.S.; Gable, W.; Zyvoloski, G.A.; and Turin, H.J. 1996. *Site-Scale Unsaturated Zone Flow and Transport Model: Modeling of Flow Radionuclide Migration, and Environmental Isotope Distributions at Yucca Mountain.* Milestone 3672. Draft. Los Alamos, New Mexico: Los Alamos National Laboratory. MOL.19971111.0625.

Robinson, B.A.; Wolfsberg, A.V.; Viswanathan, H.S.; Bussod, G.Y.; Gable, C.W.; and Meijer, A. 1997. *The Site-Scale Unsaturated Zone Transport Model of Yucca Mountain.* Milestone SP25BM3. Rev. 1. Los Alamos, New Mexico: Los Alamos National Laboratory. MOL.19980203.0570.

Rothman, A.J. 1984. *Potential Corrosion and Degradation Mechanisms of Zircaloy Cladding on Spent Nuclear Fuel in a Tuff Repository.*

UCID20172. Livermore, California: Lawrence Livermore National Laboratory. NNA.19870903.0039.

Sagar, B., ed. 1997. *NRC High-Level Radioactive Waste Program Annual Progress Report Fiscal Year 1996.* NUREG/CR-6513, No. 1, CNWRA 96-01A. San Antonio, Texas: Center For Nuclear Waste Regulatory Analyses, Southwest Research Institute. MOL.19970813.0082.

Sawyer, D.A.; Fleck, R.J.; Lanphere, M.A.; Warren, R.G.; Broxton, D.E.; and Hudson, M.R. 1994. "Episodic Caldera Volcanism in the Miocene Southwestern Nevada Volcanic Field: Revised Stratigraphic Framework, 40Ar/39Ar Geochronology, and Implications for Magmatism and Extension." *Geological Society of America Bulletin 106,* 1304–1318. Boulder, Colorado: Geological Society of America. 222523.

Sinnock, S.; Lin, Y.T.; and Brannen, J.P. 1984. *Preliminary Bounds on the Expected Postclosure Performance of the Yucca Mountain Repository Site, Southern Nevada.* SAND84-1492. Albuquerque, New Mexico: Sandia National Laboratories. NNA.19870519.0076.

Stout, R.B. and Leider, H.R., eds. 1997. *Waste Form Characteristics Report, Revision 1. UCRL-ID-108314, Version 1.2.* Livermore, California: Lawrence Livermore National Laboratory. MOL.19980512.0133.

Suzuki, T. 1983. "A Theoretical Model for Dispersion of Tephra." *Arc Volcanism: Physics and Tectonics,* 95–113. Shimozuru, D. and Yokoyama, I., eds. Tokyo, Japan: Terra Scientific Publishing Co. 238307.

Thompson, J.L.; Dozier, B.L.; Duncan, D.W.; Efurd, D.W.; Finnegan, D.L.; Kersting, A.B.; Martinez, B.A.; Ortego, P.K.; Rokop, D.J.; Smith, D.K.; and Thompson, B.K. 1998. *Laboratory and Field Studies Related to Radionuclide Migration at the Nevada Test Site, October 1, 1996 - September 30, 1997.* LA-13419-PR. Los Alamos, New Mexico: Los Alamos National Laboratory. MOL.19980625.0450.

Triay, I.; Degueldre, C.; Wistrom, A.; Cotter, C.; and Lemons, W. 1996. *Progress Report on Colloid-Facilitated Transport at Yucca Mountain.* Milestone 3383. LA-12959-MS, UIC-814. Los Alamos, New Mexico: Los Alamos National Laboratory. MOL.19970616.0061.

Triay, I.R.; Meijer, A.; Conca, J.L.; Kung, K.S.; Rundberg, R.S.; Strietelmeier, B.A.; Tait, C.D. 1997. *Summary and Synthesis Report on Radionuclide Retardation for the Yucca Mountain Site Characterization Project.* MS-3784M. LA-13262-MS. Los Alamos, New Mexico: Los Alamos National Laboratory. MOL.19971210.0177.

U.S. Department of Agriculture 1993. *Food and Nutrient Intakes by Individuals in the United States for 1 Day, 1987-88.* NFCS-87-I-1. Washington, D.C.: United States Department of Agriculture Human Nutrition Information Service. 236493.

Van Konynenburg, R.A.; McCright, R.D.; Roy, A.K.; and Jones, D.A. 1995. *Engineered Materials Characterization Report for the Yucca Mountain Site Characterization Project.* UCRL-ID-119564. Livermore, California: Lawrence Livermore National Laboratory. MOL.19960402.0547.

Van Konynenburg, R.A. 1996. "Comments on the Draft Paper, 'Underground Supercriticality From Plutonium and Other Fissile Materials,' written by C.D. Bowman and F. Venneri (LANL)." *Science and Global Security, 5(3),* 303–322. Amsterdam, Netherlands: Gordon and Breach Science. 238266.

VanSwam, L.F.P. and Shann, S.H. 1991. "The Corrosion of Zircaloy-4 Fuel Cladding in Pressurized Water Reactors." *Zirconium in the Nuclear Industry: Ninth International Symposium.,* 758–781. Euchen, C.M. and Garde, A.M., eds. Philadelphia, Pennsylvania: American Society for Testing and Materials. 237177.

Westrich, H.R. 1982. "The Solubility of LWR Core Debris in Sacrificial Floor Material." *Journal of Nuclear Materials, 110,* 324–332. Amsterdam, Holland: North-Holland Publishing Company. 234101.

Whipple, C.; Budnitz, B.; Ewing, R.; Moeller, D.; Payer, J.; and Witherspoon, P. 1997a. *First Interim Report Total System Performance Assessment Peer Review Panel.* Las Vegas, Nevada: CRWMS M&O. MOL.19971024.0188.

Whipple, C.; Budnitz, B.; Ewing, R.; Moeller, D.; Payer, J.; and Witherspoon, P. 1997b. *Second Interim Report Total System Performance Assessment Peer Review Panel.* Las Vegas, Nevada: CRWMS M&O. MOL.19980331.0294.

Whipple, C.; Budnitz, B.; Ewing, R.; Moeller, D.; Payer, J.; and Witherspoon, P. 1998. *Third Interim Report Peer Review of the Total System Performance Assessment-Viability Assessment.* Las Vegas, Nevada: CRWMS M&O. MOL.19980716.0493.

Wilson, M.L.; Gauthier, J.H.; Barnard, R.W.; Barr, G.E.; Dockery, H.A.; Dunn, E.; Eaton, R.R.; Guerin, D.C.; Lu, N.; Martinez, M.J.; Nilson, R.; Rautman, C.A.; Robey, T.H.; Ross, B.; Ryder, E.E.; Schenker, A.R.; Shannon, S.A.; Skinner, L.H.; Halsey, W.G.; Gansemer, J.D.; Lewis, L.C.; Lamont, A.D.; Triay, I.R.; Meijer, A.; and Morris, D.E. 1994. *Total System Performance Assessment for Yucca Mountain-SNL Second Iteration (TSPA-1993).* SAND93-2675. Albuquerque, New Mexico: Sandia National Laboratories. NNA.19940112.0123.

Wolery, T.J. 1992a. *EQ3/6, A Software Package for Geochemical Modeling of Aqueous Systems: Package Overview and Installation Guide.* UCRL-MA-110662, Part 1. Livermore, California: Lawrence Livermore National Laboratory. NNA.19921023.0028.

Wolery, T.J. 1992b. *EQ3NR, A Computer Program for Geochemical Aqueous Speciation-Solubility Calculations: Theoretical Manual, User's Guide, and Related Documentation, Version 7.0.* UCRL-MA-110662, Part III, Draft 1.1. Livermore, California: Lawrence Livermore National Laboratory. NNA.19921218.0010.

Wolery, T.J. and Daveler, S.A. 1992. *EQ6, A Computer Program for Reaction Path Modeling of Aqueous Geochemical Systems; Theoretical Manual, User's Guide, and Related Documentation, Version 7.0.* UCRL-MA-110662, Part IV, Draft 1.1. Livermore, California: Lawrence Livermore National Laboratory. MOL.19980218.0570.

Wronkiewicz, D.J.; Bates, J.K.; Gerding, T.J.; Veleckis, E.; and Tani, B.S. 1992. "Uranium Release and Secondary Phase Formation During Unsaturated Testing of UO_2 at 90°C." *Journal of Nuclear Materials, 190,* 107–127. Amsterdam: North Holland Publishing Company. 236558.

Yau, T.L. and Webster, R.T. 1987. "Corrosion of Zirconium and Hafnium." *Metals Handbook.* 9th ed. Volume 13, Corrosion, 707–721. Metals Park, Ohio: American Society for Metals International. 209807.

Zyvoloski, A.G.; Robinson, B.A.; Dash, Z.A.; and Trease, L.L. 1995. *Models and Methods Summary for the FEHM Application.* LA-UR-94-3787,Rev. 01. Los Alamos, New Mexico: Los Alamos National Laboratory. 222337.

7.2 STANDARDS AND REGULATIONS

Unless otherwise dated, the *Codes of Federal Regulations* cited in this document were revised as of January 1, 1998.

10 CFR (*Code of Federal Regulations*) 60. Energy: Disposal of High-Level Radioactive Wastes in Geologic Repositories; Technical Criteria; Final Rule. 238445.

40 CFR 191. Protection of Environment: Environmental Standards for the Management and Disposal of Spent Nuclear Fuel, High-Level and Transuranic Radioactive Wastes; Final Rule. 1985. 221863.

48 FR 28194 (1983). 10 CFR Part 60, Disposal of High-Level Radioactive Wastes in Geologic Repositories Technical Criteria; Final Rule. 238518.

ASTM (American Society for Testing and Materials) 1990. *Specification for Pressure Vessel Plates, Carbon Steel, for Moderate- and Lower-Temperature Service*. A516/A516M-90. Philadelphia, Pennsylvania: American Society for Testing and Materials. 237681.

ASTM 1994. *Specification for Low-Carbon Nickel-Molybdenum-Chromium and Low-Carbon Nickel-Chromium-Molybdenum Steel Alloy Plate, Sheet, and Strip*. B575-94. Philadelphia, Pennsylvania: American Society for Testing and Materials. 237683.

Energy and Water Development Appropriations Act, 1997. Public Law 104-206, 110 Stat. 2984. 104th Congress. 238115.

International Commission of Radiological Protection 1978. *Limits for Intakes of Radionuclides by Workers*. The Commission for Radiological Protection No 30. Oxford, New York: Pergamon Press. 221575.

Paperwork Reduction Act of 1995, as amended. 44 USC 3506 (1996). 237087.

APPENDIX A

GLOSSARY

APPENDIX A

GLOSSARY

The glossary is divided into two sections. Section A.1 is a general glossary of terms used in the TSPA-VA; Section A.2 contains a listing of statistical terms that are used in or are relevant to other statistical terms used in the TSPA-VA. Definitions are written with emphasis on the relationship of the term to the TSPA-VA process and are taken from previous performance-assessment documentation, where possible, or from standard reference materials.

Many of the definitions in this Glossary are Yucca Mountain Site Characterization Project specific.

A.1 GENERAL GLOSSARY

This section is a general listing of terms used in the TSPA-VA. Statistical terms are in Section A.2.

Abiotic	Characterized by the absence of living organisms.
Absorbed Dose	The energy absorbed from ionizing radiation per unit mass of irradiated material. Units of absorbed dose are the rad and the gray (Gy).
Abstracted Model	Model that reproduces, or bounds, the essential elements of a more detailed process model and captures uncertainty and variability in what is often, but not always, a simplified or idealized form. See Abstraction.
Abstraction	Distillation of the essential components of a process model into a suitable form for use in a total system performance assessment. The distillation must retain the basic intrinsic form of the process model but does not usually require its original complexity. Model abstraction is usually necessary to maximize the use of limited computational resources while allowing a sufficient range of sensitivity and uncertainty analyses.
Actinides	A series of chemically similar, mostly synthetic, radioactive elements with atomic numbers from 89 (actinium) through 103 (lawrencium).
Activity	Cumulative curie count. See Radioactivity.
Adsorb	To collect a gas, liquid, or dissolved substance on a surface as a condensed layer.
Adsorbate	A substance that is adsorbed. See Adsorb.
Adsorbent	A substance upon which another substance is adsorbed. See Adsorb.
Adsorption	Transfer of solute mass, such as radionuclides, in groundwater to the solid geologic surfaces with which it comes in contact. The term sorption is sometimes used interchangeably with this term.

Adsorption Isotherm	Relationship of the quantity of an adsorbed component to its quantity in the fluid phase (expressed in concentration) at constant temperature (i.e., under isothermal conditions).
Adsorption Coefficient	See Sorption Coefficient.
Advection	The process in which solutes are transported by the motion of flowing groundwater. Advection in combination with dispersion (hydrodynamic dispersion) controls flux into and out of the elemental volumes of the flow domain in groundwater transport models. The term convection is sometimes used for advection but is not used interchangeably in the TSPA-VA.
Advisory Committee On Nuclear Waste	A committee established under the Nuclear Regulatory Commission to provide independent reviews of, and advice on, nuclear waste facilities, including application to such facilities of 10 CFR Parts 60 and 61 (disposal of high-level radioactive wastes in geologic repositories and land disposal of radioactive waste) and other applicable regulations and legislative mandates.
Aerobic	Living or active only in the presence of oxygen, as used in reference to bacteria that require oxygen; a condition in which oxygen is present.
Air Mass Fraction	Mass of air divided by the total mass of gas (typically air plus water vapor) in the gas phase. This expression gives a measure of the "dryness" of the gas phase, which is important in waste package corrosion models.
Algorithm	(1) The set of well-defined rules that governs the solution of a problem in a finite number of steps. (2) A mathematical formulation of a model of a physical process.
Alkaline	See pH.
Alloy 22	See Inner Barrier.
Alluvium	Sedimentary material (clay, mud, sand, silt, gravel) deposited by flowing water or by wind.
Alternative	Plausible interpretations or designs based on assumptions other than those used in the base case that could also fit or be applicable based on the available scientific information. When propagated through a quantitative tool such as performance assessment, alternative interpretations can illustrate the significance of the uncertainty in the base case interpretation chosen to represent the repository's probable behavior.
Ambient	(1) Undisturbed, natural conditions such as ambient temperature caused by climate or natural subsurface thermal gradients. (2) Surrounding conditions.

Anaerobic	(1) Living or active only in the absence of oxygen; used in reference to bacteria that do not require oxygen. (2) A condition in which oxygen is absent.
Anionic	An atom or group of atoms having a negative charge.
Anisotropy	The condition in which physical properties vary when measured in different directions or along different axes. For example, in a layered rock section the permeability is often anisotropic in the vertical direction from layer to layer but is isotropic in the horizontal direction within a layer.
Annual Dose	For human exposure scenarios, a measure of an individual's exposure to radiation in a year.
Annual Committed Effective Dose Equivalent	Composed of terms in 40 CFR 191, Subpart B, in which an annual committed effective dose means the committed effective dose caused by 1-year intake from released radionuclides plus the annual effective dose caused by direct radiation from facilities or activities. See Effective Dose Equivalent and Committed Dose Equivalent.
Annual Frequency	Number of occurrences on an annual basis.
Anthropogenic	Alterations of the environment resulting from the presence or activities of humans.
Aqueous	Pertaining to water, such as aqueous phase, aqueous species, or aqueous transport.
Aquifer	A subsurface, saturated rock unit (formation, group of formations, or part of a formation) of sufficient permeability to transmit groundwater and yield usable quantities of water to wells and springs.
Areal Mass Loading	Used in thermal loading calculations, the amount of heavy metal (usually expressed in metric tons of uranium or equivalent) emplaced per unit area in the proposed repository. This number is 85 metric tons of uranium (MTU) per acre and remains a constant value over time for calculations in which the amount of waste per acre in the repository is assumed to remain constant.
AREST-CT Computer Program	A general modeling code that considers both equilibrium and kinetically controlled chemical reactions between solid phases, aqueous solutions, and gas under flowing conditions.
Average Individual	An individual representative of the life style in the Amargosa Valley with regard to eating, drinking, and other activities that may be relevant in a human exposure scenario as determined by a survey of Amargosa Valley residents by TSPA-VA researchers.

Backfill	The general fill that is placed in the excavated areas of the underground facility. If used, the backfill for the repository may be tuff or other material.
Background Radiation	Radiation arising from natural radioactive material always present in the environment, including solar and cosmic radiation, radon gas, soil and rocks, and the human body.
Basalt	A dark, fine-grained igneous rock originating from a lava flow or minor intrusion, composed mainly of plagioclase clinopyroxene and sometimes olivine, and often displaying a columnar structure.
Base Case	The sequence of anticipated conditions expected to occur in and around the proposed repository, without the inclusion of unlikely or unanticipated features, events, or processes. The components that contribute to the base case model are intended to encompass this probable behavior of the repository, based on the range of uncertainty for the various parameters and conceptual models used in constructing the base case.
Base Case Model	A computer model that represents an assessment of the most likely range of behavior for the overall repository system and is a combination of the most likely ranges of behavior for the various component models, processes, and associated parameters.
Biosphere	The ecosystem of the earth and the living organisms inhabiting it.
Biosphere Dose Conversion Factor	A multiplier used in converting a radionuclide concentration at the geosphere/biosphere interface into a dose that a human would experience for all pathways considered, with units expressed in terms of annual dose (i.e., the effective dose equivalent) per unit concentration. Depends on the radionuclide(s), pathway(s), climate, and other factors. A key assumption is that the dose is a linear function of concentration at the geosphere/biosphere interface.
Boiling Regime	One of two divisions (the other being the cooling regime) used to delineate the reactions between the gas, water, and minerals in the rock that occur as the system heats and boiling of the pore water occurs through time.
Borehole	A hole drilled from the surface for purposes of collecting information about an area's geology or hydrology. Sometimes referred to as a drillhole or well bore.
Borosilicate Glass	High-level radioactive waste matrix material in which boron takes the place of the lime used in ordinary glass mixtures.

Boundary Condition	For a model, the establishment of a set condition (set value), often at the geometric edge of the model, for a given variable. An example is using a specified groundwater flux from infiltration as a boundary condition for a flow model.
Breach	An opening in the waste package caused by gradual degradation of the outer and inner barriers that allows the waste to be exposed, and possibly released, to the external environment.
Breakthrough	The time at which the concentration of a substance, usually in groundwater, arrives at a particular point of interest after having been tracked as it moves through space.
Breakthrough Curve	A means of describing transport of radionuclides along a geosphere pathway by constructing a curve that is a cumulative probability distribution. The breakthrough curve calculation includes the effects of all flow modes, flow in rock matrix, flow in fractures, and retardation and determines the expected proportion of the radionuclide mass that has traveled the pathway at any specified time.
Buoyant Convection	Fluid movement, typically in the gas phase, in response to a density gradient in a gravitational field. An example is the rising of air when it becomes less dense because of heating followed by its subsequent fall when it cools and becomes denser.
Burnup	A measure of nuclear-reactor fuel consumption expressed either as the percentage of fuel atoms that have undergone fission or as the amount of energy produced per unit weight of fuel.
Calcite	A crystalline mineral composed of calcium carbonate ($CaCO_3$).
Calibration	The process of comparing the conditions, processes, and parameter values used in a model against actual data points or interpolations (e.g., contour maps) from measurements at or close to the site to ensure that the model is compatible with "reality" to the extent feasible. (2) For tools used for field or lab measurements, the process of taking instrument readings on standards known to produce a certain response to check the accuracy and precision of the instrument.
Canister	The structure surrounding the waste (e.g., high-level radioactive waste immobilized in glass rods) that facilitates handling, storage, transportation, and/or disposal. A metal receptacle with the following purpose: (1) a pour mold for solidified high-level radioactive waste and (2) for spent nuclear fuel, structural support for loose rods, non-fuel components, or containment of radionuclides during postclosure operations.

Capillarity	(1) A phenomenon that results from the force of mutual attraction (cohesion) between water molecules in conjunction with the force of molecular attraction (adhesion) between water and different solid materials. (2) A means by which water will rise in small diameter tubes and, in combination with the effects of gravity, a means of water movement in the unsaturated zone.
Capillary Barrier	A contact in the unsaturated zone between a geologic unit containing relatively small-diameter openings and a unit containing relatively large-diameter openings across which water does not flow.
Capillary Force	In the unsaturated zone, the forces acting on moisture that can be attributed to the attraction between rock grain, or matrix, surfaces and water.
Capillary Pressure	The difference in a fluid pressure at a given point between a nonwetting phase such as air and a wetting phase such as water.
Capillary Suction	A condition in unsaturated rocks in which the attraction of fluids to particle surfaces is stronger than the force of gravity on the fluid.
Carbon Steel	A steel that is tough but malleable and contains a small percentage of carbon. The outer barrier of waste packages is composed of carbon steel.
Carbonate	Any compound formed by the reaction of carbonic acid with either a metal or an organic compound. Any compound containing the carbonate ion.
Carbonation	A chemical process involving the change of concrete and cement into a carbonate.
Carboniferous	Producing, containing, or pertaining to carbon or coal.
Cationic	An atom or group of atoms having a positive charge.
Center For Nuclear Waste Regulatory Analyses	A federally funded research and development center in San Antonio, Texas, sponsored by the Nuclear Regulatory Commission to provide the Nuclear Regulatory Commission with technical assistance for the repository program.
Ceramic Coating	A layer of ceramic material such as alumina that has been applied to a metallic product to protect against extremely high temperatures and corrosion.
Cladding	The metallic outer sheath of a fuel element generally made of stainless steel or a zirconium alloy. It is intended to isolate the fuel element from the external environment.

Clay	A rock or mineral fragment of any composition that is smaller than very fine silt grains, having a diameter less than 0.00016 in. (1/256 mm). A clay mineral is one of a complex and loosely defined group of finely crystalline hydrous silicates formed mainly by weathering or alteration of primary silicate minerals. They are characterized by small particle size and their ability to adsorb large amounts of water or ions on the surface of the particles.
Climate	Weather conditions, including temperature, wind velocity, precipitation, and other factors, that prevail in a region.
Climate Proxies	The physical remains of substances that carry the imprint of past climates.
Climate States	Representations of climate conditions. Three different climate states are used to represent changes in climate over the time periods of interest: present-day dry climate, long-term-average climate (about twice the precipitation of dry climate), and superpluvial climate (about three times the precipitation of dry climate).
Code (Computer)	The set of commands used to solve a mathematical model on a computer.
Codisposal	A packaging method for disposal of radioactive waste in which two types of waste, such as commercial spent nuclear fuel and defense high-level radioactive waste, are combined in disposal containers. Codisposal takes advantage of otherwise unused space in disposal containers and is more cost-effective than other methods to limit the reactivity of individual waste packages.
Coefficient of Multiple Determination	See Section A.2 of this glossary.
Colloid	As applied to radionuclide migration, a colloidal system is a group of large molecules or small particles that have at least one dimension with the size range of 10^{-9} to 10^{-6}m that are suspended in a solvent. Naturally occurring colloids in groundwater arise from clay minerals such as smectites and illites. Colloids that are transported in groundwater can be filtered out of the water in small pore spaces or very narrow fractures because of the large size of the colloids.
Colloid-Facilitated, Radionuclide Transport Model	A model that represents the enhanced transport of radionuclides by particles that are colloids.
Commercial Spent Nuclear Fuel	Commercial nuclear fuel rods that have been removed from reactor use.

Committed Dose Equivalent	The dose equivalent that is committed to specific organs or tissues that will be received from an intake of radioactive material by an individual during the 50 years following the intake.
Committed Effective Dose Equivalent	The sum of the products of the weighting factors applicable to each of the body organs or tissues that are irradiated and the committed dose equivalent to these organs or tissues.
Complementary Cumulative Distribution Function	See Section A.2 of this glossary.
Component Models	The 16 process models that are run separately and then combined for running in the TSPA-VA RIP computer model.
Concentration Gradient	For a substance dissolved in a solute, the change in concentration of the substance over a distance.
Conceptual Model	A set of qualitative assumptions used to describe a system or subsystem for a given purpose. Assumptions for the model should be compatible with one another and fit the existing data within the context of the given purpose of the model.
Concrete Lining	Part of the reference design in which the large majority of emplacement drifts are lined with precast concrete segments.
Conduction	Transport of heat in static groundwater, controlled by the thermal conductivity of the geologic formation and the contained groundwater and described by a linear law relating heat flux to temperature gradient.
Confidence	See Section A.2 of this glossary.
Confidence Interval	See Section A.2 of this glossary.
Consequence	A measurable outcome of an event or process that, when combined with the probability of occurrence, gives risk.
Conservative Assumption	(1) An assumption that has the effect of maximizing the calculated amount of radionuclides released from the hypothetical repository to the accessible environment. (2) An assumption that uses uncertain inputs and does not attempt to include any potentially beneficial effects.
Conservative Tracer	Substances with no retardation effect. See Tracer.
Continuous Random Variable	See Section A.2 of this glossary.
Continuum Model	A model that represents fluid flow through numerous individual fractures and matrix blocks by approximating them as continuous flow fields.

Convection	(1) Thermally driven groundwater flow or a heat-transfer mechanism for a gas phase. The bulk motion of a flowing fluid (gas or liquid) in the presence of a gravitational field, caused by temperature differences that, in turn, cause different areas of the fluid to have different densities (e.g., warmer is less dense). (2) One of the processes that moves solutes in groundwater. See Transport.
Convolution Integral Method	(1) A computational method used to calculate the radionuclide concentration in the saturated zone as it changes with time. (2) The abstraction method for the saturated zone flow and transport component model of the TSPA-VA RIP computer model.
Cooling Regime	One of two divisions (the other being the boiling regime) used to delineate the reactions between the gas, water, and minerals in the rock, which occur as the system cools after heating and boiling of the pore water occurs through time.
Correlation Coefficient	See Section A.2 of this glossary.
Corrosion	The process of dissolving or wearing away gradually, especially by chemical action.
Corrosion Allowance Material	A material that undergoes relatively uniform corrosion penetration at relatively low and predictable rates in moderately acidic, moderately alkaline, and neutral conditions (see pH). Corrosion allowance material is used as the outer barrier of the two-layer, metallic waste-disposal container and is made of carbon steel.
Corrosion Model (for inner barrier and outer barrier)	A model that includes the time histories of first and subsequent pit and patch penetrations for the waste package layers.
Corrosion Resistant Material	A material that develops a protective film on its surface, creating a high resistance to corrosion. This material, usually the nickel-base alloy, Alloy 22 (ASTM B 575 N06022), is used as the inner barrier of the two-layer waste-disposal container.
Coupling	The ability in a performance assessment to assemble separate analyses so that information can be passed among them to develop an overall analysis of system performance.
Covariance	See Section A.2 of this glossary.
Crevice Corrosion	A type of localized corrosion that forms in splits or cracks.
Critical Event	See Criticality.

Critical Group	With regard to annual dose, the maximally exposed individuals. A group of members of the public whose exposure is reasonably homogeneous and includes individuals receiving the highest dose. The individuals making up the critical group may change with changes in source term and pathway.
Criticality	(1) A condition that would require the original waste form, which is part of the waste package, to be exposed to degradation followed by conditions that would allow concentration of sufficient nuclear fuel, the presence of neutron moderators, the absence of neutron absorbers, and favorable geometry. (2) The condition in which nuclear fuel sustains a chain reaction. It occurs when the number of neutrons present in one generation cycle equals the number generated in the previous cycle. The state is considered critical when a self-sustaining nuclear chain reaction is ongoing.
Critical Population	See Critical Group.
Cumulative Distribution Function	See Section A.2 of this glossary.
Cumulative Probability	See Section A.2 of this glossary.
Cumulative Release	The sum of the radionuclide curies released over a certain period at a specific location.
Curie	A unit of radioactivity equal to 37 billion disintegrations per second.
Darcy's Law	Used in hydrology to describe fluid flow in a porous medium. Darcy's Law states that the fluid velocity is directly proportional to the hydraulic gradient between the two locations.
Data	Facts or figures measured or derived from site characteristics or standard references from which conclusions may be drawn Parameters that have been derived from raw data are sometimes, themselves, considered to be data.
Decay	See Radioactive Decay.
Deep Percolation	Precipitation moving downward, below the plant-root zone, toward storage in subsurface strata.
Defense in Depth	The term used to describe the property of a system of multiple barriers to mitigate uncertainties in conditions, processes, and events by employing barriers that are redundant and independent, such that failure in any one barrier does not result in failure of the entire system.
Defense Spent Nuclear Fuel	See DOE Spent Nuclear Fuel.

Department of Energy, U.S. (DOE)	A Cabinet-level agency of the United States federal government charged with the responsibilities of energy security, national security, and environmental quality.
Design Concept	As mentioned in the Energy and Water Appropriations Act, consists of the subsurface repository layout, the engineered barrier segments, and the waste package.
Desorption	A physical or chemical process by which a substance that has been adsorbed or absorbed by a liquid or solid material is removed from the material.
Deterministic	A single calculation using only a single value for each of the model parameters. A deterministic system is governed by definite rules of evolution leading to cause and effect relationships and predictability. Deterministic calculations do not account for uncertainty in the physical relationships or parameter values.
Diffusion	(1) The spreading or dissemination of a substance. (2) The gradual mixing of the molecules of two or more substances due to random thermal motion.
Diffusive Transport	Movement of solutes due to their concentration gradient. The process in which substances carried in groundwater move through the subsurface by means of diffusion because of a concentration gradient.
Diffusivity	A measure of the rate of heat diffusion. It varies with the nature of the involved atoms, the structure, and changes in temperature.
Dike	A tabular body of igneous rock that cuts across the structure of adjacent rocks or cuts massive rocks. Most dikes are caused by the intrusion of magma. Some dikes occur as columnar structures.
Dimensionality	Modeling in one, two, or three dimensions.
Dimensionality Abstraction	An abstraction in which there is a change in the dimensions of a problem, such as from three dimensional to two dimensional, for modeling purposes. This is done either to simplify the problem or reduce the computational requirements of the problem to implement modeling results in a more efficient or usable form.
Discrete Heat Source	An attribute of drift-scale thermal hydrology models in which the model includes a representation of heat output for discrete waste packages with varying heat outputs depending on the type and amount of waste in the package.

Dispersion (Hydrodynamic Dispersion)	(1) The tendency of a solute (substance dissolved in groundwater) to spread out from the path it is expected to follow if only the bulk motion of the flowing fluid (defection) moved it. The tortuous path the solute follows through openings (pores and fractures) causes part of the dispersion effect in the rock. (2) The macroscopic outcome of the actual movement of individual solute particles through a porous medium. Dispersion causes dilution of solutes, including radionuclides, in groundwater and is usually an important mechanism for spreading contaminants in low flow velocity situations.
Disposal Container	The container barriers or shells, spacing structures or baskets, shielding integral to the container, packing contained within the container, and other absorbent materials designed to be placed internal to the container or immediately surrounding the disposal container (i.e., attached to the outer surface of the container). The disposal container is designed to contain spent nuclear fuel and high-level radioactive waste, but exists only until the outer lid weld is complete and accepted. The disposal container does not include the waste form or the encasing containers or canisters (e.g., high-level radioactive waste pour canisters, DOE spent nuclear fuel co-disposal canisters, multi-purpose canisters of spent nuclear fuel, etc.).
Dissolution	Change from a solid to a liquid state. Dissolving a substance in a solvent.
Distribution	See Section A.2 of this glossary.
Distribution Frequency	See Section A.2 of this glossary.
Disturbed Performance	Performance that is expected for the system if perturbed by disruptive events such as human intrusion, natural phenomena such as volcanism, or nuclear criticality. This is as used in a description of scenario.
Disruptive Event	An unexpected event that, in the case of the repository, includes human intrusion, volcanic activity, seismic activity, and nuclear criticality. Disruptive events have two possible effects: (1) direct release of radioactivity to the surface or (2) alteration of the nominal behavior or the system.
Domain (Model)	(1) The set of elements that a mathematical model describes. (2) Individual process areas, such as the unsaturated zone flow domain.
DOE Spent Nuclear Fuel	Radioactive waste created by defense activities that consists of over 250 different types of spent nuclear fuel and is expected to contribute 2,333 metric tons of heavy metal (MTHM) to the total repository. The major contributor to this waste form is the N-reactor fuel currently stored at the Hanford Site. This waste form also includes 65 MTHM of U.S. Navy spent nuclear fuel.

Dose	The amount of radioactive energy that passes the exchange boundaries of an organism (e.g., skin and mucous membranes) and is taken into living tissues. Dose arises from a combination of the energy imparted by the radiation and the absorption efficiency of the affected organism or tissues. It is expressed in terms of units of the radiation taken in, the body weight or mass impacted, and the time over which the dose occurs or the impact is measured.
Dose Conversion Factor	(1) Any factor used to change an environmental measurement to dose in the appropriate units. (2) The multipliers that convert an amount of radionuclides ingested or inhaled to an estimate of dose.
Dose Equivalent	The product of the absorbed dose in tissue, quality factor, and all other necessary modifying factors at the location of interest. See also Effective Dose Equivalent and Total Effective Dose Equivalent.
Dose Rate	An organism's exposure to radiation over time.
Downgradient	An area toward which water will tend to flow as the result of several factors. The most important factor is the elevation of water levels in wells in that area relative to other areas. The downgradient is the direction in which contaminants released from the potential repository at Yucca Mountain and migrating in the saturated zone might be expected to move. Based on current understanding of the hydraulic gradient below Yucca Mountain, downgradient is toward the south to southeast of the potential repository location in the area within about 5 km.
Drift	From mining terminology, a horizontal underground passage. The nearly horizontal underground passageways from the shaft(s) to the alcoves and rooms. Includes excavations for emplacement (emplacement drifts) and access (access mains).
Drift Scale	The scale of an emplacement drift, or approximately 5 m in diameter.
Drip Shield	A sheet of impermeable material placed above the waste package to prevent seepage water from directly contacting the waste packages.
Dripping Conditions	Assumed for a certain fraction of the waste packages based on water seepage into a drift. The following set of assumptions apply: (1) a small number of the waste packages will be emplaced in drifts with fractures that periodically drip water, and water may drip on a certain fraction of these packages after emplacement; (2) if water drips onto a waste package, it is 100 percent wet from the dripping; and (3) the dripping rate, frequency of drip periods, and water chemistry (especially pH and chloride concentration) will contribute significantly to waste package degradation.

Dry Climate	One of three sets of conditions used to represent climate changes through time. Representative of current climate conditions at Yucca Mountain. See also Long-Term-Average Climate and Superpluvial Climate.
Dual Permeability Conceptual Model	A conceptual model of groundwater flow in which fractures and rock matrix are represented as separate, interacting continua, with no assumption of pressure equilibrium between fractures and rock matrix. This concept allows modeling groundwater flow as occurring mostly in the fractures, with less flow in the rock matrix depending on the degree of connection between the rock matrix and fractures and the capillary pressure gradient. The dual permeability model is one of the conceptual models for groundwater and heat flow for fractured, porous media.
Dual Permeability/Weeps Model	A dual-permeability approximation of the Weeps Model. Also see Dual Permeability Conceptual Model and Weeps Model.
Edge Effects	Conditions at the edges of the repository that are cooler and wetter because heat dissipates more quickly than at the center of the repository.
Effective Dose Equivalent	The sum of the products of the dose equivalent to the organ or tissue and the weighting factors applicable to each of the body organs or tissues that are irradiated.
Effective Porosity	The fraction of a given medium's porosity available for fluid flow and/or solute storage, as in the saturated zone.
Electric Power Research Institute	A nonprofit organization that serves as a research and development consortium serving the entire power industry, from power generation to delivery, to end use products and services. This group has performed an independent performance assessment on the Yucca Mountain site.
Elicitation	See Expert Elicitation.
El Niño	A complex set of changes in the water temperature in the Eastern Pacific equatorial region, producing a warm current. This occurs annually to some degree between October and February, but in some years intensifies and causes unusual storms and destruction of marine life.
Empirical Model	A model whose reliability is based on observation and/or experimental evidence and is not necessarily supported by any established theory or law. Validity or applicability of such an empirical model is normally limited to situations that lie within the range of the data that were used to develop the model.
Emplacement Drift	See Drift.

Energy Policy Act of 1992, Public Law 102-486	Comprehensive energy legislation enacted in 1992. Section 801 of the Act directs the U.S. Environmental Protection Agency (EPA) to contract with the National Academy of Sciences to provide "findings and recommendations on reasonable standards...that would govern the long-term performance of a repository at the Yucca Mountain site." The EPA Administrator is to promulgate public health and safety standards after the receipt of the findings and recommendations of the National Academy of Sciences, and these shall be the only standards applicable to the Yucca Mountain site.
Energy and Water Development Appropriations Act of 1997, Public Law 104-206	Legislation that provided that "no later than September 30, 1998, the Secretary shall provide to the President and to the Congress a Viability Assessment of the Yucca Mountain site. The VA shall include: • the preliminary design concept for the critical elements for the repository and waste package • a total system performance assessment (TSPA), based upon the design concept and the scientific data and analysis available by September 30, 1998, describing the probable behavior of the repository in the Yucca Mountain geological setting relative to the overall system performance standards • a plan and cost estimate for the remaining work required to complete a license application, and • an estimate of the costs to construct and operate the repository in accordance with the design concept."
Engineered Barrier Segments	As mentioned in the 1997 Energy and Water Appropriations Act, include (1) the invert and pedestal systems to support the waste package, (2) any packing or backfill materials that may be used within the drift, (3) and any drip shield that may be placed over or around the waste package.
Engineered Barrier System	The waste packages and the underground facility. The designed, or engineered, components of the disposal system and the waste package.
Engineered Barrier System Transport Model	A computer model that includes the key processes: (1) in-drift thermal hydrology and geochemistry, (2) degradation of the drip shield (if used), (3) degradation of the waste package and cladding, (4) alteration and dissolution of the waste form, (5) degradation of the invert, (6) mobilization of the radionuclides in the waste form, and (7) transport of radionuclides in the drift.
Enrichment	The percentage of the fuel matrix that is fissile.

Environmental Impact Statement (EIS)	A detailed written statement to support a decision to proceed with major Federal actions affecting the quality of the human environment. This is required by the National Environmental Policy Act (NEPA). The environmental impact statement describes: "...the environmental impact of the proposed action; any adverse environmental effects which cannot be avoided should the proposal be implemented; alternatives to the proposed action (although the Nuclear Waste Policy Act, as amended, precludes consideration of certain alternatives); the relationship between local short-term uses of man's environment and the maintenance and enhancement of long-term productivity; and any irreversible and irretrievable commitments of resources which would be involved in the proposed action should it be implemented." Preparation of an environmental impact statement requires a public process that includes public meetings, reviews, and comments, as well as agency responses to the public comments. A final environmental impact statement for the Yucca Mountain site is to be published in fiscal year 2000.
Environmental Protection Agency (EPA), U.S.	The agency charged by the Nuclear Waste Policy Act of 1982, and subsequently by the Energy Policy Act of 1992, with promulgating generally applicable standards for protection of the general environment. The proposed repository at Yucca Mountain is overseen by this agency.
Equilibrium	The state of a chemical system in which the phases do not undergo any spontaneous change in properties or proportions with time, a dynamic balance.
Equilibrium Batch Reactor	A concept describing the conditions in a computer model cell in which the value of any given parameter is homogeneous and in equilibrium throughout the cell area. Used when referring to concentration conditions within an individual cell during modeling of engineered barrier transport.
Equivalent Continuum Model	A conceptual model of groundwater and heat flow that is also called a composite porosity model. Key assumptions are that the temperatures and capillary pressures in the rock matrix and fractures are equal. Therefore, the fractures and matrix can be treated as a single composite material, and the hydraulic properties are a combined effect of both fracture and matrix properties.
Evapotranspiration	The combined processes of evaporation and plant transpiration that remove water from the soil and return it to the air.

Event Tree	A structurally tree-like diagram that is useful in representing sequences of events and their possible outcomes. Each node, or branching point, represents an event, such as volcanic activity, and each branch from that node represents one of its possible outcomes. Each branch can continue to branch many times. Each possible pathway along the tree, from beginning to end of a given line of branching, represents a specific scenario.
Events	(1) Occurrences that have a specific starting time and, usually, a duration shorter than the time being simulated in a model. (2) Uncertain occurrences that take place within a short time relative to the time frame of the model.
Expected Behavior	The nominal behavior of the repository system and the geologic barrier in the absence of disruptive events.
Expected Value	See Section A.2 of this glossary.
Expected Value Realization	The single realization derived by sampling all uncertain input parameters in the component models at the expected values of their ranges.
Expert Elicitation	A formal process through which expert judgment is obtained.
Exploratory Studies Facility	An underground laboratory at Yucca Mountain that includes a 7.9-km (4.9-mile) main loop (tunnel), a 2.8-km (1.75-mile) cross-drift, and a research alcove system constructed for performing underground studies during site characterization. The data collected will contribute toward determining the suitability of the Yucca Mountain site. Some or all of the Exploratory Studies Facility may eventually be incorporated into the repository.
External Criticality	A condition in which a critical configuration of fissile material occurs after this material is released from the waste packages. See also Criticality.
Far-Field	With reference to processes, those occurring at the scale of the mountain. The area of the geosphere and biosphere far enough away from the repository that, when numerically modeled, releases from the repository are represented as a homogeneous, single-source effect.
Fast Path	Localized unsaturated zone flow pathways that might have high advective velocities. Fast paths move water, carrying radionuclides, through the unsaturated zone more quickly than if movement were predominantly through the pores of the rock matrix. Fractures are potential fast paths.
Fault (Geologic)	A fracture in rock along which movement of one side relative to the other has occurred.

Features	Physical, chemical, thermal, or temporal characteristics of the site or repository system.
FEHM Computer Code	The Finite Element Heat and Mass transfer computer code that is a process model for unsaturated flow and transport.
Fick's Law	The mass of solute diffusing is proportional to the concentration gradient when a solute in water moves from an area of greater concentration toward an area of lesser concentration by molecular diffusion.
Film Flow	Movement of water as a thin film along a surface.
Finite Difference Computer Code	A commonly used numerical method for solving flow problems. An approximating technique in which algebraic equations are used for approximating the partial differential equations that comprise mathematical models in order to produce a form of the problem that can be solved on a computer. For this type of approximation the real world area being modeled is formed into a grid with cubical or rectangular blocks. Values for parameters, such as head, are computed at the grid nodes with the same value also being the average for the area surrounding the node.
Finite Element Computer Code	A commonly used numerical method for solving flow problems. An approximating technique in which algebraic equations are used for approximating the partial differential equations that comprise mathematical models in order to produce a form of the problem that can be solved on a computer. For this type of approximation the real world area being model is formed into a grid with irregularly shaped blocks. This method provides an advantage in handling irregularly shaped boundaries, internal features such as faults, and simulation of point sources (of contamination), seepage faces, and moving water table elevations. Values for parameters are frequently calculated at nodes for convenience, but are defined everywhere in the blocks by means of interpolation functions.
Fissile	Sometimes used as a synonym for fissionable (see Fission). Fissile material can undergo fission with neutrons of any energy, including thermal, or slow, neutrons. The three primary materials in this category are uranium-233, uranium-235, and plutonium-239. Fissionable nuclides require fast neutrons to undergo fissions.
Fissile Material	See Fissile.
Fission	The splitting of a nucleus into at least two other nuclei, resulting in the release of two or three neutrons and a relatively large amount of energy.

Fission Products	A complex mixture of nuclides produced by the process of fission that includes radioactive (and some nonradioactive nuclides) as well as the daughter products of the radioactive decay of these nuclides, which can result in more than 200 isotopes.
Flow	The movement of a fluid such as air or water. Flow and transport are groundwater processes that can move potential contaminants; it usually means flow based on Darcy's law.
Flow Pathway	The subsurface course that a water molecule or solute (including radionuclides) would follow in a given groundwater velocity field governed principally by the hydraulic gradient.
Flux	The rate of transfer of fluid, particles, or energy passing through a unit area per unit time. For water, also known as specific discharge.
Fractures	Breaks in rocks caused by the stresses that cause folding and faulting. A fracture along which there has been displacement of the sides relative to one another is called a fault. A fracture along which no appreciable movement has occurred is called a joint. Fractures may act as fast paths for groundwater movement.
Fracture Aperture	(1) The space that separates the sides of a fracture. (2) The measured width of the space separating the sides of a fracture.
Fracture Permeability	The capacity of a rock to transmit fluid that is related to fractures in the rock.
Fracture-Matrix Exchange Coefficient	(1) A multiplier used in unsaturated groundwater flow simulations that alters the geometric conductance between fracture and matrix elements to account for reduced wetting and contact area. (2) A coefficient that assists in capturing the effect of groundwater being distributed unevenly over fracture surfaces as moves through fractured rock.
Frequency Distribution	See Section A.2 of this glossary.
Fuel Assembly	A number of fuel rods held together by plates and separated by spacers, used in a reactor. This assembly is sometimes called a fuel bundle.
Fuel Matrix	The physical form and composition of the substance that holds the fissile material.
Fugacity	A parameter that measures the chemical potential of a real gas in the same way that partial pressure measures the free energy of an ideal gas.
Galvanic	Pertaining to an electrochemical process in which electron flow is produced between two dissimilar metals when they are immersed in an electrolyte solution and placed in contact or are electrically connected. The electron flow results from the difference in electrical potential of the metals.

Galvanic Corrosion	Electrochemical corrosion (eating into a substance) caused by the flow of electricity that occurs when two dissimilar metals, with differing electrical potentials, are near each other in the presence of a conductor such as water with solutes in it.
Gaseous Diffusion	The selective transfer of gas by molecular diffusion through microporous barriers. Used to refer to the mechanism for movement of gas through concrete and rock and for movement of gas out of the waste package by means not involving water.
GENII	A deterministic computer software code that evaluates dose from the migration of radionuclides introduced into the accessible environment, or biosphere, that may eventually affect humans through ingestion, inhalation, or direct radiation. It is used to develop biosphere dose conversion factors.
GENII-S	A quasi-stochastic computer software code that can create distributions and sample them and is run in conjunction with GENII for biosphere modeling.
Geochemical	The distribution and amounts of the chemical elements in minerals, ores, rocks, soils, water, and the atmosphere, and the circulation of the elements in nature on the basis of their properties.
Geochemistry	The study of the abundance of the elements and atomic species (isotopes) in the earth. Geochemistry, or geochemical study looks at systems related to chemicals arising from natural rock, soil, soil processes such as microbe activity, and gases, especially as they interact with man-made materials from the repository system. In the broad sense, all parts of geology that involve chemical changes.
Geologic-Framework Model	A nonmathematical model of the geologic system.
Geologic Repository	A system for disposing of radioactive waste in excavated geologic media, including surface and subsurface areas of operation, and the adjacent part of the geologic setting that provides isolation of the radioactive waste.
Geologic Time	The period of time over which the earth has existed. The time scale over which geologic processes produce change. In general discussion, the term geologic time implies very long periods of time such as tens of thousands of years, hundreds of thousands of years, or millions of years.
Geosphere	The combination of the earth's rock, water, and air layers (spheres).
Glass	See High-Level Radioactive Waste Glass.

Goethite	An iron oxide mineral that is yellowish, reddish, or brownish black. It is the most common constituent of many forms of natural rust or of limonite.
Gradient	The change in value of a quantity per unit distance in a specified direction.
Groundwater	Water contained in pores or fractures in either the unsaturated or saturated zones below ground level.
Groundwater Flux	The rate of groundwater flow through a unit area of the aquifer. Means the same as specific discharge.
Groundwater Travel Time	The time required for a unit volume of groundwater to travel between two locations. The travel time is the length of the flow path divided by the velocity, where velocity is the average groundwater flux divided by the effective porosity along the flow path. If discrete segments of the flow path have different hydrologic properties, the total travel time will be the sum of the travel times for each discrete segment.
Handling Container	The container in which the fuel matrix and cladding are placed. If the waste form is solidified, this is called a pour container. In some cases, this is the only container for storage, handling, and transportation prior to disposal.
Heavy Metal	All uranium, plutonium, and thorium used in a nuclear reactor.
Herbivore	An organism that feeds on plants, especially an animal whose diet is exclusively plants.
Heterogeneity	The condition of being composed of parts or elements of different kinds. A condition in which the value of a parameter such as porosity, which is an attribute of an entity of interest such as the tuff rock containing the repository, varies over the space an entity occupies, such as the area around the repository, or with the passage of time.
High-Level Radioactive Waste	(1) The highly radioactive material resulting from the reprocessing of spent nuclear fuel, including liquid waste produced directly in reprocessing, and any solid material derived from such liquid waste that contains fission products in sufficient concentrations (2) Other highly radioactive material that the Nuclear Regulatory Commission, consistent with existing law, determines by rule requires permanent isolation.
High-Level Waste	See High-Level Radioactive Waste.
High-Level Radioactive Waste Glass	The waste form of defense high-level radioactive waste in which the radioactive waste is mixed with borosilicate glass.
Histogram	See Section A.2 of this glossary.

Homogeneous	Consisting of or composed of similar elements or ingredients.
Host Rock	The rock unit in which the repository will be located. For the repository at Yucca Mountain, the host rock would be the middle portion of the of the Topopah Spring tuff formation of the Paintbrush Group. See also tuff.
Hydraulic Conductivity	A measure of the ability to transmit water through a permeable medium. A number that describes the rate at which water can move through a permeable medium. The hydraulic conductivity depends on the size and arrangement of water-transmitting openings such as pores and fractures, the dynamic characteristics of the water such as density and viscosity, and the strength of the gravitational field.
Hydraulic Gradient	The change in the height of water levels with respect to the distance between two locations.
Hydrodynamic Dispersion	See Dispersion.
Hydrogeology	A study that encompasses the interrelationships of geologic materials and processes involving water.
Hydrologic	Pertaining to the properties, distribution, and circulation of water on the surface of the land, in the soil and underlying rocks, and in the atmosphere.
Hydrology	(1) The study of water characteristics, especially the movement of water. (2) The study of water, involving aspects of geology, oceanography, and meteorology.
Hydrostratigraphy	A stratigraphic classification of layered rocks based on rock characteristics and the hydrologic, or water-conducting, properties of the units.
Human Intrusion	The inadvertent disturbance of a disposal system by humans that could result in release of radioactive waste. Subpart B of 40 CFR 191 requires that performance assessments consider the possibility of human intrusion.
Igneous	(1) A type of rock that has formed from a molten, or partially molten, material. (2) A type of activity related to the formation and movement of molten rock either in subsurface (plutonic) or on the surface (volcanic).
Imbibition	The absorption of a fluid, usually water, by porous rock (or other porous material) under the force of capillary attraction and without pressure.
Incolloy 625	Under past reference design specifications, the corrosion resistant inner layer of the two layer metallic disposal container. The inner layer material for calculations related to disruptive scenarios.

Infiltration	The process of water entering the soil at the ground surface and the ensuing movement downward when the water input at the soil surface is adequate. Infiltration becomes percolation when water has moved below the depth at which it can be removed (to return to the atmosphere) by evaporation or evapotranspiration.
Infiltration Flux	Volumetric infiltration rate per unit area.
Infiltration Rate	See Infiltration Flux.
Inner Barrier	An inner layer of the two-layer metallic disposal container. The inner layer is constructed with corrosion-resistant material such as Alloy 22 (ASTM B575 N06022), a nickel-base, high- performance material. See also Corrosion Resistant Material.
Inner Canisters	High-level radioactive waste canisters placed within the overpack.
In Situ	In its natural position or place. The phrase distinguishes in-place experiments, conducted in the field or underground facility, from those conducted in the laboratory.
Integral-Finite-Difference Computer Code	A commonly used numerical method for solving flow problems. An approximating technique in which algebraic equations are used for approximating the partial differential equations that comprise mathematical models in order to produce a form of the problem that can be solved on a computer. Similar in capability to a finite element code in that it can handle irregularly shaped areas well. See Finite Element Computer Code.
Inventory	The amount of radioactive elements in a fuel, usually stated in curies per metric ton of heavy metal. Also termed radionuclide inventory.
Invert	A construction associated with the precast concrete structure for the purpose of providing a level drift floor and enabling transporting and support of the waste package.
Ion	(1) An atom that contains excess electrons or is deficient in electrons, causing it to be chemically active. (2) An electron not associated with a nucleus.
Ionizing Radiation	(1) Alpha particles, beta particles, gamma rays, x-rays, neutrons, high-speed electrons, high-speed protons, and other particles capable of producing ions. (2) Any radiation capable of displacing electrons from an atom or molecule, thereby producing ions.
Ionic Strength	A measure of the level of electrical force in an electrolytic solution.
Irradiated Fuel	Burned fuel. See also Burnup.
Isothermal	Pertaining to constant temperature.

Isotope	One of two or more atomic nuclei with the same number of protons (i.e., the same atomic number) but with a different number of neutrons (i.e., a different atomic weight). For example, uranium-235 and uranium-238 are both isotopes of uranium.
Isotropy	The condition wherein all significant physical properties are equal when measured in any direction or along any axes. See also Anisotropy.
Iterative	Conditions or results that are repeated in an analysis. The processes in which analysts rerun calculations or refine models as new data are gathered or new insights occur.
ITOUGH2 Computer Code	A computer code that estimates hydrogeologic model parameters for the numerical simulator TOUGH2.
J-13 Water	The groundwater taken from Wellbore J13. The chemical composition of this water is used as the standard for Yucca Mountain ambient groundwater composition for modeling purposes.
Joint	A fracture in rock, usually more or less vertical to bedding, along which no appreciable movement has occurred.
Juvenile Failure	Premature failure of a waste package because of material imperfections or damage by rockfall during emplacement.
Key Technical Issues	Issues important for assessing the long-term safety of a potential Yucca Mountain repository, as defined by the Nuclear Regulatory Commission (NRC). The issues are (1) Support Revision of the U.S. Environmental Protection Agency Standard/NRC Rule Making; (2) TSPA and Technical Integration; (3) Igneous Activity; (4) Unsaturated and Saturated Flow Under Isothermal Conditions; (5) Thermal Effects on Flow; (6) Container Life and Source Term; (7) Structural Deformation and Seismicity; (8) Evolution of Near-Field Environment; (9) Radionuclide Transport; (10) Repository Design and Thermal-Mechanical Effects.
Kinetic	Of or due to motion.
Latin Hypercube Sampling	A sampling technique that divides the cumulative distribution function into intervals of equal probability and then samples from each interval.
License Application	An application to the Nuclear Regulatory Commission for a license to construct a repository.
Line Loading Repository Design	A waste emplacement design in which waste containers are spaced very closely along the drift, with emplacement drifts relatively far apart.

Lithophysal	Pertaining to tuff units with lithophysae, voids having concentric shells of finely crystalline alkali feldspar, quartz, and other materials that were formed due to entrapped gas that later escaped.
Lithosphere	The earth's crust, as distinguished from the atmosphere or hydrosphere, and as distinguished from the deeper portion of the earth underlying the crust.
Localized Corrosion	A type of corrosion induced by local variations in electrochemical potential on a microscale over small regions. Variations in electrochemical potential may be caused by localized irregularities in the structure and composition of usually protective passive films on metal surfaces and in the electrolyte composition of the solution that contacts the metal. See Pitting Corrosion and Crevice Corrosion.
Log Normal Distribution	A distribution of a random variable X such that the natural logarithm of X is normally distributed.
Long-Term-Average Climate	One of three sets of conditions used to represent climate changes through time. Representative of the expected typical climate conditions at Yucca Mountain, with precipitation twice that of the present-day climate. See also Dry Climate and Superpluvial Climate.
Lookup Table	A multidimensional table containing columns of data representing relationships between parameters in the table. A lookup table is a convenient way to represent and implement functional relationships between parameters considered in the model.
Longitudinal Dispersion	(1) Dispersion of a solute moving in groundwater in the same direction as the groundwater flow path. (2) Spreading of a solute in the direction of bulk flow.
Magma	Molten or partially molten rock material that is naturally occurring and is generated within the earth.
Mass Balance	The procedure of accounting for conservation of mass, such as the mass of radionuclides released from waste packages, in real world processes or in models of real world processes.
Mathematical Model	A mathematical description of a conceptual model.
Matrix	Tuff rock material and its pore space exclusive of fractures. As applied to Yucca Mountain tuff, the groundmass of an igneous rock that contains larger crystals.

Matrix Diffusion	As used in TSPA-VA conceptual models, the process by which molecular or ionic solutes, such as radionuclides in groundwater, move from areas of higher concentration to areas of lower concentration. This movement is through the pore spaces of the rock material as opposed to movement through the fractures.
Matrix Permeability	The capacity of the matrix to transmit fluid.
Mean (Arithmetic)	See Section A.2 of this glossary.
Mechanistic Analysis	An analysis of processes that is based on the well established fundamentals of the processes considered, such as: thermodynamics, reaction kinetics, mass transfer laws, heat transfer laws, etc. This is as opposed to empirical analysis, which is based on a model that has been developed from the numerical value of data taken from tests or measurements of the model.
Median	A value such that half of the observations are less than that value and half are greater than the value.
Meteorological	Of, or relating to meteorology, or to weather and other atmospheric phenomena.
Metric Ton Heavy Metal (MTHM)	A metric ton is a unit of mass equal to 1,000 kg (2,205 lb). Heavy metals are those with atomic masses greater than 230. Examples include thorium, uranium, plutonium, and neptunium. When used in the Civilian Radioactive Waste Management Program, the term usually pertains to heavy metals in spent nuclear fuel in scientific text. In this document, MTHM is equal to MTU (metric tons of uranium).
Metric Ton of Uranium (MTU)	A metric ton, which is 1,000 kg, or 2,205 lb, of uranium in scientific text.
Microbe	An organism too small to be viewed with the unaided eye. Examples of microbes are bacteria, protozoa, and some fungi and algae.
Microbially Influenced Corrosion	Corrosion of the waste package that is enhanced by the activity of microbes.
Microbiologically Influenced Corrosion	See Microbially Influenced Corrosion.
Migration	Radionuclide movement from one location to another within the engineered barrier system or the environment.
Mild Steel	See Carbon Steel.
Mineral Assemblage	Minerals that compose a rock, especially an igneous or metamorphic rock. The term includes the different kinds and relative abundance of minerals but excludes the texture and fabric of the rock.

Mineralogical	Of or relating to the chemical and physical properties of minerals, their occurrence, and classification.
Mobile Radionuclides	Radionuclides that can move within a water system with little or no retardation.
Mobilization	The process of breaking down the waste form and releasing radionuclides. After its initial mobilization a radionuclide can be removed from transport by being precipitated or adsorbed and later become remobilized in a cycle of changes that can be repeated many times.
Model	A depiction of a system, phenomenon, or process including any hypotheses required to describe the system or explain the phenomenon or process.
Molal	Of a solution, containing one mole of solute per one kilogram of solvent.
Mole	The fundamental SI unit used to measure the amount of a substance. Avagadro's number of particles (6.023×10^{23}).
Monte Carlo Uncertainty Analysis	See Section A.2 of this glossary.
Mountain Scale	(1) Similar to far-field for processes that are related to the area of the geosphere and biosphere far enough away from the repository that, when numerically modeled, show that releases from the repository are represented as a homogeneous, single source term. The effects of individual, small-scale components such as individual waste packages are not modeled because they are considerably smaller than the scale of the model. (2) A scale of hundreds of meters, or even kilometers, as opposed to tens of meters.
National Academy of Sciences	A congressionally chartered, private, nonprofit, self-perpetuating organization of scientists devoted to the expansion of science and its use for the general welfare. This organization is mandated to advise the Federal Government on scientific and technical matters. Section 801 of the Energy Policy Act of 1992 directed the U.S. Environmental Protection Agency to contract with the National Academy of Sciences to provide, "findings and recommendations on reasonable standards...that would govern the long-term performance of a repository at the Yucca Mountain site."
National Research Council	The working arm of the National Academy of Sciences and the National Academy of Engineering that carries out most of the studies done on behalf of the academies. Most of the studies are done in response to specific questions presented by federal agencies or Congress.

Natural Analogs	Natural geologic systems that parallel situations that can develop in man-made systems, in which the formation and transport of minerals over hundreds of thousands and millions of years can be studied directly. An example of natural analog is the natural reactor studied at the Oklo uranium deposit in Gabon, Africa, which can be used as a source of analog data for conceptual models of criticality.
Near Field	The area and conditions within the repository including the drifts and waste packages and the rock immediately surrounding the drifts. The region around the repository where the natural hydrogeologic system has been significantly impacted by the excavation of the repository and the emplacement of waste.
Near-Field Geochemical Environment Model	A model that focuses on major-element geochemistry within the potential emplacement drifts. The boundary of the model domain is defined as the drift wall. This model includes coupling to thermohydrologic processes.
Net Infiltration	The water that has infiltrated down from the soil zone or exposed rock surface to a depth below which it cannot be removed by evapotranspiration. The amount of water that is net infiltration is the total infiltration at the surface minus water lost to evaporation and plant transpiration.
Neutron Absorber	A material such as boron or gadolinium that is placed in a radioactive waste package and that absorbs neutrons to reduce ionizing radiation and to help reduce the likelihood of criticality.
Node	A junction point in a network.
Nominal Case	The case, or conceptual model, representing the expected conditions of the disposal system as perturbed only by the presence of the repository, in the absence of disruptive events.
Nominal Conditions	The site conditions, including features and processes, which are expected, based on current site knowledge.
Nominal Behavior	(1) Expected behavior of the system as perturbed only by the presence of the repository. (2) Behavior of the system in the absence of disruptive events.
Nominal Features, Events, and Processes	Those features, events and processes expected, given the site conditions as described from current site characterization information.
Nonequilibrium Thermodynamics	The study of heat flow systems that have not stabilized (i.e., are not in equilibrium).
Nuclear Chain Reaction	A process in which some of the neutrons released in one fission event cause other fissions.

Nuclear Regulatory Commission (NRC)	Promulgates technical regulations that are consistent with standards established by the U.S. Environmental Protection Agency (EPA) and considers license applications from the U.S. Department of Energy for a proposed repository. It determines, with reasonable assurance, whether EPA standards can be met. It also has the continuing regulatory responsibility to oversee repository operation. NRC was formed by the Atomic Energy Commission with the 1974 Energy Reorganization Act, Public Law 93-438.
Nuclear Regulatory Commission Radioactive Waste Program Annual Progress Report	A status report made each fiscal year that documents the technical work performed on 10 key technical issues that are most important to performance of the proposed geologic repository at Yucca Mountain.
Nuclear Waste Policy (42 USC 10101 et seq.)	The federal statute enacted in 1982 that established the Office of Civilian Radioactive Waste Management (OCRWM) and defined its mission to develop a federal system for the management and geologic disposal of commercial spent nuclear fuel and other high-level radioactive wastes. The Act also: (i) specified other federal responsibilities for nuclear waste management, (ii) established the Nuclear Waste Fund to cover the cost of geologic disposal, (iii) authorized interim storage under certain circumstances, and (iv) defined interactions between Federal agencies and the states, local governments, and Indian tribes. The act was substantially amended in 1987 and 1992.
Nuclear Waste Policy Amendments Act of 1987, Public Law 100-203	Legislation that amended the Nuclear Waste Policy Act to: (i) limit repository site characterization activities to Yucca Mountain, Nevada, (ii) establish the Office of the Nuclear Waste Negotiator to seek a state or Indian tribe willing to host a repository or monitored retrievable storage facility, (iii) create the Nuclear Waste Technical Review Board, and (iv) increase state and local government participation in the waste management program.
Nuclear Waste Technical Review Board	An independent body established within the executive branch, created by the Nuclear Waste Policy Amendments Act of 1987 to evaluate the technical and scientific validity of activities undertaken by the U.S. Department of Energy, including site characterization activities and activities relating to the packaging or transportation of high-level radioactive waste or spent nuclear fuel. Members of this Board are appointed by the President from a list composed by the National Academy of Sciences.
NUFT Computer Code	A computer code that simulates three-dimensional flow of groundwater, heat, and contaminants in unsaturated and saturated porous and fractured media. It is named for Non-isothermal Unsaturated Flow and Transport and is used for drift scale, thermal-hydrologic calculations.

Numerical Model	An approximate representation of a mathematical model that is constructed using a numerical description method, such as finite volumes, finite differences, or finite elements. A numerical model is typically represented by a series of program statements that are executed on a computer.
Office of Civilian Radioactive Waste Management (OCRWM)	A U.S. Department of Energy office created by the Nuclear Waste Policy Act of 1982 to implement the responsibilities assigned by the Act.
One-Dimensional Model	A model that represents physical conditions and/or processes by a vertical column composed of a stack of single grid cells or by a horizontal row of single grid cells.
Order of Magnitude	A range of numbers extending from some value to ten times that value.
Outer Barrier	The outer layer of the two-layer metallic disposal container. It consists of carbon steel, which is a corrosion allowance material.
Outer Barrier and Inner Barrier Corrosion Models	See Corrosion Models.
Outer Barrier Corrosion Model	See Outer Barrier and Inner Barrier Corrosion Models.
Overburden	Geologic material of any nature, consolidated or unconsolidated, that overlies a deposit of useful materials. As used by the Yucca Mountain Site Characterization Project, this is geologic material overlying the mined repository horizon.
Oxidation	(1) A chemical reaction, such as the rusting of iron, that increases the oxygen content of a substance. (2) A reaction in which the valence of an element or compound is increased as a result of losing electrons.
Oxidation State	For an ion, expressed as a positive or negative number representing the ionic or effective charge.
Oxidize	(1) To increase the oxygen content of a substance. (2) To increase the valence of an element or compound as a result of losing electrons.
Paleoclimates	The climate of a past interval of geologic time.
Parameter	Data, or values, that are input to computer codes for a TSPA calculation.
Passive Institutional Control	From 40 CFR 191, methods of preserving information about the location, design and contents of the repository system. These include permanent markers placed around the disposal site area, public records and archives, government ownership, and regulations controlling use of land.

Patch	For corrosion modeling, one of two geometries for an opening in a waste package layer created by corrosion (the other geometry is a pit). A patch is generally wider than it is deep.
Pathway	A potential route by which radionuclides might reach the accessible environment and pose a threat to humans.
Peer Review Panel	A panel of individuals—independent of those who performed the TSPA-VA but who have technical expertise at least equivalent to those who performed the original work—who produce a documented critical review of the work.
Percentile	See Section A.2 of this glossary.
Perched Water	A saturated condition that is not continuous with the water table, because there is an impervious or semipervious layer underlying the perched zone or a fault zone that creates a barrier to water movement and perches water.
Percolation	The passage of a liquid through a porous substance. In rock or soil it is the movement of water through the interstices and pores under hydrostatic pressure and the influence of gravity. The downward or lateral flow of water that becomes net infiltration in the unsaturated zone.
Percolation Flux	Volumetric percolation rate per unit area. The flux anywhere below the root zone of plants and is no longer susceptible to removal back into the atmosphere by evapotranspiration.
Percolation Rate	See percolation flux.
Performance Assessment	An analysis that predicts the behavior of a system or system component under a given set of constant and/or transient conditions. Performance assessments will include estimates of the effects of uncertainties in data and modeling. See TSPA.
Permeability	In general terms, the capacity of a medium like rock, sediment, or soil to transmit liquid or gas. Permeability depends on the substance transmitted (oil, air, water, etc.) and on the size and shape of the pores, joints, and fractures in the medium and the manner in which they are interconnected. "Hydraulic conductivity" has replaced "permeability" in technical discussions relating to groundwater. See also Relative Permeability.
pH	A number indicating the acidity or alkalinity of a solution. A pH of 7 indicates a neutral solution. Lower pH values indicate more acidic solutions while higher pH values indicate alkaline solutions.

Phase	A physically distinct portion of matter, such as the aqueous, gas, or solid phase.
Phase Equilibria	The relationships between phases of a substance undergoing a phase change, such as from solid to liquid, under various conditions of temperature and pressure.
Phase Stability	A measure of the ability of matter to remain in a given phase.
Pit	For corrosion modeling, one of two geometries for an opening in a waste package layer created by corrosion (the other geometry is a patch). A pit is generally deeper than it is wide.
Pitting Corrosion	A type of localized corrosion that forms in indentations called pits.
Pitting Factor	A factor that is used to measure local variations of general, or uniform, corrosion penetration from corrosion allowance materials such as carbon steel.
Playa	The shallow central basin of a desert plain in which water gathers after a rain and then evaporates.
Plume	A measurable discharge of a contaminant, such as radionuclides, from a point of origin. The contaminants are usually moving in groundwater, and the plume may be defined by chemical concentration gradients.
Pluvial	(1) In climatology, relating to former periods of abundant rains, especially in reference to glacial periods. (2) In geology, said of a geologic episode, change, process, deposit, or feature caused by the action or effects of rain.
Point Loading Thermal Design	An emplacement drift design in which commercial spent nuclear fuel waste packages are spaced away from each other along the drift using emplacement drift spacing similar to the commercial spent nuclear fuel-package spacing.
Pore Fluid	The water and any material it is carrying that exist in the pore spaces of the rock matrix.
Pore Waters	Interstitial water, or subsurface water in the pores in rock or soil.
Porosity	The ratio of openings, or voids, to the total volume of a soil or rock expressed as a decimal fraction or as a percentage. See also Effective Porosity.
Pour Canister	A metallic canister into which high-level radioactive waste mixed with molten glass-making materials is poured. The material cools and solidifies in the pour canister.

Precipitate	A substance that separates as solid particles from a liquid as a result of physical or chemical changes.
Precipitation	(1) The process of depositing a substance from a solution, by the action of gravity or by a chemical reaction. (2) Any form of water particles, such as frozen water in snow or ice crystals, or liquid water in raindrops or drizzle, that fall from clouds in the atmosphere and reaches the earth's surface. (3) An amount of water that has fallen at a given point over a specified period of time, measured by a rain gauge.
Probabilistic	(1) Based on or subject to probability. (2) Involving a variate, such as temperature or porosity. At each instance of time, the variate may take on any of the values of a specified set with a certain probability. Data from a probabilistic process is an ordered set of observations, each of which is one item from a probability distribution.
Probabilistic Risk Assessment	(1) A systematic process of identifying and quantifying the consequences of scenarios that could cause a release of radioactive materials to the environment. (2) Using predictable behavior to define the performance of natural, geologic, human, and engineered systems for thousands of years into the future using probability distributions (see Section A.2 of this glossary).
Probability	See Section A.2 of this glossary.
Probability Density Function	See Section A.2 of this glossary.
Probability Distribution	See Section A.2 of this glossary.
Probability Model	A model that quantifies uncertainties in the model parameters and predicts the likelihood of the scenarios used for the model.
Probable Behavior	A combination of the concept of predicted future behavior of the various system components with the uncertainty associated with the prediction.
Process Model	A depiction or representation of a process along with any hypotheses required to describe or to explain the process.
Processes	Phenomena and activities that have gradual, continuous interactions with the system being modeled.
Pyroclastic Flow	A flow of detrital volcanic materials that have been explosively ejected from a volcanic vent. The flow is generally a dense cloud of incandescent volcanic glass, in a semimolten or viscous state, that solidifies into rock. The rock that results is chiefly a fine-grained rhyolitic tuff formed of glass shards that may be welded or nonwelded.
Quantitative	A variable that is expressed numerically.

Quality Factor	The modifying factor that is used to derive dose equivalent from absorbed dose.
Quasi-Static Thermodynamic Processes	Reversible processes resulting in a change to system or body.
Quasi-Transient	Describing the diffusive mass transport model. This means the solution used in the model incorporates steady-state diffusive mass transfer through the perforations of the failed waste container. This is combined with transient mass transfer through the spherical shell of the invert surrounding the waste container. The quasi-transient mass transfer model is used to calculate diffusive release of radionuclides at the engineered barrier system edge.
Rad	The unit of measure for the absorbed dose of radiation. Rad is short for radiation absorbed dose.
Radiation	Ionizing radiation.
Radioactive Decay	The process in which one radionuclide spontaneously transforms into one or more different radionuclides, which are called daughter radionuclides.
Radioactivity	The property possessed by some elements (i.e., uranium) of spontaneously emitting alpha, beta, or gamma rays by the disintegration of atomic nuclei.
Radiocolloid	Colloids, or colloidal systems, containing radionuclides.
Radiolysis	Chemical decomposition by the action of radiation.
Radionuclide	Radioactive type of atom with an unstable nucleus that spontaneously decays, usually emitting ionizing radiation in the process. Radioactive elements characterized by their atomic mass and number.
Random Variable	See Section A.2 of this glossary.
Range (Statistics)	See Section A.2 of this glossary.
REACT Computer Code	The reaction mass transfer code.
Reaction Kinetics	The study of the rates and mechanisms of chemical reactions.
Reaction Rate	The rate at which a chemical reaction takes place.
Realization	A complete calculation using a randomly selected value. Many of these calculations are done in a Monte Carlo analysis.
Recharge	The movement of water from the unsaturated zone to the saturated zone.

Reducing Conditions	With regard to criticality, the important aspect of reducing conditions is that they reduce the oxidation state of materials (deoxidize), and the material that is reduced becomes less soluble. Radionuclides being transported in groundwater can precipitate out and collect in an area of reducing conditions. With regard to corrosion, reducing conditions slow corrosion, because oxygen is less available, or not available, to combine with the iron and form rust.
Reference Person	With regard to dose, a hypothetical collection of human physical and physiological characteristics arrived at by international consensus. This collection may be used by researchers to relate biological damage to a stimulus such as radiation exposure. The reference adult person lives 20 km (12 miles) from Yucca Mountain and will be defined using a survey of the existing population.
Reflux Water	Water that is vaporized near waste packages, migrates to cooler areas, condenses, and then flows back toward the waste packages.
Regression Analysis	See Section A.2 of this glossary.
Relative Permeability	The permeability of rock material to a given substance compared to the absolute (total) permeability of the rock. The term is usually used to signify the permeability to one fluid when two or more fluids are present in the rock.
rem	The unit of a dose equivalent from ionizing radiation to the human body. It is used to measure the amount of radiation to which a person has been exposed) (rem means roentgen equivalent man).
Repository Layout	The host rock, depth, and areal extent of the repository facility, drift size and spacing, mechanical support system, thermal load, and ventilation system used during the operational phase of the facility. This is as mentioned in the Energy and Water Appropriations Act of 1997.
Repository Safety Strategy	A document used to assist management in prioritizing testing and analysis activities to focus on the most important issues in postclosure safety. Identification of the important issues allows resource use (e.g., sampling and testing activities) to be focused on gathering information that will reduce the uncertainty in parameters and processes related to the key issues. Key elements of the document include the following: (1) Limited water contacting waste packages (2) Long waste package lifetime (3) Low rate of release of radionuclides from breached waste packages (4) Radionuclide concentration reduction during transport from the waste packages

Retardation	Slowing or stopping of radionuclide movement in groundwater by mechanisms that include sorption of radionuclides, diffusion into rock matrix pores and microfractures, and trapping of large colloidal molecules in small pore spaces or dead ends of microfractures.
RIP Computer Program	RIP is an initialism for repository integration program, the executive TSPA "driver" program. An integrating software code into which simplified analytical expressions, or callable subroutines describing the behavior of the different components, can be placed. RIP sequentially advances through time while keeping track of the changes in environments and the fate of the radioactive constituents within the engineered and natural barriers.
Risk	The probability that an undesirable event will occur multiplied by the consequences of the undesirable event.
Risk Assessment	An evaluation of potential consequences or hazards that might be the outcome of an action. This assessment focuses on potential negative impacts on human health or the environment.
Rock Matrix	See Matrix.
Salt Deposit Effect	(1) Potential buildup of salt scales on the waste package surface from water dripping onto the waste package while its surface is at elevated temperatures. (2) The development of potentially aggressive conditions to the waste package corrosion degradation under and around the salt deposits by providing a wetter environment than the surroundings and causing concentration of aggressive species in the local salt solution.
Saturated Zone	The region below the water table where rock pores and fractures are completely saturated with groundwater.
Scenario	A well-defined, connected sequence of features, events and processes that can be thought of as an outline of a possible future condition of the repository system. Scenarios can be undisturbed, in which case the performance would be expected, or nominal, behavior for the system. The scenario can also be disturbed, if altered by disruptive events such as human intrusion, natural phenomena such as volcanism, or nuclear criticality.
Secondary Phase	Occurs when spent nuclear fuel is contacted by water and dissolves, forming uranyl minerals. The major secondary phase minerals are schoepite, uranophane, Na-boltwoodite, and soddyite.
Seepage	The inflow of groundwater moving in fractures or pore spaces of permeable rock to an open space in the rock such as a drift. Specifically, the amount of percolation flux that enters the drift in a given time period. An important factor in waste package degradation and mobilization and migration of radionuclides out of the repository.

Seepage Fraction	The fraction of the total number of waste packages that is contacted by drips from seepage into the drifts.
Seismic	Pertaining to, characteristic of, or produced by earthquakes or earth vibrations.
Sensitivity Study (Analysis)	An analytic or numerical technique for examining the effects of varying specified parameters when a model run is performed. Shows the effects that changes in various parameters have on model outcomes and can illustrate which parameters have a greater impact on the predicted behavior of the system being modeled. Also, called sensitivity analysis because it shows the sensitivity of the consequences (e.g., radionuclide release) to uncertain parameters (e.g., the infiltration rate that results from precipitation).
Simulation	The generation of a sample set by selecting a parameter value from each input distribution and calculating the consequences for the sample set. See also Realization.
Single Heater Test	A field test in the Exploratory Studies Facility that uses a single heated element emplaced directly into Yucca Mountain tuff (Topopah Spring Middle Nonlithophysal hydrogeologic unit). The test is designed to determine the thermal-hydrologic responses of the unit to heating.
Site Characterization Plan	The plan that contains the strategy for completing a detailed set of activities that was expected to provide all of the information needed to comprehensively describe the repository system. The plan also documented methods for assessing the performance of the total repository system and its individual components. This was published by the U.S. Department of Energy in 1988 with subsequent updating ongoing.
Site Recommendation	A recommendation by the Secretary of Energy to the President that the Yucca Mountain site be approved for development as the nation's first high-level radioactive waste repository. If the site is determined to be suitable, this recommendation is expected in fiscal year 2001.
Smeared Heat Source	An attribute of mountain-scale thermal hydrology models in which the model handles heat output for waste packages by using the total heat produced by all assemblies in all waste packages, arrives at the entire repository-wide thermal load, and averages the thermal load across the entire repository heat area (~740 acres).
Sorb	To undergo a process of sorption.

Sorption	The binding, on a microscopic scale, of one substance to another. A term which includes both adsorption and absorption. The sorption of dissolved radionuclides onto aquifer solids or waste package materials by means of close-range chemical or physical forces is an important process modeled in this study. Sorption is a function of the chemistry of the radioisotopes, the fluid in which they are carried, and the mineral material they encounter along the flow path.
Sorption Coefficient (K_d)	Coefficient for a term for the various processes by which one substance binds to another.
Source Term	Types and amounts of radionuclides that are the source of a potential release from the repository.
Spalling	Flaking off of corrosion products from the metal substrate as it undergoes corrosion. The layer of corroded material thickens. The spalling could be caused by an expansive action of the corrosion products because they occupy a greater volume than the uncorroded metal substrate.
Spatial Variability	A measure of how a property, such as rock permeability, varies in an object such as a rock formation.
Speciation	The existence of the elements, such as radionuclides, in different molecular forms in the aqueous phase.
Spent Nuclear Fuel	Fuel that has been withdrawn from a nuclear reactor following irradiation, the constituent elements of which have not been separated by reprocessing. Spent fuel that has been burned (irradiated) in a reactor to the extent that it no longer makes an efficient contribution to a nuclear chain reaction. This fuel is more radioactive than it was before irradiation, and it is hot. See also Burnup.
Steady-State Modeling	Modeling a system under the assumption that the variables are not changing with time. For example, flow fields can be simulated at a steady state if the boundary conditions, saturations, and fluxes are not changing with time.
Stream Tube	A modeling method used to represent the groundwater flow path from the water table to the biosphere. There are six stream tubes used for saturated zone modeling with one tube associated with and having the cross-sectional shape of, one of six regions designated at the water table. Each stream tube takes in groundwater flux and radionuclide mass flux data at the water table representing flux from the repository that has gone through the unsaturated zone.

Stochastic	Involving a variable (e.g., temperature and porosity) that may take on values of a specified set with a certain probability. Data from a stochastic process is an ordered set of observations, each of which is one item from a probability distribution. Random.
Stochastic Model	A model whose outputs are predictable only in a statistical sense. A given set of model inputs produces outputs that are not the same, but follow statistical patterns.
Stratigraphy	The branch of geology that deals with the definition and interpretation of the rock strata, the conditions of their formation, character, arrangement, sequence, age, distribution, and especially their correlation by the use of fossils and other means of identification.
Stress Corrosion Cracking	A cracking process that requires the simultaneous action of a corrosion mechanism and sustained tensile stress.
Structural Failure	Loss of waste package integrity to contain radionuclides.
Structure	In geology, the arrangement of the parts of the geologic feature or area of interest such as folds or faults. Structural features develop as a result of stresses that cause movements of the earth's crust and result in events such as earthquakes as the crust deforms.
Superpluvial Climate	One of three sets of conditions used to represent climate changes through time. Representative of wetter-than-normal climate conditions at Yucca Mountain, with precipitation three times that of the present-day climate. See also Dry Climate and Long-Term-Average Climate.
Surface Complexation	The process that describes the formation of complex molecules between the solute in the aqueous phase and the reactive groups on the solid surface, under specific chemical conditions.
Surrogate	Using one thing in place of another. An example is using a single important parameter, radionuclide travel time, as a surrogate for performance when the actual performance measure takes into account the effects of many factors. If the calculated travel time of radionuclides of interest is fast, that implies that performance of the natural and engineered barriers in containing the radionuclides is not as effective as it would be if radionuclide travel time was slow.
Tectonic	Pertaining to geologic forms or effects created by deformation of the earth's crust.
Tectonism	A general term for all movement of the earth's crust produced by tectonic processes.
Temperature Gradient	The rate of change of temperature with distance. When applied to the earth, the term geothermal gradient may be used.

Thermal-Chemical	Relating to thermal chemistry, the chemistry branch that studies heat changes that accompany chemical reactions and changes of state.
Thermal Conduction	The flow of thermal energy through a material. This conduction is affected by the amount of heat energy present, the nature of the heat carrier in the material, and the amount of dissipation.
Thermal-Hydrologic	Of or pertaining to changes in groundwater movement due to the effects of changes in temperature.
Thermal-Hydrologic Processes	Processes that are driven by a combination of thermal and hydrologic factors. These processes include evaporation of water near the repository when it is hot and subsequent redistribution of fluids by convection, condensation, and drainage.
Thermal Hydrology	The study of a system that has both thermal and hydrologic processes. A thermal-hydrologic condition, or system, is expected to occur if heat-generating waste packages are placed in the repository at Yucca Mountain.
Thermal Loading	The application of heat to a system, usually measured in terms of watt density. The thermal loading for a repository is the watts per acre produced by the radioactive waste in the active disposal area. The spatial density at which waste packages are emplaced within the repository as characterized by the areal power density and the areal mass loading.
Thermal Period	The time period in which thermal effects, such as higher temperatures or dried rock, are present in the region surrounding the repository.
Thermal Power Per Waste Package	The rate of heat released in watts by a particular waste package type. This will vary with fuel type and age, waste package capacity, and disposal configurations within waste packages.
Thermodynamic	Pertaining to the mechanical action of heat.
Thermodynamic/Kinetic Coefficients	Numbers that represent the rate of heat flow through a porous medium. An example is a coefficient that represents the rate of heat flow in a given type of rock.
Three-Dimensional Model	A three-dimensional representation of physical conditions and/or processes.
Time History	The predicted response of a system, expressed as a function of simulation time.
TOSPAC Computer Code	A computer code that simulates one-dimensional groundwater flow with the transport of decaying contaminants in partially saturated, fractured media.

Total Effective Dose Equivalent	The sum of the deep-dose equivalent, for external exposures, and the committed effective dose equivalent, for internal exposures.
Total System Performance Assessment (TSPA)	A risk assessment that quantitatively estimates how the proposed Yucca Mountain repository system will perform in the future under the influence of specific features, events, and processes, incorporating uncertainty in the models and data. Its purposes follow: (1) provide the basis for predicting system behavior and testing that behavior against safety measures in the form of regulatory standards (2) provide the results of TSPA analyses and sensitivity studies (3) provide guidance to site characterization and repository design activities (4) help prioritize testing and selection of the most effective design options.
TOUGH2 Computer Code	A computer program that simulates three-dimensional flow of groundwater and heat in unsaturated and saturated porous and fractured media. The code name is derived from Transport of Unsaturated Groundwater and Heat.
Toxicity	The ability of a substance to cause damage to cells or tissues of living organisms when the substance is inhaled, ingested, or absorbed by the skin. Acute toxicity is that which occurs over a short term of exposure, and chronic toxicity is that which occurs over a long term of exposure.
Tracer Testing	A procedure in which a soluble substance (tracer) is added to groundwater at one location, and its movement to another location is observed. Tracer testing is a technique by which groundwater flow directions and velocities and other hydrologic properties of rocks can be estimated.
Transient	Describing a variable that is changing with time. This occurs before development of a steady state condition.
Transient Modeling	Modeling of a system in which the variables are changing through time. Heating of the repository by the waste is a transient condition for which transient modeling is done.
Transparency	According to the Nuclear Waste Technical Review Board, the ease of understanding the process by which a study was carried out, which assumptions are driving the results, how they were arrived at, and the rigor of the analyses leading to the results. According to a Peer Review Panel report, transparency "requires ensuring completeness and using a logical structure that facilitates in-depth review of the relevant issues...achieved when a reader or reviewer has a clear picture of what was done in the analysis, what the outcome was, and why."

Transpiration	The process in which water enters a plant through its root system, passes through its vascular system, and is released into the atmosphere through openings in its outer covering. It is an important process for removal of water that has infiltrated below the zone where it could be removed by evaporation.
Transport	A process in which substances carried in groundwater move through the subsurface by means of the physical mechanisms of convection, diffusion, and dispersion and the chemical mechanisms of sorption, leaching, precipitation, dissolution, and complexation. Types of transport include advective, diffusive, and colloidal transport.
Transverse Dispersion	Dispersion of a solute moving in groundwater in directions transverse to the direction of the groundwater flow path. This movement may also be called lateral dispersion.
Tritium	A radioactive isotope of hydrogen that can be taken into the body easily, because it is chemically identical to natural hydrogen. Tritium decays by beta emission with a half-life of about 12.5 years.
TSPA Peer Review Panel	See Peer Review Panel.
Tuff	Igneous rock formed from compacted volcanic fragments from pyroclastic (explosively ejected) flows with particles generally smaller than 4 mm (0.16 in.) in diameter. The most abundant type of rock at the Yucca Mountain site.
Tuffaceous	A general term referring to any rock containing tuff.
Two-Dimensional Model	A two-dimensional slice through an entity, such as the earth's crust, usually in the horizontal and vertical directions, on which known features are placed and are used to predict likely features that may exist between points of known data. Mathematically, a model that represents physical conditions and/or processes; this mathematical model is composed of both horizontal rows and vertical columns of grid cells arrayed in L-shaped configurations only one grid cell thick. Also called a cross section.
Uncertainty	A measure of how much a calculated or estimated value that is used as a reasonable guess or prediction may vary from the unknown true value.
Undisturbed Performance	Refers to the expected or nominal behavior of the system as perturbed only by the presence of the repository. This is as used in description of scenarios, or features, events, or processes making up scenarios.

Unsaturated Zone	The zone of soil or rock below the ground surface and above the water table in which the pore spaces contain water, air, and other gases. Generally, the water saturation is below 100 percent in this zone, although areally limited perched water bodies (having 100 percent water saturation) may exist in the unsaturated zone. Also called the vadose zone.
Unsaturated Zone Flow	The flow of water in the unsaturated zone by downward percolation and by capillary action.
Unsaturated Zone Radionuclide Transport Model	A computer software code that defines the movement of radionuclides from the edge of the engineered barrier system, through the unsaturated zone, and to the boundary of the saturated zone.
Vadose Zone	See Unsaturated Zone.
Variable	See Section A.2 of this glossary.
Variability (Statistical)	A measure of how a quantity varies over time or space.
Velocity Field	The velocities of fluid flow, gas or liquid, in a region, which are generally depicted by arrows to indicate the direction and magnitude of the velocity.
Vitrified	Pertaining to a type of processed high-level radioactive waste where the waste is mixed with glass-forming chemicals and put through a melting process. The melted mixture is then put into a canister where it becomes a dry "log" of waste in a glassy matrix.
Vitrified Defense High-Level Radioactive Waste	A type of processed defense high-level radioactive waste that has been contained in a glass matrix.
Volcanism	Pertaining to volcanic activity.
WAPDEG Computer Code	A computer software code that was developed to model long-term corrosion degradation of waste disposal containers in the repository.

Waste Containment and Isolation Strategy	A document designed to assist the project management in prioritizing testing and analysis activities to focus on the most important issues in postclosure safety. It is also designed to help resolve uncertainty in processes and parameters of greatest significance to long-term performance. The document is still evolving. The key elements include the following: (1) Low groundwater flow amounts through storage area (2) Long-lived waste packaging (3) Cladding on the waste and low water content in waste to slow degradation (4) Engineered systems that promote slow dispersion/migration of radionuclides (5) Natural systems that promote slow dispersion/migration of radionuclides
Waste Form	A generic term that refers to radioactive materials and any encapsulating or stabilizing matrix.
Waste Package	The waste form and any containers (i.e., disposal container barriers and other canisters), spacing structures or baskets, shielding integral to the container, packing contained within the container, and other absorbent materials immediately surrounding an individual waste container placed internally to the container or attached to the outer surface of the disposal container. The waste package begins its existence when the outer lid welds are complete and accepted.
Waste Package Design Organization	The management and oversight department responsible for the waste package design and testing.
Waste Stream	Input of waste into the repository over time.
Water Flux	See Flux.
Water Table	The upper surface of a zone of saturation above which the majority of pore spaces and fracture openings are less than 100 percent saturated with water most of the time (unsaturated zone), and below which the opposite is true (saturated zone).
Weeps Model	A stochastic conceptual model of groundwater flow through fractured rock. The flow is assumed to occur through stochastically generated fracture paths, or weeps, with no interaction occurring between fracture and matrix.
Welded	Fused.
Welded Tuff	A tuff that was deposited under conditions where the particles making up the rock were heated sufficiently to cohere. In contrast to nonwelded tuff, welded tuff is considered to be denser, less porous, and more likely to be fractured (which increases permeability).

Young Spent Fuel, Old Spent Fuel	Terms used to designate groups of commercial spent nuclear fuels by their age since discharge from the power reactor. The young spent nuclear fuels are characterized by higher radiation levels and resulting higher heat outputs than the old spent nuclear fuels.
Yucca Mountain Waste Containment and Isolation Strategy	See Waste Containment and Isolation Strategy.
Zeolites	A large group of hydrous aluminosilicate minerals that act as molecular "sieves" because they can adsorb molecules with which they interact. At Yucca Mountain, they are secondary alteration products in tuff rocks when the rocks are exposed to groundwater and could act to retard the migration of radionuclides by their sieving action.
Zircaloy	An alloy material that may have any of several compositions including zirconium oxide. It is used as a cladding material.

A.2 GLOSSARY OF STATISTICS TERMS

Terms in this section are presented separately from the general glossary in Section A.1 because many of the statistical terms are defined in relation to other statistical terms. The terms are numbered to allow reference from the general glossary in Section A.1.

Coefficient of Multiple Determination	A measure of goodness of fit of a linear-regression model; a value near 1 indicates a good fit, meaning that the model is accounting for most of the uncertainty in the performance measure being analyzed.
Complementary Cumulative Distribution Function	A method of depicting the probability that a performance measure, such as dose, exceeds a given value. For most measures, the higher the value, the lower the probability.
Confidence	In statistics, a measure of how close the estimated value of a random variable is to its true value.
Confidence Interval	An interval that is believed, with a preassigned degree of confidence, to include the particular value of the random variable that is estimated.
Continuous Random Variable	Those variables whose value is determined by taking measurements and that can take <u>any</u> value of an infinite number of possible values within a certain value range. The concentration of radionuclides in water is a continuous random variable and, although ranging from zero to a value limited by the solubility of an individual radionuclide under given conditions, possible outcomes of dissolving a given radionuclide in water cannot be represented by a finite number of discrete values. This type of variable has a probability density function.

Correlation Coefficient	A coefficient (designated r) calculated in the analysis of paired data when neither of the variables can be singled out as of prior importance to the other and the study seeks to analyze their interdependence, as opposed to the dependence of one upon the other. This term is a dimensionless quantity that can be used (with certain reservations) as an absolute measure of the relationship between two variables. Mathematically, for two random variables, the ratio of their covariance to the product of their standard deviations. The correlation coefficient is also a measure of how close a scatter plot of points produced by one variable plotted against the other comes to falling on a straight line drawn through the trend of the points. In a negative correlation between the two variables, larger values of one are associated with smaller values of the other. In a positive correlation, larger values of one variable are associated with larger values of the other.
Covariance	For a pair of random variables, the expected value of the product of the deviations from their respective means. It measures the extent to which two variables vary together and if the variables are independent the covariance is zero (so is the correlation coefficient). If large values of one variable are associated with large values of the other, the covariance is positive, while if small values of one are associated with large values of another, the covariance is negative. The covariance is usually calculated to find the correlation coefficient.
Cumulative Distribution	For grouped data, a distribution that shows how many of the values are less than or more than specified values. For random variables this term is synonymous with distribution function.
Cumulative Distribution Function	For a continuous random variable, a function that quantifies the probability that the variable is no greater than any specified value of interest. The derivative of the cumulative distribution function is the probability density function. The cumulative distribution function is most commonly used to analyze continuous variables when data are not divided into categories (grouping by some qualitative description), and the probability density function is more appropriate when categorical studies of continuous random variables are performed.
Cumulative Probability	The probability that a random variable will have a value equal to or less than some specified value.
Dependent Variable	A variable whose value depends on one or more other variables. For example, the value (amount) of body weight is a variable that depends on several independent variables—the amount of calories taken in and the amount of calories burned, as well as genetics and probably other factors. As another example, the thermal load per acre of the repository is a dependent variable—it depends on the type, number, and spacing of waste packages emplaced.

Discrete Random Variables	Those variables whose values are finite, or countable in numbers. The number of waste packages of each type is a discrete variable. Discrete random variables have associated with them probability functions that tell the probability that the variable takes on any particular value. For example, in throws of two unbiased dice, the probability that the value of the numbers shown on the dice (a discrete random variable) for any throw will be two is one in 36; the probability function is 1/36.
Distribution	The overall scatter of values for a set of observed data. A term used synonymously with frequency distribution. Distributions have probability structures that are the probability that a given value occurs in the set.
Distribution Frequency	A representation of how values of an outcome or variable are distributed over the range of expected values.
Distribution Function	A function whose values are the probabilities that a random variable assumes a value less than or equal to a specified value. Synonymous with cumulative distribution.
Expected Value	A variable's mean, or average, outcome. The weighted average of the number of possible outcomes, with each outcome being weighted by its probability of occurrence. The mean of a probability distribution of a random variable that one would expect to find in a very large, random sample. The sum of the possible values, each weighted by its probability—the center of the random variable's histogram (frequency distribution).
Frequency Distribution	Formed when data are grouped into classes (or ranges of values within the overall set of values, such as 1 to 5, 5 to 10, 10 to 20, etc.), with the classes listed in a table (or other format) showing the number of data points that occur in each class.
Function (Mathematics)	A quantity that is variable and whose value depends on and varies with the value of another quantity or quantities. Functions show the mathematical relationship between dependent variables and the independent variables upon which the value of the dependent variables depend.
Histogram	A bar graph representation of a frequency distribution having frequency of occurrence as the ordinate (y axis) and classes of values observed in sampling of the variable as the abscissa (x axis). The area of each rectangle in the histogram represents the proportion of observations (relative frequency) that fall in that interval. This is the relative frequency of observations that lie between the two values that form the class boundary. It is not for a single value but is relative frequency of the class interval.
Linear Correlation	The relationship between two or more random variables for which the regression equations are linear.

Linear Regression	A regression where the relationship between the (conditional) mean of a random variable and one or more independent variables can be expressed by the mathematical equation that describes a line. A relationship between two variables such that the dependence of one variable on the other can be described by (the equation of) a straight line.
Linear Stepwise Regression	An analysis designed to determine variables that have the greatest influence on an output value (e.g., peak dose rate) when there are many variables whose input values go into the calculation. In simple terms, a linear regression is performed for a line in a multidimensional space, and the correlation of the values of different variables to the line are examined by performing the calculation multiple times and varying the value of one variable at a time while holding the others constant. This is a stepwise process in which one variable at a time is examined to determine the impact of its influence on the final outcome (peak dose rate, for instance).
Mean (Arithmetic)	For a statistical data set, the sum of the values divided by the number of items in the set. The arithmetic average.
Mode	A measure of location in a data set defined as the value which occurs with the highest frequency. For qualitative data it is the attribute which occurs most frequently. A set of data or a distribution can have more than one mode, or if no two values are alike, no mode. For the distribution of a random variable the mode is the value for which the probability function or probability density is at the relative maximum.
Monte Carlo (Uncertainty) Analysis	An analytical method that uses random sampling of parameter values available for input into numerical models as a means of approximating the uncertainty in the process being modeled. A Monte Carlo simulation comprises many individual runs of the complete calculation using different values for the parameters of interest as sampled from a probability distribution. A different final outcome for each individual calculation and each individual run of the calculation is called a realization. Each realization is equally likely to occur in the Monte Carlo process.
Percentile	For a large data set where specific values are not repeated extensively, used to indicate where a value lies in relation to the entire group of values. For example, the 25th percentile indicates that about 25 percent of the items are smaller than this value and about 75 percent are larger than this value.
Probability	The relative frequency with which an event occurs in the long run. Statistical probability is about what really happens in the real world and can be verified by observation or sampling. Knowing the exact probability of an event is usually limited by the inability to know, or compile the complete set of, all possible outcomes over time or space.

Probability-Density Function	A frequency distribution such that the bars of a histogram that would represent it are so narrow that their tops would form a smooth curve if connected by a line. The curve is the probability density function. This type of distribution can be made if the number of observations of the value of a continuous random variable increases indefinitely, and the width of the range represented by each class (class interval) becomes smaller and smaller. The area under the density function curve between any two points on the curve, such as x_1 and x_2, represents the probability that the value of the random variable will lie between these two values.
Probability Distribution	The set of outcomes (values) and their corresponding probabilities for a random variable.
Quantile	A value at or below which lies a given fraction (1/5, 30 percent, etc.) of a set of data. Also called fractile.
R^2	A correlation coefficient that quantifies the goodness of fit of a linear regression model to an output value such as peak dose rate. A value of one corresponds to a perfect fit.
R^2 - Loss	The amount of change in fit when a variable is dropped from a linear stepwise regression analysis. For example, look at a linear stepwise regression analysis such that the out put (e.g., dose) is calculated using 10 variables and the total R^2 is 0.80 (1 corresponds to a perfect fit). If the analysis is then performed with one of the variables left out and the R^2 is 0.78 (meaning it changed or lost very little), then that variable does not contribute strongly to the fit. If the loss is large such as going from 0.80 to 0.60, then the variable does contribute strongly to the fit. This is a method of showing to which variables the outcome (peak dose) is most sensitive or responsive.
Random Variable	A property that has a numerical description and is determined by the outcome of a random experiment or random sampling. The different values of the random variable have different probabilities of occurrence. Also called variates.
Range (Statistics)	The numerical difference between the highest and lowest value in any series.
Rank Transformation	A type of data transformation used either to reduce the influence of extreme values or to deal with non-linearities in data sets. Data will fit better to a non-linear curve if it is first put into ranks. In ranking, the data values of both input and input data are replaced with the rank of that data value within the data set. The smallest value of a data set is replaced with the number 1, the second smallest is replaced with the number 2, and so forth up to the largest value in the set.

Regression	The relationship between the (conditional) mean of a random variable and one or more independent variables.
Regression Analysis	The analysis of paired data such that one member of the pair is a constant and the other is a random variable. The analysis of a paired dependent variable and the independent variable upon which it depends. For example, the term was first used in a study of the heights of fathers and sons where a regression (or turning back) was observed toward the mean height of the population in the heights of sons whose fathers were taller or shorter than the mean.
Scatter Plot	(1) A set of points arrived at by plotting paired values as points in a plane. (2) A two-dimensional dot plot.
Standard Deviation	(1) For a set of observations or a frequency distribution, the square root of the average of the squared deviations from the mean divided by n-1 (where n is the sample size). (2) The square root of the variance.
Variable	A nonunique property or attribute.
Variance	(1) The square of the standard deviation. (2) The expected squared distance from the population mean of a random variable, sometimes called the population variance.

Viability Assessment of a Repository at Yucca Mountain